Free ebooks ==> www.Ebook777.com

# Dendrimers in Nanomedicine

www.Ebook777.com

Free ebooks ==> www.Ebook777.com



Taylor & Francis
Taylor & Francis Group
http://taylorandfrancis.com

www.Ebook777.com

Free ebooks ==> www.Ebook777.com

# Dendrimers in Nanomedicine

edited by
Delphine Felder-Flesch

Pan Stanford Publishing

www.Ebook777.com

Free ebooks ==> www.Ebook777.com

*Published by*

Pan Stanford Publishing Pte. Ltd.
Penthouse Level, Suntec Tower 3
8 Temasek Boulevard
Singapore 038988

Email: editorial@panstanford.com
Web: www.panstanford.com

**British Library Cataloguing-in-Publication Data**
A catalogue record for this book is available from the British Library.

**Dendrimers in Nanomedicine**

Copyright © 2016 Pan Stanford Publishing Pte. Ltd.

*All rights reserved. This book, or parts thereof, may not be reproduced in any form or by any means, electronic or mechanical, including photocopying, recording or any information storage and retrieval system now known or to be invented, without written permission from the publisher.*

For photocopying of material in this volume, please pay a copying fee through the Copyright Clearance Center, Inc., 222 Rosewood Drive, Danvers, MA 01923, USA. In this case permission to photocopy is not required from the publisher.

ISBN 978-981-4745-49-9 (Hardcover)
ISBN 978-981-4745-50-5 (eBook)

Printed in the USA

www.Ebook777.com

# Contents

*Preface* xiii

**1. General Introduction on Dendrimers, Classical versus Accelerated Syntheses and Characterizations 1**

*Audrey Parat and Delphine Felder-Flesch*

1.1 General Introduction 1
1.2 Synthesis 4
1.2.1 Classical Synthesis Pathways 5
1.2.1.1 Divergent growth 5
1.2.1.2 Convergent growth 6
1.2.1.3 Orthogonal convergent growth 8
1.2.2 Accelerated Approaches 9
1.2.2.1 Double-stage convergent method or the hypercore approach 10
1.2.2.2 Hypermonomer method or the branched monomer approach 11
1.2.2.3 Double-exponential method 12
1.2.2.4 Orthogonal coupling method or the two-step approach, the two monomers approach, and the $AB_2$–$CD_2$ approach 13
1.2.2.5 Other accelerated strategies 14
1.3 Characterization 14
1.4 Conclusion 16

**2. Dendrimer–Nanoparticle Conjugates in Nanomedicine 23**

*Catalina Bordeianu and Delphine Felder-Flesch*

2.1 Introduction 23
2.2 Why Dendrimers and Dendrons? 31

2.3 Dendrimer NPs Conjugates 32
2.3.1 Gold Nanoparticles 33
2.3.2 Quantum Dots Dendritic Nanoboxes 36
2.3.3 Iron Oxide Nanoparticles 38
2.3.3.1 NPs synthesis 39
2.3.3.2 Synthesis of dendrons 43
2.3.3.3 Nanohybrids 47
2.3.3.4 In vivo applications 54
2.3.4 Up-Conversion NPs 63
2.3.5 Manganese Oxide NPs 64
2.4 Conclusion 65

**3. Dendritic Polymers for the Repair of Tissues 77**

*Cynthia Ghobril and Mark W. Grinstaff*

3.1 Introduction 78
3.2 Synthesis and Properties of Dendritic Hydrogels 79
3.2.1 Physical Gelation 80
3.2.2 Chemical Gelation 85
3.3 Tissue Repair and Tissue Engineering Applications 92
3.3.1 Tissue Repair 92
3.3.2 Tissue Engineering 99
3.4 Conclusions 102

**4. Polyglycerols in Nanomedicine 107**

*Mohiuddin Quadir and Rainer Haag*

4.1 Introduction 108
4.2 Chemistry and Chemical Diversification of dPGs 111
4.2.1 Origin and Evolution of dPGs Structure 111
4.2.2 Chemistry of Linear PGs: Analogue Frequently Overlooked 112
4.2.3 Macromonomers of Linear PG: Building Complex Topology 116
4.2.4 Dendritic PGs: Branched Scaffold with Nanoscale Benefits 117

4.2.5 Well-Defined Hyperbranched PG: dPGs with Random Regularity 119
4.2.6 Core Variation of dPG Increases Functionality and Applicability 121
4.2.7 Block Copolymers of Dendritic Polyglycerol 123
4.2.8 Postpolymerization Modification: Tailoring the Properties of Polyglycerol 125
4.2.9 Giant Polyglycerols: Motifs Resulting in Megamers, Microgels, and Hydrogels 126
4.3 Forms Guiding Functions: Features of dPGs Architecture 128
4.4 Biocompatibility of Dendritic Polyglycerols 130
4.5 Nanomedical Applications of dPGs 131
4.5.1 Supramolecular Platforms of dPGs for Noncovalent Guest Encapsulation 132
4.5.2 Multifunctional dPG–drug Conjugates for Tumor Targeting 153
4.5.3 Designing Functional Architectures Based on PG for Multivalent Interaction 159
4.5.3.1 Neutral PGs as mimicry of oligosaccharides for surface modification 162
4.5.3.2 Negatively charged dPG derivatives 164
4.5.3.3 Applications of polycationic derivatives ofdendritic PGs 168
4.5.4 Polyglycerol Nanogel in Biomedicine 172
4.6 Opportunities 187
4.7 Conclusions 189

**5. Theranostic Potential of Dendronized Iron Oxide Nanoparticles 201**

*Aurélie Walter, Audrey Parat, Delphine Felder-Flesch, and Sylvie Begin-Colin*

5.1 Introduction 201

5.2 Influence of the NPs Synthesis Way and of the Functional Peripheral End Groups on the Grafting Conditions and Colloidal Stability 206
5.3 MRI Properties of Dendronized Iron Oxide NPs 210
5.4 Mastering Shape and Composition of Dendronized Iron Oxide Nanoparticles to Tailor Magnetic Hyperthermia Properties 213
5.5 Conclusion 220

**6. Anti-Inflammatory Dendrimers 229**

*Cédric-Olivier Turrin and Anne-Marie Caminade*

6.1 Introduction 229
6.2 Cargo-Loading Strategy: Association of Anti-Inflammatory Drugs with Dendrimers 232
6.2.1 Non-Targeted Strategies 234
6.2.1.1 Drug-dendrimer interactions 234
6.2.1.2 Surface-modified and core-modified dendrimers 236
6.2.1.3 In vivo validation of cargo-loading strategies 237
6.2.2 Targeted Strategies 238
6.3 Prodrug Strategy: Conjugation of Anti-Inflammatory Drugs on Dendrimers 240
6.3.1 Dendrimer-NSAI Drug Conjugates 241
6.3.2 Controlled Release of *N*-Acetyl-Cysteine with Dendrimer Conjugates 244
6.3.3 Glucosamine-Terminated Dendrimers 247
6.3.4 Dendrimer-Corticoid Conjugates 249
6.3.5 Targeted Strategies and Covalent Grafting 251
6.4 Dendrimers Showing Anti-Inflammatory Properties per se 252
6.4.1 Carbosilane Dendrimers 252
6.4.2 PPH Dendrimers 254
6.4.3 Other Examples 258
6.4.3.1 PAMAM 258

6.4.3.2 Click dendrimers 259
6.5 Conclusions and Perspectives 260

**7. Structurally Flexible and Amphiphilic Poly(Amidoamine) Dendrimers as Nonviral Vectors for siRNA Delivery 273**

*Xiaoxuan Liu, Yang Wang, and Ling Peng*

7.1 Introduction 273
7.2 Structurally Flexible TEA-Core PAMAM Dendrimers 276
7.3 Amphiphilic PAMAM Dendrimers 282
7.4 Conclusion and Prospects 285

**8. Dendrimers as Nanomedicine in Cancer Therapy 293**

*Keerti Jain and N. K. Jain*

8.1 Introduction 294
8.2 Cancer Targeted Drug Delivery 296
8.3 Gene Therapy: Cancer 299
8.4 Brain Delivery 300
8.5 Dendrimer Hybrids with Other Nanomaterials in Cancer Therapy 301
8.6 Theranostic Applications 302
8.7 Future Prospects 303
8.8 Conclusion 305

**9. Impact of Physicochemical Properties on Dendrimer Pharmacokinetics and Biodistribution 311**

*Orlagh Feeney, Suzanne M. Caliph, Christopher J. H. Porter, and Lisa M. Kaminskas*

9.1 Introduction 312
9.2 Understanding Pharmacokinetics 313
9.3 Intravenous Pharmacokinetics 317
9.3.1 Introduction 317
9.3.2 Effect of Size 318
9.3.3 Effect of Surface Charge 321
9.3.4 Effect of Drug Loading 324
9.3.5 Effect of Structural Flexibility 325

9.4 Tumor Biodistribution 326
9.4.1 Passive Tumor Targeting 326
9.4.2 Active Tumor Targeting 328
9.5 Subcutaneous Pharmacokinetics 329
9.5.1 Introduction 329
9.5.2 Structure of the Interstitial Space 330
9.5.3 Impact of Dendrimer Size on Absorption from Subcutaneous Injection Sites 331
9.5.4 Impact of Surface Charge on Subcutaneous Absorption 333
9.6 Oral Pharmacokinetics 335
9.7 Transdermal Pharmacokinetics 337
9.8 Pulmonary Pharmacokinetics 339
9.9 Conclusion 342

**10. Molecular Modeling of Dendrimers 353**

*Matteo Garzoni and Giovanni Pavan*

10.1 Summary 353
10.2 Introduction 354
10.2.1 Dendrimers and Their Applications 354
10.2.2 Limits of the Experiments in the Characterization of Dendrimers and the Potential of Molecular Modeling 357
10.3 Molecular Modeling of Dendrimers 358
10.3.1 First Dendrimers Models 358
10.3.2 Atomistic Simulation of dendrimers in the Gas-Phase 359
10.3.3 Characterization of the Dendrimers in Solution 361
10.3.4 Coarse Graining 367
10.3.5 Advanced Sampling Techniques: Metadynamics 369
10.4 Some Practical Applications of Molecular Modeling in the Field of Dendrimers 370

10.4.1 Dendritic Host for Small Hydrophobic Guests: Accessibility to the Dendrimer's Interior 370
10.4.2 Dendrimers' Flexibility 372
10.4.3 Dendrimers Self-Assembly Solution 379
10.4.4 Dendrimers Aggregates Responsive to External Stimuli 381
10.5 Conclusions and Future Perspectives 384

*Index* 397



Taylor & Francis
Taylor & Francis Group
http://taylorandfrancis.com

# Preface

Dendrimers are synthetically produced monodisperse polymeric nanostructures with a tree-like, highly branched architecture. They are routinely synthesized as tunable "nanostructures" that may be designed and regulated as a function of their size, shape, surface chemistry, and interior void space. The word "dendron" is also encountered and accounts for "one branch" of the tree or one elementary building block which shows a functionality at its focal point. A variety of dendrimers are available, and each has biological properties such as polyvalency, self-assembling, electrostatic interactions, chemical stability, low cytotoxicity, and solubility. Since the beginning of their history, hundreds of dendritic structures have been elaborated and some of them are now commercially available (Chapter 1). Indeed, dendrimers offer a plethora of applications deriving from the intrinsic properties of polymers but also and especially from their characteristics: on-surface easily accessible functions, porosity, flexibility of the internal branches, presence of functionalized cavities, accessibility to the core, and of course multivalency and cooperativity. These are extremely adaptable materials, with respect to their structure, flexibility, porosity or morphology, which can all be tuned at will.

Nanomaterials, and dendrimers as such, are increasingly becoming part of our daily lives as they are used as imaging agents, coatings, and wound dressings, in cosmetics, and for drug or gene delivery and photodynamic therapy. Their versatile properties lead to their desirability and exploitation in new products and, of course, in competitive production processes.

This book will appeal to anyone involved in nanobiotechnology, macromolecular science, cancer therapy, tissues repair, and siRNA delivery research as it covers research on dendrimer-based or dendrimer–nanoparticles hybrid nanodevices for use in nanomedicine, including aspects from materials sciences, biology, various diagnostic methodologies, and computer simulation.

Chapter 1 is a general introduction on dendrimers summarizing their classical (divergent, convergent, or orthogonal convergent growths) versus accelerated (hypercore approach, hypermonomer method, double-exponential method, the "two-steps approach") syntheses and main characterizations.

The second chapter covers recent advances in dendrimer–nanoparticle conjugates as efficient tools in nanomedicine. It highlights that dendrimer-based organic/inorganic hybrids made of gold, metal oxides (iron, manganese), up-conversion nanoparticles, or quantum dots represent highly advanced pharmaceutical tools, able to target a specific type of cell or organ, to be tracked while doing it, and to deliver a specific drug in situ. For example, due to their high colloidal stability, administration of dendronized hybrids of small size can be done through intravenous injection, which is less intrusive and more efficient and goes toward a "better life" medicine method.

Chapter 3 deals with dendritic polymers for the repair of tissues. As the clinical demands increase for better approaches to repair damaged or diseased tissues, so do the design requirements for the materials to be used. For tissue repair the dendrimers or dendritic macromolecules are crosslinked to form hydrogels. This chapter describes the state of the art with these different dendritic hydrogel formulations, including their design requirements, the synthetic routes, the measurement and determination of their properties, and the evaluation of their in vitro and in vivo performances for tissue repair. Chapter 4 concerns a specific class of dendritic materials called polyglycerols. It not only outlines the chemistry and structural diversification of dendritic polyglycerols (dPGs) but also highlights how forms guide functions through features of dPGs architecture, and ends up to application areas in nanomedicine. Chapter 5 reviews the theranostic potential of dendronized iron oxide nanoparticles and how to master their shapes and compositions to tailor magnetic hyperthermia properties, or how to tune their organic coating to reach efficient magnetic resonance imaging (MRI) contrast enhancement.

The search for new anti-inflammatory drugs is an area of strong interest, related to several health issues, but dendrimer-based anti-inflammatory strategies are rather scarce. Chapter 6 presents different strategies that have been proposed in the past years and among them (i) the cargo-loading approach (non-covalent

association of anti-inflammatory drugs with dendrimers), (ii) the pro-drug approach (anti-inflammatory drugs linked to dendrimers, with a possible control over the drug release), and (iii) dendrimers having intrinsic anti-inflammatory properties.

Chapter 7 is devoted to structurally flexible and amphiphilic poly(amidoamine) dendrimers as non-viral vectors for siRNA delivery. Although viral vectors are very effective for siRNA delivery, increasing concerns over their safety and immunogenicity substantiate the need to develop alternative nonviral vectors. Chapter 7 shows how structurally flexible and amphiphilic PAMAM dendrimers can outperform the commercially available siRNA delivery agents and promote functional siRNA delivery in various cells including human primary and stem cells as well as in animal models.

Chapter 8 reviews dendrimers as nanomedicine in cancer therapy (targeted drug delivery, gene therapy, brain delivery) or as efficient theranostic platforms and gives helpful future prospects.

Then, a detailed chapter on pharmacokinetics and biodistribution issues of dendrimers (Chapter 9) will help the reader choosing the right structures for successful transfer from bench to bedside. This chapter therefore gives an overview of the current understanding of the pharmacokinetic and biodistribution behavior of dendrimers, and how this can be dictated by physicochemical properties. The last chapter (10) is devoted to molecular modeling of dendrimers. Indeed, simulations can provide unique insight into shape, size, and overall features of dendrimers in different conditions, which constitutes the first milestone to understand the dendrimers' properties. In general, computer-aided simulations constitute an important platform to characterize the dendrimers' behavior on a multiscale level: from understanding the features of the dendrimer, to molecular recognition and self-assembly.

Good reading!

**Delphine Felder-Flesch**



Taylor & Francis
Taylor & Francis Group
http://taylorandfrancis.com

## Chapter 1

# General Introduction on Dendrimers, Classical versus Accelerated Syntheses and Characterizations

**Audrey Parat[a] and Delphine Felder-Flesch[a]**

[a]*IPCMS, UMR CNRS UDS 7504,*
*23 rue du loess BP 43, 67034 Strasbourg cedex 2, France*

Delphine.Felder@ipcms.unistra.fr

## 1.1 General Introduction

The word "dendrimer" comes from the Greek words, *δένδρον* or *dendros*, which translates to "tree-like" for their shape and *meros* meaning ''part of'' for the reminiscence of their chemical structure made by additional monomers.[1] In 1978, Egon Buhleier, Winfried Wehner, and Fritz Vögtle were the first to publish a paper on a new type of polymer, the polypropylene-imine (PPI), that was "capable of binding ionic guests or molecules in a Host-Guest interaction, and obtained through a synthetic pathways allowing a frequent repetition of similar steps. These new "cascade molecules," made by a repetitive monomer addition and an activation of the obtained branched molecules, gave birth to a new class of step-by-step synthesized molecules: the dendrimers.[2]

*Dendrimers in Nanomedicine*
Edited by Delphine Felder-Flesch
Copyright © 2016 Pan Stanford Publishing Pte. Ltd.
ISBN 978-981-4745-49-9 (Hardcover), 978-981-4745-50-5 (eBook)
www.panstanford.com

15:58 28 October 2016

Dendrimers are synthetically produced as monodisperse polymeric nanostructures with a tree-like, highly branched architecture. They are routinely synthesized as tunable "nanostructures" that may be designed and regulated as a function of their size, shape, surface chemistry and interior void space. The word "dendron" is also encountered and accounts for "one branch" of the tree or one elementary building block which shows a functionality at its focal point.[3,4]

The first dendrimers published by Fritz Vögtle in 1978[2] were prepared via a *divergent growth* like those elaborated by R. G. Denkewalter at Allied Corporation in 1981,[5] Donald Tomalia at Dow Chemical Co. in 1983 and 1985[1,6] and George Newkome in 1985.[7] The *convergent growth* was later introduced, in 1990, by Jean M. J. Fréchet.[8]

Dendrimers are typically 2 to 20 nm in diameter and are composed of combinations of core types such as ethylene diamine (EDA), diaminobutyl (DAB), polyamidoamine (PAMAM), polypropylimine (PPI). They also have different surface residues such as amine, carboxyl, and alcoholic groups to name but a few.

Dendrimers can be divided in three distinct regions: the core, the interior (or branches), and the periphery (surface groups).

A variety of dendrimers are available, and each has properties such as polyvalency, self-assembling, electrostatic interactions, chemical stability, low cytotoxicity, and solubility. The well-defined molecular compositions, sizes, and shapes of PAMAM dendrimers have also made them particularly attractive as (1) scaffolds for paramagnetic metal ions in magnetic resonance imaging and (2) templates for the synthesis of metal-bearing nanoparticles with tunable electronic, optical, catalytic, and biologic activity.

Since the beginning of their history, hundreds of dendritic structures have been elaborated and among them Vögtle's PPI, Tomalia's polyamidoamine (PAMAM), Denkewalter's poly(L-lysine) (PLL), Newkome's polyamide, Grinstaff's polyester (PGLSA-OH) and Hult's poly(2,2-bis(hydroxymethyl)propionic acid (bis-MPA)) structures.[9] These dendrimers are commercially available from providers like Dendritech Inc. (PAMAM), Frontier Scientific Inc. (Newkome's polyamides), Colcom (poly(L-lysine)), Polymer Factory (bis-MPA), and DSM (PPI).[10]

Dendrimers are often compared to their forebears, the polymers, but they are never obtained by polymerization. Dendritic

15:58 28 October 2016

structures can be divided into *monodisperse* dendrimers and dendrons (elementary unit) and *polydisperse* hyperbranched polymers, dendrigrafts and dendritic-linear hybrids such as dendronized polymers (Fig. 1.1).[11]

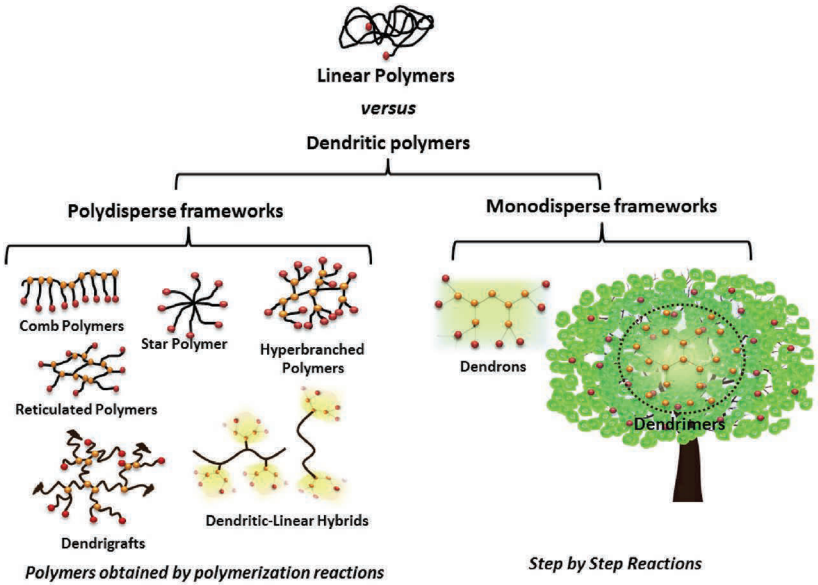



**Figure 1.1** Representative scheme of the sub-classes of dendritic versus linear polymers.

Dendrimers offer a plethora of applications deriving from the intrinsic properties of polymers but also and especially from their characteristics: on-surface easily accessible functions, porosity, flexibility of the internal branches, presence of functionalized cavities, accessibility to the core, and of course multivalency and cooperativity.[12]

Dendrimers are extremely adaptable materials, with respect to their structure, flexibility, porosity or morphology, which can all be tuned at will. Their applications rely on chemistry (synthesis, analysis, catalysis…), materials sciences (films, layers and hybrids), pharmacology (drugs, medicine), nanosciences (nanoparticles), biology, and medicine (immunology).[13]

Dendrimers are widely investigated and utilized in biomedical applications, as they have multiple surface functional groups that can be used to target or label the dendrimer for imaging and drug delivery applications.

15:58 28 October 2016

*Drug delivery*: Dendrimers have also found application in transdermal drug delivery systems and show potential in gene delivery and for enhancing the oral bioavailability of problematic drugs. The presence of numerous surface groups makes dendrimers suitable carriers for delivering high drug payloads. The interior space of dendrimers can be used to conjugate or encapsulate drugs. They are utilized for delivery vehicles of nonsteroidal anti-inflammatory drugs (NSAIDs), anticancer drugs, and other drugs such as simvastatin, famotidine, or quinolones. Drug–dendrimer conjugates show high solubility, reduced systemic toxicity, and selective accumulation in solid tumors.

*Imaging*: The multivalent character of dendrimers positioned these well-defined and hyperconnected macromolecules to the foreground in the development of new contrast agents for medical imaging or diagnosis platforms with adjustable retention times and biodistribution properties according to their generation/size, to their flexibility and/or their hydrophilicity.[14] In addition to chemistry, the characterization and the physicochemical properties of these structures were studied in detail.[15–18]

*Coatings*: PAMAM dendrimers have been applied in a variety of coating systems. Instrumental Polymer Technologies has developed dendrimers for wood coating products.

*Wound dressings*: Dendrimers have been investigated for wound dressing applications due to their high antimicrobial activity. PAMAM dendrimers also exhibit strong anti-inflammatory activity.

*Cosmetics*: Dendrimers have been incorporated into cosmetic film-forming agents. They are utilized for controlled release, to extend shelf life and enhance solubilization. L'Oreal, Unilever, and The Dow Chemical Company possess patents for dendrimers in hair care, skin care, and nail care products.

## 1.2 Synthesis

A dendrimer is a macromolecule constituted by elementary building blocks called "dendrons" which connect according to a tree-like process around a multifunctional core. These structures are synthesized in cascade by an iterative sequence of reactive steps to grow from the first generation "*n*" to the second generation "*n* + 1" and so on (Fig. 1.2). According to their perfectly branched

structure, their synthesis requires the use of robust organic reactions that can efficiently help their growth to a macromolecular level.[19]

The concept of dendrimers evoked by Flory in the 1940s,[20–22] became a reality only at the end of the 1970s and the beginning of the 1980s thanks to the groups of Vögtle,[2] Denkewalter,[5] Tomalia[1] and Newkome.[23] The 1980s were thus dedicated to the development of synthesis methods and it was only at the beginning of the 1990s that their properties began to be explored.[24]

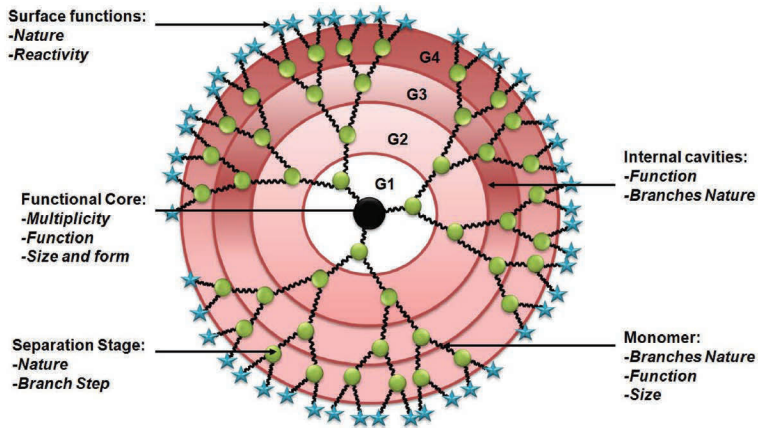



**Figure 1.2** General structure of a dendrimer.

## 1.2.1 Classical Synthesis Pathways

Dendrimers are usually synthesized according to methods allowing controlling their structure at every stage of construction. The dendritic structures are mostly synthesized by two main different approaches: divergent or convergent.

### 1.2.1.1 Divergent growth

In the *divergent approach*, the dendrimer is synthesized from the core, the starting point, and built from generation to generation toward the periphery (Fig. 1.3). So the first generation $G_1$ is obtained by coupling of an $AB_2$ unit on the central core. The second generation $G_2$ is then obtained via a sequence of "activation-coupling" reactions. The repetition of such sequence allows the synthesis of higher generations "$G_n$."

15:58 28 October 2016

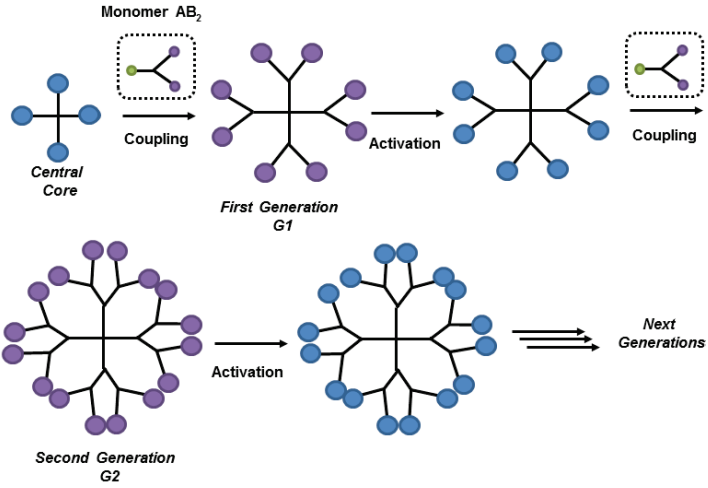



**Figure 1.3** Dendrimers synthesis method called "Divergent Growth."

However, the large number of reactions which must be made on a single molecule (with a large number of equivalent reactive sites) require quantitative transformations (more than 99% of yield) to avoid defects. Using such an approach renders a complete functionalization of the surface a difficult objective to achieve for dendrimers of the highest generations.[25]

Another difficulty ensuing from the previous one (defects can rarely be avoided) is the purification: indeed, the separation/purification of the desired dendrimer from those presenting unreacted functional surface groups proves to be quite delicate as the molar masses, the polarities, the size of these products are nearby. In order to avoid all those issues, another approach called the "*convergent growth"* appears as a good alternative.

### 1.2.1.2 Convergent growth

Such an approach was first developed by Hawker and Fréchet in 1990.[26,27] It starts from the synthesis of the branches of various generations via a "coupling and activation" sequence, which are then connected to the functional core (Fig. 1.4).

In the *convergent growth*, only a small number of reactive sites are involved in each reaction step, thus giving rise to few secondary reactions and to rather defectless structures. Every so-obtained generation can easily be purified, even if the purification becomes harder as the generation increases. Nevertheless, one

15:58 28 October 2016

issue relies on the central position of the reactive groups: indeed for higher generations the focal point is more and more isolated as buried by branches, which leads to reactivity decrease.

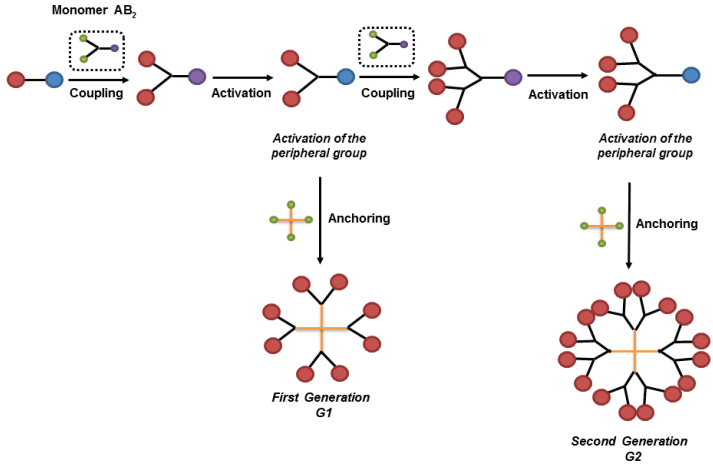



**Figure 1.4** Dendrimers synthesis method called "Convergent growth."

Through the convergent growth it is also possible to create asymmetric architectures, for example by connecting two different dendronized pieces, to lead to "*Janus" dendrimers*. There are three commonly used methods to produce such structures as shown in Fig. 1.5.

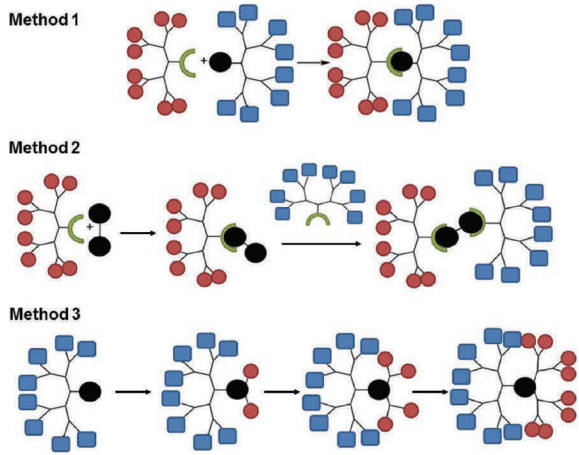



**Figure 1.5** Three commonly used methods for the elaboration of "Janus" Dendrimers.

15:58 28 October 2016

15:58 28 October 2016

The first synthesis method of Janus dendrimers consists of the reaction between two dendrons with complementary functions at their cores (method 1). The second one is based on a first connection between the focal point of a dendron and a bifunctional core. Then a second dendron is grafted, again through its focal point, to the remaining available function of the core (method 2). Finally, the last method, which has been rarely proposed, consists in using the focal point of a dendron for the growing of new branches by a divergent process (method 3).

There are different examples of Janus dendrimers in the literature.[28] Their use is very important in biomedicine, which relies essentially on their multifunctional architectures answering the current theranostic issues (Fig. 1.6).[29]

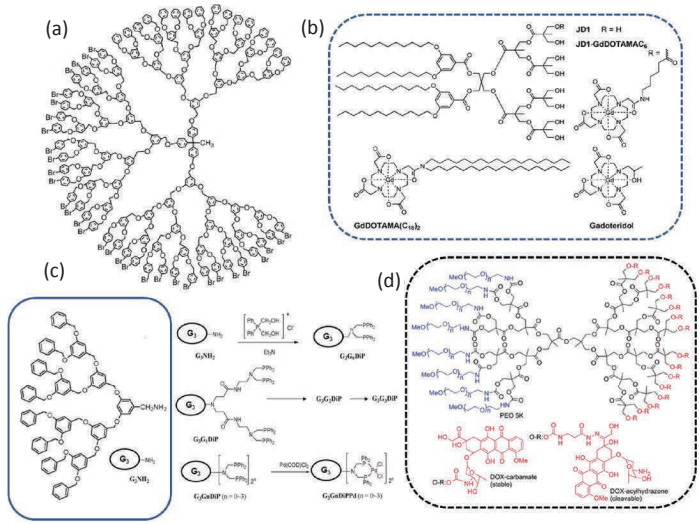



**Figure 1.6** Different literature examples of Janus Dendrimers. (a) The first Janus dendrimer reported made of poly(benzyl ether) dendrons[30]; (b) Janus dendrimer JD1 and its GdDOTAMAC$_6$, Gd-DOTAMA(C$_{18}$)$_2$ and Gadoteridol[31] conjugates; (c) Synthesis of dendritic phosphine ligands and in situ generated Pd-catalysts[32]; (d) Janus dendrimers functionalized on one side by anticancer agent doxorubicin (DOX), either through a stable (carbamate) or cleavable (acylhydrazone) bond.[33]

### 1.2.1.3 Orthogonal convergent growth

The *orthogonal approach* was described for the first time by J. M. J. Fréchet in 1993.[34] This pathway allows for the synthesis

of a new generation after each reaction step. This process requires the use of orthogonal monomers, meaning that one monomer is the activated form of the other one (Fig. 1.7). The synthesis of poly(benzyl ester) dendrimers through such "activated-monomer" approach illustrates well the accelerated process toward higher generations with good to high yields.[35]

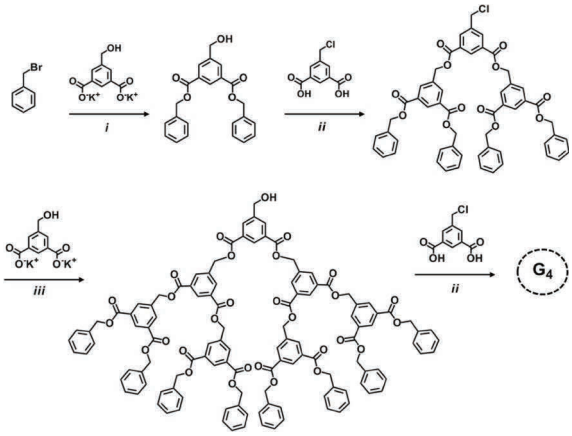



**Figure 1.7** Synthesis of poly(benzyl ester) dendrimers by the orthogonal convergent growth method. Reagents and conditions: (i) 18-C-6, $K_2CO_3$, $CH_3CN$, $\Delta$; (ii) DCC, DPTS, $CH_2Cl_2$, THF; (iii) KBr, DMF, 80°C.

Despite its advantages, the orthogonal approach seems not competing with the convergent and divergent approaches. Indeed, several issues slow down the generalization of its use and mainly the presence of activated species after each reaction, which potentially leads to secondary products. Consequently, a judicious choice of the reactive species is essential to overcome this problem.

As the dendrimers market keeps on increasing (1 ton/year planed in 2025), the challenge was to revise those traditional dendritic syntheses pathways and develop less time consuming protocols, new structures through cheaper and faster growth methods.

### 1.2.2 Accelerated Approaches

Of the large number of reports on dendrimer synthesis, only a few have reached commercial availability. This limitation can be traced back to challenges in the synthetic paths including a large

15:58 28 October 2016

15:58 28 October 2016

number of reaction steps required to obtain dendritic structures with desired features. Along with an increased number of reaction steps come not only increased waste of chemical and valuable starting materials but also an increased probability to introduce structural defects in the dendritic framework. If we take a look on the past, the synthesis of dendrimers is tedious, long and costs a lot. The most important difficulty when a high generation is synthesized is to ensure the full substitution of all reactive groups. This leads to the introduction of defects within the structure increases. To overcome those issues, accelerated approaches were developed with the aim to reduce the number of reaction steps, the reaction time, chemicals and cost.[36,37]

### 1.2.2.1 Double-stage convergent method or the hypercore approach

The *double-stage convergent method* is derived from the convergent process. This hypercore approach relies on three steps: (1) low-generation dendrons with protected terminal groups are coupled to a multifunctional core through their focal point, then (2) terminal groups of the obtained dendrimer, called *hypercore*, are deprotected, and finally (3) dendrons (same or different) are reacted with this hypercore, leading to the desired higher generation dendrimer (Fig. 1.8).

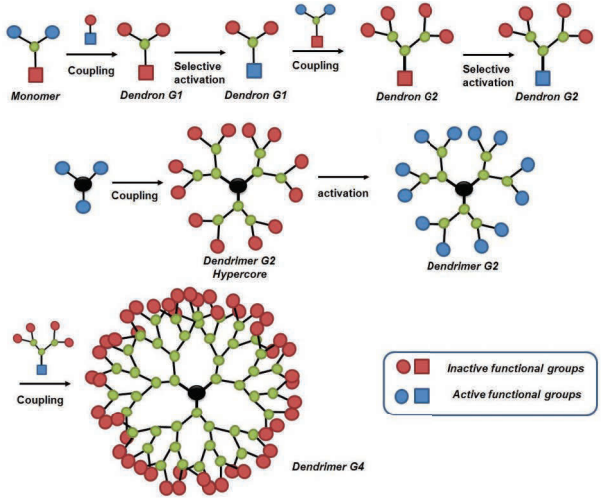



**Figure 1.8** Synthesis of dendrimers by the double-stage convergent method or the hypercore approach.

15:58 28 October 2016

Compared to the classical convergent synthesis, this approach uses a *hypercore*, which reduces steric hindrance and helps obtaining higher generation and monodisperse dendrimers. This method enables the formation of dendrimers with chemically differentiated internal and external branches, like the layer-block dendrimers,[35,38] by utilizing two different types of monomers in the synthesis of the hypercore and the dendrons. However, the hypercore method has drawbacks such as time-consuming synthesis needed to obtain the hypercore, the dendrons and the final dendrimers.

#### 1.2.2.2 Hypermonomer method or the branched monomer approach

In *the hypermonomer method*, monomers are named hypermonomers as they display a higher number of functional groups than conventional $AB_2$ or $AB_3$ monomers. Using these $AB_4$ hypermonomers (sometimes $AB_8$), dendrimers showing a high number of functional groups are obtained in few steps. For example, the preparation of a G4 dendrimer by a classical method (with a tetrafunctional core and $AB_2$ monomers) requires eight steps where the use of $AB_4$ hypermonomers results in a G4 dendrimer in only four steps (Fig. 1.9).

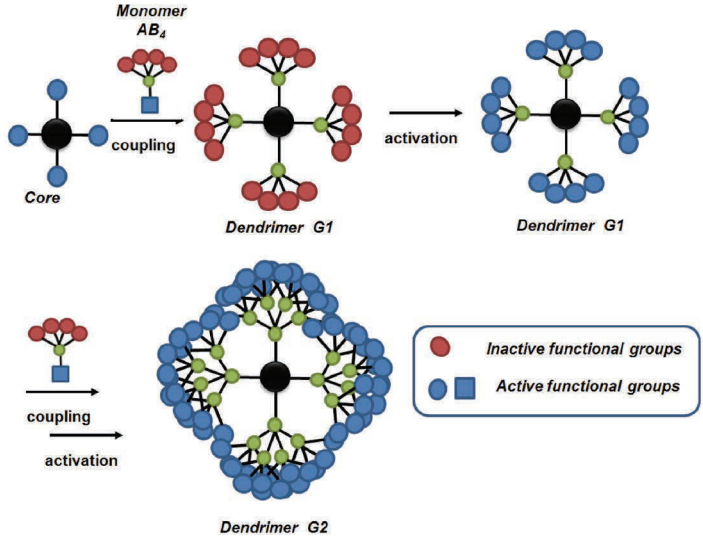



**Figure 1.9** Synthesis of dendrimers according to the hypermonomer method.

15:58 28 October 2016

Such *hypermonomer method* allows obtaining high generation dendrimers in few steps.[39,40] However, the hypermonomers are usually dendrons of low generation, whose synthesis requires several growth and activation steps. Therefore, the acceleration is in this case limited to generating dendrimers in fewer steps, without considering the time required for monomer synthesis. This strategy has been used by J. M. J. Fréchet et al.[41] in 1994 for the preparation of a G5 poly(aryl ether) dendron in three steps or by Pavan and Simanek et al. in 2013 for the synthesis of a G13 large virus dendrimer of triazines linked by diamines with a monochlorotriazine hypermonomer.[42]

### 1.2.2.3 Double-exponential method

This strategy was introduced by Moore et al. in 1995 for the synthesis of a G4 poly(phenylacetylene) dendron[43] and is particularly adapted to the elaboration of large multifunctional dendrons or dendrimers.

Technologically, the *double-exponential growth strategy* requires an $AB_2$ monomer with orthogonally protected A and B functional groups. This monomer is activated selectively (focal point or periphery) to give two differently activated monomers which are coupled together to obtain a G2 protected dendron. Repeating the selective activation/coupling process allows reaching G4, then G8, then G16 dendron. In a final step the focal points of the dendrons are activated and coupled to a multifunctional core (Fig. 1.10).

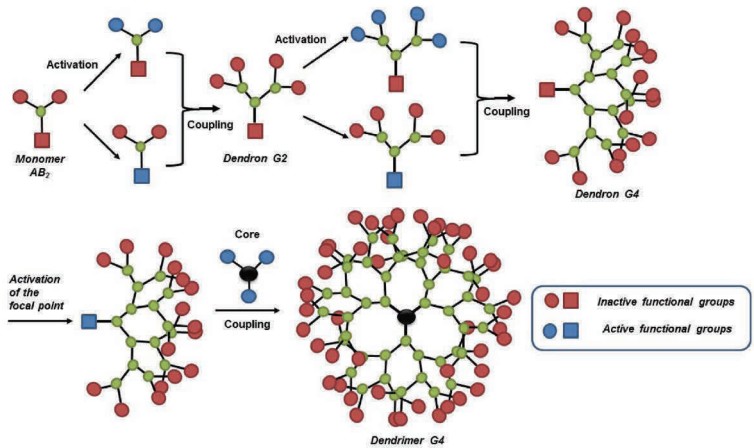



**Figure 1.10** Synthesis of dendrimers according to the double-exponential method.

15:58 28 October 2016

Theoretically, using this approach, a generation seven dendrimer can be obtained after 9 synthetic steps, whereas 14 synthetic steps would be necessary to obtain a similar structure with a conventional approach.

Poly(amide),[44] poly(ether urethane)[45] and poly(ester) dendrimers were obtained with such method. Among them the synthesis of now commercially available dendrimers based on 2,2-bis(hydroxymethyl)propionic acid (bis-MPA) monomer, performed by Hult and Gitsov et al. in 1996 is famous.[46,47]

The double-exponential method, which is similar to the convergent method, belongs to the versatile procedures enabling the preparation of classical, supramolecular, or asymmetrical (JANUS) dendrimers.

#### 1.2.2.4 Orthogonal coupling method or the two-step approach, the two monomers approach, and the $AB_2$–$CD_2$ approach

The orthogonal coupling method uses two different monomers, namely $AB_2$ and $CD_2$, with chemoselective functional groups. These monomers are selected in such a way that the focal functionality of one monomer will react specifically with the periphery of the other (A with C and D with B). Such chemoselectivity eliminates the need for activation steps and reduces the number of reaction steps by a half. Consequently, in such strategy each step gives a new generation of dendron or dendrimer (Fig. 1.11).

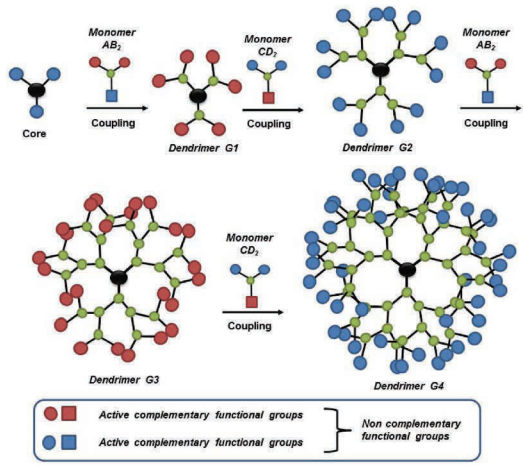



**Figure 1.11** Synthesis of dendrimers according to the orthogonal coupling method via the divergent growth.

15:58 28 October 2016

As this approach starts with two different monomers ($AB_2$ and $CD_2$), the obtained layer-block dendrimers contain different covalent linkages in their architecture.

There are different literature-reported studies related to this accelerated process: for example, the orthogonal coupling method was first reported by Spindler and Fréchet in 1993 for the one-pot synthesis of a G3 poly(ether urethane) dendron.[48] The synthesis of high generation dendrimers via the $AB_2$-$CD_2$ approach was demonstrated later by Zimmerman et al. in 1996 for G4 poly(alkyne ester) dendrimers.[49] Then, Yu et al.[50] published the first orthogonal synthesis of G4 poly(aryl alkene) dendrons with identical chemical functions in their structure. The efficiency of such orthogonal coupling method is especially high when the synthesis is performed in a one-pot system as for G4 phosphorus-containing dendrimers reported by Caminade and Majoral in 2001.[51]

To conclude, the orthogonal coupling method allows a fast synthesis of dendrimers but its limitation is caused by the need of highly efficient and orthogonal coupling reactions with specific functionalities.

#### 1.2.2.5 Other accelerated strategies

The key point of the different accelerated syntheses of dendrimers is the elimination of the iterative activation steps. Chemoselective reactions can give good results in this way through solid-phase syntheses, click chemistry, thiol-ene coupling or Diels–Alder cycloaddition.[34,35] Another possibility is to use multicomponent reactions (MCRs) combining three or more reactants in a one-pot process such as the Passerini-3CR or three component reaction and the Ugi-4CR or four component reaction.[52]

In order to facilitate the synthesis of dendrimers in fewer steps, scientists have been looking at the possibility of eliminating the need for purification steps. This was made possible through the use of one-pot synthesis (mix between the orthogonal way and the click chemistry for example) as shown by Malkoch,[53] Fréchet,[54] or Caminade[55] to obtain bifunctional dendrimers.[56]

## 1.3 Characterization

Dendrimers are synthesized by a step-by-step procedure thus displaying repetitive units in their architecture. In theory, they

15:58 28 October 2016

are monodisperse but some examples in the literature prove that this idea is false, especially for dendrimers built by a divergent approach.

As to dendrimers characterization, different used techniques give complementary information regarding chemical composition, weight, morphology, shape, size, and homogeneity.[13] Main useful analytical techniques can be divided into several categories: separation techniques (size exclusion chromatography (SEC), electrophoresis), spectroscopy/spectrometry (nuclear magnetic resonance (NMR), infrared (IR), UV-visible, fluorescence, Mass) and scattering techniques (laser light scattering (LLS), small-angle neutrons (SANS) or X-rays (SAXS)…), "electrical" techniques (electron paramagnetic resonance (EPR), electrochemistry), microscopy (transmission electron (TEM) and atomic force (AFM)), rheology (viscosity, differential scanning calorimetry (DSC)).

Nuclear magnetic resonance is certainly the most widely used in routine analysis for characterizing dendrimers, but special techniques have also been used to probe their size and morphology. Routine NMR analyses are especially useful during the step-by-step synthesis of dendrimers, even up to high generations, because they afford information about the chemical transformations undergone by the end groups. For example, this technique is the best to follow the extent of amine alkylation by methyl acrylate in PAMAM dendrimers.[1] For heteroatom-containing dendrimers, besides $^{1}H$ and $^{13}C$ NMR, the resonance of the heteroatom can afford very valuable information; this is especially true for phosphorus dendrimers.[57]

Infrared spectroscopy is mainly used for the routine analysis of the chemical transformations occurring at the surface of dendrimers, while UV–Visible spectroscopy can be used to monitor the synthesis of dendrimers, as shown for organoplatinum dendrimers in which a growth and decay of the metal to ligand charge transfer band is observed.[58]

The high sensitivity of fluorescence has been used to quantify defects during the synthesis of dendrimers, such as unreacted $CO_2H$ groups in ARB dendrimers,[59] but its main use is to characterize the structure of dendrimers having photochemical probes covalently linked to one particular section.[60]

Mass Spectrometry allows obtaining information on the molecular mass and the presence of defects in the structure, especially when the Infrared or Ultraviolet spectroscopies are

inefficient. Many type of dendrimers have been studied and well defined thanks to this technique (polyesters, poly(propylene imine), polybenzylacetylenes, PAMAM, phosphorous-containing dendrimers…).[61] However, this technique is highly sensitive to the experimental conditions, especially for the type of matrix,[62] and the presence of ions, as shown by post-source decay investigations.[63]

## 1.4 Conclusion

Dendrimers are synthetically produced as nanostructures with a tree-like, highly branched architecture. They are routinely synthesized as tunable "nanostructures" that may be designed and regulated as a function of their size, shape, surface chemistry and interior void space. They are made of three distinct regions: the core, the interior (or branches), and the periphery (surface groups).

A variety of dendrimers are available, and each has properties such as polyvalency, self-assembling, electrostatic interactions, chemical stability, low cytotoxicity, and solubility. Their well-defined molecular compositions, sizes and shapes have also made them particularly attractive as scaffolds for highly efficient medical imaging probes (in magnetic resonance imaging (MRI), in Nuclear Medicine or in optical imaging) or as templates for the synthesis of metal-bearing nanoparticles with tunable electronic, optical, catalytic, and biologic activity.

Nanomaterials, and dendrimers as such, are increasingly becoming part of our daily lives as they are used as imaging agents, coatings, and wound dressings, in cosmetics, for drug or gene delivery, photodynamic therapy. Their versatile properties lead to their desirability and exploitation in new products and of course in competitive production processes.

### References

1. Tomalia DA, Baker H, Dewald J, Hall M, Kallos G, Martin S, Roeck J, Ryder J, Smith P (1985). A new class of polymers: Starburst-dendritic macromolecules, *Polym J*, **17**, 117–132.
2. Buhleier E, Wehner W, Vögtle F (1978). "Cascade" and "Nonskid-Chain-like" syntheses of molecular cavity topologies, *Synthesis*, **2**, 155–158.

15:58 28 October 2016

3. Vögtle F, Richardt G, Werner N (2009). *Dendrimer Chemistry Concepts, Syntheses, Properties, Applications*, Wiley-VCH, ISBN 3-527-32066-0.
4. Nanjwade BK, Bechraa HM, Derkara GK, Manvia FV, Nanjwade VK (2009). Dendrimers: Emerging polymers for drug-delivery systems, *Eur J Pharm Sci*, **38**(3), 185–196.
5. US Patent, Denkewalter RG, Kolc J, Lukasavage WJ, Macromolecular highly branched homogeneous compound based on lysine units, US 4289872 A (1979). US Patent, Denkewalter RG, Kolc J, Lukasavage WJ, Macromolecular highly branched homogeneous compound, US 4410688 A (1981).
6. US Patent, Tomalia DA, Dewald JR, Dense star polymers having core, core branches, terminal groups, US 4507466 A (1983).
7. Newkome GR, Yao Z, Baker GR, Gupta VK (1985). Micelles. Part 1. Cascade molecules: A new approach to micelles. A [27]-arborol, *J Org Chem*, **50**(11), 2003–2004.
8. Hawker CJ, Fréchet JMJ (1990). Preparation of polymers with controlled molecular architecture. A new convergent approach to dendritic macromolecules, *J Am Chem Soc,* **112**(21), 7638–7647.
9. Tomalia DA (2005). Birth of a new macromolecular architecture: Dendrimers as quantized building blocks for nanoscale synthetic polymer chemistry, *Prog Polym Sci*, **30**, 294–324.
10. Mintzer MA, Grinstaff MW (2011). Biomedical applications of dendrimers: A tutorial, *Chem Soc Rev*, **40**, 173–190.
11. Schlüter AD, Rabe JP (2000). Dendronized polymers: Synthesis, characterization, assembly at interfaces, and manipulation, *Angew Chem Int Ed*, **39**, 864–883.
12. Li MH, Choi SK, Thommey PT, Desai A, Lee KH, Kotlyar A, Banaszak Holl MM, Baker, Jr. JR (2012). Dendrimer-based multivalent methotrexates as dual acting nanoconjugates for cancer cell targeting, *Eur J Med Chem,* **47C**, 560–572.
13. Caminade AM, Turrin CO, Laurent R, Ouali A, Delavau-Nicot B (2011). *Dendrimers, Towards Catalytic, Material and Biomedical Uses*, Wiley-VCH, ISBN 978-0-470-74881-7.
14. Xu H, Regino CA, Bernardo M, Koyama Y, Kobayashi H, Choyke PL, Brechbiel MW (2007). Towards improved syntheses of dendrimer-based magnetic resonance imaging contrast agents: New bifunctional diethylenetriaminepentaacetic acid ligands and nonaqueous conjugation chemistry, *J Med Chem*, **50**, 3185–3193.
15. Wiener EC, Brechbiel MW, Brothers H, Magin R L, Gansow OA, Tomalia DA, Lauterbur PC (1994). Dendrimer-based metal chelates:

15:58 28 October 2016

A new class of magnetic resonance imaging contrast agents, *Magn Res Med*, **31**, 1–8.

16. Tomalia DA, Kaplan DA, Kruper WJ Jr, Cheng RC, Tomlinson IA, Fazio MJ, Hedstrand DM, Wilson LR, U. S. Patent 5338532 (1994).
17. Tomalia DA, Wilson LR, Hedstrand DM, Tomlinson IA, Fazio MJ, Kruper WJ Jr, Kaplan DA, Edwards DS, Cheng RC, Jung CW, US Patent, 5527524 (1996).
18. Tomalia DA, Baker JR, Cheng RC, Bielinska AU, Fazio MJ, Hedstrand DM, Johnson JA, Kaplan DA, Klakamp SL, et al., US Patent, 5714166 (1998).
19. Campagna S, Ceroni P, Puntoriero F (2012). *Designing Dendrimers*, Wiley-VCH, ISBN 978-470-43355-3.
20. Flory PJ (1941). Molecular size distribution in three dimensional polymers I. Gelation, *J Am Chem Soc*, **63**, 3083–3090.
21. Flory PJ (1941). Molecular size distribution in three dimensional polymers. II. Trifunctional branching units, *J Am Chem Soc*, **63**, 3091–3096.
22. Flory PJ (1941). Molecular size distribution in three dimensional polymers II. Tetrafunctional branching units, *J Am Chem Soc*, **63**, 3096–3100.
23. Newkome GR, Yao Z, Baker GR, Gupta VK (1983). Micelles part I. cascade molecules: A new approach to micelles. A [27] arborol, *J Org Chem*, **50**, 2003–2004.
24. Tomalia DA, Fréchet JMJ (2002). Discovery of dendrimers and dendritic polymers: A brief historical perspective, *J Polym Sci Part A*, **40**, 2719–2728.
25. Hummelen JC, Van Dongen JLJ, Meijer EW (1997). Electrospray mass spectrometry of Poly(propylene imine) dendrimers: The issue of dendritic purity or polydispersity, *Chem Eur J*, **3**, 1489–1493.
26. Hawker CJ, Fréchet JMJ (1990). Preparation of polymers with controlled molecular architecture. A new convergent approach to dendritic macromolecules, *J Am Chem Soc*, **112**, 7638–7647.
27. Hawker CJ, Fréchet JMJ (1990). A new convergent approach to monodisperse dendritic macromolecules, *J Chem Soc Chem Commun*, 1010–1011.
28. Caminade AM, Laurent R, Delavaux-Nicot B, Majoral JP (2012). "Janus" dendrimers: Syntheses and properties, *N J Chem,* **36**, 217–226.

15:58 28 October 2016

15:58 28 October 2016


29. Ornelas C, Pennell R, Liebes LF, Weck M (2011). Construction of a well-defined multifunctional dendrimer for theranostics, *Org Lett*, **13**(5), 976–979.
30. Caminade AM, Laurent R, Delavaux-Nicot B, Majoral JP (2012). Janus dendrimers: Syntheses and properties, *N J Chem,* **36**, 217–226.
31. Filippi M, Martinelli G, Mulas G, Ferraretto M, Teirlinck E, Botta M, Tei L, Terreno E (2014). Dendrisomes: A new vesicular nano-platform for MR-molecular imaging applications, *Chem Commun*, **50**, 3453–3456.
32. Liu J, Feng Y, He Y, Yang N, Fan QH (2012). Janus dendritic phosphines: Synthesis and application in Suzuki coupling reactions, *N J Chem*, 2012, **36**, 380–385.
33. Caminade AM, Turrin CO (2014). Dendrimers for drug delivery, *J Mater Chem B*, **2**, 4055–4066.
34. Spindler R, Fréchet JMJ (1993). Two-step approach towards the accelerated synthesis of dendritic macromolecules, *J Chem Soc Perkin Trans,* **1**, 913–918.
35. Freeman AW, Fréchet JMJ (1999). A rapid, orthogonal synthesis of Poly(benzyl ester) dendrimers via an "activated" monomer approach, *Org Lett*, **1**, 685–687.
36. Walter MV, Malkoch M (2012). Simplifying the synthesis of dendrimers: Accelerated approaches, *Chem Soc Rev*, **41**, 4593–4609.
37. Sowinska M, Urbanczyk-Lipkowska Z (2014). Advances in the chemistry of dendrimers, *N J Chem*, **38**, 2168–2203.
38. Wooley KL, Hawker CJ, Frechet JMJ (1991). Hyperbranched macromolecules via a novel double-stage convergent growth approach, *J Am Chem Soc*, **113**, 4252–4261.
39. Morgenroth F (1998). Spherical polyphenylene dendrimers via Diels–Alder reactions: The first example of an A4B building block in dendrimer chemistry, *Chem Commun*, 1139–1140.
40. Maraval V, Caminade AM, Majoral JP, Blais JC (2003). Dendrimer Design: How to Circumvent the Dilemma of a Reduction of Steps or an Increase of Function Multiplicity?, *Angew Chem Int Ed*, **42**, 1822–1826.
41. Wooley KL, Hawker CJ, Frechet JMJ, (1994). A "branched-monomer approach" for the rapid synthesis of dendrimers, *Angew Chem Int Ed Engl*, **33**, 82–85.
42. Lim J, Kostiainen M, Maly J, Da Costa VCP, Annunziata O, Pavan GM and Simanek EE (2013). Synthesis of Large Dendrimers with the Dimensions of Small Viruses, *J Am Chem Soc*, **135**, 4660–4663.

15:58 28 October 2016


43. Kawaguchi T, Walker KL, Wilkins CL, Moore JS (1995). Double Exponential Dendrimer Growth, *J Am Chem Soc*, **117**, 2159–2165.
44. (a) Zanini D, Roy R (1996). Novel Dendritic $\alpha$-Sialosides: Synthesis of glycodendrimers based on a 3,3′-iminobis(propylamine) core, *J Org Chem*, **61**, 7348–7354; (b) Ashton PR, Anderson DW, Brown CL, Shipway AN, Stoddart JF, Tolley MS (1998). The synthesis and characterization of a new family of polyamide dendrimers, *Chemistry Eur J*, **4**, 781–795; (c) Ishida Y, Jikei M, Kakimoto M (2000). Rapid synthesis of aromatic polyamide dendrimers by an orthogonal and double-stage convergent approach, *Macromolecules*, **33**, 3202–3211.
45. Klopsch R, Franke P, and Schluter AD (1996). Repetitive strategy for exponential growth of hydroxy-functionalized dendrons, *Chemistry Eur J*, **2**, 1330–1334.
46. Ihre H, Hult A, Fréchet JMJ, Gitsov I (1998). Double-stage convergent approach for the synthesis of functionalized dendritic aliphatic polyesters based on 2,2-bis(hydroxymethyl)propionic acid, *Macromolecules*, **31**, 4061–4068.
47. Carlmark A, Malmström E, Malkoch M (2013). Dendritic architectures based on bis-MPA: Functional polymeric scaffolds for application-driven research, *Chem Soc Rev*, **42**, 5858–5879.
48. Spindler R, Fréchet JMJ (1993). Two-step approach towards the accelerated synthesis of dendritic macromolecules, *J Chem Soc*, *Perkin Trans.*, **1**, 913–918.
49. Zeng F, Zimmerman SC (1996). Rapid synthesis of dendrimers by an orthogonal coupling strategy, *J Am Chem Soc*, **118**, 5326–5327.
50. Deb SK, Maddux TM, Yu L (1997). A simple orthogonal approach to poly(phenylenevinylene) dendrimers, *J Am Chem Soc*, **119**, 9079–9080.
51. (a) Maraval V, Laurent R, Marchand P, Caminade AM, Majoral JP (2005). Accelerated methods of synthesis of phosphorus-containing dendrimers, *J Organomet Chem*, **690**, 2458–2471; (b) Brauge L, Magro G, Caminade AM, Majoral JP (2001). First divergent strategy using two AB2 unprotected monomers for the rapid synthesis of dendrimers, *J Am Chem Soc*, **123**, 6698–6699.
52 (a) Zhu J, Bienayme H (2005). *Multicomponent Reactions*, Wiley-VCH, ISBN 9783527308064; (b) Wessjohann LA, Neves Filho RAW, Rivera DG (2012). *Isocyanide Chemistry: Applications in Synthesis and Materials Science*, Wiley-VCH, ISBN 9783527330430.
53. Antoni P, Nystrom D, Hawker CJ, Hult A, Malkoch M (2007). A chemoselective approach for the accelerated synthesis of well-defined dendritic architectures, *Chem Comm*, 2249–2251.

15:58 28 October 2016


54. Lee CC, Gillies ER, Fox ME, Guillaudeu SJ, Fréchet JMJ, Dy EE, Szoka FC (2006). A single dose of doxorubicin-functionalized bow-tie dendrimer cures mice bearing C-26 colon carcinomas, *Proc Natl Acad Sci USA*, **103**, 16649–16654.

55. Maraval V, Laurent R, Donnadieu B, Mauzac M, Caminade AM, Majoral JP (2000). Rapid synthesis of phosphorus-containing dendrimers with controlled molecular architectures: First example of surface-block, layer-block, and segment-block dendrimers issued from the same dendron*, J Am Chem Soc*, **122**, 2499–2511.

56. Antoni P, Hed Y, Nordberg A, Nystrom D, von Holst H, Hult A, Malkoch M (2009). Bifunctional dendrimers: From robust synthesis and accelerated one-pot postfunctionalization strategy to potential applications, *Angew Chem Int Ed*, **48**, 2126–2130.

57. Caminade AM, Laurent R, Majoral JP (2005). Characterization of dendrimers, *Adv Drug Deliv Rev,* **57**, 2130–2146.

58. Achar S, Puddephatt RJ (1994). Organoplatinum dendrimers formed by oxidative addition*, Angew Chem Int Ed*, **33**, 847–849.

59. Newkome GR, Wies CD, Moorefield CN, Weis I (1997). Detection and functionalization of dendrimers possessing free carboxylic acid moieties, *Macromolecules,* **30**, 2300–2304.

60. Wilken R, Adams J (1997). End group dynamics of fluorescently labeled dendrimers, *Macromol Rapid Commun*, **18**, 659–665.

61. (a) Hummelen JC, van Dongen JLJ, Meijer EW (1997). Electrospray mass spectrometry of poly(propylene imine) dendrimers: The issue of dendritic purity or polydispersity, *Chem.-A Eur J*, **3**, 1489–1493; (b) Kallos GJ, Tomalia DA, Hedstrand DM, Lewis S, Zhou J (1991). Molecular weight determination of a polyamidoamine Starburst polymer by electrospray ionization mass-spectrometry, *Rapid Commun Mass Spectrom*, **5**, 383–386; (c) Tolic LC, Anderson GA, Smith RD, Brothers HM, Spindler R, Tomalia DA (1997). Electrospray ionization Fourier transform ion cyclotron resonance mass spectrometric characterization of high molecular mass Starburst (TM). dendrimers, *Int J Mass Spectrom*, **165**, 405–418; (d) Sahota HS, Lloyd PM, Yeates SG, Derrick PJ, Taylor PC, Haddleton DM (1994). Characterization of aromatic polyester dendrimers by matrix-assisted laser-desorption ionization mass-spectrometry, *J Chem Soc-Chem Commun*, 2445–2446.

62. Chessa G, Scivanti A, Seraglia R, Traldi P (1998). Matrix effects on matrix-assisted laser desorption/ionization mass spectrometry analysis of dendrimers with a pyridine-based skeleton, *Mass Spectrom*, **12**, 1533–1537.

63. Nuebert H, Knights KA, de Miguel YR, Cowan DA (2003). MALDI-TOF post-source decay investigation of alkali metal adducts of apolar polypentylresorcinol dendrimers, *Macromolecules*, **36**, 8297–8303.

15:58 28 October 2016

# Chapter 2

# Dendrimer–Nanoparticle Conjugates in Nanomedicine

**Catalina Bordeianu and Delphine Felder-Flesch**

*IPCMS, UMR CNRS UDS 7504,*
*23 rue du loess BP 43, 67034 Strasbourg cedex 2, France*

Delphine.Felder@ipcms.unistra.fr

## 2.1 Introduction

The ideas and concepts behind nanoscience and nanotechnology started with a talk entitled "There's Plenty of Room at the Bottom" by physicist Richard Feynman at an American Physical Society meeting at the California Institute of Technology (CalTech) on December 29, 1959, long before the term nanotechnology was used. In his talk, Feynman described a process in which scientists would be able to manipulate and control individual atoms and molecules. Over a decade later, in his explorations of ultra-precision machining, Professor Norio Taniguchi coined the term nanotechnology. It was not until 1981, with the development of the scanning tunneling microscope that enabled us to "see" individual atoms that modern nanotechnology began.

As one of the newest areas of science, nanoscale science and technology are seen by many as the key technology of the 21st

*Dendrimers in Nanomedicine*
Edited by Delphine Felder-Flesch
Copyright © 2016 Pan Stanford Publishing Pte. Ltd.
ISBN 978-981-4745-49-9 (Hardcover), 978-981-4745-50-5 (eBook)
www.panstanford.com

15:59 28 October 2016

century, which of course raises the question as to what role this technology will play in medicine. In general two concepts of nanomedicine can be distinguished. Some experts define nanomedicine very broadly as a technology that uses molecular tools and knowledge of the human body for medical diagnosis and treatment. Others accent the original meaning of nanotechnology as one that makes use of physical/chemical effects occurring in nanoscale objects that exist at the interface between molecular and macroscopic world in which quantum mechanics still reigns.[1] It currently relies on definitions provided by the National Nanotechnology Initiative (NNI): (1) development of research and technology at the atomic, molecular or macromolecular levels, within the scale of nanosize of approximately 1 to 100 nanometer in range; (2) devices and systems that have novel properties and functions based on nanobiomaterials, because of their small and/or intermediate size; (3) ability to control and manipulate the atomic level.[2]

The past decades surge in development, roadmaps and foresight studies in what has been termed *Nanomedicine*. The *European Science Foundation's* report calls for a coordinated strategy to deliver new nanotechnology-based medical tools for diagnostic and therapeutics. This is evidenced by the emergence within this field of many new high impact journals, international symposia, medical companies and start-ups, and an exponential growth in publications, patents, citations, clinical trials and projected global markets. At the current annual growth rate of 12.3%, global markets are projected to reach 177.6 billion $US by 2019.[3] The major nanomedicine growth areas are predicted to be primarily in neurology, oncology and cardiovascular, anti-inflammatory and anti-infective applications.

Lately, there has been a steady increase in the number of nanoparticle-based therapeutics approved by the FDA (US Food and Drug Administration), some of the products are listed in the Table 2.1. Currently, nanomedicine is dominated by drug delivery systems, accounting for more than 75% of total sales.[4] *Neulasta*, *Pegasys* and *PEG-Intron* are the therapeutics that account for most of the sales. The most widely used nanotechnology product in the field of in vitro diagnostic is colloidal gold in lateral flow assays, which is used in rapid tests for pregnancy, ovulation, HIV and other indications. Further, gold nanoparticles are also used for

cell sorting applications in clinical diagnosis. In the field of biomaterials *Filtek Supreme* was the first product introduced in 2002 as dental restoratives nanotechnologies. Furthermore, *Vitoss* has been successfully commercialized for the repair of bone defects. A commercial success story was the launch of *Acticoat* in 1998, a silver nanoparticle-based wound dressing. All of the marketed contrast agents consist of superparamagnetic iron oxide nanoparticles (SPIONs) for magnetic resonance imaging (MRI). Advanced Magnetic's *Gastromark* was the first product of this category, approved in 1993 in Europe and 1996 in the United States. The only other product was *Resovist* approved in 2000 for liver imaging on European market.[5]

15:59 28 October 2016

**Table 2.1** Nanomedicine products on the market

| Healthcare application | Composition/ active ingredient | Indications | Company/start-up |
|---|---|---|---|
| *Drug delivery* | | | |
| Abraxane | Paclitaxel protein bound nanoparticles | Cancer | Abraxis Bioscience, AstraZeneca |
| AmBisome | Liposomal Amphotericin B | Fungal infections | Gilead, Fujisawa |
| Daunoxome | Liposomal daunorubicin | Kaposi sarcoma | Gilead |
| Doxil/Caelyx | Liposomal Dexorubicin | Cancer, Kaposi sarcoma | Ortho Biotech, Schering-Plough |
| Neulasta | PEG-G-CSF | Febrile neutropenia | Amgen |
| Pegasys | PEG-$\alpha$-interferon 2a | Hepatitis C | Nektar, Hoffmann-La Roche |
| PEG-Intron | PEG-$\alpha$-interferon 2b | Hepatitis C | Enzon, Schering-Plough |
| Repamune | Nanocrystalline sirolimus | Immunosuppressant | Elan Drug Delivery, Wyeth Pharmaceuticals |
| *In vivo imaging* | | | |
| Resovist | Iron oxide nanoparticles (IONPs) | Liver tumors | Schering |

(*Continued*)

**Table 2.1** (*Continued*)

| Healthcare application | Composition/ active ingredient | Indications | Company/start-up |
|---|---|---|---|
| Feridex/ Endorem | IONPs | Liver tumors | Advanced Magnetics, Guerbet |
| Gastromark/ Lumirem | IONPs | Imaging of abdominal structures | Advanced Magnetics, Guerbet |
| *In vitro diagnostics* | | | |
| Lateral flow tests | Colloidal gold | Pregnancy, ovulation, HIV | British Biocell, Amersham/GE, Nymox |
| Clinical cell separation | Gd nanoparticles | Immunodiagnostics | Dynal/Invitrogen, Miltenyi Biotec, Immunicon |
| *Biomaterials* | | | |
| Filtek Supreme | Nanoparticle composite (NPsCo) | Dental filling material | 3M Espe |
| Vitoss | Nano-hydroxyapatite | Bone defects | Orthovita |
| Acticoat | Silver nanoparticles | Antimicrobial wound care | Nucryst |

15:59 28 October 2016

As in most areas of biotechnology, developments in nanomedicine are technology driven. However, the various unique properties of nanomaterials are beneficial towards medical applications. Drug industry shows interest in the use of nanosuspensions for increasing the solubility of certain types of small-molecule drugs. This technology is applied to drugs that are poorly water soluble and therefore cannot be administrated. At present about 40% of small molecule drugs in the pipeline of pharmaceutical companies belong to this class. This exemplifies how nanotechnology may offer solutions to fundamental problems in the pharmaceutical industry. Besides, researchers have improved on the current standards in drug delivery relating the biodistribution, intra-cellular uptake, and dosing efficacy by utilizing nanoparticles to encapsulate/absorb therapeutic agents and target sites of disease, a strategy somewhat akin to the "Trojan Horse."

Understanding the influence of nanoparticle properties—critical nanoscale design parameter (CNDPs)—on clinical translation issues, such as pharmacokinetics (PKs), pharmacodynamics (PDs), bioaccumulation, excretion modes and toxicology, is of utmost importance. These CNDPs include size, shape, surface chemistry, flexibility/rigidity, architecture and elemental composition. The ability to structure, control and engineer CNDPs is undoubtedly the major challenge in the translation of nanoparticle-based therapeutics into approved clinical applications.

Although progress in the application of nanotechnology has been dramatic and successful, substantial opportunities exist for the development of future generation nanotherapeutics by improving upon certain recognized nanoparticle limitations associated with the present prototypes.[6] Efforts are focused on creating more complex platforms that integrate real-time diagnostic, imaging, targeting and therapy delivery features. Various colloidal inorganic nanoparticles that feature properties such as: (i) luminescence (e.g. semiconductor quantum dots (QDs)[7]; up-/down-conversion nanoparticles),[8] (ii) magnetic properties (e.g. metal oxide nanoparticles)[9] and (iii) plasmonic properties (e.g. noble metal nanoparticles)[10] have been widely explored. For instance, various types of magnetic nanoparticles have a widespread range of applications such as in MRI as $T_1$ and $T_2$ contrast agent,[11] magnetically guided drug/gene delivery,[12] magnetic hyperthermia and magnetic biosensors.[13] Up-/down-conversion nanoparticles and QDs have their niche in biological and medical imaging,[14] Noble metal nanoparticles can be used for photothermal therapy,[15] and bio-sensing.[16]

Designing nanoparticles for molecular diagnosis and targeted therapy is of the utmost importance. Such systems have recently been described as *Theranostics.*[17] The fundamental advantage of theranostic nanomedicine lies in the use of patient specific test results to tailor a treatment regimen producing improved outcomes, reduced costs, and fewer side effects. While both therapeutic nanostructures and imaging nanoparticles (NPs) have a long history, they have only recently begun to coalesce into the theranostic NPs. Currently a large number of therapeutics are engaged in preclinical and clinical studies (Table 2.2).[18]

15:59 28 October 2016

15:59 28 October 2016

**Table 2.2** Examples of nanomedicine recent clinical activities involving various theranostic nanoparticles

| | Nanoparticle type | Technique | Therapeutic agent | Diagnostic agent | Disease state | Target | Reference |
|---|---|---|---|---|---|---|---|
| **Pre - Clinical** | Iron oxide | MRI | Anti-EGFR IgG | Iron Oxide | Brain CA | EGFR | Mao et al.[19] |
| | Silica | Ultrasound, MRI | Paclitaxel | Iron Oxide | Many | Folic Acid | Zink et al.[20] |
| | Liposome | Chemotherapy | Paclitaxel | pH-responsive membrane | Ovarian CA/ Many types | EPR | Langer et al.[21] |
| | Gold Nanorod | CT | Heat | Thermal/CT | Many | EPR | Bhatia et al.[22] |
| | QD | Optical | Doxorubicin | QD | Prostate CA | PSMA | Farokhzad et al.[23] |
| **Clinical Trials** | Cyclodextrin | PET/SPECT | RNAi | Transferrin/ Radiolabeled agent | Melanoma | Transferrin Receptor | Calondo Pharma (NCT00689065) |
| | Gold Nanoshell (Aurolase) | MR/Optical/CT | Nanoshell (photothermal) | Nanoshell (MR and Optical) | Head and Neck CA | EPR | NanoSpectra (NCT00848042) |
| | Silica | PET/SPECT | cRGD | $^{124}I$ | Melanoma | $\alpha_v\beta_3$ Integrin | MSKCC (NCT01266096) |
| | Iron oxide | MRI | Injected Cell | Iron oxide (Endorem) | Healthy Volunteers | None | Univ.of Edinburgh (NCT00972946) |

15:59 28 October 2016

| | Nanoparticle type | Technique | Therapeutic agent | Diagnostic agent | Disease state | Target | Reference |
|---|---|---|---|---|---|---|---|
| **Clinical Trials** | Iron oxide | MRI | Feraheme | Iron oxide (Ferumoxytol) | Pancreatic CA | EPR | Massachusetts General Hospital (NCT00920023) |
| | Iron oxide | MRI | Feraheme | Iron oxide (Ferumoxytol) | CA of lymph node | EPR | M.D. Anderson Cancer Center (NCT01815333) |
| | Iron oxide | MRI | Feraheme | Iron oxide (Ferumoxytol) | Myocardial infarction inflammation | N/A | Univ. of Edinburgh (NCT01995799) |
| | Iron oxide | MRI/ Radiotherapy | Heat | Iron oxide (NanoTherm) | Glioblastoma multiform | EPR | MagForce AG[24] |
| | Iron oxide | MRI/ Ultrasound | Doxorubicin/ Paclitaxel | Iron oxide (KER001, KER1001-1002) | Many | $\alpha_v\beta_3$ Integrin | Kereos, Inc.[25–28] |

15:59 28 October 2016

The requirements of such systems are large: they should selectively home in on the cells and organs of the body that are diseased, specifically targeting their potent healing effects on these cells and organs, while sparing healthy cells. They should be completely non-toxic, biodegradable or capable of natural excretion, not be recognized or eliminated by the body's own immune system before they have reached their target, and not induce any allergic reactions. Ideally, they are generic, i.e. they can be "programmed" to combat a wide variety of diseases by docking onto any target structures one chooses and being capable of carrying any medicines.

A proper surface coating can stabilize particles and avoid agglomeration and therefore may increase the sensitivity of NPs based sensor. In addition, a proper surface coating enables the nanoparticles to respond specifically towards biological species and avoids non-specific interactions with components in the complex matrix. Coating is also an effective manner of preventing the dissolution and release of core materials that may cause toxicity to biological system.[29] Furthermore, the steric hindrance of coating can affect the fate of NPs in biological system, such as cellular uptake and accumulation, circulation and clearance from body.[30] In addition, the surface can affect the maintenance of the intrinsic nanocrystal properties such as fluorescence and magnetic behavior. Hence, designing appropriate surface functionality is a perquisite for conjugating biomolecules to NPs for biomedical applications.

A dendritic approach as a coating strategy for the design of functional nanoparticles is particularly interesting in the field of cancer diagnostics (Fig. 2.1). The appeal of such strategy is due to the unique properties of the dendritic structures which can be chemically tuned to reach ideal biodistribution or highly and efficient targeting efficacies. Dendrimers are macromolecules consisting of multiple perfectly branched monomers and this architecture, indeed, makes them versatile constructs for the simultaneous presentation of receptor binding ligands and other biologically relevant molecules. Additionally, dendrimers might serve as promising molecular scaffolds containing a number of ligands thereby inducing an apparent increase of ligand concentration and increasing the probability of statistical rebinding. Alternatively, dendrimers may align these ligands

15:59 28 October 2016

and induce multivalency when receptor clustering occurs or is initiated after initial monovalent binding. To improve tumor targeting efficacy and to obtain better in vivo imaging properties, several studies explored the multivalency effect of dendrimers or of a dendritic surface functionalization of nanomaterials.[31] Due to their conical-like architecture and focal points, dendritic structures are of particular interest as coatings of ultrasmall NPs with very high surface curvature.[32] Certainly, such cone shapes are expected to improve steric resistance to macromolecules such as proteins while preventing better particle agglomeration by comparison with their linear counterparts.[33]

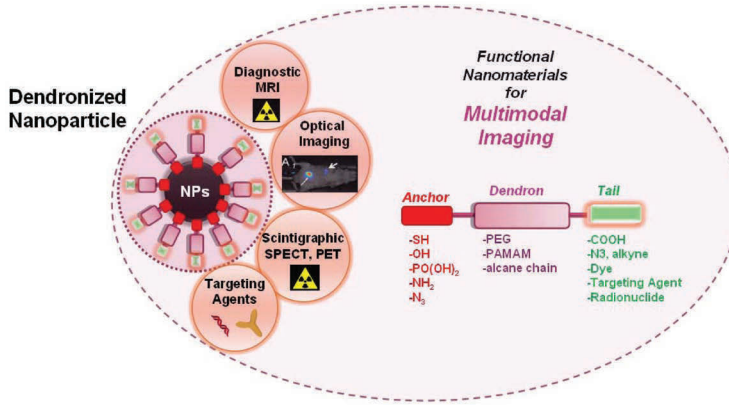



**Figure 2.1** Dendronized nanoparticles as multimodal nanoplatforms.

## 2.2 Why Dendrimers and Dendrons?

The use of dendrimers or dendritic compounds for biomedical applications is a flourishing area of research, mainly because of their precisely defined structure and composition, and also high tunable surface chemistry. Dendrimers and their elementary unit "dendrons" possess excellent symmetry in geometry morphology and good controllability on molecular weight both of which originate from their special step-by-step synthetic pattern. Besides, there are various internal cavities inside the dendritic structure and abundant functional groups on the external surface. Moreover, in addition to a controlled multifunctionalization, dendrimers and dendron units allow a versatility of size (according to the

15:59 28 October 2016

generation (G)) and of physicochemical properties (hydrophilic, lipophilic) which can be precisely tuned (Fig. 2.2). The resulting effects on stability (dendrimer effect), pharmacokinetics and biodistribution can then clearly be identified. There is no doubt that dendrimer-based organic/inorganic hybrids represent highly advanced pharmaceutical tools, able to target a specific type of cell or organ and to be tracked while doing it, and to deliver a specific drug in situ.

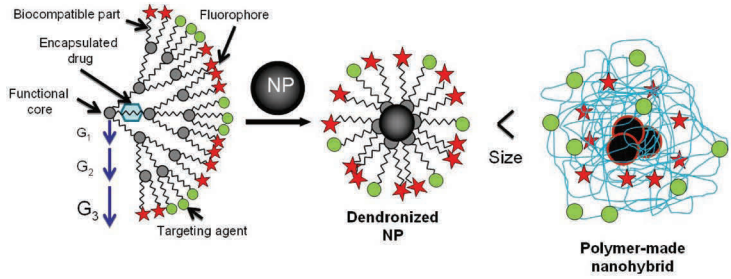



**Figure 2.2** Tuneable and small-sized dendronized nanoparticles compared to their polymer-made counterpart.

## 2.3 Dendrimer NPs Conjugates

Cancer is a worldwide disease with high mortality, accounting for about 589,430 deaths, almost 1,620 people per day in 2015 according to the statistical analysis of *American Cancer Society.*[34] About 1,658,370 new cancer cases are expected to be diagnosed in 2015. The 5-year relative survival rate for all cancers diagnosed in 2004–2010 was 68%, up from 49% in 1975–1977. The improvement in survival reflects both the earlier diagnosis of certain cancers and improvements in treatment. Therefore, early diagnosis using advanced technologies is essential. As formally introduced in 1999 and defined in 2004, molecular imaging (MI) has been emerging as a powerful tool to visualize, characterize and quantify the biological process at the molecular and cellular levels in humans and other living systems.[35] Traditional modalities such as X-rays, computed tomography (CT), and MRI produce an image of anatomy. MI modalities such as positron emission tomography (PET), single photon emission CT (SPECT), optical techniques, and contrast-enhanced CT or MRI produce an image with details on function. Molecular imaging monitors and

measures biological process in a way similar to a biopsy but is done noninvasively, in real time, and with potential for sequential and longitudinal monitoring.

### 2.3.1 Gold Nanoparticles

Recently, the use of noble metals (e.g., Au) as CT contrast agents has become a promising tool since they have a higher atomic number than iodine and consequently stronger X-rays attenuation coefficient than iodine-based CT contrast agents.

The versatile dendrimer nanotechnology enables the use of dendrimers as facile templates to synthesize Au NPs. Their unique structural characteristics provide interior or peripheral reaction sites.[36] The abundant functional groups on the surface of dendrimers and their interior space enable the dendrimer-entrapped Au NPs (Au DENPs) as well as dendrimer-stabilized Au NPs (Au DSNPs) (Fig. 2.3).[37,38] In general, Au DENPs are synthesized using fast reduction and nucleation chemistry and have a size smaller than 5 nm; Au DSNPs are synthesized under slow reduction and nucleation chemistry and have a size larger than 5 nm.[39]

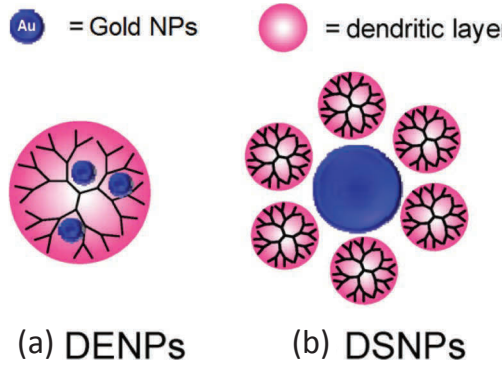



**Figure 2.3** Schematic representation of the structure of different dendritic-gold nanocomposites: (a) dendrimer-encapsulated nanoparticles (DENPs); (b) dendrimer-stabilized nanoparticles (DSNPs).

Guo et al. synthesized dendrimer-gold entrapped nanoparticles Au DENPs, by employing amine-terminated generation 5 poly (amido) amine (PAMAM) dendrimers ($G5.NH_2$) as templates and

15:59 28 October 2016

15:59 28 October 2016

explored their X-rays attenuation properties.[40] X-rays absorption coefficient measurements showed the attenuation of Au DENPs was much higher than that of *Omnipaque* (a clinically used iodinated CT contrast agent). Preliminary CT imaging experiments showed that by subcutaneous injection of Au DENPs at back of the mice, the injected area could be clearly discerned. In contrast, the injection region was not able to be discerned by injection with *Omnipaque*. In vivo micro-CT imaging results have shown that an intravenous injection of acetylated Au DENPs, prepared using G.5$NH_2$, into mice enables effective CT imaging of the pulmonary veins and the inferior vena cava of mice. Opposite, *Omnipaque* in same concentrations is unable to achieve the same blood pool CT imaging performance.[41]

Given the opportunity to link a targeting ligand onto Au DENPs, Wang et al. explored the use of folic acid (FA)-modified acetylated Au DENPs as a nanoprobe for targeting CT imaging of human lung adenocarcinoma.[42] The developed FA-Au DENPs enabled active targeted CT imaging of SPC-A1 cells overexpressing folic acid receptors (FAR) in vitro and the xenografted tumor model in vivo has been administrated with the nanoprobe through intravenous, intratumoral or intraperitoneal injection. A large amount of Au element is found in lung, spleen and liver, which are known as the reticuloendothelial system (RES) organs. Zhu et al. have shown that partial PEGylation of G5.$NH_2$ renders the formation of more stable Au DENPs with improved Au loading within the dendrimer interior, prolonged blood circulation time, reduced macrophage uptake and enhanced biocompatibility for CT imaging applications.[43] Another template was employed as efficient probe for targeted CT imaging of human hepatocellular carcinoma (HCC), constituted of lactobionic acid (LA)-modified PEGylated G5.$NH_2$.[44] Importantly, the tumor uptake through both intravenous (IV) or intraperitoneal injection (IP) of LA-modified Au DENPs was higher than for non-modified Au DENPs, further demonstrating specific tumor targeting through a receptor-mediated mechanism.

Partially PEGylated polyethyleneimine (PEI) was also used as a template for Au NPs synthesis.[45] The results showed an enhanced blood pool CT contrast at 75 min post-injection. Besides, intravenously injected PEGylated Au DENPs are able to be taken up in the tumor area via passive enhanced permeability and

15:59 28 October 2016

retention (EPR) effect, thereby enabling efficient CT imaging of tumors in vivo (Fig. 2.4a–b). At different time points post IV, the Au uptake was analyzed by inductively coupled plasma atomic emission spectroscopy (ICP-OES) (Fig. 4c). It is clear that the PEGylated Au DENPs are mainly taken up by the liver and spleen.

Instead of using dendrimers as templates to synthesize Au DENPs, under weak reducing conditions, Peng et al. reported the approach of forming dendrimer-stabilized Au DSNPs.[46] The formed Au DSNPs with Au core of 6 nm were relatively uniform and stable at different pH and temperature conditions, and showed much better in vivo performance in CT imaging of the major organs in mice (heart, liver, kidney and spleen) than *Omnipaque*.

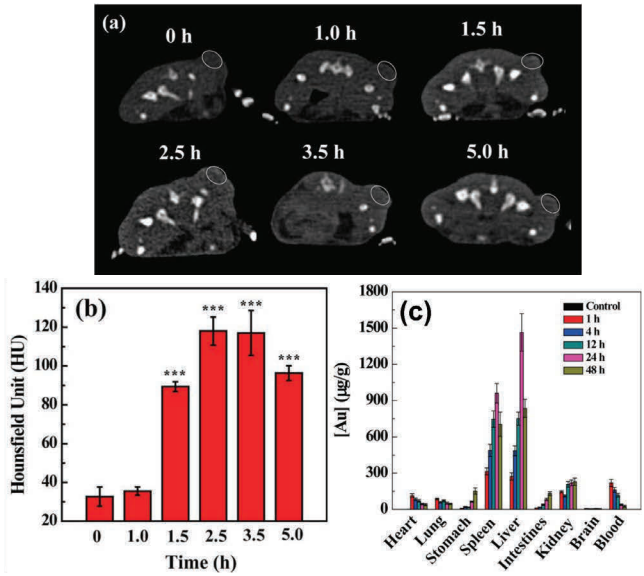



**Figure 2.4** In vivo (a) CT images and (b) CT values of the KB tumor in nude mice before and at different time points post intravenous injection of Au PEI-PEGylated NPs. (c) Biodistribution of Au element in major organs of mice. Reproduced with permission from reference 45.

For accurate detection of diseases, it would be ideal to combine multiple imaging modalities within one nanoparticle system. Hence, much effort has been devoted to developing multi-functional NPs, which enable dual mode or multimodal contrast agents for multiple imaging of different biological systems, such as

15:59 28 October 2016

MRI/fluorescence, MRI/CT and MRI/near infrared fluorescence/position emission tomography. Dual mode MRI and CT imaging is possible with core-shell $Fe_3O_4$@Au nanoparticles via the combination of layer-by-layer (LbL) self-assembly process and dendrimer chemistry.[47] $T_2$ relaxometry and X-rays attenuation measurements showed that the formed $Fe_3O_4$@Au NPs have an $r_2$ relaxivity of 71.55 $mM^{-1}$ $s^{-1}$ and enhanced X-rays attenuation property. These properties enable their use as contrast agent for dual mode MR/CT imaging, which has been demonstrated not only in imaging of cancer cells in vitro, but also in liver imaging via MR and subcutaneous CT tissue imaging. Moreover, good CT/MR dual imaging results are obtained for multifunctional Au DENPs loaded with gadolinium chelator and surface modified with RGD peptide.[48] The formed probe is water dispersible, colloidally stable at different pH and temperature conditions, non-cytotoxic, and hemocompatible in the given concentration range. Importantly, with the coexistence of Au NPs and Gd(III) ions and RGD mediated active targeting, the developed Gd-Au-DENPs-RGD nanohybrid enabled in vivo dual CT/MR imaging of a xenograft tumor model overexpressing $\alpha_v\beta_3$-integrin.

### 2.3.2 Quantum Dots Dendritic Nanoboxes

Semiconductor nanocrystals, typically referred as "quantum dots" (QDs) have shown promising applications as nanosensors, light-emitting diodes and bioprobes, especially in cellular imaging and drug delivery.[49] QDs have narrow, symmetric and size-dependent emission spectra, broad absorption spectra, high level of brightness and photostability, large Stokes shift and long fluorescence lifetime.[50] Aqueous stability is the common problem for all types of QDs when they are employed in biological researches, such as in vitro and in vivo imaging. To circumvent this problem, ligand exchange and polymer coating have proven to be effective, besides synthesizing QDs in aqueous solutions directly. Toxicity is another big concern especially for in vivo studies. Ligand protection and core/shell structure can partly solve this problem. Along with various surfactants used as stabilizing molecules in QD syntheses, an assortment of polymers has been employed as well. They include diblock ionomers, double-hydrophilic block copolymers, and block copolymer micelles.[51]

15:59 28 October 2016

Dendrimers developed for semiconductor nanocrystals have been based on thiol as the anchoring groups to the surface cations. In 2002, Wang and coworkers reported the synthesis of core-shell QDs with high relaxivity and photoluminescence.[52] Dendron ligands of different generations (G1–G3), displaying a thiol function at the focal point, are used for stabilizing CdSe and Au nanocrystals. The outer terminal groups of the dendron ligands are amines, carboxylic acids, alcohols, or esters which resemble that of a hydrophilic protein or a sugar.

Photochemical, thermal, and chemical stability of CdSe and Au dendron-nanocrystals is exceptionally good in comparison to that of nanocrystals coated by single-chain thiol ligands. The thin, about 1–2 nm, but closely packed and tangled ligand shell provides sufficient stability for the "dendron-protected nanocrystals" to withstand the rigors of the coupling chemistry and the standard separation/purification techniques. Guo and coworkers described the design of semiconductor box nanocrystals prepared via dendrimers bridging.[53,54] Cross-linking of the dendron ligands at the surface of the nanocrystals practically sealed each nanocrystal inside a dendron box, which resulted in very stable box-nanocrystals. The chemistry presented by these authors has been applied for the development of a new generation of biomedical labeling reagents.

In the last years, the use of QDs in biomedical research has grown, however successful examples of clinical translations are still lacking due to many clinical concerns. Gao et al. reported on stable and biocompatible dendron-coated InP/ZnS core/shell QD as a clinically translatable nanoprobe for molecular imaging applications.[55] The InP/ZnS core/shell nanocrystals can emit in the range of 450–750 nm, with a quantum yield as high as 40%. The bright core/shell nanocrystals are stable in air and can be dispersed in water after being coated with dendritic and PEGylated arginine-glycine-aspartic acid peptide (RGD).[55]

In vivo and ex vivo fluorescence imaging indicated that the QD-dendron-RGD2 nanoprobe clearly imaged integrin $\alpha_v\beta_3$-positive tumors (human ovarian cancer cells SKOV3) with high specificity (active targeting), while QD-dendron displayed tumor accumulation likely caused by passive targeting via EPR effect (Fig. 2.5).

The fluorescent signal in kidneys is extremely high at 4 h post injection (via tail vein), which is consistent with the biodistribution

15:59 28 October 2016

of QD-dendron and consistent with a scenario of renal excretion. The region-of-interest (ROI) signal integration analysis on the ex vivo fluorescence images is then performed to semiquantitatively study the uptake ratio of QDs in each organ. At 4 h post-injection, the ROI analysis showed that the tumor uptakes of QD-dendron-$RGD_2$ and QD-dendron under the same conditions are high, with 19.5 ± 2.2% of injected dose (ID)/g and 20.8 ± 3.5% ID/g, respectively. By comparison, at 24 h post injection (p.i) the tumor uptakes of QD-dendron-$RGD_2$ and QD-dendron are significantly different ($p < 0.05$) and 7.2 ± 1.5% ID/g and 1.1 ± 0.2% ID/g, respectively. In summary, QD-dendron and RGD-modified nanoparticles demonstrated small size, high stability, biocompatibility, favorable in vivo pharmacokinetics and successful tumor imaging properties.

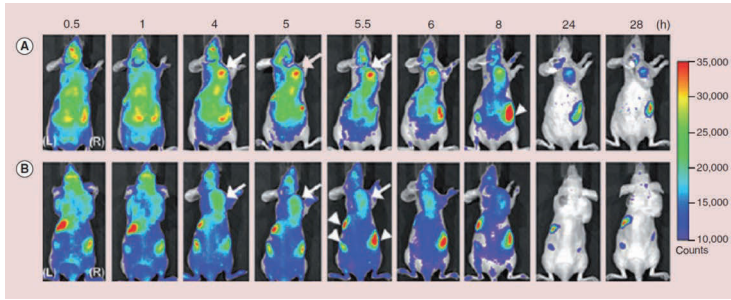



**Figure 2.5** In vivo near-infrared fluorescence imaging. The dorsal images of SKOV3 tumor-bearing (arrows) mice (L: left side; R: right side) injected with (A) QD-dendron-$RGD_2$ (200 pmol) and (B) QD-dendron (200 pmol) at different time points. Reproduced with permission from reference 55.

### 2.3.3 Iron Oxide Nanoparticles

In all biological applications, iron oxide nanoparticle (IONPs) colloidal stability is of utmost importance. It has been shown that the blood half-life, opsonization, biokinetics, and biodistribution of IONPs is determined by both the surface chemical nature and the particle size.[56] There is a group of requirements that functionalized nanoparticles need to fulfill in order to have a practical use in the biomedical field: (1) hydrophilicity and biocompatibility; (2) furtiveness; (3) colloidal stability in water and protein-rich physiological media; (4) hydrodynamic size <100 nm; (5) high multivalency and cooperative effect. Indeed,

functionalized NPs are disposed to opsonization when entering the bloodstream, a non-specific adhesion of the plasma proteins on the surface of NPs, and ingestion by the macrophages. All the physicochemical parameters of the colloids affect their extravasation by influencing, among other things, their diffusivity, their permeability through the vascular wall, their drag coefficient in the fluid and their interactions in the tumor with the cells and the extracellular matrix.[57] To this end, NPs shape, structure, composition, synthesis method and coating play a crucial role in the nontoxicity, biocompatibility, stability, reticulo-endothelial system (RES) escape, internalization by cancer cells and MRI properties of IONPs.[58]

15:59 28 October 2016

#### 2.3.3.1 NPs synthesis

IONPs are synthesized through chemical path, which provides a simple, powerful and a non-expensive way to form colloidal suspensions with dimensions below 10 nm and controlled shape, size and structure.[59] During last decades, numerous synthetic routes were developed to produce IONPs and are rundown in the Table 2.3.[60–63]

The co-precipitation method is the most efficient and simplest synthetic way to obtain magnetic nanoparticles. It is the cheapest and most environmentally friendly procedure. The synthesis involves mixing ferric and ferrous derivatives in aqueous solution at low temperatures and atmospheric pressure. The precipitation occurs after adding a base to a solution of $Fe^{2+}$ and $Fe^{3+}$ salts.The adjustment of pH, ratio between iron (II) and iron (III) concentrations, ionic strength of medium, salt type, base nature and reaction temperature, allows a better control of final characteristics of nanoparticles (size, shape and composition).[64,65] The resulting nanoparticles present a broad size distribution, a medium level of crystallinity and not well controlled shape. After the synthesis, this method requires a size selection step to reduce the size standard deviation. Other methods, such as synthesis by microemulsion,[66] hydrothermal synthesis,[67,68] polyol[69] method or sol-gel[70] have been developed and allow a better control of NPs size and morphology. Since 2000,[71–73] the synthesis by thermal decomposition is highly developed for production of magnetic nanoparticles with high level of monodispersity and size control. It consists in the decomposition of a metal complex in a high boiling

15:59 28 October 2016

**Table 2.3** Summary of synthetic methods of IONPs

| Synthetic methods | Synthesis comments | Reaction temperature | Reaction period | Solvent | Size distribution | Shape control | Yield |
|---|---|---|---|---|---|---|---|
| Co-precipitation | Very simple, ambient conditions | 20–90 | Minutes | Water | Relatively narrow | Not good | High/scalable |
| Thermal Decomposition | Complicated | 100–400 | Minutes-Hours | Organic | Very narrow | Very good | High/scalable |
| Microemulsion | Complicated, ambient conditions | 20–50 | Hours | Water/Organic | Very narrow | Very good | High/Scalable |
| Hydrothermal synthesis | Simple, high pressure | 130–250 | Hours-Days | Water or/and Organic | Relatively narrow | Good | Low |
| Polyol | Simple, high temperature and inert conditions | 120–280 | Minutes-Days | Polyol | Relatively broad | Good | High/scalable |
| Sol-gel | Complicated, high temperature | 200–400 | Minutes-Days | Water or/and organic | Relatively broad | Good | Medium |

15:59 28 October 2016

temperature organic solvent in presence of surface active agents, acting as stabilizers. This technique allows the obtaining of well-crystallized NPs and in situ functionalization with an organic hydrophobic layer ensuring their high colloidal stability in organic solvents.[74]

Begin-Colin and coworkers reported the production of monodisperse IONPs from thermal decomposition of iron (II) stearate in the presence of oleic acid in high boiling point solvents.[75] They also focused on the study of synthesis parameters to obtain a better understanding of the nanoparticle formation via this synthetic route. The structural and magnetic characterizations of NPs with sizes in the range 5–20 nm confirm that the composition of NPs evolves from maghemite for small sizes (typically <8 nm) up to a core of rather stoichiometric magnetite surrounded by an oxidized shell for larger sizes (>12 nm) via a perturbed oxidized state for intermediate sizes. These results underline that synthesis parameters affect the NPs nucleation and growth steps, by modifying the stability of iron stearate on which depend the monomer formation and concentration. The monomer formation, which is reaction time and/or temperature dependent, is thus found to vary mainly as a function of the nature of both solvents and ligands. The exact mechanism of the formation of the uniform-sized nanocrystals has still not been clarified. However, the control of the size is steered by three different processes like nucleation, growth and Ostwald ripening.[76–79]

In order to describe different stabilization methods,[80,81] it is important to define the surface nature of iron oxide nanoparticles. For all oxides, the surface of iron oxide is covered by hydroxyl groups due to the water chemisorption (Fig. 2.6a), the epoxy groups on the iron surface react with water molecules to form hydroxyl groups.

A part of hydroxyl groups exhibit amphoteric properties and their charge can be modified by varying the pH. Thus depending on the pH of the solution, the surface of iron oxide can be positively or negatively charged (Fig. 2.6b). The isoelectric point (IEP) corresponds to the pH value when the iron oxide surface carries no net electrical charges. For magnetite IEP is around 6.8.[82] Below IEP, hydroxyl sites absorb the protons and become positive by the formation of $Fe\text{-}OH_2^+$ species. Above IEP, the protons are desorbed and the deprotonation leads to negative species $Fe\text{-}O^-$. The magnitude of zeta potential (ZP) gives an indication of the stability of nanoparticle colloids. In the case of high ZP values

(negative or positive) iron oxide NPs are thus stable in suspension by electrostatic interactions. On the contrary, when low ZP values are observed, flocculation generally occurs in solution.

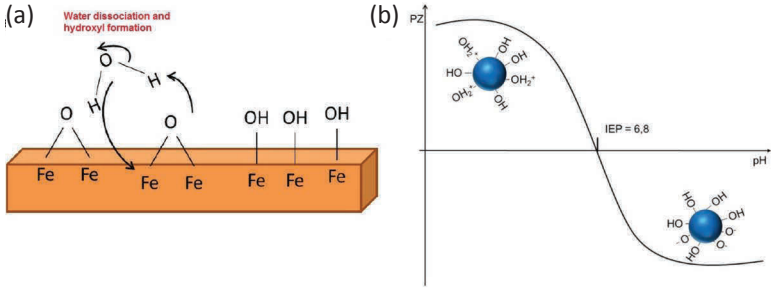



**Figure 2.6** (a) Schematic representation of hydroxyl formation on iron oxide surface; (b) Surface charge and Zeta Potential evolution according to the pH.

Moreover, iron oxide nanoparticle's IEP is exactly in the pH range of physiological media, thus for applications in biomedical field, IONPs have to be functionalized with molecules ensuring steric or/and electrostatic stabilization. The electrostatic stabilization is an effective way to disperse particles in aqueous media. The major disadvantage of charge stabilization is its great sensitivity to the ionic strength of the dispersion media, thus when the ionic strength is high, the electrostatic repulsion is insufficient to counterbalance the attractive force and consequently leads to the nanoparticle aggregation. Steric stabilization is the second method that is achieved by attaching (covalent bond or chemisorption) molecules to particle surface. The adsorbed layer on nanoparticle surface avoids direct contact between nanoparticles creating a strong steric repulsion among nanoparticles, and thus leads to a stable colloidal suspension.

The current trend is to graft molecules allowing both electrostatic and steric stabilization on the surface of NPs. These molecules are large enough to induce a steric repulsion and present charged groups on the periphery leading to electrostatic repulsion, hence the name *electrosteric* stabilization. Recently dendron molecules which display periphery charges have been shown to induce such electrosteric repulsion.[83] In the field of grafting, various procedures have been described involving bonding at the NPs surface through different types of anchoring

15:59 28 October 2016

groups (Fig. 2.7), for example catechol,[84] carboxylate[85] or stronger anchoring groups such as silane[86] or phosphonate.[87]

It has been shown that phosphonates provide a highly stable anchoring to the metal surface by forming complexes which are stable even at elevated temperature and towards enzymatic cleavage.[88,89] Therefore, we will focus here on the chemisorption of dendrons on the surface of IONPs through phosphonate anchoring groups.

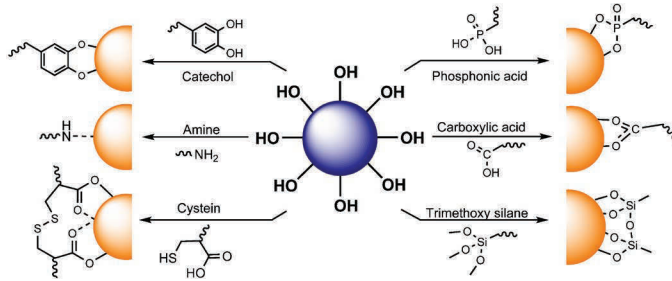



**Figure 2.7** Possible surface complexes according to the coupling agent.

### 2.3.3.2 Synthesis of dendrons

Felder-Flesch et al. reported a library of functional dendritic phosphonic acids, either fully PEGylated or derived from the poly (amido)amine (PAMAM) family.[90] Such a library of functional hydrophilic phosphonic acids opens new possibilities for the investigation of dendronized nanohybrids made from metal oxides (Fig. 2.8).

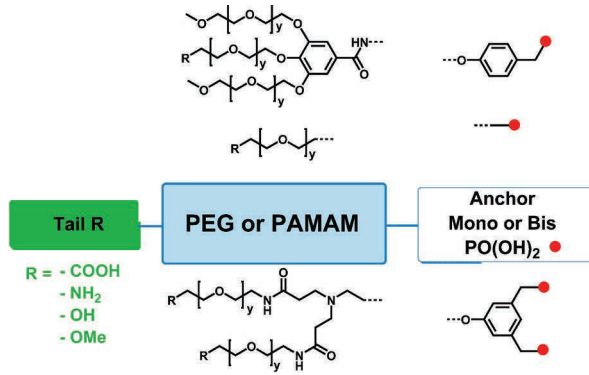



**Figure 2.8** General structure for IONPs dendritic phosphonates as coatings.

15:59 28 October 2016

15:59 28 October 2016

In the following paragraphs only a few examples of the entire library of phosphonate dendrons will be presented: one example of PEGylated monomers and another of PAMAM-OEG dendrons.

#### 2.3.3.2.1 PEGylated monomer: COOH-functionalized dendritic phosphonic acid

The synthesis of the dendritic mono-ethyl phosphonate is obtained from the key intermediate **5**, which was obtained in four steps with a 44% overall yield (Fig. 2.9). First *para*-benzylated methyl gallate **6** and tosylated tetraethyleneglycol monomethyl ether **2** are obtained in good yields from the commercially available methyl gallate and tetraethyleneoxide monomethyl ether, respectively, following a reported one-step procedure.[91] A Williamson etherification between **2** and **3** in acetone at 60°C, in the presence of potassium carbonate ($K_2CO_3$) and potassium iodide (KI), allowed the preparation of ester **5** in 75% yield.

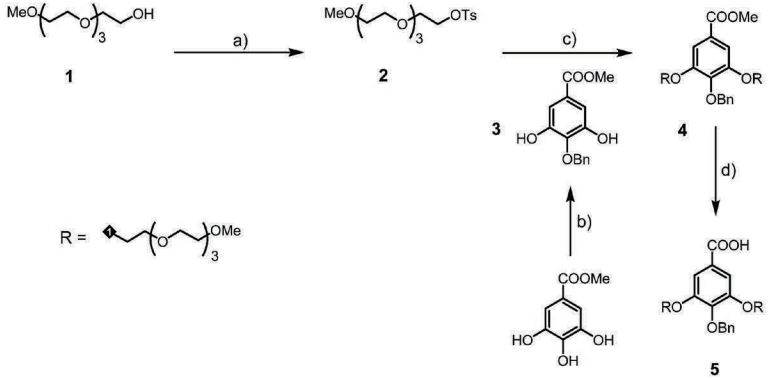



**Figure 2.9** Synthesis of *para*-benzyl (*meta*-tetraethyleneglycol monomethyl ether) methyl gallate 5: (a) TsCl, NaOH, THF/$H_2O$, rt, 24 h, 94%; (b) benzyl bromide, $KHCO_3$, KI, DMF, 30°C, 4d, 70%; (c) $K_2CO_3$, KI, acetone, reflux, 24 h, 75%; (d) NaOH, MeOH/$H_2O$, reflux, 2 h, 90%.

The synthesis of ethyl phosphonate **9** displaying an ethyl-amine linker in the *para*-position is given in Fig. 2.10. The compound is obtained in 4 steps with 54% overall yield. First, 4-(benzyloxy) benzyl chloride reacted under reflux with $P(OEt)_3$ to yield **7** (92%). Phenol **8** is obtained after hydrogenolysis in the presence of Pd/C (10%), and is next engaged in an

etherification reaction in the presence of Boc-2-bromo-ethylamine. Subsequent treatment with trifluoroacetic acid (TFA) yielded **9** (94%).

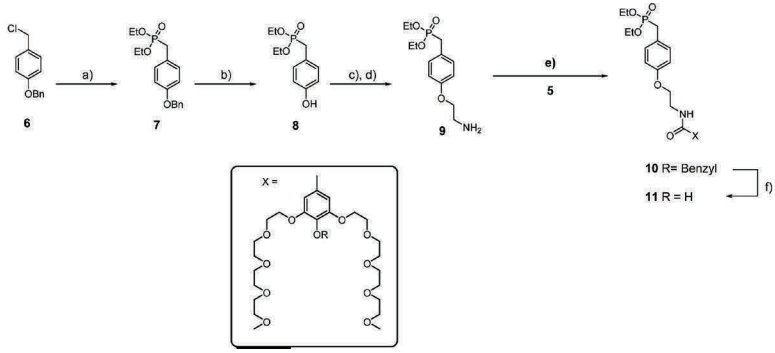



**Figure 2.10** Synthesis of mono-ethylphosphonate anchor 9: (a) $P(OEt)_3$, 160°C, 3 h, 92%; (b) Pd/C 10%, $H_2$, EtOH, rt, 16 h, 92%; (c) Boc-2-bromoethylamine, $K_2CO_3$, KI, acetone, reflux, 16 h; (d) TFA, $CH_2Cl_2$, 0°C to rt, 16 h, 94%; (e) 5, BOP, DIPEA, $CH_2Cl_2$, rt, 24 h, 70%; (f) Pd/C 10%, $H_2$, EtOH, rt, 16 h, 85%.

Amine **9** underwent a peptide coupling type reaction with carboxylic acid **5** (obtained by saponification of **4** with NaOH, Fig. 2.9) in the presence of BOP and DIPEA to obtain benzylated compounds **10** (70%). Finally, hydrogenolysis in the presence of Pd/C led to the corresponding ethyl phosphonate **11** with 85% yield.

Refluxing in concentrated hydrochloric acid (HCl) is an easy route for conversion of phosphonate esters into their acid analogues. However, for sensitive products requiring milder reaction conditions, McKenna's method[92] using bromotrimethylsilane (TMSBr) remains an efficient method which allows the obtention of trimethylsilyl phosphonate ester intermediates that hydrolyze in situ into phosphonic acids, in protic medium (water or alcohol). In order to achieve the synthesis of phosphonic acid **14** bearing a long functionalized oligoethylene glycol chain in the *para* position, the first step is the synthesis of the common intermediate **12** (Fig. 2.11), which is obtained in good yield starting from the commercially available hydroxy-dPEGs®$_8$-t-butylester.[93] **12** then underwent a Williamson reaction with ethylphosphonate **11** in acetone at 60°C in the presence of $K_2CO_3$

15:59 28 October 2016

15:59 28 October 2016

and KI to yield the corresponding dendritic ethyl phosphonate **13** in 85% yield. Treatment of **13** with a large excess of TMSBr generated a phosphonic acid function at the focal point and converted the terminal tert-butyl ester group into its corresponding carboxylic acid. This step allowed the obtention of compound **14** in 90% yield.

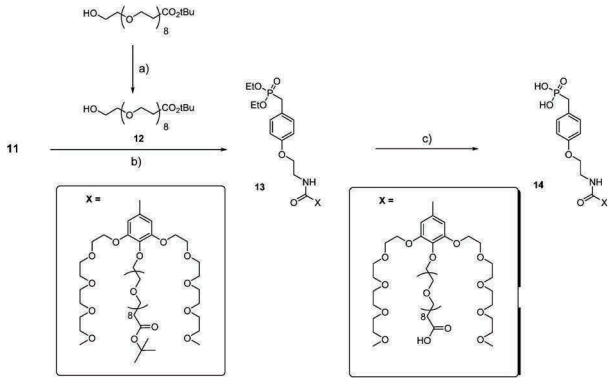



**Figure 2.11** Synthesis of COOH-functionalized dendritic mono-phosphonic acid. (a) TsCl, $NEt_3$, $CH_2Cl_2$, rt, 24 h, (85%); (b) 35, $K_2CO_3$, KI, acetone, reflux, 16 h, 70%; (c) TMSBr, $CH_2Cl_2$, rt, 16 h, 90%.

### 2.3.3.2.2 PAMAM-OEG dendron

Another design of a small-size dendron is based on a poly(amido) amine structure. Precisely, alkyne monomer **15** is synthesized following a reported procedure (Fig. 2.12).[94] After deprotection of the two methyl esters by sodium trimethyl-silanolate (TMSONa), functionalized OEG chain is introduced into the monomer by a peptide coupling reaction as shown in Fig. 2.12 to yield bifunctional acetylenic conjugate **16**. The OEG chains are chosen for their tunable length and possible derivatization.

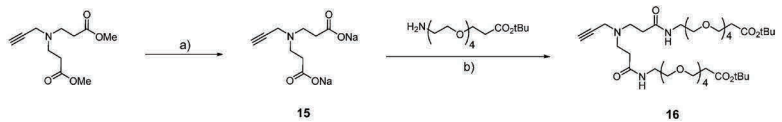



**Figure 2.12** Introduction of functional OEG chains into PAMAM monomer. (a) TMSONa 1 M, $CH_2Cl_2$, rt, 16 h, quant; (b) 1-ethyl-3-(3-dimethylaminopropyl)carbodiimide (EDCI), HOBt, DIPEA, $CH_3CN$, rt, 16 h, 67%.

In parallel, azide-derivatized ethylphosphonate precursor displaying two (**20**) phosphorus anchors is synthetized (Fig. 2.13) in a four-step procedure starting from methyl-3,5-dibromomethylbenzoate **17**.[94,95]

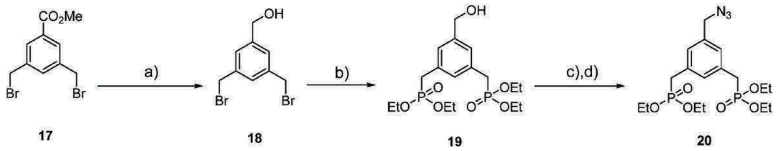



**Figure 2.13** Synthesis of bis-ethylphosphate azide precursor. (a) DIBALH, toluene, 3 h, 0 1C, 90%; (b) $P(OEt)_3$, 2 h, 140°C, quant; (c) $SOCl_2$, $CHCl_3$, 1 h, reflux, quant; (d) $NaN_3$, $CH_3CN$, reflux, 16 h, quant.

Acetylenic PAMAM monomer **16** underwent the click reaction catalyzed by $Cu(II)SO_4 \cdot 5H_2O$ in the presence of sodium ascorbate as the reducing agent with azide **20** (Fig. 2.14) to yield bis-ethylphosphonate **22**. The final deprotection of the bis-ethylphosphonate **21** is achieved in the presence of TMSBr, which allowed the simultaneous deprotection of tert-butyl esters of the compound.

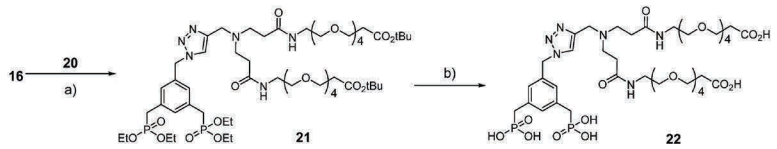



**Figure 2.14** Coupling between PAMAM monomer and azide precursor. (a) $CuSO_4 \cdot 5H_2O$/sodium ascorbate, $THF/H_2O$ (4: 1), rt, 16 h 62%; (b) TMSBr, $CH_2Cl_2$, rt, 2–4 h, 91%.

This paragraph illustrating the diversity of the structure of dendrons is absolutely not exhaustive but it gives a flavor of the synthetic aspects. Despite all the work already done about the synthesis, there is still plenty of room for improving the synthetic processes, in particular shortening the time needed at the laboratory bench.

### 2.3.3.3 Nanohybrids

Hybrid materials display strong versatility and adaptability in biomedical applications due to an appropriate organic coating.

15:59 28 October 2016

15:59 28 October 2016

Aqueous suspensions of dendronized iron oxide nanoparticles (NPs), synthesized by co-precipitation (leading to naked NPs in water) or by thermal decomposition (leading to surfactant-decorated NPs in an organic solvent), have been obtained after functionalization of NPs with phosphonic acids presented in Fig. 2.15.

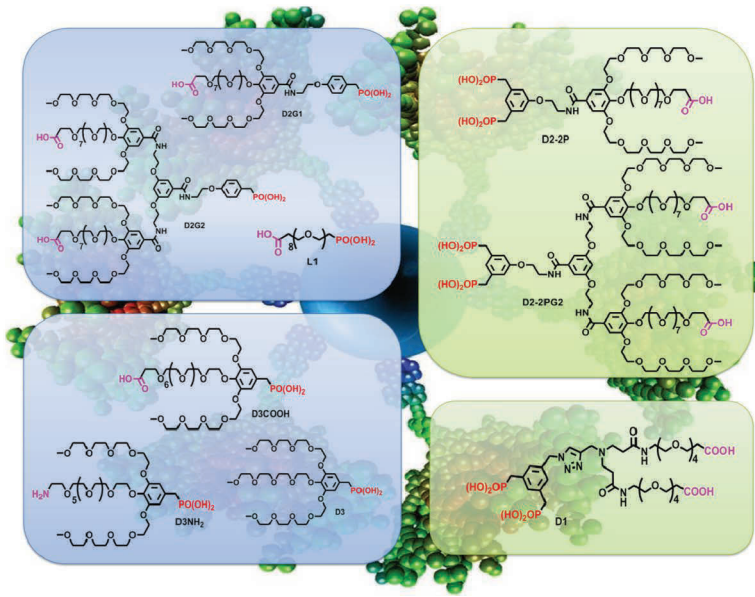



**Figure 2.15** Examples of dendritic phosphonic acids as coating for IONPs.

The next section pertains to the investigation of the colloidal stability of different nanohybrids, the influence of the synthesis route, size and morphology of nanoparticles, structure and generation of dendrons, for merging both NPs and molecules properties.

#### 2.3.3.3.1 Functionalization methods

Two methods have been developed to enable NPs functionalization according to their synthetic method: in situ functionalization (during NPs synthesis) and post-synthesis functionalization.

In situ functionalization consists in using molecules to be grafted as template for the nanoparticle synthesis. NPs nucleation therefore occurs within the functionalization material. Such strategy is mainly used with polymeric molecules.[96]

15:59 28 October 2016

In the case of post-synthesis functionalization, which is the most employed method, NPs and organic molecules are synthesized separately. However, according to their preparation method, NPs may be naked (co-precipitation route) or coated with a surfactant (thermal decomposition case). The functionalization could take place either by direct grafting, direct grafting with ligand exchange or by ligand exchange with phase transfer (Fig. 2.16).

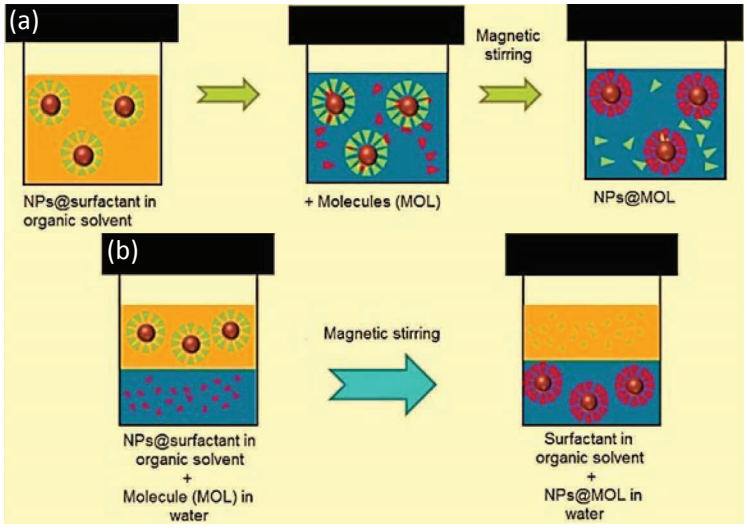



**Figure 2.16** Two synthetic pathways for the functionalization of NPs synthesized by thermal decomposition. (a) Direct ligand exchange grafting. (b) Ligand exchange with phase transfer grafting.

Direct grafting is mainly used in the case of bare NPs by introducing the molecules in IONPs suspension.[97] As NPs synthesized by co-precipitation are dispersed in water, direct grafting also occurs in water and a maximum of grafting is determined to be a function of pH. In the case of direct grafting with ligand exchange, NPs are synthesized by thermal decomposition.[75] The grafting results from mixing NPs and dendron in the presence of a polar organic solvent.[87] Afterwards, NPs are transferred into water due to dendrons hydrophilicity, but not only. The direct grafting with ligand exchange also depends on the nature of dendrons anchoring group, which should display higher affinity to the nanoparticle surface than the synthesis surfactant. Phosphonate groups show

strong complex ability with iron ions, therefore generating more stable bonds with iron oxide NPs surface then those formed with carboxylic acids.[98–100] In the case of ligand exchange with phase transfer, molecules and NPs are dispersed in two different solvents. Dendrons are dispersed in aqueous phase and nanoparticles in a water-immiscible organic solvent. The obtention of an optimal ligand exchange during a phase transfer process is pH controlled. These grafting conditions suggest that at aqueous-organic solvent interface, nanoparticles exhibit a naked part on which phosphonates in water react, thus favoring the transfer of nanoparticles in water.

15:59 28 October 2016

#### 2.3.3.3.2 Co-precipitation versus thermal decomposition IONPs synthetic path

S. Begin-Colin, D. Felder-Flesch, and coworkers studied the effect of nanoparticle synthesis method on dendronized iron oxides as MRI contrast agents (Fig. 2.17).[101] They compared microstructural, magnetic and in vitro and in vivo contrast enhancement properties of dendronized (with the same dendron $D3NH_2$ Fig. 2.15) NPs synthesized either by co-precipitation or by thermal decomposition. The thermal decomposition method led to NPs coated with oleic acid which are further dendronized by a ligand exchange with phase transfer process. NPs synthesized by co-precipitation (NPscop) are dendronized by direct grafting in water.

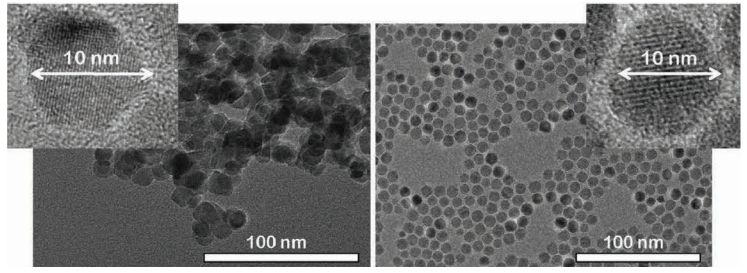



**Figure 2.17** TEM micrographs of iron oxide NPs synthesized by co-precipitation (left) and by thermal decomposition (right).

Relaxivity measurement and in vitro and in vivo MRI experiments are done. The grafting rate is similar for both types of NPs, however the anchoring of the dendron on the surface of NPcop is stronger. In vivo and in vitro MRI measurements showed that the contrast enhancement properties of the dendronized

NPs are higher than those obtained with commercial polymer-coated NPs (Endorem™, Resovist™, etc.). Moreover, if the NPs synthesized by co-precipitation displayed a higher in vitro contrast power due to their higher saturation magnetization, the NPs synthesized by thermal decomposition are more efficient in vivo. Both types of dendronized NPs are eliminated by urinary and hepatobiliary pathways without unspecific uptake especially in the RES organs (liver, lungs, spleen) and in the lungs.

#### 2.3.3.3.3 Impact of dendron architecture: G1 versus G2, G3

15:59 28 October 2016

The influence of dendron generation on nanoparticle's pharmacokinetics and pharmacodynamics has been the subject of several articles. In particular, C. Duanmu et al.[84] showed the influence of dendron generation on MRI properties of iron oxide NPs: $r_2$ increases as NPs are functionalized with higher generations. With generation increase the multivalency and the cooperative effect tend to raise.[102] Huang and coworkers studied different generations of PAMAM dendrimer–conjugated iron oxide nanoparticles, bonded with oligonucleotides via electrostatic means.[103] Such systems exhibit good gene delivery properties and have potential applications in cancer therapy and molecular imaging diagnosis. Recently D. Felder-Flesch et al. have compared linear PEG molecule and dendron of different generations grafted via a direct ligand exchange process at the surface of spherical 10 nm IONPs (NS10) synthesized by thermal decomposition (Fig. 2.18).[104]

The suspension stabilities of dendronized NS10 in water over time and phosphate buffered saline (PBS) at different concentrations are monitored. Whatever the medium and the grafted molecule at the NS10 surface, all of the suspensions preserve a monomodal distribution and a mean hydrodynamic diameter smaller than 50 nm, monitored over 3 months. Such results show that dendrons provide an electrosteric stabilization of NPs in suspension. The Nuclear Magnetic Resonance Dispersion (NMRD) profiles of the different suspensions (Fig. 2.19) were recorded and a considerable difference in the $r_{1\max}$ value was observed between the NS10 functionalized with the linear molecule (NS10@L1) and the dendronized NPs, NS10@D2-G1, NS10@D2-G2 and NS10@D2-G3.

15:59 28 October 2016

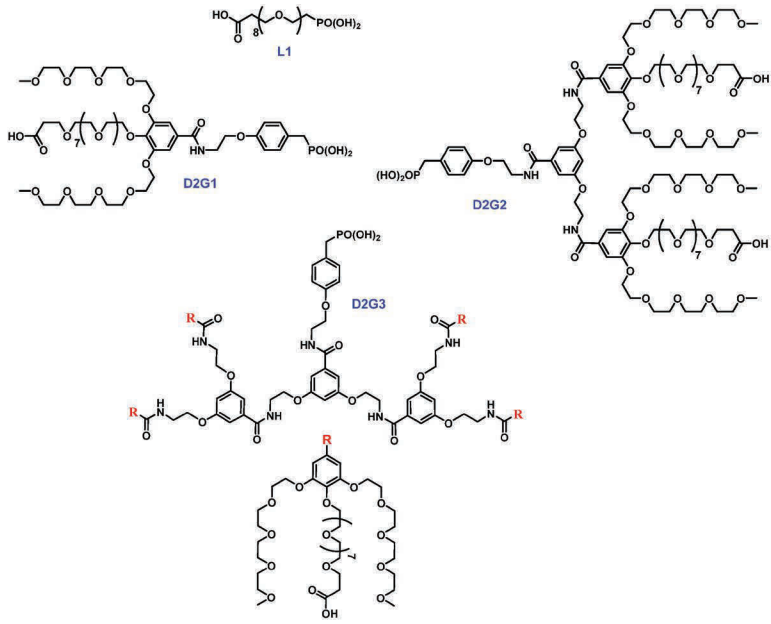



**Figure 2.18** Linear (L1) and dendritic (D2-G1, D2-G2, D2-G3) molecules grafted at the surface of spherical iron oxide nanoparticles of 10 nm (NS10).

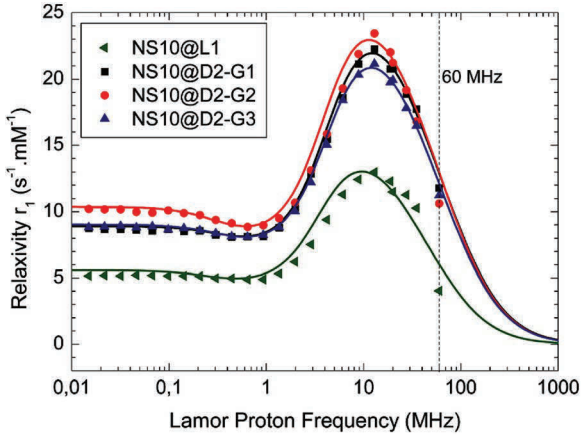



**Figure 2.19** NMRD profiles of NPs functionalized with the linear L1 and dendritic D2-G1, D2-G2, D2-G3 molecules. Reproduced from reference 104 with permission from the Royal Society of Chemistry.

15:59 28 October 2016

The difference observed in the $r_{1max}$ values can be attributed only to the nature of the surface coating: the $r_{1max}$ value for NS10@L1 is much lower, at every frequency, than the one obtained for the dendronized NPs, whatever the generation (NS10@D2-G1, NS10@D2-G2, and NS10@D2-G3). This evidences that water diffusion and circulation through the dendritic shell is much easier than through the linear organic layer. Thus, at magnetic field of medical interest, a dendritic coating of low generation (G1 or 2) seems to be more efficient in terms of magnetic relaxation.

#### 2.3.3.3.4 PAMAM versus PEG

The most commonly studied dendritic polymer is polyamidoamine PAMAM,[105] which is desirable for high drug loading, satisfactory drug release properties, reproducible in vivo behavior and cellular uptake.[106–108] Polyethylene glycol (PEG), uncharged, nontoxic and non-immunogenic water soluble polymer have found their way in diverse applications in biological science.[33,109] S. Begin-Colin et al. have compared two dendron designs: PAMAM versus PEGylated branched structures (Fig. 2.20).[110]

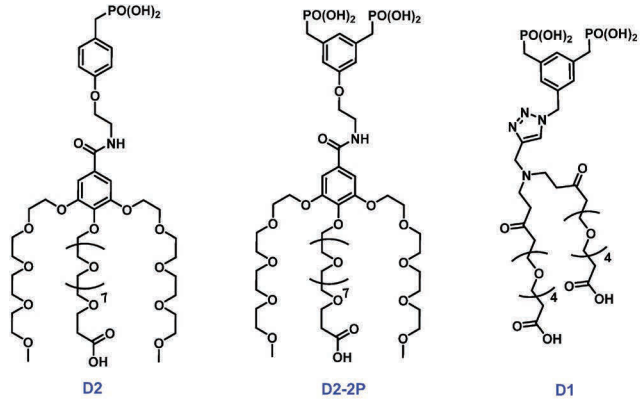



**Figure 2.20** Scheme of dendrimer phosphonates of two distinct natures.

All dendronized NPs are stable over a long period of time when suspended in water and in different physiological media. They display a mean hydrodynamic diameter smaller than 50 nm whatever the molecule architecture. Relaxivity measurements are performed for all dendronized NPs at 0.41 (20 MHz), 1.47 (60 MHz) and compared to commercially available iron oxide NPs

15:59 28 October 2016

(Ferropharm, Supravist, Sinerem, and Ferumoxyl). The values reported are higher compared to commercial products displaying similar mean hydrodynamic size. Lower relaxivity values are noticed for D1-dendronized NPs. Previous studies performed on these dendronized D1@NPs prepared by another process,[111] showed similar results and suggested that these lower values could be attributed to a lower number of PEG chains per molecule and to the presence of the triazole cycle, which confers a more hydrophobic character to this dendron. This supposition is confirmed with NMRD profiles, where $R_{1\max}$ value of NS10@D1 is lower than the $R_{1\max}$ of NS10@D2 or D2–2P. The benzylic bisphosphonate tweezer on D2–2P is also suggested to hinder the water diffusion close to the magnetic core. Good in vivo biodistribution of all dendronized NPs is confirmed by optical imaging.

#### 2.3.3.4 In vivo applications

Among the long list of nanoscale materials currently being explored for their prospective use in nanomedicine, SPIONPs are widely favored because of their unique magnetic properties,[112] nontoxicity and biodegradability.[113]

Iron oxide nanoparticles (IONPs) have been increasingly employed in MRI,[114] targeted drug delivery,[115] therapy,[116] and cell separation.[117]

##### 2.3.3.4.1 Targeted Imaging

Yang et al. reported the synthesis of a platform for targeted MRI of C6 glioma cells assembled from ultrasmall iron oxide nanoparticles and RGD-modified dendrimers G5.$NH_2$.[118] The G5.$NH_2$Ac-RGD-$Fe_3O_4$ NPs showed good water dispersibility, colloidal stability, excellent hemocompatibility and biocompatibility over a large concentration range. In vitro cellular uptake analysis suggested that G5.$NH_2$Ac-RGD-$Fe_3O_4$ NPs have high binding affinity toward C6 cells that overexpress $\alpha_v\beta_3$-integrin receptors. In vitro and in vivo tumor MR imaging experiments not only indicated good and active $T_2$-weighted MR imaging performance (Fig. 2.21) but also demonstrated the specific targeting ability; therefore, this nanoplatform can be used for targeted MR imaging of tumors via RGD-mediated pathway.

15:59 28 October 2016

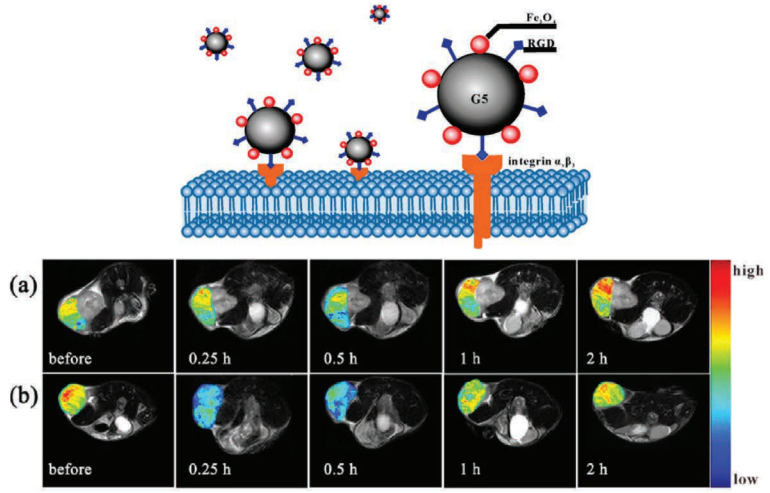



**Figure 2.21** Schematic drawing of active targeting through RGD-mediated pathway and in vivo $T_2$-weighted MR images of tumors after intravenous injections of 0.1 mL PBS solutions containing (a) G5.$NH_2$Ac-$Fe_3O_4$ NPs (b) G5.$NH_2$Ac-RGD-$Fe_3O_4$ NPs (600 µL Fe) at different times. Reproduced with permission from reference 118.

### 2.3.3.4.2 Drug delivery

IONPs have also been employed as drug delivery vehicles.[119] These systems contain three components: a therapeutic agent, a targeting moiety and a carrier. Chang et al. explored a tumor targeting and pH-responsive drug release system based on folic acid (FA) conjugated to PEGylated PAMAM dendrimer with doxorubicin and SPIONPs.[120] The cytotoxicity of the conjugate is very low on MCF7 (breast cancer cells) cells using a MTT assay. After 4 h of incubation, 85–92% cells viability is monitored, with concentrations up to 1 mg/mL. The DOX release profile results in 75% of DOX released at pH 5.03 and only 8% at pH 7.38. Due to efficient targeting through FA receptors, DOX is dissociated from the conjugates within the nuclei of tumor cells or regions nearby, thus reducing the side effects on normal tissues. In vivo MRI analyses of IONPs conjugate with FA as target molecule exhibited promising $T_2$ weighted MR-imaging results at 1 h post injection showing a great potential for application in both MRI detection and cancer therapy (Fig. 2.22).

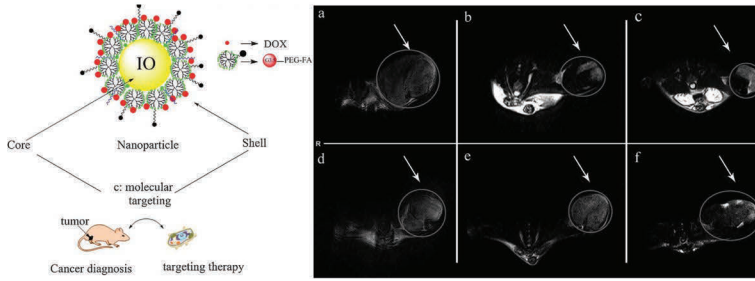



**Figure 2.22** $T_2$-weighted fast spin echo images after injection of 2.5 mg $mL^{-1}$ conjugates per mouse in 1 h (a) FA-PEG-G3.5 (b) PEG-G3.5@IONPs (c) FA-PEG-G3.5@IONPs (d) FA-PEG-G3.5-DOX (e) PEG-G3.5-DOX (f) FA-PEG-G3.5-DOX@IONPs. The arrows denote allograft tumors, which are marked by circles. Reproduced with permission from reference 120.

#### 2.3.3.4.3 Multimodal imaging

The idea of using multiple imaging techniques has recently gained in popularity, and researchers have come to realize that their complementary abilities (high sensitivity/poor resolution or high resolution/poor sensitivity) could be emphasized to great effect by using then in tandem. As the preponderance of recent reviews will attest, there has been a surge in research on multimodal imaging probes development over the past few years.[121–124]

In 2011, Begin-Colin, Felder-Flesch, and coworkers[83] investigated the synthesis of small-sized dendrons (D3, D3COOH or $D3NH_2$ Fig. 2.15) and their grafting at the surface of IONPs under optimized conditions according to the nature of the peripheral functional groups. The study had the purpose to show good colloidal stability in water and osmolar media and to ensure the possibility of tuning the organic coating characteristics (e.g. morphology, functionalities, physicochemical properties, grafting of fluorescent or targeting molecules). In vitro and in vivo MR and optical imaging are then demonstrated to be simultaneously possible using such versatile SPIONPs covered by an optimized dendritic shell displaying either carboxylate or ammonium groups at either periphery.

The very high enhancement contrast ratio (EHC) values obtained for these dendronized NPs confirmed their high contrast power at high magnetic fields (7 T). For instance, on MR $T_{2w}$ image at 7 T, EHC values were 15–17% higher than those obtained with

15:59 28 October 2016

15:59 28 October 2016

*Endorem*™. Both positive and negative EHC values are observed after injection and could be explained by local differences of concentrations: indeed, at lower concentrations (in the kidneys and initially in the bladder), the relative hyper-signal can be explained by a dominating $T_{1w}$ effect, while at high concentrations (liver, bladder and kidneys late in time), the $T_{2w}$ effect becomes very important and compensates widely for the $T_1$ effect at the origin of a decreased signal (Fig. 2.23). There is, however, a $T_{2w}$ saturation effect at very high concentrations, for example, in the liver, especially at the initial time.

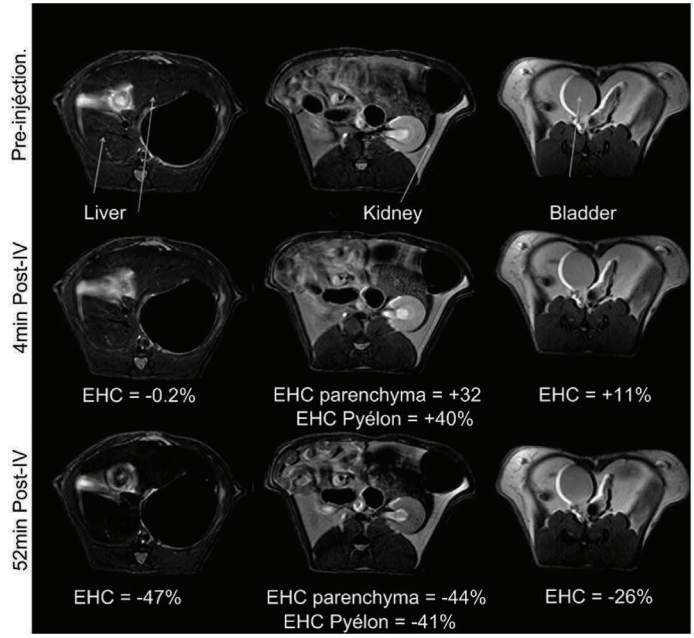



**Figure 2.23** About 4 min spin echo $T_{2w}$ axial images (RT/ET = 3000/9.5 ms, 2 slice thickness) are sequentially acquired before and immediately after IV injection of 500 µL of dendronized NPs@D3COOH at 236.4 µg/mL iron concentration at 7 T with a small animal dedicated MRI (Biospin-Brücker®) during 60 min. Reproduced with permission from reference 83.

After post-functionalization of dendronized IONPs with a fluorescent probe (Alexa-647) or with Patent Blue dye,[125] no significant liver (fluorescent intensity being equivalent to control), skin and spleen uptake is observed (no RES uptake). A very fast

urinary fluorescence indicating urinary elimination is observed (no kidney signal). In contrast, very fast (no persistent liver uptake at 20 min) and very high fluorescence signal is detected in intestinal track, indicating hepatobiliary elimination (Fig. 2.24). Observation of fluorescence in feces confirmed this hypothesis.

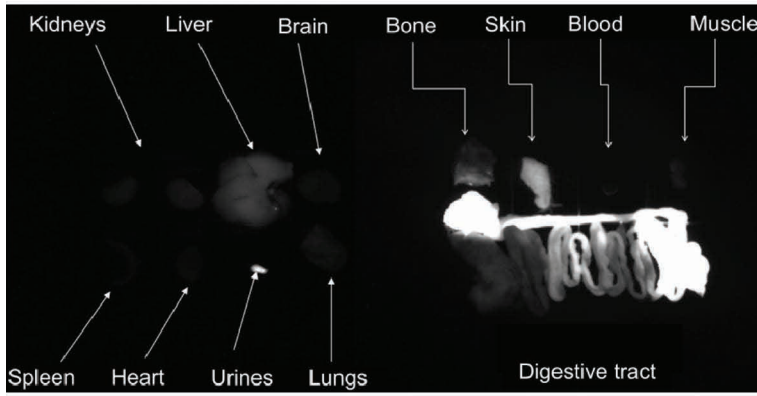



**Figure 2.24** Ex vivo optical imaging of organs removed from a rat 20 min after IV injection of Alexa-labeled NPs@D3NH2. Reproduced with permission from reference 83.

Felder-Flesch also reported in 2014 the biodistribution of Alexa-647-PAMAM-OEG decorated (D1, Fig. 2.15) IONPs of 10 nm synthesized by thermal decomposition.[111] As shown by in vivo optical imaging (Fig. 2.25), PAMAM-OEG dendronized IONPs circulate freely and without lung uptake, after IV injection thus indicating the absence of aggregates. They are eliminated both through urinary (bright signal in bladder) and hepatobiliary pathways (significant signal in the digestive tract at 30 min post IV). The urinary elimination is very rapid as evidenced by a bladder signal at 7 min post IV and is completed at 30 min. No unspecific uptake such as lung or RES uptake is observed (no signal in liver, bone marrow, spleen) leading to complete elimination of all dendronized IONPs injected within 24 h post-IV.

On the other hand, injected NPs@D1@Alexa647 shows a different biodistribution.[110] Indeed, a urinary elimination is always observed after short injection times (data not shown) but for longer imaging times, 4 and 24 h, fluorescence is observed in the digestive tract. At 4 h post injection, a weak signal is observed in

15:59 28 October 2016

15:59 28 October 2016

the intestines in accordance with complementary hepatobiliary elimination. Surprisingly, at 24 h after injection, a high fluorescence in the stomach is observed and confirms by ex vivo optical imaging. Such biodistribution is not conventional and should be related to a second internalization process. In fact, as the NPs are rapidly excreted by urine, assuming that the fluorescence in the stomach at 24 h is due to the grooming habits of mice as slight fluorescence is found at the nose. Still, no fluorescence is recorded in the tumor. These results confirm earlier studies on biodistribution of dendronized NPs: dendronized NPs are quickly eliminated through urinary and hepatobiliary pathways. It confirms as well that no EPR effect can be observed for such small sized and PEGylated dendronized hybrids.

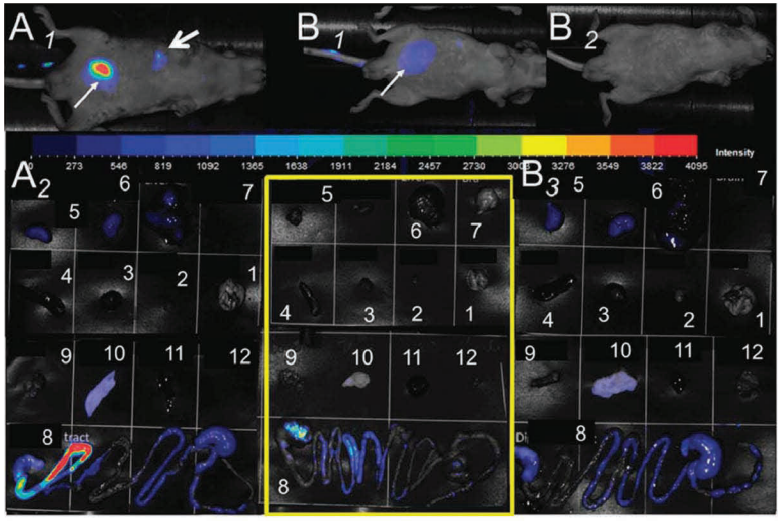



**Figure 2.25** In vivo whole body (A1, B1, and B2) and ex vivo organs (A2 and B3) optical images of NPs@D1@Alexa647 performed at 7 min (A1), 20 min (B1), 30 min (A2) and 24 h (B2 and B3) post iv injection. The yellow square includes ex vivo organ images of control mouse imaged with the same parameters [1 = lungs, 2 = urines, 3 = heart, 4 = spleen, 5 = kidney, 6 = liver, 7 = brain, 8 = digestive tract, 9 = bone sample, 10 = skin sample, 11 = blood sample, 12 = muscle sample]. Fine arrows indicate bladder signal, large arrow indicates liver signal. Reproduced from reference 111 with permission from the Royal Society of Chemistry.

15:59 28 October 2016

The effect of a linear versus a dendritic coating of low generation (generation 1 (G1), 2 (G2) or 3 (G3)) on the bio-elimination of spherical SPIONPs of 10 nm (NS10) was pointed out by Felder-Flesch and co-workers through relaxivity measurements, NMRD profiles and ex vivo biodistribution studies.[104] NS10 functionalized with the molecules L1, D2-G1, and D2-G2 are coupled to an Alexa dye (Alexa647) via carbodiimidation. Optical images of mice's organs removed 2, 4, and 6 h post IV injection are recorded (Fig. 2.26): all functionalized NPs circulated freely and without significant lung uptake post IV injection indicating the absence of large aggregates. Elimination through urinary pathway is evidenced by the fluorescent signal of urine at 2 h post IV injection of D2-G2 or by the significant decrease of the fluorescent signal in kidneys between 2 and 6 h post IV injection. Elimination through hepato-biliary pathway is also evidenced by the high fluorescent signal in the gall bladder and in the partial segment of the small bowel. However, the kinetic of the hepato-biliary elimination is both intense and fleeting for the L1-NPs, so intense but more sustainable for NP@D2-G2 and NP@D2-G1. At 6 h post IV injection, the total body elimination of NP@L2 is completed whereas a still time persistent hepato-biliary elimination process is observed for NP@D2-G1 as evidenced by the persistent fluorescent signal in the gall bladder and the digestive tract at 6 h post IV injection. At the same time delay, the NP@D2-G2 signal was still persistent and intense in kidneys and liver evocating a NPs cellular uptake.

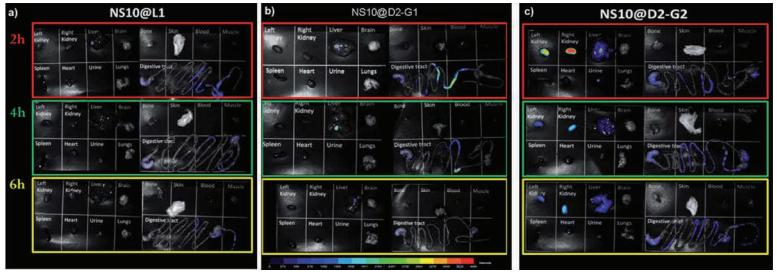



**Figure 2.26** Optical images of mice organs removed 2, 4 and 6 h post IV injection of NS10@L1 (a), NS10@D2-G1 (b) and NS10@D2-G2 (c). Reproduced from reference 104 with permission from the Royal Society of Chemistry.

To date, much research has been focused on the role of particle size as a determinant of biodistribution and clearance. These results tend to prove that there is more than just size. Indeed, both NS10@D2-G1 and NS10@D2-G2 display the same hard inorganic core, the same hydrodynamic diameter while showing different elimination rates and pathways. Yet, as underlined by H. Kobayashi,[126] other features amongst which flexibility can affect in vivo behavior of nanosized hybrids.

#### 2.3.3.4.4 Hyperthermia

IONPs are also developed for magnetic hyperthermia (MH).[124,127–129] When exposed to alternating magnetic fields of appropriate amplitude and frequency, these NPs release heat locally (where they are concentrated), which reduces the cancer cells viability. Indeed, MH is shown to enhance the tumor cells sensitivity towards chemo- or radio-therapy. Furthermore MH facilitates drug release or acts on cell membranes. However, one of the main limitations of MH is the low heating power of currently used magnetic NPs, requiring a local injection of large quantities of NPs. There is thus a great challenge for optimizing the heating power of magnetic NPs. The amount of heat generated by NPs is highly dependent on the NPs structural and magnetic properties. Preliminary studies have shown that IO NPs with a mean size around 20 nm are suitable for clinical MH.[127] Begin-Colin and coworkers reported synthesis of NPs with variable and controlled shapes and core-shell structures and functionalized with the small dendron D2G1 (Fig. 2.15).[130] The study revealed that oxidized nanocubes of 16 nm, oxNC16, displayed Specific Absorption Rates (SAR) values higher than those for spherical-shaped NPs of 19 nm, NS19, and the values of NS19 were slightly higher than those of nanocubes NC16, on low concentrated samples (Fig. 2.27). These NPs display heating capacities suitable for hyperthermia treatment, by comparison to SAR values reported for spherical single-core maghemite NPs,[127] cubic NPs,[128,131] or core–shell NPs.[11] At higher concentration, the SAR values strongly decrease for the three samples, indicating an effect of iron concentration on the magneto-thermal properties (see Fig. 2.27a). Such an effect of the concentration has already been reported with nanocubes.[128] The formation of chains[132] with

15:59 28 October 2016

core–shell nanocubes is observed at low concentration by TEM without applying a magnetic field (Fig. 2.27c), which may thus explain the high heating values at low concentration. As shown in Fig. 2.27b, the SAR values increased almost linearly with the amplitude field. This confirms an aggregation of NPs when the concentration increases.

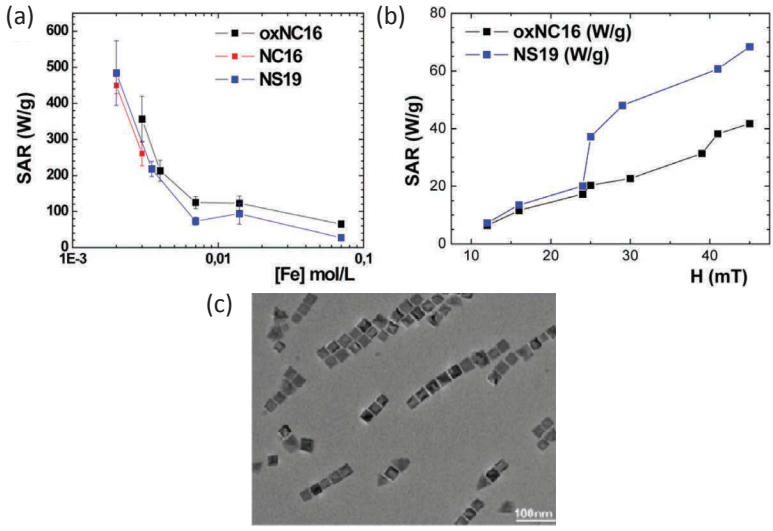



**Figure 2.27** Magneto-thermal properties of oxNC16, NC16, and NS19. (a) SAR measurements determined as a function of iron concentration at 700 kHz; (b) SAR values as a function of the magnetic field amplitude for highly concentrated oxNC16 and NS19 at 198 kHz; (c) TEM images of NC16. Reproduced with permission from reference 130.

Extensive studies of MRI properties demonstrated that core-shell $Fe_{1-x}O@Fe_{3-x}O_4$ particles display very high in vitro and in vivo MRI properties, even at very low concentrations.[130] Furthermore, oxidized nanocubes exhibited interesting positive $T_{1w}$ contrast at low concentration, allowing the envisioning of a dual contrast agent (i.e., positive contrast on $T_{1w}$ images and negative contrast on $T_{2w}$ images) with an improvement of the sensitivity related to the bright signal and thus improving the safety of the imaging interpretation procedure. In this way, the nanostructures studied here appear very promising for combining MRI and hyperthermia.

15:59 28 October 2016

15:59 28 October 2016

### 2.3.4 Up-Conversion NPs

Upconversion nanoparticles (UCNPs) are luminescent nanomaterials that generate higher energy light from lower energy radiation (usually near infrared, NIR or IR radiation), through the use of rare earth ions doped into a solid state.[133] With the development of nanotechnology, a variety of methods have been elaborated to synthesize different kinds of UCNPs, many of which are lanthanide doped nanocrystals.[134] Compared with downconversion organic fluorescent organic dyes and semiconducting nanocrystals, UCNPs have a number of advantages, such as: narrow emission peak, absence of photodamage, high photostability, very low autofluorescence background and low toxicity.[133,135,136] Since their discovery in the mid-1960s,[137] they have been pulling wide interest in many different areas, especially making them attractive contrast agents in optical biomedical imaging.[138–140]

UCNPs usually are capped with organic ligands and thus not biocompatible.[135] Surface modification is the critical step to fabricate UCNPs-based bio-probes. Water soluble and robust UCNP-g-HPG-RhB nanohybrid composed of a $NaYF_4$:Yb/Er core and tunable hyperbranched polyglycerol (HPG) shell tailored by fluorescent Rhodamine B (RhB) dye, have been recently reported to simultaneously present upconversion and downconversion luminescence in vivo.[141] In vivo studies showed good visibility at high injection depths (till 4 mm) (Fig. 2.28a–d). The standard MTT cell-viability assay displays low cytotoxicity, with a cell viability of 90% at a concentration of 0.8 mg/mL within 24 h on breast cancer cells MCF-7 (Fig. 2.28e). UCNP-g-HPG-RhB holds promise for bioimaging applications.

Regardless of encouraging results reported in the past few years in this field, there are still many challenges in applications of UCNPs-based nanohybrids in imaging and therapy. Long term toxicity of lanthanides is one of the significant concerns.[142] Another issue is the accumulation of UCNPs in RES after systemic administration.[143] Surface coating and size optimization is required to improve their pharmacokinetics and pharmacodynamics. Despite all the challenges, UCNPs have significant potential in biomedicine.

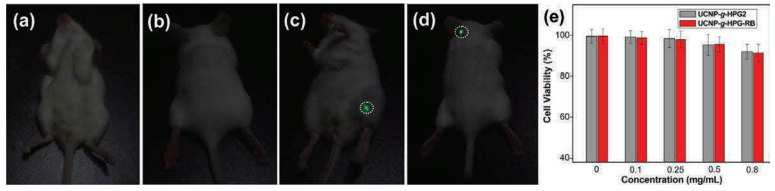



**Figure 2.28** Digital photographs of Kumming mouse after subcutaneous injection of (a) 100 μL of saline at the leg, (b) 100 μL of saline at the bottom of the ear. (c) 50 μg/L UCNPs-g-HPG-RB at the leg. (d) 50 μg/L UCNP-g-HPG-RB at the bottom of the ear under 980 nm laser illumination. (e) Cell viability of MCF-7 after incubation with UCNP-g-HPG-RB at various concentrations for 24 h. Reproduced with permission from reference 141.

15:59 28 October 2016

### 2.3.5 Manganese Oxide NPs

The development of molecular and cellular medicine has led to the recent development of a new generation of *positive* MRI contrast agents based on ultrasmall Gd, Dy or Mn-containing nanoparticles.[144,145] By opposition to iron oxide nanoparticles, ultrasmall nanoparticles made of MnO preferentially decrease the longitudinal relaxation time of hydrogen in water molecules, inducing thereby at least 1000× more sensitive MR signal enhancement in $T_1$-weighted MRI. However, the sequestration of MnO particles by the RES followed by strong uptake in the liver and in the spleen could potentially lead to $Mn^{2+}$-induced toxicity effects. Thus, for ultrasmall MnO particles to be applied in the clinics, it is necessary to develop coatings that also enable their efficient excretion within hours.

Tailored biological retention and efficient clearance of PEGylated MnO nanoparticles as positive MRI contrast agents for molecular imaging is also made possible via a dendritic approach.[146] The detection of molecular events in the nanomolar range using $T_1$-weighted MRI sequences requires the design of ultrasmall particles containing hundreds of paramagnetic ions per contrast agent unit. In 2014, Felder-Flesch, Fortin and coworkers[146] demonstrated for the first time the possibility to use MnO particles as $T_1$ vascular contrast agents, while enabling the excretion of >70% of all the Mn injected doses after 48 h. For

this, small, biocompatible and highly hydrophilic PEGylated bis-phosphonate dendrons (PDns) are grafted on MnO particles to confer colloidal stability, relaxometric performance, and fast excretion capacity. The relaxometric performance of MnO@PDns as "positive" MRI contrast agents is assessed ($r_1$ = 4.4 $mM^{-1} \cdot s^{-1}$, $r_2/r_1$ = 8.6; 1.41 T and 37°C). Mice are injected with 1.21 μg of $Mn \cdot kg^{-1}$ (22 μmol of $Mn \cdot kg^{-1}$), and scanned in MRI up to 48 h. The concentration of Mn in key organs is precisely measured by neutron activation analysis and confirmed, with MRI, the possibility to avoid RES nanoparticle sequestration through the use of phosphonate dendrons. Due to the fast kidney and hepatobiliary clearance of MnO particles conferred by PDns, MnO nanoparticles can now be considered for promising applications in $T_1$-weighted MRI requiring less toxic although highly sensitive *positive* molecular contrast agents.

15:59 28 October 2016

## 2.4 Conclusion

The universal need for improved medical care, new strategies for managing untreatable diseases and resistant pathogens, social pressure for medical needs and more cost-effective health care is demanded from current nanomedicine. The synergy between dendrimers/dendrons and nanoparticles are ensuring improved diseases management. For example, dendronized magnetic nanoparticles have a promising use for diagnosis, treatment and monitoring of the most unmanageable diseases.

However, issues associated with new nanomaterial properties, unknown toxicities and invasive therapies remain some of the greatest challenges. Thus providing support and encouraging dendrimer–nanoparticle conjugates to the clinic. Indeed, due to their high colloidal stability, administration of dendronized hybrids of small size can be done through intra-venous injection, which is less intrusive, more efficient and goes toward a "better life" medicine method.

The offspring of Nanotechnology and Medicine can hew to any challenge of human healthcare. On account of creating theranostic nanoplatforms, enabling targeted diagnosis and treatment of cancer at the same time.

15:59 28 October 2016

## References


1. Duncan, R., and Gaspar, R. (2011). Nanomedicine(s) under the microscope. *Mol. Pharm.*, **8**, 2101–2141.
2. Choi, H. S., and Frangioni, J. V. (2010). Nanoparticles for biomedical imaging: Fundamentals af clinical translation. *Mol. Imaging*, **9**, 291–310.
3. http://www.transparencymarketresearch.com.
4. Zhao, Z., et al. (2012). Nanotechnology in therapeutics: A focus on nanoparticles as a drug delivery system. *Nanomedicine*, **7**, 1253–1271.
5. Wagner, V., Dullaart, A., Bock, A.-K., and Zweck, A. (2006). The emerging nanomedicine landscape. *Nat. Biotechnol.*, **24**, 1211–1217.
6. Kannan, R. M., Nance, E., Kannan, S., and Tomalia, D. A. (2014). Emerging concepts in dendrimer-based nanomedicine: From design principles to clinical applications. *J. Intern. Med.*, **276**, 579–617.
7. Medintz, I. L., Uyeda, H. T., Goldman, E. R., and Mattoussi, H. (2005). Quantum dot bioconjugates for imaging, labelling and sensing. *Nat. Mater.*, **4**, 435–446.
8. Haase, M., and Schäfer, H. (2011). Upconverting nanoparticles. *Angew. Chem. Int. Ed. Engl.*, **50**, 5808–5829.
9. Nam, J., et al. (2013). Surface engineering of inorganic nanoparticles for imaging and therapy. *Adv. Drug Deliv. Rev.*, **65**, 622–648.
10. Kim, C., Ghosh, P., and Rotello, V. M. (2009). Multimodal drug delivery using gold nanoparticles. *Nanoscale*, **1**, 61–67.
11. Lee, J.-H., et al. (2007). Artificially engineered magnetic nanoparticles for ultra-sensitive molecular imaging. *Nat. Med.*, **13**, 95–99.
12. Thomas, C. R., et al. (2010). Noninvasive remote-controlled release of drug molecules in vitro using magnetic actuation of mechanized nanoparticles. *J. Am. Chem. Soc.*, **132**, 10623–10625.
13. Lee, H., Sun, E., Ham, D., and Weissleder, R. (2008). Chip–NMR biosensor for detection and molecular analysis of cells. *Nat. Med.*, **14**, 869–874.
14. Freeman, R., and Willner, I. (2012). Optical molecular sensing with semiconductor quantum dots (QDs). *Chem. Soc. Rev.*, **41**, 4067–4085.
15. Liu, Q., Yang, T., Feng, W., and Li, F. (2012). Blue-emissive upconversion nanoparticles for low-power-excited bioimaging in vivo. *J. Am. Chem. Soc.*, **134**, 5390–5397.
16. Jain, P. K., Huang, X., El-Sayed, I. H., and El-Sayed, M. A. (2008). Noble metals on the nanoscale: Optical and photothermal properties and some applications in imaging, sensing, biology, and medicine. *Acc. Chem. Res.*, **41**, 1578–1586.

15:59 28 October 2016

17. Sumer, B., and Gao, J. (2008). Theranostic nanomedicine for cancer. *Nanomedicine (Lond).*, **3**, 137–140.

18. Jokerst, J. V., and Gambhir, S. S. (2011). Molecular imaging with theranostic nanoparticles. *Acc. Chem. Res.*, **44**, 1050–1060.

19. Hadjipanayis, C. G., et al. (2010). EGFRvIII antibody-conjugated iron oxide nanoparticles for magnetic resonance imaging-guided convection-enhanced delivery and targeted therapy of glioblastoma. *Cancer Res.*, **70**, 6303–6312.

20. Liong, M., et al. (2008). Multifunctional inorganic nanoparticles for imaging, targeting, and drug delivery. *ACS Nano*, **2**, 889–896.

21. Harris, T. J., von Maltzahn, G., Derfus, A. M., Ruoslahti, E., and Bhatia, S. N. (2006). Proteolytic actuation of nanoparticle self-assembly. *Angew. Chem. Int. Ed. Engl.*, **45**, 3161–3165.

22. Von Maltzahn, G., et al. (2009). Computationally guided photothermal tumor therapy using long-circulating gold nanorod antennas. *Cancer Res.*, **69**, 3892–900.

23. Michalet , X., et al. (2005). Quantum dots for live cells, in vivo imaging, and diagnostics. *Science (80).*, **307**, 538–544.

24. Maier-Hauff, K., et al. (2011). Efficacy and safety of intratumoral thermotherapy using magnetic iron-oxide nanoparticles combined with external beam radiotherapy on patients with recurrent glioblastoma multiforme. *J. Neurooncol.*, **103**, 317–324.

25. Flacke, S., et al. (2001). Novel MRI contrast agent for molecular imaging of fibrin: Implications for detecting vulnerable plaques. *Circulation*, **104**, 1280–1285.

26. Winter, P. M., et al. (2003). Molecular imaging of angiogenesis in early-stage atherosclerosis with alpha(v)beta3-integrin-targeted nanoparticles. *Circulation*, **108**, 2270–2274.

27. Winter, P. M., et al. (2003). Molecular imaging of angiogenesis in nascent Vx-2 rabbit tumors using a novel targeted nanoparticle and 1.5 tesla magnetic resonance imaging. *Cancer Res.*, **63**, 5838–5843.

28. Lanza, G. M. (2002). Targeted antiproliferative drug delivery to vascular smooth muscle cells with a magnetic resonance imaging nanoparticle contrast agent: Implications for rational therapy of restenosis. *Circulation*, **106**, 2842–2847.

29. Chen, L., et al. (2013). Multifunctional nanoparticles for rapid bacterial capture, detection, and decontamination. *RSC Adv.*, **3**, 2390–2397.

30. Louie, A. (2010). Multimodality imaging probes: Design and challenges. *Chem. Rev.*, **110**, 3146–3195.

31. Nazemi, A., and Gillies, E. R. (2013). Dendritic surface functionalization of nanomaterials: Controlling properties and functions for biomedical applications. *Brazilian J. Pharm. Sci.*, **49**, 16–32.

32. Rud, O. V., et al. (2013). Dendritic spherical polymer brushes: Theory and self-consistent field modeling. *Macromolecules*, **46**, 4651–4662.

33. Gillich, T., et al. (2013). PEG-stabilized core shell nanoparticles: Impact of linear versus dendritic polymer shell architecture on colloidal properties and the reversibility of temperature-induced aggregation. *ACS Nano*, **7**, 316–329.

34. American Cancer Society (2015). *Cancer Facts & Figures 2015*.

35. Weissleder, R., and Mahmood, U. (2001). Molecular imaging. *Radiology*, **219**, 316–333.

36. Gu, Z. (John Wiley & Sons, 2015). *Bioinspired and Biomimetic Polymer Systems for Drug and Gene Delivery*. at <https://books.google.com/books?id=aJ3TBgAAQBAJ&pgis=1>

37. Lesniak, W., et al. (2005). Silver/dendrimer nanocomposites as biomarkers: Fabrication, characterization, in vitro toxicity, and intracellular detection. *Nano Lett.*, **5**, 2123–2130.

38. Shi, X., Wang, S. H., Van Antwerp, M. E., Chen, X., and Baker, J. R. (2009). Targeting and detecting cancer cells using spontaneously formed multifunctional dendrimer-stabilized gold nanoparticles. *Analyst*, **134**, 1373–1379.

39. Qiao, Z., and Shi, X. (2015). Dendrimer-based molecular imaging contrast agents. *Prog. Polym. Sci.*, **44**, 1–27.

40. Guo, R., et al. (2010). X-ray attenuation property of dendrimer-entrapped gold nanoparticles. *J. Phys. Chem. C*, **114**, 50–56.

41. Peng, C., et al. (2010). Acetylation of dendrimer-entrapped gold nanoparticles: Synthesis, stability, and x-ray attenuation properties. *J. Appl. Polym. Sci.*, **119**, 1673–1682.

42. Wang, H., et al. (2013). Folic acid-modified dendrimer-entrapped gold nanoparticles as nanoprobes for targeted CT imaging of human lung adencarcinoma. *Biomaterials*, **34**, 470–480.

43. Zhu, J., et al. (2014). Targeted cancer theranostics using alpha-tocopheryl succinate-conjugated multifunctional dendrimer-entrapped gold nanoparticles. *Biomaterials*, **35**, 7635–7646.

44. Liu, H., et al. (2014). Lactobionic Acid-modified dendrimer-entrapped gold nanoparticles for targeted computed tomography imaging of human hepatocellular carcinoma. *ACS Appl. Mater. Interfaces*, **6**, 6944–6953.

15:59 28 October 2016

15:59 28 October 2016


45. Zhou, B., et al. (2014). Synthesis and characterization of PEGylated polyethylenimine-entrapped gold nanoparticles for blood pool and tumor CT imaging. *ACS Appl. Mater. Interfaces*, **6**, 17190–17199.
46. Peng, C., et al. (2012). Facile formation of dendrimer-stabilized gold nanoparticles modified with diatrizoic acid for enhanced computed tomography imaging applications. *Nanoscale*, **4**, 6768–6778.
47. Cai, H., et al. (2012). Facile assembly of $Fe_3O_4$@Au nanocomposite particles for dual mode magnetic resonance and computed tomography imaging applications. *J. Mater. Chem.*, **22**, 15110–15120.
48. Chen, Q., et al. (2015). Multifunctional dendrimer-entrapped gold nanoparticles modified with RGD peptide for targeted computed tomography/magnetic resonance dual-modal imaging of tumors. *Anal. Chem.*, **87**, 3949–3956.
49. Wu, P., and Yan, X.-P. (2013). Doped quantum dots for chemo/biosensing and bioimaging. *Chem. Soc. Rev.*, **42**, 5489–5521.
50. Smith, A. M., Duan, H., Mohs, A. M., and Nie, S. (2008). Bioconjugated quantum dots for in vivo molecular and cellular imaging. *Adv. Drug Deliv. Rev.*, **60**, 1226–1240.
51. Zhang, J., Xu, S., and Kumacheva, E. (2004). Polymer microgels: Reactors for semiconductor, metal, and magnetic nanoparticles. *J. Am. Chem. Soc.*, **126**, 7908–7914.
52. Wang, Y. A., Li, J. J., Chen, H., and Peng, X. (2002). Stabilization of inorganic nanocrystals by organic dendrons. *J. Am. Chem. Soc.*, **124**, 2293–2298.
53. Guo, W., Li, J. J., Wang, Y. A., and Peng, X. (2003). Conjugation chemistry and bioapplications of semiconductor box nanocrystals prepared via dendrimer bridging. *Chem. Mater.*, **15**, 3125–3133.
54. Guo, W., Li, J. J., Wang, Y. A., Peng, X., and Fayette, V. (2003). Luminescent CdSe/CdS core/shell nanocrystals in dendron boxes: Superior chemical, photochemical and thermal stability. *J. Am. Chem. Soc.*, **125**, 3901–3909.
55. Gao, J., et al. (2012). A novel clinically translatable fluorescent nanoparticle for targeted molecular imaging of tumors in living subjects. *Nano Lett.*, **12**, 281–286.
56. Berry, C. C., and Curtis, A. S. G. (2003). Functionalisation of magnetic nanoparticles for applications in biomedicine. *J. Phys. D. Appl. Phys.*, **36**, R198–R206.
57. Bertrand, N., Wu, J., Xu, X., Kamaly, N., and Farokhzad, O. C. (2014). Cancer nanotechnology: The impact of passive and active targeting in the era of modern cancer biology. *Adv. Drug Deliv. Rev.*, **66**, 2–25.

15:59 28 October 2016


58. Ghobril, C., et al. (2012). Dendrimers in nuclear medical imaging. *New J. Chem.*, **36**, 310–323.
59. Jeong, U., Wang, Y., Ibisate, M., and Xia, Y. (2005). Some new developments in the synthesis, functionalization, and utilization of monodisperse colloidal spheres. *Adv. Funct. Mater.*, **15**, 1907–1921.
60. Gao, J., Gu, H., and Xu, B. (2009). Multifunctional magnetic nanoparticles: Design, synthesis, and biomedical applications. *Acc. Chem. Res.*, **42**, 1097–1107.
61. Reddy, L. H., Arias, J. L., Nicolas, J., and Couvreur, P. (2012). Magnetic nanoparticles: Design and characterization, toxicity and biocompatibility, pharmaceutical and biomedical applications. *Chem. Rev.*, **112**, 5818–5878.
62. Carrillo, A. I., Serrano, E., Luque, R., and García-Martínez, J. (2013). Microwave-assisted catalysis by iron oxide nanoparticles on MCM-41: Effect of the support morphology. *Appl. Catal. A Gen.*, **453**, 383–390.
63. Hütten, A., and Reiss, G. (2005). Applications beyond data storage. *Nat. Mater.*, **4**, 725–726.
64. Pereira, C., et al. (2012). Superparamagnetic $MFe_2O_4$ (M = Fe, Co, Mn) nanoparticles: Tuning the particle size and magnetic properties through a novel one-step coprecipitation route. *Chem. Mater.*, **24**, 1496–1504.
65. Karaagac, O., and Kockar, H. (2011). Effect of synthesis parameters on the properties of superparamagnetic iron oxide nanoparticles. *J. Supercond. Nov. Magn.*, **25**, 2777–2781.
66. Lu, A.-H., Salabas, E. L., and Schüth, F. (2007). Magnetic nanoparticles: Synthesis, protection, functionalization, and application. *Angew. Chem. Int. Ed. Engl.*, **46**, 1222–1244.
67. Grene, J. M., et al. (2006). Hydrothermal synthesis of monodisperse magnetite nanoparticles. *Chem. Mater.*, **18**, 4399–4404.
68. Chen, D., and Xu, R. (1998). Hydrothermal synthesis and sharacterization of nanocrystalline $Fe_3O_4$ powders. *Mater. Res. Bull.*, **33**, 1015–1021.
69. Joseyphus, R. J., et al. (2007). Role of polyol in the synthesis of Fe particles. *J. Magn. Magn. Mater.*, **310**, 2393–2395.
70. Solinas, S., Piccaluga, G., Morales, M. P., and Serna, C. J. (2001). sol-gel formation of $\gamma$-$Fe_2O_3/SiO_2$ nanocomposites. *Acta Mater.*, **49**, 2805–2811.
71. Sun, S., and Zeng, H. (2002). Size-controlled synthesis of magnetite nanoparticles. *J. Am. Chem. Soc.*, **124**, 8204–8205.

15:59 28 October 2016


72. Sun, S., et al. (2004). Monodisperse $MFe_2O_4$ (M) Fe, Co, Mn nanoparticles. *J. Am. Chem. Soc.*, **4**, 126–132.
73. Park, J., et al. (2004). Ultra-large-scale syntheses of monodisperse nanocrystals. *Nat. Mater.*, **3**, 891–895.
74. Jeong, U., Teng, X., Wang, Y., Yang, H., and Xia, Y. (2007). Superparamagnetic colloids: Controlled synthesis and niche applications. *Adv. Mater.*, **19**, 33–60.
75. Baaziz, W., et al. (2014). Magnetic iron oxide nanoparticles: Reproducible tuning of the size and nanosized-dependent composition, defects, and spin canting. *Phys. Chem.*, **118**, 3795–3810.
76. Wang, Y., et al. (2006). Selective heterogeneous nucleation and growth of size-controlled metal nanoparticles on carbon nanotubes in solution. *Chemistry*, **12**, 2542–2549.
77. Kashchiev, D. (2000). *Nucleation: Basic theory with Applications,* Butterworth-Heinemann.
78. Van Embden, J., Sader, J. E., Davidson, M., and Mulvaney, P. (2009). Evolution of colloidal nanocrystals: Theory and modeling of their nucleation and growth. *J. Phys. Chem. C*, **113**, 16342–16355.
79. LaMer, V. K., and Dinegar, R. H. (1950). Theory, production and mechanism of formation of monodispersed hydrosols. *J. Am. Chem. Soc.*, **72**, 4847–4854.
80. Derjaguin, B. V, Voropayeva, T. N., Titiyevskaya, A. S., and Kabanov, B. N. (1964). Surface forces and the stability of colloids and disperse systems. *J. Colloid Sci.*, **19**, 113–135.
81. Derjaguin, B. (1939). On the repulsive forces between charged colloid particules and on the theory of slow coagulation stability of lyophobe sols. *Trans. Farady Soc.*, **35**, 203–215.
82. Bacri, J.-C., Perzynski, R., and Salin, D. (1990). Ionic ferrofluids: A crossing of chemistry and physics. *J. Magn. Magn. Mater.*, **85**, 27–32.
83. Lamanna, G., et al. (2011). Dendronized iron oxide nanoparticles for multimodal imaging. *Biomaterials*, **32**, 8562–8573.
84. Duanmu, C., Saha, I., Zheng, Y., Goodson, B. M., and Gao, Y. (2006). Dendron-functionalized superparamagnetic nanoparticles with switchable solubility in organic and aqueous media: matrices for homogeneous catalysis and potential mri contrast agents. *Chem. Mater.*, **18**, 5973–5981.
85. Wu, X., et al. (2011). Water-soluble dendritic-linear triblock copolymer-modified magnetic nanoparticles: Preparation, characterization and drug release properties. *J. Mater. Chem.*, **21**, 13611–13620.

15:59 28 October 2016


86. Rouhollah, K., Pelin, M., Serap, Y., Gozde, U., and Ufuk, G. (2013). Doxorubicin loading, release, and stability of polyamidoamine dendrimer-coated magnetic nanoparticles. *J. Pharm. Sci.,* **102**, 1825–1835.

87. Basly, B., et al. (2011). Properties and suspension stability of dendronized iron oxide nanoparticles for MRI applications. *Contrast Media Mol. Imaging*, **6**, 132–138.

88. Imaging, T. M., et al. (2013). Terms of use bisphosphonate-anchored pegylation and radiolabeling of superparamagnetic iron oxide: Long-circulating nanoparticles for in vivo multimodal. *ACS Nano*, **7**, 500–512.

89. Portet, D., Denizot, B., Rump, E., Lejeune, J.-J., and Jallet, P. (2001). Nonpolymeric coatings of iron oxide colloids for biological use as magnetic resonance imaging contrast agents. *J. Colloid Interface Sci.*, **238**, 37–42.

90. Garofalo, A., et al. (2014). Efficient synthesis of small-sized phosphonated dendrons: Potential organic coatings of iron oxide nanoparticles. *N. J. Chem.*, **38**, 5226–5239.

91. Gentilini, C., Boccalon, M., and Pasquato, L. (2008). Straightforward synthesis of fluorinated amphiphilic thiols. *European J. Org. Chem.*, **2008**, 3308–3313.

92. Mckenna, C. E., Higa, M. T., Cheung, N. H., and Mckenna, M. (1977). the Facile dealkylation of phosphonic acid dialkyl ethers by bromotrimethylsilane. *Tetrahedron Lett.*, **2**, 155–158.

93. Schrigten, D., et al. (2012). A new generation of radiofluorinated pyrimidine-2,4,6-triones as MMP-targeted radiotracers for positron emission tomography. *J. Med. Chem.*, **55**, 223–232.

94. Lee, J. W., et al. (2006). Convergent synthesis of symmetrical and unsymmetrical PAMAM dendrimers. *Macromolecules*, **39**, 2418–2422.

95. Bhosale, S. V., Kalyankar, M. B., Langford, S. J., Bhosale, S. V., and Oliver, R. F. (2009). Synthesis and supramolecular properties of a novel octaphosphonate porphyrin. *European J. Org. Chem.*, **2009**, 4128–4134.

96. Dai, L., et al. (2014). One-pot facile synthesis of PEGylated superparamagnetic iron oxide nanoparticles for MRI contrast enhancement. *Mater. Sci. Eng. C. Mater. Biol. Appl.,* **41**, 161–167.

97. Daou, T. J., et al. (2009). Water soluble dendronized iron oxide nanoparticles. *Dalt. Trans.*, 4442–4449.

98. Sahoo, Y., et al. (2001). Alkyl phosphonate/phosphate coating on magnetite nanoparticles: A comparison with fatty acids. *Langmuir*, **17**, 7907–7911.

15:59 28 October 2016


99. Daou, T. J., et al. (2008). Coupling agent effect on magnetic properties of functionalized magnetite-based nanoparticles. *Chem. Mater.*, **20**, 5869–5875.

100. Daou, T., et al. (2007). Investigation of the grafting rate of organic molecules on the surface of magnetite nanoparticles as a function of the coupling agent. *Sens. Actuators B Chem.*, **126**, 159–162.

101. Basly, B., et al. (2013). Effect of the nanoparticle synthesis method on dendronized iron oxides as MRI contrast agents. *Dalt. Trans.*, **42**, 2146–2157.

102. Martin, A. L., Li, B., and Gillies, E. R. (2009). Surface functionalization of nanomaterials with dendritic groups: Toward enhanced binding to biological targets. *J. Am. Chem. Soc.*, **131**, 734–741.

103. Pan, B., et al. (2007). Dendrimer-modified magnetic nanoparticles enhance efficiency of gene delivery system. *Cancer Res.*, **67**, 8156–8163.

104. Walter, A., et al. (2015). Validation of a dendron concept to tune colloidal stability, MRI relaxivity and bioelimination of functional nanoparticles. *J. Mater. Chem. B*, **3**, 1484–1494.

105. Caminade, A.-M., Turrin, C.-O., Laurent, R., Ouali, A., and Delavaux-Nicot, B. (John Wiley & Sons, Inc., 2011). *Dendrimers*.

106. Ambade, A. V, Savariar, E. N., and Thayumanavan, S. (2005). Dendrimeric micelles for controlled drug release and targeted delivery. *Mol. Pharm.*, **2**, 264–272.

107. Eichman, J. D., Bielinska, A. U., Kukowska-Latallo, J. F., and Baker, J. R. (2000). The use of PAMAM dendrimers in the efficient transfer of genetic material into cells. *Pharm. Sci. Technolo. Today*, **3**, 232–245.

108. Kitchens, K. M., Foraker, A. B., Kolhatkar, R. B., Swaan, P. W., and Ghandehari, H. (2007). Endocytosis and interaction of poly (amidoamine) dendrimers with Caco-2 cells. *Pharm. Res.*, **24**, 2138–2145.

109. Xu, L., Shao, L., Hu, M., Chen, L., and Bi, Y. (2012). A thermoresponsive amphiphilic dendron—Synthesis, characterization, and self-assembled micelles for controlled drug release. *Can. J. Chem.*, **90**, 600–607.

110. Walter, A., et al. (2015). Modulation of relaxivity, suspension stability, and biodistribution of dendronized iron oxide nanoparticles as a function of the organic shell design. *Part. Part. Syst. Charact.*, **32**, 552–560.

111. Ghobril, C., et al. (2013). A bisphosphonate tweezers and clickable PEGylated PAMAM dendrons for the preparation of functional

iron oxide nanoparticles displaying renal and hepatobiliary elimination. *Chem. Commun. (Camb).*, **49**, 9158–9160.

112. Gupta, A. K., and Gupta, M. (2005). Synthesis and surface engineering of iron oxide nanoparticles for biomedical applications. *Biomaterials*, **26**, 3995–4021.
113. Weissleder, R., et al. (1989). Superparamagnetic pharmacokinetics iron oxide: And toxicity. *Am. J. Roentgenol.*, **152**, 167–173.
114. Huh, Y.-M., et al. (2005). In vivo magnetic resonance detection of cancer by using multifunctional magnetic nanocrystals. *J. Am. Chem. Soc.*, **127**, 12387–12391.
115. Barnett, B. P., et al. (2007). Magnetic resonance-guided, real-time targeted delivery and imaging of magnetocapsules immunoprotecting pancreatic islet cells. *Nat. Med.*, **13**, 986–991.
116. Tassa, C., Shaw, S. Y., and Weissleder, R. (2011). Dextran-coated iron oxide nanoparticles: A versatile platform for targeted molecular imaging, molecular diagnostics, and therapy. *Acc. Chem. Res.*, **44**, 842–852.
117. Bulte, J. W., et al. (2001). Magnetodendrimers allow endosomal magnetic labeling and in vivo tracking of stem cells. *Nat. Biotechnol.*, **19**, 1141–1147.
118. Yang, J., et al. (2015). Conjugation of iron oxide nanoparticles with RGD-modified dendrimers for targeted tumor MR imaging. *ACS Appl. Mater. Interfaces*, **7**, 5420–5428.
119. Chandra, S., Nigam, S., and Bahadur, D. (2013). Combining unique properties of dendrimers and magnetic nanoparticles towards cancer theranostics. *J. Biomed. Nanotechnol.*, **9**, 1–18.
120. Chang, Y., et al. (2012). Synthesis and characterization of DOX-conjugated dendrimer-modified magnetic iron oxide conjugates for magnetic resonance imaging, targeting, and drug delivery. *J. Mater. Chem.*, **22**, 9594–9601.
121. Garcia, J., Tang, T., and Louie, A. Y. (2015). Nanoparticle-based multimodal PET/MRI probes. *Nanomedicine (Lond).*, **10**, 1343–1359.
122. El-Hammadi, M. M., and Arias, J. L. (2015). Iron oxide-based multi-functional nanoparticulate systems for biomedical applications: A patent review (2008-present). *Expert Opin. Ther. Patents*, **25**, 691–709.
123. Cui, X., et al. (2016). Synthesis, characterization, and application of core-shell $Co_{0.16}Fe_{2.84}O_4$@$NaYF_4$(Yb, Er) and $Fe_3O_4$@$NaYF_4$(Yb, Tm) nanoparticle as trimodal (MRI, PET/SPECT, and optical) imaging agents. *ACS Bioconjug. Chem.*, **27**, 319–328.

15:59 28 October 2016

15:59 28 October 2016

124. Lee, N., et al. (2015). Iron oxide based nanoparticles for multimodal imaging and magnetoresponsive therapy. *Chem. Rev.*, **115**, 10637–10689.

125. Kueny-Stotz, M., Mamlouk-Chaouachi, H., and Felder-Flesch, D. (2011). Synthesis of Patent Blue derivatized hydrophilic dendrons dedicated to sentinel node detection in breast cancer. *Tetrahedron Lett.,* **52**, 2906–2909.

126. Longmire, M. R., Ogawa, M., Choyke, P. L., and Kobayashi, H. (2011). Biologically optimized nanosized molecules and particles: More than just size. *Bioconjug. Chem.*, **22**, 993–1000.

127. Gazeau, F., Lévy, M., and Wilhelm, C. (2008). Optimizing magnetic nanoparticle design for nanothermotherapy. *Nanomedicine*, **3**, 831–844.

128. Guardia, P., et al. (2012). Water-soluble iron oxide nanocubes with high values of specific absorption rate for cancer cell hyperthermia treatment. *ACS Nano*, **6**, 3080–3091.

129. Hugounenq, P., et al. (2012). Cooperative organization in iron oxide multi-core nanoparticles potentiates their efficiency as heating mediators and mri contrast agents. *ACS Nano*, **6**, 10935–10949.

130. Walter, A., et al. (2014). Mastering the shape and composition of dendronized iron oxide nanoparticles to Tailor magnetic resonance imaging and hyperthermia. *Chem. Mater.*, **26**, 5252–5264.

131. Bae, K. H., et al. (2012). Chitosan oligosaccharide-stabilized ferrimagnetic iron oxide nanocubes for magnetically modulated cancer hyperthermia. *ACS Nano*, **6**, 5266–5273.

132. de la Presa, P., et al. (2012). Study of heating efficiency as a function of concentration, size, and applied field in $\gamma$-$Fe_2O_3$ nanoparticles. *J. Physiccal Chem.*, **116**, 25602–25610.

133. Chatterjee, D. K., Gnanasammandhan, M. K., and Zhang, Y. (2010). Small upconverting fluorescent nanoparticles for biomedical applications. *Small*, **6**, 2781–2795.

134. Wang, L., et al. (2005). Fluorescence resonant energy transfer biosensor based on upconversion-luminescent nanoparticles. *Angew. Chemie Int. Ed.*, **44**, 6054–6057.

135. Cheng, L., Wang, C., and Liu, Z. (2013). Upconversion nanoparticles and their composite nanostructures for biomedical imaging and cancer therapy. *Nanoscale*, **5**, 23–37.

136. Wang, F., et al. (2010). Simultaneous phase and size control of upconversion nanocrystals through lanthanide doping. *Nature*, **463**, 1061–1065.

137. Auzel, F. (2004). Upconversion and anti-stokes processes with f and d ions in solids. *Chem. Rev.*, **104**, 139–173.

138. Zhou, J., Liu, Z., and Li, F. (2012). Upconversion nanophosphors for small-animal imaging. *Chem. Soc. Rev.*, **41**, 1323–1349.

139. Yi, G. S., and Chow, G. M. (2006). Synthesis of hexagonal-phase $NaYF_4$: Yb,Er and $NaYF_4$:Yb, Tm nanocrystals with efficient up-conversion fluorescence. *Adv. Funct. Mater.*, **16**, 2324–2329.

140. Wang, F., Banerjee, D., Liu, Y., Chen, X., and Liu, X. (2010). Upconversion nanoparticles in biological labeling, imaging, and therapy. *Analyst*, **135**, 1839–1854.

141. Zhou, L., et al. (2014). Multihydroxy dendritic upconversion nanoparticles with enhanced water dispersibility and surface functionality for bioimaging. *ACS Appl. Mater. Interfaces*, **6**, 7719–7727.

142. Xiong, L., Yang, T., Yang, Y., Xu, C., and Li, F. (2010). Long-term in vivo biodistribution imaging and toxicity of polyacrylic acid-coated upconversion nanophosphors. *Biomaterials*, **31**, 7078–7085.

143. Abdul Jalil, R., and Zhang, Y. (2008). Biocompatibility of silica coated $NaYF_4$ upconversion fluorescent nanocrystals. *Biomaterials*, **29**, 4122–4128.

144. Kueny-Stotz, M., Garofalo, A., and Felder-Flesch, D. (2012). Manganese-enhanced mri contrast agents: From small chelates to nanosized hybrids. *Eur. J. Inorg. Chem.*, **2012**, 1987–2005.

145. Tu, C., and Louie, A. Y. (2012). Nanoformulations for molecular MRI. *Wiley Interdiscip. Rev. Nanomed. Nanobiotechnol.*, **4**, 448–457.

146. Chevallier, P., et al. (2014). Tailored biological retention and efficient clearance of pegylated ultra-small MnO nanoparticles as positive MRI contrast agents for molecular imaging. *J. Mater. Chem. B*, **2**, 1779–1790.

15:59 28 October 2016

## Chapter 3

# Dendritic Polymers for the Repair of Tissues

**Cynthia Ghobril and Mark W. Grinstaff**

*Departments of Biomedical Engineering, Chemistry, and Medicine, Boston University, 590 Commonwealth Avenue, Boston, MA 02215, USA*

mgrin@bu.edu

As the clinical demands increase for better approaches to repair damaged or diseased tissues, so do the design requirements for the materials to be used. Of the materials in use or under investigation, polymers represent a significant category. Recently, dendrimers—monodisperse, highly branched, globular polymers—are being investigated for a number of biomedical applications including tissue repair. For these applications, the dendrimers or dendritic macromolecules are crosslinked to form hydrogels. Their monodispersity combined with the control of their size, architecture, density, and surface groups, makes them ideal structures for hydrogel formation. Hydrogels, either as sealants or scaffolds for cells, represent one of the most important classes of biomaterials because of their tunable mechanical properties, biocompatibility, non-toxicity, and similarity to natural soft tissues. Over the last two decades, a large number and variety

*Dendrimers in Nanomedicine*
Edited by Delphine Felder-Flesch
Copyright © 2016 Pan Stanford Publishing Pte. Ltd.
ISBN 978-981-4745-49-9 (Hardcover), 978-981-4745-50-5 (eBook)
www.panstanford.com

of dendritic-based hydrogels are reported and characterized. This chapter begins with a description of the synthetic routes and properties of these dendritic hydrogels, followed by the evaluation of their uses in tissue repair applications and ends with a summary of the field and future perspectives.

## 3.1 Introduction

The repair of damaged tissues is of utmost importance. Often, this repair involves the juxtaposition of nearby tissues to close the wound and, thus, suturing has been practiced for more than several millennia. Suture materials have progressed from collagen fibers isolated from the intestine of sheep and cows (catgut sutures) to purely synthetic sutures made from polyglycolic acid or polydioxanone. Advances in polymer chemistry and engineering, during the past 40 years have afforded these new medical device materials, and expanded the use of sutures to a wide-range of applications, practiced today. As the clinical challenges become greater—to not only repair but regenerate tissue—and the design requirements more stringent, new polymer compositions, structures, and architectures are in demand. Dendrimers are a new class of polymers that have been actively studied since their first reports in the late 1970s and early 1980s.[1–6] Dendrimers are monodisperse branched polymers possessing a focal point/core and repeat branching units that extend outward in layers or generations. The net result is a globular shaped polymer in solution with many end groups, which are available for additional chemical reactions. When dendrimers or dendritic polymers are functionalized with groups that react with other similarly (or complementarily) functionalized polymers, water-swellable crosslinked polymer networks (i.e., hydrogels) are formed. Specifically, hydrogels are composed of low-molecular-weight molecules or macromolecules linked together by multiple physical and/or covalent bonds. Hydrogels possess favorable properties and many advantages for their use in biomedicine and biomedical engineering such as ease of administration, biocompatibility, biodegradability, tunable mechanical properties, high water content, as well as a substrate for cell attachment and a matrix for drug encapsulation and delivery. Consequently, hydrogels are widely investigated for wound repair, tissue

15:59 28 October 2016

15:59 28 October 2016

engineering, and drug delivery.[7–12] The increasing need for biomaterials with unique features and mechanisms of action for specific in vitro and in vivo applications motivates the design and development of hydrogels with new chemical structures, new modes of crosslinking, and unique physicochemical properties. Hydrogels composed of dendritic macromonomers are a promising class of hydrogel-based materials. The biocompatible dendritic macromolecules of different generations $G_n$, crosslink to form the water-swellable 3D networks, with tunable physical and mechanical properties.[13] The monodispersity and low viscosity of these structures combined with the control of their size, architecture, density, and surface groups make them ideal macromonomers for the design and preparation of such materials. We begin with a discussion of the synthesis and properties of dendritic hydrogels followed by an examination of their uses in tissue repair applications, and end with a summary of the field and suggestions for future areas of application.

## 3.2 Synthesis and Properties of Dendritic Hydrogels

As shown in Fig. 3.1, dendritic hydrogels are prepared via chemical or physical gelation methods. Gelation occurs when $G_n$-dendrons/dendrimers crosslink with each other or with other multifunctional crosslinkers via physical or chemical interactions to form water-swellable 3D networks, with water filling the void spaces. The dendritic structures play unique roles in controlling the properties of the resulting hydrogels. For example, the focal point/core, the branching units and the number and composition of functional groups on the periphery of the dendrons/dendrimers can be easily varied to modify or enhance the properties of hydrogels. Additionally, $G_n$-dendritic structures possess a defined and controlled number of multivalent crosslinking units on their surface, which can lead to multiple interactions between the branched units or with other multifunctional crosslinkers, and therefore strengthen the crosslinking density of the hydrogel network, in a controlled fashion. Several literature reviews summarize the state of the art of dendritic hydrogels preparation, characterization and biological applications.[13–19] Therefore, this section will highlight

examples of the most commonly used physical and chemical linkages for the synthesis of such materials.

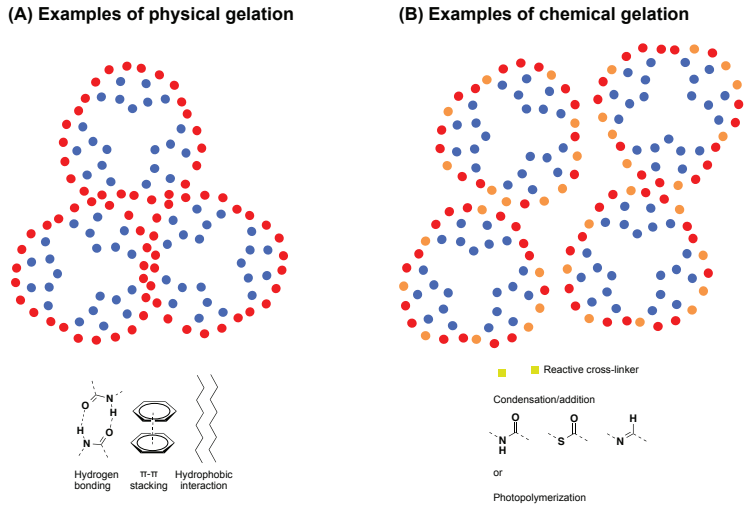



**Figure 3.1** Pictorial representations of dendritic hydrogels formed by (A) physical gelation, and (B) chemical gelation.

### 3.2.1 Physical Gelation

Physical gelation takes place when $G_n$-dendrons/dendrimers self-assemble into a 3D network through physical interactions such as hydrogen bonding, ionic association, and hydrophobic interaction (Fig. 3.1A). This type of gelation does not require the use of additives, crosslinkers or external radiation sources and often generates weak, but reversible, physical hydrogels due to the non-covalent nature of the junctions in the network, which can be disrupted under a certain physical stimuli (i.e., changes in pH, temperature, ionic strength or application of stress). As a consequence, stimuli-responsive hydrogels are explored for controlled-release type applications because they can undergo abrupt structural modifications in response to stress or environmental changes in the body, and are therefore being utilized for the design of smart devices for drug delivery, tissue engineering, immobilization of enzymes and gene carriers.

15:59 28 October 2016

15:59 28 October 2016

An early example illustrating the potential physical gelation of dendritic macromolecules was described by Newkome and co-workers in 1990.[20] Two-directional arborols **A** and **B** composed of branched domains connected by lipophilic spacers of variable lengths were synthesized (Fig. 3.2) and their gelation properties were evaluated by viscometry, optical and electronic microscopies and light scattering, after heating the solution to 80°C and cooling it to 25°C. It was observed that several of these arborols form thermally reversible hydrogels at concentrations of 1–10 weight percentage (wt%) due to their aggregation into larger rod-like structures formed via intermolecular hydrogen bonding and hydrophobic interactions between terminal hydroxyl groups of the dendrons and lipophilic chains of the spacer, respectively.

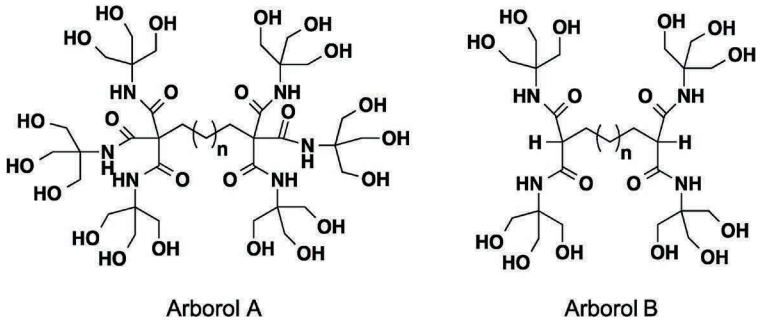
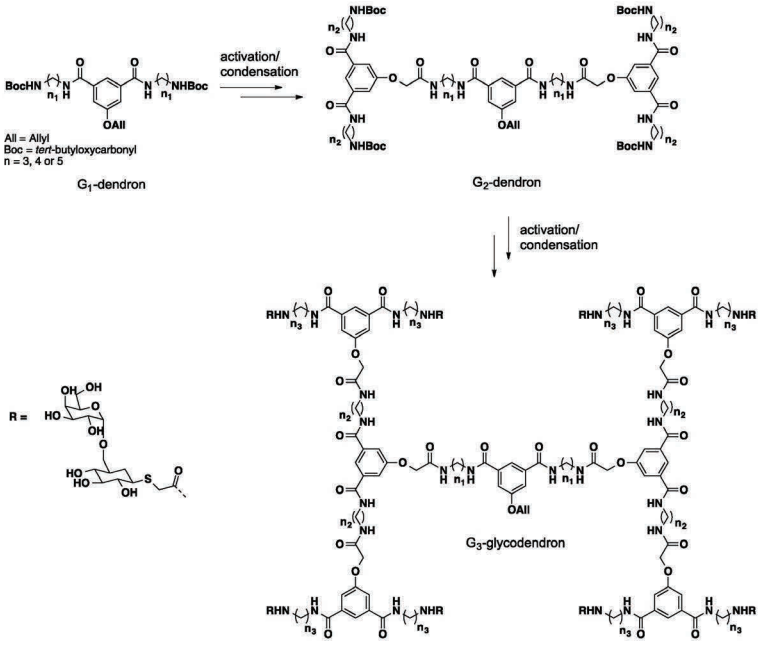



**Figure 3.2** Examples of arborols described by Newkome et al.[20]

Majoral et al. also reported the synthesis of $G_n$-organophosphorous dendrimers with cationic functional groups (pyridinium and ammonium chlorides) on their surface, which formed physical hydrogels at concentrations of 1.5–1.8 wt%, upon heating for several days at 60–65°C.[21] The gelation time strongly depended on the nature of the terminal groups as well as the experimental conditions. Hydrogels composed of pyridinium dendrimers gelled faster than their ammonium counterparts. Similarly, exchanging chloride anions with acetates in pyridinium-derived $G_1$-dendrimers accelerated the gelation process from 20 to 4 days. The internal structure of the hydrogels was evaluated using freeze-fracture electron microscopy. Before gelation, the dendritic solution exhibited a homogenous texture whereas after gelation, a non-covalent network of dendritic aggregates was observed. The physical nature of the hydrogel was due to the

intermolecular hydrogen bonding, $\pi$-$\pi$ stacking and hydrophobic effects between the amide groups and the aromatic rings within the dendrimer backbone, respectively.




**Scheme 3.1** Synthesis of $G_3$-glycodendron, as described by Boons et al.

Another group reported the gelation of glycodendrons.[22] Dendrimer growth was achieved by activation of the amino groups of the multifunctional $G_1$-dendron and the subsequent condensation of the phenol moiety to form ether linkages, as depicted in Scheme 3.1. This repetitive two-step sequence (activation/condensation) afforded higher generation dendrons onto which saccharide moieties were attached to produce water-soluble glycodendrons. Several of these dendrons formed thermally reversible hydrogels at concentrations as low as 0.33–1 wt%, when heated in water to 80°C and cooled to 4°C. It was observed that the length $n_1$ of the alkyl chain of $G_3$-dendrons had an influence on their sol-gel transition temperature ($T_{sol\text{-}gel}$), which decreased from 34–37°C for $n_1$ = 1 to 15–19°C for $n_1$ = 5. On the other hand, increasing the alkyl chain length $n_3$ of the outer shell of the dendrons resulted in an increase of $T_{sol\text{-}gel}$, which indicated

15:59 28 October 2016

15:59 28 October 2016

that structural variations in these materials strongly influenced their physical properties.

Aida et al. reported dendritic hydrogels composed of clay nanosheets (CNSs), $G_n$-dendritic binders and sodium poly(acrylates) (ASAP), which exhibited significantly strong mechanical properties. Moreover, as these gels were physically crosslinked, they were able to quickly self-heal when damaged (Fig. 3.3).[23] Upon mixing CNSs and ASAP in water, the highly entangled nanosheets tended to dissociate and disperse while being wrapped on their positively charged edges with anionic ASAP. When the $G_n$-dendritic binder composed of two guanidinium-derived dendrons linked together by a PEG spacer, was added to the mixture, a hydrogel was formed in 3 minutes (min) upon their crosslinking with the negatively charged surfaces of CNSs. Although the gel could be formed without the presence of ASAP, the polymer contributed to the increase in the mechanical strength of the network. The dendritic part as well as its telechelic structure played an important role in generating the hydrogel, as the use of guanidinium hydrochlorides or a monodendron version of the $G_n$-binder (i.e., PEG-$G_n$-dendron) instead, caused no gelation, in both cases. The rheological properties of hydrogels were evaluated while varying the $G_n$ of the dendritic binder ($n$ = 1–3) as well as the amount of CNSs, and the storage (G′) and loss (G″) moduli were measured as functions of angular frequency at a constant strain value of 1%. It was observed that G′ was always higher than G″ over the entire range of frequencies, which demonstrated an elastic or "solid-like" behavior of hydrogels. Additionally, among the three binders tested, the $G_3$-binder gave the highest G′ value due to the higher crosslinking density of the network. G″ also depended on the concentration of CNS used while forming the hydrogel, where stiffer gels were obtained with increasing amount of CNS. For example, by using CNS (5%)/$G_3$-binder (0.38%)/ASAP (0.15%), the highest G′ value of 0.5 MPa was obtained among those reported for physical hydrogels. The hydrogels were able to quickly self-heal when damaged, while exhibiting, once recovered, higher mechanical strength (G″ value 50 times bigger) than other hydrogel systems with comparable speed recovery. Finally, the hydrogels were able to incorporate and retain the activity of biologically active proteins, such as myoglobin, expanding their potential use as matrices for biological activities.

This elegant strategy contradicted the assumption that self-assembled hydrogels are weak and provided a new approach for the quick and easy development of strong physically crosslinked hydrogels for a desired property or application.

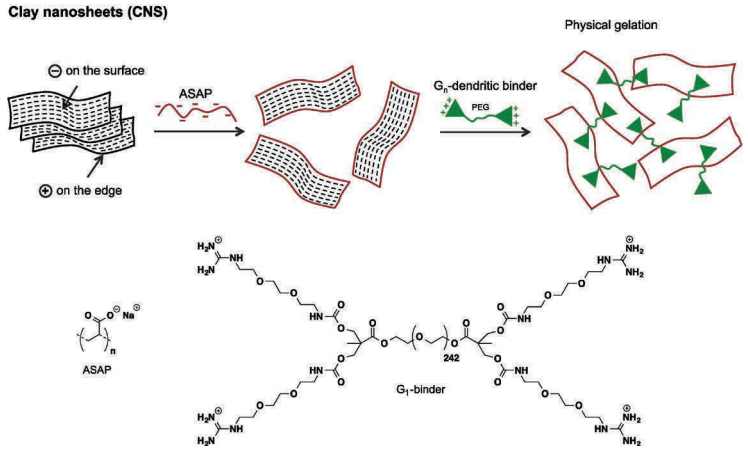



**Figure 3.3** Self-assembly of CNS/$G_n$-dendritic binder/ASAP and formation of physical hydrogels, as reported by Aida et al.[23] Adapted by permission from MacMillan Publishers Ltd: Nature (ref. 23), Copyright 2010; http://www.nature.com/nature/index.html.

Amphiphilic dendrons composed of amino acids linked to lipophilic chains have also been used for the formation of reversible hydrogels. Liu et al. designed $G_1$ and $G_2$ *L*-glutamic acid dendrons linked to $C_{18}$-alkyl chain (Fig. 3.4), which self-assembled into fiber and helical nanotube structures, respectively, and formed hydrogels, over a wide pH range from 2 to 13.[24] It was observed by atomic force microscopy (AFM) and transmission electronic microscopy (TEM) that $G_2$-dendritic amphiphiles possessed different chiral nanostructures, depending on the pH of the solution. For example, at pH 2–9, 1D right handed helical nanostructures were observed for hydrogels, whereas at pH 10–13, the hydrogels self-assembled into 2D dendritic structures. Additionally, TEM images, circular dichroism (CD) analysis, IR spectroscopic and X-ray diffraction (XRD) measurements, revealed that the dendritic amphiphiles first formed a bilayer stabilized by hydrogen bonding between the amide and carboxylic acid groups, and hydrophobic interaction between the lipophilic chains. As pH increased, a subtle change

15:59 28 October 2016

15:59 28 October 2016

in hydrogen bonding occurred, which led to various chiral nanostructures. At pH higher than 10, only the hydrogen bond sites of carboxylic acid groups were eliminated and the electrostatic interactions of carboxylates became predominant, leading to 2D dendritic structures. This work provides an example of self-assembled hydrogels with tunable architectures based on pH variation, and serves as a model system to study and understand the structure-function relationship that exists in self-assembled chiral nanostructures found in nature.

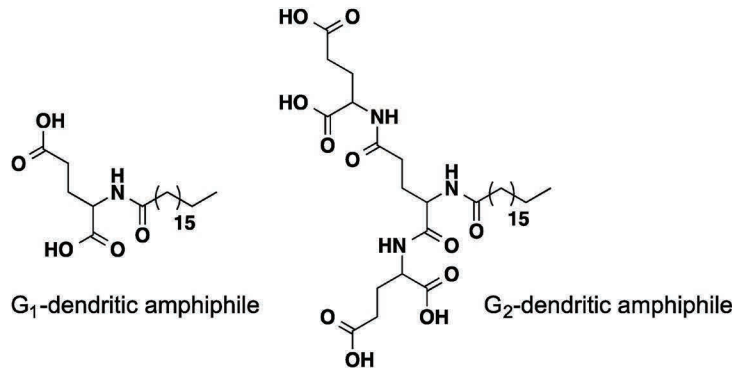



**Figure 3.4** Structures of $G_n$-dendritic amphiphiles described by Liu et al.[24]

### 3.2.2 Chemical Gelation

Chemical gelation takes place when $G_n$-dendrons/dendrimers crosslink together or with other multifunctional crosslinkers to form a water-swellable 3D network through the formation of covalent bonds such as C–C, X–C, or X–X (where C is a carbon, X is an oxygen, nitrogen or sulfur). Photopolymerization of dendritic macromolecules composed of peripheral photosensitive functional groups, or condensation/addition reactions of reactive dendritic macromolecules (e.g., esterification, amidation, click type reaction) affords covalently linked hydrogels, as depicted in Fig. 3.1B. Chemical gelation of dendritic macromolecules yields strong and stable hydrogels, due to the permanent junctions between the macromonomers in the network. These gels possess a range of properties due to the chemical diversities available with the dendritic structure (e.g., chemical composition of the focal

15:59 28 October 2016

point/core, branching units and functional groups, generation, and number of reactive moieties on the periphery), the crosslinker type and molecular weight, and the chemical crosslinking process. Chemically crosslinked hydrogels are usually more stable in vivo than their physical crosslinked counterparts and have found utility in applications where extended use of the material is required before its complete absorption, such as wound repair, drug delivery and tissue engineering.

The first dendritic hydrogel formed by photopolymerization was reported in 2002 by Grinstaff et al. as an adhesive for the repair of full-thickness corneal lacerations, and is composed of biodegradable poly(glycerol-succinic acid)-poly(ethylene glycol) dendritic-linear-dendritic (DLD) copolymers, namely ($[G_n]$PGLSA-MA)$_2$-PEG, as depicted in Fig. 3.5 (top).[25] The PEG block was selected to ensure water solubility and the branched glycerol-succinic acid provided a biodegradable unit with multiple end groups for further functionalization. Specifically, the glycerol units at the periphery of the dendrons were further derivatized with methacrylate groups (MA), which upon photopolymerization crosslinked and formed the hydrogel network in 10–30 seconds (sec). The same strategy was applied for the synthesis of carbamate-linked photo-crosslinkable dendritic macromonomers, constructed of biodegradable poly(glycerol-$\beta$-alanine)-poly(ethylene glycol) DLD copolymers, namely ($[G_n]$PGLBA-MA)$_2$-PEG, as depicted in Fig. 3.5 (bottom).[26] The carbamate linkages within the hydrogel network ensured greater in vivo stability of the gel than their ester-linked counterparts, and the material was successfully used as an adhesive for the repair of osteochondral defects.[26] Different generations of DLD copolymers ($n$ = 0–3) were synthesized and characterized and upon their photo-crosslinking with an argon ion laser and eosin-based photoinitiators, they formed hydrogels with tunable mechanical and swelling properties based on the dendrimer structure, concentration and generation. For example, ($[G_1]$-PGLSA-MA)$_2$-PEG at 5–10 wt% and ($[G_1]$-PGLBA-MA)$_2$-PEG at 5–20 wt% hydrogels exhibited minimal swelling (i.e., amount of absorbed water within the hydrogel) after 30 days incubation in phosphate buffered saline (PBS) solutions. The 20 wt% of ($[G_1]$-PGLSA-MA)$_2$-PEG hydrogel on the other hand, swelled the most, with a swelling ratio of 12%.[26] Rheological measurements

15:59 28 October 2016

evaluated on photocrosslinked ($[G_1]$PGLSA-MA)$_2$-PEG and ($[G_1]$PGLBA-MA)$_2$-PEG hydrogels significantly depended on the dendrimer concentration, with higher concentrations affording stiffer materials. Specifically, ($[G_1]$PGLSA-MA)$_2$-PEG exhibited Young's moduli $E$ of 21 ± 2 and 661 ± 13 kPa and complex shear moduli $G^*$ of 1 ± 0.1 and 45 ± 3 kPa, at 5 and 20 wt%, respectively. The ($[G_1]$PGLBA-MA)$_2$-PEG, hydrogel exhibited higher $E$ and $G^*$ values at both concentrations ($E$ = 47 ± 1 and 912 ± 16 kPa; $G^*$ = 2 ± 0.1 and 80 ± 2 kPa at 5 and 20 wt%, respectively).

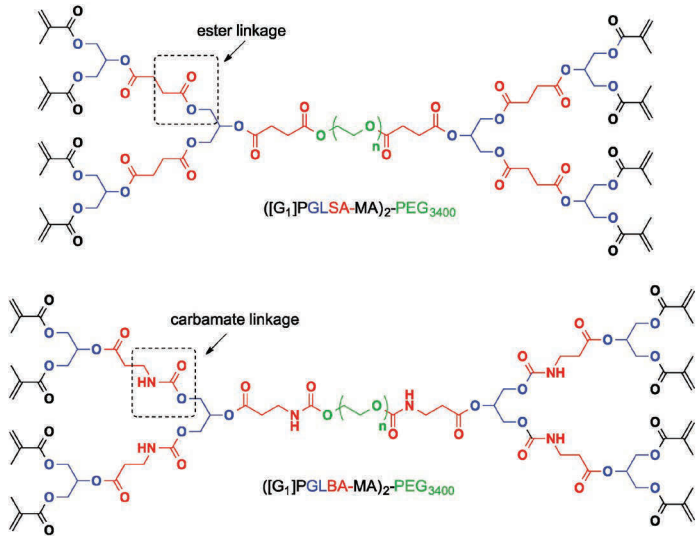



**Figure 3.5** Structures of ($[G_1]$PGLSA-MA)$_2$-PEG$_{3400}$ and ($[G_1]$PGLBA-MA)$_2$-PEG$_{3400}$ dendritic-linear-dendritic copolymers, designed by Grinstaff et al. ; G: generation ; P: poly; GL:glycerol in blue; SA/BA: succinate (top) or $\beta$-alanate (bottom) in red; MA: methacrylate in black; PEG : poly(ethylene glycol) in green. Adapted with permission from ref. 40. Copyright 2016. American Chemical Society.

The same group designed additional covalently crosslinked dendritic hydrogels based on amide and thioester linkages formed between $G_n$-peptide dendrons ($n$ = 1–2) bearing amine or thiol groups on their periphery and bis-*N*-hydroxysuccinimide ester or disuccinimidyl valerate PEG chains, respectively, as depicted in Fig. 3.6. For example, hydrogels prepared from $G_1$-lysine dendron

15:59 28 October 2016

**A** and poly(ethylene glycol bis-*N*-hydroxysuccinimide ester) (NHS-PEG-NHS (**B**); Mw = 3400), were formed in 1 min and the crosslinking reaction was monitored by FT-IR spectroscopy (Fig. 3.6.1).[27] The hydrogel swelling increased with increasing concentration of the polymers and ranged from 180% to 800%. As expected, higher generation hydrogels swelled less than lower ones, due to more efficient crosslinking and the higher density of crosslinked sites within the network. The rheological properties of the materials were measured before and after swelling, and showed strong elastic responses for all concentrations and generations. Increasing the polymer concentration (from 8 to 43 wt%) afforded **A:B** hydrogels with higher $E$ and $G^*$ (40 to 300 kPa, and 4 to 25 kPa, respectively). After swelling, the complex moduli decreased by half due to the high amount of water absorbed within the network, which decreased the hydrogels stiffness. All dendritic hydrogels were transparent, elastic, hydrophilic and, as discussed in Section 3.3, have utility for sealing ocular wounds. This work highlighted the potential use of dendritic macromonomers as multivalent crosslinkers for gel synthesis as they can be easily tuned for a desired property and application.

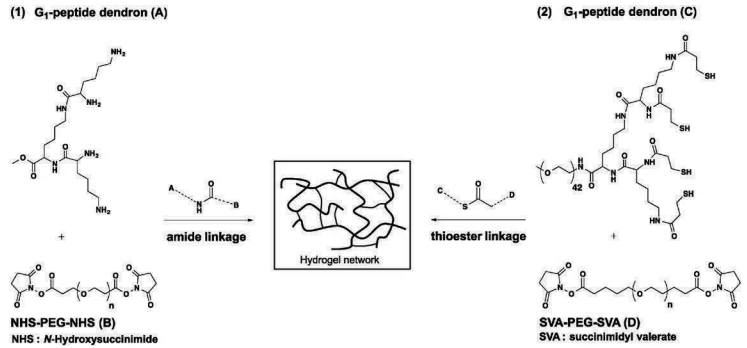



**Figure 3.6** Examples of dendritic hydrogels based on covalent crosslinking via (1) amide, and (2) thioester linkage formation. Adapted with permission from ref. 40. Copyright 2016. American Chemical Society.

Another example of a recently developed feature in a dendritic hydrogel is the on-demand dissolution.[28] The hydrogel was composed of linear-dendritic (LD) $G_1$-lysine-PEG dendron

15:59 28 October 2016

(**C**) bearing thiol moieties on the periphery, which upon crosslinking with poly(ethylene glycol disuccinimidyl valerate) (SVA-PEG-SVA (**D**); Mw = 3.4 kDa), formed the 3D network within seconds due to the rapid formation of thioester linkages (Fig. 3.6.2). The rheological properties of **C:D** hydrogels were measured using an oscillatory rheometer. Specifically, after determining the linear viscoelastic region (LVR) of the hydrogels at 10 or 30 wt%, the frequency sweep was measured at a constant oscillatory stress before and after swelling. Thioester hydrogels exhibited strong elastic properties at either concentration with low tan $\delta$ values ($\delta$ < 5°) and G′ higher than G″ moduli at frequencies between 0.1 and 10 Hz. Before swelling, G′ values for hydrogels at 10 and 30 wt% and 1 Hz of frequency, were 6 and 37 kPa, respectively, whereas after swelling to equilibrium, G″ dropped significantly to about 0.2 and 18 kPa, respectively. The on-demand dissolution of thioester hydrogels occurred via a thiol-thioester exchange reaction between an added thiol solution (e.g., cysteine methyl ester (CME)) and the thioesters present within the hydrogel network. The dissolution time of the gel depended significantly on the CME concentration and the pH of the PBS solution. For example, increasing the concentration of CME from 0.1 to 0.5 M at a constant pH of 7.4, decreased the dissolution time of the hydrogel from $t_{1/2}$ = 30 min to $t_{1/2}$ = 18 min. Additionally, when increasing the pH from 7.4 to 8.5, at a CME concentration of 0.3 M, the dissolution time decreased from $t_{1/2}$ = 25 to $t_{1/2}$ = 12 min. Interestingly, exposure of the hydrogels to a solution of lysine methyl ester (LME, 0.3 M), in PBS at pH 8.5, did not cleave the thioesters within the network, which indicated that a thiol-thioester exchange mechanism was responsible for the dissolution of the material when exposed to CME solutions.

The click chemistry concept has also been utilized for the construction of covalent hydrogels with controlled structures due to its high specificity in the presence of a variety of functional groups, its quantitative yield under physiological conditions, and its pH-insensitivity.[29] Based on this approach, Malkoch et al. and Sanyal et al. successfully described the synthesis of "clickable" hydrogels formed between acetylene-terminated-$G_n$-dendritic macromolecules, namely $G_n$-$AB_2C$ and $G_n$-DLD, and $N_3$-PEG-$N_3$ macromonomers, respectively (Fig. 3.7) (A = carboxylic acid, B =

hydroxyl, and C = acetylene; DLD = bHMPA-PEG-bHMPA where bHMPA = bis(hydroxymethyl)propionic acid); $N_3$ = azide).[30,31] The networks prepared from the $G_2$-$AB_2C$ dendrimers afforded hydrogels with 96% water uptake, which degraded within 1 hour (h) at pH 11 and 4 days (d) at pH 4, whereas hydrogels developed with $G_{2/3}$-DLD copolymers exhibited water uptake between 900 and 2000% depending on the PEG chain length and the crosslinker content. Excess alkynes from $G_n$-DLD dendrons were further functionalized with biotin for streptavidin-immobilization, and thus illustrated the possibility of protein attachment on the hydrogels.

15:59 28 October 2016

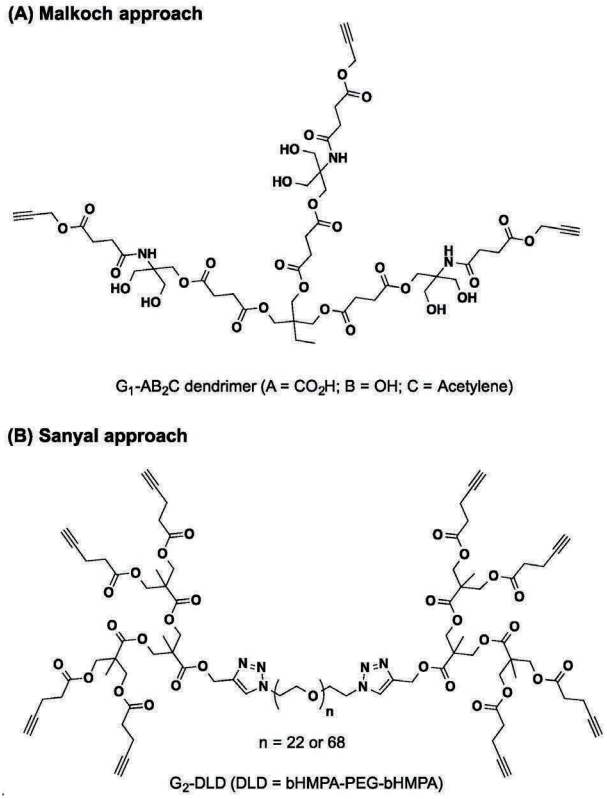



**Figure 3.7** Examples of dendritic building block structures for the formation of "clickable" hydrogels, as described by (A) Malkoch et al., and (B) Sanyal et al. Figure 3.7 (B) is reprinted with permission from ref. 40. Copyright 2016. American Chemical Society.

15:59 28 October 2016

The group of Malkoch and co-workers recently developed heterofunctional Trizma®-based dendritic scaffolds with defined orthogonal groups on the surface (i.e., alkenes and azides).[32] Alkene groups were used to crosslink with bifunctional SH-PEG-SH (SH = thiol) of 6 kDa Mw through ultra-violet (UV) initiated thiol-ene coupling (TEC) reaction and form hydrogel networks, whereas post-functionalization via copper catalyzed azide-alkyne cycloaddition (CuAAC) click reaction was used to couple D-mannose, 3,4-dihydroxyphenylalanine (DOPA) and carboxylic acid groups with the available azide functionalities, and generate bioactive materials (Fig. 3.8). For example, hydrogels (containing free azides for post hydrogel functionalization) formed within 10 min in ethanol using 0.5 wt% of Irgacure 2959 as a photoinitiator (365 nm, 9 $mW \cdot cm^{-2}$), exhibited an equilibrium swelling of 870% after solvent exchange from ethanol to water. Additionally, the gel had a Young's modulus, *E*, of 21.7 ± 2.5 kPa, close to muscle tissue (8–17 kPa). Altering the number and ratio of the azide and alkene groups within the pre-functionalized dendritic scaffold (i.e., 3 azides and 6 alkenes instead of 6 azides and 3 alkenes in Fig. 3.8) and its subsequent crosslinking with SH-PEG-SH afforded a hydrogel with higher *E* (42.8 ± 2.3 kPa), and a slight decrease in equilibrium swelling to 780%. The dendrimers were further evaluated as adhesive primers in bone fracture applications.

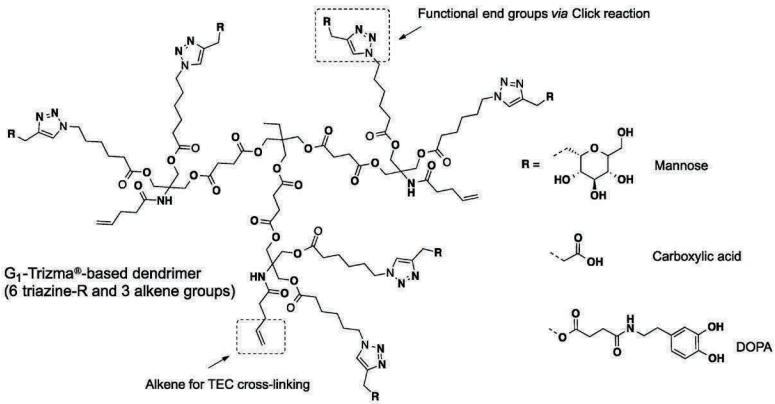



**Figure 3.8** Chemical structures of dendritic scaffolds bearing functional end groups formed through click reaction, and alkenes for TEC cross-linking, as reported by Malkoch et al.

## 3.3 Tissue Repair and Tissue Engineering Applications

The advancements in the chemical synthesis of dendrimers and dendritic macromolecules combined with new hydrogel crosslinking strategies are enabling the preparation and subsequent evaluation of hydrogels for challenges in the biomedical arena. As described in the following selected examples, dendritic hydrogels provide a wealth of opportunities to optimize the hydrogel structure and properties for a specific application.

15:59 28 October 2016

### 3.3.1 Tissue Repair

Traumatic or surgical wounds require immediate closure and repair to prevent infection and promote healing. Although sutures remain the most commonly used closure technique, their placement is time-consuming and may require the use of anesthesia (depending on the application), and they can induce infection, nerve damage and scar tissue formation. Consequently, hydrogels composed of biocompatible and biodegradable dendritic backbones have emerged as an exciting class of polymeric adhesives to supplement or replace sutures in the closure of wounds, due to their ease of administration, their non-toxicity and most importantly, their degradation, adhesive, and mechanical properties, which can be controlled at the molecular level via the composition and structure of the dendritic precursors.

One example of traumatic wounds are corneal lacerations, which are cuts in the front part of the eye caused by trauma, infection, and inflammation, and can cause blindness if untreated. Sutures are usually used to close the lacerations, in order to restore the normal intraocular pressure (IOP = 15–20 mmHg in human eye) in the eye and ensure a leak tight environment for adequate healing. However, sutures can cause additional trauma to the corneal tissue and increase the risk of infection and inflammation. Moreover, it requires removal from the wound site once the wound is healed. Therefore, the use of hydrogel sealants, which can be easily administered on the wound site and rapidly absorbed once the healing is ensured, would offer advantages over sutures.

15:59 28 October 2016

Grinstaff and co-workers investigated the use of dendritic hydrogel adhesives for the repair of ophthalmic wounds. First, they evaluated different generations of photocrosslinkable biocompatible and biodegradable DLD copolymers ($n$ = 0–3) composed of natural metabolite (succinic acid (SA) and glycerol (GL)) dendrons and linear PEGs, for the formation of hydrogel sealants for the repair of full-thickness corneal lacerations (Fig. 3.5 (top), Section 3.2).[25,33,34] Incisions (4.1 mm) were made on ex vivo human enucleated eyes and the wounds were closed either with nylon sutures or with photo-crosslinkable $(G_n\text{-PGLSA-MA})_2$-$PEG_{3400}$ copolymers. Irradiation of 20 wt% of the dendritic $G_1$-DLD copolymer with visible light in the presence of a photoinitiator generated a transparent hydrogel in situ, which adhered on the wound site and sealed it (Fig. 3.9). After injecting saline solutions into the eye via a syringe pump, the leaking pressures (LP) (i.e., maximum pressure reached before fluid leaked from the eye) for both systems were measured using a cardiac transducer probe inserted through the optic nerve. Among the generations tested, only $([G_1]\text{PGLSA-MA})_2$-PEG successfully closed the ocular wound, and prevented it from leaking.[25] Lower generation dendrons did not gel sufficiently to seal the wound, whereas higher generations either polymerized too fast and could not be delivered to the wound in a controlled fashion or were insoluble in water and thus precipitated upon application on the wound. The photocrosslinked dendritic $G_1$ copolymer adhered strongly to the wound site and was superior to conventional sutures, with a LP of 171 ± 44 mmHg as compared to 90 ± 18 mmHg for sutures.



**Figure 3.9** Photograph of a sealed corneal laceration using photo-crosslinked $([G_1]\text{PGLSA-MA})_2$-$PEG_{3400}$-based hydrogel sealant.[25]

15:59 28 October 2016

Additional corneal laceration studies were conducted in vivo using a chicken eye model over 28 days.[33,34] Similarly, 4-mm full-thickness lacerations were made in the eye of each animal and the wounds were subsequently sealed with either the photocrosslinkable $([G_1]PGLSA\text{-}MA)_2\text{-}PEG_{3400}$ or conventional sutures, and sacrificed on postoperative day 1, 3, 7, and 28. Histological examinations determined the extent of corneal healing. Both, the DLD sealant and sutures successfully secured all lacerations by post-operative day 2. However, the wounds treated with the dendritic copolymer exhibited more uniform corneal structure with less scarring than those treated with sutures. The dendrimer was gone from the wound site by day 14, and showed no toxic response during the clinical examinations. The nylon sutures were still present at day 28 and, clinically, the sutures would be removed by the physician. Additionally, the photoactivatable $G_1$-DLD copolymer was efficient in securing Laser-Assisted in situ Keratomileusis (LASIK) flaps by adequately adhering to the tissue and preventing it from displacement.[35,36]

The authors also evaluated a series of $([G_1]PGLSA\text{-}MA)_2\text{-}PEG$ macromonomers of variable PEG molecular weights (Mw from 3.4 to 20 kDa) and formulations (10–40 wt%) for the repair of 4 mm central corneal lacerations in an ex vivo porcine model.[37] The wounds were subsequently sealed with 10, 20, and 40 wt% of $([G_1]PGLSA\text{-}MA)_2\text{-}PEG_{3400}$, and 10 and 20 wt% of $([G_1]PGLSA\text{-}MA)_2\text{-}PEG_{10000/20000}$ hydrogel adhesives and compared to sutured treated eyes. All of the adhesive-repaired eyes at either formulation or concentration exhibited higher LPs than suture-treated eyes. When the DLD copolymers were used for the repair of central corneal lacerations, higher viscosities were obtained with increasing concentration of the polymer, which improved the adhesion of the material on the tissue. Similarly, higher LPs were obtained with higher concentration of copolymers at any PEG molecular weight. Finally, as the molecular weight of PEGs in $([G_1]PGLSA\text{-}MA)_2\text{-}PEG$ was increased from 3.4 to 10 kDa, the LP increased as observed for 10 and 20 wt% concentration, however, upon further increasing the molecular weight to 20 kDa, the LP decreased.

While photopolymerization of dendritic macromonomers is an efficient and rapid technique for the in situ generation of hydrogel sealants for the repair of ophthalmic wounds, the Grinstaff

15:59 28 October 2016

group also investigated alternative crosslinking strategies that did not require the use of light for crosslinking. Their strategy was to identify chemoselective organic reactions, which could form hydrogels within seconds, at room temperature, and under physiological conditions, without the generation of byproducts or with by-products that are known to be biocompatible. Therefore, the use of amide and thioester linkages formed between biocompatible peptide dendrons and PEG crosslinkers were investigated, as depicted in Fig. 3.6 (Section 3.2).

For example, Grinstaff and co-workers explored the crosslinking of amine terminated-$G_1$-peptide dendrons **A** and NHS-PEG-NHS **B** (Fig. 3.6.1, Section 3.2) to form **A:B** hydrogel sealants for the repair of scleral incisions used in pars plana vitrectomy procedures.[27] Vitrectomy is the surgical removal of the vitreous gel from the middle of the eye to correct the vision, and is usually conducted when there is retinal detachment, macular holes or vitreous hemorrhage. The surgeon makes small slits (usually three, less than 2 mm) in the side of the eye (pars plana area), in order to (1) suck out the vitreous gel, and repair the retina by removing subretinal fluids, scar tissues, and fixing macular holes, (2) insert an infusion line to replace the fluid and maintain the normal IOP, and (3) insert a light source for optical illumination. At the end of the procedure, the surgeon refills the eye with a saline solution and closes the incisions with sutures until the wound is healed. To determine whether the **A:B** hydrogels were more efficient in sealing 1.4 mm scleral wounds than sutures, a set of experiments were conducted on ex vivo enucleated pig eyes, where hydrogel precursors were first mixed at 18 wt% and quickly applied on the wounds, and the LPs were then measured after gelation and compared to 7-0 vicryl suture-treated eyes. The wounds treated with sutures had LPs of 140 ± 68 mmHg, whereas the ones treated with the bioadhesive hydrogels attained pressures higher than 250 mmHg without leakage. The hydrogel completely adhered to the tissue and prevented the wound from leaking even at high pressures. This high adhesion strength was likely due to the formation of an interpenetrating network between the gel and the host tissue, as suggested by the authors, reinforced by the possible reaction of residual NHS units of the hydrogel with amino groups of proteins presented in the extracellular matrix (ECM) of the tissue.

15:59 28 October 2016

Recently, the development of a dissolvable dendritic hydrogel sealant was reported for emergency care (e.g., arterial or hepatic bleeding), where the hydrogel was first applied on the wound to seal it and stop the bleeding, and dissolved on-demand at a later time, for wound re-exposure and further surgical treatment. The hydrogel was formed within seconds, at room temperature, via the crosslinking of thiol-terminated-$G_1$-lysine dendrons **C** with SVA-PEG-SVA **D**, as depicted in Fig. 3.6.2 (Section 3.2), and the formation of reversible thioester linkages within the 3D network.[28]

The hydrogel was not toxic to NIH3T3 murine fibroblast cells nor induced an immune response when exposed to macrophages. Additionally, the gel adhered strongly to ex vivo human skin tissues and was completely dissolved upon exposure to CME solutions. As a first step toward the development of a dissolvable hydrogel hemostat for emergency care, the adhesion and sealing efficiency of thioester **C:D** hydrogels were investigated on ex vivo jugular vein punctures (Fig. 3.10). First, the precursors of the gel (30 wt%) were mixed at room temperature, and quickly applied on a 2.5 mm hole made on the vein (Figs. 3.10a,b). A transparent hydrogel was formed on the incision within seconds, and completely closed it without leakage, as the pressure in the syringe pump continuously increased to 250 mmHg. When the hydrogel was exposed to CME solution, it dissolved due to the thiol-thioester exchange mechanism between the thioester linkages in the network and the added thiolate, and the wound leaked again (Figs. 3.10c,d). This work highlighted the first example of a hydrogel sealant that adhered strongly to skin tissues, secured the wound at high

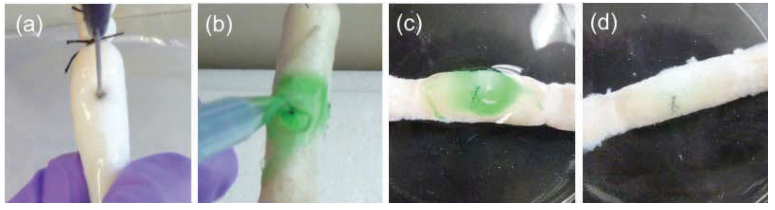



**Figure 3.10** Photographs of (a) punctured jugular vein, (b) hydrogel sealant, dyed in green, applied on the puncture, (c) hydrogel sealant exposed to cysteine methyl ester (CME) solution, and (d) dissolution of the hydrogel sealant. Adapted with permission from ref. 28. Copyright 2013 Wiley-VCH.

15:59 28 October 2016

pressures without breakage or leakage (good mechanical properties), and dissolved on demand for controlled wound re-exposure and definitive surgical care.

Malkoch et al. evaluated the use of Trizma®-based dendritic crosslinkers, with clickable azide and alkene groups, as adhesive primers in bone fracture applications (Fig. 3.11).[32] Surgical treatment of bone injuries relies on the use of screws and metal plates and requires harsh surgeries and general anesthesia. Additionally, bone fractures near sensitive tissues cannot be treated with conventional techniques due to the fragility of these areas. Consequently, minimally invasive adhesive implants have emerged as an alternative approach to replace conventional fixation techniques in the repair or stabilization of bone fractures. However, it was reported that the direct application of adhesives on fractured areas interfered with the natural bone healing process as well as resulted in an insufficient adhesive area. Therefore, the adhesives were incorporated in composite materials (a fiber reinforced adhesive patch (FRAP)), which were applied on the outside of the fractured sites as opposed to the inside, in order to circumvent and minimize their interference with the healing process and increase their contact with bone surface areas. The strategy consisted of a dendritic azide/triazine-alkene based layer (primer) that contained adhesive peripheral groups (e.g., DOPA, $CO_2H$) capable of binding to bone tissues in wet conditions, as well as alkenes that further crosslinked, upon exposure to UV, with a thiol-ene-based matrix and E-glass fiber layers, which provided reinforced adhesive strength (Fig. 3.12). A variety of $G_1$-Trizma®-based dendritic crosslinkers were tested as primers in FRAPs and their shear strengths (maximum shear attained before the adhesive broke) were measured on fractured bones and compared to a free-primer FRAP. All patches exhibited higher shear strengths when dendritic primers were incorporated within the composites, which demonstrated their enhanced adhesion to fractured bones in wet conditions, as opposed to patches without primers. Surprisingly, polar triazine-based dendritic crosslinkers functionalized with six DOPA or carboxylic acid ($CO_2H$) and three alkene groups exhibited the lowest shear strength values of 0.6 and 0.8 MPa, respectively, among all primers (Fig. 3.8, Section 3.2), whereas less polar dendrimers with switched functionalities

15:59 28 October 2016

(i.e., three DOPA or $CO_2H$ and six alkene groups), exhibited higher shear strengths of 3.2 and 1.8 MPa, respectively. However, none of these dendritic primers exhibited shear strength as high as the commercially available wound closure adhesive, Histoacryl®, with a shear strength value of 3.8 MPa. Finally, when using the dendritic primers with three azide and six alkene groups, compared to six azide and three alkene groups (Fig. 3.11), shear strength values of 3 and 4.2 MPa were reached, respectively, which highlighted the important role of azide moieties in increasing significantly the shear strength of the FRAP. This result was explained by the possible rearrangement of azides into reactive imines and nitrogen upon exposure to UV light, which further reacted with themselves leading to higher molecular weight primers. These macromolecules have shown to exhibit higher shear strength due to their stronger binding to bone surfaces, as opposed to low molecular weight counterparts. Additionally, upon contact with water, imines also hydrolyze to aldehydes, hydrates, or acetals, which can react with amino acids present in the ECM of bone tissues and further increase the covalent attachment of primers to bones in wet conditions. The FRAP did not show any toxic signs towards MG63 osteoblast cells and its use is a promising strategy for the stabilization of fractured bones.

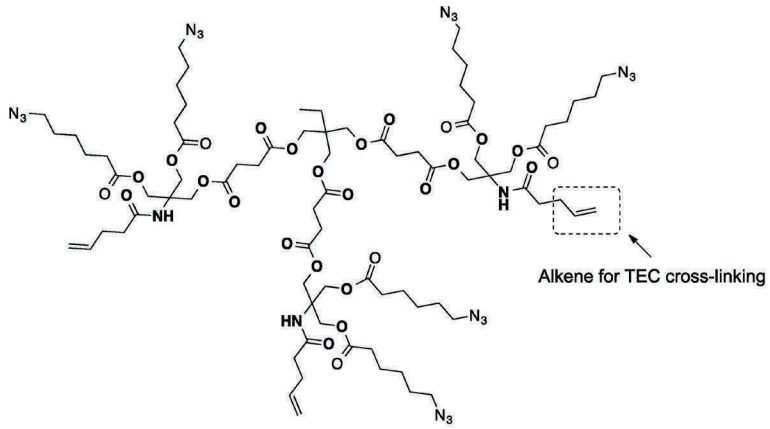



**Figure 3.11** $G_1$-Trizma®-based dendrimer evaluated as an adhesive primer for the repair of bone fractures.

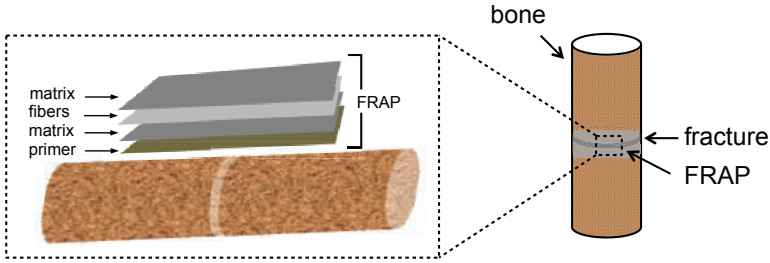



**Figure 3.12** Schematic representation of the FRAP on fractured bones. Adapted with permission from ref. 32. Published by the Royal Society of Chemistry.

15:59 28 October 2016

### 3.3.2 Tissue Engineering

Organ or tissue transplantation remains the common therapy to treat patients who suffer from organ or tissue failure due to accidents or diseases. However, the shortage of donated organs severely limits the number of transplants performed each year. One exciting approach is the use of implantable engineered organs or tissues that are fabricated from the patient's own cells encapsulated within 3D polymeric scaffolds that mimic the role of natural ECM found in tissues. These scaffolds allow cell adhesion, proliferation, and interaction with other components in the matrix, as well as diffusion of nutrients, proteins, and metabolites, while enhancing and controlling the tissue regeneration. Among various polymeric scaffolds investigated for tissue engineering, dendritic hydrogels are specifically appealing because they are biocompatible, and are synthesized with a precise control of their structure, crosslinking density, porosity, and mechanical and degradation properties. In addition, dendritic macromonomers allow the conjugation of various bioactive molecules that can interact with cells in the matrix. These characteristics are important for the development of 3D scaffolds for tissue engineering because they will impact the adhesion, migration and differentiation of encapsulated cells within the network as well as the degradation rate of the synthetic material once the ECM is deposited and the desired tissue is formed.

Grinstaff and co-workers also investigated the use of $([G_1]PGLSA\text{-}MA)_2\text{-}PEG_{3400}$ macromonomers as in situ photo-

15:59 28 October 2016

crosslinkable scaffolds for articular cartilage tissue engineering, and evaluated their efficacy in supporting articular chondrocytes and ECM synthesis in vitro.[38] The in situ photopolymerization technique is highly favorable for tissue engineering applications, because it allows the spatial and temporal control of hydrogel crosslinking while providing better adhesion of the material on defected sites (precursors have time to spread and fill the holes in defected sites prior to gelation). The hydrogels were biocompatible and biodegradable because they were composed of naturally occurring metabolites and linked by ester groups, respectively. Although the gels exhibited lower $G^*$ and $E$ moduli than native cartilage tissue, they were able to encapsulate chondrocytes within their network without any signs of toxicity, and promote the production of type II collagen and proteoglycans-rich ECM similar to native articular cartilage. It was observed that hydrogels at low macromonomer concentration (7.5 wt%) afforded more protein-rich ECM than the ones at higher concentration (15 wt%), and degraded in 5–6 weeks when ECM was deposited, whereas the latter did not decompose even after 12 weeks, delaying cell proliferation and matrix formation. Additionally, the hydrogels possessed low swelling ratios due to the multivalent nature of the dendritic macromonomers, which made them ideal materials for use in confined areas, such as cartilage trauma sites.

Jia et al. have recently reported the synthesis of photo-crosslinked dendritic hydrogels as mimics of ECMs, composed of linear poly(lactic acid)-*b*-poly(ethylene glycol)-*b*-poly(lactic acid) (PLA-PEG-PLA) copolymers with acrylate end-groups, and $G_4$-PAMAM dendrimers functionalized with PEGs containing terminal arginine-glycine-(aspartic acid)-(D-tyrosine)-cysteine (RGDyC) and acryloyl groups (Fig. 3.13).[39] The conjugation of the dendritic macromolecules with bioactive molecules (i.e., RGDyC) afforded enhanced stem-cell adhesion, differentiation, and proliferation. Furthermore, the advantage of this system as compared to PLA-PEG-PLA hydrogels was the introduction of PAMAM dendrimers, which provided hydrogels with higher mechanical properties and lower swelling ratios, due to the increase in crosslinking density of the network resulting from the multivalent crosslinking units available on the surface of the dendrimer. This characteristic is particularly important when applying the material in confined areas of the body, where

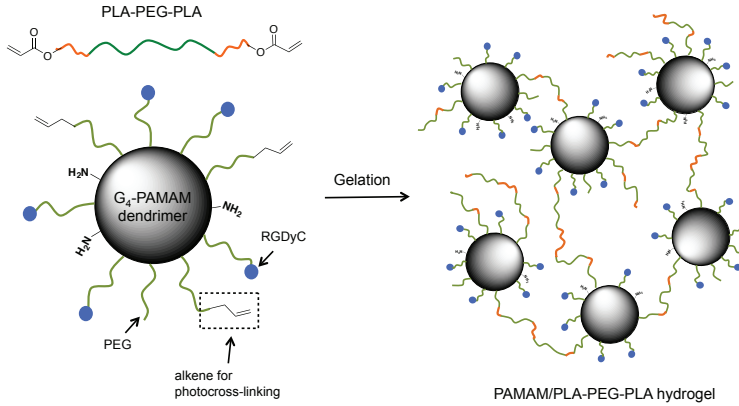



**Figure 3.13** Bioactive PAMAM/PLA-PEG-PLA hydrogel formed via the photo-crosslinking of acrylated PLA-PEG-PLA with alkene-terminated PAMAM dendrimers.[39]

excessive swelling can cause tissue compression, or detachment of the gel from the wound site. However, at higher PAMAM:PLA-PEG-PLA ratios (e.g., 0.5, 1, and 2), intramolecular and/or intermolecular crosslinking between the acryloyl groups on PAMAM dendrimers can also occur leading to softer hydrogels. Extended degradation times of hydrogels were observed with increasing PAMAM:PLA-PEG-PLA ratios in the scaffolds. For example, PLA-PEG-PLA hydrogels degraded in 27 days whereas the degradation time of PAMAM/PLA-PEG-PLA hydrogels at a PAMAM:PLA-PEG-PLA ratio of 1/10, 1/5, 1/2, and 1/1 was measured to be 30, 36, 39, and 45 days, respectively. Next, mouse bone marrow mesenchymal stem cells (mMSCs) were encapsulated in hydrogels at a PAMAM:PLA-PEG-PLA ratio of 1/5 to evaluate whether they can stimulate stem-cells proliferation and differentiation, similarly to ECMs of native tissues. It was observed that hydrogels with RGDyC moieties increased cell attachment and proliferation, whereas hydrogels without RGDyC caused reduction in cell viability. Moreover, it was reported that the activation of $\alpha_5\beta_1$ integrin receptor in mMSCs can be triggered by RGDyC, which further promotes osteogenic differentiation and leads to bone tissue regeneration. Consequently, enhanced gene expression of osteogenic markers of mMSC differentiation such as alkaline phosphatase (ALP), osterix (OSX), parathyroid hormone 1 receptor (PTH1R), and osteocalcin (OC) was observed by real-time

15:59 28 October 2016

polymerase chain reaction (PCR) in cells cultured within the bioactive hydrogels at 4 and 7 days, as compared to hydrogels without RGDyC moieties. The enhanced promotion of mMSCs proliferation and differentiation within PAMAM/PLA-PEG-PLA hydrogels due to the presence of multivalent RGDyC moieties supported the strategy of using dendritic macromolecules for the introduction of these bioactive molecules, and further demonstrated the potential use of these materials in tissue engineering.

15:59 28 October 2016

## 3.4 Conclusions

Dendritic macromonomers are monodisperse and can be constructed with defined compositions, shapes, molecular sizes (generations), molecular weights, structures, viscosities, solubilities, and functional groups. Due to their multivalent crosslinking units within their structures, and the type of linkages that can be formed, hydrogels possessing a range of properties are attainable. The diversity of structures and resulting hydrogels provides a platform for the determination of structure-activity relationships and the preparation of hydrogels based on the design requirements for a specific application. Examples of both covalently and physically crosslinked dendritic-based hydrogels are described, including those that undergo self-repair or self-healing when broken. Consequently, dendritic hydrogels are being evaluated for a variety of biomedical uses. For example, tissue repairing sealants or scaffolds based on these materials are reported for ocular, bone and cartilage applications. However, significant opportunities still remain in this tissue repair space. Given the control to tune the chemical composition and mechanical properties, these types of hydrogels may find utility as scaffolds for stem cell isolation and/or differentiation. Finally, when combined with other components (e.g., particles) to create composite materials, new properties may be garnered such as mechanically tough physical hydrogels, as reported by Aida et al.

Despite the significant progress achieved with dendritic hydrogels in the last decade, the potential of dendritic macromonomers has not yet been fully explored. One limiting factor to their investigation is the time-consuming and expensive synthesis and purification, as compared to linear polymers, which

can be formed in one step and easily isolated by precipitation. However, the synthetic routes to dendrimers are improving and becoming more facile as a consequence of highly efficient and selective reactions, where monomers with complimentary functional groups, for example, can interact specifically with each other avoiding side product formation (accelerated dendritic synthesis), or reactions that proceed with high yields without the generation of by-products. It is therefore evident that with the advances in dendrimer syntheses and crosslinking strategies, new dendritic macromonomers and hydrogel compositions will be studied. Given the number of unmet clinical needs that can be addressed using hydrogels, we are optimistic that hydrogels composed of dendritic macromonomers will continue to play a critical role.

15:59 28 October 2016

## Acknowledgment

This work was supported in part by Boston University, the Coulter Foundation, and NIH R21 EB013721.

## References

1. Caminade A-M, Yan D, Smith DK (2015) Dendrimers and hyperbranched polymers, *Chem Soc Rev*, DOI: 10.1039/C5CS90049B.
2. Grayson SM, Fréchet JMJ (2001) Convergent dendrons and dendrimers: From synthesis to applications, *Chem Rev*, **101**, 3819–3868.
3. Majoral J-P, Caminade A-M (1999) Dendrimers containing heteroatoms (Si, P, B, Ge, or Bi), *Chem Rev*, **99**, 845–880.
4. Mintzer MA, Grinstaff MW (2011) Biomedical applications of dendrimers: A tutorial, *Chem Soc Rev*, **40**, 173–190.
5. Newkome GR, He E, Moorefield CN (1999) Suprasupermolecules with novel properties: metallodendrimers, *Chem Rev*, **99**, 1689–1746.
6. Esfand R, Tomalia DA (2001) Poly(amidoamine) (PAMAM) dendrimers: from biomimicry to drug delivery and biomedical applications, *DDT*, **6**, 427–436.
7. Kopeček J (2009) Hydrogels from soft contact lenses and implants to self-assembled nanomaterials, *J Polym Sci Part A: Polym Chem*, **47**, 5929–5946.
8. Vermonden T, Censi R, Hennink WE (2012) Hydrogels for protein delivery, *Chem Rev*, **112**, 2853–2888.

15:59 28 October 2016


9. Yu L, Ding J (2008) Injectable hydrogels as unique biomedical materials, *Chem Soc Rev*, **37**, 1473–1481.
10. Ghobril C, Grinstaff MW (2015) The chemistry and engineering of polymeric hydrogel adhesives for wound closure: A tutorial, *Chem Soc Rev*, **44**, 1820–1835.
11. Moon HJ, Ko DY, Park MH, Joo MK, Jeong B (2012) Temperature-responsive compounds as in situ gelling biomedical materials, *Chem Soc Rev*, **41**, 4860–4883.
12. Lee KY, Mooney DJ (2001) Hydrogels for tissue engineering, *Chem Rev*, **101**, 1869–1880.
13. Smith DK (2006) Dendritic gels-many arms make light work, *Adv Mater*, **18**, 2773–2778.
14. Grinstaff MW (2008) Dendritic macromers for hydrogel formation: Tailored materials for ophthalmic, orthopedic, and biotech applications, *J Polym Sci Part A: Polym Chem*, **46**, 383–400.
15. Gitsov I (2008) Hybrid linear dendritic macromolecules: From synthesis to applications, *J Polym Sci Part A: Polym Chem*, **46**, 5295–5314.
16. Kojima C, Tsumura S, Harada A, Kono K (2009) A collagen-mimic dendrimer capable of controlled release, *J Am Chem Soc*, **131**, 6052–6053.
17. Oberg K, Hed Y, Joelsson Rahmn I, Kelly J, Lowenhielm P, Malkoch M (2013) Dual-purpose PEG scaffolds for the preparation of soft and biofunctional hydrogels: the convergence between CuAAC and thiol-ene reactions, *Chem Commun*, **49**, 6938–6940.
18. Tamesue S, Ohtani M, Yamada K, Ishida Y, Spruell JM, Lynd NA, Hawker CJ, Aida T (2013) Linear versus dendritic molecular binders for hydrogel network formation with clay nanosheets: Studies with ABA triblock copolyethers carrying guanidinium ion pendants, *J Am Chem Soc*, **135**, 15650–15655.
19. Whitton G, Gillies ER (2015) Functional aqueous assemblies of linear-dendron hybrids, *J Polym Sci Part A: Polym Chem*, **53**, 148–172.
20. Newkome GR, Baker GR, Arai S, Saunders MJ, Russo PS, Thierot KJ, Moorefield CN, Rogers EL, Miller JE (1990) Cascade molecules. Part 6. Synthesis and characterization of two-directional cascade molecules and formation of aqueous gels, *J Am Chem Soc*, **112**, 8458–8465.
21. McWatt M, Boons G-J (2001) Parallel combinatorial synthesis of glycodendrimers and their hydrogelation properties, *Eur J Org Chem*, **2001**, 2535–2545.

22. Marmillon C, Gauffre F, Gulik-Krzywicki T, Loup C, Caminade A-M, Majoral J-P, Vors J-P, Rump E (2001) Organophosphorus dendrimers as new gelators for hydrogels, *Angew Chem Int Ed*, **40**, 2626–2629.
23. Wang Q, Mynar JL, Yoshida M, Lee E, Lee M, Okuro K, Kinbara K, Aida T (2010) High-water-content mouldable hydrogels by mixing clay and a dendritic molecular binder, *Nature*, **463**, 339–343.
24. Duan P, Qin L, Zhu X, Liu M (2011) Hierarchical self-assembly of amphiphilic peptide dendrons: Evolution of diverse chiral nanostructures through hydrogel formation over a wide pH range, *Chem–Eur J*, **17**, 6389–6395.
25. Carnahan MA, Middleton C, Kim J, Kim T, Grinstaff MW (2002) Hybrid dendritic–linear polyester–ethers for in situ photopolymerization, *J Am Chem Soc*, **124**, 5291–5293.
26. Degoricija L, Bansal PN, Söntjens SHM, Joshi NS, Takahashi M, Snyder B, Grinstaff MW (2008) Hydrogels for osteochondral repair based on photocrosslinkable carbamate dendrimers, *Biomacromolecules*, **9**, 2863–2872.
27. Wathier M, Johnson MS, Carnahan MA, Baer C, McCuen BW, Kim T, Grinstaff MW (2006) In situ polymerized hydrogels for repairing scleral incisions used in pars plana vitrectomy procedures, *Chem Med Chem*, **1**, 821–825.
28. Ghobril C, Charoen K, Rodriguez EK, Nazarian A, Grinstaff MW (2013) A dendritic thioester hydrogel based on thiol–thioester exchange as a dissolvable sealant system for wound closure, *Angew Chem Int Ed*, **52**, 14070–14074.
29. Malkoch M, Vestberg R, Gupta N, Mespouille L, Dubois P, Mason AF, Hedrick JL, Liao Q, Frank CW, Kingsbury K, Hawker CJ (2006) Synthesis of well-defined hydrogel networks using click chemistry, *Chem Commun*, **26**, 2774–2776.
30. Antoni P, Hed Y, Nordberg A, Nyström D, von Holst H, Hult A, Malkoch M (2009) Bifunctional dendrimers: From robust synthesis and accelerated one-pot postfunctionalization strategy to potential applications, *Angew Chem Int Ed*, **48**, 2126–2130.
31. Altin H, Kosif I, Sanyal R (2010) Fabrication of "clickable" hydrogels via dendron–polymer conjugates, *Macromolecules*, **43**, 3801–3808.
32. Hed Y, Oberg K, Berg S, Nordberg A, von Holst H, Malkoch M (2013) Multipurpose heterofunctional dendritic scaffolds as crosslinkers towards functional soft hydrogels and implant adhesives in bone fracture applications, *J Mater Chem B*, **1**, 6015–6019.

15:59 28 October 2016

33. Grinstaff MW (2007) Designing hydrogel adhesives for corneal wound repair, *Biomaterials*, **28**, 5205–5214.

34. Oelker AM, Grinstaff MW (2008) Ophthalmic adhesives: A materials chemistry perspective, *J Mater Chem*, **18**, 2521–2536.

35. Luman NR, Kim T, Grinstaff MW (2004) Dendritic polymers composed of glycerol and succinic acid: Synthetic methodologies and medical applications, *Pure Appl Chem*, **76**, 1375–1385.

36. Kang PC, Carnahan MA, Wathier M, Grinstaff MW, Kim T (2005) Novel tissue adhesives to secure laser in situ keratomileusis flaps, *J Cataract Refract Surg*, **31**, 1208–1212.

37. Degoricija L, Johnson CS, Wathier M, Kim T, Grinstaff MW (2007) Photo cross-linkable biodendrimers as ophthalmic adhesives for central lacerations and penetrating keratoplasties, *Invest Ophthalmol Vis Sci*, **48**, 2037–2042.

38. Söntjens SHM, Nettles DL, Carnahan MA, Setton LA, Grinstaff MW (2006) Biodendrimer-based hydrogel scaffolds for cartilage tissue repair, *Biomacromolecules*, **7**, 310–316.

39. Wang Y, Zhao Q, Zhang H, Yang S, Jia X. (2014) A novel poly(amidoamine)-dendrimer-based hydrogel as a mimic for the extracellular matrix, *Adv Mater*, **26**, 4163–4167.

40. Ghobril C, Rodriguez EK, Nazarian A, Grinstaff MW. (2016) Recent advances in dendritic macromonomers for hydrogel formation and their medical applications, *Biomacromolecules*, DOI: 10.1021/acs.biomac.6b00004.

15:59 28 October 2016

## Chapter 4

# Polyglycerols in Nanomedicine

**Mohiuddin Quadir[a,b] and Rainer Haag[c]**

[a]*Koch Institute for Integrative Cancer Research, Massachusetts Institute of Technology, Massachusetts 02139, USA*
[b]*Current Address: Department of Coatings and Polymeric Materials, North Dakota State University, North Dakota 58108, USA*
[c]*Institut für Chemie und Biochemie, Freie Universitaet Berlin, 14195 Berlin, Germany*

haag@chemie.fu-berlin.de

The application area of nanomedicine in human health and diseases is expanding at an unprecedented rate, and its overwhelming success critically hinges on discovery of novel polymers and materials with unique structural and biochemical properties. Synthesized from commercially available monomers and FDA-approved oligoglycerols, polyglycerols (PGs) have claimed a separate domain within the realm of nanomedicine by their distinctive traits of (1) well-defined topological uniformity (2) biocompatibility, and (3) multi-functionality. Over the last decades, a diverse assortment of PG motifs has been synthesized ranging from linear and dendritic (tree-like) unimolecular structures, to highly-branched, yet finitely monodispersed, cross-linked macromolecular aggregates. Owing to their nanoscale features and presence of multivalent functional groups, both linear and dendritic PGs have

*Dendrimers in Nanomedicine*
Edited by Delphine Felder-Flesch
Copyright © 2016 Pan Stanford Publishing Pte. Ltd.
ISBN 978-981-4745-49-9 (Hardcover), 978-981-4745-50-5 (eBook)
www.panstanford.com

enabled the power of multivalency to be harnessed at cellular level. No wonder that PG analogues have been ceaselessly utilized for drug and cell delivery, tissue-regeneration, and in coating applications throughout the past two decades, and the endeavor continues. This chapter presents, in a tutorial fashion, the primary synthetic routes to PGs and structural variants thereof, methods to modify the parent PG scaffolds, and a case-by-case analysis of their major discovery and application areas. We are hoping to provide the reader, in a nutshell, the broader picture of research that has been conducted over dendritic PGs (dPGs) in past years, thereby to elaborate the dazzling capacity of this multi-purpose, multivalent macromolecule in the field of nanomedicine.

15:59 28 October 2016

## 4.1 Introduction

One of the grand challenges in the field of nanomedicine is the ability to generate synthetic macromolecules that is structurally stable, functionally programmable and capable to perform therapeutically desired task at defined physio-pathological space and time. Identifying an intelligent polymer scaffold that can be prepared in a facile synthetic route, with control over composition, conformation, and hence on function, is a critical subset of obstacles that impedes the path towards generating smart nanobiomaterials. With the advent of newer catalyst systems and routes to generate innovative monomers, cutting-edge polymers have constantly been added to the nanomedical repository. However, many of these materials, in spite of their structural novelty and diversity, do not demonstrate desirable gain of function that can confirm their global applications in nanomedicine. Dendritic polyglycerols, and their linear analogues are polyether-based scaffolds derived from sustainable materials as glycerol and glycerol-based compounds such as, glycidol, which are the by product of biofuel production. Owing to their condensed three-dimensional structures, intrinsic molecular confinement capabilities, presence of large number of modifiable, peripheral functional groups and inertness to ubiquitous biological components such as protein and phospholipid membranes, these highly branched polyols have established themselves as a novel molecular platform in nanomedicine research. For ease of discussion, both perfectly branched dendritic polyglycerols as well as their hyperbranched

15:59 28 October 2016

analogues will be considered as dendritic polyglycerols throughout this chapter.

Dendritic polyglycerols (dPGs) come in many sizes and shapes. In spite of their heavily branched structural pattern, dPGs show narrow distributions in their molecular weight (MW) with a well-defined hydrodynamic size range that directly affects their physical and chemical properties. Their surface multi-functionality offers the option of application-guided tailoring that is required for multivalent interactions with biological substrates and tissue-microenvironment.[1] Compared to linear polymers of analogues molecular weight, spatially globular architecture of dPGs gives rise to a number of interesting properties such as reduced viscosities and enhanced water solubility, both of which can be readily modulated by postsynthetic functionalization of peripheral hydroxyl functional group through classical alcohol-group chemistry.[2–4] Another salient feature that makes dPGs unique from its linear analogues is the fact that these macromolecules exhibit a distinct "interior" supramolecular space, sterically shielded from the topological "exterior" of the scaffold.[5] This feature has been one of the fundamental properties that fueled the use of dPGs as transport systems in nanomedicine. It is, therefore, not surprising that, dendritic molecules, and dPGs in particular, caught interest of the scientific community that was desperately looking for a poly (ethylene glycol)-like inert, multi-functional molecule.[6] Not only the three-dimensional diversity that reflects the underlying structural strength of dPG, but also the synergy between dPGs' multivalency and nanoscopic size can be utilized to impart chemical intelligence along their molecular scaffold, making these macromolecules an invaluable addition towards designing advanced therapeutic materials and diagnostic modalities. Since dPGs inception in the late nineties, this class of functional macromolecule has been greatly shaping up the nanomedical landscape. With time, the molecular size and architecture of dPGs have evolved from molecular length scale (1–10 nm) to 100 nm multimolecular assembly constituting nano- and microgels (Fig. 4.1).[7]

A range of desirable therapeutically functional properties such as, high transport capacity, low toxicity, molecular confinement and predefined release, multivalent charge display and protein resistance profile, can be efficiently engineered into dPGs

nanoplatform with relative ease, rendering them critically useful for life science applications. As a result, dPGs have been investigated as therapeutic components in the treatment of cancer and inflammation, for targeting biological cells and tissues, and for generating responsive surfaces. In this chapter, we begin our discussion of how dPGs are synthesized and how the macromolecule is chemically modulated towards application-specific, three-dimensional hierarchy. The next section elaborates the intrinsic structural features that define dPGs' gain of nanomedical function and finally we will summarize the recent developments in terms of structural diversity that has been achieved, and functional versatility that has been included within the dPGs scaffold in relevance to specific biomedical purpose.

15:59 28 October 2016

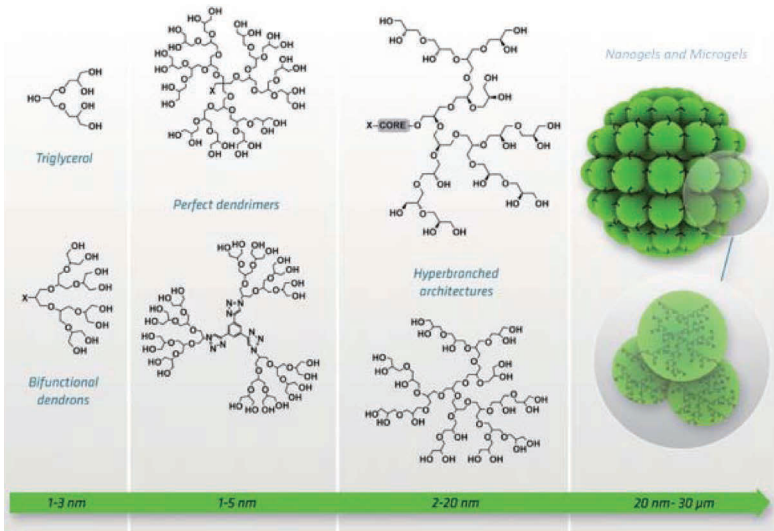



**Figure 4.1** Evolution of dPGs: from dendrons, perfect dendrimers, hyperbranched structures to megamers. Adapted with permission from John Wiley & Sons, Inc., Copyright 2010.

**Outline of the Chapter**

4.2 Chemistry and Structural Diversification of dPGs
4.3 Forms Guiding Functions: Features of dPGs Architecture
4.4 Biological and Chemical Compatibility
4.5 Application Areas in Nanomedicine

## 4.2 Chemistry and Chemical Diversification of dPGs

### 4.2.1 Origin and Evolution of dPGs Structure

Classically, dPGs that are aliphatic, dendritic polyethers with terminal hydroxy groups are prepared from an entirely biocompatible molecule, glycerol, either by convergent[8] or divergent synthetic approaches resulting in perfect dendrimers, pseudo-dendrimers and hyperbranched polymers.[9] It is noteworthy to mention that glycerol is also the sustainable monomer used for the preparation of oligoglycerols and is an increasingly economic byproduct of biodiesel production (via trans-esterification of vegetable oils).[10] Hyperbranched PGs, on the other hand, represents the randomly branched polymer that can be prepared in a controlled synthesis via anionic or cationic ring-opening multibranching polymerization (ROMBP) using glycidol as a latent $AB_2$ monomer (Fig. 4.2). A number of excellent reviews have been published which elaborates the synthetic routes and properties of hyperbranched polyglycerols.[7,11]

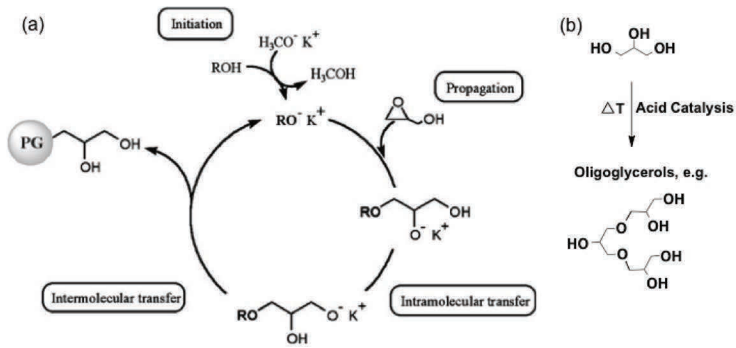



**Figure 4.2** (a) Mechanism of anionic polymerization of glycidol to synthesize well-defined hyperbranched PGs under slow monomer addition condition. (b) Thermal acid catalysis of triglycerol have also been utilized to yield a regioisomeric mixture of oligoglycerol. Adapted with permission from John Wiley & Sons, Inc., Copyright 2010.

Both perfect dendrons and hyperbranched systems are characterized by the combination of a stable, polyether scaffold,

15:59 28 October 2016

15:59 28 October 2016

high-end group functionality and a compact, well-defined dendrimer-like architecture. These molecular properties have been harnessed at multifarious levels to design nano-, micro-, and macroscopic devices and materials that can create extremely high local concentrations of drugs, molecular labels, or probe moieties at biological interfaces and surfaces, modulate therapeutic efficacy of the active molecules and engage cell-surface attached, or freely circulating biomolecules inside a living system. Relatively recently, it was reported that the branching reaction of glycidol that accompanies the polymerization process can be suppressed by protecting the hydroxyl function, a discovery that gave access to highly diversified architectures ranging from linear structures to macromolecules of complex topological features.[12] Hence, the chemistry of glycidol and its protected derivatives can give rise to a practically limitless number of structurally different macromolecules with complex form and function that can be orthogonally and selective amended to gain specific biomedical advantage.

Historically, polymerization of glycidol dates back to the earlier work of Sandler and Berg[13] followed by several efforts to polymerize glycidol to linear products in the presence of various catalyst systems.[14,15] Polymerization of protected glycidols and 3-hydroxyoxetane[15,16] resulted in the generation of linear PG. Cationic polymerization of glycidol under the influence of Lewis acids (i.e., $BF_3OEt_2$, $SnCl_4$) and protonic acids (such as $CF_3COOH$, $CF_3SO_3H$) have been carried out by Dwork and coworkers.[17,18] The molecular weight of the resulting polymers varied from 2500 to 6000 g $mol^{-1}$. Subsequently, Deffieux and coworkers[19] described a new initiation system for the monomer activated anionic polymerization of propylene oxide (PO) using onium salts/triisobutylaluminium to polymerize glycidyl methyl ether, and with Deffieux protocol, linear poly(glycidyl methyl ether) with high molar masses (up to 100,000 g $mol^{-1}$) was achievable in a relatively controlled pattern at low to moderate temperature.

### 4.2.2 Chemistry of Linear PGs: Analogue Frequently Overlooked

Although dPGs are the major focus area of this chapter, but it should be kept under consideration that linear PGs also

15:59 28 October 2016

constitutes an attractive molecular platform due to their sustainable scalability and biocompatibility.[20] As with dPGs, a series of chemical diversification can be included into linear PG scaffolds during polymerization or postpolymerization process, usually resulting in the synthesis of multifunctional materials with substantial hydrophilic property. Synthesis of linear poly (glycidyl ether) by anionic polymerization and copolymerization of allyl glycidyl ether, tert-butyl glycidyl ether, and ethoxyethyl glycidyl ether (EEGE) using potassium 3-phenyl-1-propanol as initiator have been reported by Keul et al.[21] These structures have been investigated for "core-fatty acid shell type" encapsulation platform for model hydrophobic guest molecule such as Congo red; however, it was later found that molecular encapsulation was not an inclusive property of linear PGs.[22] Haag et al. carried out a systematic synthesis of linear methylated and hydroxylated oligo (glycidyl ethers) which was found to reduce adsorption of single proteins on surfaces which are modified with these oligomers.[23] Poly(glycidol)-poly(propylene oxide)-poly(glycidol) block copolymers, which are structurally analogous to well-studied block copolymer, Pluronic®, composed of poly (ethylene oxide)-poly (propylene oxide)-poly (ethylene oxide), has been synthesized by Rangelov and coworkers. These PG-based triblock copolymers were found to self-assemble in to stable micelles above certain critical micellar concentration (CMC), which in turn was found to depend on temperature and PG-content.[24] This is important to note that CMC of amphiphilic polymers is the indication of stability of self-assembled systems in aqueous in vivo conditions. Klock et al. recently reported the synthesis of amine-initiated polyglycerols of different architectures through anionic ring opening polymerization of EEGE. An assortment of linear polyglycerols with end- or mid-chain amino functional groups, originated from the methoxybenzyl protected aminoethanol or serinol as initiators were synthesized along this strategy.[25] Figure 4.3a summarizes the anionic ring-opening approaches towards amino-functional linear polyglycerols for surface modification and bioconjugation as developed by Haag et al. and Klok et al., respectively. Möller et al. reported the synthesis and characterization of poly(glycidol-coglycidyl amine), poly(glycidol)-block-poly(glycidyl amine), and poly-(glycidol) end-capped with a glycidyl amine unit.[26] The synthetic route to realize this class of

15:59 28 October 2016

polyglycerols involved copolymerization of ethoxyethyl glycidyl ether with epichlorohydrin using tetraoctylammonium bromide/ triisobutylaluminiumas catalyst resulting in statistical or block copolymers, thus providing access to prepare multifunctional macromolecules since amine and alcohol groups of the polyglycerol derivatives can be addressed selectively by electrophiles (Fig. 4.3b).

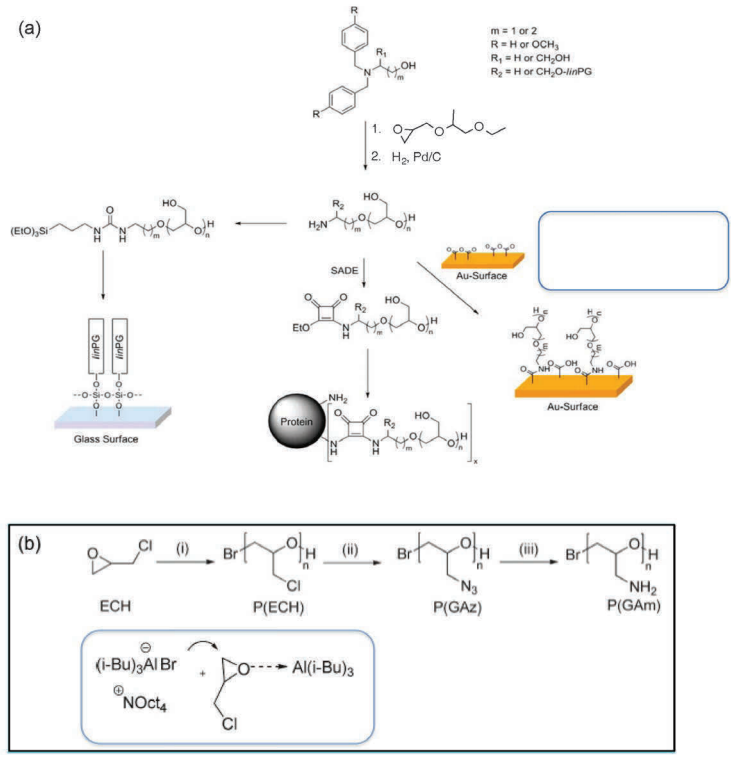



**Figure 4.3** (a) Summary of anionic ring-opening approaches targeting amino-functional linear polyglycerols for surface modification and bioconjugation developed by Haag et al. and Klok et al., respectively (SADE = squaric acid diethyl ester). (b) Reaction Sequence for the Synthesis of Poly(glycidyl amine), P(Gam) starting from Epichlorohydrin (ECH) through poly(epichlorohydrin), P(ECH) and poly(glycidyl azide), P(GAz). Key: (i) $NOct_4Br$, $iBu_3Al$, 0°C, room temperature, toluene; (ii) $NaN_3$, DMF, 110°C (iii) 1. $PPh_3$, DMF, room temperature. 2. $H_2O$, DMF, room temperature. In inset activation of the monomer and the initiator with $Al(i\text{-}Bu)_3$ has been shown.

15:59 28 October 2016

A set of biologically important proteins, i.e., bovine serum albumin (BSA), and lysozyme were PGylated, i.e., connected chemically to linear PGs following the similar approach of PEGylation. Generally, PEGylation is a well established and value-adding synthetic modification usually performed to improve the pharmacokinetic properties, i.e., circulatory time, metabolic stability and urinary clearance of therapeutic proteins. An interesting set of linear PGs generated by bioactive initiator such as catechol or cholesterol has been reported recently.[27] Catechols, which are abundantly present in nature, mostly as molecular constituent of neurotransmitters and biological polyphenols, show brilliant biosimilar activity in adhesion control. Marine mussels use the noncatechol analogue, L-DOPA as the major constituent of their structural protein that is responsible for their universal adhesion properties. Frey's group has designed a catechol-bearing functional polyether structure (both linear and hyperbranched) via anionic ring opening polymerization.[28,29] Postsynthetically, it was possible to immobilize the catechol bearing polyethers onto manganese oxide (MnO) nanoparticles, resulting in their improved and efficient dispersion. The coated MnO nanoparticles was investigated as nontoxic contrast agents for magnetic resonance imaging. In a different communication, the same group has also studied anionic ring-opening approach initiated by cholesterol. These linear polyglycerols have been prepared from EEGE followed by acidic cleavage of the acetal-protecting groups,[30] Due to the presence of cholesterol, a liquid crystalline order was observed within the resulting polymeric structure in a broad temperature range up to 260°C for a series of molecular weights,[31] The oxyanionic polymerized product of various epoxides initiated by the same monomer, resulted in polymer architectures with "stealth" like capability to evade immune surveillance as frequently observed with PEGylated lipids.[32] For generating exclusive polymer architecture driven by supramolecular recognition among the constituent components, Frey and coworkers have recently reported the synthesis of adamantly methanol-initiated polyglycerol which can be used to form complex supramolecular graft copolymer structures where cyclodextrin-functional poly (methacrylate) backbone is supramolecularly linked polyglycerol side chains,[33] and

using "hyper-grafting" strategies, the same group was also able to generate more complex linear-hyperbranched architectures.[34]

When compared and contrasted with heavily studied, biocompatible polymers like PEG, water-soluble linear PGs exhibited a similar or even slightly superior biocompatibility profile of the former, which is currently the candidate of choice for generating biologically active polymer-based therapeutics and devices. Linear polyglycerols did not trigger any significant effect on immune systems, coagulation pathways or on cellular health reflecting the long-standing fidelity of oligoglycerol esters (with a degree of polymerization up to 10) as Food and Drug Administration (FDA)-approved consumable excipient. A head-to-head comparative studies of antifouling properties between linear PGs and PEGs employed for surface modification were undertaken by Haag and co-workers where linear PGs showed similar antifouling properties as that of PEG.[23b,36,37]

15:59 28 October 2016

### 4.2.3 Macromonomers of Linear PG: Building Complex Topology

Either through "end-capping method" (where an activated chain end is allowed to react with a polymerizable end group) or the "initiator method" (cases in which a polymerizable units is built-in within the preformed polymer), linear PGs have been utilized as macromonomers to generate complex PG-based materials, hence combining the best of both scaffolds, i.e., branched and linear. Dworak's forwarding work[38] on end-capping of living P(EEGE) chains with p-chloromethylstyrene to obtain $\omega$-vinylbenzyl-functional macromonomers has been investigated later by Basinska and Slomkowski et al., and the resulting structures have been utilized for surface modifications, controlling protein adsorption and potential biomedical applications and have been discussed at full length in a comprehensive set of publications[39–41] Frey group reported a straightforward approach in which alkoxide initiators were used to polymerize EEGE to obtain well-defined precursor oligomers.[42] Direct end-capping of the living chain ends was carried out by sequential addition of excess triethylamine and methacrylic anhydride to the reaction mixture. Subsequent homopolymerization of the narrowly distributed macromonomers ($M_w/M_n$ < 1.30) by ATRP and subsequent deprotection resulted

in water-soluble and well-defined graft copolymers ($M_w/M_n$ < 1.31) containing a methacrylate backbone and densely grafted oligoglycerol side chains.

A partial esterification of the hydroxyl groups of linear PGs can be modified with aliphatic acyl chlorides, e.g., palmitoyl chloride. The resulting architecture has been compared with their hyperbranched analogues for their nanoencapsulation capability, although it was observed that, linear PGs did not show significant encapsulation efficiency.[43,44] Linear PG structures can also be modified using acetic acid[38a,45] and acetic anhydride[46] yielding poly(glycerol-co-glycerol acetate)s with an LCST behavior (LCST = 4 to 100°C) which is governed by degree of functionalization. Linear polyglycerol have been decorated by bioactive and hydrophilic functional groups to render the scaffold applicable towards biomedical applications. Both phosphonic and carboxylic acid groups along the polyglycerol backbone were introduced by Penczek et al. by via Michael addition of the hydroxyl groups of linear PG with diethyl vinylphosphonate, followed by hydrolysis.[47–49]

15:59 28 October 2016

### 4.2.4 Dendritic PGs: Branched Scaffold with Nanoscale Benefits

Different research groups around the globe have adopted a variety of approaches to design dPG architectures with assortment of sizes, branching density, surface topology and chemical properties. A systematic library of PG architectures with varying properties was synthesized using a careful selection of starting materials through an economic synthetic route that provided an option to perform postmodification on the PG scaffold. The synthetic progress of PG-based architectures as presented in Fig. 4.1 and will be discussed throughout this section. In a pioneering work in this field, Haag et al. reported the synthesis of amino PG dendrons that have been synthesized by a completely divergent approach using 2-aminopropane-1,3 diol or D,L-serine.[50] Allylation of alcohol functionalities under phase-transfer conditions followed by catalytic dihydroxylation and subsequent catalytic hydrogenation yielded the desired generations of monoamino glycerol dendrons (Fig. 4.4), which was one of the first of its class dPGs with perfect dendritic architecture.

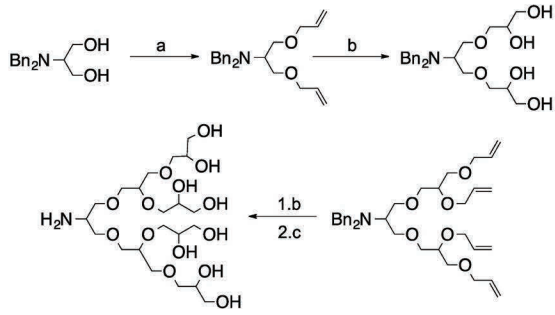



**Figure 4.4** Exemplary synthesis of generation 2.0 monoamino PG dendrons. Reagents and conditions: (a) allyl bromide, 50% NaOH, TBAI, 40°C, 18 h; (b) 1 mol % $K_2OsO_4$, NMO, acetone/water/tert-butyl alcohol, 40°C, 18 h; (c) 10% Pd/C, MeOH, 5 bar $H_2$, 24 h. Adapted with permission from John Wiley & Sons, Inc., Copyright 2010.

15:59 28 October 2016

In an alternate approach, commercially available triglycerol can also be utilized as starting material for synthesizing dendrons of multiple generations using iterative chemical synthesis. Following this approach, Haag et al. synthesized polyols that were consecutively attached to the 4,4-biphenyldicarboxylic acid cores by carbodiimide mediated coupling to generate triblock amphiphiles. Zimmerman et al. have synthesized azide-cored PG dendrons in an attempt to generate porphyrin cored dendrimers by clicking the dendrons with octa-alkynylporphyrin.[51] The synthetic simplicity of copper (I)-catalyzed 1,3-dipolar cycloaddition, known as "click" chemistry has been widely investigated to generate PGs with dendritic architectures. Different generations of glycerol dendrons have been synthesized using 3-chloro-2-chloromethyl-1-propene (methallyl chloride or MDC) and acetal-protected triglycerol as starting material. Using the Williamson ether synthesis and an ozonolysis/reduction sequence as activation and growth promotion steps, PG dendrons up to the fourth generation have been synthesized.[52] Perfect glycerol dendrimers and pseudo-dendritic PGs first appeared in the literature back in 2004. Haag group described the initial synthetic approach through a divergent pathway that was chosen to synthesize dendrimers with glycerol units as building blocks starting from trimethylolpropane (TMP)[53] (Fig. 4.5). An improved synthetic approach to glycerol dendrimers of multiple generations and

15:59 28 October 2016

their covalent modification to contain perfluorinated shell has also been reported subsequently which showed interesting physicochemical properties in the field of fluorous phase chemistry. It also yielded useful properties for surface coating for polymers, such as PMMA.[54]

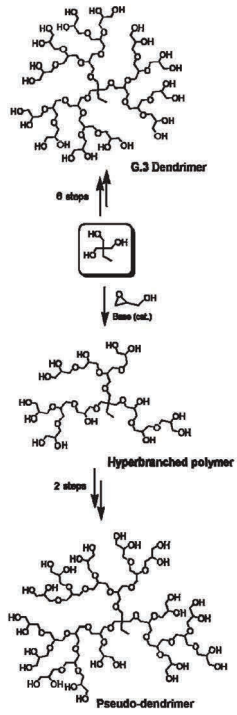



**Figure 4.5** Synthesis of glycerol dendrimer and the pseudo dendritic analogue: (a) allyl bromide, NaOH, TBAB, water; (b) NMO, OsO4 (cat), water, acetone, t-BuOH. Reprinted with permission from Ref. 53. Copyright (2000) American Chemical Society.

### 4.2.5 Well-Defined Hyperbranched PG: dPGs with Random Regularity

As mentioned previously, hyperbranched PG is typically synthesized from the commercially available and highly reactive hydroxy epoxide, glycidol which serves as a latent $AB_2$ monomer by utilizing the ROMBP process.[9b] An advantageous feature of this pathway lies in the fact that the route avoided the problem of high

15:59 28 October 2016

polydispersity associated with the synthesis of hyperbranched polymers by polycondensation of $AB_m$ monomers[55] or self-condensing vinyl polymerization (SCVP).[56,57] Controlled anionic ring-opening polymerization of glycidol is generally carried out utilizing partially deprotonated TMP as the initiator. Slow addition of the monomer to establish a rapid cation-exchange equilibrium and to minimize polymerization without initiator resulting in cyclization, favors the formation of hyperbranched polyols with a well-defined polyether structure. Due to controlled polymerization conditions, the monomer exclusively reacts with the growing multifunctional hyperbranched polymer, leading to a "living" type growth of the macromolecule (Fig. 4.6).

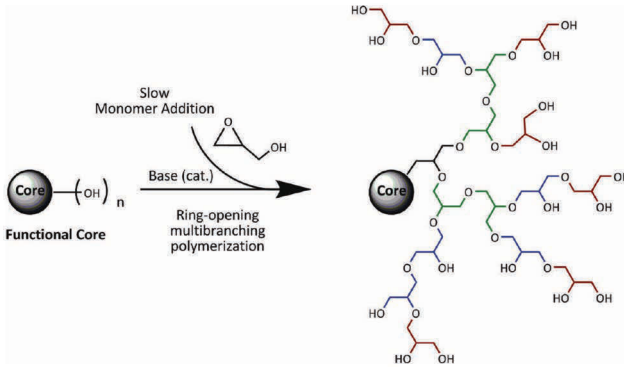



**Figure 4.6** Synthesis of hyperbranched polyglycerols by anionic ring-opening multibranching polymerization.

Fast proton exchange equilibrium maintains all hydroxyl groups present as potentially active propagation sites, thus leading to random branching.[5] Computer simulation carried out by Frey and coworkers confirmed that polyfunctional initiators such as TMP and slow monomer addition provide a rigid control over the molecular weight and suppress the polydispersity of the resulting polymer.[58] The degree of branching for these polymers varies between 0.53 and 0.59, with a controllable degree of polymerization ranging from 15 to approx. 100 and a polydispersity index typically within 1.2–1.7, which is exceptionally low for hyperbranched architectures. Detailed structural investigation revealed that such hyperbranched PG contains linear 1,3- and 1,4-units, terminal and dendritic units, and carries the initiator

15:59 28 October 2016

(TMP) incorporated as core functionality in every PG molecule. The scale up of this polymerization technology with technical details under economic aspects has also been documented.[59]

A very high molecular weight (up to 700 kDa) and narrowly dispersed (PDI 1.1–1.4) hyperbranched PG generated via ROMBP of glycidol, using dioxane as an emulsifying agent has been reported for the first time by Brooks and coworkers.[60] A mechanism that involves faster cation exchange in the presence of dioxane has been proposed by these authors to generate hyperbranched PG with low polydispersities. These high molecular weight PGs showed low intrinsic viscosities, with very small hydrodynamic radii with dimensions similar to those of high generation dendrimers (5–10 nm). The use of a macroinitiator was found to be an attractive way to control the molecular weight limitations associated with the synthesis of hyperbranched PG up to molecular weight of 24,000 g $mol^{-1}$. Frey and coworkers have harnessed the capability of using low-molecular-weight PG and slow monomer (glycidol) addition technique to generate very high molecular weight of PG up to 24 kDa for the first time with polydispersity ranging from 1.3–1.8 and degree of branching from 0.60 to 0.63, which parallels with the theoretical limit of 0.66 for slow monomer addition condition.[61]

### 4.2.6 Core Variation of dPG Increases Functionality and Applicability

Application-guided modification of dPG-scaffold can be easily carried out either by a variation in the core, or by modification of the peripheral functional groups to fine tune the resulting functional architecture (Fig. 4.7). In an attempt to overcome the extremely high polarity of hyperbranched PG, which creates compatibility and solubility issues, the hydroxyl groups of the molecule can be hydrophobized by “capping” the end groups with a few units of propylene oxide to suppress hydrophilicity.[9c] The degree of propoxylation that can be carried out in the same polymerization vessel subsequent to the glycidol polymerization does not affect the inherently narrow polydispersity of the structures, but decreases instead the glass-transition temperature ($T_g$) significantly.

15:59 28 October 2016

Extension of the concept led to the development of multiarm triblock, all-ether-based copolymers formed by block-copolymerization with ethylene oxide (EO) with unaffected polydispersity and high functionality of the PG.[62] Haag group reported an efficient approach towards hyperbranched monoamino dendrons (X = $NH_2$) by an efficient polymerization/deprotection process to generate more complex core/multishell (CMS) architectures (see below).[63] A systematic investigation of utilizing different functional cores such as mono- and bifunctional n-alkyl amines, photoreactive benzylamine and 1-naphthylmethylamine, primary amines and bisglycidolized amines within hyperbranched PGs has been carried out by Frey et al.[64] Brooks et al. reported an efficient synthesis of hydrophobically modified as well as PEG-grafted hyperbranched PGs using 1,2-epoxyoctadecane and $\alpha$-epoxy, $\gamma$-methoxy PEG 350 (MPEG-epoxide) as the monomer, respectively (Fig. 4.8).[65] Anionic ROMBP of glycidol was employed to generate hyperbranched PG of molecular weight of 7 kDa, followed by a partial dervatization of PG hydroxyl group with C18 alkyl chain and mPEGs carried out by sequential addition of the corresponding epoxides.

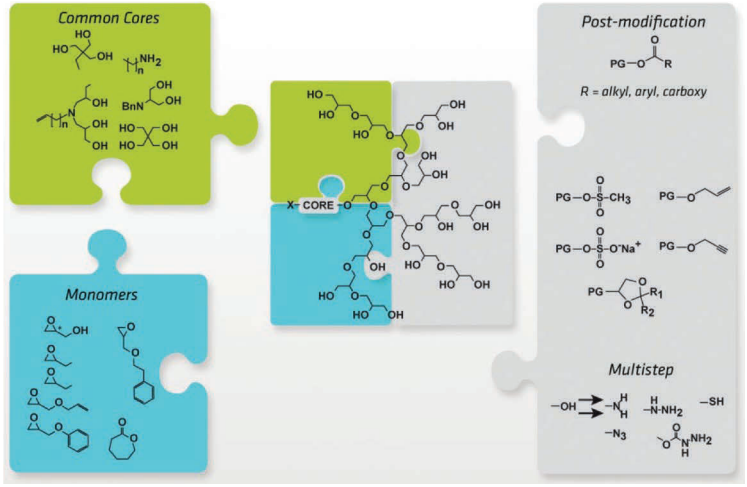



**Figure 4.7** Synthetic diversification of PG scaffolds: a modular toolbox that can be used for application-guided synthesis of dPG-based functional architectures. Adapted with permission from John Wiley & Sons, Inc., Copyright 2010.

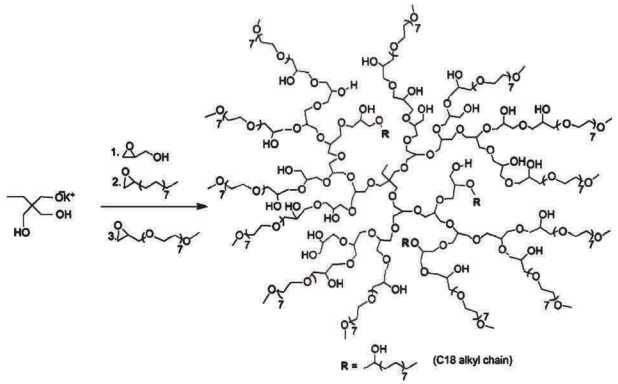



**Figure 4.8** Synthetic scheme for the hydrophobically derivatized dPGs. Reprinted from Biomaterials, 29, Kainthan, R. K., Janzen, J, Kizhakkedathu, J. N., Devine, D. V., Brooks, D. E., Hydrophobically derivatized hyperbranched polyglycerol as a human serum albumin substitute, 1693–1704, Copyright (2008), with permission from Elsevier.

15:59 28 October 2016

### 4.2.7 Block Copolymers of Dendritic Polyglycerol

Block copolymers of glycerol have also been extensively investigated to generate diversified PG-based structures. Double hydrophilic linear hyperbranched block copolymers based on PEO and PG have been reported by Frey and coworkers.[66] These polymers, which essentially contain an aliphatic polyether structure, were prepared from linear PEO-b-(linear PG) precursor block copolymers, obtained by anionic polymerization of EO and subsequently of ethoxyethyl glycidyl ether. Partial deprotonation of the linear PG block with cesium hydroxide permitted hypergrafting of glycidol onto the alkoxide initiating sites using the slow monomer addition technique (Fig. 4.9). The resulting linear-hyperbranched PEO-b-PG block copolymers exhibited low polydispersities ranging from 1.09 to 1.25, based on the molecular weight of the hyperbranched block. Depending on the linear PEO segment and hyperbranched segment, it was possible to attain the MW as high as 15.7 kDa.

Frey and coworkers also reported the synthesis and characterization of poly (glyceryl glycerol) block copolymers prepared from PEO and poly (glyceryl glycerol) that can be viewed as a perfect first-generation dendronized polymer based on PG.[66]

15:59 28 October 2016

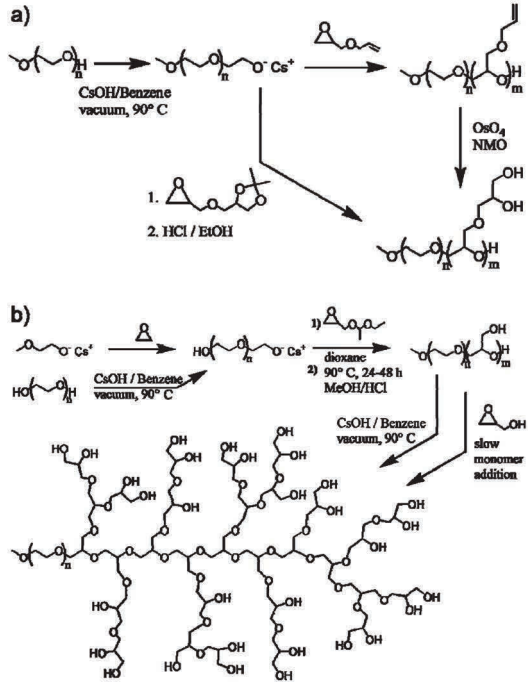



**Figure 4.9** (a) Synthesis of poly (glyceryl glycerol). (b) Synthesis of linear-hyperbranched PEO–PG block copolymers as well as dendronized PG. Reprinted with permission from Ref 66. Copyright (2008) American Chemical Society.

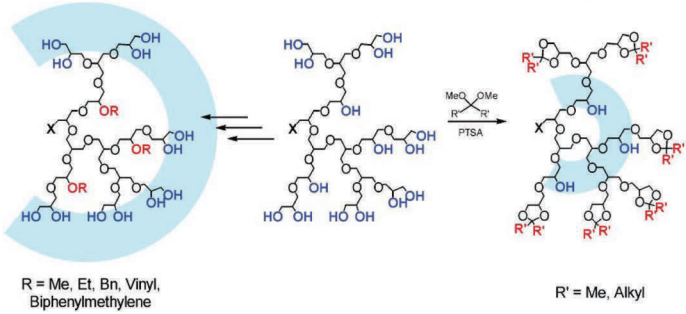



**Figure 4.10** Selective functionalization of hyperbranched PG scaffolds: (a) Hydrophilic outer shell. (b) dPGs and (c) Hydrophobic outer shell. Adapted with permission from John Wiley & Sons, Inc., Copyright 2010.

15:59 28 October 2016

This synthesis can be realized either by anionic polymerization of D,L-1,2-isopropylidene glyceryl glycidyl ether and conversion into well-defined block copolymers, or in another approach, by consecutive polymerization of EO and allyl glycidyl ether, followed by a subsequent dihydroxylation step using osmium tetroxide (Fig. 4.10). Copolymerization of $\varepsilon$-caprolactone with hyperbranched PG as an initiator, in the presence of a tin catalyst, has been carried out to yield multiarm star polymers with biodegradable poly($\varepsilon$-caprolactone) arms.[67] In another approach, hyperbranched PG has also been used as a macroinitiator for atom transfer radical polymerization (ATRP) by conjugating an initiator moiety to the hydroxyl end groups.[68] Frey group introduced double-hydrophilic linear-hyperbranched block copolymers with PEG and polyglycerol segments, where PEG-linear Poly (EEGE) block copolymer was deprotected under acidic conditions, providing PEG-b-linear PG copolymers with 13–40 hydroxyl groups. Slow addition of glycidol to partially protonate linear PG block, the so-termed "hypergrafting process," yielded linear-hyperbranched PEG-b-hyperbranched PG copolymers,[34] and in a similar fashion ABA-type block copolymer of (hyperbranched PG)-b-PEG-b-(hyperbranched PG) has been prepared. Linear-hyperbranched PEG-polyglycerols have been investigated for noncovalent protein conjugation using avidin-biotin system for supramolecular bioconjugation and solubilization of carbon nanotube.[69,70] The double hydrophilic linear-hyperbranched systems (i.e., PEG-b-hyperbranched PG) have been used for preparing pH-responsive nanoscale drug conjugates of doxorubicin intended for use in cancer setting.[71]

### 4.2.8 Postpolymerization Modification: Tailoring the Properties of Polyglycerol

Postpolymerization modification of the linear monohydroxyl, and terminal dihydroxyl functional groups of dendritic polyglycerol scaffold can be carried out following classical hydroxyl group chemistry. Such modification generates a wide-spectrum of polymer architectures with high drug loading capacity, solvent-specific solubility and biocompatibility. A subset of the large amount of research that has been devoted towards designing different architectures by selective modification of PG hydroxyl group into different functionalities is illustrated in Fig. 4.7.[72]

15:59 28 October 2016

Although dPGs, of hyperbranched motif, show no distinguishable interior or periphery as dendrimers, they possess two distinct types of hydroxyl functionalities, linear hydroxyl groups in proximity to the core as well as terminal hydroxyl groups in the periphery of the macromolecule originating from linear and terminal glycerol units present in the monomer (Fig. 4.10). Haag et al. proposed an elegant selective protection/deprotection strategy where these two types of hydroxyl group can be chemically differentiated yielding a core/shell type architecture.[73] The procedure allowed tailoring of the PG scaffold to contain hydrophobic substituents in the interior and/or targeting agents in the periphery, thereby modulating the distribution coefficients and diversification of the generated structure between organic and aqueous phase.

### 4.2.9 Giant Polyglycerols: Motifs Resulting in Megamers, Microgels, and Hydrogels

A larger dPG analogue with an optimum diameter ranging from 20–100 nm, the so-called PG nanogel have been proposed by Haag group.[74] The fundamental concept of preparation of these nanogels, which evolved with time fundamentally depends on the cross-linking of preformed dPGs (2–3 nm diameter, MW 5 kDa) to higher homologues using the miniemulsion polymerization technique, whereby the surfactant-stabilized dispersed droplets act as "nanoreactors." The cross-linking reactions have initially been achieved by "click" type alkyne/azide Huisgen cycloaddtion, either mediated by copper or simply by thermal cycloaddition reaction at 80°C. Both direct and inverse miniemulsion processes have been adopted which generated both hydrophilic and hydrophobic nanoparticles. As evident from TEM and GPC, for hydrophobic nanosystems, particles showed average diameter between 25 and 85 nm while for hydrophilic ones, nanoparticle size could be varied from 45–90 nm depending on the amount of surfactant used.[74] Since this initial work, high molecular weight analogues of hyperbranched PGs have been prepared using the nanoreactor and a wide variety of orthogonal reactions have been used to achieve cross-linking, as we will encounter in later sections. A new idea where functional PG nanogels were synthesized by an acid catalyzed polyaddition of glycerol to trisglycidyl glycerol ether utilizing the inverse miniemulsion technique has been developed by Haag laboratory. In this approach, polar reactants

were dispersed in nonpolar cyclohexane and a poly (ethylene-co-butylene)-block-poly (ethylene oxide) surfactant was used as a stabilizer and a small amount of DMSO was added to prevent Ostwald ripening. In a different approach, multifunctional alcohols were used as monomers and di- and triepoxides as cross-linking agents. The amount of monomers and cross-linkers, and their chemistry were found to govern the physicochemical properties of the nanogels, such as, size, degree of branching, viscosity and swelling behavior. The procedure for the preparation of nanogel that has been reported in the original work of Haag et al. is presented in Fig. 4.11.

Bulk PG hydrogels have been synthesized, on the other hand, harnessing the capability of low viscosity of dPGs in aqueous environment. By cross-linking methacrylated hyperbranched PG derivatives using potassium peroxodisulfide as an initiator and tetramethylethylenediamine as catalyst, the preparation of the bulk hydrogel has been realized. Hyperbranched PG methacrylate has also been photopolymerized using Irgacure 2959 (2-hydroxy-1-[4-(2-hydroxyethoxy)phenyl]-2-methyl-1-propanone) to generate gel structure with high shear storage modulus and limited swelling. Microparticulate hydrogel structures have also been prepared from methacrylated hyperbranched PG structures by micromolding and photolithography techniques. This strategy, as proposed by Hennink et al., generated hyperbranched PG microgels within the size range of 200 to 1400 nm.[76]

15:59 28 October 2016

**Key Ideas of Section 4.2**

- Perfectly dendritic PGs are aliphatic, polyethers with terminal hydroxy groups, and are prepared from biocompatible molecule, glycerol, by either convergent or divergent approach.
- Hyperbranched PGs (hPGs) represents the randomly branched polyether polymers prepared in a controlled synthesis via anionic or cationic ring-opening multibranching polymerization (ROMBP) using glycidol as a latent $AB_2$ monomer.
- Both perfect dendrons and hyperbranched systems are characterized by the combination of a stable, polyether scaffold, high-end group functionality and a compact, well-defined dendrimer-like architecture, and are termed as dendritic PGs (dPGs) in the following sections.
- Both linear PGs and dPGs can be modified in an application-guided manner by core variation, copolymerization, peripheral functional groups modification, and cross-linking chemistry to generate nano-, micro-, and macroscale hierarchical structures.

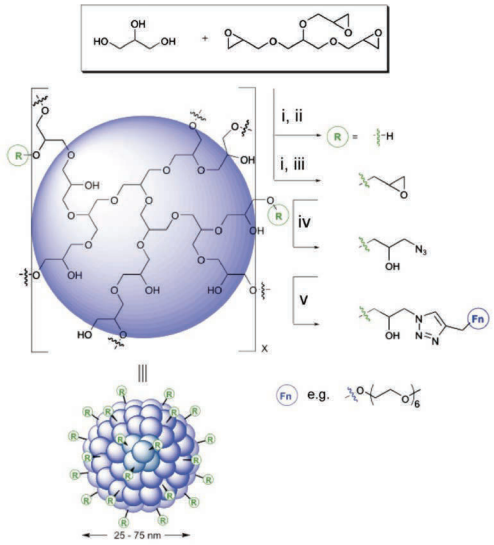



**Figure 4.11** Synthetic pathways toward pure dPG microgel particles and their surface functionalized analogues: (i) cyclohexane/MSO/block copolymer surfactant, sonic tip mini-emulsification 4 × 1 min; (ii) p-TSA (cat.), 115°C, 16 h; (iii) p-TSA (cat.), 115°C, varied time; (iv) $NaN_3$, DMF, 60°C, 24 h; (v) propargyl derivative, $CuSO_4$. $5H_2O$, sodium ascorbate, $H_2O$, 24 h. Adapted with permission from John Wiley & Sons, Inc., Copyright 2009.

## 4.3 Forms Guiding Functions: Features of dPGs Architecture

A set of properties that arises as the direct consequence of the three dimensional structure of dPGs play a critical role in their applications in nanomedicine. These properties include (1) molecular weight (2) polydispersity and (3) degree of branching, and govern not only the interaction of dendritic systems in a living system, but also their clinical efficiency and their prospective usage in medical ecosystem. Among these properties, molecular weight and polydispersities are closely and intricately related. Multifunctional polycondensation reaction, which is the major pathway towards the synthesis of dendritic polymers, is fundamentally related to high polydispersity of the resulting macromolecule. To this end, the slow addition of highly reactive

15:59 28 October 2016

15:59 28 October 2016

branching monomer to a polyfunctional core, as described earlier is an attractive approach that renders the polymer to grow following chain-growth kinetics. Extensive theoretical and experimental studies by Frey group and others revealed that, the advantage of slow addition of suitable $AB_m$ type monomers to multifunctional core not only includes a robust control over molecular weight but also over reducing polydispersity significantly.[58] Degree of branching (DB) of a dendritic polymer is essentially related with the spatial distribution of the terminal functional group that are in close contact with the surrounding environment of the macromolecules.[77] In case of polyglycerol, based on branching multiplicity of $AB_2$ type monomer glycidol, three different building units can be identified by NMR spectroscopy and the DB can be calculated under inverse gated condition, namely branched (dendritic, D) units, linear (L) unites and terminal (T) units (Fig. 4.12).

Although perfectly branched polyglycerols do not have any linear units, and for such maximally branched structures, the degree of branching is generally considered to be 1 (i.e., 100%) compared to linear polymers which has DB = 0. Hyperbranched polyglycerols shows an intermediate DB between 0–1, which reflects its dendritic structural features.[78] With postsynthetic modification, the polyglycerol DB can be increased up to values close or equal to 1. For hyperbranched polyglycerol, using glycidol as the reactive monomer and under slow monomer addition condition, the DB was found to increase with $DP_n$ until it reaches a plateau value, with a DB between 0.53 and 0.59 (slightly below the value of 0.66 for ideal slow addition mode).[79] In an attempt to reduce polydispersity without compromising the molecular weight, Brooks et al. reported the unexpected formation of very narrowly dispersed, high molecular weight PG when using dioxane as an emulsifying agent of low polarity. Molecular weights of several 100 kDa were reported with immense application prospect in a variety of biomedical setting.[80] Degree of branching has a series of consequences on nanomedical application of dPGs. First of all, the higher the degree of branching, the more is the number of the modifiable functional group amenable towards attachment of targeting groups, peptides or aptamers with relatively less steric constraints. Second, increasing the number of peripheral

functional groups also control the rules-of-engagement through which the dendritic molecules interact with the biological surrounding and with the circulatory components.

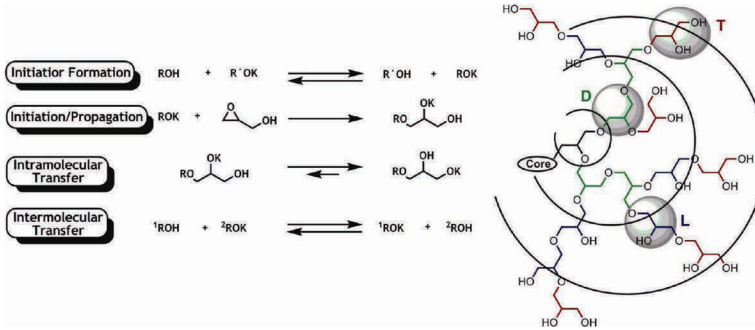



**Figure 4.12** Dendritic, linear and terminal units within dPG structure (small fragment of the actual polymer structure).

## 4.4 Biocompatibility of Dendritic Polyglycerols

To ensure the biological compatibility of dPGs as a nanomedical material, a cohort of closely related bioefficacy studies has been conducted, and the results were compared and contrasted with benchmark biomaterial, PEG. At cellular level, dPG with hyperbranched motif and molecular weight of 5 kDa did not show any cytotoxicity.[5] In an extensive study conducted by Brook et al. using dPGs of broad MW distribution and composition,[81–83] it was found that both linear and hyperbranched PGs have similar or even improved biocompatibility profile than PEG with MW ranging from 4.2 to 670 kDa. Little or no effects on blood compatibility, viscosity, complement activation, platelet activation and in plasma protein precipitation was observed with dPG analogues. Both linear and dPGs of hyperbranched motif were reported to have a similar or even better biocompatibility profile than PEG with MW ranging from 4.2 to 670 kDa. Samples of dPGs were found to have no effect on normal aggregation when polymer concentrations from 0.01 to 10 mg $mL^{-1}$ were used. However, PEG ($M_n$ 40,000) at concentrations of 1 and 10 mg $mL^{-1}$ was found to enhance aggregation of the red cells which can be attributed to their large hydrodynamic radii. In vivo studies conducted on mice revealed no sign of toxicity after i.v. Injection of a dose up to 1 g $kg^{-1}$.

15:59 28 October 2016

For a period of 28 days no sign of weight fluctuation or undesired side effects were observed. The structural differences of the dPGs obtained by the cationic approach did not seem to have an effect on the in vitro compatibility of the polymer as well. The results indicated a comparable toxicity of these structures with PEG against human peripheral blood mononuclear cells and tumor derived human B cell line. Low toxicity, multiple, peripheral functionality, and a relatively high thermal and oxidative stability compared to PEG make dendritic PG a promising material for medical applications at nano- to micro-scale.

15:59 28 October 2016

**Key Ideas of Sections 4.3 and 4.4**

- Molecular weight, polydispersity, and degree of branching are the three primary structural feature of dPG that govern their interaction with nanomedical ecosystem.
- Degree of branching (DB) of a dendritic polymer is essentially related with the spatial distribution of the terminal functional group that are in close contact with the surrounding micro-environment of the macromolecule.
- Biocompatibility-wise, dPGs have similar or even improved biocompatibility profile than PEG considering the parameters of blood compatibility, viscosity, complement activation, platelet activation and in plasma protein precipitation.
- Low toxicity, multiple, peripheral functionality, and a relatively high thermal and oxidative stability compared to PEG make dPGs a promising material for medical applications at nano- to micro-scale.

## 4.5 Nanomedical Applications of dPGs

Structurally compact, biologically inert, dPGs indeed find a broad-spectrum of powerful application in nanomedicine. The prospect of using these macromolecular scaffold in therapeutics stems from their spatial 3D-arrangement, presence of multiple and amenable functional groups, and significant biocompatibility. The application areas where dPGs have shown progress and promise includes, but not limited to, designing of core–shell type, stimuli-sensitive smart drug and gene delivery systems, enabling hydrophilization of relatively water-insoluble drug molecules, bioactive scaffolds for surfaces, and in regenerative therapy.[9b,84,85] For example, dPGs are considered as new delivery enhancers for many bio-

15:59 28 October 2016

actives that could substantially increase the internalization of active components specifically into targeted cells. Such targeted cellular uptake guarantees the enhancement of drug activity and efficacy.[86] Postsynthetically modified dPGs bearing biocompatible modalities can be designed with sufficiently low zeta potentials through surface modification, thereby resulting in lower interactions with serum albumin, enhanced cellular uptake, and high cellular viability on humanized cell lines.[87] Dendritic polyglycerol scaffolds with average MW between 10 and 20 kDa, and surface functionalities suitable for further drug encapsulation or conjugation were found to be comparable with linear PEG polymer or dextran, indicating the suitability of dPG derivatives in delivering therapeutic agents systemically.[85] Hence dPG is an ideal nanomedical platform due to its: (a) unique architectural and chemical tunability, (b) optimizable surface charge for cellular uptake, (c) controllable interactions with plasma proteins, (d) variability in the size and architecture toward favorable of cellular internalization and passive accumulation in damage tissues. A broad-spectrum of approaches and initiatives have been undertaken to engineer and diversify PG-architecture to fit into specific application areas. As a result of these efforts, dPGs with a wide range of size and molecular weight, surface topology and chemical properties have been synthesized. Along with the synthesis of dendritic PG, fabrication routes to perfect dendrimers, dendrons, microgels, and nanogels have also been devised and evolved over the last decades. Noteworthy to mention that, this very large library of dPG architectures were exclusively synthesized using a careful selection of starting materials through a sustainable synthetic route, and with an option to perform facile postmodification on the resulting scaffold.[53,86a] The following sections deals with the major application areas where dPGs have been modified in an application-guided pattern, hence to provide an idea about its suitability in nanomedicine:

### 4.5.1 Supramolecular Platforms of dPGs for Noncovalent Guest Encapsulation

Physical encapsulation of drugs and/or other bioactive molecules within polymeric networks by noncovalent interaction between complementary functional modalities of the involved species is

the most fundamental and facile approach to design nanoscale drug delivery systems (Fig. 4.13).

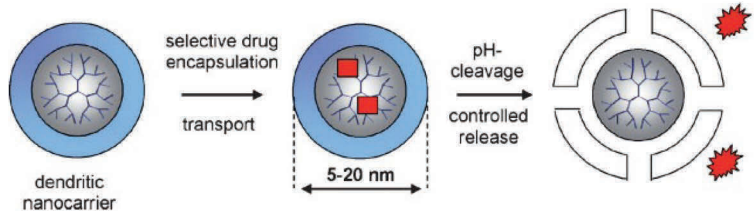



**Figure 4.13** Unimolecular dendritic nanocarriers for encapsulation of biologically active compounds followed by controlled release after triggered shell cleavage. Reprinted from Ref. 86, Copyright (2009), with permission from Elsevier.

15:59 28 October 2016

Dendritic polymers as that of dPGs attracted attention of Park and coworkers[88–90] to investigate the effect of generation numbers of perfect dendritic architectures on aqueous solubilization and release of paclitaxel, a poorly water-soluble drug widely used for cancer chemotherapy. Improvement of solubility profile of a poorly water-soluble drug is a critical formulation-wide challenge. A number of potent drugs fail in their clinical translation owing to their high octanol-water partition co-efficient, and hence need a solubility-enhancer, which are most often polymeric materials that aid the drug molecule to supramolecularly stabilize in an aqueous environment. Comparison between perfect PG dendrimers (generation 3–5) with star-shaped PEGs, as carried out in Park et al.'s experiment, showed a higher ability of the dendritic structures to enhance the solubility of paclitaxel. The results clearly demonstrated the generation and concentration dependent enhancement of paclitaxel solubility as exhibited by dPG scaffold. NMR studies revealed the presence of hydrophobic segments of paclitaxel within the dendritic structure thereby exerting the so-called "hydrotropic effect". The results, however, suggested that the probable mechanism of solubilization is likely to happen through aggregate formation. Haag group, in parallel to spearheading the synthesis and diversification of dPGs architecture, also pioneered the approach of designing dPG-based core/shell scaffold by attaching a variety of aromatic cores connected to different generations of PG dendrons and investigating the scaffold's ability to encapsulate hydrophobic guest molecules

15:59 28 October 2016

(Fig. 4.14).[50,52] The synthetic protocol towards such structures included the linking of the dendrons through amide chemistry or Cu-mediated azide-alkyne type click coupling. These dendritic architectures were evaluated as solubilizing agents for the hydrophobic dye Nile red.

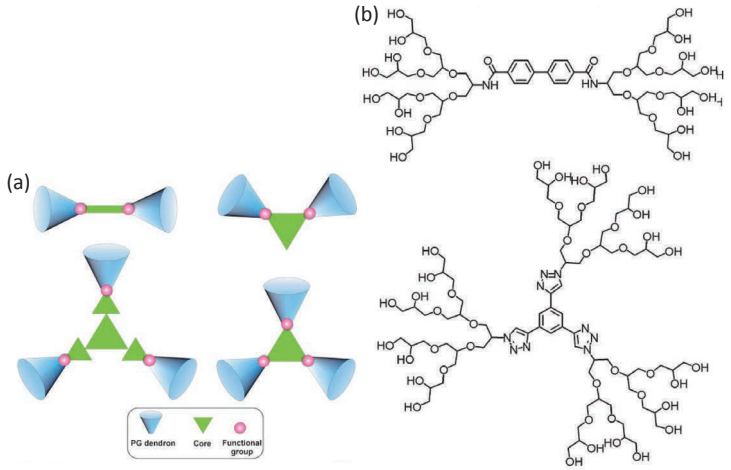



**Figure 4.14** Structural variety of core/shell architectures based on PG dendrons. Adapted with permission from John Wiley & Sons, Inc., Copyright 2010.

As mentioned earlier, Pegylation of nanoparticles and polymer-conjugates is a powerful approach to mimic the structure of "stealth" liposome which results in improved water-solubility, minimized immunogenicity, and increased blood circulation half-life of the resulting nanocarriers.[91] Pegyation of dPGs, along the same mechanistic route, resulted in efficient encapsulation. However, for dPGs, release rate of the encapsulated guest needs to be adjusted to overcome the strong host–guest interaction, as illustrated by the work of Paleos and coworkers.[92] The group has prepared pegylated dPGs with folic acids as targeting ligands, and showed that PEG chains attached to the surface of hyperbranched PG enhanced the encapsulation of fluorescent probes, pyrene, and the anticancer drug tamoxifen. Dynamic light scattering (DLS) revealed unimolecular encapsulation of the guest molecules within the PG–PEG structure. A salt-triggered release was observed upon addition of sodium chloride. Haag group has introduced a PG-

15:59 28 October 2016

based core/shell structure where a tri-PEGylated benzaldehydes of varying lengths were attached to dPG amines through pH-labile imine bonds as shown in Fig 4.15a.[86a]

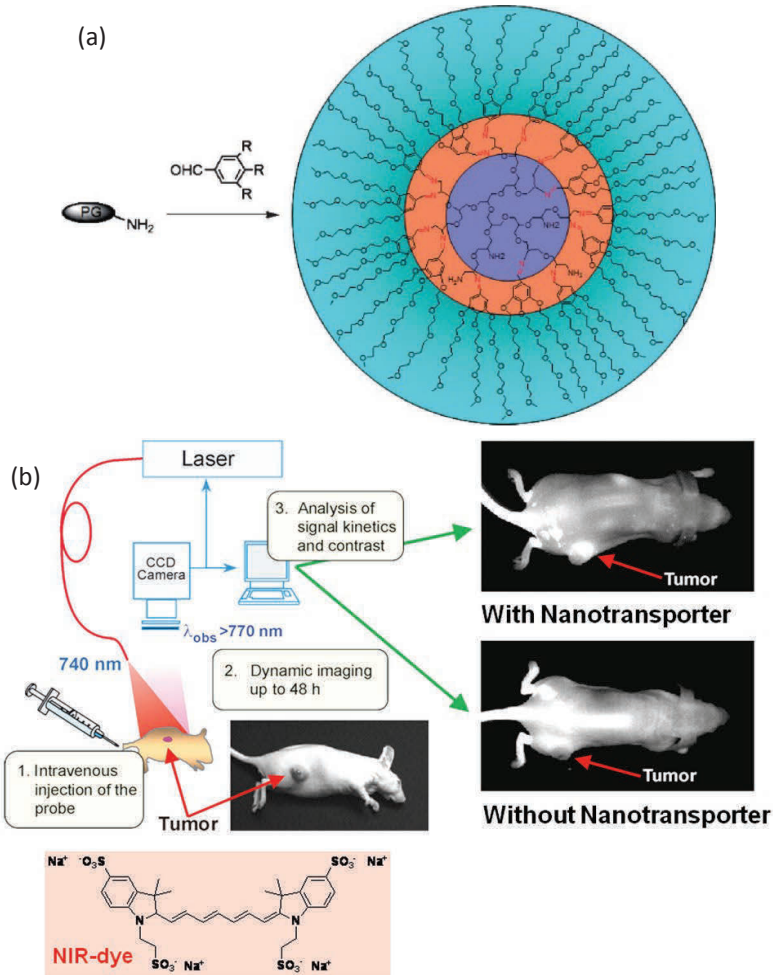



**Figure 4.15** Structure of an idealized fragment of the pH labile core/shell architecture with R = $O(CH_2CH_2O)_nCH_3$ with $n$ = 4, 7, 16, and 24. (b) Laser diode/camera assembly to image the dynamic accumulation of ITCC-loaded nanoparticles in the tumor tissues of F9 teratocarcinoma bearing mice. Reprinted from Ref. 86, Copyright (2009), with permission from Elsevier.

15:59 28 October 2016

The designed structures as shown in Fig. 4.15 were able to encapsulate the anticancer agent doxorubicin and indotricarbocyanine, a near-infrared (NIR) imaging dye. The nanocarriers with the shortest PEG chain ($n$ = 4) and a denser shell was found to demonstrate the best encapsulation efficiency (up to 5 molecules/pegylated PG) showing the critical interplay between PEG-length and surface density. In a nude mice model, the doxorubicin nanocarrier could be dosed up to 24 mg $kg^{-1}$ free doxorubicin equivalents as an intravenous administration that was a significant increase in the maximum tolerated dose (MTD) compared to free doxorubicin MTD. The ability of the nanocarriers to localize in tumors in vivo was demonstrated by fluorescence imaging of tumor-bearing mice with the indotricarbocyanine–nanocarrier complex (Fig. 4.15, lower panel). The near-infrared fluorescence imaging allowed an easy visualization of the tumor-accumulation of the dye–PG complexes since near-infrared and far-red light (650–900 nm) can avoid strong absorption by RBC and water (the so-termed "auto-fluorescence") to allow light to pass through the body of the mice in the depth of several centimeters. In an attempt to design a universal nanocarrier, Haag laboratory has engineered a novel class of CMS architecture that was inspired by the molecular mimicry of a liposome, and based on a dPG core surrounded by double-layered shell motif.[93,94] The synthesis of such dendritic multishell architectures was performed by coupling an alkyl chain to monomethylated PEGs which were in turn coupled to hyperbranched PG amine as shown in Fig. 4.16.

Above a critical concentration, these "Haag-type" nanocarriers with a size range of 8–9 nm coexisted with their larger aggregates with diameters of 20–50 nm. The supramolecular aggregates were found to encapsulate and transport a wide variety of compounds ranging from nonpolar to ionic species in a broad matrix spectrum including nonpolar and polar organic as well as aqueous environments. In contrast to already existing micelle-analogue systems, this new architecture mimics the structure of a liposome on a unimolecular basis and has found extensive applications in dermatological research-space. Dendritic terminal groups of dPGs can also be used to ionically anchor drug molecules. Cisplatin [cis-diamminedichloroplatinum (II)], a potent anticancer compound, has been shown to form strongly bound complexes with succinic acid ester of hyperbranched PG with a stable

15:59 28 October 2016

complex for over 5 days at 37°C,[95] resulting in a sustained release of cisplatin into physiological saline over 7 days.

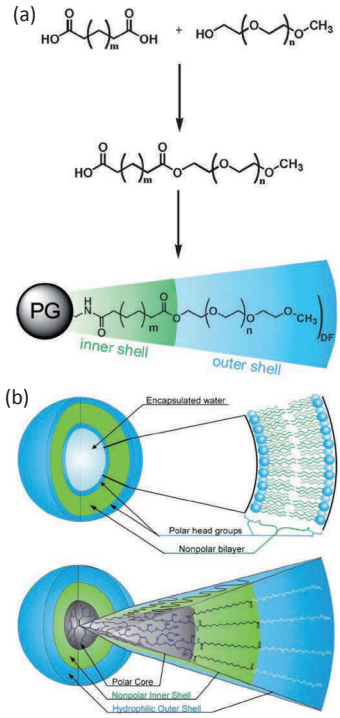



**Figure 4.16** (a) Synthesis of CMS architecture. (b) Schematic representation of a typical liposome structure (top) and the dendritic multishell architecture (bottom).

In an attempt to include a stimuli-responsive modality that can sense local changes of environmental stimulus to trigger drug release from a supramolecular scaffold, Kono et al. incorporated a pH- and temperature-responsive modalities dendritic PG structure. The resulting properties were prospective for different fields in biomedical applications.[96] The group reported the preparation of dPGs connected with NIPAM moieties that imparted thermal-sensitivity and pH-responsiveness to the PG scaffold. In a different approach, Huang and coworkers prepared nanoparticles by postmodification of hyperbranched PG with *N*,*N*-dimethylaminoethyl acrylate (DMA) followed by polymerization and intra-molecular cross-linking.[97] The hydroxyl groups of PG were converted to

15:59 28 October 2016

trithiocarbonates, and the later were used to mediate the surface graft polymerization of DMA. The poly (DMA) shell was cross-linked by 1,6-dibromohexane and then parted from the core by the cleavage of trithiocarbonates with sodium borohydride to yield particles with thiol groups located on the interface between PG core and poly (DMA) shell. The synthetic pathway towards unimolecular micelles as developed by Brooks and coworkers[83] and as shown in earlier section (cf. Fig. 4.8) resulted in structures that carried alkyl chains at the core and PEG moieties grafted on the shell. The unimolecular micellar nature of the molecules with different alkyl chains/PEG composition was probed by multi-angle laser light scattering (MALLS). Due to low intrinsic viscosity, these scaffolds were found to be a specially promising candidate for human serum albumin (HSA) substitutes.[65] The encapsulation efficiency of "Brooks-type construct" was evaluated using paclitaxel and pyrene as model compounds. Since these structures presented mucoadhesive properties, their complex with paclitaxel was evaluated as an intravesical agent against non-muscle-invasive bladder cancer.[98] Though the encapsulated paclitaxel was slightly less potent than the free drug in vitro, the in vivo studies showed that the mucoadhesive formulation of paclitaxel was significantly more effective in reducing orthotopic bladder tumor growth than the standard Cremophor-EL formulation of paclitaxel. Relative tumor growth with paclitaxel complex was reduced to 15% of the control compared to 66% for the free paclitaxel group. The complex was well tolerated in mice and the resulting stabilized level of hematuria and body weight with zero mortality indicated no sign of systemic toxicity.

Several groups have investigated polyglycerol scaffolds and nanoparticles for topical drug delivery applications where the drug is loaded onto dPG scaffold through noncovalent binding. The impact of structural modifications on the nanoparticles' properties, drug delivery potential, and biocompatibility have been assessed in great details. Hedtrich et al. explored the structure-activity relationships of polyglycerol-based nanoparticles on dermal drug delivery efficiency and biocompatibility. The dPG-PEG particles were synthesized via random and controlled alkylated chemo-enzymatic approaches resulting in significantly varying particle sizes and interaction-profile with guest molecules. Considerably improved dermal drug delivery was observed with

15:59 28 October 2016

the smallest particle size dPG nanoparticles (11 and 14 nm) that was well correlated with the surface properties. Biocompatibility for all PG-PEG particles was mainly attributed to the neutral surface charge while no irritation potential, major cytotoxicity or genotoxicity was observed.[99] To gain insight into the factors that affect stability and transport efficiency under dilution conditions, dendronized and hyperbranched multifunctional amphiphilic polymers are synthesized following the "grafting to" approach. Varied amounts of propargylated alkyl chain with perfect and hyperbranched polyglycerol dendrons were attached on the base copolymer of PEG with $M_n$ = 1000 g mol$^{-1}$ diethylester and 2-azidopropane-1, 3-diol following the "bio-catalytic method" and "click approach". The dendronized and hyperbranched polymeric systems were found to form supramolecular aggregates and exhibited an efficient transport potential for the model dye "Nile red" in low μm range. The core–shell-type architecture provided with distinct amphiphilicity as required for encapsulation. Cytotoxicity studies showed that the polymeric systems do not trigger adverse reactions over a wide concentration range. The cellular internalization of Nile-red-encapsulated supramolecular micelles was also studied using cellular fluorescence microscopy and fluorescence-activated cell sorting (FACS) measurements that showed the potential of these polymeric systems as prospective nanocarriers.[100] Grozdova et al. have investigated the use of dPGs as chemosensitizers. As of the present state-of-the-art, most of the polymeric chemosensitizers have a linear poly (ethylene glycol) (PEG) hydrophilic block. In an exploratory approach, a series of novel block copolymers containing a hyperbranched polyglycerol segment as a hydrophilic block (known as PPO-NG copolymers) was prepared and their effect on multi-drug-resistant (MDR) tumor cells in culture have been assessed. PPO-NG copolymers inhibited MDR of three cell lines, indicating that the linear PEG can be substituted for a hyperbranched polyglycerol block without loss of the polymers' chemosensitizing activity. The extent of MDR reversal increased with the polymers affinity toward the cells and the expression level of P-glycoprotein. In contrast with Pluronic® L61, which increases viability of tumor cells in the absence of drugs, PPO-NG chemosensitizers were completely devoid of this property undesired in cancer therapy, making them promising candidates for application as novel MDR reversal agents.[101]

15:59 28 October 2016

Kim et al. have constructed light-responsive polymeric micelles from dPGs. To this end, spiropyran (SP), a well-known photochromic molecule, was used to initiate the ring-opening multibranching polymerization of glycidol to afford a series of hyperbranched polyglycerols (Fig. 4.17). The micelle assembly and disassembly were induced by an external light source owing to the reversible photo-isomerization of hydrophobic SP to hydrophilic merocyanine (MC). The structures and optical responsiveness was evaluated spectroscopically, and critical micellar concentrations for these systems were found to be within the range of 13 to 20 mg/L that critically depends on the length of polarity of the dPG backbone. In parallel to the cytotoxicity pattern observed with other reports, these authors did not found any harmful effect of these nanosystems when subjected to WI-38 and HeLa cells.[102]

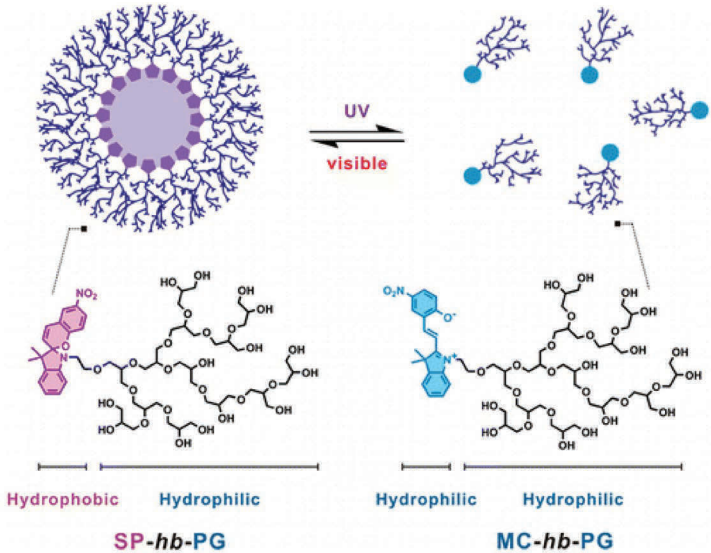



**Figure 4.17** light-responsive polymeric micelles composed of dPG conjugated to spiropyran. Reprinted with permission from Ref. 102. Copyright (2014) American Chemical Society.

Supramolecular recognition is a powerful tool to generate higher order structures with programmable functionalities. A detailed biocompatibility testing of a novel class of hybrid nanostructures based on hyperbranched polyglycerol and $\beta$-

15:59 28 October 2016

cyclodextrin has been carried out. This highly water soluble nanostructure with size of less than 10 nm, polydispersity of less than 1.3 were used as a carrier in drug delivery systems. To this end, extensive studies in vitro, such as cytotoxicity tests based on MTT and Neutral Red assay and blood biocompatibility tests such as effects on coagulation cascade, and complement activation have been studied. The results show that these hybrid nanostructures, which can be prepared in a simple reaction, are considerably biocompatible. In vivo studies showed that the hybrid nanostructure is well tolerated by rats even in high doses of 10 mg $ml^{-1}$. After necropsy, the normal structure of liver tissue was observed; which reveals high biocompatibility and their potential applications of these supramolecular structures in drug delivery and nanomedicine.[103]

To generate fully supramolecular dendrosomes (FSD) for bi-phase drug delivery systems, amphiphilic linear-dendritic supramolecular systems have been synthesized via host-guest interactions between hyperbranched polyglycerol having $\beta$-cyclodextrin core and bi-chain polycaprolactone with a fluorescine focal point. The work carried out by Bani et al. showed that, through supramolecular self-assembly it was possible to generate dPG-based FSD in aqueous environment, which were able to encapsulate paclitaxel with a high loading capacity. The dendrosome-based drug delivery systems were highly sensitive to pH and temperature and were stable at 20–37°C and pH 7–8, but dissociated and released drug at temperatures lower than 20°C or higher than 37°C and pH lower than 7.[104] Very recently, Haag et al. reported an interesting amphiphilic structure (Fig. 4.18) generated through microwave-assisted synthesis of polyglycerol dendron functionalized cyclodextrin (CD) with hydrophobic tails. These amphiphilic CDs consisted of seven polyglycerol dendrons and fourteen alkyl chains on the primary and secondary rims of the cyclodextrin core, respectively. These amphiphilic structures were found to self-assemble in aqueous solutions and efficiently encapsulate hydrophobic aromatic guests. The size and shape of the self-assemblies and also their ability to encapsulate guest molecules were found to depend on the generation of conjugated polyglycerol dendrons.[105]

15:59 28 October 2016

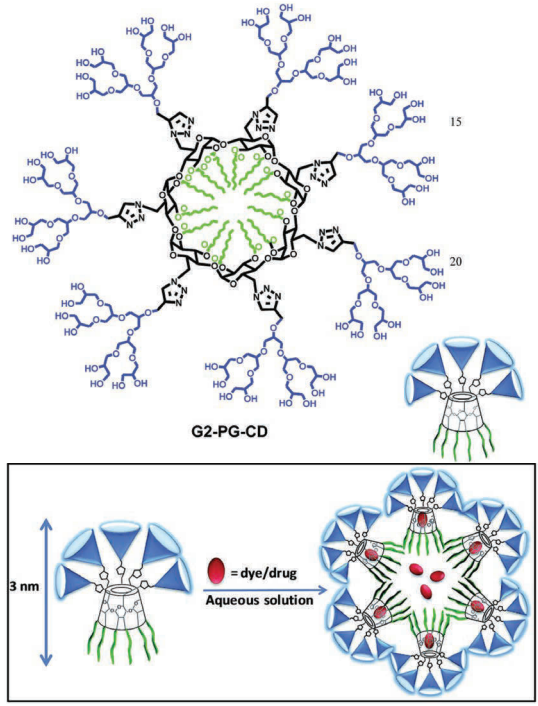



**Figure 4.18** Generation 2 polyglycerol dendron immobilized on cyclodextrin (G2PG-CD dendrimer). In inset, the mechanism of hydrophobic guest encapsulation by G2PG-CD is illustrated.

Shibasaki et al. described a one-pot synthesis of a dPG-based, poly (ethoxyethyl glycidyl ether) (PEEGE)-b-[hyperbranched polyglycerol] and studied its capacity to form micelles and to encapsulate model therapeutic molecules. These amphiphilic block copolymers were prepared by the sequential addition of ethoxyethyl glycidyl ether (EEGE) to glycidol, and the micelles were formulated by injection of deionized water into a tetrahydrofuran solution of the block copolymer. Using pyrene as the hydrophobic guest molecule, the critical micelle concentration was found to be 18.2–30.9 mg/L, and the micelle size was within the range of 100–250 nm. The pyrene-containing micelle was found to collapse rapidly on exposure to acidic pH, allowing conversion of hydrophobic PEEGE to hydrophilic PG, thus, facilitating the release of the encapsulated pyrene. These amphiphilic block copolymers

15:59 28 October 2016

also showed insignificant cytotoxicity and substantially high biocompatibility, suggesting their potential as a drug delivery carrier.[106]

Biodegradable multi-functional polymeric scaffold that undergo controlled degradation in response to physiological cues are important in numerous biomedical applications including drug delivery, bio-conjugation and tissue engineering. A dPG-based, new class of water soluble multi-functional, branched biodegradable polymer with high molecular weight and biocompatibility has been prepared by Kizhakkedathu et al., which demonstrates good correlation of in vivo biodegradation and in vitro hydrolysis. Main chain degradable hyperbranched polyglycerols within the size range of 20–100 kDa were synthesized by the introduction of acid labile groups within the polymer structure by an anionic ring opening copolymerization of glycidol with ketal-containing epoxide monomers having different ketal structures (Fig. 4.19).

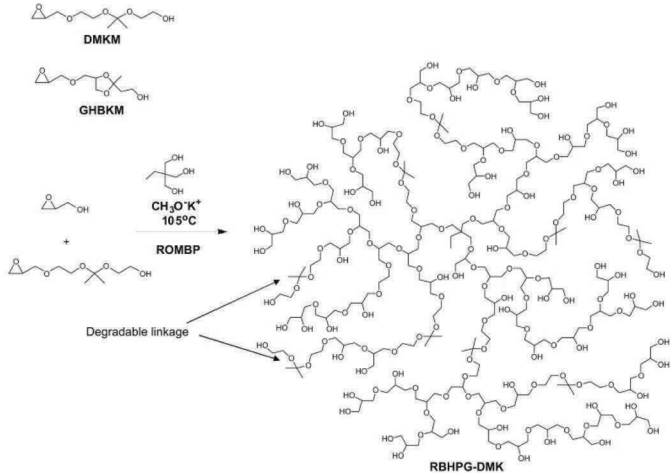



**Figure 4.19** Chemical structure of the acid cleavable ketal monomers and synthesis of biodegradable hyperbranched polyglycerols with randomly distributed ketal groups (RBHPGs) by the ROMBP of glycidol and ketal monomer. Reprinted from *Biomaterials*, **34**(25), Shenoi, R. A., Lai, B. F.L., Imran ul-haq, M., Brooks, D. E., Kizhakkedathu, J. N., Biodegradable polyglycerols with randomly distributed ketal groups as multi-functional drug delivery systems, 6068–6081, Copyright (2013), with permission from Elsevier.

15:59 28 October 2016

The water-soluble biodegradable dPGs with randomly distributed ketal groups showed controlled degradation profiles in vitro, depending on solution pH, temperature and the structure of incorporated ketal groups, and resulted in nontoxic degradation products. The dPG-based scaffolds and their degradation products exhibited excellent blood compatibility and tissue compatibility. When administered intravenously in mice, tritium labeled dPG derivatives of molecular weight 100 kDa with dimethyl ketal group showed a circulation half life of 2.7 ± 0.3 h, correlating well with the in vitro polymer degradation half life (4.3 h) and changes in the molecular weight profile during the degradation (as measured by gel permeation chromatography) in buffer conditions at 37°C. The degraded products of low-molecular-weight fragments cleared from circulation rapidly. The biodistribution and excretion studies demonstrated that these responsive dPG scaffolds exhibited significantly lower tissue accumulation and enhanced urinary and fecal excretion when compared to nondegradable dPGs of similar molecular weight.[107]

In recent nanotechnology-enabled medicine is heavily exploring the possibility of using nanoparticles (NPs) for delivering drug and genetic materials to target cells. Mixed copolymer NPs have been prepared from self-assembly driven association of $\beta$-cyclodextrin-grafted hyperbranched polyglycerol (HPG-g-CD) and lactobionic acid (LA)-grafted hyperbranched polyglycerol (HPG-g-LA) and were investigated as carriers for a hydrophobic antitumor drug, paclitaxel for designing hepatocellular carcinoma-targeted delivery. The resulting NPs exhibited high drug loading capacity and desirable stability in aqueous solution. In vitro drug release studies demonstrated a controlled rate of release with an increment in acidic pH. Remarkably, tumor proliferation assays showed that drug-loaded mixed copolymer NPs inhibited asialoglycoprotein (ASGP) receptor positive HepG2 cell proliferation in a concentration-dependent manner in comparison with ASGP receptor negative BGC-823 cells. Moreover, the competition assay demonstrated that the small molecular LA inhibited the cellular uptake of the PTX-loaded mixed copolymer NPs, indicating the ASGP receptor-mediated endocytosis in HepG2 cells. In addition, the intracellular uptake tests by confocal laser scanning microscopy showed that the mixed copolymer NPs were more efficiently taken up by HepG2 cells compared with HPG-g-CD NPs, suggesting

15:59 28 October 2016

the potential use of the dPG-based mixed copolymer NPs as nanocarriers for hepatoma-targeted delivery of potent antitumor drugs.[108] The availability of long circulating, multifunctional polymers is critical to the development of drug delivery systems and bioconjugates. The ease of synthesis and functionalization make linear polymers attractive but their rapid clearance from circulation compared to their branched or cyclic counterparts, and their high solution viscosities restrict their applications in certain settings. Hence, harnessing the unusual compact nature of high molecular weight linear polyglycerols (LPGs) of different MW in aqueous solutions were compared with dPG and matched molecular weight of PEG, as a function of their impact on solution properties, blood compatibility, cell compatibility, in vivo circulation, biodistribution and renal clearance. The hydrodynamic size and the intrinsic viscosity of LPG in water were considerably lower compared to PEG. The Mark–Houwink parameter of LPG was almost 10-fold lower than that of PEG. LPG and dPG of hyperbranched origin demonstrated excellent blood and cell compatibilities. Unlike LPG and dPG, high MW PEG showed dose dependent activation of blood coagulation, platelets and complement system, severe red blood cell (RBC) aggregation and hemolysis, and cell toxicity. The long blood circulation of LPG was found to be 31.8 ± 4 h as demonstrated in mice; however, it was shorter compared to dPGs (39.2 ± 8 h). The shorter circulation half life of LPG was correlated with its higher renal clearance and deformability. Relatively lower organ accumulation was observed for LPG and dPG with some influence of on the architecture of the polymers. Since LPG showed better biocompatibility profiles, longer in vivo circulation time compared to PEG and other linear drug carrier polymers along with its multiple functionalities for conjugation, makes LPG a potential candidate for developing long circulating multifunctional drug delivery systems similar to dPG.[109] Sun et al. reported a biodegradable dPGs (Fig. 4.20), which were synthesized through oxyanionic initiating hybrid polymerization of glycerol and glycidyl methacrylate. Due to the introduction of ester linkages into the hyperbranched polyglycerol backbone, these dendritic polymers showed good biodegradability and low cytotoxicity. A potent anticancer drug, i.e., methotrexate (MTX) and a fluorescent probe Rhodamine-123 were conjugated onto the surface of dPGs. The resultant MTX-conjugated dPGs

exhibited an amphiphilic character, resulting in the formation of micelles in an aqueous solution. The release of MTX from micelles was significantly faster at mildly acidic pH of 5.0 compared to physiological pH of 7.4. Cancer cells efficiently internalized the conjugated dPG-MTX micelles while the MTT assay showed high activity of the conjugate against cancer cells.[110]

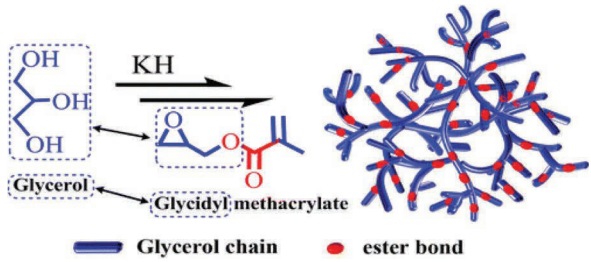



**Figure 4.20** Synthetic scheme towards the preparation of biodegradable dPG structure through oxyanionic initiating hybrid polymerization of glycerol and glycidyl methacrylate. Reprinted with permission from Ref. 110. Copyright (2012) American Chemical Society.

Kizhakkedathu has also reported the synthesis of biodegradable dPG-motif having acid-cleavable core structure by anionic ROMBP of glycidol using initiators bearing dimethyl and cyclohexyl ketal groups. The group has synthesized different multifunctional initiators carrying one to four ketal groups and two to four hydroxyl groups per molecule. The hydroxyl carrying initiators containing one ketal group per molecule were synthesized from ethylene glycol. An alkyne-azide click reaction was used for synthesizing initiators containing multiple cyclohexyl ketal linkages and hydroxyl groups. The synthesized dPG-based polymers exhibited monomodal molecular weight distributions and polydispersity in the range of 1.2 to 1.6, indicating the controlled nature of the polymerizations. The polymers were relatively stable at physiological pH but degraded at acidic pH values. The decrease in the polymer molecular weights upon degradation was correlated well with the number of ketal groups in their core structure. The polymers and their degradation products were highly biocompatible, as measured by blood coagulation, complement activation, platelet activation, and cell viability assays, while controlled degradation profiles of

15:59 28 October 2016

15:59 28 October 2016

these polymers together with their excellent biocompatibility rendered them as a suitable for drug delivery and bioconjugation candidate.[111] To address the possibility of using dPG-like structure in neurological field, Liu et al. designed a novel nanoparticles-based brain drug delivery system composed of hyperbranched polyglycerol-conjugated to poly (lactic-co-glycolic acid, PLGA). The resulting structure was surface functionalized with transferrin antibody (OX26) and the copolymer was synthesized, characterized and prepared into nanoparticles by double emulsion solvent evaporation technique. Transmission electron micrograph and dynamic light scattering showed that these dPG-based nanoparticles had a round and regular shape with a mean diameter of 170 ± 20 nm. As a model drug, Endomorphin was encapsulated in the nanoparticles. In vitro drug release study showed that endomorphins was released continuously for 72 h. Cellular uptake study showed that the uptake of nanoparticles by the brain microvascular endothelial cells was both time- and concentration-dependent. An uptake inhibition study indicated that the internalization of nanoparticles was mediated via a caveolae-mediated endocytotic pathway. In vivo endomorphins brain delivery ability was evaluated based upon the rat model of chronic constriction injury of sciatic nerve. OX26 modified nanoparticles had achieved better analgesic effects, compared with other groups indicating the use of OX26 modification of dPG-based scaffold as a promising brain drug delivery carrier.[112]

Recent trend indicates a series of investigations, which has been aimed at evaluating dPGs structure for a number of novel applications such as in dialysis and blood transfusion. It has been observed that, patients requiring chronic RBC transfusions for inherited or acquired anemia are at risk of developing transfusional iron overload, which may impact negatively on organ function and survival. Current iron chelators are suboptimal due to the inconvenient mode of administration and/or side effects. A dPG-based strategy to engineer low-molecular-weight iron chelators with long circulation lifetime for the removal of excess iron in vivo has been reported by Kizhakkedathu et al. To realize this purpose, desferoxamine (DFO) was conjugated to dPGs (Fig. 4.21) resulting in a 484-fold increase in $t_{1/2}$ between the free DFO (5 min) and dPG conjugated-DFO (44 h). In an iron overloaded mouse model, statistically efficient iron excretion by

15:59 28 October 2016

DFO conjugated dPG scaffold was observed in the urine and feces, as was the reduction in liver, heart, kidney, and pancreas iron content, and plasma ferritin level compared to free DFO. No apparent toxicity in several analyses including body weight, serum lactate dehydrogenase level, necropsy analysis, and by histopathological examination of organs was observed with the conjugates. This dPG-based chelating system has been a novel structure of its kind and application, that has prospective benefit towards patients suffering from transfusional iron overload.[113]

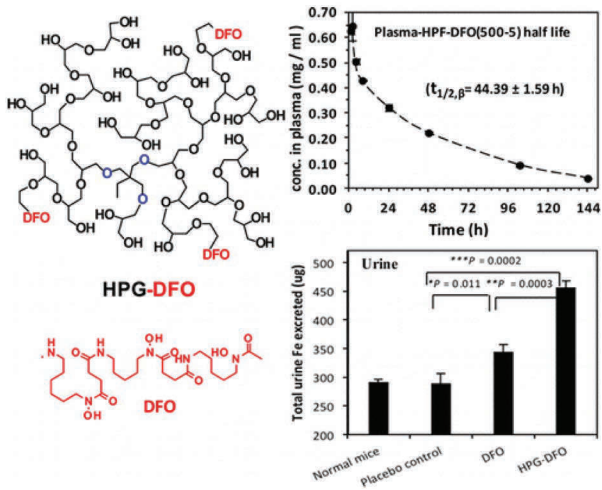



**Figure 4.21** DFO conjugated to dPG structure towards preparation of novel dPG-based iron chelating agents with prolonged half-life. Reprinted with permission from Ref. 113. Copyright (2013) American Chemical Society.

In an earlier communication, to enhance the effectiveness of peritoneal dialysis (PD) and design a new biocompatible PD solutions the same group have synthesized and tested the efficacy and biocompatibility of dPG as a nontoxic, nonimmunogenic water-soluble polyether polymer for PD applications. To establish the proof-of-concept, Kizhakkedathu group instilled adult Sprague-Dawley rats with 30 mL dPG solution (molecular weight 3 kDa; 2.5–15%) or control glucose PD solution. Intraperitoneal fluid was recovered and peritoneal injury and cellular infiltration were determined by histologic and flow cytometric analysis. Human peritoneal mesothelial cells (PMCs) were also assessed for viability

15:59 28 October 2016

in vitro after 3 h of PD fluid exposure. It was found that, 15% polymeric solution achieved a 4 h dose-related ultrafiltration up to 43.33 ± 5.24 mL and a dose-dependent urea clearance up to 39.17 ± 5.21 mL, results that were superior to those with control PD solution at statistically significant level. Although the dialysate-to-plasma (D/P) ratios of urea with 7.5% and 15% polyglycerol solution were not statistically different from those with control PD solution, fluid recovered from the dPG administered group contained proportionally fewer neutrophils (3.63% ± 0.87% vs. 9.31% ± 2.89%, $p < 0.0001$) compared to the fluid recovered from the control group. Detachment of mesothelial cells positive for human bone marrow endothelial protein 1 did not increase in the dPG-treated group compared with the control ($p = 0.1832$), but it was elevated in the control PD solution group (1.62% ± 0.68% vs. 0.41% ± 0.31%, $p = 0.0031$). Peritoneal biopsies from animals in the dPG-treated PD group, compared with those from control PD animals, demonstrated less neutrophilic infiltration and reduced thickness. Human peritoneal mesothelial cell survival after dPG exposure was also superior in vitro. It was found that exposure to glucose PD solution induced cytoplasmic vacuolation and caspase 3-independent necrotic cell death that was not observed with dPG solution. Hence, the novel dPG-based PD solution demonstrated effective ultrafiltration and waste removal with reduced peritoneal injury in a rodent model of PD.[114] To substitute glucose as a common osmotic agent for peritoneal dialysis (PD), the prospect of dPG has also been tested as an alternative osmotic agent. The efficiency and biocompatibility of dPG as an agent for PD was studied as a function of their molecular weights in a preclinical rodent model of PD, and compared with directly to conventional glucose-based Physioneal™ PD solution (PYS). The efficacy of polyglycerol solutions was measured by their ultrafiltration (UF) capacity, solute removal, and free water transport while the biocompatibility was determined in vivo by the histological analysis of the peritoneal membrane and the cell count of detached PMCs and neutrophils, and in vitro cytotoxicity to cultured human PMCs. All the different sized dPGs induced higher UF and sodium removal over a sustained period of time (up to 8 h) compared to PYS. Urea removal was significantly higher for 1–3 kDa than PYS, and was similar for 0.5 kDa. It was found that the peritoneal membrane exhibited more tolerance to

15:59 28 October 2016

the polyglycerol solutions compared to PYS, evidenced by less submesothelial injury and neutrophil infiltration in vivo, and less cell death in cultured human peritoneal mesothelial cells due to dPGs intrinsic biocompatiblity. Free water transport analysis of dPG indicated that these molecules functioned as colloids and induced osmosis mainly through capillary small pores. The superior osmotic activity of different sized dPGs was explained in terms of polymer bound water, as measured by differential scanning calorimetry. These preclinical data indicated that compared to PYS, low MW dPGs (0.5–3 kDa) are able to produce superior fluid and waste removal with better biocompatibility profile, suggesting their prospective use as osmotic agents for PD.[115] In an interesting approach, dPGs and polyethylene glycol (PEG) polymers with similar solution hydrodynamic sizes were grafted to red blood cells (RBCs) to investigate the impact of polymer architecture on the cell structure and function. It was found that dPG grafted RBCs showed much higher electrophoretic mobility values than PEG grafted RBCs at similar grafting concentrations and hydrodynamic sizes indicating differences in the structure of the polymer exclusion layer on the cell surface. PEG grafting impacted the deformation properties of the membrane to a greater degree than brought about by dPGs. The complement-mediated lysis of the grafted RBCs was found to depend on the type of polymer, grafting concentration and molecular size of grafted chains. At higher molecular weights and graft concentrations both dPG and PEG triggered complement activation. The magnitude of activation was higher with dPG possibly due to the presence of many hydroxyl groups per molecule. RBCs, which were grafted with dPGs, showed significantly higher levels of CD47 self-protein accessibility than PEG grafted RBCs at all grafting concentrations and molecular sizes. PEG grafted polymers provided, in general, a better shielding and protection to ABO and minor antigens from antibody recognition than dPG-based polymers; however, the compact dPGs provided greater protection of certain antigens on the RBC surface. It was found that, that dPGs of 20 and 60 kDa grafted RBCs exhibited properties that are more comparable to the native RBC than PEG 5 and 10 kDa grafted RBCs of comparable hydrodynamic sizes. The study showed that small compact polymers such as hyperbranched polyglycerol of 20 kDa have a greater

potential in the generation of functional RBC for therapeutic delivery applications. The concept is illustrated in Fig. 4.22.[116]

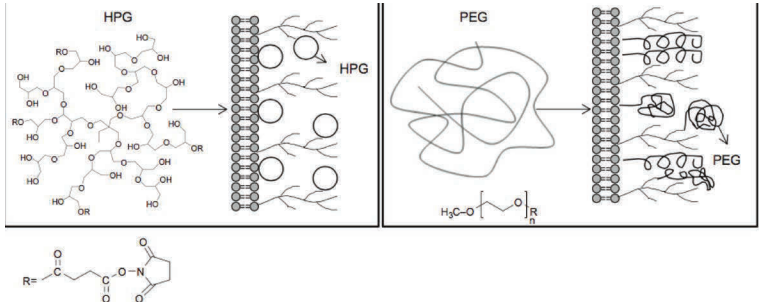



**Figure 4.22** Proposed conjugated architecture of dPG and PEG on RBCs. dPG has a compact spherical shape in water, and it maintains its confirmation after grafting. PEG has a loose random coil structure that can have an extended structure on RBC surface. A tree shape structures on the lipid bilayer represent glycoproteins on the surface of RBCs (sizes not to scale). Reprinted from *Biomaterials*, 33(31), Chapanian, R., Constantinescu, I., Rossi, N. A. A., Medvedev, N., Brooks, D. E., Scott, M. D., Kizhakkedathu, J. N., Influence of polymer architecture on antigens camouflage, CD47 protection and complement mediated lysis of surface grafted red blood cells, 7871–7883, Copyright (2012), with permission from Elsevier.

Including more than one imaging modalities on a polymeric platform often leads to acquisition of complementary information and synergistic advantages. A trimodal long-circulating imaging agent tagged with radioactive, magnetic resonance, and fluorescence markers will be able to combine the high sensitivity of SPECT with the precised resolution of MRI over hours and days. To make a trimodal long-circulating probe, high-molecular-weight dPGs with hyperbranched motif were modified with a suitable ligand for (111) In radiolabeling and Gd coordination, and additionally tagged with a fluorescent dye. The resulting radiopharmaceutical and contrast agent platform was nontoxic and hemocompatible. Measured radioactively, the total tumor uptake of the platform was increased from 2.6% at 24 h to 7.3% at 72 h, which is twice the enhancement expected due to tumor growth in this time period. Both in vivo MRI and subsequent histological analyses

15:59 28 October 2016

15:59 28 October 2016

of the same tumors confirmed maximum polymer accumulation at 3 days post injection. Furthermore, Gd-derivatized dPGs showed an excellent contrast enhancement on T1-weighted MRI at 10 × lower molar concentrations than commercially available Galbumin. Multimodal imaging with dPGs are thus found to be long-circulating macromolecules with great potential for imaging of healthy and leaky blood vessels using overlapping and orthogonal imaging approaches through passive targeting of tumors as showed in this work by Häfeli et al.[117] Currently, in vivo or in vitro (99m) Tc-radiolabeled red blood cells are the standard blood pool imaging agents. To counteract the risks associated with handling of blood and the problems with the current (99m) Tc shortage, the same group designed a long-circulating biocompatible synthetic macromolecule that can be easily prepared, and could also be used for PET imaging. To this end, a high molecular weight hyperbranched polyglycerol of 500 kDa was derivatized to coordinate radioactive gallium. The resulting radiopharmaceutical in a kit form was labeled rapidly within a couple of minutes at room temperature, was stable in transferrin and EDTA challenge tests, and was nontoxic in both cell viability and different hemocompatibility assays. A pharmacokinetic biodistribution study showed that the gallium loaded dPG platform was confined to the blood compartment with a biological half-life of 50.7 h thus providing a facile strategy to prepare blood pool imaging agent for applications where a long biological half-life is essential, for example, in the diagnosis of internal bleeding.[118]

**Key Ideas of Section 4.5.1**

- Spatial 3D-arrangement, presence of multiple and amenable functional groups, and significant biocompatibility are the major driving force for applying dPGs in biomedical setting.
- Physical encapsulation of drugs and/or other bioactive molecules within dPGs' supramolecular cavity enables non-covalent stabilization of the guest, rendering dPGs as an attractive scaffold for drug/biomolecular encapsulation.
- Pegylated dPGs mimic the structure of "stealth" liposome with improved water-solubility, minimized immunogenicity, and increased blood circulation half-life.
- Stimuli-responsive modalities that can sense local changes of environmental stimulus, i.e., pH-, temperature, and enzyme status can be included through classical or supramolecular chemical approaches to design to generate dPG-based smart drug delivery systems.

15:59 28 October 2016

### 4.5.2 Multifunctional dPG–drug Conjugates for Tumor Targeting

To enhance the stability unachievable with supramolecular and multimolecular encapsulation via scaffolding mechanism, as well as to induce programmability in function, covalent attachment of drugs and bioactive molecules to dendritic polymer has become an established route towards designing controlled-release polymer therapeutics. Such systems can spatially and temporally modulate the loading and release of active species. Chemical conjugation using classical functional group chemistry allows covalent attachment of different kinds of active molecules (imaging agents, drugs, targeting moieties, or peptides and proteins) to a dendritic scaffold in a stoichiometrically controlled ratio. Polymer–drug conjugates show several advantages over supramolecularly encapsulating polymer assembly in terms of programmable stability and release. In case of polymer–drug conjugate, the drug molecule can be connected to the macromolecular scaffold through a cleavable bond which can be degraded under specific conditions present at the site of action (endogenous stimuli, e.g., acidic pH, overexpression of specific enzymes, or reductive conditions as well as exogenous stimuli, such as light, salt concentration, electrochemical potential) as shown in Fig. 4.23, in compared to supramolecular encapsulation).

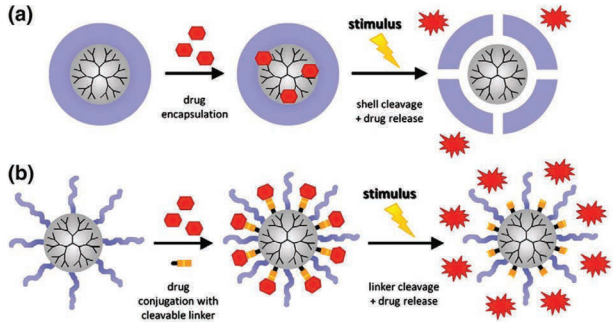



**Figure 4.23** Different mechanisms for stimuli-responsive release of active agents from nanocarriers: (a) supramolecular complexes like dendritic core-shell particles with a cleavable shell and (b) dendritic scaffolds with attached solubilizing/stealth groups using cleavable linkers for the drug conjugation. Reprinted from Ref. 119a, Copyright (2012), with permission from Elsevier.

15:59 28 October 2016

Kannan and coworkers presented the first example of using dPGs as a scaffold in the synthesis of polymer–drug conjugate containing high ibuprofen loading for enhancement of cellular uptake.[119] By a postmodification of the scaffold with an average MW of 6 kDa, a multiple functional system bearing 67% w/w of drug conjugated to PG by an ester linkage was obtained. The scaffold also contained fluorescein isothiocyanate (FITC) as a fluorescent marker. The conjugate was able to rapidly deliver the drug inside the cells after distribution into the cytosol. The anti-inflammatory activity of the conjugate, as investigated by monitoring prostaglandin inhibition, was considerably faster than the free drug. Haag et al. extensively studied maleimide-bearing, dendritic PG-based prodrug concept.[120] To this end, thiolated PG nanocarriers have been synthesized as a general, flexible platform to couple diagnostic or therapeutic agents under physiological conditions (Fig. 4.24). In an early communication, Haag group reported the use of the dPG platform for conjugation to maleimide bearing prodrugs of doxorubicin or methotrexate which incorporates either a self-immolative para-aminobenzyloxycarbonyl (PABC) spacer coupled to the dipeptide Phe–Lys or the tripeptide D-Ala-Phe-Lys as the protease substrate. Both prodrugs were cleaved by cathepsin B, an enzyme overexpressed by several solid tumors, to release doxorubicin or a methotrexate lysine derivative.

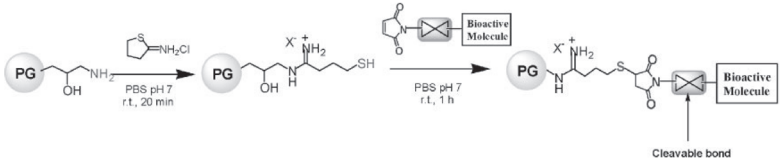



**Figure 4.24** Synthetic scheme for the immobilization of bioactive molecule on to PG scaffold through orthogonal thiol maleimide coupling. Adapted with permission from John Wiley & Sons, Inc., Copyright 2010.

Cytotoxicity of these conjugates against human tumor cell lines showed that the activity of the drugs was primarily retained, which confirmed the macromolecular prodrug concept.[120] Thiolated hyperbranched polyglycerols have been designed to couple either diagnostics or therapeutic agents.[75] The synthetic protocol

15:59 28 October 2016

consists of four steps. The first three steps for the synthesis of polyglycerolamine with average molecular weights between 10 and 500 kDa, and up to 20% of total hydroxyl groups functionalized to amine groups. For the synthesis of the thiolated derivatives, three different pathways have been established using 3-(tritylthio) propionic acid, 2-iminothiolane, or acetyl thiopropionic acid. Among all the thiolation reactions studied, the 2-iminothiolane pathway was found to be the most reproducible for in situ Michael reaction with maleimide derivatives as the following step. This modular approach proved to be flexible for coupling different drugs, solubilizing agents, as well as imaging and targeting moieties.[121,122] In a subsequent example the concept has been explored to prepare PG doxorubicin prodrug that were flexible for drug loading by using an acid-sensitive hydrazone linker and further postmodification with poly(ethylene glycol) shell. The resulting drug polymer conjugates showed optimal properties for in vitro and in vivo applications because of their high water solubility, an appropriate size for passive tumor toxicity, a high stability at physiological conditions, pronounced acid-sensitive properties, cellular internalization, and a favorable toxicity profile. Doxorubicin polyglycerol conjugates with a high drug-loading ratio showed clearly improved antitumor efficacy over doxorubicin in an ovarian xenograft tumor model (A2780) as shown in Fig. 4.25. This induced transient complete remissions and thus demonstrated its potential for development of an efficient multifunctional dendritic drug delivery using our modular approach.[123] To determine the optimal size of the conjugates for achieving enhanced permeability and retention (EPR) mediated targeting of the drug, the molecular weight of the PG scaffold was varied systematically. Using the same synthetic strategy, indotricarbocyanin–maleimide was coupled to these dendritic PG scaffolds. These conjugates were injected i.v. in tumor bearing mice and the systemic localization and tumor accumulation was observed by fluorescence imaging technique. The results from the in vivo imaging study showed an increased half-life of the conjugates compared to the dye coupled to a small PG dendron, since the fluorescence signal was still measurable 24 h after the administration.

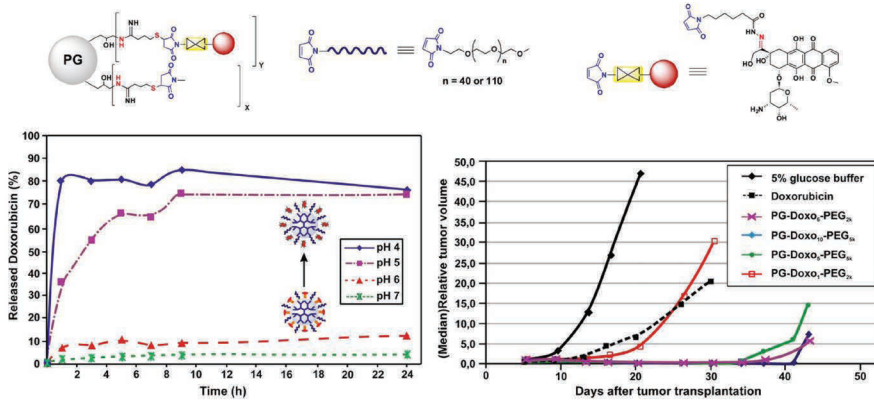



**Figure 4.25** Schematic structure of doxorubicin–polyglycerol conjugates. The curves depict the pH-release profile and the tumor growth inhibition of subcutaneously growing A2780 xenograft under therapy with doxorubicin and the conjugates. Reprinted from Ref. 120b, Copyright (2011), with permission from Elsevier.

Photodynamic therapy (PDT) is a stimuli-responsive system where the light of specific wavelengths is imposed upon a polymer–drug conjugate to trigger therapeutic activity. In a preliminary study, the PDT efficacy of tetrapyrrols coupled to dPGs was evaluated. The RGD peptides are not suitable for clinical applications due to their high inhibitory concentration as indicated by $IC_{50}$ and low in vivo residence times. Gyongyossy-Issa and coworkers[124] presented a method to improve the activities of RGD peptide by conjugation to a dPG structural motif via a divinyl sulfone linker. The conjugates showed an increased platelet inhibitory function of RGD by two to three orders of magnitude, thereby increasing RGD's local concentration as well as decreasing its dissociation kinetics. The effectiveness of the dPG–RGD conjugate was dependent upon MW and the number of RGD peptides attached to each PG molecule. These multivalent inhibitors of platelet aggregation decreased the $IC_{50}$ of RGD in an inverse linear manner based on the number of RGD peptides per PG.

Harnessing the multivalency and compact 3D architecture of hyperbranched polyglycerol, Kizhakkedathu and Straus reported the synthesis of dPG conjugates of antimicrobial peptides (AMPs). Aurein 2.2 peptide was conjugated to high molecular weight

15:59 28 October 2016

15:59 28 October 2016

hyperbranched polyglycerol with a varying number of peptides per polymer, and the biocompatibility and antimicrobial activity of the conjugates were investigated. The antimicrobial activity of the peptide and its conjugates were determined by measuring the minimal inhibitory concentration (MIC) against Staphylococcus aureus and Staphylococcus epidermidis. The interaction of aurein 2.2 peptide and the conjugates with a model bacterial biomembrane was investigated using CD spectroscopy to understand the mode of action of the conjugates. The biocompatibility of the AMP-polymer conjugates was investigated by measuring red cell lysis, platelet activation and aggregation, complement activation, blood coagulation, and cell toxicity. The report showed that the size of the conjugates and the peptide density influence the biocompatibility of the antimicrobial conjugates which set the stage for further structural modification of polyglycerol-AMP conjugates.[125] To design targeted anticancer therapeutics, Kang et al. grafted hyperbranched polyglycerol on superparamagnetic nanoparticles. Polyglycerols with dendritic architectures have also been conjugated with methotrexate (MTX). The successful grafting of MTX and dPG onto the nanoparticles was confirmed by X-ray photoelectron spectroscopy (XPS), Fourier transform infrared (FT-IR) spectroscopy, and UV-visible spectroscopy. The dPG-grafted layer confers the magnetic nanoparticles with good dispersibility and stability in aqueous medium and macrophage-evasive property while the MTX acts as a chemotherapeutic drug as well as a tumor targeting ligand. The dose-dependent targeting and anticancer effect of the dPG-coated nanoparticles were evaluated, and the results showed that depending on the amount of conjugated MTX and the concentration of the incubated nanoparticles, the uptake of nanoparticles by human head and neck cancer (KB) cells can be eight times higher than that exhibited by 3T3 fibroblasts and RAW macrophages. As a result, dPG coated nanoparticles were capable of killing <50% of the KB cells while at the same time exhibiting low cytotoxicity towards 3T3 fibroblasts and RAW macrophages which is a desirable property for successful design of targeted nanoparticles.[126]

Polymer–protein conjugates generated from side chain functional synthetic polymers are attractive platforms because they can be easily further modified, for example, with labeling groups or targeting ligands. The residue-specific modification

15:59 28 October 2016

of proteins with side chain functional synthetic polymers using the traditional coupling strategies may be compromised due to the nonorthogonality of the side-chain and chain-end functional groups of the synthetic polymer leading to side reactions. The feasibility of the squaric acid diethyl ester mediated coupling as an amine selective, hydroxyl tolerant, and hydrolysis insensitive route for the preparation of side-chain functional, hydroxyl group bearing, polymer–protein conjugates were studied by Klok et al. The hydroxyl side chain functional polymers selected for this study composed of library of amine end-functional, linear, mid-functional, hyperbranched, and linear-block-dPGs copolymers (Fig. 4.26). These synthetic polymers have been used to prepare a diverse library of BSA and lysozyme polymer conjugates. In addition to exploring the scope and limitations of the squaric acid diethylester-mediated coupling strategy, the use of the library of polyglycerol copolymers also allows to systematically study the influence of molecular weight and architecture of the synthetic polymer on the biological activity of the protein. Comparison of the activity of PG-lysozyme conjugates generated from relatively low-molecular-weight PG copolymers did not reveal any obvious structure-activity relationships. Evaluation of the activity of conjugates composed of PG copolymers with molecular weights of 10,000 or 20,000 g/mol, however, indicated significantly higher activities of conjugates prepared from mid-functional synthetic polymers as compared to linear polymers of similar molecular weight.[127]

**Key Ideas of Section 4.5.2**

- To enhance the stability unachievable with supramolecular and multimolecular encapsulation via scaffolding mechanism, as well as to induce programmability in function, covalent attachment of drugs and bioactive molecules to dendritic polymer has become an established route.
- The peripheral hydroxyl groups of dPGs can be utilized to construct dPG-conjugates of small molecular drugs, peptides, antibodies and proteins with high-molecular loading and biological inertness.
- Through the design of the linker, drug and other bioactive molecules can be attached to dPG scaffold which are release in a programmed and controlled pattern only at the site of action.

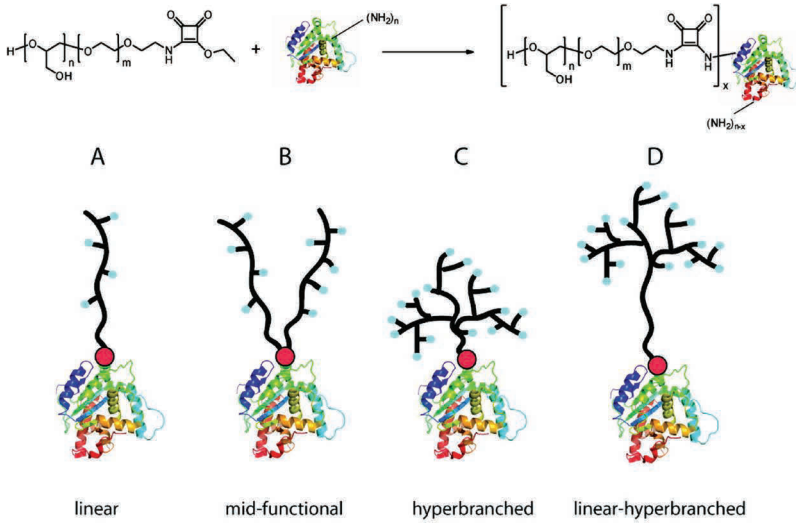



**Figure 4.26** Top panel: Squaric Acid mediated attachment of PG copolymers to Proteins; (Bottom). Architectural diversity of different protein-polymer conjugates from linear to linear-hyperbranched system. Reprinted with permission from Ref. 127. Copyright (2012) American Chemical Society.

### 4.5.3 Designing Functional Architectures Based on PG for Multivalent Interaction

As mentioned previously, dendritic PG has distinct linear, monohydroxyl and terminal, dihydroxyl functionalities within their scaffold. These hydroxyl groups can be converted to desirable functional groups following established hydroxyl group chemistry, resulting in generation of broad-spectrum of products with high molecular loading capacity, a variety of peripheral functional groups and selective solvent solubility. A substantial amount of research has been directed to design different architectures by modification of dPG hydroxyl groups into different functionalities as illustrated in Fig. 4.27.[7a]

The resulting architectures are capable of demonstrating a diversified set of biological effect, which can be utilized in therapeutics and medicine. These effects are originated from the inherent multi-functional nature of dPGs that gives rise to

15:59 28 October 2016

15:59 28 October 2016

multivalency, and reinforced by the nanoscale dimension of the dendritic molecule per se. Theoretically, multivalency describes the binding of two or more entities that involves the simultaneous interaction between multiple and complementary functionalities. Multivalent interactions (Fig. 4.28) are considerably stronger than the individual bonding of a corresponding number of monovalent ligands to a multivalent receptor and are the most predominant phenomena in biological systems, particularly for recognition and attachment, signal transduction, and numerous cellular interactions.[85,128] The driving potential of multivalent systems is the high entropic gain in the formation of multivalent complex. For example, the binding constants of bivalent interactions can be a factor of 1000-fold higher than the corresponding monovalent binding, and for tri- and pentavalent interaction, values up to $10^8$ have been reported. This intrinsic multivalency, which is a built-in feature of dPGs has been used to mimic functional biomacromolecules which exhibit multivalent interactions with biological substrates, i.e., cell-surface receptors. It has been an experimentally evident fact that such multivalent interaction can be exploited to enhance or regulate the down-stream effect of such ligand-receptor engagement.

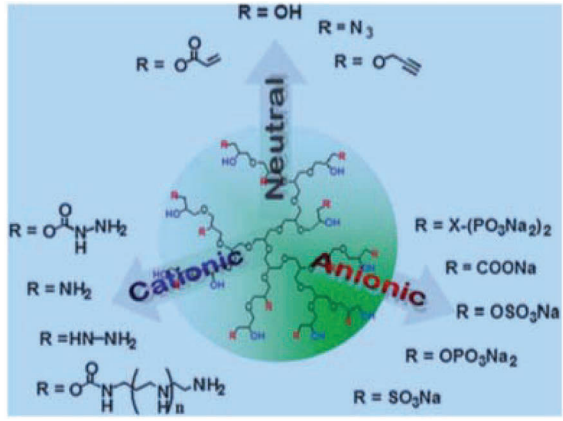



**Figure 4.27** Schematic representation of dPG derivatives used for the development of functional materials in the field of nanomedicine. Reprinted from Ref. 121. Copyright (2010), with permission from Elsevier.

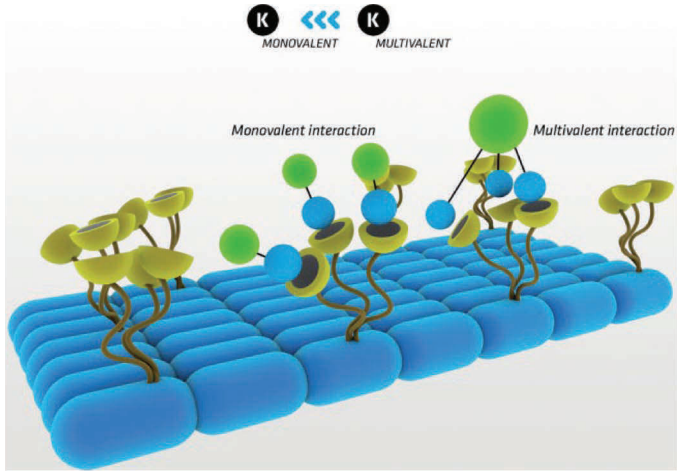



**Figure 4.28** Schematic representation of monovalent and multivalent interaction. Adapted with permission from John Wiley & Sons, Inc., Copyright 2010.

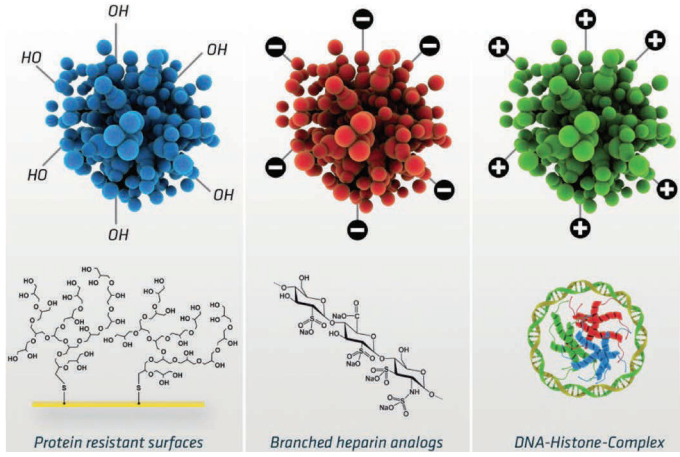



**Figure 4.29** Biologically active macromolecules (lower panel) that have been mimicked through dPGs modification (top panel). Adapted with permission from John Wiley & Sons, Inc., Copyright 2010.

DNA-binding proteins such as histones, or polysaccharides like heparin are biological macromolecules of critical capacity which, due to their surface charge, and secondary and tertiary

15:59 28 October 2016

conformation and multivalency, control and regulate vital cellular and biochemical function such as protection of DNA or modulation of blood coagulation process. A concerted effort has been made to render dPGs mimicking these bioactive proteins and carbohydrates, mostly by postpolymerization modification (Fig. 4.29). Dendritic PGs with cationic groups, such as primary, tertiary and quaternary amines have been synthesized which represents histone-like macromolecule for compacting DNA. A broad range of dendritic PGs with anionic functional end groups have been synthesized that mimic negatively charged polysaccharides as heparin or poly(sialic) acid, and have been investigated for applications such as modulating coagulation pathways and stimulating anti-inflammatory actions.

15:59 28 October 2016

#### 4.5.3.1 Neutral PGs as mimicry of oligosaccharides for surface modification

Biomaterials that can resist nonspecific adsorption of protein can find prospective applications in designing prostheses, sensors, substrates for enzyme-linked immunosorbent assays (ELISAs) and in contact lenses, and implanted devices.[129] More recent applications include systems for patterned cell cultures,[130] tissue regeneration,[131] microfluidic systems,[132] drug delivery[133] and systems for high throughput screening of proteins[134] or cells.[135] With the development of new biomedical applications, there is a great need to develop new biomaterials with novel structures and properties. In recent years a variety of substances have been studied for their resistance to protein adsorption.[136,137] PEG is one of the most commonly used biomaterials because of its exceptional biocompatibility. It shows unsurpassed resistance to nonspecific protein binding. Polyethylene glycol also meets the four molecular-level characteristics defined by Whitesides et al. for resisting the adsorption of proteins because it is hydrophilic, includes hydrogen-bond acceptors, does not include hydrogen bond donors, and is neutral. However, PEGs can only be functionalized at the chain ends and the polymer is not biodegradable. Based on the analysis of the best protein resistant surfaces known in literature, it becomes apparent that branched architectures, for example with highly flexible aliphatic polyethers and hydrophilic

15:59 28 October 2016

H-donor groups, are some of the critical structural features that enable protein resistance. This, in addition to the higher thermal stability compared to PEG makes the dPGs optimal candidates for surface modification with the scope of getting a biocompatible surface.[138] In addition, dPGs resemble the structure of polysaccharides, which is a major constituents of the extracellular glycomatrix, hence preventing unspecific adhesion of cells. In this context, several disulfide-functionalized hyperbranched PGs by coupling of thioctic acid has been synthesized by Haag group which spontaneously formed self-assembled monolayers (SAMs) on a gold surface and prevented the adsorption of proteins to the same level as for PEG SAMs, and significantly better than that of dextran. A systematic structure–activity relationship revealed that the more globular the structures, the more inert the assembly is towards protein adsorption, while the molecular weight changes did not appear to have a significant effect. Substitution of acidic hydrogen atoms by methyl groups resulted in small improvement in the protein resistance which was in agreement with the hypothesis referring to the absence of hydrogen-bond donors[136] A different synthesis for a thiolated dPG was reported by ring-opening polymerization of glycidol from partially deprotonated 2,20-dihydroxyethane disulfide as the initiator and the subsequent reduction of the disulfide group.[139] Two molecular weights (1.59 and 4.26 kDa) were obtained by varying the initiator to glycidol ratio. By a comprehensive study, it was shown that the branched polymers produced more uniform structures on gold surfaces with low surface roughness. Although the low-molecular-weight species gave a higher graft density, the high MW coated surface was much more resistant to protein adsorption than the PEG coated surface. In addition, the protein repulsion of PG-coated surfaces was found to increase with increasing graft density of chains on the surface. It can be stipulated that, dPGs can place themselves, as superior candidates for surface coating than PEG so far the higher thermal and oxidative stability of the former is concerned. As an added advantage, and unlike PEG, dPGs provides multiple free hydroxyl groups for further functionalization with ligands that will result in targeted protein or cellular interaction. The conjugation of PG to proteins may be an elegant solution for systems where proteins to be immobilized, e.g., for biosensors. For

15:59 28 October 2016

example, streptokinase, glucose oxidase, and phosphorylcholine have been conjugated to dPG to construct a glucose biosensor. For example, in an earlier study, Queiroz and coworkers conjugated streptokinase, a thrombolytic enzyme, to hyperbranched PG. In a careful study of the platelet adhesion and thrombus formation on polystyrene surfaces, it was found that the conjugate can lyse blood clots.[140] This indicates that the conjugation process does not affect the fibrinolytic property of the enzyme. This concept was transferred to design a biosensor,[141] where the PG–streptokinase conjugate was linked to glucose oxidase and phosphorylcholine and further entrapped in polyaniline nanotubes. After deposition in an aluminum electrode, the platelet adhesion, fibrinolytic activity, protein adsorption, and amperometric response to glucose were studied to examine the interaction of blood with the PG-based biosensor, and the electrochemical response. The in vitro results on the blood compatibility and glucose sensing properties suggest that the bioconjugated PG could be a very useful material for development of implantable glucose biosensor.

#### 4.5.3.2 Negatively charged dPG derivatives

Dendritic PGs have been extensively used to mimic multivalent carbohydrate-binding proteins, such as lectin, which specifically bind different sugar structures. Lectins have received considerable attention recently due to their importance in cell surface interaction and biological recognition, and multivalency in lectins has been discussed in detail by different authors. For dendritic PGs with negatively charged functional groups, lectins provide a robust model for studying multivalency of dendritic polymer derivatives. Haag group has extensively explored the use of dendritic PGs to mimic multivalent glycoarchitectures (Fig. 4.30) for the inhibition of L- and P-selectins, a general class of receptors which displays a selective adhesion and includes a lectin-like domain.[142] Two structures were compared, namely, free PG–galactose (R = H in Fig. 4.30) and PG–sulfated galactose (R = $SO_3Na$). Selectin inhibition studies carried out with SPR measurements indicated a clear enhanced effect due to multivalency. Using L-selectin, the nanomolar binding affinity of PG–galactose was observed. Notably, sulfated dendritic galactose showed a further enhancement with an $IC_{50}$ of 1 nM. This indicates the importance of negatively charged sulfate groups on the surface of these polysaccharide analogues.

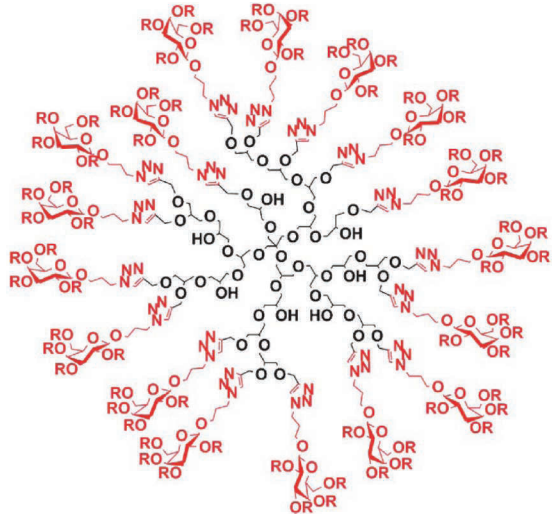


**Figure 4.30** Multivalent glycoarchitectures based on PG-galactose (R = H) and PG-sulfated galactose (R = $SO_3Na$). Adapted with permission from John Wiley & Sons, Inc., Copyright 2010.

As a continuation of their work, Haag group generated dPG sulfates as a heparin analogue. These structures were found to prolong the time of activated partial thromboplastin as well as thrombin and to inhibit both the classical and alternative complement activation more effectively than heparin.[143] On the other hand, the biocompatible and well tolerated PG sulfate has been synthesized that act as multivalent selectin ligand mimetic and efficiently blocks leukocyte migration. L- and P-selectin binding to immobilized ligands was drastically reduced by the PG sulfates in vitro and gave $IC_{50}$ values in the low nanomolar range. The inhibition was strongly dependent on core size and degree of sulfation for different derivatives.[144] Among the polyanionic PG candidates, i.e., carboxylates, sulfonate, phosphate and phosphonates, only dPG sulfates demonstrated a nanomolar binding to L-selectins.[145] Administration of dPG sulfates in a contact dermatitis in vivo model suppressed leukocyte extravasation in a comparable extent to that of glucocorticoids, and also significantly reduced edema formation. Complement factors such as C3 and C5 were found to interact with dPG sulfates, where the anionic macromolecule significantly reduced C5a levels in a mouse model for complement activation.[146] To translate the idea towards

15:59 28 October 2016

15:59 28 October 2016

diagnostics in an effort to investigate whether dPG sulfate can target inflamed tissue, the dendritic system was labeled with a NIR dye indocyanine green (ICG) and injected to a rheumatoid arthritis (RA) animal model. In vivo experimentation revealed that dPGs exhibit a rapid and selective uptake in inflammation areas triggering differentiation of disease scores and allowing identification of joints with early signs of inflammation. Fluorescent histology studies clearly showed that the dendritic PG sulfates are mainly deposited in the inflammatory infiltrate in the synovial membrane in contrast to the nonsulfated control (Fig. 4.31).[144,147]

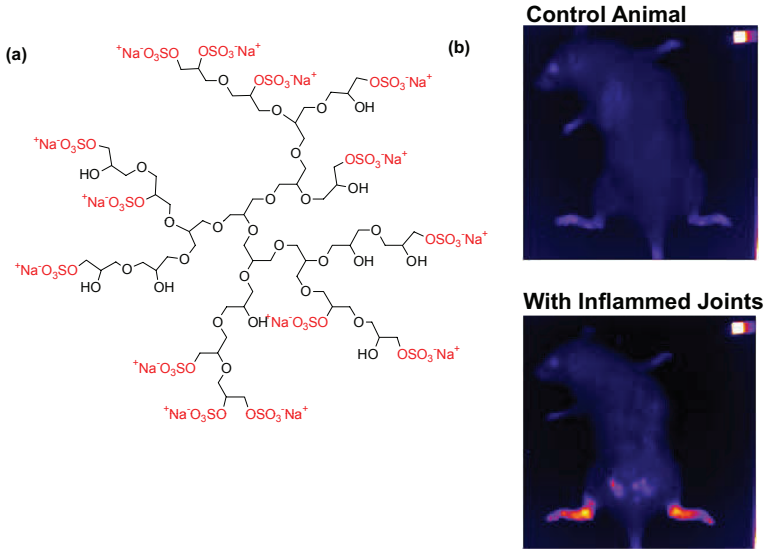



**Figure 4.31** (a) Schematic representation of endritic polyglycerol sulfate. (b) In vivo fluorescence imaging of rats with joint inflammation (collagen-induced); i.v. injection of dPGS-dye (2 mg/kg); recorded after 1 h (irradiation at 760 nm). Reprinted with permission from Ref. 147. Copyright (2011) American Chemical Society.

As the immune response required for designing successful antitumor vaccine depends strongly on the class and presentation of the tumor-associated antigen, Frey and Kunz has utilized "click chemistry" to immobilize a tumor-associated MUC1 glycopeptide combined with a immune-stimulating T-cell epitope P2 (from tetanus toxoid) to a multi-functionalized dPG architecture with

15:59 28 October 2016

hyperbranched motif. This globular polymeric carrier has a flexible structure, which allowed optimal antigen presentation to the immune system, and the resulting synthetic vaccine induced strong immune responses in mice and IgG antibodies recognizing human breast-cancer cells.[148] Haag group has thoroughly investigated the extent to which the scaffold architecture of dPG sulfates affects inflammatory processes and hemocompatibility. Competitive L-selectin binding assays, cellular uptake studies, and blood compatibility readouts were done to evaluate distinct biological properties. Fully glycerol-based dPG architectures which were obtained by either homopolymerization of glycidol (60% branching) or a new copolymerization strategy of glycidol with EEGE. Two dPGs with 24% and 42% degree of branching (DB) were synthesized by using different monomer feed ratios. A perfectly branched polyglycerol dendrimer is synthesized according to an iterative two-step protocol based on allylation of the alcohol and subsequent catalytic dihydroxylation. All the polyglycerol sulfates were synthesized with a comparable molecular weight and degree of sulfation.[149]

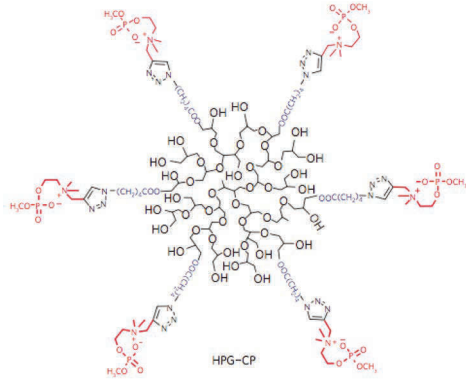



**Figure 4.32** Choline phosphate conjugated to dPG: a universal biomembrane adhesive can electrostatically bind to a variety of cell membranes and to PC-containing liposomes. Reprinted by permission from Macmillan Publishers Ltd: Nature Materials (Ref. 150), Copyright (2012).

Phospholipids in the cell membranes of all eukaryotic cells contain phosphatidyl choline (PC) as the head group. In an interesting study, Brooks lab has generated dPGs decorated with

15:59 28 October 2016

the "PC-inverse" choline phosphate (CP) in a polyvalent fashion, which can electrostatically bind to a variety of cell membranes and to PC-containing liposomes (Fig. 4.32). The binding strength was found to depend on the number density of CP groups per macromolecule. It was also shown that CP conjugated dPGs can cause cells to adhere with varying affinity to other cells, and that binding can be reversed by subsequent exposure to low-molecular-weight hyperbranched polyglycerols carrying small numbers of PCs. Moreover, PC-rich membranes adsorb and rapidly internalize fluorescent CP conjugated polyglycerol but not PC conjugated macromolecules, which suggests that CP-conjugated species could be used as drug-delivery agents. CP-decorated polymers can be considered as a prospective candidate also as tissue sealants and in the self-assembly of lipid nanostructures.[150]

#### 4.5.3.3 Applications of polycationic derivatives of dendritic PGs

The terminal hydroxyl group of dPGS can be converted to cationic charged group enabling them to interact multivalently with polyanions. Such interaction of dendritic, cationic polyamines with polynucleotides can be harnessed for stable and targeted delivery of genes, DNA and siRNA. The electrostatic interaction between the negative phosphates backbones of the DNA/RNA strand with agents that carry multiple positively charged groups has long been used in nonviral gene delivery (Fig. 4.33). Cationic lipids and cationic polymers are the best studied compounds for this purpose.[151,152] Several amine functionalized hyperbranched PGs have been reported as potential gene vectors.

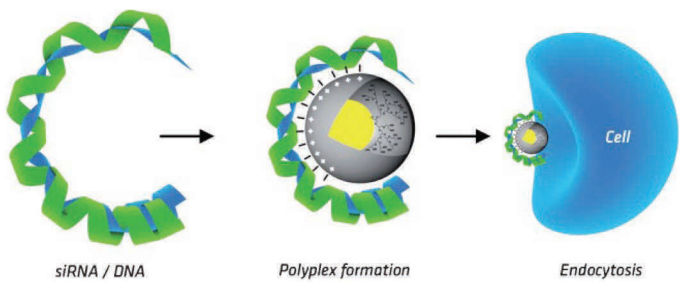



**Figure 4.33** Schematic representation of dendritic nanocarriers for cell internalization of gene vectors. Adapted with permission from John Wiley & Sons, Inc., Copyright 2010.

15:59 28 October 2016

By comparison with standard cationic polymers like PEI, a much lower cytotoxicity of the PG derivatives was observed so far as the cellular internalization of genetic materials is concerned. In DNA binding, a high affinity in the nanomolar range was found at low levels of quaternization, comparable to the binding affinities of cationic multivalent dendrimers with their much lower biocompatibility.[153] In a different approach, dPGs was partially functionalized with quaternary and tertiary ammonium groups with different loading degrees, and the resultant polymers showed interaction with DNA and formed neutral polyplexes.[146] These quarternized PG-derivatives showed similar transfection efficiency as PEI but with significantly diminished cytotoxicity in mammalian cells. In a recent investigation, Haag group synthesized several dPG constructs that were postmodified with spermine, spermidine, and pentaethylenehexamine. These dendritic polyamine compounds were clearly multivalent in gene complexation (Fig. 4.34).[154] By an ethidium bromide displacement assay, it was possible to demonstrate the high affinity of these amine functionalized PGs towards DNA. The affinity of the amine moieties increased significantly after their attachment onto the PG scaffold. Preliminary cytotoxicity studies showed that the dendritic nanocarriers exhibited a safe profile at the required concentrations and have decreased bioluminescence in U87-luciferase cell lines by 50–80%. In a preliminary in vivo experiment significant gene silencing of some of the structures tested was observed. Compared to other dendritic structures, dendritic PGs demonstrate added advantage of structural flexibility and low toxicity. Facile postmodification methodology that can be carried out over dendritic PG scaffold allows an easy control of transfection/toxicity ratio as a function of surface chemistry. Among the various candidates tested, dPG-amine demonstrated the highest affinity towards DNA fragments as evident from ethidium bromide displacement assay, and so far siRNAs are concerned, the dendritic scaffold were able to complex the polynucleotide as slightly positively charged globular polyplexes. The knockdown efficiency of the siRNA-polyplex was comparable to Hiperfect® in suppressing proteins like Lamin, CDC2 and MAPK2 in HeLAS3 cell lines. Dendritic PG amines showed superior safety profile compared to poly (ethylene imine) (PEI) derivatives at relevant concentration optimum for activity. The time for internalization

15:59 28 October 2016

for siRNA-PG-amine polyplexes was found to be 24 h in glioblastoma cells via endosome-lysosomal pathway (Fig. 4.34A). When administered intravenously or intratumorally, these polyplexes significantly silenced the target genes without any toxicity (Fig. 4.34B). Fluorescently labeled siRNAs were detected in the tumor but not in other major organs, which essentially reflects the passive targeting capability of dendritic PG-amines mediated by EPR effect.

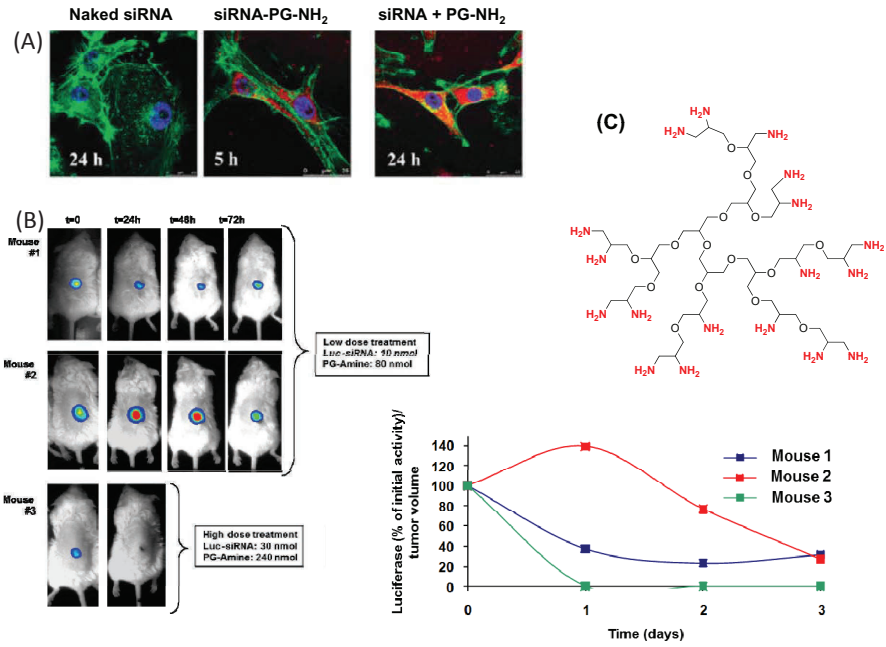



**Figure 4.34** siRNA-PG amine polyplex intracellular uptake. U87-Luc cells were incubated with TRITC-labeled siRNA (red) either alone (naked siRNA) or complexed with dPG-amine (siRNA + dPG-$NH_2$). Actin filaments were stained with phaolloidin (green). Scale ar represents 25 mm. (B) Therapeutic response of SCID mice bearing U87-Luc tumors treated with differnet amounts of PG-$NH_2$, complexed with siRNA and (C) Idealized fragment of polyglycerolamine.

In a different communication, Haag group has successfully used dPG-amine in xenograft model to delivery siRNA in the form of a polyplex. The result showed that, dPG-amine polyplexes are able to down regulate mRNA expression of ferrochelatase (FECH), an enzyme that completes the heme-synthetic pathway by

15:59 28 October 2016

incorporating iron into protoporphyrin IX (PpIX).[155] Precise and efficient inhibition of FECH, resulting blockage of heme synthesis and subsequent accumulation of PpIX within xenotransplanted human tumor was observed when dPG-amine was used to cargo siRNA inside xenograft microenvironment. To translate such series of inspiring results in gene therapy using dPG scaffold in clinical setting, Kizhakkedathu et al. reported a complete study of blood compatibility and DNA binding of dPGs decorated with PEG chains and tris (2-aminoethyl) amine.[156a] Surprisingly, the scaffolds with different degrees of amine quaternization showed insignificant effects on hemolysis, erythrocyte aggregation, complement activation, platelet activation, and coagulation.

**Key ideas of Section 4.5.3**

- Multivalency is defined as the binding of two or more entities that involves the simultaneous interaction between multiple and complementary functionalities.
- The intrinsic multivalency, which is a built-in feature of dPGs owing to the presence of multiple peripheral hydroxyl groups of dPGs, can be utilized advanced nanomedical setting, particularly for recognition and attachment, signal transduction, and numerous cellular interactions.
- Dendritic PGs have been extensively used to mimic multivalent carbohydrate-binding proteins, heparin analogue, "PC-inverse" choline phosphate (CP) as biological sealant, and as epitope-bearing scaffold.
- The terminal hydroxyl group of dPGs can be converted to cationic charged group enabling them to interact multivalently with polyanions such as genes, DNA and siRNA.

Transgene transfection techniques using cationic polymers such as polyethylenimines (PEIs) and PEI derivatives as gene vectors have shown efficacy, although they also have shortcomings such as high toxicity. PEIs have decent DNA-binding capability and good cell internalization performance, but they cannot deliver gene payloads very efficiently to cell nuclei. Wu et al. developed a set of dPGs connected to polyethylenimine polymers, which were functionalized with myo-inositol (INO) molecules. The resulting polymer constructs have an increased number of INO ligands per molecule. Mixing the dPG-PEI constructs with DNA produced compact nanocomposites. Colocalization study conducted with fluorescence microscopic technique showed that,

accumulation of polymers in 293T cell nuclei were enhanced as the number of conjugated inositol ligands increased in the polymeric architecture. It was also found that, extracellular adenosine triphosphate (eATP) inhibited the transgene efficiency of polymers, as compared with PEI and dPG-PEI that were not conjugated with inositol, indicating the possibility of using inositol as an effective ligand for transgene expression.[156b]

### 4.5.4 Polyglycerol Nanogel in Biomedicine

Nanogels are highly-monodispersed polymeric nano-aggregates cross-linked under template conditions. Nanogel technology has gained much acceleration in recent years as it enables the generation of advanced materials with desired size and physicochemical properties. Haag group has initially reported the fabrication of nanogels as drug delivery vehicles, which has later been extended to cover broader application areas of regenerative therapy, tissue-engineering and for generation of biomimetic extracellular matrix materials. The hydrophilic, hydroxyl-rich structural scaffold and their size at optimal nanoscale range, provides the PG-based nanogels with enhanced properties to interact with biological microenvironment.[157]

In a systematic exploratory study, Haag group synthesized dPG-based nanogels in different size ranges to find out the goldilocks' spot of nanogel size range on cellular internalization. It was found that nanogels within the size range of 25–350 nm were rapidly internalized within cellular cytoplasm, and primarily accumulates in the perinuclear region (Fig. 4.35). Apparently, the extent of internalization was found to be depend on nanogel particle size, with almost no apparent cytotoxicity in the mg/mL range.[158]

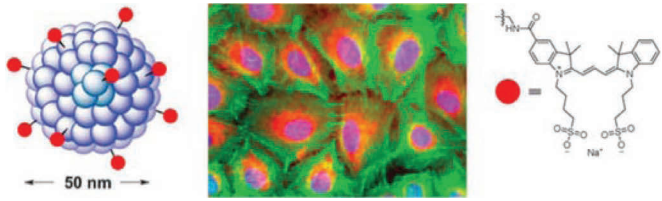



**Figure 4.35** Fluorescence microscopy shows clear evidence for cellular uptake of fluorescently labeled PG microgels via an endocytotic pathway. Adapted with permission from John Wiley & Sons, Inc., Copyright 2009.

15:59 28 October 2016

15:59 28 October 2016

As a logical consequence of this initial study, biodegradable PG nanogels and hydrogels were prepared through an acid-catalyzed ring-opening polyaddition of disulfide containing polyols and polyepoxides (Fig. 4.36) to generate programmable nanogel scaffold that breaks down within the systemic circulation after a specified period of time.[159,160] The particle size and polydispersity were found to depend on reaction conditions and disulfide content within the polymer network. In reducing environment, disulfide containing oligoglycerols nanogels were smoothly degraded, and were found to be highly biocompatible. The nanogel network can also be used to encapsulate and release a near-infrared fluorescent dye in a fairly controlled fashion. Groll and coworkers utilized a miniemulsion condition to generate biocompatible and degradable nanogels built on thiol-functional monomer. In this case, thiol modified star-shaped poly (ethylene oxide-stat-propylene oxide) and linear polyglycerol were cross-linked, which showed glutathione dependent biodegradation.[161]

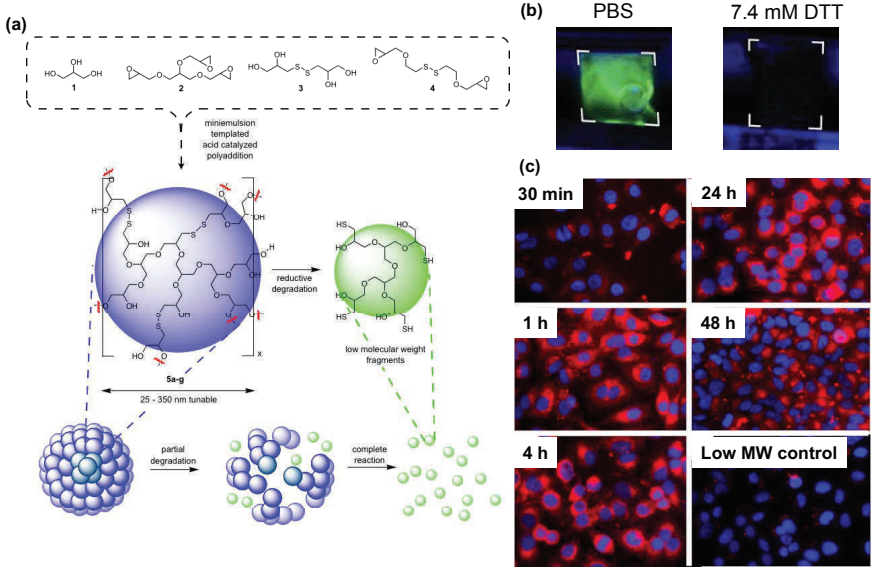



**Figure 4.36** (a) Synthetic route to biodegradable polyglycerol nanogel. (b) Degradation of the nanogel in reducting envrionment compared to PBS control. (c) Intracellular uptake of nanogels as a function of time (DAPI was used as the nuclear stain). Adapted with permission from John Wiley & Sons, Inc., Copyright 2010.

15:59 28 October 2016

The exactly match the nanogel dimensions with biomacromolecular components such as prokaryotic and eukaryotic cells, membrane structures and organelles, a wide-spread scientific interest has been evident from early 2010 to study the impact of nanogel scaffold on biological interaction. In an extensive study, dendritic PG nanogels were utilized to design a multivalent glycoarchitectures for inhibition of the influenza virus.[162] Nanogels composed of dPGs were fabricated in a broad range of sizes and degree of functionalization to fit to the corresponding virus size and receptor multiplicity to ensure maximum binding efficiency. The study revealed that larger the size of the macromolecular glycoconjugate, stronger the inhibitory activities they demonstrate against viral interaction. It was found that dPGs nanogels with 50 nm diameters showed 7 × $10^3$ fold more efficiency in inhibiting the binding and fusion to influenza virus than hyperbranched PG with a diameter of 3 nm. The nanogels were also found to reduce the viral activity by up to 80% and demonstrated the importance of size-multiplicity relationship towards therapeutically purposeful intervention of biological attachments (Figure 4.37).

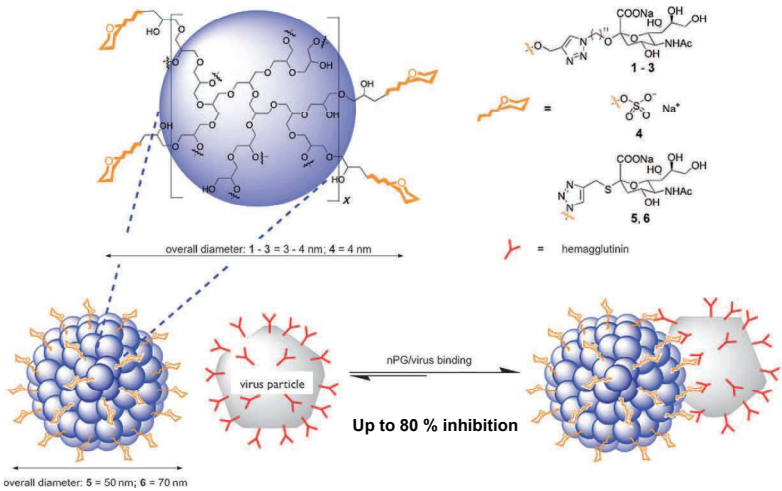



**Figure 4.37** Schematic representation of sialic acid conjguated PG nanoparticles that match influenza virus size and multiplicity. Adapted with permission from John Wiley & Sons, Inc., Copyright 2011.

15:59 28 October 2016

Dendritic PG nanogels have recently been prepared with stimuli-responsive properties. Calderon et al. developed dendritic nanogels where PG units are cross-linked by thermoresponsive n-isopropylacrylamide (NIPAM), and the resulting 50–200 nm particles were isolated by precipitation polymers.[163] As a continuation of their work, the group has synthesized doxorubicin-loaded nanogels with multiple stimuli-responsive properties, which were prepared using dPGs as a biocompatible scaffold. The nanogels are synthesized in a single step combining free-radical polymerization and a mild nanoprecipitation technique. The nanogels respond to different biological stimuli such as low pH and reductive environments, resulting in a more efficient cell proliferation inhibition in A549 cells.[164] Haag et al. developed a novel pH and redox-responsive prodrug nanogel was prepared by an inverse nanoprecipitation method, which is mild and surfactant free, and based on a thiol-disulfide exchange reaction and thiol-Michael addition reaction. Highly biocompatible dPGs were cross-linked with disulfide bonds, to obtain biodegradable nanogels, which degrades under intracellular reductive conditions. Doxorubicin (DOX) was conjugated to the biodegradable nanogel matrix via an acid-labile hydrazone linker. This is the first dual-responsive prodrug nanogel system that shows very low unspecific drug leaching, but efficient intracellular release of the payload triggered by the intracellular conditions. Two different prodrug nanogels were prepared with a size of approximately 150 nm, which is big enough to take the advantage of the enhanced permeation and retention (EPR) effect in tumor tissue. Cell culture analysis by microscopy and flow cytometry revealed that the prodrug nanogels were efficiently internalized by tumor cells. Distinct release profiles of DOX were achieved by adjusting the nanogel architecture, and online detection of cytotoxicity showed that, unlike free DOX, the dual-responsive prodrug nanogels exhibited a delay in the onset of toxicity, indicating the different uptake mechanism and the need for prodrug activation to induce cell death.[165] Although several strategies are now available to enzymatically cross-link linear polymers to hydrogels for biomedical use, little progress has been reported on the use of dendritic polymers for the same purpose. To this direction, Haag laboratory demonstrated that horseradish peroxidase (HRP)

15:59 28 October 2016

successfully catalyzes the oxidative cross-linking of a dendritic polyglycerol functionalized with phenol groups to hydrogels. The tunable cross-linking results in adjustable hydrogel properties. As the obtained materials are cytocompatible, the candidates showed a great potential for encapsulating living cells for regenerative therapy. The gel formation can be triggered by glucose and could be controlled under various environmental conditions.[166] In an attempt to generate micrometer-sized hydrogel, Haag and Seiffert fabricated particles that contain living cells with exquisite control through the use of droplet-based microfluidics and biocompatible polymers such as poly (ethylene glycol) (PEG) and dPGs. Currently established techniques involve the use toxic reactions with free radical for microgel gelation, which is severely detrimental for the viability of the encapsulated cells. To overcome this limitation, a novel technique was devised in this work that combines droplet microfluidic templating with bio-orthogonal thiol-ene click reactions to fabricate monodispersed, cell-laden microgel particles (Fig. 4.38). The gelation of these microgels is achieved via the nucleophilic Michael addition of dithiolated PEG macro cross-linkers to acrylated dPG building blocks and does not require any initiator. Microgel properties were systematically studied as a function of PEG linkers and macromonomer concentration to investigate the influence of these parameters on the viability and proliferation of encapsulated yeast cells. The encapsulation of mammalian cells including fibroblasts and lymphoblasts was also possible within these scaffolds.[167]

Higher ordered self-assembled architectures with functional importance have been fabricated using dPGs as the structural materials. The highly hydrophilic nature of dPGs, together with the high multi-functionality of the dendritic structures, allows the use of this polymer to design a new generation of hydrogels. Application of dendritic PG was reported in the field of tissue engineering as illustrated by the work of Alblas and coworkers who encapsulated bone marrow derived multipotent stromal cells (MSC) in a photopolymerizable hydrogel for the development of printed bone grafts.[168] They demonstrated the adverse effects of photopolymerization on the viability and cell cycle progression of exposed MSC monolayers, but their differentiation potential remained intact. The hydrogel with incorporated MSC supported

15:59 28 October 2016

survival and osteogenic differentiation of the embedded cells to a variable degree. Queiroz et al. prepared a novel bone scaffolding material by electrospinning solutions of dPGs that contained nanoparticles of hydroxyapatite (HA).[141] The potential use of the electrospun fibrous dPG–HA scaffolds for bone regeneration was evaluated in vitro with human osteoblasts ($SaSO_2$) in terms of alkaline phosphatase (ALP) activity of the cells and cytotoxicity. The biocompatibility evaluation of the dPG–HA provided encouraging indications for long-term safety. The electrospun fibers exhibited highest ALP activity and appeared to promote both proliferation and differentiation of human osteoblasts.

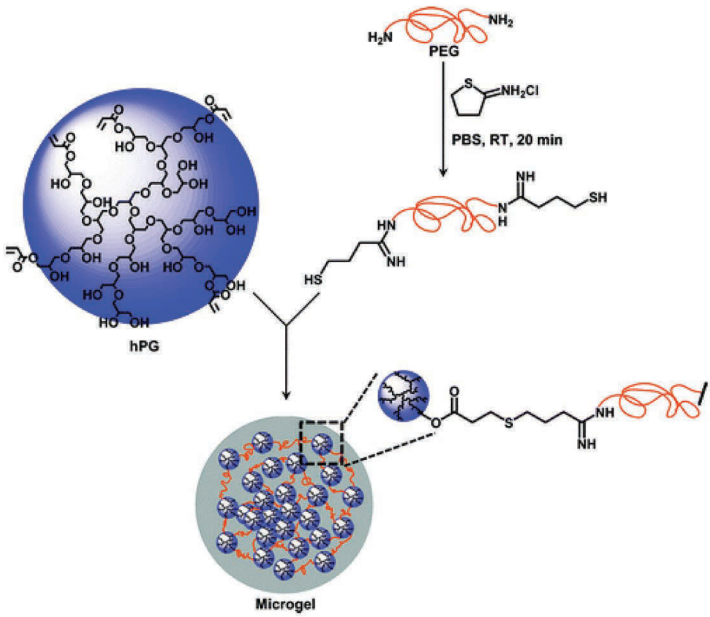



**Figure 4.38** Formation of Gel Particles by Cross-Linking of dPGs and PEG. Reprinted with permission from Ref. 167. Copyright (2012) American Chemical Society.

## Hierarchical application of dPGs to design nanomedical materials

Currently, aside from scaffolding and drug and gene delivery applications, dPGs have been introduced in the field of blood transfusion, organ preservation, antifouling surface coatings,

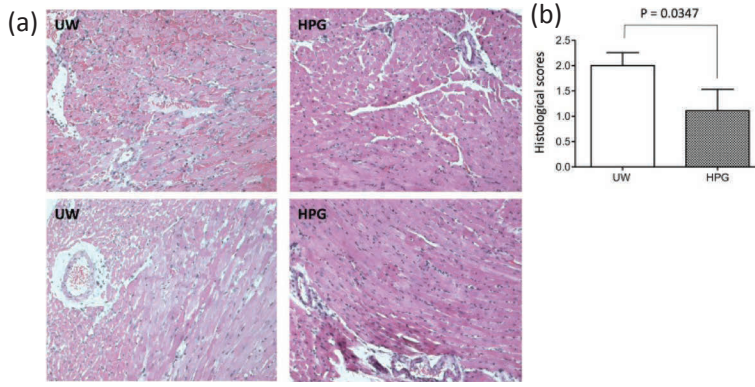



**Figure 4.39** Cold preservation with the dPG solution reduces cardiac inflammation and cell death in heart transplants. Donor hearts were treated with prolonged cold preservation in dPG solution vs. UW solution and transplanted. The grafts were harvested at 24 h after transplantation, and were formalin-fixed and paraffin-embedded. The graft injury was examined in H&E stained sections. Data are presented as a typical image of light microscopy, showing perivascular inflammation and cardiomyocyte necrosis.

15:59 28 October 2016

dialysis and in bioimaging. The following section highlights a subset of such research effort to illustrate the recent trend of dPG research. For example, hydroxyethyl starch (HES) has been used as a standard common colloid in organ preservation solutions, such as in University of Wisconsin (UW) solution, for preventing graft interstitial edema and cell swelling during cold preservation of donor organs. However, HES has undesirable characteristics, such as high viscosity leading to kidney injury, and aggregation of erythrocytes. The low intrinsic viscosity and compact, branched topology of dPGs have been utilized by Kizhakkedathu laboratory to design a potential alternative to HES for cold organ preservation. To this end, dPGs (MW—0.5 to 119 kDa) were synthesized by ring-opening multibranching polymerization of glycidol. As in vitro models, rat myocardiocytes and human endothelial cells were used and heart transplantation in mice was adopted as an in vivo model. Tissue damage or cell death was determined by both biochemical and histological analysis. Polyglycerol-based macromolecules were more compact with relatively low polydispersity index than HES in UW solution. Cold preservation

15:59 28 October 2016

of mouse hearts ex vivo in dPG solutions reduced organ damage in comparison to those in HES-based UW solution. Both size and concentration of dPGs contributed to the protection of the donor organs, for example, 1 kDa dPG at 3-wt% solution was superior to HES-based UW solution and other dPGs. Heart transplants preserved with dPG solution (1 kDa, 3%) as compared with those with UW solution were found to have a better functional recovery, less tissue injury and neutrophil infiltration in syngeneic recipients that survived longer in allogeneic recipients (Fig. 4.39). In cultured myocardiocytes or endothelial cells, significantly more cells survived after cold preservation with the dPG solution than those with the UW solution, which was positively correlated with the maintenance of intracellular adenosine triphosphate and cell membrane fluidity. It was conclusively shown that, dPG solution significantly enhanced the protection of hearts or cells during cold storage, suggesting that dPG is a promising colloid for the cold storage of donor organs and cells in transplantation.

Use of dPGs in preparation of antifouling surface coatings is historic, and has been constantly evolving. Recently, Haag and Grunwald combined nature's amazing bioadhesive catechol with biocompatible dPGs to prepare antifouling surfaces. Different amounts of catechol groups were immobilized on dPG structure for multivalent anchoring and cross-linking. The catecholic dPGs were coated on various surfaces including metal oxides, noble metals, ceramics, and polymers via simple incubation procedures. The effect of the catechol amount on the immobilization, surface morphology, stability, and antifouling performance of the coatings were studied. It was found that, both anchoring and cross-linking interactions provided by catechols can enhance the stability of the coatings. When the catechol groups on the dPG are underrepresented, the tethering of the coating is not effective, while an overrepresentation of catechol groups leads to protein adsorption and cell adhesion. Hence, only a critical amount of catechols were optimized that provided the coatings with both robust stability and optimum antifouling ability.[169] In a similar context, chemically active catecholic dPGs were used by Haag group to form a foundation layer on a versatile surface via multivalent anchoring and cross-linking, the activity of which was shielded by the bioinert catecholic hPGs. Mono-catecholic dPGs were able to terminate all of the free catechols to build a flexible bio-neutral

top layer. These coatings were found to prevent protein and cell adhesion with high efficiency (Fig. 4.40).[169]

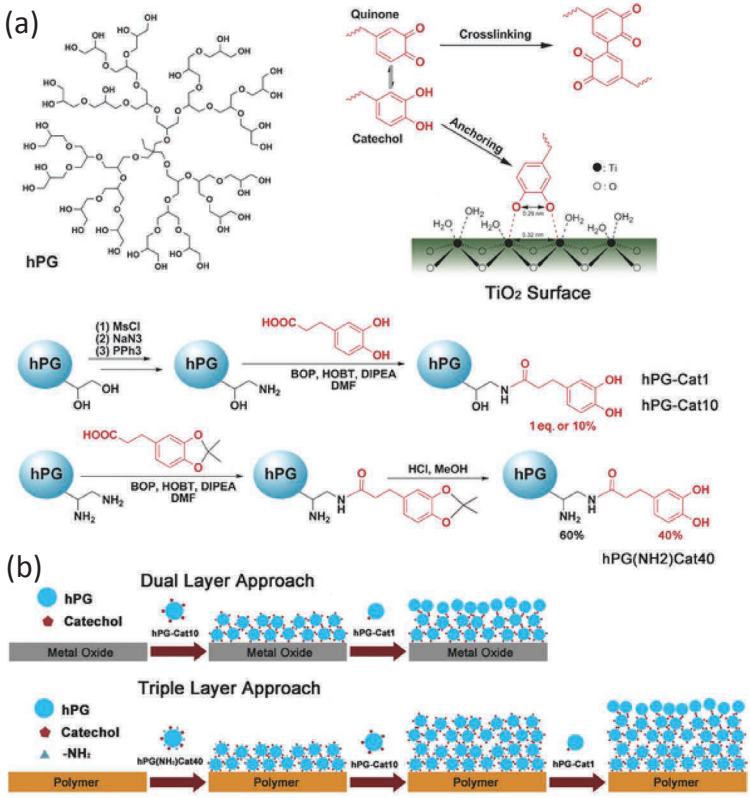



**Figure 4.40** (a) Synthesis of catechol functionalized dPGs and the mechanism of catechol anchoring and cross-linking. (b) Preparation of the dual layer and triple layer architecture coatings on metal oxide or polymer surfaces, respectively. Adapted with permission from John Wiley & Sons, Inc., Copyright 2014.

Voelcker et al. demonstrated a patterned biofunctionalization of antifouling dPG coatings on silicon and glass substrates. The ultra low-fouling dPG coatings afforded straightforward chemical handles for rapid bioconjugation of amine containing biomolecular species as realized by sodium periodate oxidation of terminal dPG diols to yield reactive aldehyde groups. Patterned microprinting of sodium periodate and cell adhesion mediating cyclic peptides

15:59 28 October 2016

containing the RGD sequence resulted in an array of covalently immobilized bioactive signals. When incubated with mouse fibroblasts, the dPG background resisted cell attachment whereas high-density cell adherence was observed on the peptide spots, resulting in high-contrast cell microarrays. It was also showed that a single-step, in situ functionalization of the dPG coatings by printing periodate and peptide concurrently was achievable, demonstrating the effectiveness of antifouling property of functionalized dPG graft polymer coatings in microarray applications for the first time.[170]

A key attribute for nanoparticles (NPs) that are used in medicine is the ability to avoid rapid uptake by phagocytic cells in the liver and other tissues. Poly (ethylene glycol) (PEG) coatings has been the gold standard in this regard for several decades. Saltzman et al. examined dPGs as an alternate to PEG coating on NPs. In earlier work, dPG was modified with amines and subsequently conjugated to poly (lactic acid) (PLA), but that approach compromised the ability of dPG to resist nonspecific adsorption of biomolecules. Hence a new synthetic approach was developed where a copolymer of PLA-dPG was synthesized by a one-step esterification. NPs were produced from a single emulsion using this copolymer and a fluorescent dye or an antitumor agent camptothecin (CPT) were encapsulated at high efficiency within the NPs. The nanoparticle efficiency was quantitatively compared to PLA-PEG NPs, produced through approaches that have been extensively optimized for drug delivery in humans. It was found that, in spite of being similar in size, drug release profile and in vitro cytotoxicity of dPG-based NPs showed significantly longer blood circulation and significantly less liver accumulation than PLA-PEG. CPT-loaded dPG-based nanoparticles showed higher stability in suspension and better therapeutic effectiveness against tumors in vivo than CPT-loaded PLA-PEG NPs indicating dPG as a suitable alternate to PEG as a surface coating for NPs in drug delivery.[171] In bioimaging territory, upconversion nanoparticle (UCNP) has been a new class of agent that is gaining prominence because of its unique optical properties. An ideal UCNP for bioimaging should simultaneously possess fine water dispersibility and favorable functional groups. Wei et al. presented a simple but effective method to synthesize an UCNP-based nanohybrid bearing a multihydroxy hyperbranched polyglycerol shell by combining

15:59 28 October 2016

a "grafting from" strategy with a ring-opening polymerization technique. The structure and morphology of the resulting UCNP-dPG nanohybrid were characterized in detail by Fourier transform infrared, $^{1}$H NMR, thermogravimetric analysis, and transmission electron microscopy measurements. The results showed that the amount of grafted dPG could be manipulated to control the thickness of the polymer layer on upconversion nanoparticles. The dPG coated nanoparticles showed high water dispersibility and strong and stable upconversion luminescence. Due to multiple surface hydroxyl groups, upconversion nanoparticles could be tailored by a representative fluorescent dye rhodamine B to afford a nanohybrid that simultaneously presents upconversion and downconversion luminescence. Preliminary biological studies demonstrate that dPG coated UCNP shows low cytotoxicity, high luminescent contrast, and deep light penetration depth showing their applicability in the field of bioimaging (Fig. 4.41).[172]

15:59 28 October 2016

Research to render nanodiamond as a useful materials scaffold has been gaining pace in recent years, in an effort to utilize them in bioimaging applications. Chen et al. used dPGs to coat nanodiamond for designing targeted drug delivery device for cancer chemotherapy which are capable to avoid nonspecific uptake by scavenging monocyte-macrophage system. To this purpose, a platform based on detonation nanodiamond with dPGs coating was prepared and was shown to be noninteracting with U937 macrophages. Targeting ligands, such as RGD peptide was then conjugated to dPG coated nanodiamond through multistep organic transformations. The resulting RGD conjugated nanodiamond was found to evade macrophage uptake but preferentially taken up by targeted A549 cancer cells that expresses RGD peptide receptors. Coated nanodiamonds were biocompatible with satisfactory hydrophilicity, owing to dPG coating. Frontline anticancer agent such as doxorubicin was loaded on to such dPG-coated nanodiamond through acid-labile hydrazone linkage. When the cellular uptake and cytotoxicity were compared against doxorubicin in A549 cells and U937 macrophages, it was observed that RGD conjugated nanodiamond scaffold showed superior cellular uptake and improved cytotoxicity selectively in A549 cells over U937 macrophages. Although nanodiamond coated with dPGs showed a slight increase of TNF-$\alpha$ production, highly selective

15:59 28 October 2016

drug delivery in tumor cells through specific uptake mechanisms indeed confirmed the potential of dPG as coating materials for generating compatible scaffolds for biomedical applications.[172] For modifying the surface of fluorescent silicon nanoparticles in an attempt to construct NPs with substantial hydrophilicity and high colloidal stability, Jana et al. utilized ring-opening polymerization of glycidol for generating dPG grafted silicon nanoparticles. The resultant hydrophilized nanoparticles were found to have hydrodynamic diameter within the range of 25 nm, showed low surface charge, and broad emission within the range of 450–700 nm with a fluorescence quantum yield of 6–9%. The dPG coated silicon nanoparticles were immobilized with cyclic RGD peptide using the conventional bioconjugation chemistry, and used for specific targeting to $\alpha v\beta_3$ integrin overexpressed cervical cancer cells and glioblastoma cells, indicating their potential application for in vivo bioimaging applications.[173] Muller et al. covalently grafted dPGs on the surface of superparamagnetic iron oxide nanoparticles. In the first stage, superparamagnetic magnetite nanoparticles were prepared by co-precipitation technique in aqueous media, followed by the surface modification of the nanoparticle with reactive groups that allow grafting of oligoglycerols by ring-opening anionic polymerization mediated by n-bulyllithium as initiator. The magnetometry, relaxometry and phantom MRI experiments of this highly stable ferrofluid showed its high potential as a negative MRI contrast agent. Calculated $r_1$ and $r_2$ relaxivities at different magnetic fields were higher than the values reported for commercially available iron oxide contrast agents. The in vivo MRI studies showed that, after intravenous injection into mice, the particles produced a strong negative contrast in liver and kidneys, which persisted for 80 min (in liver) to 110 min (in kidneys). The negative contrast of the liver and kidneys weakened over the time, suggesting that polyglycerol coating renders the nanoparticles stealth and possibly optimal for renal excretion.[174]

Proteins are surface-active molecules that undergo nonspecific adsorption when getting in contact with surfaces such as the primary packaging material. This process is critical as it may cause a loss of protein content or protein aggregation. To prevent unspecific adsorption, protein repellent coatings are of high

15:59 28 October 2016

interest. Towards this direction, coating of industrially relevant borosilicate glass vials with linear methoxylated polyglycerol, methoxylated and nonmethoxylated dendritic polyglycerol was performed. Although all the coatings provide excellent protein repellent effects, the nonmethoxylated dPG coating performed best. The protein repellent properties were maintained also after applying industrial relevant sterilization methods (≥200°C). Marginal differences in antibody stability between formulations stored in bare glass vials and coated vials were detected after 3 months' storage and the protein repellent effect remained largely stable. The results indicated that, dPG can be suitable new material candidate for the coating of primary packaging material of proteins which significantly reduces protein adsorption and enhances product shelf-life of biologics.[175]

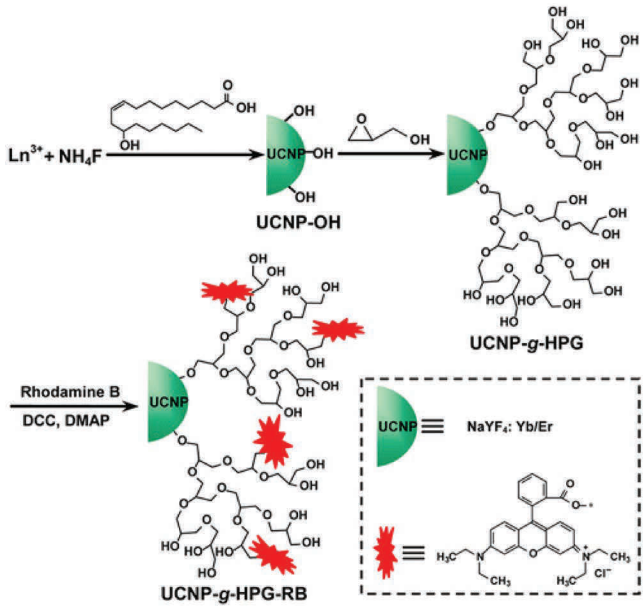



**Figure 4.41** Synthetic Route to UCNP-g-dPG and Modification of the Grafted dPG with Fluorescent Dye. Reprinted with permission from Ref. 172b. Copyright (2014) American Chemical Society.

The formation of hydrogels on surfaces is a frequently used strategy to render the surfaces biorepulsive, and towards this direction Layering with dPGs have become an attractive strategy

15:59 28 October 2016

alternative to the frequently used PEGs. A facile strategy was adopted by Terfort et al. to covalently graft polyglycerol layers onto surfaces by first depositing an aminopropylsiloxane layer, which acts as an initiator layer for the ring-opening polymerization of 2-(hydroxymethyl) oxirane (glycidol). For silicon surfaces, the resulting polyglycerol layers started inhibiting for E. coli build-up at a thickness of 2 nm and reached their highest bacterial repulsion (98%) at thicknesses of 7 nm or larger. This deposition strategy promises general applicability because the formation of aminopropylsiloxane layers has already been established with a broad-spectrum of materials.[176] Modulation of cell surface properties via functional modification is of great interest in cell-based therapies, drug delivery, and in transfusion. In an elegant study, Red Blood Corpuscles have been modified with dPGs, and in vivo circulation, immunogenicity, and mechanism of clearance of dPG-modified red blood cells (RBCs) were evaluated. The circulation half-life of modified cells can be modulated by controlling the polymer graft concentration on RBCs; low graft concentrations (0.25 and 0.5 mM) showed normal circulation as that of control RBCs. Molecular weight of dPG did not found to affect the circulation of modified RBCs. Grafting of dPG on RBCs reduced CD47 self-protein accessibility in a graft concentration-dependent fashion. Modified RBCs were not observed to be immunogenic, as is evident from their similar circulation profile upon repeated administration in mice and monitoring over 100 days. Histological examination of the spleen, liver, and kidneys of the mice injected with dPG-modified RBCs revealed distinct differences, such as elevated iron deposits and an increase in the number of CD45 expressing cells at high graft concentration of dPGs (1.5 mM); no changes were seen at low graft concentration. The absence of iron deposits in the white pulp region of the spleen and its presence in the red pulp region indicates that the clearance of functional RBCs occurs in the venous sinuses mechanical filtering system, similar to the clearance of unmodified senescent RBCs. Modification of RBCs with dPGs were found to provide camouflage of a large number of minor blood group antigens on human RBCs, hence demonstrating the utility of the approach in chronic transfusion. The normal circulation, nonimmunogenic nature, and the potential to modulate the circulation time of modified cells without toxicity

make this dPG-based cell surface modification an attractive strategy for drug delivery and other cell-based therapies.[177]

Since stem cells emerged as a new generation of medicine, there are increasing efforts to deliver stem cells to a target tissue via intravascular injection. However, the therapeutic stem cells lack the capacity to detect and adhere to the target tissue. Therefore, Zimmerman and Kong et al. synthesized a bioactive dPG scaffold that can noninvasively associate with stem cells and further guide them to target sites, such as inflamed endothelium. The overall process is analogous to the way in which leukocytes are mobilized to the injured endothelium as illustrated in Fig. 4.42.[178]

15:59 28 October 2016

**Key Ideas of Section 4.5.4**

- Nanogels are highly-monodispersed polymeric nano-aggregates cross-linked under template conditions and have prospective applications in the areas of regenerative therapy, tissue-engineering and for generation of biomimetic extracellular matrix materials.
- Biodegradable dPG nanogels and hydrogels were prepared through an acid-catalyzed ring-opening polyaddition of disulfide containing polyols and polyepoxides to generate programmable nanogel scaffold that breaks down within the systemic circulation after a specified period of time. Nanogels have been prepared with dPGs within the size range of 25–350 nm, which were rapidly internalized within cellular cytoplasm, and primarily accumulates in the perinuclear region.
- It was found that dPGs nanogels with 50 nm diameters showed 7 × 103 fold more efficiency in inhibiting the binding and fusion to influenza virus than hyperbranched PG with a diameter of 3 nm. PG nanogels have recently been prepared with stimuli-responsive properties.
- Using droplet microfluidic templating, combined with bio-orthogonal thiol-ene click reactions, monodispersed nanogels based on dPGs have been fabricated encapsulating living cells avoiding the currently established techniques that involve the use toxic reactions of using free-radicals for microgelation.
- Currently, aside from scaffolding and drug and gene delivery applications, dPGs have been introduced in the field of blood transfusion, organ preservation, anti-fouling surface coatings, dialysis and in bioimaging.

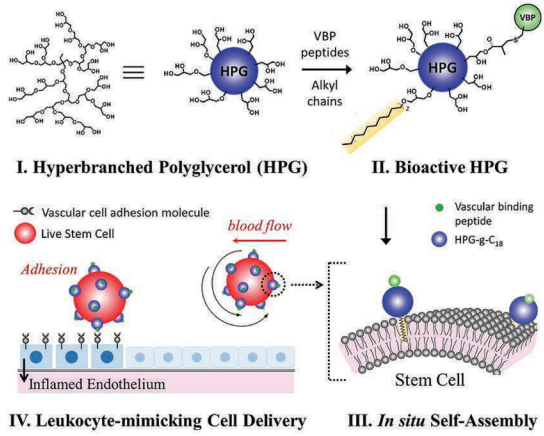



**Figure 4.42** A bioactive dPG scaffold covalently modified with octadecyl chains and vasculature-binding peptides (VBPs) was utilized as a novel Cell-Guidance Molecule that can associate with stem cells and further guide them to target defective vasculature. Reprinted with permission from Ref. 178. Copyright (2013) American Chemical Society.

## 4.6 Opportunities

The overwhelming promise of nanotechnology in medical application critically relies upon the availability of sustainable materials that permits control and adjustment at molecular, synthetic, assembly and function level. Materials that can be synthesized in an economic, low cost route and provide a postsynthetic flexibility towards facile bottom-up approach to generate value-added hierarchical materials are of particular necessity. Such systems will definitely gain strategic advantage to meet the exclusive demands of nanotechnology. As scaffold materials for fabricating diversified nanostructures, dPGs has proved its suitability in the areas of drug delivery, pharmaceutical excipient and disease sensors. In the next couple of decades, a range of medical applications at the nanoscale will be developed, where dPG can easily and efficiently fit in. Several challenges and opportunities exist in developing dPG-based architectures, including but not limited to its biodegradability and biodistribution. To this end, nanogels of dPG are undoubtedly superior candidate

15:59 28 October 2016

15:59 28 October 2016

as they can be designed with responsive cross-linkers that can be cleaved off by enzyme action resulting in smaller oligoglycerols, which in turn can be eliminated through renal and metabolic clearance. Generation of dPGs with such programmable degradation can definitely provide a strategic advantage so far nonspecific accumulation in normal and hepatic tissues is concerned. Incorporating tissue-targeting motif onto the PG surface can further minimize the off-target toxicity of dPG–drug conjugate. Such motif might include simple small molecules such as folic acid, or larger peptides, antibodies and aptamers that can selectively recognize diseased areas. Changing peripheral functional group, size and shape of the nano-architecture can further enhance the targeting capacity of dendritic PG-conjugates. Such modulation of intrinsic structural properties of dPGs will not only enable them to engage a specific cluster of cells but also allow them to partition between physiological membranes and disease micro-environment in a controlled fashion. With orthogonal stimuli-responsive modalities, dPGs can constitute an intelligent platform to deliver multiple drugs at temporally and spatially differentiated kinetics. In the realm of hydro- and nanogels, dPGs have already been used for regenerative medicine and for cellular encapsulation. The affinity of cellular growth within the gel network can be further reinforced by incorporating proliferative peptides and growth factors along the dendritic scaffold. Hybridization of dPGs with linear architectures has generated a number of interesting molecular motifs, and surely these structures can be further investigated for their biocompatibility and efficiency as drug delivery vehicles in unimolecular or multimolecular format. Although a series of new architectures can be potentially constructed based on dPGs with unforeseen activity and topology, selection of an appropriate disease and biological model will always remain a challenge. Inclusion of dPG in a solid-pharmaceutical formulation is another broad field of studies, which has remained mostly unexplored. Extensive structure-activity studies of dPG under GMP-conditions might be a pre-requisite to utilize this highly branched macromolecule more ubiquitously in drug and consumer applications. As a PEG-like molecule with multiple functionalities, dPGs clearly exhibit promise and prospect as a new platform molecule for bridging the gap between chemical sciences, functional materials, and polymer therapeutics. Intriguingly, by breaking new

grounds in the above-mentioned areas, dPGs can be utilized for bringing about conspicuous difference in nanomedicine delivery, distribution and efficacy.

## 4.7 Conclusions

As the emergence and translation of nanomedicine into the clinics continue, the demand for smart and innovative polymeric materials also becomes inevitable and quite critical. Not only as scaffold materials, but also as a macromolecule with biocompatibility, functionality and sustainable scalability, the rise and evolution of dPGs continues in a robust and recognizable pace. It can be perceived that, the use of dPGs in nanomedicine will increase in the foreseeable future because of its sustainable synthesis and postsynthetic modifications. The sheer amount of research that has been conducted on the prospect of using dPGs in biomedical setting clearly reflects the fact that the scientific community is desperately looking forward for a suitable advanced materials that can combine multivalency with biocompatibility, a combination that is difficult to achieve by many, if not the most, of the established material systems. Although a number of multivariate, well-controlled toxicity and metabolic studies are yet to be performed, this chapter clearly shows the suitability of dPG in medical applications, and that their clear placement in the future arsenal of nanomedicine is certainly confirmed.

15:59 28 October 2016

## References

1. (a) Tomalia, D. A., Reyna, L. A., Svenson, S., *Biochem. Soc. Trans.*, 2007, 35(Pt 1), 61–67; (b) Klajnert, B., Bryszewska, M., *Acta Biochim. Pol.*, 2001, 48(1), 199–208; (c) Zeng, F., Zimmerman, S. C., *Chem. Rev.*, 1997, 97(5), 1681–1712.
2. Wooley, K. L., Fréchet, J. M. J., Hawker, C. J., *Polymer*, 1994, 35, 4489–4495.
3. (a) Hawker, C. J., Malmström, E., Frank, C. W., Kampf, J. P., *J. Am. Chem. Soc.*, 1997, 119, 9903–9904; (b) Mourey, T. H., Turner, S. R., Rubinstein, M., Fréchet, J. M. J., Hawker, C. J., Wooley, K. L., *Macromolecules*, 1992, 25, 2401–2406; (c) Wooley, K. L., Hawker, C. J., Pochan, J. M., Fréchet, J. M. J., *Macromolecules*, 1993, 26, 1514–1519.

15:59 28 October 2016


4. (a) Hawker, C. J., Farrington, P. J., Mackay, M. E., Wooley, K. L., Fréchet, J. M. J., *J. Am. Chem. Soc.*, 1995, 117, 4409–4410; (b) Grayson, S. M., Fréchet, J. M. J., *Chem. Rev.*, 2001, 101, 3819–3867.
5. Frey, H., Haag, R., *J. Biotechnol.*, 2002, 90(3–4), 257–267.
6. Stiriba, S. E., Frey, H., Haag, R., *Angew. Chem.*, 2002, 114, 1385–1390.
7. (a) Calderon, M., Quadir, M. A., Sharma, S. K., Haag, R., Dendritic polyglycerol for biomedical applications. *Adv. Mater.*, 2010, 22, 190–218; (b) Khandare, J., Calderon, M., Dagia, N., Haag, R., *Chem. Soc. Rev.*, 2012, 41, 2824–2848.
8. (a) Jarayaman, M., Fréchet, J. M. J., *J. Am. Chem. Soc.*, 1998, 120, 12996; (b) Ihre, H., De Jesus, O. L. P., Fréchet, J. M. J., *J. Am. Chem. Soc.*, 2001, 123, 5908; (c) Grayson, S. M., Fréchet, J. M. J., *J. Am. Chem. Soc.*, 2000, 122, 10335–10344; (d) Cho, B.-K., Jain, A., Nieberle, J., Mahajan, S., Wiesner, U., *Macromolecules*, 2004, 37, 4227.
9. (a) Sunder, A., Türk, H., Mülhaupt, R., Haag, R., Frey, H., *Macromolecules*, 2000, 33, 7682–7692; (b) Sunder, A., Hanselmann, R., Frey, H., Mülhaupt, R., *Macromolecules*, 1999, 32, 4240–4246; (c) Sunder, A., Mülhaupt, R., Frey, H., *Macromolecules*, 2000, 33, 309–314; (d) Magnusson, H., Malmström, E., Hult, A., *Macromol. Rapid Commun.*, 1999, 20, 453; (e) Magnusson, H., Malmström, E., Hult, A., *Macromolecules*, 2001, 34, 5786; (f) Bednarek, M., Biedron, T., Helinski, J., Kaluzynski, K., Kubisa, P., Penczek, S., *Macromol. Rapid Commun.*, 1999, 20, 369; (g) Xu, Y., Gao, C., Kong, H., Yan, D., Luo, P., Li, W., Mai, Y., *Macromolecules*, 2004, 37, 6264.
10. (a) Dodds, D. R., Gross, R. A., *Science*, 2007, 318(5854), 1250–1251; (b) Pagliaro, M., Ciriminna, R., Kimura, H., Rossi, M., Della Pina, C., *Angew. Chem. Int. Ed.*, 2007, 46(24), 4434–4440.
11. Wilms, D., Stiriba, S. E., Frey, H., *Acc. Chem. Res.*, 2010, 43, 129–141.
12. Thomas, A., Müller, S. S., Frey, H., *Biomacromoleules*, 2014, 15, 1935–1954.
13. Sandler, S. R., Berg, F. E., *J. Polym. Sci., Polym Chem. Ed.*, 1966, 4, 1253.
14. Tsuruta, T., Inoue, S., Koinuma, H., *Macromol. Chem.*, 1968, 112, 58.
15. Haouet, A., Sepulchrre, M., Spassky, N., *Eur. Polym. J.*, 1983, 19, 1089.
16. (a) Taton, D., Le Borgne, A., Sepulchre, M., Spassky, N., *Macromol. Chem. Phys.*, 1994, 195, 139; (b) Vandenberg, E. J., Mullis, J. C., Juver, R. S., Miller, T., Nieman, R. A., *J. Polym. Sci., Polym. Chem. Ed.*, 1989, 27, 3113.
17. Dworak, A., Wałach, W., Trzebicka, B., *Macromol. Chem. Phys.*, 1995, 196, 1963–1970.

15:59 28 October 2016


18. Tokar, R., Kubisa, P., Penczek, S., Dworak, A., *Macromolecules*, 1994, 27, 320–322.
19. Labbé, A., Carlotti, S., Deffieux, A., Hirao, A., *Macromol. Symp.*, 2007, 249–250, 392–397.
20. Thomas, A., Müller, S., Holger, F., *Biomacromolecules*, 2014, 15, 1935–1954.
21. Erberich, M., Keul, H., Möller, M., *Macromolecules*, 2007, 40, 3070–3079.
22. (a) Stiriba, S. E., Kautz, H., Frey, H., *J. Am. Chem. Soc.*, 2002, 124(33), 9698–9699; (b) Kumar, K. R., Brooks, D. E., *Macromol. Rapid Commun.*, 2005, 26, 155–159.
23. (a) Haag, R., Wyszogrodzka, M., Heek, T., Mivenion, G., *Europäische Patentanmeldung EP08152554.5. Internationale Patentanmeldung PCT/EP2009/052786* 2007; (b) Wyszogrodzka, M., Haag, R., *Langmuir*, 2009, 25(10), 5703–5712.
24. Halacheva, S., Rangelov, S., Tsvetanov, C., *Macromolecules*, 2006, 39, 6845–6852.
25. Wurm, F., Dingels, C., Frey, H., Klok, H.-A., Wurm, F., Dingels, C., Frey, H., Klok, H.-A. *Biomacromolecules*, 2012, 13(4), 1161–1171.
26. Meyer, J., Keul, H., Moller, M., *Macromolecules*, 2011, 44, 4082–4091.
27. (a) Sedo, J., Saiz-Poseu, J., Busque, F., Ruiz-Molina, D. A. M., *Adv Mater*, 2013, 25(5), 653–701; (b) Faure, E., Falentin-Daudre, C., Jerìôme, C., Lyskawa, J., Fournier, D., Woisel, P., Detrembleur, C., *Prog. Polym. Sci.*, 2013, 38(1), 236–270.
28. Thomas, A., Bauer, H., Schilmann, A.-M., Fischer, K., Tremel, W., Frey, H., *Macromolecules*, 2014, 47(14), 4557–4566.
29. Wilms, V. S., Bauer, H., Tonhauser, C., Schilmann, A.-M., Müller, M.-C., Tremel, W., Frey, H., *Biomacromolecules*, 2013, 14(1), 193–199.
30. Hofmann, A. M., Wurm, F., Frey, H., *Macromolecules*, 2011, 44(12), 4648–4657.
31. Hofmann, A. M., Wipf, R., Stühn, B., Frey, H., *Macromolecules*, 2011, 44(17), 6767–6775.
32. Hofmann, A. M., Wurm, F., Hühn, E., Nawroth, T., Langguth, P., Frey, H., *Biomacromolecules*, 2010, 11(3), 568–574.
33. Moers, C., Nuhn, L., Wissel, M., Stangenberg, R., Mondeshki, M., Berger-Nicoletti, E., Thomas, A., Schaffel, D., Koynov, K., Klapper, M., Zentel, R., Frey, H., *Macromolecules*, 2013, 46, 9544–9553.
34. Wurm, F., Kemmer-Jonas, U., Frey, H., *Polym. Int.*, 2009, 58(9), 989–995.

35. O'Brien, R. D., *Fats and Oils: Formulating and Processing for Applications*, 2nd ed.; CRC Press, LLC: Boca Raton, FL, 2004.

36. Weinhart, M., Grunwald, I., Wyszogrodzka, M., Gaetjen, L., Hartwig, A., Haag, R., *Chem. Asian J.*, 2010, 5(9), 1992–2000.

37. Weinhart, M., Becherer, T., Schnurbusch, N., Schwibbert, K., Kunte, H.-J., Haag, R., *Adv. Eng. Mater.*, 2011, 13(12), B501–B510.

38. (a) Dworak, A., Panchev, I., Trzebicka, B., Walach, W., *Macromol. Symp.*, 2000, 153, 233–242; (b) Dworak, A., Panchev, I., Trzebicka, B., Walach, W., *Polym. Bull.*, 1998, 40(4–5), 461–468.

39. Basinska, T., Slomkowski, S., Dworak, A., Panchev, I., Chehimi, M. M., *Colloid Polym. Sci.*, 2001, 279(9), 916–924.

40. (a) Basinska, T., Slomkowski, S., Kazmierski, S., Dworak, A., Chehimi, M. M., *J. Polym. Sci. Part A: Polym. Chem.*, 2004, 42(3), 615–623; (b) Basinska, T., Slomkowski, S., Kazmierski, S., Chehimi, M. M., *Langmuir*, 2008, 24(16), 8465–8472; (c) Basinska, T., Krolik, S., Slomkowski, S., *Macromol. Symp.*, 2009, 281(1), 96–105.

41. (a) Slomkowski, S., Basinska, T., *Macromol. Symp.*, 2010, 295(1), 13–22; (b) Basinska, T., Slomkowski, S., *Chem. Pap.*, 2012, 66(5), 352–368.

42. Thomas, A., Wolf, F. K., Frey, H., *Macromol. Rapid Commun.*, 2011, 32(23), 1910–1915.

43. Stiriba, S. E., Kautz, H., Frey, H., *J. Am. Chem. Soc*, 2002, 124(33), 9698–9699.

44. Kumar, K. R., Brooks, D. E., *Macromol. Rapid Commun.*, 2005, 26(3), 155–159.

45. Dworak, A., Trzebicka, B., Wałach, W., Utrata, A., Tsvetanov, C., *Macromol. Symp.*, 2004, 210, 419–426.

46. Dworak, A., Trzebicka, B., Utrata, A., Walach, W., *Polym. Bull.*, 2003, 50(1–2), 47–54.

47. Penczek, S., Pretula, J., Kaluzynski, K., *J. Polym. Sci., Part A: Polym. Chem.*, 2004, 42(3), 432–443.

48. (a) Köhler, J., Keul, H., Möller, M., *Chem. Commun.*, 2011, 47(28), 8148–8150; (b) Köhler, J., Marquardt, F., Keul, H., Möller, M., *Macromolecules*, 2013, 46(10), 3708–3718.

49. Köhler, J., Marquardt, F., Teske, M., Keul, H., Sternberg, K., Möller, M., *Biomacromolecules*, 2013, 14(11), 3985–3996.

50. Wyszogrodzka, M., Möws, K., Kamlage, S., Wodzinska, J., Plietker, B., Haag, R., *Eur. J. Org. Chem.*, 2008, 53–63.

51. Elmer, S. L., Man, S., Zimmerman, S. C., *Eur. J. Org. Chem.*, 2008, 2008, 3845–3851.

15:59 28 October 2016

15:59 28 October 2016


52. Wyszogrodzka, M., Haag, R., *Chem. Eur. J.*, 2008, 14, 9202–9214.
53. Haag, R., Sunder, A., Stumbé, J. F., *J. Am. Chem. Soc.*, 2000, 122, 2945–2955.
54. (a) Garcia-Bernabé, A., Krämer, M., Olàh, B., Haag, R., *Chemistry*, 2004, 10, 2822–2830; (b) Thomann, Y., Haag, R., Brenn, R., Delto, R., Weickman, H., Thomann, R., Mülhaupt, R., *Macromol. Chem. Phys.*, 2005, 206, 135–141.
55. (a) Kim, Y. H. J., *Polym. Sci. Polym. Chem.*, 1998, 36, 1685; (b) Voit, B. I., *Acta Polym.*, 1995, 46, 87.
56. Frechet, J. M., Henmi, M., Gitsov, I., Aoshima, S., Leduc, M. R., Grubbs, R. B., *Science*, 1995, 269(5227), 1080–1083.
57. Hawker, C. J., Fréchet, J. M. J., Grubbs, R. B., Dao, J. J., *J. Am. Chem. Soc.*, 1995, 117, 10763.
58. Hanselmann, R., Holter, D., Frey, H., *Macromolecules*, 1998, 31, 3790–3801.
59. Haag, R., Mecking, S., Türk, H., *Deutsche Patentanmeldung DE 10211664 A1* 2004.
60. Kainthan, R. K., Muliwan, E. B., Hatzikiriakos, S. G., Brooks, D. E., *Macromolecules*, 2006, 39, 7708–7717.
61. Wilms, D., Wurm, F., Nieberle, J., Böhm, P., Kemmer-Jonas, U., Frey, H., *Macromolecules*, 2009, 42, 3230–3236.
62. Knischka, R., Lutz, P. J., Sunder, A., Frey, H., *Polym. Mater. Sci. Eng.*, 2001, 84, 945.
63. Burakowska, E., Haag, R., *Macromolecules*, 2009, 42, 5545–5550.
64. Barriau, E., Pastor-Perez, L., Berger-Nicoletti, E., Kilbinger, A. F. M., Frey, H., Stiriba, S. E., *J. Polym. Sci., Polym. Chem.*, 2008, 46, 2049–2061.
65. Kainthan, R. K., Janzen, J., Kizhakkedathu, J. N., Devine, D. V., Brooks, D. E., *Biomaterials*, 2008, 29(11), 1693–1704.
66. Wurm, F., Nieberle, J., Frey, H., *Macromolecules*, 2008, 41, 1184–1188.
67. Burgath, A., Sunder, A., Neuner, I., Mülhaupt, R., Frey, H., *Macromol. Chem. Phys.*, 2000, 2000, 792–797.
68. Maier, S., Sunder, A., Frey, H., Mülhaupt, R., *Macromol. Rapid Commun.*, 2000, 21, 226–230.
69. Wurm, F., Klos, J., Raeder, H. J., Frey, H., *J. Am. Chem. Soc.*, 2009, 131(23), 7954–7955.
70. Wurm, F., Hofmann, A. M., Thomas, A., Dingels, C., *Macromol. Chem. Phys.*, 2010, 211(8), 932–939.

15:59 28 October 2016


71. Lee, S., Saito, K., Lee, H.-R., Lee, M. J., Shibasaki, Y., Oishi, Y., Kim, B.-S., *Biomacromolecules*, 13(4), 1190–1196.
72. Roller, S., Zhou, H., Haag, R., *Mol. Divers.*, 2005, 9(4), 305–316.
73. Haag, R., Stumbé, J. F., Sunder, A., Frey, H., Hebel, A., *Macromolecules*, 2000, 33, 8158–8166.
74. Sisson, A. L., Papp, I., Landfester, K., Haag, R., *Macromolecules*, 2009, 42, 556–559.
75. Calderon, M., Welker, P., Licha, K., Graeser, R., Kratz, F., Haag, R., *J. Control. Release*, 2010, 148, e24–e25.
76. Oudshoorn, M. H., Penterman, R., Rissmann, R., Bouwstra, J. A., Broer, D. J., Hennink, W. E., *Langmuir*, 2007, 23(23), 11819–11825.
77. Radke, W., Litvinenko, G., Muller, A. H. E., *Macromolecules*, 1998, 31, 239–248.
78. Holter, D., Burgath, A., Frey, H., *Acta Polym.*, 1997, 48, 30–35.
79. Lach, C., Frey, H., *Macromolecules*, 1998, 31, 2381–2383.
80. Kainthan, R. K., Muliawan, E. B., Hatzikiriakos, S. G., Brooks, D. E., *Macromolecules*, 2006, 39, 7708–7717.
81. Kainthan, R. K., Janzen, J., Levin, E., Devine, D. V., Brooks, D. E., *Biomacromolecules*, 2006, 7(3), 703–709.
82. (a) Kainthan, R. K., Hester, S. R., Levin, E., Devine, D. V., Brooks, D. E., *Biomaterials*, 2007, 28(31), 4581–4590; (b) Kainthan, R. K., Brooks, D. E., *Biomaterials*, 2007, 28(32), 4779–4787.
83. Kainthan, R. K., Mugabe, C., Burt, H. M., Brooks, D. E., *Biomacromolecules*, 2008, 9(3), 886–895.
84. Calderon, M., Quadir, M. A., Sharma, S. K., Haag, R., *Adv. Mater.*, 2010, 22, 190–218.
85. Haag, R., Kratz, F., *Angew. Chem. Int. Ed.*, 2006, 45(8), 1198–1215.
86. Xu, S., Luo, Y., Graeser, R., Warnecke, A., Kratz, F., Hauff, P., Licha, K., Haag, R., *Bioorg. Med. Chem. Lett.*, 2009, 19, 1030–1034.
87. Khandare, J., Mohr, A., Calderon, M., Welker, P., Licha, K., *Biomaterials*, 2010, 31, 4268–4277.
88. Ooya, T., Huh, K. M., Saitoh, M., Tamiya, E., Park, K., *Sci. Technol. Adv. Mater.*, 2005, 6, 452–456.
89. Ooya, T., Lee, J., Park, K., *J. Control. Release*, 2003, 93, 121–127.
90. Ooya, T., Lee, J., Park, K., *Bioconjug. Chem.*, 2004, 15, 1221–1229.
91. Allen, T. M., Cullis, P. R., *Science*, 2004, 303(5665), 1818–1822.

15:59 28 October 2016


92. Tziveleka, L.-A., Kontoyianni, C., Sideratou, Z., Tsiourvas, D., Paleos, C. M., *Macromol*. *Biosci*., 2005, 6, 161–169.

93. Kuchler, S., Radowski, M. R., Blaschke, T., Dathe, M., Plendl, J., Haag, R., Schafer-Korting, M., Kramer, K. D., *Eur*. *J*. *Pharm*. *Biopharm*., 2009, 71(2), 243–250.

94. Radowski, M. R., Shukla, A., von Berlepsch, H., Böttcher, C., Pickaert, G., Rehage, H., Haag, R., *Angew*. *Chem*. *Int*. *Ed*., 2007, 46(8), 1265–1269.

95. Haxton, K. J., *Dalton Trans*., 2008, 5872–5875.

96. Kojima, C., Yoshimura, K., Harada, A., Sakanishi, Y., Kono, K., *Bioconjug*. *Chem*., 2009.

97. Wan, D., Li, Z., Huang, J., *J*. *Polym*. *Sci*. *Part A: Polym*. *Chem*., 2005, 43, 5458–5464.

98. Mugabe, C., Hadaschik, B. A., Kainthan, R. K., Brooks, D. E., Al, S., Gleave, M. E., Burt, H. M., *BJU Int*., 2009, 103 (7), 978–986.

99. Kumar, S., Alnasif, N., Fleige, E., Kurniasih, I., Kral, V., Haase, A., Luch, A., Weindl, G., Haag, R., Schäfer-Korting, M., Hedtrich, S., *Eur*. *J*. *Pharm*. *Biopharm*., 2014, 88(3), 625–634.

100. Kumari, M., Gupta, S., Achazi, K., Böttcher, C., Khandare, J., Sharma, S. K., Haag, R., *Macromol*. *Rapid Commun*., 2015, 36(2), 254–261.

101. Demina, T. V., Budkina, O. A., Badun, G. A., Melik-Nubarov, N. S., Frey, H., Müller, S. S., Nieberle, J., Grozdova, I. D., *Biomacromolecules*, 2014, 15(7), 2672–2681.

102. Son, S., Shin, E., Kim, B. S., *Biomacromolecules*, 2014, 15(2), 628–634. *doi: 10.1021/bm401670t*.

103. Zarrabi, A., Shokrgozar, M. A., Vossoughi, M., Farokhi, M., *J*. *Mater*. *Sci*. *Mater*. *Med*., 2014, 25(2), 499–506.

104. Adeli, M., Fard, A. K., Abedi, F., *Nanomedicine*, 2013, 9(8), 1203–1213.

105. Rodrigo, A. C., Malhotra, S., Böttcher, C., Adeli, M., Haag, R., *RSC Adv*., 2014, 4, 61656–61659.

106. Oikawa, Y., Lee, S., Kim do, H., Kang, D. H., Kim, B. S., Saito, K., S., S., Oishi, Y., Y., S., *Biomacromolecules*, 2013, 14(7), 2171–2178.

107. Shenoi, R. A., Lai, B. F., Imran ul-haq, M., Brooks, D. E., Kizhakkedathu, J. N., *Biomaterials*, 2013, 34(25), 6068–6081.

108. Zhang, X., Zhang, X., Yu, P., Han, Y., Li, Y., Li, C., *J*. *Pharm*. *Sci*., 2013, 102(1), 145–153. *doi: 10.1002/jps.23344*. *Epub 2012 Nov 6*.

109. Imran ul-haq, M., Lai, B. F., Chapanian, R., Kizhakkedathu, J. N., *Biomaterials*, 2012, 33(35), 9135–9147. doi: 10.1016/j.biomaterials. 2012.09.007. Epub 2012 Sep 25.

15:59 28 October 2016


110. Hu, M., Chen, M., Li, G., Pang, Y., Wang, D., Wu, J., Qiu, F., Zhu, X., Sun, J., *Biomacromolecules*, 2012, 13(11), 3552–3561.

111. Shenoi, R. A., Lai, B. F., Kizhakkedathu, J. N., *Biomacromolecules*, 2012, 13(10), 3018–3030.

112. Bao, H., Jin, X., Li, L., Lv, F., Liu, T., *J. Mater. Sci. Mater. Med.*, 2012, 23(8), 1891–1901.

113. Imran ul-haq, M., Hamilton, J. L., Lai, B. F., Shenoi, R. A., Horte, S., Constantinescu, I., Leitch, H. A., Kizhakkedathu, J. N., *ACS Nano*, 2013, 7(12), 10704–10716.

114. Mendelson, A. A., Guan, Q., Chafeeva, I., da Roza, G. A., Kizhakkedathu, J. N., Du, C., *Perit. Dial. Int.*, 2013, 33(1), 15–27.

115. Du, C., Mendelson, A. A., Guan, Q., Chapanian, R., Chafeeva, I., da Roza, G., Kizhakkedathu, J. N., *Biomaterials*, 2014, 35(5), 1378–1389.

116. Chapanian, R., Constantinescu, I., Rossi, N. A., Medvedev, N., Brooks, D. E., Scott, M. D., Kizhakkedathu, J. N., *Biomaterials*, 2012, 33(31), 7871–7883.

117. Saatchi, K., Soema, P., Gelder, N., Misri, R., McPhee, K., Baker, J. H., Reinsberg, S. A., Brooks, D. E., Häfeli, U. O., *Bioconjug. Chem.*, 2012, 21(3), 372–381.

118. Saatchi, K., Gelder, N., Gershkovich, P., Sivak, O., Wasan, K. M., Kainthan, R. K., Brooks, D. E., Häfeli, U. O., *Int. J. Pharm.*, 2012, 422(1–2), 418–427.

119. (a) Fliege, E., Quadir, M., Haag, R., *Adv. Drug Deliv. Rev.*, 2012, 64, 866–884. (b) Kolhe, P., Khandare, J., Pillai, O., Kannan, S., Lich-Lai, M., Kannan, R., *Pharm. Res.*, 2004, 21, 2185–2195.

120. (a) Calderon, M., Graeser, R., Kratz, F., Haag, R., *Bioorg. Med. Chem. Lett.*, 2009, 14, 3725. (b) Calderón, M., Welker, P., Licha, K., Fichtner, I., Graeser, R., Haag, R., Kratz, F., *J. Control. Release*, 2011, 151, 295–301.

121. Khandare, J., Mohr, A., Calderon, M., Welker, P., Licha, K., Haag, R., *Biomaterials*, 2010, 31, 4268–4277.

122. Reichert, S., Calderon, M., Khandare, J., Welker, P., Mangoldt, D., Licha, K., Kainthan, R. K., Brooks, D. E., Haag, R., *Small*, 2011, 7, 820–829.

123. Calderon, M., Welker, P., Licha, K., Fichtner, I., Graeser, R., Haag, R., Kratz, F., *J. Control. Release*, 2011, 151, 295–301.

124. Zhang, J. G., Krajden, O. B., Kainthan, R. K., Kizhakkedathu, J. N., Constantinescu, I., Brooks, D. E., Gyongyossy-Issa, M. I. C., *Bioconjug. Chem.*, 2008, 19, 1241–1247.

125. Kumar, P., Shenoi, R. A., Lai, B. F., Nguyen, M., *Biomacromolecules*, 2015, 16(3), 913–923.

15:59 28 October 2016

126. Li, M., Neoh, K. G., Wang, R., Zong, B. Y., Tan, J. Y., ET., K., *Eur*. *J*. *Pharm*. *Sci*., 2013, 48(1–2), 111–120.

127. Wurm, F., Dingels, C., Frey, H., Klok, H. A., *Biomacromolecules*, 2012, 13(4), 1161–1171. *doi: 10.1021/bm300103u*. *Epub 2012 Mar 20*. Squaric acid mediated synthesis and biological activity of a library of linear and hyperbranched poly(glycerol)-protein conjugates. Wurm F(1), Dingels C, Frey H, Klok HA. (4), 1161–1171.

128. Mammen, M., Choi, S.-K., Whitesides, G. M., *Angew*. *Chem*. *Int*. *Ed*. *Engl*., 1998, 37, 2754.

129. Ratner, B. D., Hoffmann, F. J., Schoen, J. E., Lemons, F., *Biomaterials Science*. *An Introduction to Materials in Medicine; Academic Press: New York* 1996.

130. Chen, C. S., Mrksich, M., Huang, S., Whitesides, G. M., Ingber, D. E., *Science*, 1997, 276, 1425–1428.

131. Niklason, L. E., Gao, J., Abbott, W. M., Hirschi, K. K., Houser, S., Marini, R., Langer, R., *Science*, 1999, 284(5413), 489–493.

132. Manz, A., Becker, H., *Microsystem Technology in Chemistry and Life Sciences; Springer-Verlag: Berlin*, *Germany* 1998.

133. Santini, J. T., Jr., Cima, M. J., Langer, R., *Nature*, 1999, 397(6717), 335–338.

134. Lee, K. B., Park, S. J., Mirkin, C. A., Smith, J. C., Mrksich, M., *Science*, 2002, 295(5560), 1702–1705.

135. Whitney, M., Rockenstein, E., Cantin, G., Knapp, T., Zlokarnik, G., Sanders, P., Durick, K., Craig, F. F., Negulescu, P. A., *Nat*. *Biotechnol*., 1998, 16(13), 1329–1333.

136. Chapman, R. G., Ostuni, E., Takayama, S., Holmlin, R. E., Yan, L., Whitesides, G. M., *J*. *Am*. *Chem*. *Soc*., 2000, 122, 8303–8304.

137. Chapman, R. G., Ostuni, E., Yan, L., Whitesides, G. M., *Langmuir*, 2000, 16, 6927–6936.

138. Sieger, C., Biesalski, M., Haag, R., *Chem*. *Eur*. *J*., 2004, 10, 2831–2838.

139. PY, J. Y., Kainthan, R. K., Zou, Y., Chiao, M., Kizhakkedathu, J. N., *Langmuir*, 2008, 24(9), 4907–4916.

140. Ramos-Fernandes, E. G., Queiroz, A. A. A. D., Abraham, G. A., Roman, J. S., *J*. *Mater*. *Sci*.*: Mater*. *Med*., 2006, 17, 105–111.

141. Ramos-Fernandes, E. G., Queiroz, A. A. A. D., *J*. *Mater*. *Sci*.*: Mater*. *Med*., 2009, 20, 473–479.

142. Papp, I., Dernedde, J., Enders, S., Haag, R., *Chem*. *Commun*., 2008, 44, 5851–5853.

15:59 28 October 2016

143. Dernedde, J., Rausch, A., Weinhart, M., Enders, S., Tauber, R., Licha, K., Schirner, M., Zugel, U., von Bonin, A., Haag, R., *Proc. Natl. Acad. Sci. U. S. A.*, 2010, 107, 19679–19684.

144. Weinhart, M., Groger, D., Enders, S., Riese, S. B., Dernedde, J., Kainthan, R. K., E., B. D., Haag, R., *Macromol. Biosci.*, 2011, 11, 1088–1098.

145. Weinhart, M., Groger, D., Enders, S., Dernedde, J., Haag, R., *Biomacromolecules*, 2011, 12, 2502–2511.

146. Tziveleka, L. A., Psarra, A. M., Tsiourvas, D., Paleos, C. M., *Int. J. Pharm.*, 2008, 356, 314–324.

147. Licha, K., Welker, P., Weinhart, M., Wegner, N., Kern, S., Reichert, S., Gemeinhardt, I., Weissbach, C., Ebert, B., Haag, R., Schirner, M., *Bioconjug. Chem.*, 2011, 22 (12), 2453–2460.

148. Glaffig, M., Palitzsch, B., Hartmann, S., Schüll, C., Nuhn, L., Gerlitzki, B., Schmitt, E., Frey, H., Kunz, H., *Chemistry*, 2014, 20(15), 4232–4236.

149. Paulus, F., Schulze, R., Steinhilber, D., Zieringer, M., Steinke, I., Welker, P., Licha, K., Wedepohl, S., Dernedde, J., R., H., *Macromol Biosci.*, 2014, 14(5), 643–654.

150. Yu, X., Liu, Z., Janzen, J., Chafeeva, I., Horte, S., Chen, W., Kainthan, R. K., Kizhakkedathu, J. N., Brooks, D. E., *Nat Mater.*, 2012, 11(5), 468–476.

151. Karmali, P. P., Chaudhuri, A., *Med. Res. Rev.*, 2007, 27, 696–722.

152. Vijayanathan, V., Thomas, T., Shirahata, A., Thomas, T. J., *Biochemistry*, 2001, 40(45), 13644–13651.

153. Ganguli, M., Jayachandran, K. N., Maiti, S., *J. Am. Chem. Soc.*, 2004, 126(1), 26–27.

154. Fischer, W., Calderon, M., Haag, R., *Top. Curr. Chem.*, 2010, 296, 95–129.

155. Wan, K., Ebert, B., Voigt, J., Wang Q., Dai, Y., Haag, R. Kemmer, W. *Nanomedicine*, 2012, 9(4), 393–398.

156. (a) Kainthan, R. K., Gnanamani, M., Ganguli, M., Ghosh, T., Brooks, D. E., Maiti, S., Kizhakkedathu, J. N., *Biomaterials*, 2006, 27, 5377–5390. (b) Zhang, S., Bellis, S.L., Fan, Y., Wu, Y. Int J. Nanomedicine, 2015, 10, 2871–2884.

157. Sisson, A. L., Haag, R. A. R. H., *Soft Matter*, 2010, 6, 4968–4975.

158. Sisson, A. L., Steinhilber, D., Rossow, T., Welker, P., Licha, K., Haag, R., *Angew. Chem. Int. Ed.*, 2009, 48(41), 7540–7545.

159. Steinhilber, D., Sisson, A. L., Mangoldt, D., Welker, P., Licha, K., Haag, R., *Adv. Funct. Mater.*, 2010, 20, 4133–4138.

15:59 28 October 2016

160. Steinhilber, D., Haag, R., Sisson, A. L., *Int. J. Artif. Organs*, 2011, 34, 118–122.

161. Groll, J., Singh, S., Albrecht, K., Moeller, M., *J. Polym. Sci. Part A: Polym. Chem.*, 2009, 47, 5543–5549.

162. Papp, I., Sieben, C., Sisson, A. L., Kostka, J., Bottcher, C., Ludwig, K., Herrmann, A., Haag, R., *ChemBioChem*, 2011, 12, 887–895.

163. Cuggino, J. C., Alvarez, C. I., Strumia, M. C., Welker, P., Licha, K., Steinhilber, D., Mutihac, R.-C., Calderon, M., *Soft Matter*, 2011, 7, 11259–11266.

164. Sousa-Herves, A., Wedepohl, S., Calderón, M., *Chem Commun (Camb).*, 2015, 51(25), 5264–5267.

165. Zhang, X., Achazi, K., Steinhilber, D., Kratz, F., Dernedde, J., Haag, R., *J. Control. Release*, 2014, 174, 209–216.

166. Wu, C., Strehmel, C., Achazi, K., Chiappisi, L., Dernedde, J., Lensen, M. C., Gradzielski, Ansorge-Shumacher, M. B., Haag, R. *Biomacromolecules*, 2014, 15 (11), 3881–3890.

167. Rossow, T., Heyman, J. A., Ehrlicher, A. J., Langhoff, A., Weitz, D. A., Haag, R., Seiffert, S., *J. Am. Chem. Soc.*, 2012, 134(10), 4983–4989.

168. Fedorovich, N. E., Oudshoorn, M. H., van Geemen, D., Hennink, W. E., Alblas, J., Dhert, W. J., *Biomaterials*, 2009, 30(3), 344–353.

169. Wei, Q., Becherer, T., Noeske, P. L., Grunwald, I., Haag, R., *Adv Mater.*, 2014 26(17), 2688–2693.

170. Moore, E., Delalat, B., Vasani, R., Thissen, H., Voelcker, N. H., *Biomacromolecules*, 2014, 15(7), 2735–2743.

171. Deng, Y., Saucier-Sawyer, J. K., Hoimes, C. J., Zhang, J., Seo, Y. E., Andrejecsk, J. W., Saltzman, W. M., *Biomaterials*, 2014, 35(24), 6595–6602.

172. (a) Zhao, L., Xu, Y. H., Akasaka, T., Abe, S., Komatsu, N., Watari, F., Chen, X., *Biomaterials*, 2014, 35(20), 5393–5406. (b) Zhou, L., He, B., Huang, J., Cheng, Z., Xu, X., Wei, C. *ACS Applied Mater Interfaces*, 2014, 6(10), 7719–7727.

173. Das, P., Jana, N. R., *ACS Appl. Mater. Interfaces*, 2014, 6(6), 4301–4309.

174. Arsalani, N., Fattahi, H., Laurent, S., Burtea, C., Vander Elst, L., Muller, R. N., *Contrast Media Mol. Imaging*, 2012, 7(2), 185–194.

175. Höger, K., Becherer, T., Qiang, W., Haag, R., Friess, W., Küchler, S., *Eur. J. Pharm. Biopharm.*, 2013, 85(3 Pt A), 756–764.

176. Weber, T., Gies, Y., Terfort, A., *Langmuir*, 2012, 28(45), 15916–15921.

177. Chapanian, R., Constantinescu, I., Medvedev, N., Scott, M. D., Brooks, D. E., Kizhakkedathu, J. N., *Biomacromolecules*, 2013, 14(6), 2052–2062.

178. Jeong, J. H., Schmidt, J. J., Kohman, R. E., Zill, A. T., DeVolder, R. J., Smith, C. E., Lai, M. H., Shkumatov, A., Jensen, T. W., Schook, L. G., Zimmerman, S. C., Kong, H., *J. Am. Chem. Soc.*, 2013, 135(24), 8770–8773.

15:59 28 October 2016

## Chapter 5

# Theranostic Potential of Dendronized Iron Oxide Nanoparticles

**Aurélie Walter, Audrey Parat, Delphine Felder-Flesch, and Sylvie Begin-Colin**

*Institut de Physique et de Chimie des Matériaux de Strasbourg IPCMS, UMR CNRS-Unistra 7504, 23 rue du Loess, BP 43, 67034 STRASBOURG cedex 2, France*

Sylvie.Begin@unistra.fr

## 5.1 Introduction

Although much progress has been made in cancer treatment through the most common conventional therapies currently applied (surgery, chemotherapy, and radiotherapy), new approaches are necessary to minimize deleterious side effects and to increase the patient survival rates. Nanomedicine and nano-objects offer several advantages to address this challenge: (i) with tailored dimensions in the range of 10–100 nm, they are small enough to circulate in every capillary of the organism allowing a non-invasive approach, (ii) unlike usual chemotherapeutic molecules (size ca. 1 nm) they are big enough to avoid renal elimination, (iii) with their modular design and broad spectrum of functionalization, they have potential to simultaneously deliver drug and allow imaging, to achieve specific cell-targeting while maintaining stability in the blood which remains challenging with other molecular, remote

*Dendrimers in Nanomedicine*
Edited by Delphine Felder-Flesch
Copyright © 2016 Pan Stanford Publishing Pte. Ltd.
ISBN 978-981-4745-49-9 (Hardcover), 978-981-4745-50-5 (eBook)
www.panstanford.com

15:59 28 October 2016

or surgical approaches. Therefore, there is currently a well-identified medical need to develop novel efficient nanovectors for cancer treatment. Additionally with the aim to collect real-time data during a cancer treatment and understand how the nanovectors interact with a patient, the development of nanovectors allowing imaging is also crucial for the development of image-guided therapy. Active diagnostic tools especially for oncology are based on computed tomography (CT-scan), single photon emission computed tomography (SPECT) and MRI. If SPECT imaging brings the most sensitive approach, MRI imaging gives a spatial resolution by far more important to insure, through a minimally invasive way and at anatomic scale, visualization of the therapeutic effect. The development of new MRI contrast agents (CAs) in oncology for the detection of tumors represents also a valuable market.

Among currently developed nano-objects, iron oxide NPs, due to their intrinsic properties, are extensively studied for different applications in the biomedical field (Fig. 5.1).[1–3] They are used for diagnosis as contrast agent for MRI, or as biosensors. In therapy, magnetic NPs are used as heating medium for hyperthermia treatment or as a platform for drug delivery. Iron oxide NPs are also used for purification and cell isolation.

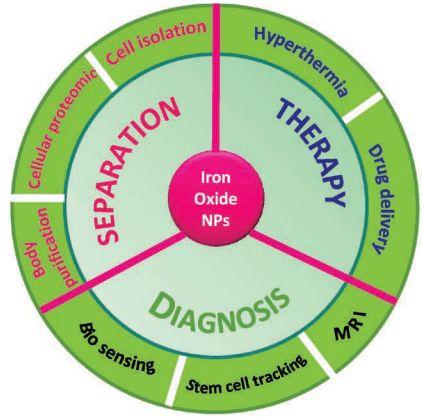



**Figure 5.1** Main applications of functionalized iron oxide NPs in the biomedical field.

In the case of biomedical applications, the functionalization of NPs is of major importance and must meet a set of specific characteristics[4]:

- bring biocompatibility and hydrophilicity to NPs
- ensure stealth NPs
- allow the colloidal stability of NPs in water, in physiological media rich in proteins and in the presence of high electrolyte concentration without desorption of molecules
- conduct to a mean hydrodynamic size less than 100 nm after functionalization to ensure a good biodistribution
- provide functional groups for coupling of bioactive molecules (dye, targeting ligands, drug.)

15:59 28 October 2016

The nature of the surface functionalization of the NPs and the grafting method will condition these parameters. The hydrodynamic diameter of the NPs after functionalization is an important parameter, especially if intravenous injection is envisioned. Thus, it is more favorable to graft small molecules to the surface of the NP that will cover uniformly the surface while minimizing their final size: this is not always possible when grafting polymers to the surface of NPs. Considering these parameters, the grafting of dendron (elementary unit of a dendrimer) appears as a good approach for the functionalization of NPs for biomedical applications. Indeed, their small size ensures a final low hydrodynamic diameter, their tree structure provides high stability in suspension and their various functional groups allow providing additional multifunctionality to the final nano-object. It has been shown that a dendritic coating allows fast bioelimination of functionalized NPs and good MRI properties (contrast enhancement).

The use of dendrimers or dendrons in the biomedical field has been motivated by the many advantages they provide through their tree-like structure:

- the conformation and the size can be easily controlled by varying the generation (G) of the dendrimer (or dendron) or the nature and number of peripheral chains. It is then possible to control the pharmacokinetics and biodistribution.
- their biological properties may be attributed to a single molecular entity rather than a random distribution as in the case of polymers.
- the dendron generation can be adapted with a nanometer precision to the size of the NPs and thus minimize the thickness of the organic layer.

- the peripheral chains or the cavities can be functionalized with drugs, chromophores, or other ligands, which provide additional functionality to the dendron.

Since the early work of Vögtle and innovative studies in the field of branched molecules, dendrimer/dendrons have attracted the attention of many scientists in various fields such as catalysis and biomedicine. The dendrons have been used to functionalize gold NPs,[5–7] quantum dots,[8] polymeric NPs,[9] carbon nanotubes,[10–11] surfaces,[12] recently MnO NPs[13] and in particular iron oxide NPs.[9,14–28]

Although dendritic molecules are used to functionalize various supports, the advantages of a dendron versus a linear molecule are not clearly shown in the literature. The team of Marcus Textor[15] has recently made an interesting contribution to the discussion. By comparing the colloidal stability of iron oxide NPs functionalized with linear molecules or with PEG dendrons of various molecular weight, they were able to demonstrate the reversible aggregation of NPs functionalized with dendrons during an increase of temperature, while NPs functionalized with linear molecules aggregate and sediment irreversibly. The group of Na et al.[14] has, in the meanwhile, compared two branched versus two linear structures, bearing carboxylic acids or catechol as coupling agents: the branched structure increases the colloidal stability in water, in a 1M NaCl solution, and in a medium used for cell culture. Recently, Walter et al.[28] functionalized iron oxide NPs of 10 nm with a linear PEG monophosphonate or with PEGylated mono-phosphonated dendrons of growing generations: dendritic nano-objects with a mean hydrodynamic size smaller than 50 nm, stable in physiological media and showing both renal and hepatobiliary elimination have been obtained. The colloidal stability is induced by combined electrostatic and steric interactions when only electrostatic interactions are involved in the colloidal stability of hybrids grafted with a linear molecule. These last nano-objects were less stable in biological media at high ionic concentration and NMRD profiles and relaxivity measurements highlighted the influence of the molecule architecture on the water diffusion close to the magnetic core thus influencing the relaxation properties at low magnetic field.[28]

The influence of the dendron generation was the subject of several articles. The increase in generation also increases the

15:59 28 October 2016

15:59 28 October 2016

functionality of the NPs.[9,17] In 2012, the team of Kenji Kono[29] showed that transfection activity of PAMAM dendron bearing lipids depends on the dendron generation. Duanmu et al.[16] have particularly shown the influence of the dendron generation on the MRI properties of iron oxide NPs: the $r_2$ relaxivity increased with dendron generation. Walter et al. confirmed this result (Table 5.1 and Fig. 5.2) and showed that the dendron hydrophilicity was also an important parameter when comparing dendron CYNCOOH (PAMAM-based) and D2 (Fréchet-type).[28]

**Table 5.1** Longitudinal ($r_1$) and transverse ($r_2$) relaxivities ($s^{-1}$. $mM^{-1}$) calculated from the total amount of iron in dendronized iron oxide NPs as a function of the type of dendron and dendron generation

| | $\Phi_{hydro}$ (nm) | $r_1$ ($s^{-1} \cdot mM^{-1}$) | $r_2$ ($s^{-1} \cdot mM^{-1}$) | $r_2/r_1$ |
|---|---|---|---|---|
| CYNCOOH | 14 | 11 ± 0.5 | 46 ± 11 | 4 ± 1 |
| D2 | 18 | 10 ± 1 | 52 ± 7 | 5 ± 1 |
| D2-G2 | 18 | 9 ± 1 | 51 ± 7 | 6 ± 1 |
| D2-G3 | 32 | 9 ± 0.5 | 81 ± 4 | 9 ± 0.5 |

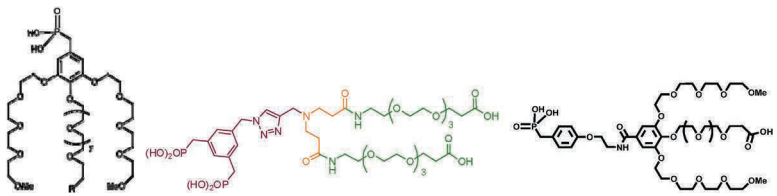


**Figure 5.2** Dendron molecules named ANA with R = –COOH (ANACOOH), $-CH_3$ ($ANACH_3$), $-NH_2$ ($ANANH_2$) (left), CYNCOOH (middle) and dendron D2 (right).

Iron oxide NPs can be used for magneto-transfection. Huang et al.[18] have studied 6 generations of PAMAM dendrimers grafted on iron oxide NPs with polyethyleneimine (PEI)/DNA polyplexes to increase the PEI transfection using a magnetic field. In other studies, the delivery of gene,[19] or doxurubicine[20,21] and streptavidin[30] using dendron-functionalized iron oxide NPs was also studied. In particular, Liu et al.[19] linked covalently iron oxide NPs, through a silane, to PAMAM dendrimer of different generations and used them for binding of *survivin* (asODN) antisense oligonucleotides to inhibit breast cancer cells growth.

15:59 28 October 2016

Such results proved the efficiency of modified iron oxide NPs-PAMAM dendrimer for gene delivery as well as for cancer therapy. However, the most widely studied application of dendronized NPs is their use as MRI contrast agent.[22–28]

If dendrons can be considered as promising molecules to functionalize NPs for a large panel of biomedical applications, the properties of the iron oxide core, as well as the grafting strategy at the NP surface, are key parameters to ensure small hydrodynamic size, in vivo MRI contrast enhancement and possibly magnetic hyperthermia properties. The dendronization of a magnetic core displaying MRI and magnetic hyperthermia (MH) properties is very promising for the elaboration of efficient theranostic nano-objects. We will describe our concept based on the grafting, at the NPs surface, of dendrons via a phosphonate coupling agent (allowing a direct grafting and a strong binding of the dendron at the NPs surface)[23]; show the influence of the synthesis method of iron oxide NPs (co-precipitation versus thermal decomposition) and of the dendron architecture (functional PAMAM-PEG or Fréchet-type) on the grafting conditions, on the resulting colloidal stability and on the structural and magnetic properties. Then relaxivity measurements, in vivo tests and MRI measurements will demonstrate both the impact of the dendron architecture and the NPs properties and the great potential of these dendronized NPs for MRI. Finally the design of the magnetic iron oxide core will be shown promising to provide also therapeutic properties to the nano-objects.

## 5.2 Influence of the NPs Synthesis Way and of the Functional Peripheral End Groups on the Grafting Conditions and Colloidal Stability

Iron oxide NPs synthesized by thermal decomposition (NPStd) and co-precipitation (NPSco) (Fig. 5.3) have been synthesized and characterized (Table 5.2). Then both NPs were functionalized with dendron molecules whose structures are depicted in Fig. 5.2. The influence of the nature of the end group R ($-NH_2$, $-CH_3$ or $-COOH$)[24,26] and of the NPs synthesis way[24] on the colloidal stability of NPs suspension after grafting was investigated.

15:59 28 October 2016

**Table 5.2** Characteristics of iron oxide NPs synthesized by coprecipitation and thermal decomposition

| Synthesis way | Composition | Molecules | Diameter (nm) | Mean hydrodynamic size | Saturation magnetization |
|---|---|---|---|---|---|
| Coprecipitation | $Fe_{2.73}O_4$ | Naked | 11.6 | Aggregated 600 nm | 65 emu/g |
| Thermal decomposition | $Fe_{2.78}O_4$ | Oleates | 11.3 | 12 nm | 55 emu/g |

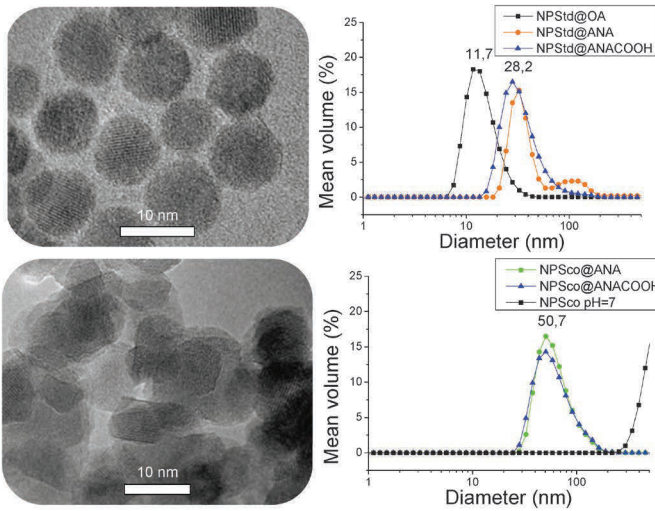



**Figure 5.3** TEM image (left) and size distributions in water at pH = 7 (right) before and after dendronization of iron oxide NPs synthesized by thermal decomposition (top) and co-precipitation (down).

When NPs are synthesized by co-precipitation (NPSco), they are naked and aggregated through van der Waals interactions at physiological pH. Their functionalization by dendrons occurs through direct grafting by directly introducing the dendrons in a water suspension of NPs at a given pH. This grafting step was found highly dependent towards the nature of the dendron functional end-groups.[23,26,31] Earlier studies on interaction of phosphates with the surface of iron oxide NPs have demonstrated that electrostatic interactions between negatively charged phosphates and the positively charged iron oxide surface (due to

15:59 28 October 2016

the presence of amphoteric OH groups at the surface[31]) favors the grafting.[32] Thus, the best conditions for the grafting of dendron bearing a methyl end group (ANACH3, Fig. 5.2) were found around pH = 5–6 (above the pKa of the phosphonate anchoring group and below the isoelectric point of iron oxide which is around 7). The elemental analyses and the calculated grafting rate showed that the surface was totally covered by the dendron ANACH3. When the dendron bearing a carboxylate group, ANACOOH, was grafted in the same conditions, a lower grafting rate was noticed and explained by the competitive interactions of deprotonated carboxylate and phosphonate groups with the positively charged surface of iron oxide and/or to the fact that the chain bearing the carboxylate group was longer thus leading to steric hindrance.[26] The first pKa of the phosphonate (3.1) being lower than the pKa of the carboxylate (4), the grafting has been conducted at a pH between both pKas (around pH 3.5 ) and a larger grafting rate was obtained, closed to that of ANACH3 (Table 5.3). When the dendron bears an ammonium group, the ammonium group is positively charged up to pH around 10 and the grafting has been conducted at the same pH as the dendron $ANACH_3$.[26]

**Table 5.3** Properties of dendronized iron oxide NPs

| **Synthesis way of NPs** | **(Co)-precipitation** | | | **Thermal decomposition** | | |
|---|---|---|---|---|---|---|
| Dendron | ANA | ANACOOH | $ANANH_2$ | ANA | ANACOOH | CYNCOOH |
| Grafting way | Direct | | | Ligand exchange | | |
| Name | NPSco@ ANA | NPSco@ ANACOOH | NPSco@ $ANANH_2$ | NPStd@ ANA | NPStd@ ANACOOH | NPS@CYN COOH |
| Grafting rate (dendrons/$nm^2$ ) | 1.30 | 1.01 | 0.8 | 1.33 | 1.06 | 1.8 |
| Saturation magnetization | ~70 emu/g | | | ~55 emu/g | | |
| $r_2$ ($mM^{-1}\cdot s^{-1}$), 1.5 T | 265 | 213 | | 130 | 91 | 54 |
| $r_2/r_1$ | 25 | 23 | | 12 | 15 | 7 |
| Mean hydrodynamic size | 50 nm | | | 30 nm | | 20 nm |

15:59 28 October 2016

Stable and concentrated suspensions (monomodal size distribution) of dendronized NPs were obtained with dendrons bearing the carboxylic acid (ANACOOH) and the methyl group ($ANACH_3$) at the chain end (Fig. 5.3 and Table 5.3). However, no stable suspensions could be prepared with the dendron carrying an ammonium group ($ANANH_2$) and a lower grafting rate was noticed with this dendron due to intramolecular interactions between the ammonium and phosphonate groups at the studied pH (5–6).

The NPs synthesized by thermal decomposition (NPStd) were dendronized either by direct ligand exchange in THF and then transfer in water or by a one-step ligand exchange and phase transfer process (the NPs coated with oleic acid are in suspension in hexane and are put into contact with a water suspension of dendron by magnetic stirring).[24]

After purification of dendronized NPs water suspensions, the dendron grafting was confirmed by IR spectroscopy, thermogravimetry (TGA) measurements, elemental analyses, zeta potential measurements and photoemission spectroscopy.[22,24–26,28,31,33] The grafting rate of dendrons was similar whatever the NPs synthesis way and depended mainly on the dendrons nature (Table 5.3).[26] It was very close to the theoretical one (1.35 dendrons/$nm^2$) with ANACH3 and slightly lower with ANACOOH due to grafting conditions close to the pKa of the carboxylate end group and to the longer PEG chain bearing the carboxylate group (steric hindrance). A modification of the infrared (IR) bands of the phosphonate in the range 1200–850 $cm^{-1}$ and the observed shift, in XPS spectra, of the P2p (P2p3/2 and P2p1/2) peaks towards lower binding energies after the grafting step confirmed grafting through the phosphonate.[24,31]

The oxidation state of iron oxide NPs after this dendronization step has been checked by x-ray diffraction (XRD) measurements, IR spectroscopy and Mössbauer spectroscopy and a slight oxidation of NPs was observed with a mean composition of $Fe_{2.72}O_4$. Indeed, it is now well established that the $Fe^{2+}$ ions located at the surface of magnetite $Fe_3O_4$ NPs are very sensitive to oxidation and when the size decreases, their sensitivity to oxidation increases. Magnetite displays a saturation magnetization higher (92 emu/g) than its oxidized form, Maghemite $\gamma Fe_2O_3$ (76 emu/g).

15:59 28 October 2016

Then oxidation of magnetite at the nanoscale reduces the saturation magnetization values. In addition, iron oxide NPs display a surface spin canted layer, induced by the nanosize, which lowers also their saturation magnetization by comparison with bulk iron oxides.[34] However, magnetic measurements showed that despite this slight oxidation, the saturation magnetization (Tables 5.1 and 5.2) of both NPs is preserved and even slightly enhanced for NPs synthesized by co-precipitation after the dendronization step.[22,24] The lower saturation magnetization of NPs synthesized by thermal decomposition by comparison with those synthesized by coprecipitation is explained by the larger thickness of their surface spin canted shell as determined by Mössbauer spectroscopy.[34] The preservation of the magnetic properties of the iron oxide core is explained by the strong anchoring of the phosphonate group to the iron oxide surface which induces a surface magnetic ordering decreasing the surface spin canting.[35]

After dendronization, NPs synthesized by co-precipitation display an average hydrodynamic size of ~50 nm, whereas 30 nm dendronized NPs are obtained when synthesized by thermal decomposition (Fig. 5.3, Table 5.3). This difference is a direct result of their aggregation state before the grafting reaction: NPs synthesized by co-precipitation are naked and aggregated at neutral water pH (close to the isoelectric point of iron oxide) while NPs synthesized by thermal decomposition are coated with oleic acid and well dispersed in an organic solvent (Fig. 5.3). The suspension stability of these dendronized NPs in physiological media was investigated and a greater stability was demonstrated for NPs functionalized with a dendron bearing a carboxylic group at the end of the central PEG chain.[24–26]

Therefore whatever the synthesis method of iron oxide NPs, by controlling the grafting conditions, NPs may be coated with dendron at a high grafting rate (very close to the theoretical one) leading to high colloidal stability of nano-objects displaying a mean hydrodynamic size lower than or equal to 50 nm.

## 5.3 MRI Properties of Dendronized Iron Oxide NPs

The development of new MRI contrast agents (CAs) represents a valuable market and ultra-small iron oxide NPs, which are commercially used as T2 contrast agents for MRI,[36] are of particular

15:59 28 October 2016

interest as biodegradable and non-toxic nano-objects compared to other CAs families such as Gadolinium macromolecular complexes. A good T2 contrast agent displays high $r_2$ value and $r_2/r_1$ ratio. These values depend mainly on the saturation magnetization of NPs, their aggregation state and organic coating. Indeed besides providing a good colloidal stability of NPs in physiological media, the organic coating should favor the water molecules diffusion around and close to the magnetic core and affect a large amount of water molecules.

Preliminary in vitro and in vivo MRI studies on dendronized NPs were performed on NPs grafted with ANACOOH (Fig. 5.2). Indeed, the presence of the carboxylate peripheral group was found important to ensure a good colloidal stability in physiological media.[26,28] In vitro relaxivity values of both types (NPSco and NPStd) of dendronized NPs (Table 5.3) were higher than those of commercial contrast agents displaying similar mean hydrodynamic size. Figure 5.4 shows ghost images obtained with a dendron similar to ANACOOH (dendron D2, Fig. 5.2 and Table 5.1) confirming the good dark contrast properties of these dendritic hybrids.

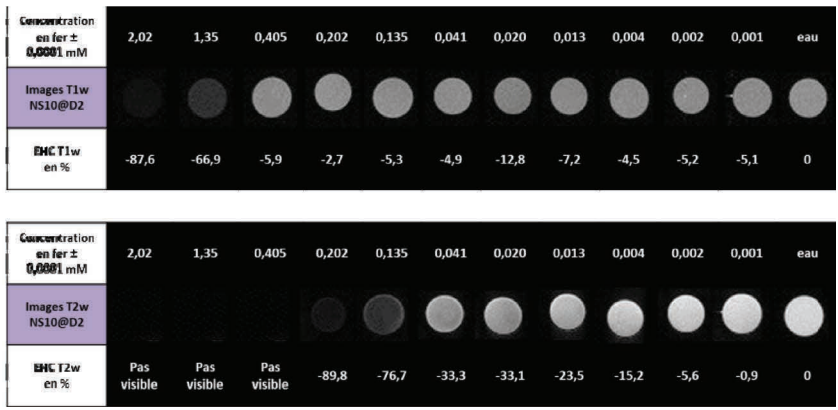



**Figure 5.4** T1w and T2w ghost images of iron oxide NPs coated with dendron D2 (Fig. 5.2) as the function of iron concentration. Top: D2@NPStd, Bottom: D2@NPSco.

In Table 5.3 are also reported the relaxivity values obtained with a PAMAM-based dendron named CYNCOOH: the lower relaxivity value $r_2$ and $r_2/r_1$ ratio compared to D2@NPs cannot be explained by the magnetic properties of the core as the NPs for both syntheses were similar. Even if the hydrodynamic size is

15:59 28 October 2016

lower for CYNCOOH@NPs, the lower relaxivity values were related to the diffusion of water around the magnetic core: indeed, water diffusion around CYNCOOH involves less water molecules than around D2 due to its less arborescent and also more hydrophobic structure.[33]

Dendronized NPStd showed a lower in vitro $r_2$ value than NPsco. This trend was attributed to the difference in hydrodynamic size after functionalization of the two NPs types, but also to the lower saturation magnetization of NPStd: indeed, relaxivity values increase with the saturation magnetization and aggregation state of NPs. However, during in vivo MRI studies, no difference was observed following both types of NPs and even better contrast was noticed with dendronized NPStd.[24] Figure 5.5 shows MRI images in liver at different time points after *iv* injection: A high enhanced contrast (EHC) value is observed at 39 minutes post *iv*.

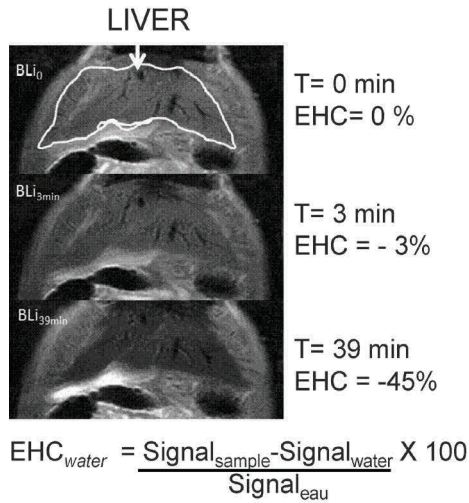



**Figure 5.5** T2w images centered on liver together with contrast enhancement (EHC) values obtained after iv injection of D2@NPStsd.

The coupling of a fluorophore on the functional end group of D2@NPS allowed monitoring biodistribution by optical imaging (Fig. 5.6): D2@NPStd were rapidly excreted by urinary and hepatobiliary pathways without reticulo-endothelial system (RES) uptake.[24,26,28]

15:59 28 October 2016

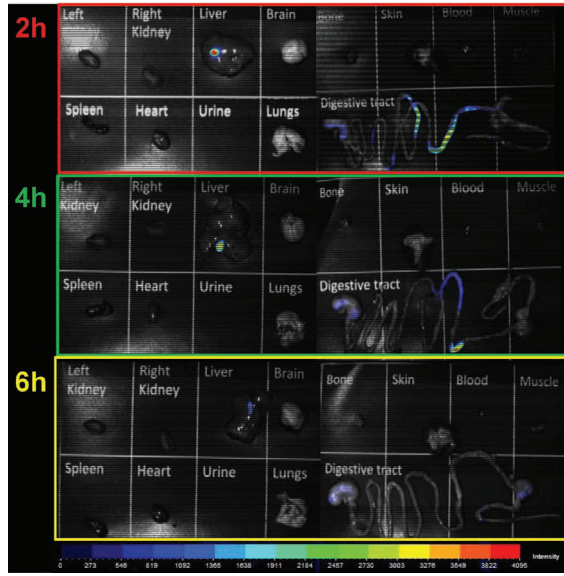



**Figure 5.6** Ex vivo optical images of mice organs removed 2, 4 and 6 h post intravenous (iv) injection of D2@NPStd.

## 5.4 Mastering Shape and Composition of Dendronized Iron Oxide Nanoparticles to Tailor Magnetic Hyperthermia Properties

Besides MRI, iron oxide NPs are also currently developed for magnetic hyperthermia (MH). When exposed to alternating magnetic fields of appropriate amplitude and frequency, these NPs release heat locally (where they are concentrated), which reduces the viability of cancer cells. The MH potential is demonstrated with the favorable recent results of the "nanothermotherapy" study in clinical phase II led by a German company MagForce Nanotechnology (hospital Charité in Berlin),[37] which has led to a European market authorization.[38–40] MH has been demonstrated to enhance the sensitivity of tumor cells towards chemo- or radio-therapies, to trigger a thermally-induced release of drugs or to act on cell membranes.[41]

However, one of the limitations of MH is the low heating power of usual magnetic NPs, requiring a local injection of large quantities of NPs. Given the clinical importance of these results,

15:59 28 October 2016

there is thus currently a crucial need to design optimized NPs for efficient MH.[42,43] However, optimization is not yet well-understood and experimental results from NPs systems vary widely. Indeed in MH, very specific physical properties are required for an optimal conversion of the supplied magnetic energy into heat. Three independent mechanisms result in thermal energy upon stimulation: Neel relaxation (internal friction with respect to the crystal lattice of NPs), Brown relaxation (internal friction of the NPs in the surrounding medium) and hysteresis loss (shift of domain walls).[44,45] The relative contribution of each is strongly dependent on size, shape, crystalline anisotropy and degree of aggregation or agglomeration of NPs. Hysteresis loss deals with large multi-domain particles. Single domain magnetic superparamagnetic NPs, which display smaller size than that of multi-domain particles absorb much more power at biologically tolerated magnetic fields and frequencies and form more easily stable suspensions. For these small sized NPs, the Neel and Brown relaxations are the main heating mechanisms. Neel and Brown relaxation times are mainly governed by the magneto-crystalline anisotropy (a property of the material which gives a preferred orientation to the magnetic moment), the NPs volume and the viscosity of the media. Brownian relaxation will tend to dominate at larger particle volume and lower viscosities while the Neel relaxation will at smaller NPs volumes and in viscous solutions. The occurrence of these relaxation phenomena depends also strongly on the NPs anisotropy[42] and there is currently a key challenge to overcome in the design of NPs with magnetic properties specifically tailored for hyperthermia related applications.[42,45,48]

The heating efficiency of an ensemble of magnetic NPs depends not only on their structural and magnetic properties but also on the magnitude and frequency of the applied magnetic field. Indeed the heating performance is usually assessed by determining the specific absorption rate (SAR) which is the power dissipated by magnetic NPs per mass unit[46]: SAR = $C/m \times \mathrm{d}T/\mathrm{d}t$, with $C$, the water specific heat per volume unit, $m$ the iron concentration in suspension (Fe g/L) and $\mathrm{d}T/\mathrm{d}t$ the increase in measured temperature. SAR (in W/g) values depend on the structure and composition of the NPs but also on the frequency ($f$) and amplitude of the magnetic field ($H$) applied during the measurements.[42,44] For an efficient heat treatment with minimal

15:59 28 October 2016

invasiveness for the patient, the search for new magnetic nanomaterials which show the highest SAR values at the lowest NPs dose administered and at the lowest frequency and/or magnetic field amplitude applied is of paramount relevance.[42,47,54] For superparamagnetic NPs, SAR values usually increase by increasing either the frequency or the magnetic field amplitude (or both) applied during the measurements. For a safe application of hyperthermia to patients, it was experimentally found that the product of the frequency and the magnetic field amplitude (Hf) should be smaller than $5 \times 10^9$ A $m^{-1}s^{-1}$.[47] However, many of the published SAR values reported for magnetic NPs are measured at frequencies between 500 and 700 kHz and fields between 10 and 30 kA $m^{-1}$, resulting in Hf factors which are mostly largely above this limit (ca. 2–4 times higher). Furthermore, the lack of standard devices or established measurement protocols contribute to an increase of the variability of the SAR values reported in the literature so far.[36]

For frequencies of the magnetic field used in hyperthermia studies compatible with clinical use, most models indicate an optimal diameter of 14 nm for standard spherical NPs but, given the variation in the anisotropy of the different synthesized magnetite ($Fe_3O_4$) NPs, the experimental optimal diameter appears to fall between a broad range between 12 and 20 nm.[42,48] Indeed magnetic properties of iron oxide NPs strongly depends on their synthesis way[49] and SAR values depend strongly on the measurement parameters (field frequency and amplitude, viscosity, NPs concentration) which vary from one paper to another: this makes the published SAR values very difficult to compare. The highest SAR values for standard spherical NPs obtained in conditions compatible with clinical uses ($Hf < 5 \times 10^9$ $Am^{-1}s^{-1}$) reported so far were obtained either for 30 nm iron oxide NPs synthesized by chemical methods followed by a size selection process (600 W/g at 400 kHz, 13 mT) or for magnetite NPs produced by bacteria (magnetosomes, 960 W/g at 410 kHz, 12.5 mT).[50] One may just conclude at this point that by imposing hyperthermia measurement conditions compatible with clinical uses, NPs'magneto-crystalline anisotropy, saturation magnetization and size would be the key parameters to consider for optimizing their heat capacity.

Doping iron oxide with Co or Mn has been proposed as a way to improve SAR values.[42,51] For example, cobalt ferrite NPs were

15:59 28 October 2016

found to have very large SAR values (up to 720 W/g).[45] However, up to now most works were devoted to iron oxide NPs[52] because of their proven biocompatibility, ease of synthesis and size tuning with narrow size distribution. Despite their high potential, the development of doped ferrites was thus limited, their synthesis being generally more complex (chemical heterogeneities)[53] and their biocompatibility being a concern.

Nevertheless, current progress in synthesis methods allows now synthesizing NPs with different shapes and core–shell structures that are highly promising to optimize heat efficacy. By playing on the NPs shape e.g. via the synthesis of cubic iron oxide NPs (Fig. 5.7)[54,55] or flower-shaped nanostructures which enable cooperative magnetism,[56,57] the heating power was recently considerably improved. Besides, the capping of inorganic shells on magnetic core allows shielding non-biocompatible doped-ferrites NPs by a protecting shell such as silica, or modifying the magneto-crystalline anisotropy of the resulting core–shell systems. Indeed, a very important anti-tumor effect induced by MH has been noticed with core–shell NPs consisting of a core with a high magnetic anisotropy and of a shell with a small magnetic anisotropy.[43]

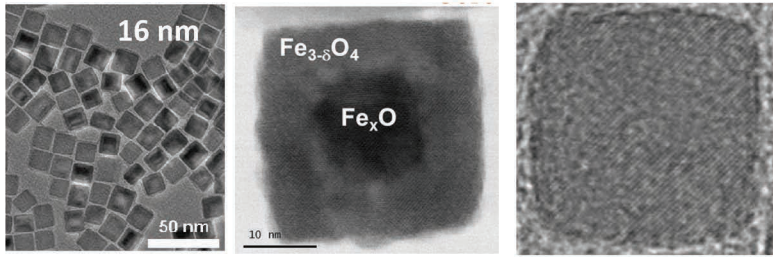



**Figure 5.7** Transmission electron microscopy (TEM) images of 16 nm nanocubes (left); 16 nm core–shell $FeO@Fe_{3-\delta}O_4$ nanocubes (middle); 16 nm oxidized nanocubes (right).

In that context, spherical NPs[58] with a mean diameter of 22 nm have been synthesized as well as cubic-shaped homogeneous $Fe_{3-x}O_4$ and core–shell $FeO@Fe_{3-x}O_4$ NPs[59] (Figs. 5.7 and 5.8). Their size and mean composition in magnetite have been determined by TEM and by analysis of the X-ray diffraction pattern knowing that only the magnetic magnetite fraction will contribute to MRI properties (FeO is antiferromagnetic) (Table 5.4).[60] NPs have been

15:59 28 October 2016

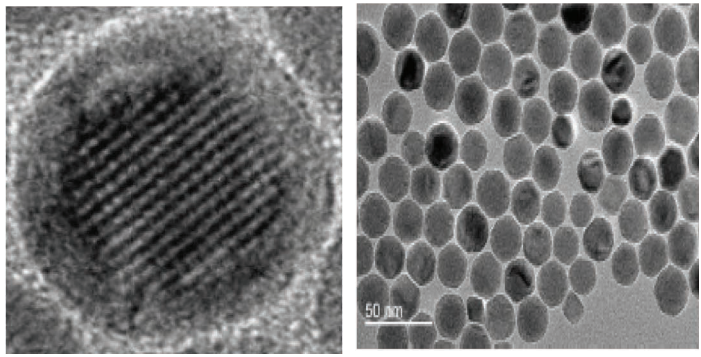



**Figure 5.8** Transmission electron microscopy (TEM) images of 19 nm core–shell FeO@$Fe_{3-\delta}O_4$ nanospheres, 22 nm $Fe_{3-\delta}O_4$ nanospheres.

**Table 5.4** Properties of D2-dendronized iron oxide NPs as a function of their size, shape and composition (Φ = mean diameter determined from TEM images, $\Phi_{Hydro}$ = mean hydrodynamic diameter)

| | Φ (nm) | $\%Fe_{3-x}O_4$ | $\Phi_{Hydro}$ (nm) | $r_1$ ($mM^{-1}\cdot s^{-1}$) | $r_2$ ($mM^{-1}\cdot s^{-1}$) | $r_2/r_1$ |
|---|---|---|---|---|---|---|
| | 19 | 72 | 42 | 7 | 202 | 28 |
| | 16 | 66 | 66 | 5 | 116 | 23 |
| | 16 | 100 | 42 | 8 | 222 | 27 |
| | 10 | 100 | 30 | 6.1 | 91 | 15 |
| | 20 | 100 | 45 | 4 | 126 | 31 |
| Endorem | — | — | 120–130 | 10 | 141 | 13 |

coated with D2 dendrons (Fig. 5.2) and their MRI contrasting properties have been evaluated at first by relaxivity measurements. All these results are given in Table 5.4. One may notice that a modification of the size or shape or composition does not affect the in vitro relaxivity properties of dendronized NPs and even

the measured values and ratio are very high especially for homogeneous nanocubes and core–shell spherical NPs. Ghost images (Fig. 5.9) confirm the very strong T2 effect of these NPs even at low iron concentration (0.02 mM in Fe). The very good contrasting properties of these dendronized NPs were also highlighted in vivo after intravenous injection of homogeneous nanocubes and FeO@$Fe_{3-x}O_4$ nanospheres.[60]

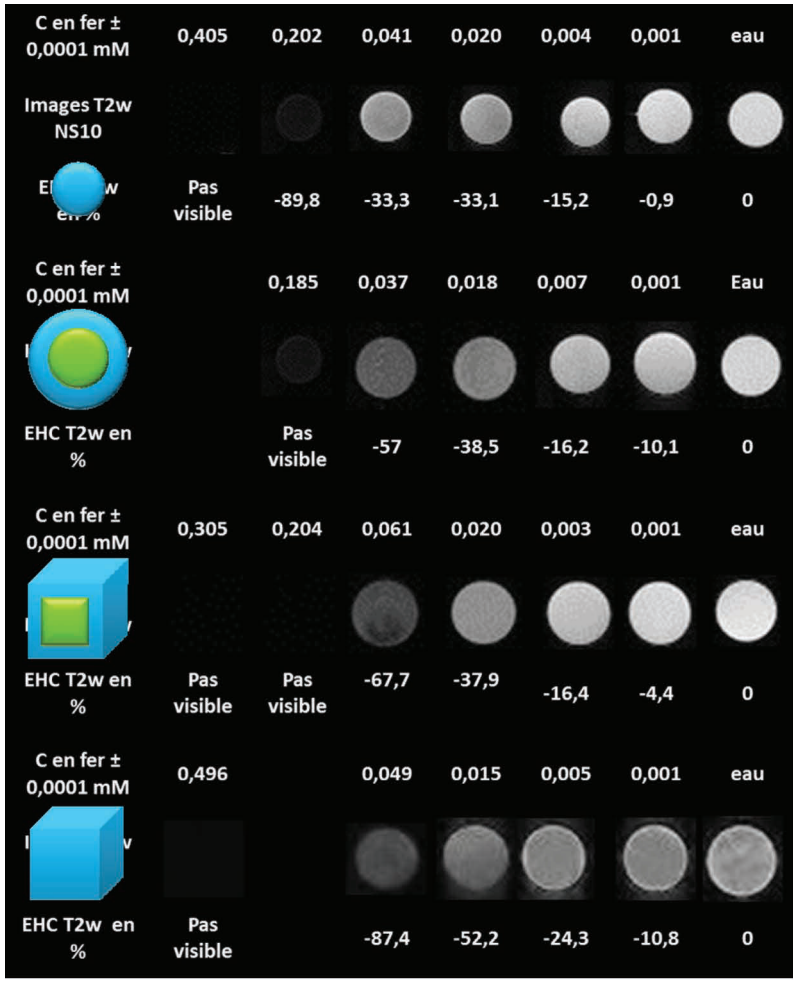



**Figure 5.9** T2w ghost images of D2-dendronized NPs at 7T and 25°C together with EHC values as a function of the iron concentration.

15:59 28 October 2016

15:59 28 October 2016

Magnetic hyperthermia measurements at a field frequency of 700 kHz and amplitude of 27 mT were performed on suspensions of core–shell and homogeneous nanocubes and core shell nanospheres as a function of the iron concentration (Table 5.5). At first, one may notice a decrease of the SAR values when the iron concentration increases. On low concentrated samples, oxidized nanocubes display SAR values higher than those of core–shell nanospheres, which display slightly higher values than those of oxidized nanocubes. The good hyperthermia properties of these dendronized NPs at low concentration were confirmed with SAR values obtained for homogeneous 22 nm nanospheres at a lower concentration and with a lower frequency (Table 5.5). Theses SAR values are difficult to compare to published results as the measurement parameters such as concentration, field amplitude or frequency vary a lot in the literature.[54] However, the NPs considered here display heating capacities suitable for hyperthermia treatment, by comparison to SAR values reported for spherical single-core maghemite NPs[15,55–57] or cubic NPs[17,58] or core–shell NPs.[32]

**Table 5.5** SAR values obtained for homogenenous and core–shell nanocubes or nanospheres at a field frequency of 700 kHz and amplitude of 27 mT and for 22 nm sized homogeneous nanospheres at field frequency of 571 kHz and amplitude of 24 mT

| | **19 nm core–shell FeO@$Fe_{3-\delta}O_4$ nanospheres** | | | | | **16 nm core–shell FeO@$Fe_{3-\delta}O_4$ nanocubes** | | **16 nm oxidized nanocubes** | | | | | **22 nm $Fe_{3-\delta}O_4$ nanospheres 571 kHz, 24 mT** |
|---|---|---|---|---|---|---|---|---|---|---|---|---|---|
| [Fe] mmol | 2 | 4 | 7 | 14 | 70 | 2 | 3 | 3 | 4 | 7 | 14 | 70 | 1.34 |
| SAR (W/g) | 484 | 218 | 73 | 94 | 27 | 450 | 261 | 356 | 213 | 125 | 123 | 65 | 360 |

At higher concentration, the SAR values strongly decrease for the three samples indicating an iron concentration effect on magneto-thermal properties. Indeed, the heat released by magnetic NPs does not depend only on their intrinsic properties but also on magnetic interaction between individual NPs as the NPs concentration increases.[61] The role that dipolar interactions might have on SAR values is not completely understood at present and has not been properly addressed in the past years.[55,62,63]

15:59 28 October 2016

Indeed, contradictory experimental studies reported either a decrease or an increase of SAR with those interactions.[55,61,62,64,65] In fact, depending on the NPs anisotropy, dipolar interactions may act differently on the clustering/spatial arrangement of NPs under an applied magnetic field leading either to their aggregation or to their alignment in chains. Very recent evaluations of these interaction effects[55,62] and studies on magnetosomes synthesized by bacteria[50] pointed out that chains of magnetic NPs are ideal for reaching very high SAR values. Furthermore, cubic-shaped NPs would favor geometrical arrangement compared to spherical shape. Indeed chains of nanocubes can form due to strongly anisotropic dipolar forces mediating nanoparticle attachment.[55,62] Serantes et al. reported the positive effect of oriented attachment of 44 nm NPs on hyperthermia properties.[65] In our case, the formation of chains with core–shell nanocubes at low concentration was observed by TEM without applying any magnetic field.[60] These observations may thus explain the high heating values obtained at low concentration. At high concentration, aggregates form due to enhanced dipolar interactions and then the benefit effect of the geometric arrangement is lost.

Such good hyperthermia properties at low iron concentration are promising to envision therapy after *iv* injection and targeting of organs as the amount of NPs accumulated in organs will be lower than after intratumoral injection. Few in vivo MH studies have been reported so far and in these studies, NPs had to be injected intratumorally.

## 5.5 Conclusion

Dendron molecules were found very suitable to develop smart nano-objects for in vivo MRI with a very good biodistribution and bioelimination without RES uptake. Such improved in vivo and MRI properties are attributed to the good magnetic properties of the inorganic core and to the dendron anchoring through phosphonate functions, but mainly to the optimal design of the small-sized dendritic organic shell. The design of the core was also found of great importance as it provides therapeutic properties through magnetic hyperthermia leading thus to theranostic dendronized nano-objects showing great promise for imaging-guided therapy.

## References


1. Laurent, S. et al. (2008). Magnetic iron oxide nanoparticles: Synthesis, stabilization, vectorization, physicochemical characterizations, and biological applications. *Chem. Rev.*, **108**(6), 2064–2110.
2. Gupta, A. K., Gupta, M. (2005). Synthesis and surface engineering of iron oxide nanoparticles for biomedical applications. *Biomaterials*, **26**(18), 3995–4021.
3. Neuberger, T., Schöpf, B., Hofmann, H., Hofmann, M., and von Rechenberg, B. (2005). Superparamagnetic nanoparticles for biomedical applications: Possibilities and limitations of a new drug delivery system. *J. Magn. Magn. Mater*., **293**(1), 483–492.
4. Nguyen, N. T. K. eds. (2012) In *Magnetic Nanoparticles: from Fabrication to Clinical Applications*, CRC Press, Taylor and Francis.
5. Tomalia, D. A., and Fréchet, J. M. J. (2002). Discovery of dendrimers and dendritic polymers: A brief historical perspective. *J. Polymer Sci. Part A: Polymer Chem.*, **40**(16), 2719–2728.
6. Love, C. S., Chechik, V., Smith, D. K., and Brennan, C. (2004). Dendron-stabilized gold nanoparticles: Generation dependence of core size and thermal stability. *J. Mater. Chem.,* **14**(5), 919–923.
7. Paez, J. I., Coronado, E. A., and Strumia, M. C. (2012). Preparation of controlled gold nanoparticle aggregates using a dendronization strategy. *J. Colloid Interf. Sci.*, **384**(1), 10–21.
8. Huang, B., and Tomalia, D. A. (2005). Dendronization of gold and CdSe/cdS (core–shell) quantum dots with tomalia type, thiol core, functionalized poly(amidoamine) (PAMAM) dendrons. *J. Lumin.,* **111**(4), 215–223.
9. Martin, A. L., Li, B., and Gillies, E. R. (2009). Surface functionalization of nanomaterials with dendritic groups: Toward enhanced binding to biological targets. *J. Am. Chem. Soc.,* **131**(2), 734–741.
10. Sun, Y.-P., Weijie, H., Yi, L., Kefu, F., Kitaygorodskiy, A., Riddle, L. A., Joy, Y., and Carroll, D. L. (2001). Soluble dendron-functionalized carbon nanotubes: Preparation, characterization, and properties. *Chem. Mater.,* **13**(9), 2864–2869.
11. Lamanna, G., Garofalo, A., Popa, G., Wilhelm, C., Bégin-Colin, S., Felder-Flesch, D., Bianco, A., Gazeau, F., and Ménard-Moyon, C. (2013). Endowing carbon nanotubes with superparamagnetic properties: Applications for cell labeling, MRI cell tracking and magnetic manipulations. *Nanoscale*, **5**(10), 4412–4421.


15:59 28 October 2016

15:59 28 October 2016

12. Benhabbour, S. R., Sheardown, H., and Adronov, A. (2008). Protein resistance of PEG-functionalized dendronized surfaces: Effect of PEG molecular weight and dendron generation. *Macromolecules*, **41**(13), 4817–4823.

13. Chevallier, P., Walter, A., Garofalo, A., Veksler, I., Lagueux, J., Bégin-Colin, S., Felder-Flesch, D., and Fortin, M.-A. (2014). Tailored biological retention and efficient clearance of pegylated ultra-small MnO nanoparticles as positive MRI contrast agents for molecular imaging. *J. Mater. Chem. B*, **2**, 1779–1790.

14. Na, H. B., Palui, G., Rosenberg, J. T., Ji, X., Grant, S. C., and Mattoussi, H. (2012). Multidentate catechol-based polyethylene glycol oligomers provide enhanced stability and biocompatibility to iron oxide nanoparticles. *ACS Nano*, **6**(1), 389–399.

15. Gillich, T., Acikgöz, C., Isa, L., Dieter Schlüter, A., Spencer, N. D., and Textor, M. (2012). PEG-stabilized core–shell nanoparticles: Impact of linear versus dendritic polymer shell architecture on colloidal properties and the reversibility of temperature-induced aggregation. *ACS Nano*, **7**(1), 316–329.

16. Duanmu, C., Saha, I., Zheng, Y., Goodson, B. M., and Gao, Y. (2006). Dendron-functionalized superparamagnetic nanoparticles with switchable solubility in organic and aqueous media: Matrices for homogeneous catalysis and potential mri contrast agents. *Chem. Mater.,* **18**(25), 5973–5981.

17. Heuze, K., Rosario-Amorin, D., Nlate, S., Gaboyard, M., Bouter, A., and Clerac, R. (2008). Efficient strategy to increase the surface functionalization of core-shell superparamagnetic nanoparticles using dendron grafting. *New J. Chem.*, **32**(3), 383–387.

18. Pan, B., Cui, D., Sheng, Y., Ozkan, C., Gao, F., He, R., Li, Q., Xu, P., and Tuo, H. (2007). Dendrimer-modified magnetic nanoparticles enhance efficiency of gene delivery system. *Cancer Res.*, **67**(17), 8156–8163.

19. Liu, W.-M., Xue, Y.-N., Peng, N., He, W.-T., Zhuoa, R.-X., and Huang, S.-W. (2011). Dendrimer modified magnetic iron oxide nanoparticle/DNA/PEI ternary magnetoplexes: A novel strategy for magnetofection. *J. Mater. Chem.,* **21**(35), 13306–13315.

20. Chandra, S., Mehta, S., Nigam, S., and Bahadur, D. (2010). Dendritic magnetite nanocarriers for drug delivery applications. *New J. Chem.,* **34**(4), 648–655.

21. Rouhollah, K., Pelin, M., Serap, Y., Gozde, U., and Ufuk, G. (2013). Doxorubicin loading, release, and stability of polyamidoamine dendrimer-coated magnetic nanoparticles. *J. Pharm. Sci.,* **102**(6), 1825–1835.

15:59 28 October 2016

22. Felder-Flesch, D., Perriat, P., Pourroy, G., and Bégin-Colin, S. (2011). Properties and suspension stability of dendronized iron oxide nanoparticles for MRI applications. *Contrast Media Mol. Imaging,* **6**(3), 132–138.

23. Basly, B., Felder-Flesch, D., Perriat, P., Billotey, C., Taleb, J., Pourroy, G., and Begin-Colin, S. (2010). Dendronized iron oxide nanoparticles as contrast agents for MRI. *Chem. Comm.,* **46**(6), 985–987.

24. Basly, B., Popa, G., Fleutot, S., Pichon, B., Garofalo, A., Ghobril, C., Billotey, C., Berniard, A., Bonazza, P., Martinez, H., Felder-Flesch, D., and Begin-Colin, S. (2013). Effect of the nanoparticle synthesis way on dendronized iron oxides as MRI contrast agents. *Dalton Trans.*, **42**, 2146–2157.

25. Ghobril, C., Popa, G., Parat, A., Billotey, C., Taleb, J., Bonazza, P., Begin-Colin, S., and Felder-Flesch, D. (2013). A bisphosphonate tweezers and clickable PEGylated PAMAM dendrons for the preparation of functional iron oxide nanoparticles displaying renal and hepatobiliary elimination. *Chem. Commun.,* **49**(80), 9158–9160.

26. Lamanna, G., Kueny-Stotz, M., Mamlouk-Chaouachi, H., Basly, B., Ghobril, C., Billotey, C., Berniard, A., Pourroy, G., Begin-Colin, S., and Felder-Flesch, D. (2011). Dendronized iron oxide nanoparticles for multimodal imaging. *Biomaterials*, **32**(33), 8562–8573.

27. Arsalani, N., Fattahi, H., Laurent, S., Burtea, C., Vander Elst, L., and Muller, R. N. (2012). Polyglycerol-grafted superparamagnetic iron oxide nanoparticles: Highly efficient MRI contrast agent for liver and kidney imaging and potential scaffold for cellular and molecular imaging. *Contrast Media Mol. Imaging*, **7**(2), 185–194.

28. Walter, A., Garofalo, A., Bonazza, P., Parat, A., Taleb, J., Jouhannaud, J., Pourroy, G., Voirin, E., Laurent, S., Vander Elst, L., Muller, R. N., Billotey, C., Begin-Colin, S., and Felder-Flesch, D. (2015). Validation of a dendron concept to tune colloidal stability, MRI relaxivity and bioelimination of functional nanoparticles. *J. Mater. Chem. B*, **3**, 1484–1494.

29. Kono, K., Ikeda, R., Tsukamoto, K., Yuba, E., Kojima, C., and Harada, A. (2012). Polyamidoamine dendron-bearing lipids as a nonviral vector: Influence of dendron generation. *Bioconjug. Chem*., **23**(4), 871–879.

30. Gao, F., Pan, B. F., Zheng, W. M., Ao, L. M., and Gu, H. C. (2005). Study of streptavidin coated onto PAMAM dendrimer modified magnetite nanoparticles. *J. Magn. Magn. Mater.,* **293**(1), 48–54.

15:59 28 October 2016


31. Walter, A., Garofalo, A., Parat, A., Martinez, H., Felder-Flesch, D., and Begin-Colin, S. (2015). Functionnalization strategies and dendronization of iron oxide nanoparticles. *Nanonotechnol. Rev.*, in press.
32. Daou, T. J., Bégin-Colin, S., Grenèche, J. M., Thomas, F., Derory, A., Bernhardt, P., Legaré, P., and Pourroy, G. (2007). Phosphate adsorption properties of magnetite nanoparticles. *Chem. Mater.,* **19**, 4494–4505.
33. Walter, A., Parat, A., Garofalo, A., Laurent, S., Vander Elst, L., Muller, R. N., Wu, T., Heuillard, E., Robinet, E., Meyer, F., Felder-Flesch, D., and Begin-Colin, S. (2014). Modulation of relaxivity, suspension stability, and biodistribution of dendronized iron oxide nanoparticles as a function of the organic shell design. *Part. Part. Syst. Charact.*, DOI: 10.1002/ppsc.201400217.
34. Baaziz, W., Pichon, B., Fleutot, S., Liu, Y., Lefevre, C., Greneche, J.-M., Toumi, M., Mhiri, T., and Begin-Colin, S. (2014). Magnetic iron oxide nanoparticles: Tuning of the size and nanosized-dependent composition, defects and spin canting. *J. Phys. Chem C*, **118**(7), 3795–3810.
35. Daou, T. J., Grenèche, J. M., Pourroy, G., Buathong, S., Derory, A., Ulhaq-Bouillet, C., Donnio, B., Guillon, D., and Begin-Colin, S. (2008). Coupling agent effect on magnetic properties of functionalized magnetite-based nanoparticles. *Chem. Mater.,* **20**(18), 5869–5875.
36. Bin Na, H., Chan Song, I., and Hyeon, T. (2009). Inorganic nanoparticles for MRI contrast agents. *Adv. Mater.*, **21**, 2133–2148.
37. http://www.magforce.de/en/home.html.
38. Thiesen, B., and Jordan, A. (2008). Clinical applications of magnetic nanoparticles for hyperthermia. *Int. J. Hyperther*., **24**, 467–474.
39. Maier-Hauff, K., Rothe, R., Scholz, R., Gneveckow, U., Wust, P., Thiesen, B., Feussner, A., von Deimling, A., Waldoefner, N., and Felix, R. (2007). Thermotherapy using magnetic nanoparticles combined with external beam radiotherapy: Results of a feasibility study on patients with glioblastoma multiform. *J. Neuro-Oncol.*, **81**, 53–60.
40. Maier-Hauff, K., Ulrich, F., Nestler, D., Niehoff, H., Wust, P., Thiesen, B., Orawa, H., Budach, V., and Jordan, A. (2011). Efficacy and safety of intratumoral thermotherapy using magnetic iron-oxide nanoparticles combined with external beam radiotherapy on patients with recurrent glioblastoma multiform. *J. Neuro-Oncol.*, **103**(2), 317–324.
41. Goya, G. F., Asin, L., and Ibarra, M. R. (2013). Cell death induced by AC magnetic fields and magnetic nanoparticles: Current state and

15:59 28 October 2016

perspectives. *Int. J. Hyperther.*, **1–9**, DOI: 10.3109/02656736.2013.838646.

42. Deatsch, A. E., and Evans, B. A. (2014). Heating efficiency in magnetic nanoparticle hyperthermia. *J. Magn. Magn. Mater.,* **354**, 163–172; Kolosnjaj-Tabi, J., Di Corato, R., Lartigue, L., Marangon, I., Guardia, P., Silva, A. K. A., Luciani, N., Clément, O., Flaud, P., Singh, J. V., Decuzzi, P., Pellegrino, T., Wilhelm, C., and Gazeau, F. (2014). Heat-Generating iron oxide nanocubes: Subtle "destructurators" of the tumoral microenvironment, *ACS Nano*, **8**, 4268–4283.
43. Lee, J.-H., Jang, J.-T., Choi, J.-S., Moon, S. H., Noh, S.-H., Kim, J.-W., Kim, J.-G., Kim, I.-S., Park, K. I., and Cheon, J. (2011). Exchange-coupled magnetic nanoparticles for efficient heat induction. *Nature Nanotech.,* **6**, 418–422.
44. Glöckl, G., Hergt, R., Zeisberger, M., Dutz, S., Nagel, S., and Weitschies, W. (2006). The effect of field parameters, nanoparticle properties and immobilization on the specific heating power in magnetic particle hyperthermia. *J. Phys. Condens. Matter,* **18**, S2935.
45. Hergt, R., Dutz, S., Müller, R., and Zeisberger, M. (2006). Magnetic particle hyperthermia: Nanoparticle magnetism and materials development for cancer therapy. *J. Phys. Condens. Matter*, **18**, S2919.
46. R. E. Rosensweig (2002). Heating magnetic fluid with alternating magnetic field. *J. Magn. Magn. Mater.,* **252**, 370–374.
47. Hergt, R., and Dutz, S. (2007). Magnetic particle hyperthermia-biophysical limitations of a visionary tumour therapy. *J. Magn. Magn. Mater.*, **311**, 187–192.
48. Gazeau, F., Lévy, M., and Wilhelm, C. (2008). Optimizing magnetic nanoparticle design for nanothermotherapy. *Nanomedicine*, **3**, 831–844.
49. Daou, T. F., Pourroy, G., Bégin-Colin, S., Grenèche, J.-M., Ulhaq-Bouillet, C., Legaré, P., Bernhardt, P., Leuvrey, C., and Rogez, G. (2006). Hydrothermal synthesis of monodisperse magnetite nanoparticles. *Chem. Mater.*, **18**, 4399–4404; Jaime Santoyo Salazar, J., Perez, L., de Abril, O., Truong Phuoc, L., Ihiawakrim, D., Vazquez, M., Greneche, J.-M., Begin-Colin, S., and Pourroy, G. (2011). Magnetic iron oxide nanoparticles in 10–40 nm range: Composition in terms of magnetite/maghemite ratio and effect on the magnetic properties. *Chem. Mater.*, **23**, 1379–1386.
50. Alphandéry, E., Faure, S., Seksek, O., Guyot, F., and Chebbi, I. (2011). Chains of magnetosomes extracted from AMB-1 magnetotactic

bacteria for application in alternative magnetic field cancer therapy. *ACS Nano*, **5**, 6279–6296.

51. Kumara, S. S. R., and Mohammad, F. (2011). Magnetic nanomaterials for hyperthermia-based therapy and controlled drug delivery. *Adv. Drug Deliv. Rev.*, **63**, 789–808.
52. Laurent, S., Dutz, S., Häfeli, U. O., and Mahmoudid, M. (2011). Magnetic fluid hyperthermia: Focus on superparamagnetic iron oxide nanoparticles. *Adv. Colloid Interface Sci.*, **166**, 8–23.
53. Baaziz, W., Pichon, B. P., Lefevre, C., Ulhaq-Bouillet, C., Greneche, J.-M., Toumi, M., Mhiri, T., and Bégin-Colin, S. (2013). High exchange bias in $Fe_{3-\delta}O_4$@CoO core shell nanoparticles synthesized by a one-pot seed-mediated growth method. *J. Phys. Chem. C,* **117**(21), 11436–11443.
54. Guardia, P., Di Corato, R., Lartigue, L., Wilhelm, C., Espinosa, A., Garcia-Hernandez, M., Gazeau, F., Manna, L., and Pellegrino, T. (2012). Water-soluble iron oxide nanocubes with high values of specific absorption rate for cancer cell hyperthermia treatment. *ACS Nano*, **6**, 3080–3091.
55. Martinez-Boubeta, C., Simeonidis, K., Makridis, A., Angelakeris, M., Iglesias, O., Guardia, P., Cabot, A., Yedra, L., Estradé, S., Peiró, F., Saghi, Z., Midgley, P. A., Conde-Leborán, I., Serantes, D., and Baldomir, D. (2013). Learning from nature to improve the heat generation of iron-oxide nanoparticles for magnetic hyperthermia applications. *Sci. Rep.*, **3**, 1652.
56. Hugounenq, P., Levy, M., Alloyeau, D., Lartigue, L., Dubois, E., Cabuil, V., Ricolleau, C., Roux, S., Wilhelm, C., Gazeau, F., and Bazzi., R. (2012). Iron oxide monocrystalline nanoflowers for highly efficient magnetic hyperthermia. *J. Phys. Chem. C*, **116**, 15702–15712.
57. Lartigue, L., Hugounenq, P., Alloyeau, D., Clarke, S. P., Lévy, M., Bacri, J.-C., Bazzi, R., Brougham, D. F., Wilhelm C., and Gazeau, F. (2012). Cooperative organization in iron oxide multi-core nanoparticles potentiates their efficiency as heating mediators and mri contrast agents. *ACS Nano*, **6**(12), 10935–10949.
58. Demortière, A., Panissod, P., Pichon, B. P., Pourroy, G., Guillon, D., Donnio, B., and Bégin-Colin, S. (2011). Size-dependent properties of magnetic iron oxide nanocrystals. *Nanoscale*, **3**, 225–232.
59. Pichon, B. P., Gerber, O., Lefevre, C., Florea, I., Fleutot, S., Baaziz, W., Pauly, M., Ohlmann, M., Ulhaq, C., Ersen, O., Pierron-Bohnes, V., Panissod, P., Drillon, M., and Begin-Colin, S. (2011). Microstructural

15:59 28 October 2016

and magnetic investigations of wüstite-spinel core-shell cubic-shaped nanoparticles. *Chem. Mater.,* **23**, 2886–2900.

60. Walter, A., Billotey, C., Garofalo, A., Ulhaq-Bouillet, C., Lefèvre, C., Taleb, J., Laurent, S., Vander Elst, L., Muller, R. N., Lartigue, L., Gazeau, F., Felder-Flesch, D., and Begin-Colin, S. (2014). Mastering shape and composition of dendronized iron oxide nanoparticles to tailor magnetic resonance imaging and hyperthermia. *Chem. Mater.*, **26**(18), 5252–5264.
61. Dennis, C. L., Jackson, A. J., Borchers, J. A., Hoopes, P. J., Strawbridge, R., Foreman, A. R., van Lierop, J., Grüttner, C., and Ivkov, R. (2009). Nearly complete regression of tumors via collective behavior of magnetic nanoparticles in hyperthermia. *Nanotechnology*, **20**, 395103–395110.
62. Mehdaoui, B., Tan, R. P., Meffre, A., Carrey, J., Lachaize, S., Chaudret, B., and Respaud, M. (2013). Increase of magnetic hyperthermia efficiency due to dipolar interactions in low-anisotropy magnetic nanoparticles: Theoretical and experimental results. *Phys. Rev. B*, **87**, 174419.
63. Burrows, F., Parker, C., Evans, R. F. L., Hancock, Y., Hovorka, O., and Chantrell, R. W. (2010). Energy losses in interacting fine-particle magnetic composites. *J. Phys. D: Appl. Phys.,* **43**, 474010.
64. de la Presa, P., Luengo, Y., Multigner, M., Costo, R., Morales, M. P., Rivero, G., and Hernando, A. (2012). Study of Heating efficiency as a function of concentration, size, and applied field in $\gamma$-$Fe_2O_3$ nanoparticles. *J. Phys. Chem. C*, **116**, 25602–25610.
65. Serantes, D., Simeonidis, K., Angelakeris, M., Chubykalo-Fesenko, O., Marciello, M., del Puerto Morales, M., Baldomir, D., and Martinez-Boubeta, C. (2014). Multiplying magnetic hyperthermia response by nanoparticle assembling. *J. Phys. Chem. C*, **118**, 5927–5934.

15:59 28 October 2016

15:59 28 October 2016



Taylor & Francis
Taylor & Francis Group
http://taylorandfrancis.com

## Chapter 6

# Anti-Inflammatory Dendrimers

**Cédric-Olivier Turrin and Anne-Marie Caminade**

*CNRS, LCC (Laboratoire de Chimie de Coordination),*
*205, route de Narbonne, F-31077 Toulouse, France*
*Université de Toulouse, UPS, INPT, LCC, F-31077 Toulouse, France*

cedric-olivier.turrin@lcc-toulouse.fr

The search for new anti-inflammatory drugs is an area of strong interest, related to several health issues, but dendrimer-based anti-inflammatory strategies are rather scarce. This chapter presents different strategies that have been already proposed in the past years for many of them. These strategies include (i) the cargo-loading approach (non-covalent association of anti-inflammatory drugs with dendrimers), (ii) the pro-drug approach (anti-inflammatory drugs linked to dendrimers, with a possible control over the drug release), and (iii) dendrimers having intrinsic anti-inflammatory properties.

## 6.1 Introduction

Inflammation (from the Latin *inflammare*, set on fire) processes are defense mechanisms that are onset in order to protect higher

*Dendrimers in Nanomedicine*
Edited by Delphine Felder-Flesch
Copyright © 2016 Pan Stanford Publishing Pte. Ltd.
ISBN 978-981-4745-49-9 (Hardcover), 978-981-4745-50-5 (eBook)
www.panstanford.com

15:59 28 October 2016

organisms from infection and injury. This protective response is associated to specific purposes like elimination of the initial cause of cell injury, removal of necrotic or damaged tissues and initiation of the process of repair. Despite the impressive complexity of inflammatory processes and the related immune responses, the onset of inflammation is schematically mediated by an increase in permeability of blood vessels, and the migration of proteins and white blood cells from the circulation to the site of tissue damage (Fig. 6.1).

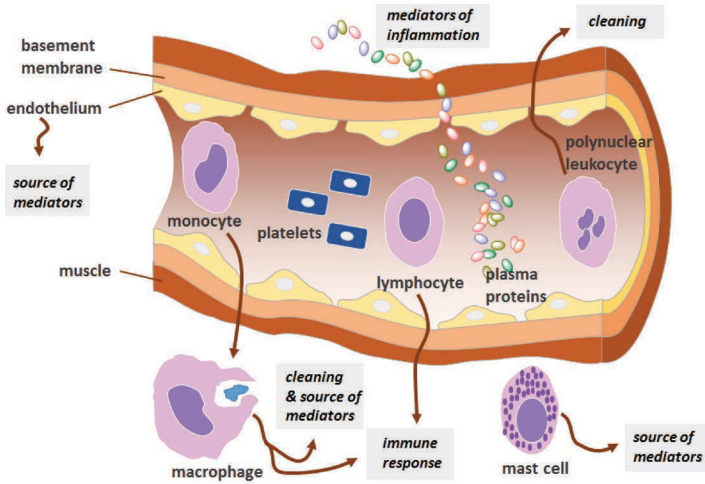



**Figure 6.1** Components of acute and chronic inflammation transiting in the blood stream.

Acute inflammation refers to rapid inflammatory, relatively nonspecific, responses that last few days, and originates from infections, tissue necrosis (thermal injury for example), foreign bodies or immune reactions related to hypersensitivity reaction (allergy, autoimmune diseases). In this regard, acute inflammation can be considered as an appropriate host response to infection or injury. Chronic inflammation refers to progressive, relatively specific and often severe inflammatory responses that may last over a long duration. Chronic inflammation may result from persistent injury or infection (ulcer), prolonged exposure to toxic agents or autoimmune diseases.

Chronic inflammation appears then as a dysregulated, inappropriate response which is not only associated to autoimmune

chronic inflammatory diseases (CIDs), but also underlies the genesis and progression of a broad range of pathological processes, like type 2 diabetes and cancers,[1] in particular during the aging process. As a matter of fact, chronic inflammatory diseases are an important cause of death and disability, with significant societal costs and a dramatic impact on patient's life. As such, many efforts have been devoted to bring new therapeutic strategies to suppress inflammation, and there still exists an unmet medical need for new effective therapies.

Treatment of inflammation is often a gradual response involving a wide range of drugs. Non-steroidal anti-inflammatory (NSAI) drugs are widely used and inhibit the prostaglandin synthase, also name cyclooxygenase (COX) involved in the first step of synthesis of some inflammation mediators. Glucocorticoid derivatives are steroidal hormone analogous to endogenous cortisol, which affect several physiological processes, including immune response, regulation of inflammation, carbohydrate and protein metabolisms. Biologics or biological products refer to as blood components, cells tissues and recombinant proteins, and contrarily to synthetic drugs, these complex mixtures produced by living organisms are not easily identified or characterized. Biologics like soluble receptors or monoclonal antibodies (MoAbs) that target a specific cell-derived or plasma protein-derived chemical mediators of inflammatory processes are widely used in first-line treatments for CIDs.

Despite the fact that the search for new anti-inflammatory drugs is an area of strong interest, it should be noted that the literature related to dendrimer-based anti-inflammatory strategies is rather scarce, although it has been significantly increasing over the last few years. This observation can possibly be related to the fact that traditional drug discovery like structure-based drug design, has been moderately successful in satisfying the unmet needs related to chronic inflammation, possibly because of the extreme complexity of immune responses underlying inflammatory processes and the high development costs associated to traditional drug discovery pathways. Drug repositioning, that is finding new uses for existing drugs, is actually an option that is preferred by big pharmaceutical companies and smaller biotechnology companies, because it offers faster development times and costs. This tendency can be illustrated by the presence of many MoAbs

15:59 28 October 2016

originating from the oncology pipeline in several clinical assays for the treatment of CIDs, despite the severe and deleterious side effects associated to these biologics-based treatments.

The first use of dendrimers for anti-inflammatory purposes was described in the late 1990s. These strategies are related to drug delivery and they involve either the encapsulation of known anti-inflammatory drugs within dendrimers or the conjugation of these drugs on dendrimers. These strategies are generally based on a simple rational, with a key issue related to drug solubility or its transportation to the site of action, and the presence of the dendrimer is justified by its ability to solve this pivotal problem. Conversely, the discovery of dendrimers having intrinsic anti-inflammatory properties resembles in some aspect to a serendipitous process and it is much less documented. These aspects, which have been partially surveyed in two recent reviews,[2,3] are also developed in this chapter dedicated to recent examples.

15:59 28 October 2016

## 6.2 Cargo-Loading Strategy: Association of Anti-Inflammatory Drugs with Dendrimers

The encapsulating properties of dendrimers have been early uncovered in pioneering studies showing that it was possible to solubilize lipophilic molecules in water in the presence of water-soluble dendrimers.[4,5] These studies revealed dynamic processes associated to this strategy and the possibility that encapsulated molecules could escape the host. The dendritic box developed in the group of Meijer,[6] allowed to prevent passive diffusion outside the dendrimer thanks to an adapted steric hindrance of the dendrimer surface. The underlying fundamentals related to dendrimer-base encapsulation and solubilization of active molecules has been since then described in several reviews,[7–11] and this strategy is still generating a considerable number of publications. Basically, it is generally admitted that the simple encapsulation inside dendrimers occurs thanks to lipophilic and/or electrostatic interactions between the dendrimer structure (internal scaffold and surface functions) and the drug, which can be a neutral lipophilic drug or a more complex charged architecture (DNA, RNA, SiRNA).[12] In the case of charged molecules, the interactions between the dendrimer and the encapsulated

drug often result in poorly-defined supramolecular assemblies, which have been coined as "dendriplexes" in the case of genetic materials complexed by dendrimers (Fig. 6.2).[13,14]

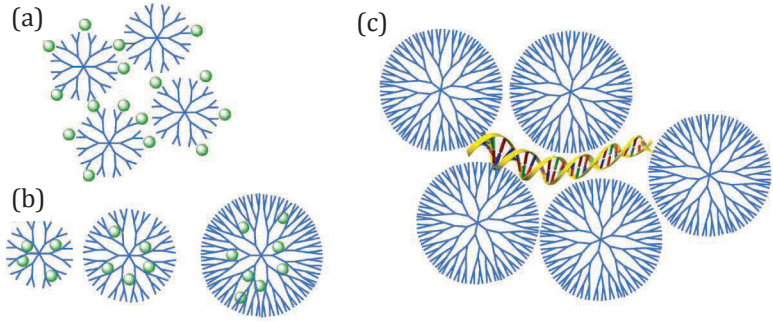



**Figure 6.2** Encapsulation of drugs with dendrimers through surface ionic interactions (a) or lipophilic interactions (b) and schematic representation of a dendriplex (DNA fragment complexed with dendrimers (c)).

Considering the high versatility of dendrimer chemistry, their surface can be easily engineered to favor the access to the suitable site of action of the drug or to escape the immune system. In the case of anti-inflammatory strategies, these issues are sometimes less important, mostly because the question of the target can be less pivotal than for other organ-dependent pathologies. Additionally, it should be noted that escaping the immune system might be contradictory regarding the importance of the latter in the inflammatory response. Nevertheless, these surface modifications are connected to the general concept of bioavailability, which is generally admitted to be the portion of unchanged drug that reaches its site of action, whereas it is *stricto sensu* the portion of unchanged drug that reaches the bloodstream after a non-intravenous administration. Considering that the advent of a drug is at least related to its solubility, the question of bioavailability remains a key concern, which has been addressed in some cases by PEGylation of the dendrimer surface in order to increase the drug solubility and/or the cargo loading capacities rather that for escaping the reticuloendothelial system. It can be noticed that the number of studies related to organ-oriented or targeted anti-inflammatory strategy with dendrimers bearing specific groups on their surface is very low.

15:59 28 October 2016

15:59 28 October 2016

### 6.2.1 Non-Targeted Strategies

Several examples of non-targeted formulations are based on ionic interactions between acidic NSAI drugs and amine-terminated dendrimers. Most examples deal with commercially available PAMAM, either in their native or surface-engineered forms, and core-modified PolyAmidoAmine (PAMAM) or PEI dendrimers with PEG or PPO (polypropylene oxide) moieties. The poor water solubility of NSAI drugs often requires high doses, which are responsible for side effects affecting the gastrointestinal tract, as this side effect is dose-dependent and related to their therapeutic target, the cyclooxygenase (COX) enzyme. The issue of the bioavailability of these drugs and their ability to cross natural barrier is then highly related to their side effect issues. In the absence of specific surface function modification, it should be noted that the cargo-loading strategy also presents the advantage to reduce the charge-related intrinsic cytotoxic effects of polycationic dendrimers.[15] In this regard, it is noteworthy that drug-dendrimer interactions may significantly affect the toxicity of both components,[16] as stated above in the case of NSAI drugs.

#### 6.2.1.1 Drug-dendrimer interactions

The question of the host-guest interactions ruling the association depends on the nature of both components, and subtle combinations of ionic and lipophilic interactions as demonstrated by several theoretical and experimental studies.[17–21] The formulation of well-known acidic NSAI drug ibuprofen produced at 13000 t per year with PAMAM dendrimers was initially found to proceed through ionic surface interaction. The complexation was found to be dependent on pH values, with a significant solubility enhancement at basic and neutral pH and no solubility change at acidic pH in comparison with the plain drug.[22] Although this macroscopic observation was confirmed by UV-vis, FTIR and NMR studies,[21] the encapsulation of ibuprofen within the dendrimer structure was also found to increase moderately its water solubility.[21] Fully atomistic molecular dynamic simulations of PAMAM-ibuprofen complexes revealed that at low pH values (pH < 4) the hydrophobic ibuprofen molecules form clusters in water rather than interacting with the dendrimer, despite a more open conformation of the latter. At physiological pH, dendrimer/ibuprofen stable complexes

15:59 28 October 2016

are favored by hydrogen bonding.[19] Despite the fact that the authors concluded that this study could probably be extended to other NSAI drugs, a recent theoretical and experimental study based on Metropolis Monte Carlo algorithm calculations and mass spectrometry revealed some significantly different behavior for diflunisal, ibuprofen, ketoprofen, and naproxen in the presence of generation 4 PAMAM dendrimers. The affinity degree of the drug for the dendrimer (naproxen > ketoprofen > ibuprofen > diflunisal) was found to be governed by the interaction of the drugs with the lipophilic interior of the dendrimer in addition to the ionic interactions between the PAMAM amino terminal groups and the acidic fragments of the drugs.[23] These theoretical results were confirmed by ESI-MS/MS analysis of drug-dendrimer competitive complexation, in which the affinity of the drug was correlated to a more abundant presence of the drug/dendrimer fragments in the gas phase. Interestingly, this strategy is also amenable to non-acidic but ionizable NSAI drugs like phenylbutazone, for which both lipophilic and surface electrostatic interactions between the enol form and the dendrimer surface allow efficient drug solubilization in water,[24] confirming the importance of the internal structure of the carrier to achieve efficient loading.

In vitro, it was shown that these transportation strategies resulted in increased cellular entry in epithelial cell lines,[21,25] and paved the way for other studies on analogous NSAI drugs[26–29] (Fig. 6.3). In all studies, formulation of these NSAI drugs with PAMAM dendrimers increased their water solubility and reduced the hemolytic cytotoxicity of the polycationic drug delivery system by charge masking.

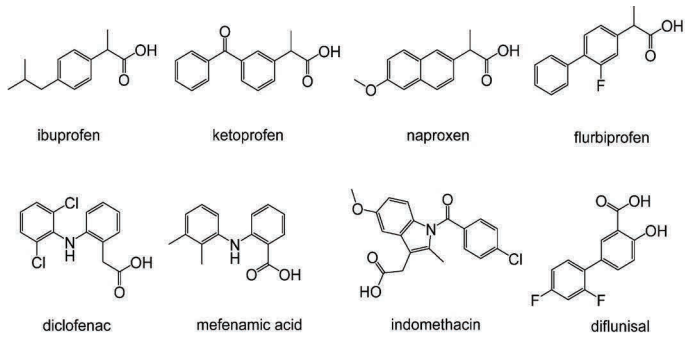



**Figure 6.3** Examples of NSAI drugs formulated with dendrimers.

In another study, PAMAM dendrimers were used to increase the water solubility of celastrol,[30] a pentacyclic triterpenoïd extracted from *Tripterygium wilfordii* which is used in traditional Chinese medicine. Celastrol showed in vivo and in vitro anti-inflammatory properties,[31] and *Tripterygium wilfordii* extracts were found to be as good as methotrexate to treat rheumatoid arthritis according to a recent clinical trial.[32] The use of generation 3 PAMAM dendrimers with amine or hydroxyl end groups allowed to increase the solubility of the drug by 7 and 12 fold, respectively. In the case of celastrol formulated with hydroxyl-terminated PAMAM, the intrinsic toxicity of celastrol towards microglia was significantly reduced and promising anti-inflammatory modulation of microglia, the primary monocytic immune cells of the central nervous system (CNS), was observed in vitro by suppressing their pro-inflammatory signaling. It should be noticed that this study also revealed the intrinsic anti-inflammatory properties of hydroxy-terminated PAMAM dendrimers (see Section 6.4) towards microglial cells.

15:59 28 October 2016

#### 6.2.1.2 Surface-modified and core-modified dendrimers

Despite the importance of lipophilic interactions in the loading efficacy, some surface engineering strategies have also been developed to increase the loading ability of PAMAM dendrimers, by either grafting PEG moieties or charged entities prone to form stable interactions with the transported drug.

In this regard, a generation 3 PPI dendrimer was quaternized with glycidyltrimethyl ammonium chloride. The resulting QPPI (quaternized PPI) dendrimer was found to increase the water solubility of anti-inflammatory drug nimesulide (NMD) up to 72 folds in comparison with the intrinsic solubility of the free lipophilic neutral drug. Despite the fact that this value was lower than the one obtained with native PPI dendrimer (108 folds), the QPPI dendrimer was found to be a better candidate than its parent compound. Actually, QPPI was able to sustain for a longer time the in vitro drug release: in 5 h 33% of NMD was release from QPPI dendrimer, whereas 90% was released from PPI dendrimer at the same time point. Additionally, the cytotoxicity of dendrimer, as measured by MTT assay on HBL cell line, was significantly reduced (at least one order of magnitude) upon glycidyltrimethyl ammonium grafting.[33]

15:59 28 October 2016

Although surface PEGylation mostly intends to increase the biocompatibility by escaping the reticuloendothelial system, PEGylation of dendrimers can provide structural modification that may increase their encapsulating properties. For optimized drug loading, the PEG or PPO entity can be placed at the core of the dendrimer. For instance, mefenamic acid and diclofenac NSAI drugs have been formulated with PEG-cored dendrimers[34] built from biocompatible citric acid.[35] The resulting system was found to be stable for several months and the release was found to be moderately accelerated at low pH. Analogous study on PPO-cored PAMAM dendrimers showed that the encapsulating properties of these systems towards the solubilization of NSAI drugs like ibuprofen, ketoprofen, and diflunisal was increased by a factor 4 in comparison with native PAMAM dendrimers. In another example, PPI dendrimers capped with PEG chains have been used to formulate a diclofenac prodrug.[36] The loading capacity of the PPI dendrimers was significantly increased upon PEGylation, indicating a possible interaction between the drug and the PEG-capping. The in vivo reduction of paw edema was more efficient in the presence of the dendrimer carrier in comparison with the plain drug.[37]

#### 6.2.1.3 In vivo validation of cargo-loading strategies

In a pioneering study published in 2005, the group of Baker compared the cargo-loading strategy versus the prodrug strategy (covalent conjugation on the surface of the dendrimer) towards the in vitro release kinetics of methotrexate,[38] an anti-cancer drug, which is also used to treat autoimmune CIDs like rheumatoid arthritis. The complexation of methotrexate (MTX) within PAMAM dendrimers changes it into a water-soluble species. Nevertheless, the complex rapidly disassembles in a solution of phosphate buffered saline, with immediate release of free MTX. Contrarily, covalent coupling of MTX leads to stable conjugates under the same conditions. Analogously, the burst release of dendrimer-complexed drug in the blood stream is actually an issue that is mentioned in many in vivo experiments. This strategy should then be considered as formulation strategy intending to allow the administration of an insoluble, which is already a valuable intention, rather than a real drug delivery strategy that should also include the proper delivery of the drug to its site of action.

15:59 28 October 2016

In the special case of anti-inflammatory drugs formulations, this consideration is more questionable and depends on the type of drug and its cellular target. Actually the site of action of anti-inflammatory drugs may be located in the bloodstream, as well as other nonspecific tissues, as in the case of drugs targeting immune cells or chemical mediators of inflammation like cyclooxygenase or glucocorticoid receptors.

An exhaustive survey of the literature shows that a few studies including in vivo studies have demonstrated that the cargo-loading strategy can significantly increase the mean residence time and half-life of the dendrimer-formulated drug in comparison with the plain drug after intravenous administration, despite the rapid burst release[29] that is observed in many cases.[39,40] More interestingly, the effect can also be observed following oral administration. It was actually shown that a *per os* administration of dendrimer-ketoprofen formulations on mice (stomach pH between 3 and 5)[41] leads to higher plasma drug concentration in animals treated with dendrimer-ketoprofen formulations.[28] Despite the known pH-sensitivity of these ionic formulations, these results unambiguously show the improved drug bioavailability following oral absorption. Nevertheless, translation to human digestive tract should be considered with great care considering the lower pH value of the human stomach.

In another example, partially PEGylated PPI dendrimers were used to formulate aceclofenac, a diclofenac pro-drug. In addition to the solubility enhancement provided by the PEG capping, in vivo studies on the reduction of paw edema following IV administration showed an increased efficiency of the drug dendrimer complex in comparison with the plain drug.

### 6.2.2 Targeted Strategies

As mentioned above, the number of examples of targeted strategies for the delivery of anti-inflammatory drugs formulated with dendrimers is rather scarce. For example, the targeting abilities of folate-functionalized dendrimers towards Chlamydia-infected tissues in a mouse model of reactive arthritis have been assayed with PAMAM structures. The results suggested that the concentration of folate-modified dendrimers on the site of infections was 3 to 4 times higher than the dendrimers lacking

15:59 28 October 2016

the folate capping.[42] In a recent study by N. K. Jain and coworkers, PPI dendrimers modified by fucose groups on their surface were assayed for the solubilization and in vivo delivery of the anti-inflammatory lipophilic drug sulfasalazine to liver macrophage, which are responsible for liver inflammation through the production and release of pro-inflammatory cytokines in the case of chronic liver diseases.[43] Macrophages being equipped with a large number of carbohydrate receptors, fucose has been shown to be an efficient targeting moiety to reach this cell population. Fucose-terminated PPI dendrimers actually proved to be good candidates to achieve the delivery of sulfasalazine in vivo, as demonstrated by high liver and spleen uptakes in comparison with the plain drug or the drug formulated with amine-terminated native PPI dendrimers. Basic pharmacodynamics data such as maximum plasma concentration, half-life, and mean residence time were found to be interestingly increased in animals treated with the fucose-PPI/sulfasalazine formulations in comparison with animals treated with the PPI/sulfasalazine formulations or the plain drug. The in vivo results were comforted by in vitro reduction of the production of pro-inflammatory cytokine IL-12 by macrophages cell lines. Cell viability assays and measurement of hematological parameters in animal models also demonstrated that the fucose-capping also decreased the intrinsic cytotoxicity of the carrier. Despite the specific liver-targeting strategy, these results could also open interesting perspectives for other autoimmune inflammatory conditions that are in the scope of sulfasalazine like Crohn's disease or rheumatoid arthritis.

Recently, some dendrimer-based systems have also been designed to propose alternative therapeutic strategies to address complex neuro-inflammation issues. Neuro-inflammation involves several mechanisms and cellular or molecular actors and mediators, among which microglia plays a pivotal role. Microglial cells are immune components that regulate many inflammatory processes in the CNS (central nervous system), and their regulation is actually at the center of many therapeutic issues related to neuro-inflammation and/or neurodegeneration. One of the key issues when addressing the regulation of microglia is the crossing of the blood–brain barrier (BBB) that separates the CNS from the bloodstream. Carboxymethylchitosan-modified PAMAM-based nanoparticles have been shown to efficiently target glial cells

and neurons in vitro and in vivo, proving their ability to cross the BBB and reach the desired target.[44] These systems with a diameter of a few hundred of nanometers can be equipped with targeting antibody,[45] and they have been tested in vitro for the delivery of methylprednisolone to microglial cells, and to treat lateral hemisection lesions in rats, an animal model of secondary injury following spinal cord injury (SCI), a major CNS trauma. In vitro delivery proved to be sustained over 14 days. The nanoparticles were found to be non-toxic at the concentration of 200 $\mu g \cdot mL^{-1}$, but significantly higher concentrations were used to observe efficient cellular uptake by CNS populations such as astrocytes, microglia and oligodendrocytes and subsequent modification of their metabolic activities. Nanoparticle uptake in the damaged spinal tissue was found to be effective in vivo within 3 h after a local administration realized close to and just after the lateral hemisection injury, and the functional outcome of treated rats was significantly improved in comparison with the control animals. It should be noticed that in a separate study these chitosan-PAMAM vehicles loaded with dexamethasone have been successfully assayed ex vivo to promote the osteogenic differentiation of rat marrow stromal cells,[46] opening new strategies in the field of regenerative medicine.[47]

15:59 28 October 2016

## 6.3 Prodrug Strategy: Conjugation of Anti-Inflammatory Drugs on Dendrimers

The prodrug strategy[48] consisting in attaching covalently a drug to a dendrimer has reached a high a level of sophistication with the advent of multifunctional targeted devices, as those developed by the group of J. R. Baker.[49–51] Despite a significant number of promising studies and demonstration of batch to batch consistency,[52] the issue related to the molecular definition of these dendrimers bearing on their surface a stochastic distribution of an active compound, a fluorescent tag and a targeting moiety has not been completely addressed.[53] Most studies are actually centered on the development dendrimeric systems for the delivery of MTX. MTX is a cytostatic drug acting on cells having a rapid proliferation, like myeloid and malignant cells, and it is used to treat several cancer conditions and chronic inflammatory diseases like

rheumatoid arthritis, psoriasis or Crohn's disease. Other examples can also be found in the literature, but many reports deal with non-targeted systems. The encapsulation and/or adsorption of anti-inflammatory drugs within and/or on the surface of dendrimers preserves the chemical integrity and pharmacological properties. On the contrary, the prodrug strategy involving a covalent attachment can alter its integrity, but it can provide a better control over drug release as demonstrated in some isolated comparative studies. It can be noticed that the issue of the drug release, which is highly dependent on the nature of the covalent link used to attach the drug to the dendrimer is not systematically discussed, although it can preclude further development.

15:59 28 October 2016

### 6.3.1 Dendrimer-NSAI Drug Conjugates

As stated previously, NSAI drugs are poorly soluble in water, and the interest of formulating them with dendrimers, in a non-covalent or a covalent fashion, resides mainly in increasing their bioavailability, which is, literally, their plasma concentration as an available active ingredient, following an oral administration. This increase is expected to be achieved through water solubility enhancement and increased crossing ability of the epithelial barrier. Despite the relative small number of studies, it can be noticed that most of them include information related to the stability of these systems and their ability to release the free drugs, in vitro or in vivo.

In a pioneering study, Wiwattanapatapee and colleagues described the grafting of 5-amino salicylic acid (5-ASA), the metabolite of sulfasalazine anti-inflammatory drug used in the treatment of colon inflammatory disorders, onto the surface of a generation 3 PAMAM dendrimer. 5-ASA was attached through azo-bond using *p*-aminobenzoic acid (PABA) or *p*-aminohippuric acid (PAH), and a release was expected to occur in the colon thanks to azoreductase enzymes. The conjugates were incubated with rat cecal contents at 37°C. The amount of drug released in one day was 45% and 57% for PABA and PAH linkers, respectively, whereas the release of 5-ASA from commercial sulfazaline was 80% in 6 h under the same conditions. This observation was explained by a steric hindrance of the enzyme sites in the case

of dendrimer-supported-5-ASA.[54] The group of D'Emanuele described the conjugation of naproxen on a generation 0 PAMAM dendrimer by amide bond or by ester bond thanks to L-lactic acid or PEG spacer.[55] The amide linker was found to be stable in various pH conditions, and in human plasma the ester bond was found to be cleaved resulting in a 20% release of naproxen after 16 h. The conjugates were non-toxic when exposed to Caco-2 cells for 3 h and the dendrimers significantly increased the transport of naproxen across this model barrier.[44] It was also found that the grafting of one lauroyl chain on the surface group of the diethylene glycol ester conjugate resulted in a higher permeability into Caco-2 cells.

Salicylic acid, another common NSAI drug, has also been used as a building block to prepare polyester dendrimers, containing up to 60 salicylate moieties per dendrimer (generation 3). Despite promising drug delivery properties associated to sustain delivery profiles through hydrolytic disassembly processes, these systems have not been further assayed. More recently, methyl, ethyl and isopropyl salicylate esters have been grafted onto the surface of polyether Fréchet-like dendrimers.[56] Despite an expected low-water solubility due to the absence of hydrophilic group, these systems presented fairly good anti-arthritic activity as measured by the inhibition of protein denaturation method, in comparison to the reference drug diclofenac.

In another early example reported by the group of Kannan,[57] 58 molecules of ibuprofen have been attached to a generation 4 OH-terminated PAMAM dendrimer (64 OH groups) through an ester linkage, and fluorescein isothiocyanate (FITC) labeling was achieved on the remaining non-esterified OH groups. The authors observed a rapid internalization of theses conjugates into lung epithelial cancer cell lines through a lysozome-endosome internalization pathway. Assuming a hydrolytic release of ibuprofen giving rise to a high local concentration of active compound, the dendrimer–drug conjugate was found to be more efficient than the small molecular weight ibuprofen-FITC analog in inhibiting the production of prostaglandin $PGE_2$.

The drug release properties of analogous systems have been studied with various linkers including amide, ester and glycine-phenylalanine-leucine-glycine (GFLG) tetrapeptide (Fig. 6.5), and compared to a monofunctional PEG linked to one molecule of ibuprofen.[58] Interestingly, the drug payload of the dendrimers

15:59 28 October 2016

15:59 28 October 2016

had to be maintained in the 4–9% range (in weight) in order to maintain a good solubility in the buffer solution, indicating that solubility issues had been encountered in the previous study reported above. Hydrolytic and enzymatic release profiles of these systems confirmed that ester linkage shows a pH-dependent hydrolytic release, with 36% of ibuprofen released at pH = 1.2 (human stomach pH) and only 4% of ibuprofen released within 10 days at pH = 5 (late endosome pH). The peptide linkages (simple amide or GFLG sequence) were quite stable against hydrolytic cleavage over a 10-daytime period and released less than 3% of the conjugated drug at pH = 1.2. The enzymatic release was found to be efficient only in the case of the PEG conjugated ibuprofen, a rather simple system in comparison with dendrimer conjugates which on the contrary afforded a sustained delivery over long periods of time, indicating a steric blockage of the esterase and protease active sites in the case of the dendrimer conjugates.

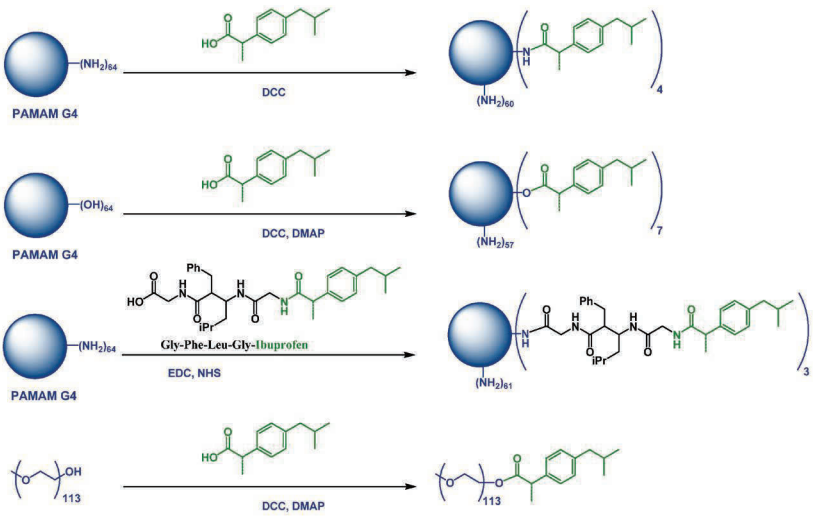



**Figure 6.4** Ibuprofen conjugates.

Aceclofenac, an analog of diclofenac used for the relief of pain and inflammation in chronic inflammatory diseases like rheumatoid arthritis, osteoarthritis and ankylosing spondylitis, has also been grafted on a generation 0 PAMAM dendrimer and a 40 KDa dextran polymer for comparison purposes, through an amide and an ester linkage, respectively.[59] The statistical grafting

led to comparable drug payload of 12.5% and 7.5%, respectively, as determined by proton NMR. In vitro studies in simulated gastric fluid (pH = 1.2) revealed that no amount of the drug was regenerated. In vivo assays showed that the anti-inflammatory and analgesic activities of the PAMAM conjugate were comparable to those of the standard drug. Interestingly, chronic ulcerogenic activity, an impairing side effect of the drug, was significantly reduced for the PAMAM dendrimer and dextran conjugates.

### 6.3.2 Controlled Release of *N*-Acetyl-Cysteine with Dendrimer Conjugates

*N*-acetyl cysteine (NAC) is a readily available, inexpensive amino-acid derivative that has been used for decades as a mucolytic agent, among other indications. It is a glutathione precursor having intrinsic antioxidant properties. It also has promising anti-inflammatory properties[60,61] related to the inhibition of the transcription of the NF-κB factor, and the resulting down-regulation of several pro-inflammatory genes.[62] NAC has a high plasma affinity requiring high doses and associated side effects when administrated intravenously.

In this context, its conjugation to suitable carriers could improve its bioavailability, its free circulation and interaction with plasma, in particular for the treatment of neuro-inflammation in perinatal applications. In this regard, the group of Kannan has devoted significant efforts to develop PAMAM-based NAC conjugates for the treatment of several conditions related to neuro-inflammation.

The grafting of NAC to amine (generation 1.5) and acid terminated (generation 3.5) PAMAM dendrimers has been designed through cleavable disulfide linkages (Fig. 6.5) for intracellular delivery based on glutathione levels.[63,64] It should be noticed that this strategy can be considered as non-conventional targeted strategy, as the drug is expected to be released within the cells. Actually, the issue of drug delivery also embraces questions related to the release of the drug. A statistical grafting strategy led to cationic G4 and anionic G3.5 PAMAM dendrimers having 16 and 18 NAC molecules on their surface, respectively. Some unreacted surface functions were subsequently involved into the grafting of FITC for imaging purposes. Release studies in buffer solutions showed by means of reverse phase High Pressure Liquid Chromatography

15:59 28 October 2016

15:59 28 October 2016

(HPLC) analysis that a fast release of NAC occurs at intracellular glutathione concentration (10 mM), while the conjugates are stable at extracellular glutathione levels (2 μM). Microglial cells are a key cell population involved in neuro-inflammation and the target cells of NAC. The FITC-labeled conjugates were found to enter rapidly and localize in the cytoplasm of these cells, following a lipopolysaccharide activation to trigger their pro-inflammatory response. The anti-oxidative property of the drug, as measured by the nitrite inhibition in the cell culture medium, was found to be significantly enhanced in the case of the conjugates as compared to free NAC. This improvement indicates that PAMAM dendrimers are responsible for higher intracellular NAC concentration, and that glutathione (GSH)-sensitive disulfide linker efficiently enables a rapid release of the drug. Additionally, the cationic PAMAM-NAC conjugate showed slightly better efficacy than the anionic PAMAM–NAC conjugate at equivalent concentrations, despite comparable drug payload.[51]

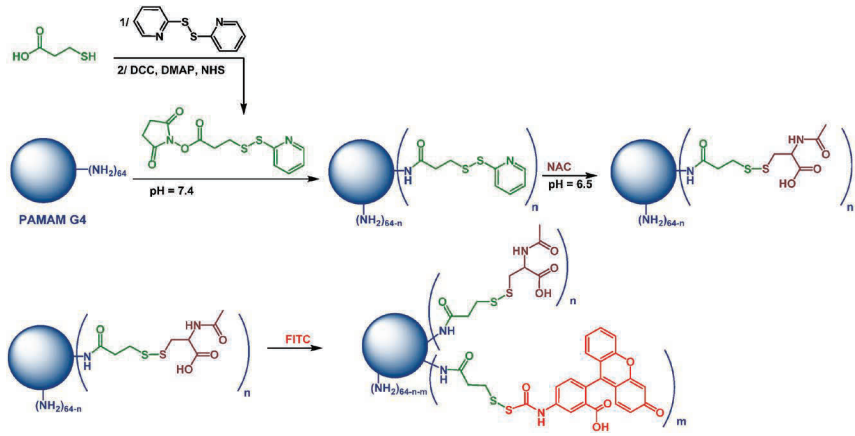



**Figure 6.5** PAMAM-NAC conjugates with glutathione sensitive linkers.

Further evaluation of the anionic G3.5 PAMAM dendrimers having 18 NAC on its surface on BV-2 microglial cells confirmed the rapid entry of the conjugate into the cells and its localization in the cytoplasm. The conjugate was found to be non-toxic and more efficient than the free NAC to reduce ROS, NO and TNF-alpha, a pro-inflammatory cytokine.[65] Interestingly, a comparable study was designed with PEG star compounds (6 or 8 arms).[66] The PEG stars showed comparable NAC release profile to those of PAMAM-NAC

15:59 28 October 2016

conjugates, but the efficacy was not comparable for all biological markers (NO, ROS, TNF alpha release), proving the influence of the scaffold on the overall activity, as already observed in above-mentioned study involving amine-terminated and carboxyl-terminated PAMAM dendrimers.[51] The group of R. Kannan also explored the potential of these systems to address cerebral palsy (CP) which is a chronic childhood disorder without effective cure. CP is highly related to neuro-inflammation caused by activated microglia and other cells located in the CNS like astrocytes. Exhaustive in vivo study in a newborn rabbit model, where CP is induced by maternal intrauterine endotoxin administration showed that the PAMAM scaffold used to prepare the dendrimer-NAC conjugates is able to cross blood–brain barrier and then localize in astrocytes and microglia in animal models with CP, but not in healthy animals. Following intravenous injection at day one of life to the kits, the PAMAM conjugates were found to significantly improve their motor functions and to decrease the neuro-inflammation and oxidative injury markers 5 days later.[67] Another severe health issue with no effective therapeutic response is brain injury following circulatory arrest. The authors studied the combined effects of PAMAM-NAC conjugates to reduce neuro-inflammation, and valproic acid-PAMAM conjugates to reduce excitotoxicity resulting from a neuronal hyperactivity due to excess of neurotransmitter glutamate. Hydroxyl-terminated PAMAM dendrimers (generation 4) were statistically functionalized with an Fmoc protected $\gamma$-aminobutyric acid (GABA) spacer (40 out of 62 surface functions).[68] Fmoc removal resulted in partial removal of the GABA spacer and afforded dendrimers equipped with 21 to 24 free GABA groups (Fig. 6.6) which were statistically functionalized with a 2-pyridyldithio-propionate spacer able to react either with NAC or mercapto-PEG-modified valproic acid affording disulfide glutathione-sensitive linker for fast intracellular delivery in the target cells (microglia).

Systemic administration of these conjugates to canine animal models resulted after one day in the improvement of neurological deficit scores, comparable to those obtained with the free drugs NAC and valproic acid (VPA) drugs used at higher concentrations (ten folds), while the impairing side effects of the drugs were significantly reduced. This study also included a biodistribution study of the fluorescently labeled vehicle dendrimer (hydroxyl-terminated PAMAM) on these large animal models, which showed

a small, yet detectable brain uptake (0.02% of the injected dose) and localization of the vehicle in injured neurons and microglia. Although these results are in good agreement with previous studies on small animal models,[67] they are not transferable to the dendrimer–drug conjugates taking into account the importance of surface functions that may rule protein interactions and other surface function-related parameters affecting biodistribution.

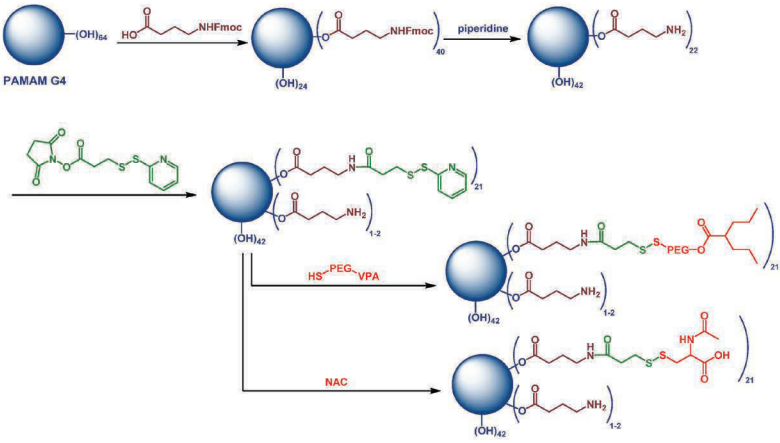



**Figure 6.6** PAMAM-NAC and PAMAM-VPA conjugates with glutathione–sensitive linkers.

NAC has also been grafted on the surface of a generation 3.5 poly(ethylene glycol)-block-poly(ester sulfide) dendrimer prepared via a divergent approach with methoxypoly(ethylene glycol) (mPEG), 4-pentenoyl chloride and 3-mercapto-1,2-propanediol as building blocks, but the release of the drug, covalently bond to alkene groups via thiol-ene Michael reaction was not investigated.[69,70]

### 6.3.3 Glucosamine-Terminated Dendrimers

The corneal surface epithelium that covers the eye surface is practically impermeable. Taking into account the mechanical and lachrymal washing of this surface, the trans-corneal delivery of drug is a challenging issue to treat inflammatory contexts that may affect the eye integrity and visual recovery following injury or surgery. In this regard, the group of S. Shaunak has described the stochastic grafting of d-(+)-glucosamine and d-(+)-glucosamine-

15:59 28 October 2016

15:59 28 October 2016

6-sulfate onto the surface of a generation 3.5 carboxyl-terminated PAMAM dendrimer. d-(+)-Glucosamine is an anti-inflammatory agent that inhibits the synthesis of pro-inflammatory cytokines like TNF-alpha, presumably through interactions with a receptor located on the surface of monocytes (namely TLR4). d-(+)-glucosamine-6-sulfate has anti-angiogenic properties by interacting with fibroblast growth factor 2 (FGF2) receptor. Both of these carbohydrates can reduce tissue scarring formation after glaucoma surgery, a process related to excessive pro-inflammatory signalization and FGF-mediated proliferation of endothelial cells. Remarkably, combination of both glucosamine terminated PAMAM dendrimers dramatically increased the long-term success of glaucoma filtration surgery on rabbit models from 30% to 80%, and no toxicity was found after one month.[71] Molecular modeling studies revealed that the flexibility and polarity of these systems were gradually modified upon incremental glucosamine grafting and that peripheral glucosamine moieties remained available on the dendrimer's outer shell for interaction with the biological targets.[72] Additionally, it was shown that the activity of this dendrimer was highly related to its ability to block the formation of the TLR4-MD2-LPS complex involving Toll-Like receptor 4 (TLR4) associated to MD 2 surface protein and lipopolysaccharide (LPS).[73] This finding was further utilized for the design of triazine-PAMAM dendrimer constructs as antagonists of the TLR4-MD2-LPS complex.[74]

Despite the fact that the initial preclinical case study did not led to further development, it should be noted that the glucosamine-terminated PAMAM dendrimers have recently inspired a successful in vivo study on rabbit models to prevent excessive inflammatory cytokine response and related to gut inflammation caused by intestinal pathogen. Pathogens responsible for severe infectious diarrheal diseases actually use the mass release of pro-inflammatory cytokines IL-6 and IL-8 and the associated tissue injury to promote their tissue invasion. Having in hand the activity of the glucosamine-terminated PAMAM dendrimer on human monocytes and its ability to modulate their pro-inflammatory response and taking into account that its large size (13.6 kDa) could probably impair to affordably scale-up its synthesis and development, a smallest analog dendrimer was semi-empirically designed. Modeling and experimental studies

15:59 28 October 2016

suggested that an anionic PETIM (polyamine and polyether scaffold (Fig. 6.7)) having 12 peripheral carboxylic acids and four glucosamine molecules statistically grafted on its surface would have comparable flexibility, surface glucosamine density, electrostatic charge and hydrophilicity in comparison with the glucosamine-terminated PAMAM dendrimer model. This elegant structure refinement allowed to show that this dendrimer administered orally strongly inhibited epithelial gut wall damage induced by Shigella pathogen and reduced IL-6 and IL-8 expression. These effects resulted in a significant decrease of the bacterial invasion, showing that this preclinical candidate could be useful for preventing gut wall tissue damage associated to infectious diarrheal diseases.[75]

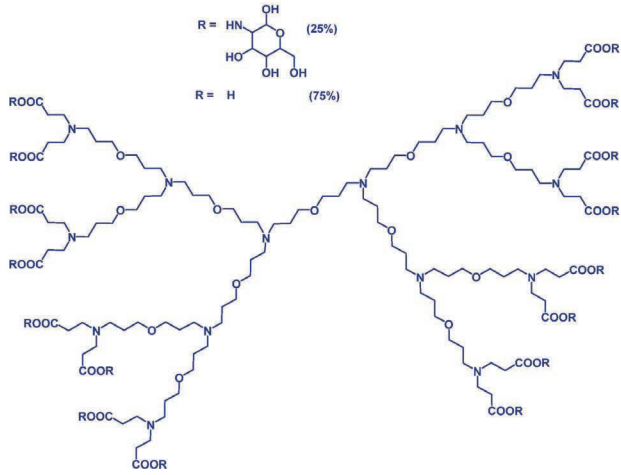



**Figure 6.7** Anionic PETIM dendrimer randomly grafted with glucosamine.

### 6.3.4 Dendrimer-Corticoid Conjugates

Methylprednisolone (MP) has been grafted on the surface on generation 4 hydroxy-terminated PAMAM dendrimers via a double ester involving a glutaric acid spacer (Fig. 6.8). MP is a glucocorticoid drug used for the treatment of asthma-related acute lung inflammation by airway administration. NMR and mass spectrometry analyses of the conjugate revealed a stochastic distribution of 12 MP molecules[76] per dendrimer, resulting in

15:59 28 October 2016

water-insoluble systems. To circumvent the solubility issue, conjugates were formulated with cyclodextrin or lysine. Cyclodextrin formulations resulted in lung inflammation when administrated to mice. The lysine formulations required high quantities of lysine (10 fold excess) to solubilize the dendrimer-MP conjugate, and resulted in safe administrations, but no data regarding the effect of the formulation process on the ester linkage integrity was presented.[77]

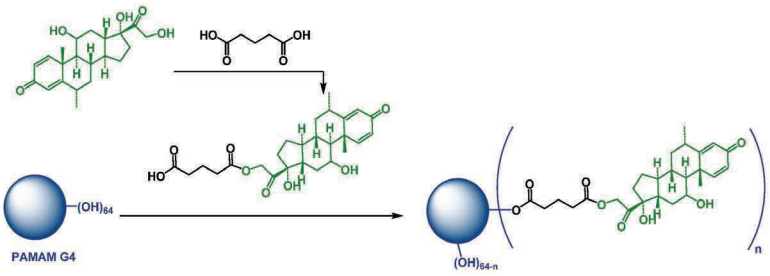



**Figure 6.8** PAMAM-methylprednisolone conjugates.

Trans-nasal administration of these formulations significantly reduced the ovalbumin-induced airway inflammatory response in a mouse model, and the dendrimer pro-drug approach allowed for lower MP concentrations in comparison with MP alone. Repeated administrations did not produce any undesired effects or non-specific inflammation. A FITC-dendrimer conjugate was also designed for biodistribution purposes. This fluorescent conjugate was structurally different from the active MP-conjugate as it was conceived from amine-terminated PAMAM dendrimers lacking the MP moieties. Comparison with FITC alone revealed that FITC-dendrimer conjugate had a significantly longer residence time in the lungs. In a complementary study, the same group reported on the influence of branching architecture and linker on the activity of these conjugates.[78] Unsurprisingly, a polyol hyperbranched polymer having twice the number of surface function (128) of the PAMAM dendrimer (64 functions) was found to attach more MP molecules than the latter. Glutaric acid spacers allowed higher payloads than succinic acid linkers. This observation was correlated to a lowered steric hindrance authorized by the supplementary methylene group of the glutarate, allowing a higher drug payload than hydroxyl-

terminated PAMAM dendrimers. It was also observed that glutaric acid spacers allowed higher payloads than succinic acid linkers. Both vehicles increase the cellular uptake of MP in A549 cell lines, and the anti-inflammatory activity of both conjugates after 4 h was comparable to the one of the free drug. At shorter times (1 h) the polyol conjugate was found to be significantly more efficient than the dendrimer conjugate and the free drug.

Another comparative study on the anti-inflammatory activity of a generation 4 PAMAM dendrimer-dexamethasone (DEX) conjugates having succinic acid spacer with DEX-liposomes showed significant efficacy differences.[79] The drug encapsulation efficiency in liposomes was found to be 14% (w/w) and it was correlated to a dose-dependent inhibition of TNF-$\alpha$ ranging from 39% to 57%. The drug loading of the dendrimer-DEX conjugates was estimated by UV absorption spectroscopy at 78%. At comparable DEX concentrations, these dendrimer-DEX conjugates presented higher TNF-$\alpha$ inhibition in LPS-activated human PBMC cultures, in the 67–71% range.

15:59 28 October 2016

### 6.3.5 Targeted Strategies and Covalent Grafting

As already mentioned, the number of examples of anti-inflammatory pro-drugs related to dendrimer-based targeted strategies is rather scarce. The stochastic approach developed by the group of J. Baker was early exemplified with cytostatic drug MTX, mostly for anti-cancer purposes. Prior to the development of J. Baker's group, the group of Wiener reported first the grafting of FA to Gd-containing PAMAM dendrimer for the MRI imaging of cancer cells.[80] Folic acid (FA) is the vitamin $B_9$ and it is essential to cell division processes. FA receptors (FAR) are overexpressed in several epithelial tumor cells, making FA a suitable targeting agent for selective delivery of anticancer AIs.[81] It should be noted that FA targeting is often associated with high liver uptake due to the overexpression of FAR in hepatic cells.[82,83] Interestingly, FA is also overexpressed on activated macrophages.[81] FA-targeting strategies could also open new perspectives for the treatment or diagnostic of macrophage-related chronic inflammatory diseases such as rheumatoid arthritis, Crohn's disease, and atherosclerosis. Considering that MTX is also a reference treatment for chronic inflammatory diseases like rheumatoid arthritis,[81] all the work

developed on FA targeted dendrimer-MTX conjugated could then find new application in the treatment of CID, as demonstrated by several recent reports.[84,85] In another example reported earlier, FA-functionalized PAMAM dendrimers have also been conjugated to indomethacin, another anti-inflammatory drug used in the treatment of arthritis. These systems showed promising in vitro targeting properties.[86]

## 6.4 Dendrimers Showing Anti-Inflammatory Properties per se

15:59 28 October 2016

Unlike dendrimers that are structurally modified with known drugs according to a rational design, dendrimers lacking specific known anti-inflammatory functions may present anti-inflammatory properties which discovery is generally the result of serendipitous processes. Few examples have been uncovered recently, in particular hydroxyl-terminated PAMAM dendrimers, carbosilane dendrimers, and polyphosphorhydrazone (PPH) dendrimers, all of them having non-similar backbones and surface functions. Some of these results have already been reviewed in the past years.[2,3]

### 6.4.1 Carbosilane Dendrimers

Carbosilane dendrimers developed in the group of R. Gomez and F. J. de la Mata have a versatile scaffold that can be capped with a variety of surface functions. For instance, ethylene-diammonium-capped carbosilane dendrimers have been evaluated for the delivery of antisense oligonucleotides and small interference RNA. The intrinsic toxicity of these transfecting agents was assessed by a global gene expression profiling method. The results showed that these dendrimers induce gene expression modifications in human primary macrophages.[87] In particular, these modifications were correlated to immune response, proliferation and transcription regulation pathways, and a significant down-regulation of the expression of cytokines involved in autoimmune diseases, like interleukin (IL) 17F, IL23R, and IL23 A, was observed. Among the carbosilane (CBS) dendrimers, compound 2G-NN16 (Fig. 6.9) equipped with ethylene diammonium salts proved to be of particular interest due to its transfecting properties and ability

15:59 28 October 2016

to cross the blood–brain barrier.[88] In order to further evaluate its potential as a vehicle for gene therapy or as medication, its effects on several subpopulations of the immune system have been studied in depth. For instance, it was shown that 2G-NN16 has no adverse effect on the pivotal functions of dendritic cells in which it can deliver anti-HIV peptides as it does not induce changes in maturation markers levels on the surface of dendritic cells derived from human monocytes.[89]

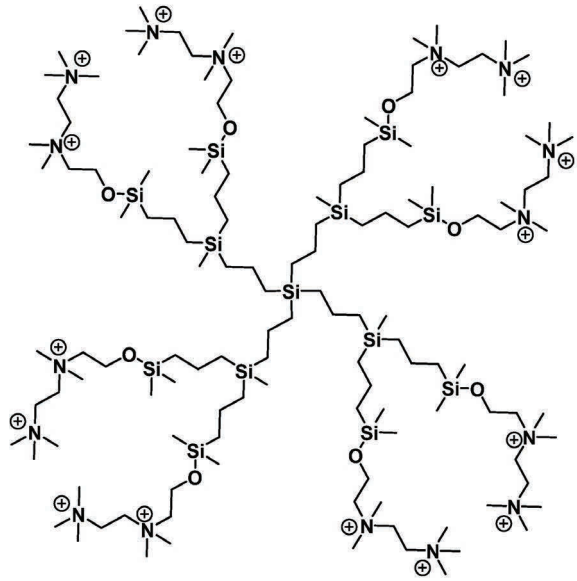


**Figure 6.9** 2G-NN16 carbosilane (CBS) dendrimer.

The same compound was also found to repress Tc17 differentiation in primary TCD8+ lymphocytes,[90] as demonstrated by the modification of the gene expression of TC8+ cells. Taking into account that IL17 secreting Tc17 lymphocytes are a unique subset of TCD8+ lymphocytes that are involved in the maintenance of inflammation in some autoimmune chronic inflammatory disease, these compounds could be of interest for the treatment of such diseases driven by Tc17 cells. Recently, another generation 2 CBS dendrimer having 24 diammonium salts on its surface was found to modify the behavior of M2 macrophages and to turn them to an M1-like polarization state.[91] Basically, the M1 phenotype is associated to high levels of pro-inflammatory cytokines,

production of reactive nitrogen and oxygen intermediates, promotion of Th1 response, and marked microbicidal and tumoricidal activity, whereas in contrast, M2 macrophages are likely to favor parasite containment and promote tissue remodeling and tumor progression with immuno-regulatory functions. M2 polarized macrophages and tumor-associated macrophages sharing many functional features, this finding could open new perspective in oncology.

### 6.4.2 PPH Dendrimers

15:59 28 October 2016

Polyphosphorhydrazone (PPH) dendrimers covered with phosphonic acid derivatives have also been identified as an emerging class of small dendrimers having per se, intrinsic, immuno-modulatory and anti-inflammatory properties, as their surface functions lack the biological activities when there are not grafted on dendrimer scaffolds.[92–96] These researches led by the groups of Caminade and the groups of Fournié and Poupot, have been initiated in the early 2000s and led initially to the identification of G1-ABP (Fig. 6.10), a first-generation PPH dendrimer terminated with 12 amino-bis(methylene phosphonic acids), as a natural killer (NK) cells amplifier.[97]

Searching for cellular events that could rationalize the expansion of NK cells, further studies on the PBMC sub-populations that could be related to this event showed that monocytes were activated by this dendrimer after a short contact time.[93] Both NK cells and monocytes play important roles in the primary immune response. NK cells are part of the innate immune system and they belong to the first line of defense of human organisms against all pathogens including bacteria, fungi, viruses, parasites and also cells lacking the self-markers like tumor cells. Monocytes are part of the innate immune system, and these phagocytic cells are precursors of macrophages which diffuse in tissues and organs. Monocytes are involved in the triggering and the control of the immune response against infection before cells of the adaptative immune system take over. The ex vivo activation of monocytes by G1-ABP was associated to the down-regulation of two surface proteins, CD14 and HLA-DR, longer lifetimes in cultures, size, and granulosity increase as well as increased phagocytic activity.

15:59 28 October 2016

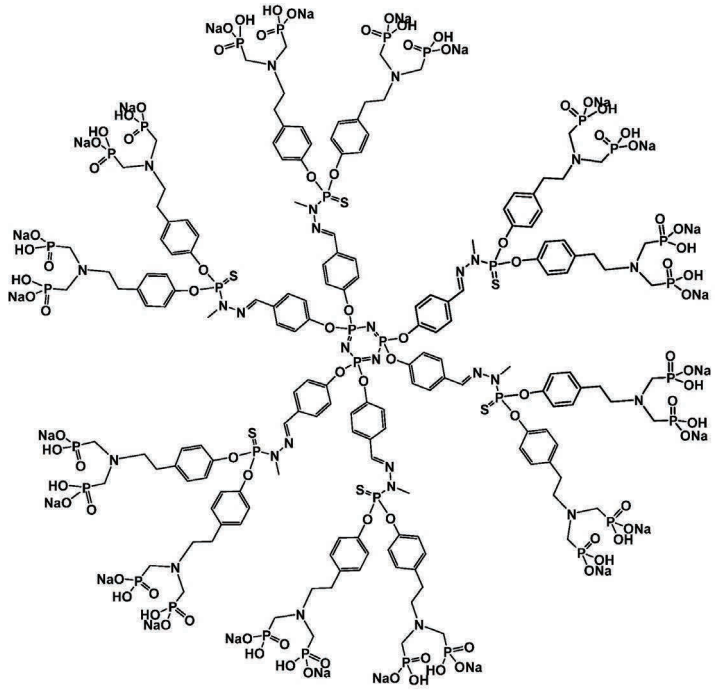


**Figure 6.10** PPH dendrimer G1-ABP with 12 tyramine-derived aminobis (methylenephosphonic acid) surface functions.

Further studies confirmed that the interaction processes between monocytes and dendrimer G1-ABP involve some specific, receptor-mediated, interactions, in addition to non-specific interaction processes.[98] Elucidation of the monocytes activation pathway by genomic and proteomic analysis also showed that dendrimer G1-ABP activates human monocytes according to an alternative-like pathways leading to anti-inflammatory and immunosuppressive dendrimer-activated monocytes,[99] and complementary analysis revealed that several receptors might be involved. Despite the complexity of the rational ruling the dendrimer-monocyte interactions, these studies paved the way for the evaluation of this dendrimer in several preclinical studies for the treatment of uncontrolled inflammatory events in autoimmune diseases. Indeed, the consortium latter correlated the monocyte-triggered ex vivo expansion of NK cells from PBMCs[97] to a specific inhibition of $CD4^+$ lymphocytes, which are also pro-

15:59 28 October 2016

inflammatory monocytes.[100] This inhibition of pro-inflammatory TCD4+ lymphocytes is another immuno-modulatory and anti-inflammatory feature of this dendrimer G1-ABP.

The effects of dendrimer G1-ABP on monocytes and NK cells result from several direct and indirect interactions with different subpopulations of PBMCs. These events are generated by indirect balances between dendrimer-induced activating and deactivating signals among these subpopulations. In the absence of a defined unambiguous receptor, quantitative structure-activity relationship can hardly be predicted as there is no well-defined process to describe the biological activities. Despite these difficulties, a structure optimization based on simple dendrimer main structural feature was designed. Accordingly, key structural parameters of G1-ABP, namely the chemical nature of surface functions, the size and the generation, along with the chemical nature of the dendritic skeleton and the density of the functional outer-shell, were modified in order to optimize them independently and sequentially. For instance, a significant variety of surface functions was assayed, including neutral surfaces, cationic entities and acids,[93] such as functionalized phosphonic acids, amino-phosphonic acids, amino-bisphosphonic acids,[96] as well as isosters of the surface function of the dendrimer hit.[95] The generation number was also optimized in preliminary studies and set to generation 1.[93] The influence of the chemical nature of the dendrimer's skeleton was analyzed by comparing the activities of PEI, thiophosphate, Poly-L-Lysine (PLL), carbosilane, PAMAM, and other PPH-like dendrimers having approximately the same size and the same number of amino bis-methylene phosphonate surface functions. In a study recently published, it was shown thanks to molecular modeling that one criterion ruling the activity of these dendrimer was related to the directionality of the dendrimeric scaffold,[101] a topological parameter that is somehow related to the local density of surface functions and is reminiscent to multivalency considerations. Other studies aiming only at the optimization of the local density of outer shell were performed independently on PPH structures having the same size and a controlled numbered of surface functions by selective locking reactions on the hexafunctional core of PPH dendrimers.[94]

Dendrimer G1-ABP being identified as a lead compound, these findings led to a preclinical evaluation of this dendrimer in

15:59 28 October 2016

a rheumatoid arthritis (RA) mouse model, namely the IL-1RA KO model in which mice lack the receptor for interleukin 1. RA is an autoimmune disease associated to a chronic inflammatory context due to the activation of T $CD4^+$ lymphocytes and bone resorption related to an increased activity of osteoclasts, which are giant multinuclear cells resulting from the trans-differentiation of monocytes. The IL-1RA KO murine model is a clinically relevant model of RA-like chronic inflammation which results in the development of physio-pathological issues which resemble the human pathology. The dendrimer-based treatment was initiated after 8 weeks, once the disease is significantly installed in all animals, and it consisted in the IV or oral administration of 1 or 10 mg/Kg of G1-ABP (in saline solution), every week. In all animals, a complete inhibition and remission of arthritis was observed (Fig. 6.11), and no adverse effect was detected. The suppression of disease was evidenced by normal synovial membranes, reduced levels of inflammatory cytokines, absence of cartilage destruction and absence of bone erosion.[102]

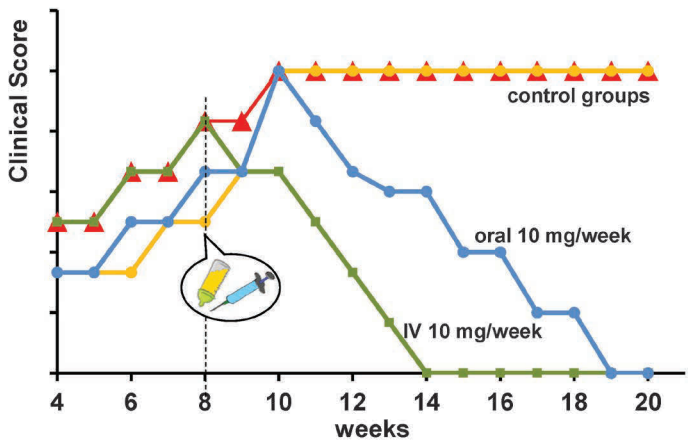



**Figure 6.11** Efficacy of dendrimer G1-ABP in a RA mouse model (IV and oral absorption).

Further studies on this murine model and on biopsies of RA patient showed that the dendrimer G1-ABP was also capable to inhibit the trans-differentiation of monocytes to osteoclasts. Accordingly, the G1-ABP dendrimer lead is (i) anti-inflammatory (alternative activation of monocytes), (ii) immuno-suppressive

15:59 28 October 2016

(inhibition of $CD4^+$ lymphocytes) and (iii) anti-osteoclastic. These gathered properties rationalize the unprecedented results obtained on this RA murine model, considering that rheumatoid arthritis (RA) is an autoimmune disease associated to a chronic inflammatory context due to the activation of T $CD4^+$ lymphocytes and bone resorption related to an increased activity of osteoclasts. Other preclinical assessments have been initiated recently for the treatment of other CIDs, including uveitis,[103] psoriasis, and multiple sclerosis.[104]

In another study by the same group, PPH dendrimers capped with mannose have been designed to mimic *Mycobacterium tuberculosis* mannose-capped lipoarabinomannan, which is able to inhibit the release of pro-inflammatory cytokines by activated human dendritic cells (DCs) via targeting the C-type lectin receptor DC-SIGN. Among this series of mannodendrimers, a generation 3 PPH dendrimer with 48 trimannoside caps and a generation 4 PPH dendrimer with 96 dimannosides showed a high binding avidity for DC-SIGN and were found to inhibit the production of pro-inflammatory cytokines production by activated human DCs. The generation 3 mannodendrimer equipped with 48 trimannosides was found to dramatically reduce acute lung inflammation following oral administration in mice in which lung inflammation had been triggered by aerosolized lipopolysaccharide (LPS). The in vivo results were in good agreement with cellular experiments as the anti-inflammatory in mice was correlated to the targeting of the murine DC-SIGN homolog.[105]

### 6.4.3 Other Examples

#### 6.4.3.1 PAMAM

PAMAM dendrimers used for the conjugation of anti-inflammatory drug indomethacin[106] have been found to possess unexpected anti-inflammatory properties in the absence of the Indomethacin moieties.[107] Indeed, plain hydroxy-terminated PAMAM dendrimers were found to exhibit better anti-inflammatory properties than the PAMAM-indomethacin conjugates or indomethacin alone. In a preliminary structure/activity exploratory study, a set of generation 4 and generation 4.5 PAMAM dendrimers capped with various

surface functions (Fig. 6.12) were assayed in vivo in rats in different anti-inflammatory assay methods including carrageenan-induced paw edema model, cotton pellet test, and adjuvant-induced arthritis assay.

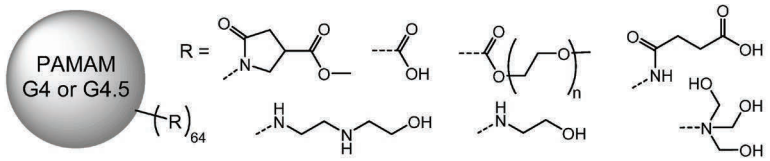



**Figure 6.12** PAMAM dendrimers having intrinsic anti-inflammatory properties.

15:59 28 October 2016

Amine and hydroxy terminated PAMAM dendrimers showed better activity in reducing inflammation than carboxylic acid capped PAMAM. Considering that the most active surface functions of this series somehow resemble the polar head of the agonistic prodrug Fingolimod™ (FTY720) developed by Novartis which is the first oral treatment of multiple sclerosis, these compounds could inspire new strategies for the design of multivalent drugs targeting the sphingolipid signaling pathway.[108]

### 6.4.3.2 Click dendrimers

Kakkar's group is utilizing alkyne-azide "click" chemistry to prepare small generation dendrimers that can be elegantly functionalized.[109–111] Some of these compounds have recently shown promising anti-inflammatory properties.[110,112,113] In particular, in vitro studies on rat microglial cells have shown that small generation dendrimers terminated with acetylene and hydroxyl groups can inhibit the LPS-induced production of nitric oxide and also to inhibit COX-2, an enzyme involved in inflammation and pain signaling. Complementary computational studies recently highlighted that the anti-inflammatory effect of these dendrimers is related to a direct binding to the active site of the enzyme, responsible for the synthesis of nitric oxide species, namely inducible nitric oxides synthases (iNOS) and COX-2 enzyme.[114] These results could possibly lead to novel strategies for the design of anti-inflammatory dendrimers.

## 6.5 Conclusions and Perspectives

Dendrimers show interesting properties for the transport and delivery of drugs, and it has been demonstrated that their structural features can be adapted to facilitate their passage through different membranes like the intestinal barriers or the blood–brain barrier. Drug complexation or encapsulation and drug conjugation provide different advantages for the solubilization and delivery, and their differences are related mostly to the sustainability of the delivery and the fundamentals underlying these approaches. In a simplified point of view, the conjugation of a drug to a dendrimer can be considered as a multivalent prodrug approach, whereas drug complexation/encapsulation with dendrimers can be considered as a formulation. As discussed in this chapter, these remarks also apply to dendrimers and anti-inflammatory drugs. Persistent or chronic inflammation is a common feature in the genesis, onset and symptomatology of many diseases and cancers. The treatment of inflammation is then highly related to the treatment or diagnosis of several age-associated pathological conditions such as autoimmune and neurodegenerative diseases as well as many cancers. Interestingly, it can be noticed that despite the relatively scarce number of examples related to anti-inflammatory dendrimers, many studies have been conducted in vivo on clinically relevant animal models, and in some cases, in depth preclinical studies could eventually end up to clinical assays. The advent of dendrimers having intrinsic anti-inflammatory properties could also open new perspectives for macromolecular drug design, as demonstrated by recent findings on different dendrimeric scaffolds.

15:59 28 October 2016

## References

1. Coussens, L. M. and Werb, Z. (2002). Inflammation and cancer, *Nature*, **420**, pp. 860–867.
2. Atvi, P. K. and Kakkar, A. (2013). Dendrimers as anti-inflammatory agents, *Braz. J. Pharm. Sci.*, **49**, pp. 57–65.
3. Hayder, M., Fruchon, S., Fournié, J.-J., Poupot, M. and Poupot, R., (2011). Anti-inflammatory of dendrimers per se, *Scientific World J.*, **11**, pp. 1367–1382.

15:59 28 October 2016


4. Naylor, A. M., Goddard, W. A., Kiefer, G. E. and Tomalia, D. A. (1989). Starburst dendrimers. 5. Molecular shape control, *J. Am. Chem. Soc.*, **111**, pp. 2339–2341.
5. Turrin, C.-O. and Caminade, A.-M., Encapsulation of drugs inside dendrimers," in *Dendrimers*, A. M. Caminade, C. O. Turrin, R. Laurent, A. Ouali, and B. Delavaux-Nicot (eds.), John Wiley & Sons, Ltd, 2011.
6. Jansen, J. F. G. A., de Brabander-Van den Berg, E. M. M. and Meijer, E. W. (1994). Encapsulation of guest molecules into a dendritic box, *Science*, **266**, pp. 1226–1229.
7. D'Emanuele, A. and Attwood, D. (2005). Dendrimer-drug interactions, *Adv. Drug Delivery Rev.*, **57**, pp. 2147–2162.
8. Svenson, S. and Chauhan, A. S. (2008). Dendrimers for enhanced drug solubilization, *Nanomedicine*, **3**, pp. 679–702.
9. Svenson, S. (2009). Dendrimers as versatile platform in drug delivery applications, *Eur. J. Pharm. Biopharm.*, **71**, pp. 445–462.
10. Medina, S. H. and El-Sayed, M. E. H. (2009). Dendrimers as carriers for delivery of chemotherapeutic agents, *Chem. Rev.*, **109**, pp. 3141–3157.
11. Cheng, Y. Y., Xu, Z. H., Ma, M. L. and Xu, T. W. (2008). Dendrimers as drug carriers: Applications in different routes of drug administration, *J. Pharm. Sci.*, **97**, pp. 123–143.
12. Caminade, A.-M. and Turrin, C.-O. (2014). Dendrimers for drug delivery, *J. Mater. Chem. B*, **2**, pp. 4055–4066.
13. Caminade, A. M., Turrin, C. O. and Majoral, J. P. (2008). Dendrimers and DNA: Combinations of two special topologies for nanomaterials and biology, *Chem. Eur. J.*, **14**, pp. 7422–7432.
14. Dufes, C., Uchegbu, I. F. and Schatzlein, A. G. (2005). Dendrimers in gene delivery, *Adv. Drug Delivery Rev.*, **57**, pp. 2177–2202.
15. Chauhan, A. S., Jain, N. K. and Diwan, P. V. (2010). Pre-clinical and behavioural toxicity profile of PAMAM dendrimers in mice, *Proc. R. Soc. A*, **466**, pp. 1535–1550.
16. Madaan, K., Kumar, S., Poonia, N., Lather, V. and Pandita, D. (2014). Dendrimers in drug delivery and targeting: Drug-dendrimer interactions and toxicity issues, *J. Pharm. Bioall. Sci.*, **6**, pp. 139–150.
17. Cheng, Y. Y., Li, Y. W., Wu, Q. L., Zhang, H. H. and Xu, T. W. (2009). Generation-dependent encapsulation/electrostatic attachment of phenobarbital molecules by poly(amidoamine) dendrimers: Evidence from 2D-NOESY investigations, *Eur. J. Med. Chem.*, **44**, pp. 2219–2223.

18. Cheng, Y. Y., Wu, Q. L., Li, Y. W. and Xu, T. W. (2008). External electrostatic interaction versus internal encapsulation between cationic dendrimers and negatively charged drugs: Which contributes more to solubility enhancement of the drugs? *J. Phys. Chem. B*, **112**, pp. 8884–8890.

19. Tanis, I. and Karatasos, K. (2009). Association of a weakly acidic anti-inflammatory drug (ibuprofen) with a poly(amidoamine) dendrimer as studied by molecular dynamics simulations, *J. Phys. Chem. B*, **113**, pp. 10984–10993.

20. Milhem, O. M., Myles, C., McKeown, N. B., Attwood, D. and D'Emanuele, A. (2000). Polyamidoamine Starburst (R) dendrimers as solubility enhancers, *Int. J. Pharm.*, **197**, pp. 239–241.

21. Kolhe, P., Misra, E., Kannan, R. M., Kannan, S. and Lieh-Lai, M. (2003). Drug complexation, in vitro release and cellular entry of dendrimers and hyperbranched polymers, *Int. J. Pharm.*, **259**, pp. 143–160.

22. Milhem, O. M., Myles, C., McKeown, N. B., Attwood, D. and D'Emanuele, A. (2000). Polyamidoamine Starburst dendrimers as solubility enhancers, *Int. J. Pharm.*, **197**, pp. 239–241.

23. Avila-Salas, F., Sandoval, C., Caballero, J., Guinez-Molinos, S., Santos, L. S., Cachau, R. E. and Gonzalez-Nilo, F. D. (2012). Study of interaction energies between the PAMAM dendrimer and nonsteroidal anti-inflammatory drug using a distributed computational strategy and experimental analysis by ESI-MS/MS, *J. Phys. Chem. B*, **116**, pp. 2031–2039.

24. Yang, W. J., Li, Y. W., Cheng, Y. Y., Wu, Q. L., Wen, L. P. and Xu, T. W., (2009). Evaluation of phenylbutazone and poly(amidoamine) dendrimers interactions by a combination of solubility, 2D-NOESY NMR, and isothermal titration calorimetry studies, *J. Pharm. Sci.*, **98**, pp. 1075–1085.

25. Kannan, S., Kolhe, P., Raykova, V., Glibatec, M., Kannan, R. M., Lieh-Lai, M. and Bassett, D. (2004). Dynamics of cellular entry and drug delivery by dendritic polymers into human lung epithelial carcinoma cells, *J. Biomater. Sci., Polym. Ed.*, **15**, pp. 311–330.

26. Cheng, Y. Y. and Xu, T. W. (2005). Dendrimers as potential drug carriers. Part I. Solubilization of non-steroidal anti-inflammatory drugs in the presence of polyamidoamine dendrimers, *Eur. J. Med. Chem.*, **40**, pp. 1188–1192.

27. Cheng, Y. Y., Xu, T. W. and Fu, R. Q. (2005). Polyamidoamine dendrimers used as solubility enhancers of ketoprofen, *Eur. J. Med. Chem.*, **40**, pp. 1390–1393.

15:59 28 October 2016

15:59 28 October 2016

28. Man, N., Cheng, Y. Y., Xu, T. W., Ding, Y., Wang, X. M., Li, Z. W., Chen, Z. C., Huang, G. Y., Shi, Y. Y. and Longping, W. (2006). Dendrimers as potential drug carriers. Part II. Prolonged delivery of ketoprofen by in vitro and in vivo studies, *Eur. J. Med. Chem.*, **41**, pp. 670–674.

29. Asthana, A., Chauhan, A. S., Diwan, P. V. and Jain, N. K. (2005). Poly(amidoamine) (PAMAM) dendritic nanostructures for controlled site-specific delivery of acidic anti-inflammatory active ingredient, *AAPS PharmSciTech*, **6**, pp. E536–E542.

30. Boridy, S., Soliman, G. M. and Maysinger, D. (2012). Modulation of inflammatory signaling and cytokine release from microglia by celastrol incorporated into dendrimer nanocarriers, *Nanomedicine*, **7**, pp. 1149–1165.

31. Venkatesha, S. H., Yu, H., Rajaiah, R., Tong, L. and Moudgil, K. D., (2011). Celastrus-derived celastrol suppresses autoimmune arthritis by modulating antigen-induced cellular and humoral effector responses, *J. Biol. Chem.*, **286**, pp. 15138–15146.

32. Lv, Q.-W., Zhang, W., Shi, Q., Zheng, W.-J., Li, X., Chen, H., Wu, Q.-J., Jiang, W.-L., Li, H.-B., Gong, L., Wei, W., Liu, H., Liu, A.-J., Jin, H.-T., Wang, J.-X., Liu, X.-M., Li, Z.-B., Liu, B., Shen, M., Wang, Q., Wu, X.-N., Liang, D., Yin, Y.-F., Fei, Y.-Y., Su, J.-M., Zhao, L.-D., Jiang, Y., Li, J., Tang, F.-l., Zhang, F.-C., Lipsky, P. E. and Zhang, X. (2015). Comparison of Tripterygium wilfordii Hook F with methotrexate in the treatment of active rheumatoid arthritis (TRIFRA): A randomised, controlled clinical trial, *Ann. Rheum. Dis.*, **74**, pp. 1078–1086.

33. Murugan, E., Rani, D. P. G. and Yogaraj, V. (2014). Drug delivery investigations of quaternised poly(propylene imine) dendrimer using nimesulide as a model drug, *Colloids Surf., B*, **114**, pp. 121–129.

34. Alavidjeh, M. S., Haririan, I., Khorramizadeh, M. R., Ghane, Z. Z., Ardestani, M. S. and Namazi, H. (2010). Anionic linear-globular dendrimers: Biocompatible hybrid materials with potential uses in nanomedicine, *J. Mater. Sci. Mater. Med.*, **21**, pp. 1121–1133.

35. Namazi, H. and Adell, M. (2005). Dendrimers of citric acid and poly (ethylene glycol) as the new drug-delivery agents, *Biomaterials*, **26**, pp. 1175–1183.

36. Gajbhiye, V., Kumar, P. V., Sharma, A. and Jain, N. K. (2008). Novel PEGylated PPI dendritic nanostructures for sustained delivery of anti-inflammatory agent, *Curr. Nanosci.*, **4**, pp. 267–277.

37. Koc, F. E. and Senel, M. (2013). Solubility enhancement of non-steroidal anti-inflammatory drugs (nsaids) using polypolypropylene oxide core PAMAM dendrimers, *Int. J. Pharm.*, **451**, pp. 18–22.

15:59 28 October 2016

38. Patri, A. K., Kukowska-Latallo, J. F. and Baker, J. R. (2005). Targeted drug delivery with dendrimers: Comparison of the release kinetics of covalently conjugated drug and non-covalent drug inclusion complex, *Adv. Drug Delivery Rev.*, **57**, pp. 2203–2214.

39. Sun, Q., Radosz, M. and Shen, Y. (2012). Challenges in design of translational nanocarriers, *J. Controlled Release*, **164**, pp. 156–169.

40. Mody, N., Tekade, R. K., Mehra, N. K., Chopdey, P. and Jain, N. K., (2014). Dendrimer, liposomes, carbon nanotubes and PLGA nanoparticles: One platform assessment of drug delivery potential, *AAPS Pharm Sci Tech*, **15**, pp. 388–399.

41. Kararli, T. T. (1995). Comparison of the gastrointestinal anatomy, physiology, and biochemistry of humans and commonly used laboratory animals, *Biopharm. Drug Dispos.*, **16**, pp. 351–380.

42. Benchaala, I., Mishra, M. K., Wykes, S. M., Hali, M., Kannan, R. M. and Whittum-Hudson, J. A. (2014). Folate-functionalized dendrimers for targeting Chlamydia-infected tissues in a mouse model of reactive arthritis, *Int. J. Pharm.*, **466**, pp. 258–265.

43. Gupta, R., Mehra, N. K. and Jain, N. K. (2014). Development and characterization of sulfasalazine loaded fucosylated PPI dendrimer for the treatment of cytokine-induced liver damage, *Eur. J. Pharm. Biopharm.,* **86**, pp. 449–458.

44. Cerqueira, S. R., Oliveira, J. M., Silva, N. A., Leite-Almeida, H., Ribeiro-Samy, S., Almeida, A., Mano, J. F., Sousa, N., Salgado, A. J. and Reis, R. L. (2013). Microglia response and in vivo therapeutic potential of methylprednisolone-loaded dendrimer nanoparticles in spinal cord injury, *Small*, **9**, pp. 738–749.

45. Cerqueira, S. R., Silva, B. L., Oliveira, J. M., Mano, J. F., Sousa, N., Salgado, A. J. and Reis, R. L. (2012). Multifunctionalized CMCht/PAMAM dendrimer nanoparticles modulate the cellular uptake by astrocytes and oligodendrocytes in primary cultures of glial cells, *Macromol. Biosci.*, **12**, pp. 591–597.

46. Oliveira, J. M., Sousa, R. A., Kotobuki, N., Tadokoro, M., Hirose, M., Mano, J. F., Reis, R. L. and Ohgushi, H. (2009). The osteogenic differentiation of rat bone marrow stromal cells cultured with dexamethasone-loaded carboxymethylchitosan/poly(amidoamine) dendrimer nanoparticles, *Biomaterials*, **30**, pp. 804–813.

47. Oliveira, J. M., Salgado, A. J., Sousa, N., Mano, J. F. and Reis, R. L. (2010). Dendrimers and derivatives as potential therapeutic tool in regenerative medicine strategies: A review, *Prog. Polym. Sci.*, **35**, pp. 1163–1194.

15:59 28 October 2016

48. Najlah, M. and D'Emanuele, A. (2007). Synthesis of dendrimers and drug-dendrimer conjugates for drug delivery, *Curr. Opin. Drug Discovery Dev.*, **10**, pp. 756–767.

49. Kukowska-Latallo, J. F., Candido, K. A., Cao, Z. Y., Nigavekar, S. S., Majoros, I. J., Thomas, T. P., Balogh, L. P., Khan, M. K. and Baker, J. R. (2005). Nanoparticle targeting of anticancer drug improves therapeutic response in animal model of human epithelial cancer, *Cancer Res.*, **65**, pp. 5317–5324.

50. Majoros, I. J., Thomas, T. P., Mehta, C. B. and Baker, J. R. (2005). Poly(amidoamine) dendrimer-based multifunctional engineered nanodevice for cancer therapy, *J. Med. Chem.*, **48**, pp. 5892–5899.

51. Myc, A., Kukowska-Latallo, J., Cao, P., Swanson, B., Battista, J., Dunham, T. and Baker, J. R., Jr. (2010). Targeting the efficacy of a dendrimer-based nanotherapeutic in heterogeneous xenograft tumors in vivo, *Anticancer Drugs*, **21**, pp. 186–192.

52. Myc, A., Douce, T. B., Ahuja, N., Kotlyar, A., Kukowska-Latallo, J., Thomas, T. P. and Baker, J. R., (2008). Preclinical antitumor efficacy evaluation of dendrimer-based methotrexate conjugates, *Anti-Cancer Drugs*, **19**, pp. 143–149.

53. Turrin, C.-O. and Caminade, A.-M., Dendrimer conjugates for drug delivery, in *Dendrimers*, A. M. Caminade, C. O. Turrin, R. Laurent, A. Ouali and B. Delavaux-Nicot (eds.), John Wiley & Sons, Ltd, 2011.

54. Wiwattanapatapee, R., Lomlim, L. and Saramunee, K. (2003). Dendrimers conjugates for colonic delivery of 5-aminosalicylic acid, *J. Controlled Release*, **88**, pp. 1–9.

55. Najlah, M., Freeman, S., Attwood, D. and D'Emanuele, A. (2006). Synthesis, characterization and stability of dendrimer prodrugs, *Int. J. Pharm.*, **308**, pp. 175–182.

56. RSC Advances Journal of Macromolecular Science, P. A. P. A. A. C., Mani and Rajakumar, P. (2014). Synthesis and analysis of in vitro anti-arthritic activity of dendrimers with methyl, ethyl and isopropyl salicylates as surface groups, *RSC Adv.*, **4**, pp. 63208–63215.

57. Kolhe, P., Khandare, J., Pillai, O., Kannan, S., Lieh-Lal, M. and Kannan, R. M. (2006). Preparation, cellular transport, and activity of polyamidoamine-based dendritic nanodevices with a high drug payload, *Biomaterials*, **27**, pp. 660–669.

58. Kurtoglu, Y. E., Mishra, M. K., Kannan, S. and Kannan, R. M., (2010). Drug release characteristics of PAMAM dendrimer-drug conjugates with different linkers, *Int. J. Pharm.*, **384**, pp. 189–194.

59. Shrivastava, P., Singh, R. and Shrivastava, S. (2010). Polyamidoamine dendrimer and dextran conjugates: Preparation, characterization, and in vitro and in vivo evaluation, *Chem. Pap.*, **64**, pp. 592–601.

60. Rocksen, D., Lilliehook, B., Larsson, R., Johansson, T. and Bucht, A. (2000). Differential anti-inflammatory and anti-oxidative effects of dexamethasone and N-acetylcysteine in endotoxin-induced lung inflammation, *Clin. Exp. Immunol.*, **122**, pp. 249–256.

61. Berk, M., Malhi, G. S., Gray, L. J. and Dean, O. M. (2013). The promise of *N*-acetylcysteine in neuropsychiatry, *Trends Pharmacol. Sci.*, **34**, pp. 167–177.

62. Verhasselt, V., Vanden Berghe, W., Vanderheyde, N., Willems, F., Haegeman, G. and Goldman, M. (1999). *N*-acetyl-*L*-cysteine inhibits primary human T cell responses at the dendritic cell level: Association with NF-kappaB inhibition, *J. Immunol.*, **162**, pp. 2569–2574.

63. Navath, R. S., Kurtoglu, Y. E., Wang, B., Kannan, S., Romero, R. and Kannan, R. M. (2008). Dendrimer-drug conjugates for tailored intracellular drug release based on glutathione levels, *Bioconjugate Chem.*, **19**, pp. 2446–2455.

64. Kurtoglu, Y. E., Navath, R. S., Wang, B., Kannan, S., Romero, R. and Kannan, R. M. (2009). Poly(amidoamine) dendrimer-drug conjugates with disulfide linkages for intracellular drug delivery, *Biomaterials*, **30**, pp. 2112–2121.

65. Wang, B., Navath, R. S., Romero, R., Kannan, S. and Kannan, R. (2009). Anti-inflammatory and anti-oxidant activity of anionic dendrimer-N-acetyl cysteine conjugates in activated microglial cells, *Int. J. Pharm.*, **377**, pp. 159–168.

66. Navath, R. S., Wang, B., Kannan, S., Romero, R. and Kannan, R. M. (2009). Stimuli-responsive star poly(ethylene glycol) drug conjugates for improved intracellular delivery of the drug in neuroinflammation, *J. Control. Release*, **142**, pp. 447–456.

67. Kannan, S., Dai, H., Navath, R. S., Balakrishnan, B., Jyoti, A., Janisse, J., Romero, R. and Kannan, R. M. (2012). Dendrimer-based postnatal therapy for neuroinflammation and cerebral palsy in a rabbit model, *Sci. Trans. Med.*, **4**, pp. 130ra46.

68. Mishra, M. K., Beaty, C. A., Lesniak, W. G., Kambhampati, S. R., Zhang, F., Wilson, M. A., Blue, M. E., Troncoso, J. C., Kannan, S., Johnston, M. V., Baumgartner, W. A. and Kannan, R. M. (2014). Dendrimer brain uptake and targeted therapy for brain injury in a large animal model of hypothermic circulatory arrest, *ACS Nano*, **8**, pp. 2134–2147.

15:59 28 October 2016

15:59 28 October 2016

69. Fury, J. J., Altenhofer, E. F. and Sedaghat-Herati, R. (2009). Synthesis of new poly(ethylene glycol)-block-poly(ester sulfide) dendrimers, *Tetrahedron Lett.*, **50**, pp. 4205–4207.

70. Fury, J. J., Robison, J. and Sedaghat-Herati, R., (2013). Synthesis and self-assembly of new poly(ethylene glycol)-block-poly(ester-sulfide) dendrimers, *J. Macromol. Sci., Part A: Pure Appl. Chem.*, **50**, pp. 1113–1120.

71. Shaunak, S., Thomas, S., Gianasi, E., Godwin, A., Jones, E., Teo, I., Mireskandari, K., Luthert, P., Duncan, R., Patterson, S., Khaw, P. and Brocchini, S. (2004). Polyvalent dendrimer glucosamine conjugates prevent scar tissue formation, *Nat. Biotechnol.*, **22**, pp. 977–984.

72. Barata, T. S., Shaunak, S., Teo, I., Zloh, M. and Brocchini, S. (2011). Structural studies of biologically active glycosylated polyamidoamine (PAMAM) dendrimers, *J. Mol. Model.*, **17**, pp. 2051–2060.

73. Barata, T. S., Teo, I., Brocchini, S., Zloh, M. and Shaunak, S. (2011). Partially glycosylated dendrimers block MD-2 and prevent TLR4-MD-2-LPS complex mediated cytokine responses, *PLoS Comput. Biol.*, **7**, e1002095.

74. Barata, T., Teo, I., Lalwani, S., Simanek, E., Zloh, M. and Shaunak, S. (2011). Computational design principles for bioactive dendrimer based constructs as antagonists of the TLR4-MD-2-LPS complex, *Biomaterials*, **32**, pp. 8702–8711.

75. Teo, I., Toms, S. M., Marteyn, B., Barata, T. S., Simpson, P., Johnston, K. A., Schnupf, P., Puhar, A., Bell, T., Tang, C., Zloh, M., Matthews, S., Rendle, P. M., Sansonetti, P. J. and Shaunak, S. (2012). Preventing acute gut wall damage in infectious diarrhoeas with glycosylated dendrimers, *EMBO Mol. Med.*, **4**, pp. 866–881.

76. Khandare, J., Kolhe, P., Pillai, O., Kannan, S., Lieh-Lai, M. and Kannan, R. M. (2005). Synthesis, cellular transport, and activity of polyamidoamine dendrimer-methylprednisolone conjugates (vol 16, pg 336, 2005), *Bioconjugate Chem.*, **16**, pp. 1049–1049.

77. Inapagolla, R., Guru, B. R., Kurtoglu, Y. E., Gao, X., Lieh-Lai, M., Bassett, D. J. P. and Kannan, R. M. (2010). In vivo efficacy of dendrimer-methylprednisolone conjugate formulation for the treatment of lung inflammation, *Int. J. Pharm.*, **399**, pp. 140–147.

78. Perumal, O., Khandare, J., Kolhe, P., Kannan, S., Lieh-Lai, M. and Kannan, R. M. (2009). Effects of branching architecture and linker on the activity of hyperbranched polymer-drug conjugates, *Bioconjugate Chem.*, **20**, pp. 842–846.

15:59 28 October 2016

79. Choksi, A., Sarojini, K. V. L., Vadnal, P., Dias, C., Suresh, P. K. and Khandare, J. (2013). Comparative anti-inflammatory activity of poly(amidoamine) (PAMAM) dendrimer-dexamethasone conjugates with dexamethasone-liposomes, *Int. J. Pharm.*, **449**, pp. 28–36.

80. Wiener, E. C., Konda, S., Shadron, A., Brechbiel, M. and Gansow, O. (1997). Targeting dendrimer-chelates to tumors and tumor cells expressing the high-affinity folate receptor, *Invest. Radiol.*, **32**, pp. 748–754.

81. Low, P. S., Henne, W. A. and Doorneweerd, D. D. (2008). Discovery and development of folic-acid-based receptor targeting for imaging and therapy of cancer and inflammatory diseases, *Acc. Chem. Res.*, **41**, pp. 120–129.

82. Fernandes-Costa, F. and Metz, J. (1979). Role of serum folate binders in the delivery of folate to tissues and to the fetus, *Br. J. Haematol.*, **41**, pp. 335–342.

83. Corrocher, R., De Sandre, G., Pacor, M. L. and Hoffbrand, A. V. (1974). Hepatic protein binding of folate, *Clin. Sci. Mol. Med.*, **46**, pp. 551–554.

84. Thomas, T. P., Goonewardena, S. N., Majoros, I. J., Kotlyar, A., Cao, Z., Leroueil, P. R. and Baker, J. R., Jr. (2011). Folate-targeted nanoparticles show efficacy in the treatment of inflammatory arthritis, *Arthritis Rheum*, **63**, pp. 2671–2680.

85. Qi, R., Majoros, I., Misra, A. C., Koch, A. E., Campbell, P., Marotte, H., Bergin, I. L., Cao, Z., Goonewardena, S., Morry, J., Zhang, S., Beer, M., Makidon, P., Kotlyar, A., Thomas, T. P. and Baker, J. R., Jr. (2015). Folate receptor-targeted dendrimer-methotrexate conjugate for inflammatory arthritis, *J. Biomed. Nanotechnol.*, **11**, pp. 1431–1441.

86. Chandrasekar, D., Sistla, R., Ahmad, F. J., Khar, R. K. and Diwan, P. V. (2007). The development of folate-PAMAM dendrimer conjugates for targeted delivery of anti-arthritic drugs and their pharmacokinetics and biodistribution in arthritic rats, *Biomaterials*, **28**, pp. 504–512.

87. Gras, R., Almonacid, L., Ortega, P., Serramia, M. J., Gomez, R., Javier de la Mata, F., Lopez-Fernandez, L. A. and Angeles Munoz-Fernandez, M. (2009). Changes in gene expression pattern of human primary macrophages induced by carbosilane dendrimer 2G-NN16, *Pharm. Res.*, **26**, pp. 577–586.

88. Jimenez, J. L., Clemente, M. I., Weber, N. D., Sanchez, J., Ortega, P., de la Mata, F. J., Gomez, R., Garcia, D., Lopez-Fernandez, L. A. and Munoz-Fernandez, M. A. (2010). Carbosilane dendrimers to transfect human astrocytes with small interfering RNA targeting human immunodeficiency virus, *BioDrugs*, **24**, pp. 331–343.

15:59 28 October 2016

89. Pion, M., Serramia, M. J., Diaz, L., Bryszewska, M., Gallart, T., García, F., Gómez, R., de la Mata, F. J. and Muñoz-Fernandez, M. Á. (2010). Phenotype and functional analysis of human monocytes-derived dendritic cells loaded with a carbosilane dendrimer, *Biomaterials*, **31**, pp. 8749–8758.

90. Gras, R., Garcia, M. I., Gomez, R., de la Mata, F. J., Munoz-Fernandez, M. A. and Lopez-Fernandez, L. A. (2012). Carbosilane dendrimer 2G-NN16 represses Tc17 differentiation in primary T CD8+ lymphocytes, *Mol. Pharm.*, **9**, pp. 102–110.

91. Perise-Barrios, A. J., Gomez, R., Corbi, A. L., de la Mata, J., Dominguez-Soto, A. and Munoz-Fernandez, M. A. (2015). Use of carbosilane dendrimer to switch macrophage polarization for the acquisition of antitumor functions, *Nanoscale*, **7**, pp. 3857–3866.

92. Rolland, O., Turrin, C. O., Caminade, A. M. and Majoral, J. P. (2009). Dendrimers and nanomedicine: Multivalency in action, *New J. Chem.*, **33**, pp. 1809–1824.

93. Poupot, M., Griffe, L., Marchand, P., Maraval, A., Rolland, O., Martinet, L., L'Faqihi-Olive, F. E., Turrin, C. O., Caminade, A. M., Fournie, J. J., Majoral, J. P. and Poupot, R. (2006). Design of phosphorylated dendritic architectures to promote human monocyte activation, *FASEB J.*, **20**, pp. 2339–2351.

94. Rolland, O., Griffe, L., Poupot, M., Maraval, A., Ouali, A., Coppel, Y., Fournié, J. J., Bacquet, G., Turrin, C. O., Caminade, A. M., Majoral, J. P. and Poupot, R. (2008). Tailored control and optimisation of the number of phosphonic acid termini on phosphorus-containing dendrimers for the ex-vivo activation of human monocytes, *Chem. Eur. J.*, **14**, pp. 4836–4850.

95. Rolland, O., Turrin, C. O., Bacquet, G., Poupot, R., Poupot, M., Caminade, A. M. and Majoral, J. P. (2009). Efficient synthesis of phosphorus-containing dendrimers capped with isosteric functions of amino-bismethylene phosphonic acids, *Tetrahedron Lett.*, **50**, pp. 2078–2082.

96. Marchand, P., Griffe, L., Poupot, M., Turrin, C. O., Bacquet, G., Fournie, J. J., Majoral, J. P., Poupot, R. and Caminade, A. M. (2009). Dendrimers ended by non-symmetrical azadiphosphonate groups: Synthesis and immunological properties, *Bioorg. Med. Chem. Lett.*, **19**, pp. 3963–3966.

97. Griffe, L., Poupot, M., Marchand, P., Maraval, A., Turrin, C. O., Rolland, O., Métivier, P., Bacquet, G., Fournié, J. J., Caminade, A. M., Poupot, R. and Majoral, J. P. (2007). Multiplication of human natural killer cells by nanosized phosphonate-capped dendrimers, *Angew. Chem. Int. Ed.*, **46**, pp. 2523–2526.

15:59 28 October 2016

98. Ledall, J., Fruchon, S., Garzoni, M., Pavan, G. M., Caminade, A.-M., Turrin, C.-O., Blanzat, M. and Poupot, R. (2015). Specific receptor(s) is (are) involved in the recognition of an anti-inflammatory phosphorus-containing dendrimer by human monocytes, *Nanoscale*, **7**, pp 17672–17684.

99. Fruchon, S., Poupot, M., Martinet, L., Turrin, C. O., Majoral, J. P., Fournie, J. J., Caminade, A. M. and Poupot, R. (2009). Anti-inflammatory and immunosuppressive activation of human monocytes by a bioactive dendrimer, *J. Leukocyte Biol.*, **85**, pp. 553–562.

100. Portevin, D., Poupot, M., Rolland, O., Turrin, C.-O., Fournié, J.-J., Majoral, J.-P., Caminade, A.-M. and Poupot, R. (2009). Regulatory activity of azabisphosphonate-capped dendrimers on human CD4+ T cell proliferation for ex-vivo expansion of NK cells from PBMCs and immunotherapy, *J. Trans. Med.*, **7**, p. 82.

101. Caminade, A. M., Fruchon, S., Turrin, C. O., Poupot, M., Ouali, A., Maraval, A., Garzoni, M., Maly, M., Furer, V., Kovalenko, V., Majoral, J. P., Pavan, G. M. and Poupot, R. (2015). The key role of the scaffold for designing efficient dendrimer nanodrugs, *Nat. Commun.,* **6**, pp. 7722.

102. Hayder, M., Poupot, M., Baron, M., Nigon, D., Turrin, C.-O., Caminade, A.-M., Majoral, J.-P., Fournié, J.-J., Cantagrel, A., Poupot, R. and Davignon, J.-L. (2010). Phosphorus-based dendrimer as nanotherapeutics targeting both inflammation and osteoclastogenesis in experimental arthritis, *Science Trans. Med.*, **3**, pp. 81–35.

103. Fruchon, S., Caminade, A.-M., Abadie, C., Davignon, J.-L., Combette, J.-M., Turrin, C.-O. and Poupot, R. (2013). An azabisphosphonate-capped poly(phosphorhydrazone) dendrimer for the treatment of endotoxin-induced uveitis, *Molecules*, **18**, pp. 9305–9316.

104. Hayder, M., Varilh, M., Turrin, C.-O., Saoudi, A., Caminade, A.-M., Poupot, R., Liblau, R. S. (2015). The phosphorus-based dendrimer ABP treats neuroinflammation by promoting IL-10-producing $CD4^+$ T cells *Biomacromolecules* DOI:10.1021/acs.biomac.5b00643.

105. Blattes, E., Vercellone, A., Eutamene, H., Turrin, C. O., Theodorou, V., Majoral, J. P., Caminade, A. M., Prandi, J., Nigou, J. and Puzo, G., (2013). Mannodendrimers prevent acute lung inflammation by inhibiting neutrophil recruitment, *Proc. Natl. Acad. Sci. U. S. A.*, **110**, pp. 8795–8800.

106. Chauhan, A. S., Jain, N. K., Diwan, P. V. and Khopade, A. J. (2004). Solubility enhancement of indomethacin with poly(amidoamine) dendrimers and targeting to inflammatory regions of arthritic rats, *J. Drug Targeting*, **12**, pp. 575–583.

107. Chauhan, A. S., Diwan, P. V., Jain, N. K. and Tomalia, D. A., (2009). Unexpected in vivo anti-inflammatory activity observed for simple, surface functionalized poly(amidoamine) dendrimers, *Biomacromolecules*, **10**, pp. 1195–1202.

108. Marsolais, D. and Rosen, H. (2009). Chemical modulators of sphingosine-1-phosphate receptors as barrier-oriented therapeutic molecules, *Nat. Rev. Drug. Discov*., **8**, pp. 297–307.

109. Franc, G. and Kakkar, A. (2008). Dendrimer design using Cu-I-catalyzed alkyne-azide "click-chemistry", *Chem. Commun.*, pp. 5267–5276.

110. Hourani, R. and Kakkar, A. (2010). Advances in the elegance of chemistry in designing dendrimers, *Macromol. Rapid Commun.*, **31**, pp. 947–974.

111. Hourani, R., Sharma, A. and Kakkar, A. (2010). Designing dendritic frameworks using versatile building blocks suitable for CuI-catalyzed alkyne azide "click" chemistry, *Tetrahedron Lett.*, **51**, pp. 3792–3795.

112. Castonguay, A., Wilson, E., Al-Hajaj, N., Petitjean, L., Paoletti, J., Maysinger, D. and Kakkar, A. (2011). Thermosensitive dendrimer formulation for drug delivery at physiologically relevant temperatures, *Chem. Commun.*, **47**, pp. 12146–12148.

113. Sharma, A., Khatchadourian, A., Khanna, K., Sharma, R., Kakkar, A. and Maysinger, D. (2011). Multivalent niacin nanoconjugates for delivery to cytoplasmic lipid droplets, *Biomaterials*, **32**, pp. 1419–1429.

114. Neibert, K., Gosein, V., Sharma, A., Khan, M., Whitehead, M. A., Maysinger, D. and Kakkar, A. (2013). "Click" dendrimers as anti-inflammatory agents: With insights into their binding from molecular modeling studies, *Mol. Pharm.*, **10**, pp. 2502–2508.

15:59 28 October 2016

15:59 28 October 2016



Taylor & Francis
Taylor & Francis Group
http://taylorandfrancis.com

Chapter 7

# Structurally Flexible and Amphiphilic Poly(Amidoamine) Dendrimers as Nonviral Vectors for siRNA Delivery

**Xiaoxuan Liu,[a] Yang Wang,[b] and Ling Peng[c]**

[a]*State Key Laboratory of Natural Medicines and Jiangsu Key Laboratory of Drug Discovery for Metabolic Diseases, Center of Advanced Pharmaceuticals and Biomaterials, 24 Tong Jia Xiang, 210009 Nanjing, P. R. China*
[b]*Humanwell Healthcare Group Co., Ltd., 430075 Wuhan, Hubei, P. R. China*
[c]*Aix-Marseille Université, CNRS, Centre Interdisciplinaire de Nanoscience de Marseille, UMR 7325, "Equipe Labellisée Ligue Contre le Cancer," 163, avenue de Luminy, 13288 Marseille, France*

ling.peng@univ-amu.fr

## 7.1 Introduction

The ability of small interfering RNA (siRNA) to specifically and efficiently turn off gene expression has provided an enormous opportunity for exploitation in biomedical applications such as gene-based disease treatment. However, siRNA molecules are highly negatively charged and hydrophilic and hence do not readily cross the cell membrane to enter into cells. In addition, unprotected naked siRNAs are not stable and can be rapidly

*Dendrimers in Nanomedicine*
Edited by Delphine Felder-Flesch
Copyright © 2016 Pan Stanford Publishing Pte. Ltd.
ISBN 978-981-4745-49-9 (Hardcover), 978-981-4745-50-5 (eBook)
www.panstanford.com

15:59 28 October 2016

degraded by enzymes such as nucleases and esterases in biological fluids. Consequently, safe and efficient delivery systems, which could prevent siRNA degradation and bring siRNA to the site of interest and enter into cells, are highly demanded.

Although viral vectors are very effective for siRNA delivery, increasing concerns over their safety and immunogenicity substantiate the need to develop alternative nonviral vectors. A variety of natural and synthetic nonviral vectors, including lipids, polymers, and inorganic materials (e.g., carbon nanotubes, quantum dots, gold nanoparticles) have been developed and tested for siRNA delivery.[1–3] Among them, dendrimers, a special type of synthetic polymers, represent a promising delivery platform for the RNAi therapeutics[4–6] by virtue of their precisely-controlled structure as well as their unique multivalency and cooperativity confined within a nanoscale volume. Unlike traditional polymer vectors, dendrimers have a well-defined molecular architecture composed of three distinct domains: (1) a central core, (2) branching units allowing dendrimer growth in a geometrically organized radial layers called generations (**G**), and (3) a large number of terminals on the surface (Fig. 7.1).[7] The structure of a dendrimer can be precisely controlled during its stepwise synthesis either via divergent or convergent strategies or combination of both.[7] Up to now, a multitude of dendrimers have been explored for siRNA delivery.[4,5]

Among all the dendrimers, poly(amidoamine) dendrimers, also called PAMAM dendrimers, are the most extensively explored for siRNA delivery. PAMAM dendrimers bear primary amine terminals on the dendrimer surface, which are positively charged under physiological condition and ready to interact and condense with the negatively charged siRNA molecules through electrostatic interaction. These dendrimers also harbor tertiary amines in the interior, which are beneficial for the intracellular release of siRNA via the "proton sponge" effect.[8,9] The released siRNA molecules will then eventually join the RNAi machinery to activate the gene silencing process. The first study on PAMAM dendrimers for siRNA delivery was reported in 2005 by Juliano and co-workers using commercially available ethylenediamine (EDA)-core PAMAM

15:59 28 October 2016

dendrimer.[10] Nevertheless, the employed PAMAM dendrimer and its related conjugates were not effective for functional siRNA delivery. In 2006, we reported the first successful dendrimer–based siRNA delivery[11] using structurally flexible PAMAM dendrimers.[12,13] These flexible dendrimers have a triethanolamine (TEA) core (Fig. 7.2) and are excellent vectors for the delivery of various RNAi molecules in vitro and in vivo.[14,15] Recently, we have further explored amphiphilic dendrimers[16–18] for siRNA delivery. Some of these amphiphilic dendrimers outperform the commercially available siRNA delivery agents and promote functional siRNA delivery in various cells including human primary and stem cells as well as in animal models. In this chapter, we will mainly focus on the structurally flexible and amphiphilic PAMAM dendrimers developed in our group and their siRNA delivery feature and potency.

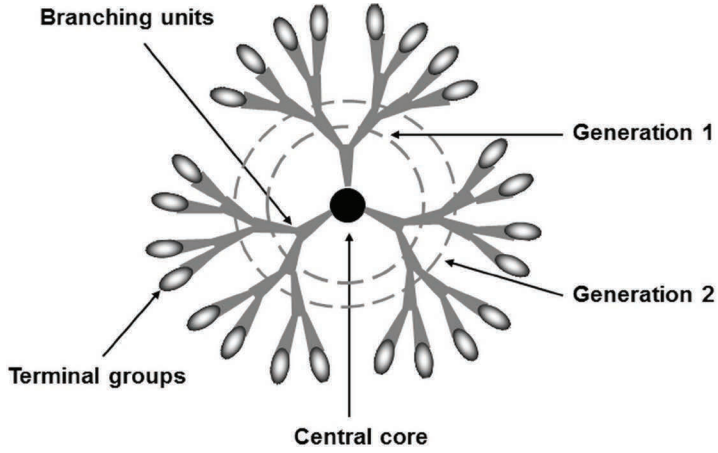



**Figure 7.1** Schematic presentation of a dendrimer, a special class of synthetic macromolecule possessing well-defined molecular architecture composed of three distinct domains: (1) a central core, (2) branching units that are repeated in a geometrically organized fashion resulting in a series of radial layers called generations (**G**), and (3) a large number of terminals on the outer surface. Adapted from *New J Chem*, 2012, **36**, 256–263, with permission of The Royal Society of Chemistry (RSC) on behalf of the Centre National de la Recherche Scientifique (CNRS) and the RSC.

15:59 28 October 2016

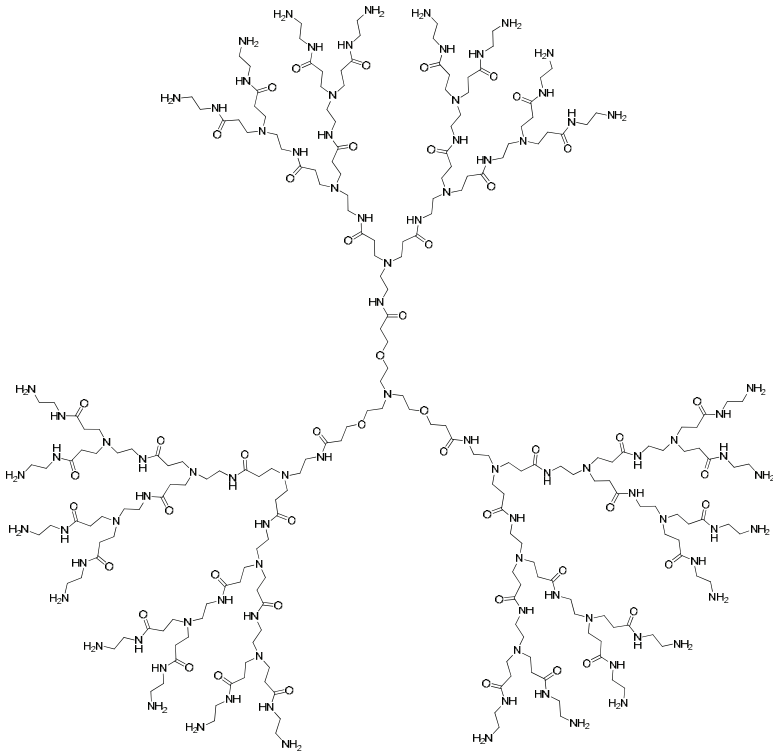


**Figure 7.2** Structurally flexible triethanolamine (TEA) core PAMAM dendrimer of generation 3. Adapted with permission from *Mol Pharmaceutics*, 2012, **9**, 470–481. Copyright 2012 American Chemical Society.

## 7.2 Structurally Flexible TEA-Core PAMAM Dendrimers

Poly(amidoamine) (PAMAM) dendrimers were first reported by Tomalia and co-cworkers in 1985.[19] They have been extensively investigated as nanovectors for DNA delivery.[20] Nowadays, these dendrimers have been commercialized as DNA transfection reagent. The active ingredient of the commercial reagent is composed of fractured and degraded dendrimers rather than intact PAMAM dendrimers. This is because fractured and degraded dendrimers have greater structural flexibility, allowing better and more efficient interaction with DNA, hence better DNA delivery

15:59 28 October 2016

efficiency. The fractured dendrimers are prepared either via thermal degradation or alkaline hydrolysis of the intact dendrimers.[21] This degradation process is neither economically nor ecologically sound as the preparation of intact dendrimers is time-consuming, and requires strictly controlled stepwise synthesis and laborious purification. Most importantly, the precise control over structure is lost during this degradation process, which may raise the problem of batch consistence and reproducibility as well as eventual FDA approval for biomedical applications.

With the aim to overcoming these drawbacks, we have developed genuine, structurally flexible triethanolamine (TEA) core PAMAM dendrimers (Fig. 7.2) for nucleic acid delivery, in particular for siRNA delivery.[11,15] Importantly, the dendrimer core, triethanolamine (TEA) has a considerably extended structure compared to $NH_3$, the core of the first PAMAM dendrimers developed by Tomalia et al.[22] This TEA core grants the corresponding PAMAM dendrimers with much more internal space to accommodate the branching units, thereby imparting structural flexibility to the resulting dendrimers. In other words, TEA-core based dendrimers bear less densely packed branching units and offer greater access for water and siRNA molecules, favoring both siRNA binding and release processes. This structural feature has been further affirmed by multiscale molecular modeling investigation.[13,23,24]

Effective protection of siRNAs from degradation during the extra- and intra-cellular traffic and eventually transporting them to cytoplasm for RNAi machinery is critical for siRNA delivery. Our structurally flexible TEA-core dendrimers are able to bind siRNA to form stable nanoparticles,[12,25] leading to effective protection of siRNA from degradation and significant promotion of cellular uptake via endocytosis, in particular, macropinocytosis. After entering into the cells, the siRNA molecules will be escaped from the endosome through endosomal swelling and breakage caused by the "proton sponge" effect which benefits from the presence of tertiary amines in the interior of the PAMAM dendrimers. In a proof of principle study, the generation 7 of our PAMAM dendrimer family ($\mathbf{G_7}$) was the most effective for siRNA delivery and gene silencing of the luciferase gene in A549Luc cells which stably express the GL3 luciferase gene.[11] The excellent siRNA delivery capacity of this dendrimer was further confirmed

15:59 28 October 2016

by its effective delivery of a siRNA targeting heat shock protein 27 (Hsp27) in human castration-resistant prostate cancer PC-3 cells, generating potent down-regulation of Hsp27.[26] Hsp27 is a molecular chaperone which plays an important role in drug resistance, and has been recently considered as a novel target for treating drug-resistant prostate and other cancers.[27–29] Following the gene silencing of Hsp27 by the siRNA/$\mathbf{G_7}$ complexes, an effective anticancer activity was achieved in prostate cancer models, which could be ascribed to the caspase-dependent apoptosis induction.[26]

Recently, we also demonstrated that the generation 6 of this PAMAM dendrimer family ($\mathbf{G_6}$) could also effectively deliver a siRNA molecule targeting Akt,[30] a key oncogene that contributes to tumorigenesis and constitutes an attractive therapeutic target for cancer therapy.[31,32] In addition, this $\mathbf{G_6}$-mediated Akt gene silencing approach in combination with paclitaxel based chemotherapy could significantly and synergistically enhance anticancer potency in ovarian cancer models in vitro and in vivo.[30]

Nevertheless, the large-scale synthesis of the High-generation dendrimers are prerequisites with required quality for clinical translation is technically demanding. Therefore, it is desirable and preferable to explore small dendrimers of low generations with effective siRNA delivery capacity. With this in mind, we have actively pursued our efforts in molecular engineering of either siRNA or dendrimer to attain the goal.

It is to mention that both the RNA molecular size and the dendrimer generation play a crucial role on the construction of stable and uniform nanoscale RNA/dendrimer complexes: High-generation dendrimers are prerequisite for effective interaction with small siRNA molecules, whereas low-generation dendrimers are sufficient to generate strong interaction with large RNA molecules.[25] On the other hand, Behr et al. reported the sticky siRNA concept: siRNA molecules with short complementary $A_n/T_n$ ($n$ = 5–8) 3′ overhangs, named "sticky" siRNA (ssiRNA), are able to self-assemble into "gene-like" double-stranded large RNAs (Fig. 7.3).[33] Based on the sticky siRNA concept together with our finding on size-dependence of RNA and dendrimer, we explored the capacity of lower generation dendrimers for the delivery of sticky siRNA molecules. Indeed, the generation 5 dendrimer ($\mathbf{G_5}$) could effectively deliver sticky siRNA targeting Hsp27 and achieve

15:59 28 October 2016

potent gene silencing and the consequent anticancer activity in prostate cancer models in vitro and in vivo.[23] This could be reasonably explained by self-assembling of the sticky siRNAs into large RNA molecules, therefore even the smaller dendrimer $\mathbf{G_5}$ could produce strong interact and deliver ssiRNA effectively. Additionally, the two complementary $A_n/T_n$ overhangs of the sticky siRNAs could also act as a pair of protruding molecular arms, allowing the siRNA molecule to enwrap the spherical, low-generation dendrimers with higher binding affinity compared with a conventional siRNA with two short $T_2/T_2$ overhangs. This binding and interaction mode was revealed by computer modeling and could also contribute towards the enhanced delivery activity of $\mathbf{G_5}$.[23]

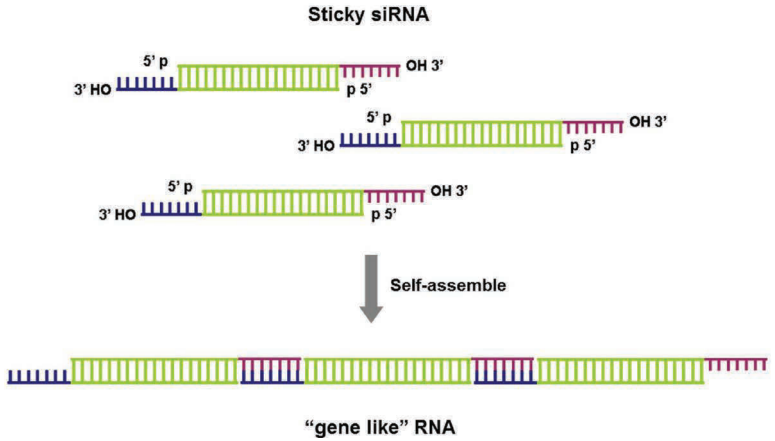



**Figure 7.3** Cartoon presentation of self-assembly of sticky siRNA into "gene-like" longer double stranded RNA. Adapted with permission from *Mol Pharmaceutics*, 2012, **9**, 470–481. Copyright 2012 American Chemical Society.

Besides sticky siRNA concept, another strategy for siRNA engineer is to design dicer substrate siRNA (dsiRNA) which is consist of asymmetric 25-/27-mer duplexes having 3′ two-nucleotide overhang and two 3′-DNA residues on the blunt end (Fig. 7.4). Such Dicer-generated siRNAs can generate better gene silencing effect than the conventional siRNA when targeted to the same sequence location.[34–37] Indeed, the generation 5 dendrimer ($\mathbf{G_5}$) could effectively deliver dsiRNA into human prostate cancer

15:59 28 October 2016

PC-3 cells, human T cells and human primary PBMC cells, resulting in cogent gene silencing.[38,39] Importantly, this dendrimer was able to deliver a cocktail of dsiRNA molecules for targeting multiple genes in order to achieve synergic effect. For example, our dendrimer $\mathbf{G_5}$ effectively delivered siRNA cocktails to target both HIV replication and host HIV infection in an HIV-infected humanized RAG-hu mice model. The resulting gene silencing led to extraordinary anti-HIV activity, with significant suppression of viral loads by several orders of magnitude. Moreover, host CD4 T-cell depletion and viral escape could be effectively prevented.[39]

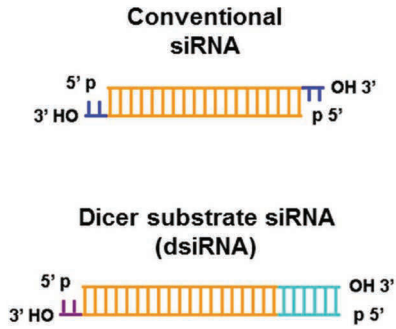



**Figure 7.4** Asymmetric Dicer substrate siRNA design in comparison to that of conventional siRNA. Adapted with permission from *Biotech Adv*, 2014, **32**, 844–852. Copyright 2014 Elsevier.

In addition to above different strategies to improve siRNA potency, microRNA (miRNA) also emerged as novel potential RNA molecules to down-regulate gene expression. We demonstrated that our $\mathbf{G_5}$ dendrimer could successfully deliver the mature miR-124 RNA duplexes into glioblastoma stem cells (GSC1),[40] resulting in down-regulating NRAS, a small guanine-nucleotide bindingprotein belonging to one of the three RAS (KRAS, NRAS, HRAS) isoforms.[41] It is well known that the RAS signaling pathway plays a crucial role in many cancers by regulating cell proliferation, differentiation, and survival, thus constitutes a promising anticancer target.[40]

Further efforts have been also made to use short-activating RNA (saRNA) which is design to target sequences in gene promoters, readily upregulating target gene expression called dsRNA-induced transcriptional activation (RNAa).[42,43] Our results

15:59 28 October 2016

also demonstrated that our $\mathbf{G_5}$ dendrimer was able to deliver saRNA targeting C/EBP$\alpha$ (CCAAT/enhancer-binding protein-$\alpha$), a transcriptional regulator and activator of albumin gene expression. Functional delivery of this saRNA led to enhanced endogenous albumin production, reducing tumor burden and simultaneously improving liver function in a clinically relevant liver cirrhosis/HCC model.[44]

Apart from employing different small RNA molecules, molecular engineering of dendrimer is rather a direct approach to confer low-generation dendrimers for the effective siRNA delivery by imparting better delivery feature. It is well known that cell-penetrating peptides bear arginine-rich motif can favorably interact with cell membrane through divalent H-bonding of the guanidinium moiety in arginine residue with the phosphate/carboxylate/sulfate group on cell surface. We hence reasoned that appending arginine residues to the terminals of our TEA-core dendrimers might also improve cell penetration and cell uptake of the siRNA/dendrimer complexes, hence better siRNA delivery efficiency by harnessing the cell-penetrating advantages of the arginine-rich motif and the unique siRNA delivery properties of the flexible TEA-core PAMAM dendrimers. The results correlated well with our expectation: A generation 4 dendrimer of this family (**$\mathbf{G_4}$Arg**) (Fig. 7.5) formed stable dendriplexes with siRNA, resulting in significantly improved cell uptake of siRNA compared to the nonarginine counterpart $\mathbf{G_4}$.[45] The consequent gene silencing of Hsp27 using **$\mathbf{G_4}$Arg** led to potent anticancer effects in prostate cancer models in vitro and in vivo yet with no adverse effects.

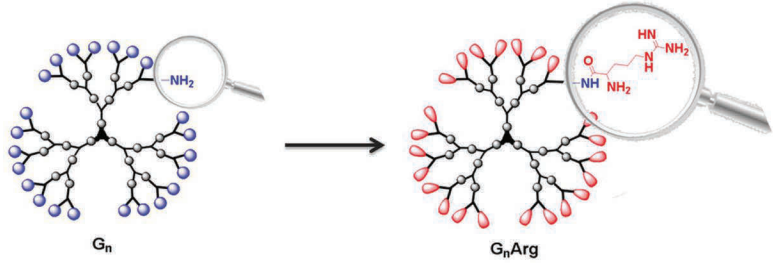



**Figure 7.5** Arginine-decorated dendrimer $\mathbf{G_n}$**Arg** based on the amine-terminated TEA-core PAMAM dendrimer ($\mathbf{G_n}$). Adapted with permission from *Bioconjugate Chem*, 2014, **25**, 521–532. Copyright 2014 American Chemical Society.

15:59 28 October 2016

Collectively, all these results demonstrate that our structurally flexible TEA-core dendrimers hold great promise for siRNA delivery for further clinical translation to treat diseases. Indeed, the $\mathbf{G_5}$ dendrimer was scheduled for clinical trial to deliver siRNA for cancer therapy in USA and UK, but unfortunately the project was delayed due to the shortage of dendrimer reaching "Good Manufacturing Practice (GMP)" quality. We are working actively to promote the translation of our dendrimer research into real clinical implementations.

## 7.3 Amphiphilic PAMAM Dendrimers

As we mentioned above, although structurally flexible PAMAM dendrimers of generations 5, 6, and 7 ($\mathbf{G_5}$, $\mathbf{G_6}$, and $\mathbf{G_7}$) are excellent vectors for siRNA delivery, their large scale synthesis in high-quality is far from trivial, impeding their further translation in clinical applications. To overcome this problem, we wanted to develop small-molecular-weight dendrimers that can be easily synthesized. We therefore came up with the idea to construct supramolecular dendrimers through self-assembling of small amphiphilic dendrimer units (Fig. 7.6), in the hope that the noncovalently created supramolecular dendrimers could mimic the covalently constructed high-generation dendrimers in structure, size, and function, in particular, siRNA delivery in our study.

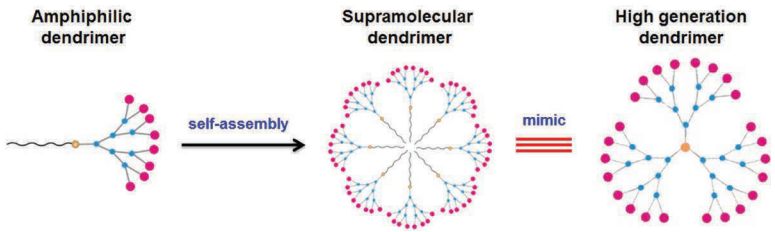



**Figure 7.6** Self-assembling of small amphiphilic dendrimers leading to the formation of supramolecular dendrimers, which could mimic the covalently constructed high-generation dendrimers. Adapted with permission from *Small*, 2016, in revision. Copyright 2016 Wiley-VCH Verlag GmbH & Co.

Regarding the small molecular dendrimer building units for constructing supramolecular dendrimers, we have developed a series of amphiphilic dendrimers that are able to self-assemble into supramolecular dendrimers, with size and shape similar to that of

15:59 28 October 2016

the structurally flexible TEA-core dendrimers.[16–18,46] Indeed, the amphiphilic dendrimer (**AD1**) composed of a hydrophobic alkyl chain and a hydrophilic PAMAM dendron with 8 amine terminals (Fig. 7.7A), is able to deliver siRNA, with comparable potency as our structurally flexible high-generation dendrimer $\mathbf{G}_7$.[16] In addition, this dendrimer is capable of combining the advantageous delivery features of lipid and dendrimer vectors, effectively deliver siRNA with potent gene silencing effect both in vitro and in vivo.[16] This is the first report on small amphiphilic dendrimer able to deliver siRNA and generate gene silencing in vitro and in vivo.

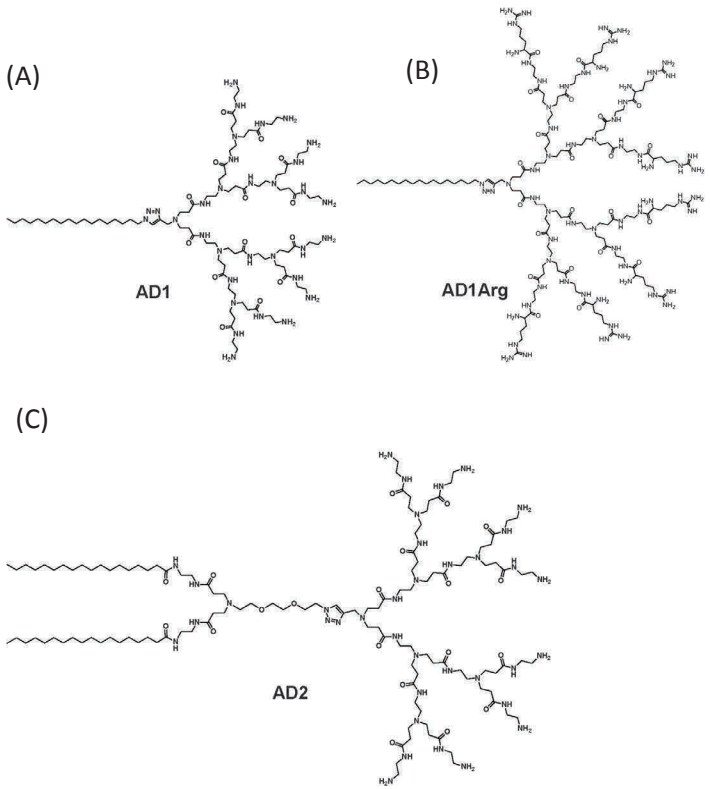



**Figure 7.7** Amphiphilic dendrimers reported in this work. (A) Amphiphilic dendrimer **AD1** featuring a low-generation hydrophilic PAMAM dendron and a hydrophobic alkyl chain. (B) Arginine terminated amphiphilic dendrimer **AD1Arg** derived from amphiphilic dendrimer **AD1**. (C) Amphiphilic dendrimer **AD2** bearing a low-generation hydrophilic PAMAM dendron and two hydrophobic alkyl chains.

15:59 28 October 2016

In order to further improve the delivery efficiency of this amphiphilic dendrimer **AD1** via increased cellular uptake of siRNA, we also employed the cell-penetration peptide mimicry by conjugating this amphiphilic dendrimer with arginine terminals (**AD1Arg**) (Fig. 7.7B).[46] Indeed, the arginine-terminated dendrimer (**AD1Arg**) was granted with significantly enhanced cellular uptake of siRNA, leading to more efficient siRNA delivery and better gene silencing in human prostate cancer PC-3 cells and human hematopoietic $CD34^+$ stem cells, compared to the corresponding nonarginine counterpart **AD1**.[46]

Instead of decorating dendrimer surface with arginine residues for better siRNA delivery, we further modified the hydrophobic component of the amphiphilic dendrimer **AD1** by appending two long hydrophobic alkyl chains. To our great interest, this amphiphilic dendrimer **AD2** (Fig. 7.7C) could self-assemble into vesicle-like dendrimersome nanostrcutures (Fig. 7.8).[18] Instead of the micellar structures formed by **AD1**. This finding is somehow reminiscent of lipids and detergents, with lipids often generating versicular structures whereas detergents forming preferentially micelles. Most importantly, the vesicle-like dendrimersome formed by **AD2**, is able to undergo spontaneous structural rearrangement into small and spherical micelles upon interaction with siRNA (Fig. 7.8).[18] This vesicular to micellar structural transition will allow **AD2** to maximally expose the positively charged terminals and provide stronger stabilizing electrostatic interactions with the negatively charged siRNA, hence effectively interacting, entrapping and condensing the negatively charged siRNAs into nanoparticles in order to protect siRNA from degradation and deliver siRNA to the desired site. The resulting nanoparticles is able to harness the delivery advantages of both lipid and dendrimer vectors, and successfully deliver siRNA into a wide range of cell types including the highly challenging human primary cells and stem cells, largely outperforming the currently available nonviral vectors for siRNA delivery. They are also effective for in vivo delivery. The peculiar feature of **AD2** to dynamically self-assemble into adaptive supramolecular assemblies upon response to siRNA alongside its advantageous combination of lipid and polymer vector delivery is evocative of virus-like delivery. This robust, versatile and non-toxic delivery activity of **AD2**, coupled with its easy formulation, yields a promise for a new, highly effective and

cell type independent nanovector for efficient and safe siRNA delivery, heralding a new age of self-assembling dendrimer based drug delivery in biomedical applications. We are currently undertaking a structure/activity relationship study on amphiphilic dendrimers in order to gain insightful understanding and enhance our knowledge for molecular technology of dendrimer nanovectors for siRNA delivery.[48]

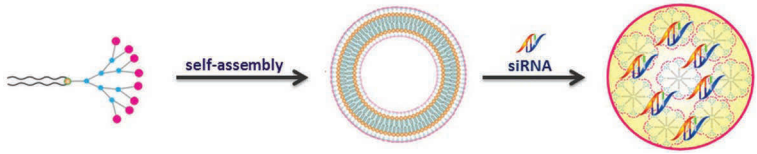



**Figure 7.8** Amphiphilic dendrimer **AD2** forms the vesicle-like dendrimersome nanostructure, which upon interaction with siRNA, undergoes spontaneous structural rearrangement into smaller, spherical micelles, in order to provide maximal exposure of the positively charged dendrimer terminal amines for better and stronger interaction with the negatively charged siRNAs. Adapted with permission from *Angew Chem Int Ed*, 2014, **53**, 11822–11827. Copyright 2014 Wiley-VCH Verlag GmbH & Co.

## 7.4 Conclusion and Prospects

Dendrimers are speculated as ideal delivery platforms for diverse therapeutic agents thanks to their well-defined structure and spherical architecture bearing unique radiating branching units in the interior and numerous end groups on the surface yet within the nanometric size. Over the past decade, dendrimers have emerged as effective nonviral vectors for siRNA delivery. In particular, we have established bioinspired structurally flexible high-generation dendrimer and self-assembling amphiphilic dendrimer based supramolecular dendrimers, which are excellent vectors for siRNA delivery in cell based experiments and in various animal models.

Delivery of siRNA therapeutics should not only be efficient but also home to the right site in order to achieve better efficacy and lower toxicity. In this regards, we have been developing a targeted delivery strategy by decorating the siRNA/dendrimer nanoparticulate system with the targeting peptide $E_{16}G_6$RGDK

15:59 28 October 2016

15:59 28 October 2016

(Fig. 7.9).[38,47] The peptide $E_{16}G_6RGDK$ contains three distinct segments: the targeting warhead (RGDK) for binding with integrins and neuropilin-1 receptors expressed on the cancer cell surface, the negatively charged sequence ($E_{16}$) for cargo carrying through electrostatic interaction with the positively charged siRNA/dendrimer nanoparticle, and the neutral linker ($G_6$) to bridge the targeting unit and the cargo carrying entity. Indeed, the so-devised system led to significantly improved receptor-mediated cell uptake, enhanced gene silencing and anticancer activity in prostate cancer and glioblastoma models in vitro and in vivo.[38,47]

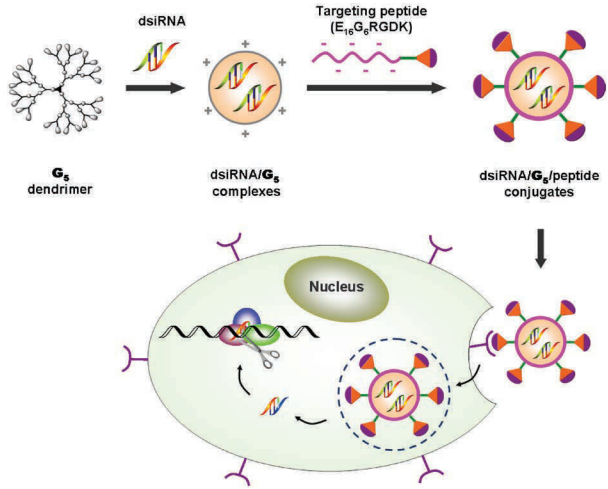



**Figure 7.9** Cartoon presentation of the siRNA/dendrimer nanoparticle decorated with the targeting peptide $E_{16}G_6RGDK$, which is composed of three distinct segments: RDGK sequence for dual targeting of the integrin and the neuropilin-1 receptor, the negatively charged oligopeptide $E_{16}$ for binding to the positively charged siRNA/dendrimer nanoparticles, and the neutral sequence of $G_6$ to bridge the binding and targeting components. Adapted with permission from *Nanomedicine NBM*, 2014, **10**, 1627–1636. Copyright 2014 Elsevier.

While considerable basic knowledge has been acquired and significant advances have been made for dendrimer-mediated siRNA delivery and gene silencing, translation to the clinical setting represents a challenging road ahead. Our goal is to develop multifunctional biocompatible dendrimeric delivery platforms for

siRNA delivery while respecting the need to maximize the efficacy and specificity of delivery and minimize the complicated side effects. We are pursuing actively in this direction.

## Acknowledgement

We acknowledge financial support from the international ERA-Net EURONANOMED European Research projects DENANORNA and Target4Cancer, Ligue Nationale Contre le Cancer, Association pour la Recherche sur les Tumeurs de la Prostate, Association Française contre les Myopathies, INCa, Canceropôle PACA, CNRS and INSERM. We thank all of our former and present team members as well as our collaborators who have participated and contributed to the work presented in this short review. We are also grateful of Dr. Cheng Liu for preparing some of the figures.

15:59 28 October 2016

## References

1. Yin H, Kanasty RL, Eltoukhy AA, Vegas AJ, Dorkin JR, Anderson D (2014) Non-viral vectors for gene-based therapy, *Nat Rev Genet*, **15**, 541–555.
2. Daniela C, Rossi JJ (2009) The promises and pitfalls of RNA-interference-based therapeutics, *Nature*, **457**, 8331–8340.
3. Kanasty R, Dorkin JR, Vegas A, Anderson D (2013) Delivery materials for siRNA therapeutics, *Nat Mater*, **12**, 967–977.
4. Liu X, Rocchi P, Peng L (2012) Dendrimers as non-viral vectors for siRNA delivery, *New J Chem,* **36**, 256–263.
5. Ravina M, Paolicelli P, Seijo B, Sanchez A (2010) Knocking down gene expression with dendritic vectors, *Mini-Rev Med Chem*, **10**, 73–86.
6. Khandare J, Calderon M, Dagia NM, Haag R (2012) Multifunctional dendritic polymers in nanomedicine: opportunities and challenges, *Chem Soc Rev*, **41**, 2824–2848.
7. Vögtle F, Richardt G, Werner N (eds) (2009). *Dendrimer Chemistry: Concepts, Syntheses, Properties, Applications*, Wiley-VCH, Weinheim, Germany.
8. Behr JP (1997) The proton sponge: a trick to enter cells the viruses did not exploit, *Chimia*, **51**, 34–36.

15:59 28 October 2016


9. Kukowska-Latallo JF, Bielinska AU, Johnson J, Spindler R, Tomalia DA, Baker JR, Jr (1996) Efficient transfer of genetic material into mammalian cells using Starburst polyamidoamine dendrimers, *Proc Natl Acad Sci U S A*, **93**, 4897–4902.
10. Kang H, DeLong R, Fisher MH, Juliano RL (2005) Tat-conjugated PAMAM dendrimers as delivery agents for antisense and siRNA oligonucleotides, *Pharm Res*, **22**, 2099–2106.
11. Zhou J, Wu J, Hafdi N, Behr JP, Erbacher P, Peng L (2006) PAMAM dendrimers for efficient siRNA delivery and potent gene silencing, *Chem Commun,* 2362–2364.
12. Wu J, Zhou J, Qu F, Bao F, Zhang Y, Peng L (2005) Polycationic dendrimers interact with RNA molecules: Polyamine dendrimers inhibit the catalytic activity of Candida ribozymes, *Chem Commun*, 313–315.
13. Liu X, Wu J, Yammine M, Zhou J, Posocco P, Viel S, et al. (2011) Structurally flexible triethanolamine core PAMAM dendrimers are effective nanovectors for DNA transfection in vitro and in vivo to the mouse thymus, *Bioconjugate Chem*, **22**, 2461–2473.
14. Liu X, Posocco P, Liu C, Yu T, Wang Q, Dal Col V, et al. (2013) Poly(amidoamine) dendrimers as non-viral vectors for the delivery of RNA therapeutics, in *Dendrimers in Biomedical Applications* (Cena V, Klajnert B, and Peng L, eds), RSC publishing, pp. 73–83.
15. Liu X, Liu C, Catapano CV, Peng L, Zhou J, Rocchi P (2014), Structurally flexible triethanolamine-core poly(amidoamine) dendrimers as effective nanovectors to deliver RNAi-based therapeutics, *Biotech Adv*, **32**, 844–852.
16. Yu T, Liu X, Bolcato-Bellemin AL, Wang Y, Liu C, Erbacher P, et al. (2012) An amphiphilic dendrimer for effective delivery of small interfering RNA and gene silencing in vitro and in vivo, *Angew Chem Int Ed*, **51**, 8478–8484.
17. Wei T, Chen C, Liu J, Liu C, Posocco P, Liu X et al. (2015) Anticancer drug nanomicelles formed by self-assembling amphiphilic dendrimer to combat cancer drug resistance, *Proc. Natl. Acad. Sci. U S A*, 112, 2978–2983.
18. Liu X, Zhou J, Yu T, Chen C, Cheng Q, Sengupta K, et al. (2014) Adaptive amphiphilic dendrimer-based nanoassemblies as robust and versatile siRNA delivery systems, *Angew Chem Int Ed*, **53**, 11822–11827.
19. Tomalia DA, Naylor AM, Goddard III WA (1990) Starburst dendrimers: molecular-level control of size, shape, surface chemistry, topology,

15:59 28 October 2016

and flexibility from atoms to macroscopic matter, *Angew Chem Int Ed Engl*, **29**, 138–175.

20. Guillot-Nieckowski M, Eisler S, Diederich F (2007) Dendritic vectors for gene tranfection, *New J Chem*, **31**, 1111–1127.
21. Tang MX, Redemann CT, Szoka FC, Jr. (1996) In vitro gene delivery by degraded polyamidoamine dendrimers, *Bioconjugate Chem,* **7**, 703–714.
22. Tomalia DA, Baker H, Dewald J, Hall M, Kallos G, Martin S, et al. (1985) A new class of polymers: starburst-dendritic macromolecules, *Polym J*, **17**, 117–132.
23. Liu X, Liu C, Laurini E, Posocco P, Pricl S, Qu F, et al. (2012) Efficient delivery of sticky siRNA and potent gene silencing in a prostate cancer model using a generation 5 triethanolamine-core PAMAM dendrimer, *Mol Pharmaceutics*, **9**, 470–481.
24. Posocco P, Liu X, Laurini E, Marson D, Chen C, Liu C, et al. (2013) Impact of siRNA overhangs for dendrimer-mediated siRNA delivery and gene silencing, *Mol Pharmaceutics*, **10**, 3262–3273.
25. Shen XC, Zhou J, Liu X, Wu J, Qu F, Zhang ZL, et al. (2007) Importance of size-to-charge ratio in construction of stable and uniform nanoscale RNA/dendrimer complexes, *Org Biomol Chem*, **5**, 3674–3681.
26. Liu XX, Rocchi P, Qu FQ, Zheng SQ, Liang ZC, Gleave M, et al. (2009) PAMAM dendrimers mediate siRNA delivery to target Hsp27 and produce potent antiproliferative effects on prostate cancer cells, *Chem Med Chem*, **4**, 1302–1310.
27. Cornford PA, Dodson AR, Parsons KF, Desmond AD, Woolfenden A, Fordham M, et al. (2000). Heat shock protein expression independently predicts clinical outcome in prostate cancer, *Cancer Res*, **60**, 7099–7105.
28. Rocchi P, So A, Kojima S, Signaevsky M, Beraldi E, Fazli L, et al. (2004) Heat shock protein 27 increases after androgen ablation and plays a cytoprotective role in hormone-refractory prostate cancer, *Cancer Res*, **64**, 6595–6602.
29. Xia Y, Rocchi P, Iovanna JL, Peng L (2012) Targeting heat shock response pathways to treat pancreatic cancer, *Drug Discov Today*, **17**, 35–43.
30. Kala S, Mak ASC, Liu X, Posocco P, Pricl S, Peng L, et al. (2014). Combination of dendrimer-nanovector-mediated small interfering RNA delivery to target Akt with the clinical anticancer drug

15:59 28 October 2016

Paclitaxel for effective and potent anticancer activity in treating ovarian cancer, *J Med Chem*, **57**, 2634–2642.

31. Testa JR, Bellacosa A (2001) AKT plays a central role in tumorigenesis, *Proc Natl Acad Sci U S A*, **98**, 10983–10985.
32. Luo J, Manning BD, Cantley LC (2003) Targeting the PI3K-Akt pathway in human cancer: rationale and promise, *Cancer Cell*, **4**, 257–262.
33. Bolcato-Bellemin AL, Bonnet ME, Creusat G, Erbacher P, Behr JP (2007) Sticky overhangs enhance siRNA-mediated gene silencing, *Proc Natl Acad Sci U S A*, **104**, 16050–16055.
34. Kim DH, Behlke MA, Rose SD, Chang MS, Choi S, Rossi JJ (2005) Synthetic dsRNA Dicer substrates enhance RNAi potency and efficacy, *Nat Biotechnol*, **23**, 222–226.
35. Amarzguioui M, Lundberg P, Cantin E, Hagstrom J, Behlke MA, Rossi JJ (2006) Rational design and in vitro and in vivo delivery of dicer substrate siRNA, *Nat Protoc*, **1**, 508–517.
36. Amarzguioui M, Rossi JJ (2008) Principles of Dicer substrate (D-siRNA) design and function, *Methods Mol Biol*, **442**, 3–10.
37. Rose SD, Kim DH, Amarzguioui M, Heidel JD, Collingwood MA, Davis ME, et al. (2005) Functional polarity is introduced by Dicer processing of short substrate RNAs, *Nucleic Acids Res*, **33**, 4140–4156.
38. Liu X, Liu C, Chen C, Bentobji M, Cheillan FA, Piana J T et al. (2014) Targeted delivery of Dicer-substrate siRNAs using a dual targeting peptide decorated dendrimer delivery system, *Nanomedicine NBM*, **10**, 1627–1636.
39. Zhou J, Neff CP, Liu X, Zhang J, Li H, Smith DD, et al. (2011). Systemic administration of combinatorial dsiRNAs via nanoparticles efficiently suppresses HIV-1 infection in humanized mice, *Mol Ther*, **19**, 2228–2238.
40. Lang MF, Yang S, Zhao C, Sun G, Murai K, Wu X, et al. (2012) Genome-wide profiling identified a set of miRNAs that are differentially expressed in glioblastoma stem cells and normal neural stem cells, *PLoS One*, **7**, e36248.
41. Ma L, Teruya-Feldstein J, Weinberg RA (2007) Tumour invasion and metastasis initiated by microRNA-10b in breast cancer, *Nature*, **449**, 682–688.
42. Portnoy V, Huang V, Place RF, Li LC (2011) Small RNA and transcriptional upregulation, *Wiley Interdiscip Rev RNA*, **2**, 748–760.

43. Li LC, Okino ST, Zhao H, Pookot D, Place RF, Urakami S et al. (2006) Small dsRNAs induce transcriptional activation in human cells, *Proc Natl Acad Sci U S A*, **103**, 17337–17342.

44. Reebye V, Sætrom P, Mintz PJ, Huang KW, Swiderski P, Peng L, et al. (2014) Novel RNA oligonucleotide improves liver function and inhibits liver carcinogenesis in vivo, *Hepatology*, **59**, 216–227.

45. Liu C, Liu X, Rocchi P, Qu F, Iovanna JL, Peng L (2014) Arginine-terminated generation 4 PAMAM dendrimer as an effective nanovector for functional siRNA delivery in vitro and in vivo, *Bioconjugate Chem*, **25**, 521–532.

46. Liu X, Liu C, Zhou J, Chen C, Qu F, Rossi JJ, et al (2015) Promoting siRNA delivery via enhanced cellular uptake using an arginine-decorated amphiphilic dendrimer, *Nanoscale*, **7**, 3867–3875.

47. Cui Q, Yang S, Ye P, Tian E, Sun G, Zhou J et al. (2016) Downregulation of TLX induces TET3 expression and inhibits glioblastoma stem cell self-renewal and tumorigenesis, *Nature Commun*, **7**, 10637.

48. Chen C, Posocco P, Liu X, Cheng Q, Zhou J et al. (2016) Mastering dendrimer self-assembly for efficient siRNA delivery: from conceptual design to in vivo efficient gene silencing, *Small*, in revision. DOI: 10.1002/smll.201503866R1.

15:59 28 October 2016

15:59 28 October 2016



Taylor & Francis
Taylor & Francis Group
http://taylorandfrancis.com

## Chapter 8

# Dendrimers as Nanomedicine in Cancer Therapy

**Keerti Jain[a,b] and N. K. Jain[a]**

[a]*Pharmaceutical Nanotechnoloagy Research Laboratory, ISF College of Pharmacy, Moga, Punjab 142001, India*
[b]*National Institute of Pharmaceutical Education and Research (NIPER-Raebareli), Raebareli, Uttar Pradesh 229010, India*

dr.jnarendr@gmail.com

In recent years, dendrimers have attracted scientists particularly in various facets of cancer therapy. The application of dendrimers in cancer therapy ranges from improved pharmacokinetic profile of poorly permeable anticancer drug, increased aqueous solubility of hydrophobic drugs to targeted drug delivery, gene therapy, cancer imaging, photodynamic therapy (PDT), boron neutron capture therapy (BNCT), etc. Dendrimers have shown passive targeting via the enhanced permeation retention (EPR) effect and pH-sensitive drug release as well as active targeting using various ligands such as mannose, folic acid, transferrin, antibodies, and peptides, etc. In this review, we have summarized latest advances in dendrimer-mediated cancer therapy for speculated clinical applications of dendrimers.

*Dendrimers in Nanomedicine*
Edited by Delphine Felder-Flesch
Copyright © 2016 Pan Stanford Publishing Pte. Ltd.
ISBN 978-981-4745-49-9 (Hardcover), 978-981-4745-50-5 (eBook)
www.panstanford.com

04:36 30 October 2016

## 8.1 Introduction

Serious side effects and resistance to anticancer chemotherapy are two major limitations for cancer therapy and hence most of the cancers are fatal due to ineffectiveness of antineoplastic drugs in controlling tumor without causing toxicity. The prime aim in cancer treatment is to kill selectively the cancer cells, sparing normal host cells and their physiology. Nanomedicines based on nanomaterials having size in the range of nanometers are providing a new platform for designing drug for rational and effective individualized treatment protocol (Jain et al., 2013a,b; Markman et al., 2013; Kumari et al., 2015). Recent decades have witnessed the introduction of a large number of nanomaterials in the field of medicine and hence a new branch of science known as nanomedicine has emerged as a prospective tool for personalized medicine system.

Dendrimers, carbon nanotubes, quantum dots, micelles, and several other nanoparticles are being investigated for drug delivery, as diagnostic agents, as tool for photodynamic therapy, boron neutron capture therapy, etc. (Fig. 8.1). Further, nanomaterials are also being explored as a hybrid system, i.e., combination of two or more nanomaterials in the field of medicine. A few of these nanomaterials are based on polymeric systems like dendrimers, micelles, nanoparticles, polymeric drug conjugates, etc. One of the recently emerging nanomaterials, 21st century polymer, dendrimers constitute a novel class of macromolecular systems, recently being explored for drug delivery and other biomedical applications (Mehra et al., 2015; Jain and Jain, 2014a). Dendrimers are essentially defined as nearly monodispersed macromolecules with well-defined globular multi-branched architecture consisting of a central focal point known as core, repeated branching units, and multivalent surface functional groups, which can either interact electrostatically with polar drug molecules or encapsulate non-polar drug molecules within their hydrophobic internal cavities (Fig. 8.2). Further, their surface could be engineered to control delivery of drug molecules, which could be triggered by specific stimuli like pH, specific enzymes, targeting ligands, etc. (Markman et al., 2013; Jain et al., 2014a).

04:36 30 October 2016

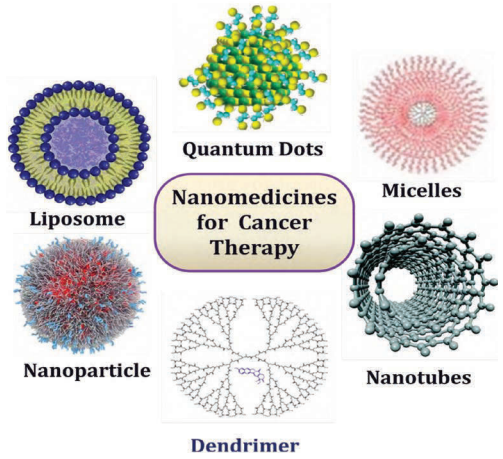



**Figure 8.1** Nanomaterials for cancer therapy.

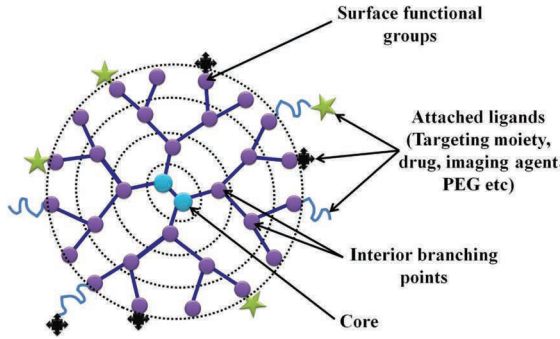



**Figure 8.2** Typical structure of a dendrimer.

In oncology, dendrimers are being explored in every facet of cancer therapy. Dendrimers are being investigated to solubilize poorly soluble anticancer drugs and developing an oral formulation for injectable drug as well as improving pharmacokinetic profile and bioavailability. Further, the multivalent surface of dendrimers could be conjugated with a number of bioactives, including therapeutic moiety, targeting ligand, spacer like PEG, diagnostic agent, antibody and nucleic acids, etc. The severe side effects of anticancer drugs could also be alleviated by dendrimer -mediated delivery to improve anticancer efficacy. Recently dendrimers are also being used simultaneously for the delivery

of neoplastic agents and imaging of cancer cells, the approach known as theranostic applications (Kojima, 2015; Jain et al., 2012; Jain et al., 2014b; Jain and Jain, 2014b). At present dendrimers are extensively being explored for various applications in cancer therapy, and a brief summary of applications of dendrimers as nanomedicine in cancer therapy is given in Table 8.1. In this chapter, we have summarized the latest updates on the role of dendrimers in cancer therapy.

## 8.2 Cancer Targeted Drug Delivery

04:36 30 October 2016

The availability of a large number of functional groups on the surface of dendrimers renders them a suitable platform for linking a large number of homing ligands that can deliver the anticancer therapeutic agent selectively to cancer cells. In this context, a large number of ligands varying from vitamins to monoclonal antibodies, hormones to nucleic acid, etc., has been conjugated with dendrimers. Some of the most explored ligands used in dendrimer-mediated drug targeting include folic acid, mannose, galactose, RGD peptide, estradiol, aptamers, vitamin E derivatives, etc. Somani and Dufes (2015) highlighted the potential applications of dendrimers particularly conjugated with transferrin (TfR) or ligand specific for transferrin receptor for treatment of cancer. The scientists added that these transferrin receptor anchored dendrimers were found to be very efficient in targeting genes, chemotherapeutic drugs to cancer cells and hence may be developed as a safe and targeted drug delivery system in cancer therapy (Somani and Dufes, 2015).

Zhang et al. (2015b) designed DNA aptamer conjugated dendrimers for targeted delivery of anticancer agent as well as for targeted imaging of cancer cells. For this investigation, they exploited multivalent nanoscaffold of dendrimers to conjugate with a number of bioactives, including anticancer drug doxorubicin, targeting aptamer DNA, and fluorophore. The efficiency of this nanoconstruct was evaluated in two cell lines, including human T cell acute lymphoblastic leukemia cell line and human Burkitt's lymphoma cell line. The results depicted that these dendrimers selectively targeted the anticancer drug and imaging agent to conjugated aptamer specific cancer cells, which was human T cell acute lymphoblastic leukemia cell line in this case (Zhang et al., 2015b).

04:36 30 October 2016

**Table 8.1** Applications of dendrimer-based nanomedicines in cancer therapy

| Dendrimers | Ligands | Bioactive | Objective | Results | Reference |
|---|---|---|---|---|---|
| PPI | Lactoferrin, Lactoferricin | DNA encoding TNFα | To increase tumor selective gene expression with reduction in liver associated non-specific gene expression | Targeted dendriplexes showed complete suppression of 60% of A431 tumors and up to 50% of B16-F10 tumors over one month. | Lim et al., 2015 |
| PPI | anti-ITCH siRNA and shRNA | Gemcitabine | Co-administration of RNA interference agents targeting the ubiquitin ligase ITCH with Gemcitabine to prevent loss of efficacy with prolonged treatment | (i) Significant uptake by human pancreatic cancer cells<br>(ii) A 40–60% decrease in ITCH RNA and protein expression in vitro (si/shRNA) and in a xenograft model of pancreatic cancer (shRNA).<br>(iii) Complete regression of tumor growth on co-administration of subtherapeutic dose of gemcitabine (100 mg/kg/week) with ITCH-shRNA (3 × 50 mg/week) for 17 days | de la Fuente et al., 2015 |
| Poly(ether imine) | Dendriplex (dendrimer-DNA complex) | pIRES-Rgp (Rabies plasmid vaccine construct) | To increase efficacy and immunogenicity of plasmid-based rabies vaccine | Dendriplex with poly(ether imine) dendrimers can produce earlier onset of a high-titer protective antibody response to a plasmid-based rabies vaccine and may emerge as effective nonviral genetic vaccination | Ullas et al., 2014 |
| Boltorn® H40* | PLA (poly-D,L-lactide) | Docetaxel (DTX) | To investigate the fate of nanohybrid after internalization by cells | Increased in vitro cancer cell cytotoxicity and delayed tumor growth in immune-deficient mice observed after co-delivery of chloroquine | Zhang et al., 2014 |

(*Continued*)

04:36 30 October 2016

**Table 8.1** (*Continued*)

| Dendrimers | Ligands | Bioactive | Objective | Results | Reference |
|---|---|---|---|---|---|
| | | | and speculate that these nanoparticles are sequestered by autophage followed by fusion with lysosomes in MCF-7 cells | (autophagy inhibitor) and DTX suggested promising clinical applications of dendrimeric copolymer-based nanoparticles. | |
| PAMAM | PEG, lactobionic acid | Astrocyte elevated gene-1 (AEG-1) siRNA | Effective treatment of Hepatocellular Carcinoma (HCC) | Delayed tumor growth, increased necrosis, inhibition of proliferation, and increased apoptosis. | Rajasekaran et al., 2015 |
| ALA# dendrimers | — | Protoporphyrin IX | To investigate efficacy and efficiency of ALA dendrimers to photosensitize cancer cells | ALA dendrimer was mainly uptaken in macrophages by caveloae-mediated endocytosis. ALA dendrimers are effective for cancer as well as vascular PDT. | Rodriguez et al., 2015 |
| Dendrimer (5.0G PAMAM)-entrapped gold nanoparticles (Au DENPs) | alpha-tocopheryl succinate (α-TOS) and arginine-glycine-aspartic acid (RGD) | — | Targeted chemotherapy and computed tomography (CT) imaging of cancer cells | Increased generation of reactive oxygen species leading to enhanced ability to induce apoptosis. These nanocomposites may emerge as potential nanoplatform for cancer targeting and imaging. | Zhu et al., 2015 |

*A dendritic polyester with 64 hydroxyl terminal groups per molecule; $M_n$ 2833.

#ALA: 5-aminolaevulinic acid.

04:36 30 October 2016

Apart from targeting achieved by ligand receptor interactions, dendrimers are also being investigated for cancer targeting via various physical stimuli. The presence of amino groups on the surface of dendrimers like PPI, PAMAM, PLL facilitated pH-sensitive drug release due to protonation of the amino groups at acidic pH of tumor environment (Jain et al., 2014a). The effect of osmotic pressure on lymphatic targeting potential was investigated and it was observed that the increase in osmotic pressure could increase the lymphatic targeting potential of dendrimers (Yang et al., 2015). Dendrimers have shown promising results in the scenario of anticancer drug targeting, which depends on their generations, functional groups, and attached ligand (Fig. 8.2 and Fig. 8.3).

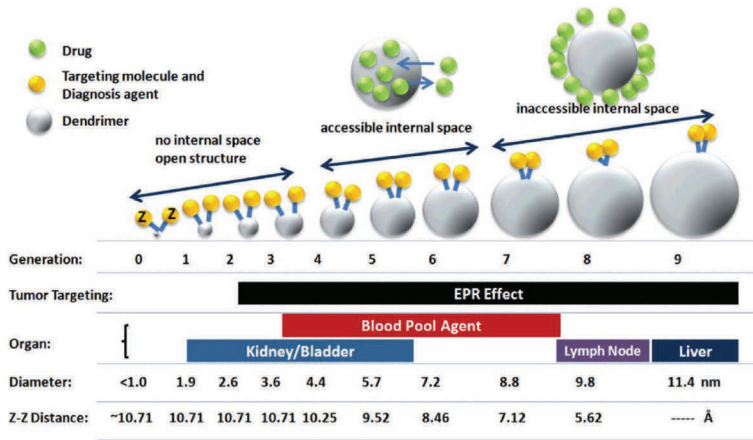



**Figure 8.3** Schematic representation of variation in the properties of dendrimers with increasing generation along with different biomedical application in respect of PAMAM-DTPA (Gd) complex developed as MRI contrast agent. Adapted with permission from Lo et al. (2013).

## 8.3 Gene Therapy: Cancer

Dendrimers are being investigated to overcome the problems related to gene therapy of cancer (Lim et al., 2015). Lactoferrin and lactoferricin conjugated PPI dendrimers have been investigated by scientists for tumor-targeted delivery of gene to enhance therapeutic efficacy against liver cancer cell lines

overexpressing receptors for these ligands. It was observed that these surface engineered-dendrimers could increase gene delivery efficiency revealed by significant increase in gene expression, being well tolerated by experimental animals, and may serve as promising gene delivery vectors for clinical applications (Lim et al., 2015).

Complexes of PAMAM, carbosilane, and phosphorus dendrimers having cationic surface functional groups with anticancer siRNAs (Bcl-xl, Bcl-2, Mcl-1) for gene therapy of cancer have been designed and investigated by scientists. Further formation of dendriplexes as well as integrity of siRNA released from dendrimers was investigated using heparin, and it was confirmed that siRNAs formed complexes with dendrimers, the integrity and activity was unaffected by dendrimers, siRNA could be released after treatment with heparin and moreover dendrimers protected siRNA from activity of RNase enzyme. Transfection efficiency of these dendriplexes was examined in HeLa and HL-60 cell lines and phosphorous-based dendriplexes were found to most cytotoxic as well as efficient transfection agents among all tested siRNA dendrimer complexes (Dzmitruk et al., 2015; Ionov et al., 2015).

Urbiola et al. (2015) investigated the efficiency of transferrin conjugated PAMAM dendrimers for gene delivery in cancer cells. Developed polyplex was found to be stable and protected from DNAse I enzyme degradation and showed superior transfection efficiency in HepG2, CT26 and HeLa cell lines as compared to plain dendriplexes and branched polyethyleneimine complexes of DNA.

## 8.4 Brain Delivery

Effective penetration of blood–brain tumor barrier and uniform distribution in brain tumor is prerequisite for the treatment of glioblastoma. Zhang et al. (2015a) examined hydroxylated 4.0G PAMAM dendrimers for targeted delivery of immunomodulators to tumor associated microglia/macrophages (TAMs) for the therapy of glioblastoma and observed that after systemic administration these dendrimers were distributed homogeneously within the solid tumor having diameter around 6 mm along with peritumoral area in a short time period of 15 min

04:36 30 October 2016

followed by accumulation and retention within TAMs (Zhang et al., 2015a). Carbosilane dendrimers showed successful gene silencing achieved by successful transfection of siRNA to HIV-infected human primary astrocytes without causing cytotoxicity for the treatment of neurological disorders (Serramía et al., 2015).

## 8.5 Dendrimer Hybrids with Other Nanomaterials in Cancer Therapy

04:36 30 October 2016

Nanotechnology is emerging as a novel platform for personalized and controlled drug delivery with ability to provide selective biological response and improved therapeutic activity. In this context, more than one nanomaterial is also being investigated in combination for improved treatment strategy of different ailments. One of the examples of such hybrid nanomaterials is combination of dendrimers with nanoparticles. Nanoparticles are showing excellent potentials in drug delivery as well as in various diagnostic and biomedical applications yet it is indispensable to modify the surface of nanoparticles to make them biocompatible and target specific (Parat et al., 2015; Kesharwani et al., 2014; Bagre et al., 2013).

Cai et al. (2015) designed nanocomposites consisting of $Fe_3O_4$ nanoparticles and dendrimers for dual-mode imaging of tumors using computed tomography (CT) scanning and magnetic resonance imaging (MRI) techniques. A layer-by-layer self-assembly technique was used by scientists to develop multilayered assembly of poly($\gamma$-glutamic acid) (PGA)/poly(l-lysine)/PGA/folic acid (FA)-modified dendrimer-entrapped gold nanoparticles. These nanocomposites were found to be cytocompatible and hemocompatible and showed fine X-ray attenuation properties. Further, presence of folic acid made these nanocomposites to be selectively uptaken by folic acid receptor overexpressing cancer cells as depicted by in vitro cell line studies and in vivo xenografted tumor model (Cai et al., 2015).

Taratula et al. (2015) designed graphene nanosheets modified with PPI dendrimers loaded with a photosensitizer, phthalocyanine (Pc), as nanomedicines for targeted phototherapy of ovarian cancer. Further, this hybrid carrier was conjugated with PEG and LHRH to improve biocompatibility and tumor-targeted

delivery of photosensitizer, respectively. This nanohybrid made up of dendrimers and graphene sheets inhibited the fluorescence quenching of phthalocyanine with increased cancer cytotoxicity attributed to synergistic effect of ROS and hyperthermia (Taratula et al., 2015).

## 8.6 Theranostic Applications

04:36 30 October 2016

The term "theranostics" includes concurrent assimilation of therapy and diagnosis. Further, nanotheranostic means application of nanomaterials such as polymeric nanoparticles, polymeric conjugates, metal nanoparticles, liposomes, micelles, dendrimers, quantum dots and carbon nanotubes in theranostics via simultaneous delivery of therapeutic and diagnostic agents for treatment and diagnosis of various ailments (Muthu et al., 2014; Lo et al., 2013). Although this concept seems interesting and converting it to reality is still a big challenge, yet scientists are investigating the strategy to design, develop and characterize multifunction theranostic nanoscaffolds (Zhu et al., 2014). Taratula et al. (2013) developed complex of phthalocyanine and 4.0G PPI dendrimers for theranostic applications and found these phthalocyanine-based dendrimers promising in near infrared imaging purposes and photodynamic therapy (Taratula et al., 2013).

Grünwald et al. (2013) developed dendrimer-coated adenovirus carrying hNIS gene encoding the sodium iodide symporter (NIS) as theranostic gene for combined NIS-mediated radiotherapy and oncolytic virotherapy. In the result of this study, scientists found this dendrimer-coated adenovirus as promising nanoscaffold for tumor radiotherapy and imaging (Grünwald et al., 2013). Dendrimers entrapping gold nanoparticles functionalized with multiple ligands, including polyethylene glycol (PEG)-modified $\alpha$-TOS, PEGylated folic acid, and fluorescein isothiocyanate (FI), were reported by Zhu and coworkers for targeted cancer therapy and diagnosis via computed tomography (CT) imaging. In vitro and in vivo study with cancer cell lines and xenografted tumor model, respectively, showed that these multifunctional dendrimer entrapped nanoparticles were targeted towards cancer cells for effective cancer therapy and imaging (Zhu et al., 2014). In this context the unique properties of dendrimers, i.e., multifunctional

surface and availability of large number of interior cavities render them suitable nanoplatform for theranostic applications (Fig. 8.4).

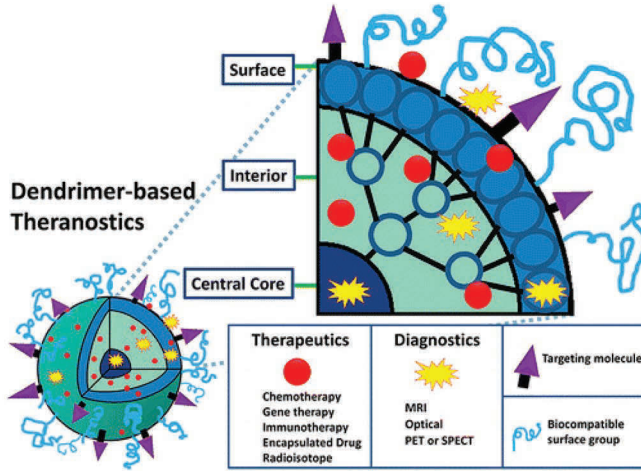



**Figure 8.4** Schematic presentation of theranostic application.s of dendrimers. Adapted with permission from Lo et al. (2013).

## 8.7 Future Prospects

Dendrimers are emerging as promising nanomedicine for the treatment of various ailments, including cancer, parasitic diseases, and neurodegenerative disorders (Ardestani et al., 2015; Sepúlveda-Crespo et al., 2015a,b; Milowska et al., 2015). In our laboratory, we have designed dendrimers with antiangiogenic activity to synergize anticancer activity of antineoplastic drugs (Jain et al., 2014a; Jain and Jain, 2014b). Apart from this, dendrimers are also being investigated for their potential antimicrobial activity as well as promising drug delivery applications in treatment of various infectious diseases (Xue et al., 2015; Jain et al., 2015a,b). VivaGel®, a product based on dendrimers is in phase 3 clinical trial for its topical microbicidal activity (Starpharma, 2012). Recently Starpharma got the approval to commence phase 1 clinical trial of dendrimer-based product of anticancer drug, docetaxel (Table 8.2). In future, it could be expected that dendrimers will also play crucial role in the nanomedicine-based theranostic applications (Fig. 8.5).

04:36 30 October 2016

04:36 30 October 2016

**Table 8.2** Market status of dendrimer-based formulations

| Product/ formulation | Activity | Status | Specifications | Manufacturer |
|---|---|---|---|---|
| DEP™-Docetaxel | Anticancer | Phase 1 clinical trial | Dendrimer-enhanced docetaxel (Taxotere®) chemotherapeutic product | Starpharma, Australia |
| VivaGel® | Topical microbicide | Phase 3 clinical trial | An innovative antimicrobial agent (SPL7013, or astodrimer sodium) has been successfully tested in clinical studies to relieve the signs and symptoms of bacterial vaginosis (BV), and to reduce risk of recurrence of BV, in clinical studies, to prevent recurrence of BV | Starpharma, Australia |
| Superfect® | Gene transfection agent | Marketed | Based on activated-dendrimer technology for Plasmid transfection, protein overexpression applications | Qiagen, Netherlands |
| Alert Ticket™ | Anthrax detection | Marketed | Dendrimer-based product for anthrax detection | US army research laboratory, USA |
| Stratus® CS | Analyzer | Marketed | Acute care diagnostic system based on quantitative cardiac assays for fast, accurate evaluation of patients suspected of having myocardial ischemia. | Dade Behring, UK |

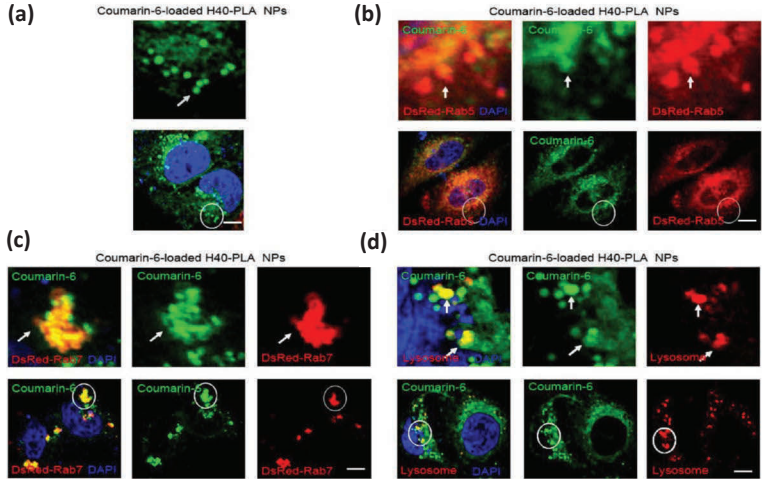



**Figure 8.5** Dendritic copolymer H40-PLA were uptaken through endocytosis by the CF-7 cells, DsRed-Rab5 transfected MCF-7 cells and DsRed-Rab7 transfected MCF-7 cells treated with 100 μg/mL coumarin-6-loaded H40-PLA NPs for 2 h. For lysosome detection, the MCF-7 cells were treated with 100 μg/mL coumarin-6-loaded H40-PLA NPs for 2 h, and then co-treated with Lyso-Tracker Red probes for 30 min. Adapted with permission from Zhang et al. (2014).

## 8.8 Conclusion

Dendrimers, the polymer of the 21st century, are showing tremendous potential applications in cancer therapy. Theranostic applications of dendrimers are paving the new way for the prognosis of cancer and a systematic evaluation of dendrimers in this regard could lead to potential clinical applications. Intrinsic therapeutic activity of dendrimers, including anticancer activity, antimicrobial activity, and antiangiogenic activity, also needs to be investigated thoroughly and completely to broaden the range of available therapeutic moieties. Although, application of dendrimers as drug is a distant dream, yet the entry of dendrimer-based marketed formulation, i.e., VivaGel™, into phase 3 clinical trial could be an indication of the shortening of the journey from designing of dendrimers to their promising clinical applications.

04:36 30 October 2016

## References

Ardestani MS, Fordoei AS, Abdoli A, Ahangari Cohan R, Bahramali G, Sadat SM, Siadat SD, Moloudian H, Nassiri Koopaei N, Bolhasani A, Rahimi P, Hekmat S, Davari M, Aghasadeghi MR. Nanosilver based anionic linear globular dendrimer with a special significant antiretroviral activity. *J Mater Sci Mater Med*, 2015; 26(5): 5510.

Bagre AP, Jain K, Jain NK. Alginate coated chitosan core shell nanoparticles for oral delivery of enoxaparin: in vitro and in vivo assessment. *Int J Pharm*, 2013; 456(1): 31–40.

Cai H, Li K, Li J, Wen S, Chen Q, Shen M, Zheng L, Zhang G, Shi X. Dendrimer-assisted formation of $Fe_3O_4$/Au nanocomposite particles for targeted dual mode CT/MR imaging of tumors. *Small*, 2015; doi: 10.1002/smll.201500856.

de la Fuente M, Jones MC, Santander-Ortega MJ, Mirenska A, Marimuthu P, Uchegbu I, Schätzlein A. A nano-enabled cancer-specific ITCH RNAi chemotherapy booster for pancreatic cancer. *Nanomedicine*, 2015; 11(2): 369–377.

Dzmitruk V, Szulc A, Shcharbin D, Janaszewska A, Shcharbina N, Lazniewska J, Novopashina D, Buyanova M, Ionov M, Klajnert-Maculewicz B, Gómez-Ramirez R, Mignani S, Majoral JP, Muñoz-Fernández MA, Bryszewska M. Anticancer siRNA cocktails as a novel tool to treat cancer cells. Part (B). Efficiency of pharmacological action. *Int J Pharm*, 2015; 485(1–2): 288–294.

Grünwald GK, Vetter A, Klutz K, Willhauck MJ, Schwenk N, Senekowitsch-Schmidtke R, Schwaiger M, Zach C, Wagner E, Göke B, Holm PS, Ogris M, Spitzweg C. Systemic image-guided liver cancer radiovirotherapy using dendrimer-coated adenovirus encoding the sodium iodide symporter as theranostic gene. *J Nucl Med*, 2013; 54(8): 1450–1457.

Ionov M, Lazniewska J, Dzmitruk V, Halets I, Loznikova S, Novopashina D, Apartsin E, Krasheninina O, Venyaminova A, Milowska K, Nowacka O, Gomez-Ramirez R, de la Mata FJ, Majoral JP, Shcharbin D, Bryszewska M. Anticancer siRNA cocktails as a novel tool to treat cancer cells. Part (A). Mechanisms of interaction. *Int J Pharm*, 2015; 485(1–2): 261–269.

Jain K, Gupta U, Jain NK. Dendronized nanoconjugates of lysine and folate for treatment of cancer. *Eur J Pharm Biopharm*, 2014a; 87(3): 500–509.

Jain K, Jain NK. Dendrimer: A 21st century nanobiopolymer. 2014a; http://www.pharmabiz.com/ArticleDetails.aspx?aid=81282&sid=21.

04:36 30 October 2016

04:36 30 October 2016

Jain K, Jain NK. Dendrimers as nanobiopolymers in cancer chemotherapy. *In Nanobiomed.*, 2014b, Vol. III, M/s Studium Press LLC, USA, 65–90.

Jain K, Jain NK. Surface engineered dendrimers as antiangiogenic agent and carrier for anticancer drug: dual attack on cancer. *J Nanosci Nanotechnol*, 2014b; 14(7): 5075–5087.

Jain A, Jain K, Kesharwani P, Jain NK. Low density lipoproteins mediated nanoplatforms for cancer targeting. *J Nanopart Res*, 2013a; 15: 1888.

Jain A, Jain K, Mehra NK, Jain NK. Lipoproteins tethered dendrimeric nanoconstructs for effective targeting to cancer cells. *J Nanopart Res*, 2013b; 15: 2003.

Jain K, Kesharwani P, Gupta U, Jain NK. A review of glycosylated carriers for drug delivery. *Biomaterials*, 2012; 33(16): 4166–4186.

Jain K, Mehra NK, Jain NK. Potentials and emerging trends in nanopharmacology. *Curr Opin Pharmacol*, 2014b; 15C: 97–106.

Jain K, Verma AK, Mishra PR, Jain NK. Characterization and evaluation of amphotericin B loaded MDP conjugated poly(propylene imine) dendrimers. *Nanomedicine*, 2015a; 11(3): 705–713.

Jain K, Verma AK, Mishra PR, Jain NK. Surface engineered dendrimeric nanoconjugates for macrophage targeted delivery of amphotericin B: formulation development, in vitro and in vivo evaluation. *Antimicrob Agents Chemother*, 2015b; 59(5): 2479–2487.

Kesharwani P, Jain K, Jain NK. Dendrimer as nanocarrier for drug delivery. *Prog Polym Sci,* 2014; 39(2): 268–307.

Kojima C. Preclinical studies of dendrimer prodrugs. *Expert Opin Drug Metab Toxicol*, 2015; DOI:10.1517/17425255.2015.1052404.

Kumari P, Ghosh B, Biswas S. Nanocarriers for cancer-targeted drug delivery. *J Drug Target*, 2015; PMID: 26061298.

Lim LY, Koh PY, Somani S, Robaian MA, Karim R, Yean YL, Mitchell J, Tate RJ, Edrada-Ebel R, Blatchford DR, Mullin M, Dufès C. Tumor regression following intravenous administration of lactoferrin- and lactoferricin-bearing dendriplexes. *Nanomedicine*, 2015; DOI: 10.1016/j.nano.2015.04.006.

Lo ST, Kumar A, Hsieh JT, Sun X. Dendrimer nanoscaffolds for potential theranostics of prostate cancer with a focus on radiochemistry. *Mol Pharm*, 2013; 10(3): 793–812.

Markman JL, Rekechenetskiy A, Holler E, Ljubimova JY. Nanomedicine therapeutic approaches to overcome cancer drug resistance. *Adv Drug Deliv Rev*, 2013; 65(13–14): 1866–1879.

Mehra NK, Jain K, Jain NK. Pharmaceutical and biomedical applications of surface engineered carbon nanotubes. *Drug Discov Today*, 2015; 20(6): 750–759.

Milowska K, Szwed A, Mutrynowska M, Gomez-Ramirez R, de la Mata FJ, Gabryelak T, Bryszewska M. Carbosilane dendrimers inhibit $\alpha$-synuclein fibrillation and prevent cells from rotenone-induced damage. *Int J Pharm*, 2015; 484(1–2): 268–275.

Muthu MS, Leong DT, Mei L, Feng SS. Nanotheranostics Application and further development of nanomedicine strategies for advanced theranostics. *Theranostics*, 2014; 4(6): 660–677.

Parat A, Bordeianu C, Dib H, Garofalo A, Walter A, Bégin-Colin S, Felder-Flesch D. Dendrimer-nanoparticle conjugates in nanomedicine. *Nanomedicine* (*Lond*), 2015; 10(6): 977–992.

Rajasekaran D, Srivastava J, Ebeid K, Gredler R, Akiel M, Jariwala N, Robertson CL, Shen XN, Siddiq A, Fisher PB, Salem AK, Sarkar D. Combination of nanoparticle-delivered siRNA for astrocyte elevated gene-1 (AEG-1) and all-trans retinoic acid (ATRA): An effective therapeutic strategy for hepatocellular carcinoma (HCC). *Bioconjug Chem*, 2015; DOI: 10.1021/acs.bioconjchem.5b00254.

Rodriguez L, Vallecorsa P, Battah S, Di Venosa G, Calvo G, Mamone L, Sáenz D, Gonzalez MC, Batlle A, MacRobert AJ, Casas A. Aminolevulinic acid dendrimers in photodynamic treatment of cancer and atheromatous disease. *Photochem Photobiol Sci*, 2015; DOI: 10.1039/C5PP00126A.

Sepúlveda-Crespo D, Gómez R, De La Mata FJ, Jiménez JL, Muñoz-Fernández MÁ. Polyanionic carbosilane dendrimer-conjugated antiviral drugs as efficient microbicides: Recent trends and developments in HIV treatment/therapy. *Nanomedicine*, 2015a, DOI: 10.1016/j.nano.2015.03.008.

Sepúlveda-Crespo D, Sánchez-Rodríguez J, Serramía MJ, Gómez R, De La Mata FJ, Jiménez JL, Muñoz-Fernández MÁ. Triple combination of carbosilane dendrimers, tenofovir and maraviroc as potential microbicide to prevent HIV-1 sexual transmission. *Nanomedicine* (*Lond*), 2015b; 10(6): 899–914.

Serramía MJ, Álvarez S, Fuentes-Paniagua E, Clemente MI, Sánchez-Nieves J, Gómez R, de la Mata J, Muñoz-Fernández MÁ. In vivo delivery of siRNA to the brain by carbosilane dendrimer. *J Control Release*, 2015; 200: 60–70.

Somani S, Dufès C. Transferrin-bearing dendrimers for cancer therapy: An update. *Nanomedicine* (*Lond*), 2015; DOI: 10.2217/nnm.14.93.

04:36 30 October 2016

04:36 30 October 2016

Taratula O, Patel M, Schumann C, Naleway MA, Pang AJ, He H, Taratula O. Phthalocyanine-loaded graphene nanoplatform for imaging-guided combinatorial phototherapy. *Int J Nanomed.*, 2015; 10: 2347–2362.

Taratula O, Schumann C, Naleway MA, Pang AJ, Chon KJ, Taratula O. A multifunctional theranostic platform based on phthalocyanine-loaded dendrimer for image-guided drug delivery and photodynamic therapy. *Mol Pharm*, 2013; 10(10): 3946–3958.

Ullas PT, Madhusudana SN, Desai A, Sagar BK, Jayamurugan G, Rajesh YB, Jayaraman N. Enhancement of immunogenicity and efficacy of a plasmid DNA rabies vaccine by nanoformulation with a fourth-generation amine-terminated poly(ether imine) dendrimer. *Int J Nanomed.*, 2014; 9: 627–634.

Urbiola K, Blanco-Fernández L, Navarro G, Rödl W, Wagner E, Ogris M, Tros de Ilarduya C. Evaluation of improved PAMAM-G5 conjugates for gene delivery targeted to the transferrin receptor. *Eur J Pharm Biopharm*, 2015; DOI: 10.1016/j.ejpb.2015.05.007.

Starpharma. 2012. http://www.starpharma.com/news/139. (accessed on 29.06.2015).

Xue XY, Mao XG, Li Z, Chen Z, Zhou Y, Hou Z, Li MK, Meng JR, Luo XX. A potent and selective antimicrobial poly(amidoamine) dendrimer conjugate with LED209 targeting QseC receptor to inhibit the virulence genes of gram negative bacteria. *Nanomedicine*, 2015; 11(2): 329–339.

Yang R, Mao Y, Ye T, Xia S, Wang S, Wang S. Study on enhanced lymphatic exposure of polyamidoamin-alkali blue dendrimer for paclitaxel delivery and influence of the osmotic pressure on the lymphatic targeting. *Drug Deliv*, 2015; DOI:10.3109/10717544.2015.1041577.

Zhang H, Ma Y, Xie Y, An Y, Huang Y, Zhu Z, Yang CJ. A controllable aptamer-based self-assembled DNA dendrimer for high affinity targeting, bioimaging and drug delivery. *Sci Rep*, 2015b; 5: 10099.

Zhang F, Mastorakos P, Mishra MK, Mangraviti A, Hwang L, Zhou J, Hanes J, Brem H, Olivi A, Tyler B, Kannan RM. Uniform brain tumor distribution and tumor associated macrophage targeting of systemically administered dendrimers. *Biomaterials*, 2015a; 52: 507–516.

Zhang X, Yang Y, Liang X, Zeng X, Liu Z, Tao W, Xiao X, Chen H, Huang L, Mei L. Enhancing therapeutic effects of docetaxel-loaded dendritic copolymer nanoparticles by co-treatment with autophagy inhibitor on breast cancer. *Theranostics*, 2014; 4(11): 1085–1095.

Zhu J, Fu F, Xiong Z, Shen M, Shi X. Dendrimer-entrapped gold nanoparticles modified with RGD peptide and alpha-tocopheryl succinate enable targeted theranostics of cancer cells. *Colloids Surf B Biointerfaces*, 2015; 133: 36–42.

Zhu J, Zheng L, Wen S, Tang Y, Shen M, Zhang G, Shi X. Targeted cancer theranostics using alpha-tocopheryl succinate-conjugated multifunctional dendrimer-entrapped gold nanoparticles. *Biomaterials*, 2014; 35(26): 7635–7646.

04:36 30 October 2016

## Chapter 9

# Impact of Physicochemical Properties on Dendrimer Pharmacokinetics and Biodistribution

**Orlagh Feeney, Suzanne M. Caliph, Christopher J. H. Porter, and Lisa M. Kaminskas**

*Monash Institute of Pharmaceutical Sciences, Monash University, 381 Royal Parade, Parkville, Victoria 3052, Australia*

lisa.kaminskas@monash.edu

Given that dendrimers are macromolecular entities with a highly defined structure and low polydispersity, there has been increasing interest over the past 20 years in developing dendrimer-based drug delivery and imaging systems. The significant potential of dendrimers to modulate and improve the biological and pharmacokinetic properties of associated drugs and imaging moieties has inspired the synthesis of some very elegant and elaborate constructs with multiple in vivo functionalities. The translatability of these novel constructs into clinical application is ultimately, however, dependent largely upon their chemical and biological reproducibility, toxicological and pharmacokinetic properties. The pharmacokinetic and biodistribution behavior of dendrimers in particular is largely dictated by physicochemical properties, such as size, hydrophilicity, surface charge, functionality,

*Dendrimers in Nanomedicine*
Edited by Delphine Felder-Flesch
Copyright © 2016 Pan Stanford Publishing Pte. Ltd.
ISBN 978-981-4745-49-9 (Hardcover), 978-981-4745-50-5 (eBook)
www.panstanford.com

flexibility and core or scaffold structure. As a general guideline, very large, hydrophobic or anionic dendrimers avidly target organs of the mononuclear phagocyte system which contain high levels of macrophages, such as the liver, spleen, lungs and lymphoid tissue. Small hydrophilic, flexible or uncharged systems are more readily eliminated from the body via urinary excretion, whilst larger hydrophilic and uncharged systems tend to remain in the body for prolonged periods of time and facilitate uptake into solid tumors or areas of inflammation and increased angiogenesis. This chapter therefore gives an overview of our current understanding of the pharmacokinetic and biodistribution behavior of dendrimers, and how this can be dictated by physicochemical properties.

04:32 30 October 2016

## 9.1 Introduction

The number of new small molecule drugs or chemical entities (NCEs) that eventually succeed in being approved for clinical use is less than 10%.[14] NCEs fail in preclinical and clinical trials for a wide variety of reasons which can include unacceptable toxicity, poor activity and inappropriate pharmacokinetic profiles.[70] Restrictions surrounding the approval of chemotherapeutic drugs (which include antibiotics and cancer chemotherapeutics) are less stringent than most NCEs, however, since the successful treatment of the disease and survival of the patient take precedence above toxic side effects and sub-optimal pharmacokinetics. Altogether, this has driven a rapid expansion in the development of nanometer sized colloidal, polymeric and nanoparticle-based drug delivery systems which can be used to tailor the pharmacokinetic behavior of loaded drugs. Although to date, liposome-based delivery systems are leading the field of "nanomedicine," we are seeing increasing interest in the development of dendrimer-based drug vectors. Numerous literature examples demonstrate improved pharmacokinetic behavior and activity of small molecule drugs in preclinical rodent models as a result of their covalent or non-covalent association with dendrimer-based carriers. To this point, however, dendrimer-based nanomedicines for internal use have not yet reached the market, although Starpharma Pty Ltd currently has a dendrimer-based formulation of docetaxel in Phase I clinical trials in Australia.

04:32 30 October 2016

The intent of this chapter is to describe the pharmacokinetic behavior of dendrimers after intravenous (IV), interstitial (subcutaneous [SC], intramuscular [IM]), oral, transdermal and pulmonary administration. We describe how the physicochemical properties of dendrimers impact their pharmacokinetic behavior and provide some guidance on properties that achieve prolonged circulation in blood, uptake into solid tumors and absorption across membrane barriers. It should be noted at this point, however, that "dendrimer pharmacokinetics" have historically been described by following a radioactive tracer attached to the scaffold and by following the pharmacokinetics of covalently and non-covalently associated drugs. The latter, however, does not provide an accurate detail of dendrimer behavior in vivo, since the pharmacokinetics of the associated drug will be dictated by liberation from the dendrimer scaffold, dendrimer biodegradation and patterns of drug disposition and is expanded on somewhat in the next section. In this chapter, we have therefore focused specifically on describing the pharmacokinetic behavior of the dendrimer (by tracing the scaffold) rather than on associated drugs.

## 9.2 Understanding Pharmacokinetics

As efforts to better define candidate nanomedicines increase, attention has increasingly focused on accurately quantifying the absorption, distribution, metabolism and elimination (ADME) properties of the delivery system, and any associated drugs. In large part the methods employed are an extension of traditional pharmacokinetic profiling techniques, although the complexity of dendrimer–drug conjugates dictates some modifications to standard practice. The following section very briefly summarizes the most common approaches that can be taken to define the pharmacokinetics of dendrimers and dendrimer associated drugs. The interested reader is directed to any one of a number of classical pharmacokinetic texts for more details.[17,62]

Classically, pharmacokinetics provides a means to quantify and model the fate of a drug after administration into the body. This may be simplified to suggest that pharmacokinetics describes "what the body does to a drug" rather than pharmacodynamics that instead defines "what the drug does to the body." Direct

04:32 30 October 2016

application of these principles to drug delivery systems rather than simply to drugs provides some complexity and indeed has led to some controversy as to whether pharmacokinetics is the right term to describe the movement of a drug delivery system rather than a drug through the body. For the purpose of this discussion, however, we will refer to the pharmacokinetics of a dendrimer as meaning the ADME properties of the carrier, whether conjugated to a drug or not, realizing that it is possible to separately define the pharmacokinetics of a drug that is initially conjugated to a dendrimer carrier, but is subsequently released and processed as free drug. In large part, the distinction between these two is determined by the analytical method and whether what is being measured is the concentration of the carrier, the concentration of total drug (i.e., free and dendrimer conjugated) or free drug alone. All provide useful information, but the data are not interchangeable.

The first parameters to be assessed for a dendrimer intended for intravenous injection are the systemic pharmacokinetic parameters, i.e., the parameters that describe the kinetics of removal of the delivery system from the general (systemic) circulation. These are obtained by administering the carrier intravenously and taking blood samples as a function of time post administration. Assuming a means by which the concentration of the carrier in the blood (in fact the concentration in plasma is usually measured since this is easier analytically) can be calculated, a measure of overall exposure of the carrier to the systemic circulation can be obtained by measuring the area under the blood level versus time curve (AUC). Thus, nanomaterials that persist for longer in the blood have larger AUCs at a given dose and those that persist for shorter periods have lower AUCs. From this piece of information the two primary pharmacokinetic parameters can be calculated: clearance (Cl) and volume of distribution (Vd). Clearance is calculated simply from the dose divided by the AUC and provides a measure of how quickly drug delivery systems are removed from the blood. Thus, materials that are removed quickly have lower AUCs at a fixed dose and therefore higher clearance and vice versa. However, clearance must be viewed together with volume of distribution to provide a more complete understanding of systemic pharmacokinetics. The need to assess Cl and Vd stems from the realization that the concentration of a drug delivery system in the blood is reduced not only by mechanisms that

04:32 30 October 2016

change it into something else (such as enzymatic breakdown) or remove it from the body completely (such as excretion into urine via the kidney), but also by any process that leads to transfer (or distribution) of the delivery system out of the blood into the tissues. A detailed discussion of volume of distribution is beyond the scope of the current article (indeed there are a number of different volumes of distribution that can be defined). But in simple terms Vd provides a measure of the degree to which a drug (or a delivery system) distributes out of the blood. Thus, delivery systems that distribute more effectively (for example, those that are smaller and cross the endothelial cells that line the blood vessels more easily) will have higher volumes of distribution than larger macromolecules that diffuse across vascular endothelial cells less readily. Indeed, for many high molecular weight dendrimers the volume of distribution is close to the blood volume, suggesting that distribution out of the blood stream is limited. Collectively, Vd and Cl dictate the half life of a delivery system in the plasma where half life = 0.693 × Vd/Cl. Thus, where the volume into which a delivery system distributes is high it takes longer to clear at fixed clearance. Drugs with low Cl or high Vd therefore persist for long periods and have long half lives, whereas those with low Vd and high Cl have short half lives. It is important to realize that whilst Cl, Vd and half life are mathematically related, mechanistically, Cl and Vd together dictate half life (rather than, for example, half life and clearance dictating Vd). Cl can be further characterized to provide an indication of the proportion of total clearance made up by excretion into the urine by the kidney—or by other processes. These are the renal clearance and non-renal clearance respectively. Renal clearance is calculated by collecting the total quantity of a delivery system recovered (unchanged) in the urine after a single dose and then expressing this as a fraction of the dose. Where, for example, 50% of the dose is recovered in the urine, then renal clearance is 50% of total clearance.

In all the above scenarios, there is one major proviso and that is that what is measured in the blood is intact delivery system. For example, where a drug delivery system is quantified by using a radiolabel it is important to confirm that the label is still associated with the dendrimer. In our laboratories we confirm this routinely using size exclusion chromatography (SEC) to show

04:32 30 October 2016

that the label is still associated with a macromolecule with a molecular weight consistent with that of the original dendrimer. In contrast, where the label leaches from the dendrimer or is cleaved, this is apparent from the SEC trace and the kinetics of clearance and distribution of the label no longer reflect that of the delivery system.

Having defined the systemic pharmacokinetics, the pharmacokinetics after non-intravenous administration can then be assessed. Most commonly this is employed to quantify the efficiency of absorption after e.g., oral, subcutaneous or pulmonary administration. In reality, what is more commonly calculated is bioavailability after non-IV administration. Bioavailability defines the fraction of the dose that is absorbed from the administration site and transported intact through to the general circulation. So in addition to absorption it also takes into account any breakdown that might occur on transport from the absorption site to the general circulation. This is typically most prevalent after oral administration (although this would be an unusual situation for macromolecules such as a dendrimer, since oral absorption is commonly very low) since absorbed materials must pass through the liver before reaching the general or systemic circulation and the liver is highly metabolically active. However, the same principles apply after e.g., subcutaneous administration if the delivery system is broken down at the injection site or degraded on transport through the blood or the lymph to the systemic circulation.

Bioavailability (more accurately absolute bioavailability by this definition) is calculated by administering a fixed dose via a non-IV route (e.g., subcutaneously) and then measuring the AUC and comparing this to the AUC obtained after intravenous administration of the same dose. Thus, if the AUC obtained after subcutaneous administration is 50% of that obtained after IV injection of the same dose, the data suggest that only 50% of the dose is absorbed and transported through to the systemic circulation after SC administration, or the bioavailability is 50%.

Importantly, whilst simple comparison of the AUC obtained after pulmonary administration of one dendrimer with the AUC obtained after pulmonary administration of another does provide an indication of differences in relative exposure, it does not provide any understanding of absolute bioavailability. For example, pulmonary administration of 5 mg of dendrimer 1 might

04:32 30 October 2016

lead to an AUC of 500 units and administration of the same dose of dendrimer 2 might lead to an AUC of 1000. This suggests that the exposure obtained from dendrimer 2 is twice that of dendrimer 1. But without an understanding of systemic pharmacokinetic parameters we cannot say that the absolute bioavailability of dendrimer 2 is higher than that of dendrimer 1. It is possible, for example, that the high exposure of dendrimer 2 may reflect the fact that this dendrimer is cleared very slowly when it gets into the systemic circulation rather than the fact that a large proportion of the dose is absorbed. Similarly, dendrimer 1 might be cleared much faster and in fact is more bioavailable. Thus, if the AUC of dendrimer 1 after IV administration of the same dose is 750, and that of dendrimer 2 is 2000 (i.e., the clearance of dendrimer 2 is less than that of dendrimer 1), then the bioavailability of dendrimer 1 is 500/750 or 67%, and of dendrimer 2 is 1000/2000 or 50%. Thus dendrimer 2 has higher exposure (due to low clearance) but lower bioavailability. These concepts are important in separating overall exposure from absorption and bioavailability.

In summary, by calculating a few simple pharmacokinetic parameters a much better quantitative understanding of the rates of absorption, distribution, metabolism and excretion of a dendrimer-based delivery system can be gained. Far more information can be obtained by applying any one of a number of pharmacokinetic modeling techniques, notably compartmental pharmacokinetic models or physiologically based pharmacokinetic models; however, discussion of these approaches is beyond the brief description here. The interested reader is directed to the following general text for more details.[17,62,79]

## 9.3 Intravenous Pharmacokinetics

### 9.3.1 Introduction

As discussed in earlier sections, dendrimers are similar in size (both molecular weight and hydrodynamic diameter) to many globular plasma proteins. As a result, dendrimers have the capacity to evade rapid clearance from the body and passage through epithelial barriers, such as the vascular wall. This, however, also restricts how dendrimers can be administered (with the intent of administration as a drug or drug delivery system). For small

04:32 30 October 2016

molecule drugs, the "gold standard" of drug administration is via the oral route. For dendrimers and other macromolecular drugs and drug carriers, however, administration is usually limited to parenteral (e.g., intravenous, subcutaneous and intramuscular) injection. Once dendrimers reach the blood, they are subjected to in vivo clearance processes that define how rapidly the dendrimer escapes from the vasculature as described above, the patterns of distribution in the body, rates of catabolism (for biodegradable dendrimers) and excretion (via the urine and feces). These are classically defined by the size of the dendrimer and how it interacts with cells and tissues of the body (commonly dictated by surface charge, lipophilicity, structural flexibility, shape, etc.). This first section therefore describes how dendrimer size, surface charge and drug loading impacts on the intravenous pharmacokinetics of dendrimers.

### 9.3.2 Effect of Size

The size of dendrimers is commonly increased in two main ways: by increasing dendrimer generation and by increasing the degree of surface PEGylation. For instance, as dendrimer generation increases or the molecular weight of surface PEG increases, the effective molecular weight and hydrodynamic diameter also increase in turn. In terms of discussing the impact of dendrimer size on pharmacokinetics, in the most part, work in this area has focused mainly on PEGylated dendrimers. Hence, much of this section describes the impact of PEG size on intravenous pharmacokinetics rather the impact of dendrimer generation alone. It should be noted at this stage, however, that the relationship between molecular weight (commonly used to describe the "size" of polymers) and hydrodynamic diameter (more commonly used to describe the size of nanoparticles and colloids) is not necessarily linear. In general though, an increase in molecular weight or hydrodynamic diameter typically has the effect of limiting urinary excretion by restricting permeability through glomerular filtration slits in the kidney (that are approximately 25 nm in diameter)[18] that typically begin to restrict the passage of globular macromolecules larger than approximately 20 kDa (Fig. 9.1). This ultimately has the effect of prolonging blood circulation times.

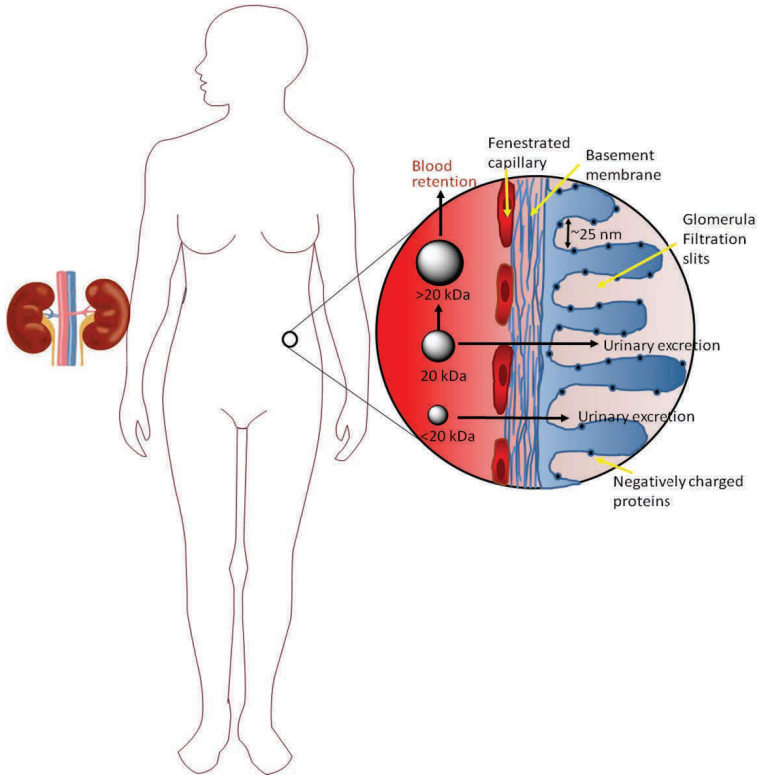



**Figure 9.1** Diagrammatic representation of the renal filtration of macromolecules in the kidneys.

As a general rule, therefore, dendrimers smaller than approximately 20 kDa are rapidly and almost exclusively eliminated from blood via the urine, and blood retention progressively increases above 20 kDa as urinary elimination slows.[19,25,27,29,35,49,53] For uncapped dendrimers (e.g., those terminating in a primary amine, hydroxyl or carboxy group) dendrimers of G5 or lower are generally cleared rapidly from blood via the urine.[43,44,46] A caveat to this, however, is that glomerular filtration slits are negatively charged and tend to more strongly restrict the passage of anionic proteins and dendrimers.[24,28] The exclusion limit of glomerular filtration is approximately 68 kDa and as a result, dendrimers larger than this display prolonged blood circulation times, commonly with terminal half lives of longer that 1 day, and rely on other processes for in vivo elimination.[19,25,51,54] This is best represented in Fig. 9.2 which shows a strong correlation between

04:32 30 October 2016

dendrimer molecular weight and the proportion of a dose excreted via urine. For dendrimers that have no appreciable affinity for cells and tissues of the body, urinary excretion is therefore commonly the primary process that drives blood exposure and circulation times.

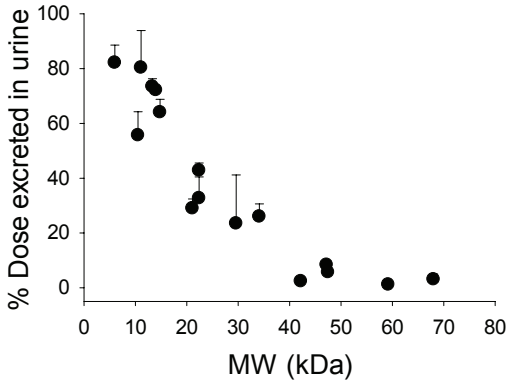



**Figure 9.2** Correlation between dendrimer molecular weight and urinary excretion of PEGylated polylysine dendrimers. Data represent mean ± s.d. Adapted from ref. 26.

For large dendrimers that are not eliminated via the urine and which cannot rely upon biodegradation to smaller fragments, the primary mechanism for blood clearance becomes the much slower process of uptake via organs of the reticuloendothelial system (RES; also referred to as the mononuclear phagocyte system). These organs include the liver, spleen, lungs, lymph nodes, bone marrow and thymus and are rich in macrophages that over time, recognize dendrimers as "foreign" and remove them from blood largely via phagocytosis. For very large dendrimers, however (e.g., G9 dendrimers or dendrimers with molecular weights of several hundred kDa), the rate of RES mediated clearance can increase as a result of the more rapid recognition of dendrimers via macrophages (particularly in the liver and spleen).[43,44,46] For instance, a study by Kobayashi demonstrated that an increase in generation for Gd-conjugated PAMAM dendrimers from 6 to 7, resulted in increased blood residence times. However, beyond G7 (hydrodynamic diameter >10 nm, >100 kDa), blood residence times decreased and uptake into the liver and spleen increased.[44] While PEGylation can reduce RES

04:32 30 October 2016

clearance, it is not known to this point how large a PEGylated dendrimer can be constructed before accelerated clearance via the RES becomes evident.

There is also some evidence to suggest that dendrimers can be excreted via the feces after intravenous administration, although this has not been extensively evaluated and to date, only the excretion of PEGylated dendrimers via feces has been examined. Elimination via the feces relies upon initial retention in the liver and subsequent deposition into the gallbladder and bile. In the most part, dendrimers are relatively stable in the gastrointestinal tract of rodent models used to evaluate pharmacokinetics, and resultantly, the proportion of the dose excreted via the feces is a good indicator of the exposure of dendrimers to bile fluid. Less than 2% of an intravenous dendrimer dose is generally recovered in feces excreted over 48 h after intravenous administration and there appears to be little correlation between molecular weight and the proportion of the dose excreted.[19,25,43,51] The largest proportion of an administered dendrimer dose ever quantified in feces after intravenous delivery was 37–47% after administration of PEGylated G1 polyester "bow-tie" dendrimers ranging in molecular weight from 22 to 44 kDa.[19] Interestingly, as dendrimer generation (and molecular weight) increased, the proportion of the dose excreted via the feces over 48 h decreased to approximately 25% for G2 dendrimers (23–87 kDa) and approximately 10% for G3 dendrimers (45–160 kDa). This simply serves to highlight the significant differences that can exist in the pharmacokinetics and elimination profile of dendrimers with different scaffolds and surface construction.

### 9.3.3 Effect of Surface Charge

For largely uncharged dendrimers or dendrimers bearing only a partial overall charge, clearance from blood after intravenous delivery is dictated mainly by the size of the construct as described above, as well as the construction of the scaffold and surface functionality. For dendrimers bearing highly charged surface functionality (such as amine- or carboxy-terminated dendrimers) surface charge together with dendrimer generation drive pharmacokinetic behavior. Dendrimer generation is also important

04:32 30 October 2016

04:32 30 October 2016

when discussing the impact of charge on pharmacokinetics, since increasing dendrimer generation effectively increases the number of charged groups on the dendrimer surface. The importance of surface charge is that it is a critical determinant of how the dendrimer surface interacts with membranes, cells and plasma proteins, which have a significant impact on the dendrimers in vivo behavior.

The most significant differences between uncharged and charged dendrimers are observed for dendrimers bearing a cationic charge, such as amine terminated systems. Cationic dendrimers have a strong affinity for anionic charges present on membrane and cell surfaces and it is this interaction that has driven much of the interest in cationic dendrimers as in vitro transfection reagents (e.g., Priofect™ and SuperFect®). The interaction, however, is driven by (1) the number of surface charges (where increasing the number of charges increases electrostatic interactions with membranes) and (2) the presence or absence of uncharged polymers such as PEG which can mask surface charge and block interactions with membranes.[8,29,35,53,57] The strong affinity of cationic dendrimers with membranes, though, has also been linked to increased cytotoxicity, which has limited in vivo application somewhat.[23] In vivo, however, cationic dendrimers (that do not bear surface PEG) adhere rapidly to vascular membranes after intravenous administration, leading to very rapid initial clearance from blood which restricts their use as drug delivery vehicles.[8] They do, however, have some potential as gene transfection reagents, although this utility is limited largely to local administration rather than systemic (intravenous) administration. Biodistribution patterns for cationic dendirmers also typically reflect how well perfused individual organs are, such that higher biodistribution is normally seen in the liver, which contains approximately 20–30% w/w of blood.[6,8,53] Cationic dendrimers also display reduced excretion into the urine and feces when compared to uncharged and anionic dendrimers due to this strong vascular interaction, since only free, unbound dendrimer in circulation is available for elimination via these pathways.[8,57] PEG groups, however, can block these electrostatic interactions without reducing surface charge and lead to pharmacokinetic

04:32 30 October 2016

profiles that more closely match that of fully PEGylated/uncharged systems, where pharmacokinetics are driven in large part by size.[29,35]

Interestingly, however, dendrimers with an overall anionic surface display longer circulation times than cationic dendrimers, since their interaction with cells and membranes is reduced.[24,53] This is strongly determined, though, by the nature of the anionic surface functionality. For instance, dendrimers bearing surface functionalities with relatively high pKa values (such as those that bear surface carboxyl functions) and which are therefore less highly charged at physiological pH are cleared via the urine and RES organs as a function of size.[24] Thus, their intravenous pharmacokinetic profiles (at least for non-biodegradable dendrimers) would be expected to reflect those of similar sized PEGylated systems. For anionic dendrimers bearing surface functionalities with much lower pKa value (such as arylsulphonate-conjugated systems), pharmacokinetic profiles change considerably as a result of increased binding to plasma proteins (termed opsonization). For these systems that are bear a significant number of surface anionic charges at physiological pH, the extent of plasma protein binding increases with increasing surface charge which has the ultimate effect of promoting clearance via the RES organs. Thus, a G4 polylysine dendrimer bearing 32 benzenedisulphonate groups was previously shown to display more avid opsonization in plasma and biodistribution towards the liver and spleen when compared to a G4 dendrimer bearing 32 benzenesulphonate groups[24] (Fig. 9.3). Interestingly, the plasma profiles also showed a unique convex shape, with slower initial plasma clearance resulting from the formation of high molecular weight protein conjugates, followed by increasing rates of plasma clearance as the protein-bound species were removed by the liver and spleen. Extensive plasma protein binding does not always lead to extensive liver targeting, however, since the propensity for opsonized dendrimers to be removed via the liver is dictated by not only how extensively the dendrimers are bound to plasma proteins but also which plasma proteins are involved.[24,28] This is since some plasma proteins promote liver targeting (opsonins), while others prevent liver targeting (dysopsonins).

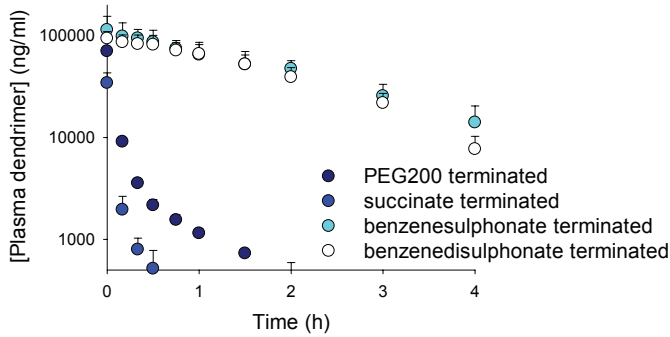



**Figure 9.3** Plasma concentration-time profile of $^{3}$H-labeled G4 polylysine dendrimers capped with PEG200 (uncharged) or anionic surface functions after intravenous administration of 5 mg/kg dendrimer to rats. The degree of plasma protein binding (opsonization) and liver biodistribution for the dendrimers is in the order PEG200 terminated < succinate terminated < benzenesulphonate terminated < benzenedisulphonate terminated. Data are represented as mean ± s.d. ($n$ = 3).

04:32 30 October 2016

### 9.3.4 Effect of Drug Loading

The earlier sections of this chapter highlight the importance of surface properties in dictating the pharmacokinetics of dendrimers. Not surprisingly, therefore, the covalent association of drugs onto the surface of a dendrimer-based drug carrier can also have an impact on pharmacokinetics. This is an important consideration since much of the initial development of dendrimer-based drug delivery systems is based on first understanding the in vitro and in vivo behavior of the non-drugylated species.

Since most drugs do not possess a significant charge, drug effects on pharmacokinetics are largely driven by changes to aqueous solubility and specific drug–receptor interactions. For instance, by replacing 50% PEG chains on the surface of a fully PEGylated dendrimer with the folic acid analogue methotrexate, plasma clearance increases by virtue of increased uptake by the liver and spleen, despite no significant change in molecular weight.[27] This has been attributed to a decrease in hydrophilicity and more avid binding to plasma proteins when compared to fully PEGylated counterparts. The extent of the increase in

04:32 30 October 2016

plasma clearance, however, is dependent upon the affinity of the methotrexate molecule with folate receptors. Specifically, the alpha carboxyl group of methotrexate has previously been shown to be an important mediator of the binding affinity between folic acid analogues and folate receptors. Thus, when the carboxyl group remains unprotected, methotrexate-conjugated dendrimers are cleared rapidly from plasma and display terminal half lives of only around half an hour, presumably as a result of rapid binding to folate receptors throughout the body.[28] In contrast, by protecting the alpha carboxyl with an –OtBu functionality, this interaction is reduced and the dendrimer displays more prolonged blood exposure. However, the same effect on plasma pharmacokinetics is not necessarily seen for other drugs with limited aqueous solubility. Doxorubicin conjugation, for instance, does not have a significant impact on the pharmacokinetics of PEGylated dendrimers,[29] which may be due in part to the fact that doxorubicin-conjugated dendrimers do not display significant binding to plasma proteins. Thus, the pharmacokinetic behavior of dendrimers can in part be predicted by first understanding their interaction with plasma proteins and, as described above, cells and membranes.

### 9.3.5 Effect of Structural Flexibility

In most cases, dendrimers are globular in construction with limited structural flexibility. A number of factors, however, can have a significant impact on how well these structures conform to fit through membrane pores, including the number and length of PEG chains, construction of the scaffold and scaffold components. For instance, it is already well established that linear polymers are cleared from blood more rapidly than more rigid, branched polymers (such as dendrimers) of similar size by virtue of the ability of linear polymers to better maneuver through glomerular filtration slits in the kidneys to be excreted via the urine.[67]

Even within a given class of dendrimer, significant differences in blood clearance can be evident by introducing small changes in the scaffold or surface structure that impact on flexibility. A good example of this was demonstrated by Gillies et al.[19] using polyester bow-tie dendrimers. They showed that smaller

04:32 30 October 2016

generation (G1, G2) dendrimers conjugated with several long PEG chains to give final molecular weights of between 45 and 85 kDa, displayed shorter plasma half lives and greater urinary excretion than similar MW G3 dendrimers with more, but shorter PEGs (Fig. 9.4). Differences in plasma pharmacokinetics and urinary excretion have also been observed following a more subtle modification of a 22 kDa PEGylated G4 polylysine dendrimers.[27] In this case, replacement of the G4 lysine layer on a polylysine dendrimer with the symmetrical lysine analogue succinimyldipropyldiamine resulted in a 10% reduction in hydrodynamic volume, but a decrease in plasma clearance and urinary excretion. This was explained by the succinimyldipropyldiamine layer introducing increased structural rigidity, which limited the capacity of the dendrimer to traverse vascular and renal membrane barriers.




| | G1 (2 X 20k PEG) | G2 (4 X 10k PEG) | G3 (8 X 5k PEG) |
|---|---|---|---|
| kDa | 44.2 | 43.0 | 44.7 |
| t½ (h) | 1.4 ± 0.4 | 26 ± 6 | 31 ± 2 |
| % in urine (24h) | 20 | 16 | 1 |

**Figure 9.4** Structure of PEGylated polyester bow-tie dendrimers and correlation between structural "flexibility" (where increasing the number of PEG chains is expected to increase structural rigidity) and plasma elimination half lives and urinary excretion. Data from Gillies et al.[19]

## 9.4 Tumor Biodistribution

### 9.4.1 Passive Tumor Targeting

The targeting and treatment of cancer is one of the primary intended clinical applications of dendrimer-based nanomedicines. Small molecule chemotherapeutics administered intravenously are potent anticancer agents that are inherently associated with significant systemic side effects as a result of the widespread distribution of cytotoxic anticancer agents throughout the body.

04:32 30 October 2016

Clearly, this can severely limit the utility of cancer therapies since the dose of the drug must be kept high enough to kill the cancer, but low enough to avoid severe and life threatening side effects, which can be difficult. The advent of nanomedicines, however, has facilitated a shift towards the sequestration of these chemotherapeutics within drug carriers, reducing free concentrations in the blood and in turn minimizing systemic toxicity associated with whole body exposure of the toxic drug.[58] The liberation of cytotoxic drugs from dendrimers may be via either the release of non-covalently entrapped dendrimer down a concentration gradient, or via the cleavage of covalent bonds by enzymes that are overexpressed specifically in the tumor environment or by acid-mediated hydrolysis (since the tumor interstitium and endosomal vesicles are slightly acidic). A discussion of chemotherapeutic drug association approaches and mechanisms of tumor-specific drug liberation is beyond the scope of this chapter, but the interested reader is directed towards the following reference for further information.[26]

In the most part, the improved biodistribution of dendrimer-associated drugs and other nanomedicines has been facilitated by significant differences in the architecture of solid tumors when compared to normal tissue. Notably, tumor-associated blood and lymph vessels have structural irregularities that alters their function in tumor tissue. Rapid angiogenesis and lymphangiogenisis, for instance, results in the formation of hyperpermeable blood and lymph capillaries within the tumoral stroma (Fig. 9.5). These leaky vessels facilitate the increased extravasation of macromolecular therapeutics from the blood and restricted lymphatic drainage which collectively leads to the passive accumulation of nanomaterials in tumors (but limited extravasation from normal tissues, coupled with efficient clearance of extravasated material via the lymphatic system).[32] This phenomenon was coined the enhanced permeation and retention (EPR) effect by Maeda and colleagues in 2001 and remains a cornerstone of long circulating nanoparticulate drug delivery.[52] It should be pointed out at this time though, that the EPR effect also takes place in other areas of inflammation, such as around sites of rheumatoid arthritis and infarction.

Blood circulation half-life is critical to the success of EPR targeting, where tumor accumulation has been correlated with

04:32 30 October 2016

the plasma elimination half life of dendrimers.[26] Specifically, dendrimers with longer circulation times tend to display higher accumulation in tumors than dendrimers with shorter circulation times. As discussed in earlier sections, this therefore dictates that passive tumor biodistribution will be, in large part, a function dendrimer size. However, while the EPR effect provides a facile means of directing dendrimers to solid tumors, this approach could also limit the tumor distribution or dendrimers in instances where other concurrent pathologies induce hypervascularization, and therefore increased intratumoral pressure.[2,69]

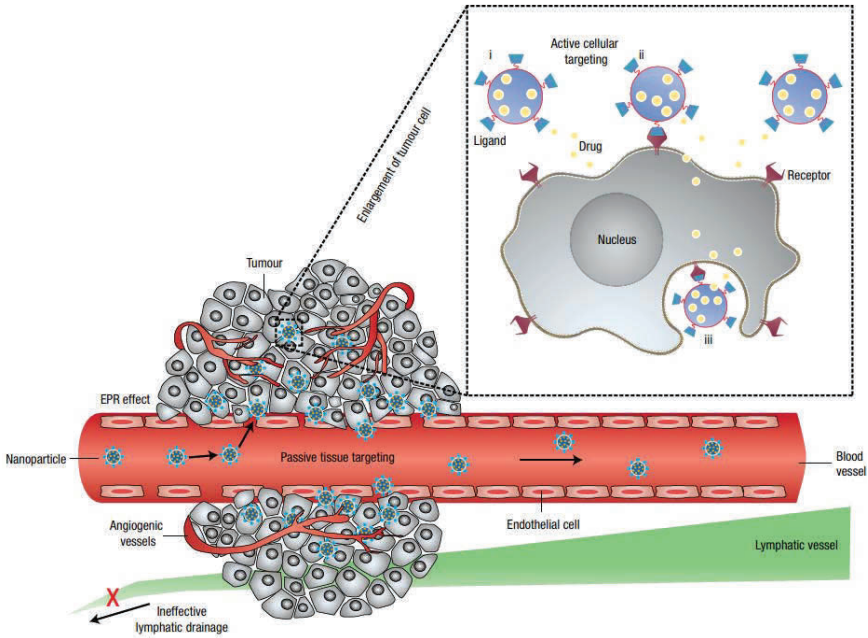



**Figure 9.5** Schematic representation of passive targeting to tumors by the EPR effect (main) and active targeting to sites on tumor cells (insert). Reproduced with permission from.[58]

## 9.4.2 Active Tumor Targeting

Conjugation of dendrimers to ligands or antibodies which bind receptors that are overexpressed on tumor cells provides a means of further increasing tumor targeting and cancer cell internalization specificity though the active uptake of the construct (Fig. 9.5 insert). In these instances targeting commonly

04:32 30 October 2016

overexpressed receptors (for instance to folate,[11,47,56,71,74,85] epidermal growth factor,[75,83,84] transferring,[20] integrin $\alpha 5\beta 3$[80] and luteinizing hormone releasing hormone[5,73]) can improve tumor uptake. Folic acid-conjugation has most commonly been utilized to improve the tumor disposition of dendrimers, this it is a small and readily available molecule that is relatively simple to handle and attach.[1,47,60] As an example, by decorating the surface of PAMAM dendrimers with folic acid, the dendrimers have exhibited threefold greater tumor uptake than similar constructs not conjugated with folic acid.[47] However, it must be noted that the receptor targets mentioned above are not exclusively overexpressed in cancerous tissue and in the case of folate, concurrent uptake into the lungs and kidneys occurs and can pose a significant problem for nanoparticles bearing these targeting moieties. Antibody targeting to HER-2 has also been employed to improve the tumor targeting of dendrimers.[61] However, the large size of antibodies (approx. 150 kDa) compared to much smaller peptide (up to several hundred Da)-based ligands may significantly alter the dynamics of intertumoral diffusion and pharmacokinetics are ultimately expected to reflect the antibody, rather than the dendrimer.

In summary, the active or passive accumulation of dendrimers in cancerous tissue to deliver conjugated chemotherapeutics provides a means of circumventing toxicity issues associated with small molecule cytotoxic drugs. However, the targeting strategies employed are dependent on the surface chemistry, size and presence of targeting ligands. Increased plasma circulation times induced by polymeric surface coatings can result in improved tumor colocalization but steric effects may preclude efficient internalization of the dendrimer. On the other hand, surface decoration with targeting ligands may slow dendrimer ingress into the tumor mass, reducing efficacy. These passive and active targeting strategies must be balanced in order to maximize the tumoral uptake of dendrimers.

## 9.5 Subcutaneous Pharmacokinetics

### 9.5.1 Introduction

Nanoparticulate drug carriers such as dendrimers are becoming increasingly common as pharmaceutical therapeutic candidates.

04:32 30 October 2016

However, their high molecular weights and resultant low diffusion rates across epithelial barriers can pose a significant challenge to uptake when compared to small molecule drugs. As a result, these formulations are typically dosed parenterally (i.e., via intravenous, subcutaneous or intraperitoneal injection) as described earlier in this chapter. However, while avoiding epithelial barriers can improve the likelihood of dendrimer uptake, the extent of absorption of macromolecular or nanoparticulate constructs from the interstitium is also influenced by the physicochemical properties of the dendrimer administered, as well as the volume and site of administration. This section will therefore discuss the barriers to the interstitial (e.g., subcutaneous, intramuscular) absorption of dendrimers and the kinetics of dendrimer absorption from these sites. Specifically, we will discuss the absorption of dendrimers from subcutaneous injection sites, since much of the literature surrounding the interstitial administration of dendrimers has centered around subcutaneous injection and because subcutaneous administration can be performed at home without medical supervision or significant training, unlike intramuscular or intravenous administration.

### 9.5.2 Structure of the Interstitial Space

The extracellular matrix (ECM) in healthy interstitium served as a structural scaffold, water reservoir and regulator of osmotic pressure. The balance between interstitial fluid pressure (IFP) and intravascular pressure (IVP) in healthy tissue is slightly negative and favors convection from higher pressure blood capillaries (28 mm Hg) towards the lower pressure interstitium (1–3 mm Hg).[21] Blood capillaries in the interstitium possess a continuous basement membrane (Fig. 9.6) and absorption is mediated via tight junctions between adjacent endothelial cells. As a result, the interstitial space serves as a sink for extravasated fluids with the potential for vascular reuptake limited to small molecules and nanoparticles smaller than 10 nm.

By contrast, macromolecules in the interstitium are able to be taken up by blind-ended initial lymphatic capillaries comprising an intermittent basement membrane and large interendotheial junctions (Fig. 9.1). This relatively porous, tethered capillary system can also be manipulated with movement or increases in IFP to further promote uptake of material from the interstitium.

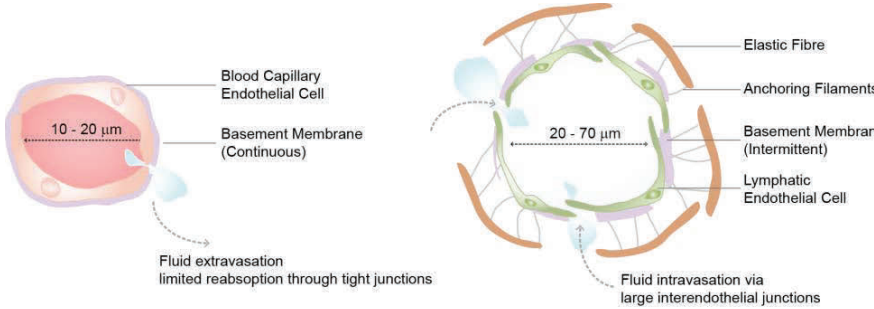



**Figure 9.6** Cross-sectional view of the interstitial microvasculature. (a) blood vessel capillary with complete basement membrane. Adapted from ref. 72. (b) Initial lymphatic capillary with intermittent basement membrane and endothelial cells anchored to surrounding elastic tissue via microfilaments. Adapted from ref. 86.

04:32 30 October 2016

The lymphatic system differs from the circulatory system in that it is a conduit of unidirectional flow which redistributes and filters extravasated fluid and material away from tissues to the systemic circulation via a series of capillaries, valved lymphatic vessels, lymph nodes and large lymph ducts which anastomose to the systemic circulation at the subclavian and internal jugular veins.[65] Given the role of the lymphatics in tissue homeostasis, administration of dendrimers at sites that are drained by initial lymphatic vessels provides a second and oftentimes competing route to dendrimer absorption.

### 9.5.3 Impact of Dendrimer Size on Absorption from Subcutaneous Injection Sites

Absorption of nanomedicines from the interstitium can occur via the circulatory system or the lymphatic system. In the simplest terms, these two absorptive processes can be assumed to preferentially discriminate based on size, with larger dendrimers (greater than approximately 8 nm) taken up by the lymphatics,[40] while smaller dendrimers with hydrodynamic radii of less than approximately 8 nm can be taken up by the circulatory system[34] (Fig. 9.7).

This size relationship has been exemplified in a series of experiments conducted on gadolinium-labeled PAMAM dendrimers

04:32 30 October 2016

as magnetic resonance lymphaniography (MRI) agents. Kobayashi and coworkers demonstrated that dendrimer generation influences both subcutaneous diffusion rates and lymphatic uptake.[40–42,45] Smaller dendrimers (G2 and G4) showed significant nonspecific diffusion at the injection site, presumably due to poor retention within the highly permeable lymphatic capillaries, whereas larger scaffold G6 dendrimers (hydrodynamic radii greater than 10 nm) were largely retained in the early lymphatics resulting in improved resolution of the draining lymph vessels and downstream lymph nodes. Interestingly, as the size (and generation) of the dendrimers further increased to G8, the benefit of retention in the early lymphatics was offset by slower diffusion through the interstitial space. Increased hydrophobicity of similarly sized dendrimers has also been shown to increase lymphatic drainage and imaging resolution for a G5 polypropyleneimine (PPI) dendrimer with a diaminobutane (DAB) core when compared to a G4 dendrimer of comparable molecular weight.[40]

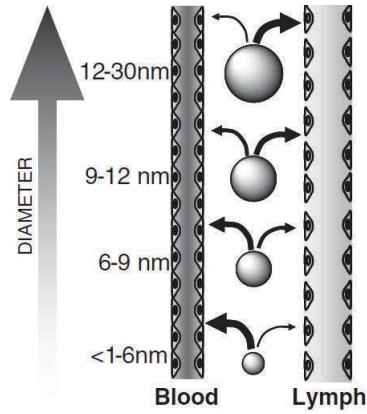



**Figure 9.7** Diagrammatic visualization showing the contribution of dendrimer size to the relative uptake of dendrimer via the lymph and blood from the interstitium. Reproduced with permission from Kaminskas and Porter.[34]

Other studies have utilized surface modification to increase the size of administered dendrimers, thereby shifting the dominating absorption pathway towards lymphatic uptake. In studies conducted with PEGylated G4 polylysine dendrimers,

Kaminskas and colleagues showed that by increasing PEG molecular weight and consequently, increasing hydrodynamic radius, the route of dendrimer absorption shifted from primarily vascular uptake for small (11 kDa) dendrimers, to primarily lymphatic uptake (for larger 68 kDa dendrimers).[30] The bioavailability of these PEGylated dendrimers was also reported to be close to 100%. Crucially these studies also highlighted the importance of redistribution of dendrimers from the systemic circulation back to the interstitium and again to the lymphatics. This multimodal recirculation of dendrimers appears to provide a means to prolonging their systemic exposure and also suggests that there is the potential for altered dendrimer pharmacokinetics in subjects with altered lymphatic function.

04:32 30 October 2016

### 9.5.4 Impact of Surface Charge on Subcutaneous Absorption

The subcutaneous space is made up of a structural scaffold of collagens, elastins, fibrins and polyanionic glycosaminoglycans (GAGs).[81] The net negative charge conferred by GAGs renders charged drug delivery systems vulnerable to unwanted electrostatic interactions. Cationic species may interact directly with the GAGs preventing diffusion to the vasculature, while anionic species are repelled from the GAG-rich matrix.

There are only a few examples of subcutaneously administered cationic dendrimers, primarily due to the inherent cytotoxicity associated with cationic species.[50] However, a cationic L-arginine-grafted polyamidoamine (PAM-RG4) dendrimer has recently been successfully used as a ~100 nm polyplex to deliver nonviral gene therapy for the treatment of diabetic skin wounds in mice.[48] While these studies did not investigate the systemic exposure of the PAM-RG4 dendrimers, they were reliant on local retention of dendrimer associated plasmid DNA for upregulation of VEGF expression. Thus it can be postulated that increased skin wound healing was attributable in part to colocalization of the cationic dendrimer DNA polyplex with proliferating cells at the injection site, i.e., the cationic dendrimer did not diffuse into the systemic or lymphatic circulation. However, it must also be noted that the

04:32 30 October 2016

100 nm polyplexes described in these studies would have inherently slow diffusion from the injection site and deconvolution of size and charge effects in this study is difficult.

More recently, a partly PEGylated G5 polylysine dendrimer was administered subcutaneously to rats.[31] The dendrimer, with 50% PEG surface coverage and 50% uncapped primary amines had a bioavailability of 76% which was lower than that of a similar fully PEGylated dendrimer.[30] The interaction of the cationic surface functional groups with anionic GAGs may have impeded efficient transport through the interstitium. Counterintuitively, when the amine groups of this dendrimer were conjugated with the peptide GILGVP-glutamic acid (to give a partially anionic dendrimer that terminated in carboxyl groups) the absorbed dose was further reduced to 50%, indicating that charge repulsion was not sufficient to improve dendrimer uptake from SC absorption sites.

Dendrimers with 100% anionic surface coverage also have poor absorption from SC injection sites when compared to neutral or partly PEGylated counterparts. Benzenesulphonate decorated polylysine dendrimers were administered subcutaneously to male rats and compared to a similarly sized PEGylated polylysine dendrimer.[30] The data showed that in the absence of significant size differences, the negative surface charge of the sulphonated dendrimer had a detrimental impact on dendrimer absorption (~25% bioavailability) from the interstitium when compared to the uncharged PEGylated dendrimer (~100% bioavailability). This poor diffusivity from the SC site could in part be attributable to interaction with plasma proteins in the interstitium resulting in the formation of high molecular weight, slow diffusing aggregates.

Generally, it can be conceded that neutral surface coatings provide improved dendrimer diffusion from subcutaneous injection sites. However, the studies described above have also investigated downstream lymph node disposition of dendrimers and while uncharged species are typified by long circulation and recirculation behavior, their PEG coatings can also preclude efficient targeting to the site of action due to steric shielding. As a result, dendrimer surface chemistry requires a balance between sufficient surface coating to facilitate diffusion through the interstitium, longevity in the systemic circulation and adequate targeting to ensure the carrier is effective at the site of action.

Dendrimers therefore have significant potential for systemic administration via subcutaneous injection, which avoids the need for clinical visits that are required for intravenous administration. In general, uncharged dendrimers display good bioavailability from subcutaneous injection sites, and the route of absorption shifts from the vascular to lymphatic routes upon increasing site. This highlights the further potential to utilize dendrimers as lymphatic contrast agents for cancer staging and for the localized treatment of lymph-resident diseases, such as lymph node metastases. Bioavailability, however, tends to decrease with increasing charge, although PEGylation provides a means to limit interstitial interactions and maximize absorption from an injection site.

04:32 30 October 2016

## 9.6 Oral Pharmacokinetics

Oral drug administration is simple, convenient and in general, offers better compliance and outcomes, at least for small molecule drugs. In recent times, however, oral drug delivery has become increasingly challenging with the emergence of new generations of highly potent, but poorly water soluble and poorly bioavailable compounds. Thus, appropriate formulation of these compounds with drug carriers may enhance oral bioavailability. Dendrimers have been suggested to enhance oral bioavailability by promoting drug solublization in the intestinal lumen, inhibit drug-efflux transporter interactions, prevent intestinal elimination of drugs and enhance drug permeability by disrupting epithelial tight junctions in the intestines. The use of dendrimers for oral drug delivery, however, is challenging as a result of their macromolecular size and hydrophilicity that ultimately limits intestinal permeability, together with poorly controllable drug release profiles in the gastrointestinal tract. Nevertheless, there have been some, despite few, important examples of enhanced in vivo bioavailability of drugs when associated with dendrimers. As an example, the bioavailability of doxorubicin has been shown to be enhanced 300-fold when delivered as a complex with an amine-terminated G3 PAMAM dendrimer, compared to delivery of the free drug.[36] The mechanism by which this increase in bioavailability occurred was not clear but may have been due to reduced interaction of

04:32 30 October 2016

doxorubicin with intestinal efflux transporters, increased drug solubility or altered mechanisms of drug transport across the intestine. More recently, both cationic and anionic G4 PAMAM dendrimers were shown to improve the oral bioavailability of camptothecin in mice by 2- to 3-fold.[68]

Much of the literature surrounding the intestinal transport of dendrimers, however, has been based on in vitro studies which provide mechanistic insights into dendrimer trafficking through intestinal membranes and physicochemical properties that are likely to promote gastrointestinal absorption. Specifically, these studies largely involve the use of Caco-2 cell monolayers. The Caco-2 model is based on a colon cell line that differentiates to form polarized cell layers and a brush border, similar to the intestinal lumen. Whilst this model is generally considered to be useful for examining the mechanisms of drug permeability across the intestinal epithelium, it does not accurately reflect the more complex in vivo conditions. For instance, it lacks a defined mucous membrane and unstirred water layer, which have been suggested to have a significant influence on intestinal drug absorption. Never the less, charged dendrimers have in general been shown to display more efficient transcellular and paracellular transport than uncharged dendrimers in the order cationic > anionic > uncharged.[66] The mechanisms proposed to explain this observation include enhanced electrostatic binding of charged dendrimers to cell membranes, which promotes cellular endocytosis and disruption of interendothelial tight junctional proteins. The impact of dendrimer size, however, is more complex. For instance, increases in the size of anionic dendrimers (up to G4) was shown to correlate with increased Caco-2 permeability, whereas increasing the size of cationic dendrimers tends more to cause cytotoxicity and a loss of membrane integrity.[37–39,82] Intestinal membrane permeability can also be enhanced by increasing dendrimer lipophilicity.[13,16,59]

In general, dendrimers may have some potential to improve the oral bioavailability of poorly soluble and poorly permeable drugs, but at present, in vivo evidence of significant benefit is lacking. Since most of the evidence for the improved gastrointestinal permeability of dendrimers is based on charged (largely cationic) systems, utility may be limited by the inherent toxicity of the dendrimers, particularly over prolonged use.

## 9.7 Transdermal Pharmacokinetics

Although not considered a mainstream route of systemic drug administration, dendrimers have been explored for their potential to enhance the transdermal absorption of a number of drugs including cancer chemotherapeutics and analgesics (specifically non-steroidal anti-inflammatory drugs; NSAIDs). One advantage of drug delivery via this route is that it avoids first pass metabolism after gastric absorption that limits the utility of oral delivery for some drugs and can also limit gastrointestinal irritation caused by most NSAIDs.

The major barrier to transdermal drug delivery is penetration through the outer barrier of the skin (the stratum corneum). Once drugs reach the underlying epidermis, however, access to blood capillaries to facilitate systemic absorption is more readily facilitated. In general, therefore, the penetration of small molecule drugs through the skin and towards blood capillaries is limited to slightly lipophilic molecules with low melting points that have sufficient chemical stability to withstand degradation on the surface of the skin and within the epidermis.[9] While in many cases the chemical properties of drugs cannot be optimized for transdermal delivery whilst also retaining biological activity, association with dendrimers (which can be tailored to display defined chemical properties) can potentially facilitate better membrane permeation. In the most part, the transdermal penetration of dendrimers has not been examined in a whole animal setting, but rather in vitro using excised portions of pig or rat skin. There are, however, a few exemplary in vivo studies that demonstrate improved percutaneous absorption of drug when associated with a dendrimer carrier and improved in vivo activity.[7,12]

In most cases, the transport of the dendrimer itself has not been measured, only non-covalently associated drugs and so solid conclusions cannot be made in regards to “dendrimer” penetration through the skin. Never the less, as a general rule, smaller dendrimers appear to promote the more effective penetration of loaded drugs through the skin when compared to larger dendrimers, presumably due to their ability to more effectively pass between cells.[76] There is, however, some discrepancy with regards to what dendrimer charges promote the best transdermal

04:32 30 October 2016

04:32 30 October 2016

penetration. In the most part, cationic dendrimers generally promote better transdermal absorption of loaded drugs than uncharged dendrimers, which promote better penetration than anionic dendrimers.[10,77] This has been suggested to be a result of the ability of cationic dendrimers to adhere more effectively to lipid bilayers of the skin. In contrast, another study traced the penetration of FITC-labeled dendrimers through the skin and reported that cationic change in fact reduces the penetration of dendrimers through the skin when compared to anionic and uncharged dendrimers.[78] This was proposed to be a result of the strong binding of cationic dendrimers with cells, which promoted enhanced retention in cells, but limited permeation through the skin. Additionally, a more recent study has shown that increasing the number of cationic charged beyond 8 may reduce drug penetration through the skin (using 5-fluorouracil as a model, Fig. 9.8).[55] This suggests that partial cationic charge may promote

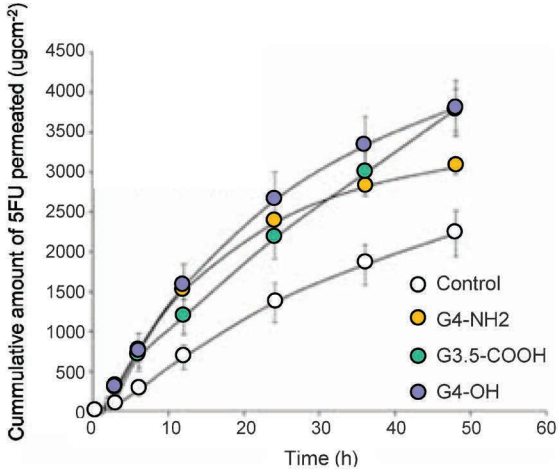



**Figure 9.8** Permeability of 5-fluorouracil (5FU) through pig skin after pretreatment with phosphate buffered saline (control) or PAMAM dendrimers bearing different surface functionalities for 24 h. Modified from Venuganti et al.[77]

good adherence of dendrimers to, and penetration through the skin, but increasing cationic charge beyond a certain point is likely to hinder dendrimer and drug penetration and access to underlying vascular capillaries.

## 9.8 Pulmonary Pharmacokinetics

In recent years, there has been accelerating increase in the development of dendrimers for the inhaled delivery of drugs and genetic material. Inhaled delivery has a number of advantages over other means of administration, including (1) the ability to improve drug or siRNA exposure specifically to the lungs while avoiding systemic exposure, (2) the avoidance of first pass metabolism that can limit the utility of oral delivery for some drugs, and (3) provides a needle-free means to deliver drugs and macromolecules to the systemic circulation. In contrast to other means of drug administration, inhaled delivery is more complex since the site of drug or macromolecule deposition in the deep lungs (alveolar region), airways (trachea, bronchi, bronchioles) or the back of the mouth and throat is dictated by the size and aerodynamic properties of the inhaled aerosol or dry powder. The importance of site of deposition is that the site of a lung disease to be targeted may reside either in the deep lung (e.g., cancer or pneumonia) or in the airways (e.g., asthma or chronic obstructive pulmonary disease). Also, absorption from the lung is thought to be most efficient from the deep lung which has a rich vascular supply and thin epithelial barrier. As a general rule, droplets or particles of less than 0.5 μm in size are generally exhaled and are not retained in the lungs, while 1–5 μm particles are deposited primarily in the alveolar region. As particle size increases beyond this, particles are increasingly deposited in the upper airways and the back of the mouth and throat for very large (>5 μm) particles.[63]

For small molecule drugs, absorption across the alveolar epithelium is generally very rapid as a result of the thin epithelium and extensive vascular supply of the lungs, to the point where in some cases, plasma concentration-time profiles almost reflect the profiles obtained after intravenous administration. By associating small molecule drugs with macromolecular drug carriers, however, drug retention in the lungs can be prolonged and drug liberation can be tuned to provide sustained lung exposure. It is worth noting at this stage, though, that macromolecules need to overcome 3 distinct barriers in the lungs before gaining access to the systemic circulation, including (1) passage through the fluid/mucus lining of the lungs, (2) passage through the alveolar epithelium and (3)

04:32 30 October 2016

04:32 30 October 2016

passage through the underlying pulmonary vascular or lymphatic epithelia. The alveolar epithelium, however, is approximately 10-fold less permeable to macromolecules than pulmonary vascular capillaries as a result of the larger number of tight junctions. Macromolecule absorption from the lungs is therefore much less efficient when compared to interstitial administration. Despite this, several studies have demonstrated that dendrimers can be absorbed from the lungs in a size-dependent manner and improve the absorption of co-formulated drugs and proteins.[3,4,15,33,64] For instance, a recent study has shown that small approximately 11 kDa PEGylated polylysine dendrimers are efficiently absorbed (approximately 30%) from the lungs of rats via both direct absorption of the intact dendrimer as well as absorption of products of dendrimer catabolism.[64] A slightly larger 22 kDa dendrimer also displayed similar absorption from the lung, but absorption was slower and a larger proportion of intact dendrimer was absorbed as a result of greater steric shielding of the polyamino acid core by the larger PEG. A much larger 77 kDa dendrimer, however, was retained in the lung for a prolonged period of time and was cleared from the lungs mainly via cilia in the airways that promotes the expulsion of mucus and trapped particles from the lungs into the throat, where they are swallowed and eventually excreted via the feces. This suggests the potential to tailor dendrimers to act as systemic drug delivery vectors or drug depots to promote prolonged drug retention in the lungs. More recently, the transport of G3 amine-terminated dendrimers across a Calu-3 monolayer model of the pulmonary epithelium was shown to be improved by increasing the degree of PEGylation as a result of masking the cationic charge on the dendrimer.[4] In a related study, the coadministration of G0-G3 PAMAM dendrimers to the lungs improved the absorption insulin and calcitonin in rats by disrupting gap junctions and increasing the permeability of the pulmonary epithelium.[15]

Pharmacodynamic data have also been generated which support the use of dendrimers as inhalable drug delivery systems. For instance, an early study showed that G3 PAMAM-PEG micelles enhanced the bioavailability of entrapped low molecular weight heparin from the lungs (60%) and the pulmonary delivery of the dendrimer formulation resulted in similar or better anticoagulant activity in a rat model of thrombosis when compared to the

04:32 30 October 2016

subcutaneous delivery of heparin alone.[3] Conversely, a hydroxyl-terminated G4 PAMAM dendrimer containing methylprednisolone prolonged the retention of the drug in the lungs after pulmonary administration when compared to administration of the drug alone and improved the reduction in experimental airway inflammation when compared to the drug in a rat model of lung inflammation.[22] More recently, the pulmonary administration of a 56 kDa PEGylated G5 polylysine dendrimer conjugated with the chemotherapeutic drug doxorubicin displayed 13% absorption from the lungs of rats and prolonged retention of drug in the lungs.[33] When administered to the lungs of rats with experimentally induced lung metastases of breast cancer, anticancer activity was significantly improved when compared to the intravenous administration of the dendrimer or doxorubicin alone (Fig. 9.9). Lung related toxicity was also reduced when compared to the pulmonary administration of the drug. The mechanism of action was proposed to be due to enhanced permeation and retention of the dendrimer from the blood into the tumors, as well as convection of the dendrimer from the airways into the tumor, where drug was liberated.

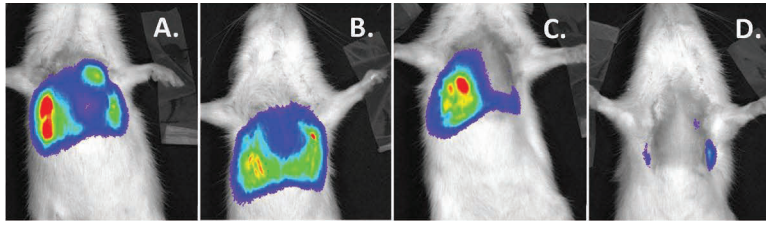



**Figure 9.9** In vivo bioluminescence images of lung tumor burden in rats treated for 2 weeks with intratracheal saline vehicle (a), intravenous doxorubicin (b), intravenous doxorubicin-dendrimer (c) and intratracheal doxorubicin-dendrimer (d). Lung tumors were induced via the intravenous injection of firefly-luciferase expressing rat breast MAT13762 IIIB cells. Adapted and modified from Kaminskas et al.[33]

Dendrimers therefore have considerable utility as inhalable drug delivery vectors, although more work will be needed to thoroughly evaluate the long-term safety of dendrimers in the lungs, particularly given current concerns over the potential toxic effects of airborne nanoparticles on the lungs.

## 9.9 Conclusion

Dendrimers have clear potential for a range of biomedical applications, most notably as drugs, drug delivery systems and imaging agents. In order for dendrimers to be translated successfully into the clinic as systemically administered entities, their in vivo and pharmacokinetic behavior must first be understood. This chapter provided a brief overview of the pharmacokinetic behavior of dendrimers after administration via a range of injectable and non-invasive routes, and discussed how the physicochemical properties of dendrimers drive this behavior. Information gained thus far, however, has largely been obtained from rodent models which enable high throughput screening of expected in vivo dispositional behavior, but examination in larger animal models and humans is still lacking. Human data is expected to emerge, however, as dendrimers begin to make significant headway in clinical trials.

04:32 30 October 2016

## References

1. Abolmaali, S. S., Tamaddon, A. M., and Dinarvand, R. (2013) A review of therapeutic challenges and achievements of methotrexate delivery systems for treatment of cancer and rheumatoid arthritis, *Cancer Chemother. Pharmacol.*, **71**, pp. 1115–1130.
2. Azzopardi, E. A., Ferguson, E. L., and Thomas, D. W. (2013) The enhanced permeability retention effect: A new paradigm for drug targeting in infection, *J. Antimicrob. Chemother.*, **68**, pp. 257–274.
3. Bai, S., Thomas, C., and Ahsan, F. (2007) Dendrimers as a carrier for pulmonary delivery of enoxaparin, a low-molecular weight heparin, *J. Pharm. Sci.*, **96**, pp. 2090–2106.
4. Bharatwaj, B., Mohammad, A. K., Dimovski, R., Cassio, F. L., Bazito, R. C., Conti, D., Fu, Q., Reineke, J., and da Rocha, S. R. (2015) Dendrimer nanocarriers for transport modulation across models of the pulmonary epithelium, *Mol. Pharm.*, **12**, pp. 826–838.
5. Bi, X., Shi, X., and Baker, J. R., Jr. (2008) Synthesis, characterization and stability of a luteinizing hormone-releasing hormone (LHRH)-functionalized poly(amidoamine) dendrimer conjugate, *J. Biomater. Sci.*, **19**, pp. 131–142.

04:32 30 October 2016

6. Blustajn, J., Cuenod, C. A., Clement, O., Siauve, N., Vuillemin-Bodaghi, V., and Frija, G. (1997) Measurement of liver blood volume using a macromolecular MRI contrast agent at equilibrium, *Magn. Res. Imaging*, **15**, pp. 415–421.
7. Borowska, K., Wolowiec, S., Glowniak, K., Sieniawska, E., and Radej, S. (2012) Transdermal delivery of 8-methoxypsoralene mediated by polyamidoamine dendrimer G2.5 and G3.5--in vitro and in vivo study, *Int. J. Pharm.*, **436**, pp. 764–770.
8. Boyd, B. J., Kaminskas, L. M., Karellas, P., Krippner, G., Lessene, R., and Porter, C. J. (2006) Cationic poly-L-lysine dendrimers: Pharmacokinetics, biodistribution, and evidence for metabolism and bioresorption after intravenous administration to rats, *Mol. Pharm.*, **3**, pp. 614–627.
9. Calpena, A. C., Blanes, C., Moreno, J., Obach, R., and Domenech, J. (1994) A comparative in vitro study of transdermal absorption of antiemetics, *J. Pharm. Sci.*, **83**, pp. 29–33.
10. Chauhan, A. S., Sridevi, S., Chalasani, K. B., Jain, A. K., Jain, S. K., Jain, N. K., and Diwan, P. V. (2003) Dendrimer-mediated transdermal delivery: Enhanced bioavailability of indomethacin, *J. Control. Release*, **90**, pp. 335–343.
11. Chen, W. T., Thirumalai, D., Shih, T. T., Chen, R. C., Tu, S. Y., Lin, C. I., and Yang, P. C. (2010) Dynamic contrast-enhanced folate-receptor-targeted MR imaging using a Gd-loaded PEG-dendrimer-folate conjugate in a mouse xenograft tumor model, *Mol. Imaging Biol.*, **12**, pp. 145–154.
12. Cheng, Y., Man, N., Xu, T., Fu, R., Wang, X., Wang, X., and Wen, L. (2007) Transdermal delivery of nonsteroidal anti-inflammatory drugs mediated by polyamidoamine (PAMAM) dendrimers, *J. Pharm. Sci.*, **96**, pp. 595–602.
13. D'Emanuele, A., Jevprasesphant, R., Penny, J., and Attwood, D. (2004) The use of a dendrimer-propranolol prodrug to bypass efflux transporters and enhance oral bioavailability, *J. Control. Release*, **95**, pp. 447–453.
14. Dickson, M., and Gagnon, J. P. (2004) The cost of new drug discovery and development, *Disc. Med.*, **4**, pp. 172–179.
15. Dong, Z., Hamid, K. A., Gao, Y., Lin, Y., Katsumi, H., Sakane, T., and Yamamoto, A. (2011) Polyamidoamine dendrimers can improve the pulmonary absorption of insulin and calcitonin in rats, *J. Pharm. Sci.*, **100**, pp. 1866–1878.

04:32 30 October 2016

16. Florence, A. T., Sakthivel, T., and Toth, I. (2000) Oral uptake and translocation of a polylysine dendrimer with a lipid surface, *J. Control. Release*, **65**, pp. 253–259.
17. Gabrielsson, J., and Weiner, D. (2000) *Pharmacokinetic and Pharmacodynamic Data Analysis. Concepts and Applications* (Swedish Pharmaceutical Press, Stockholm).
18. Gagliardini, E., Conti, S., Benigni, A., Remuzzi, G., and Remuzzi, A. (2010) Imaging of the porous ultrastructure of the glomerular epithelial filtration slit, *J. Am. Soc. Nephrol.*, **21**, pp. 2081–2089.
19. Gillies, E. R., Dy, E., Frechet, J. M., and Szoka, F. C. (2005) Biological evaluation of polyester dendrimer: Poly(ethylene oxide) "bow-tie" hybrids with tunable molecular weight and architecture, *Mol. Pharm.*, **2**, pp. 129–138.
20. Han, L., Huang, R., Liu, S., Huang, S., and Jiang, C. (2010) Peptide-conjugated PAMAM for targeted doxorubicin delivery to transferrin receptor overexpressed tumors, *Mol. Pharm.*, **7**, pp. 2156–2165.
21. Heldin, C. H., Rubin, K., Pietras, K., and Ostman, A. (2004) High interstitial fluid pressure-an obstacle in cancer therapy, *Nat. Rev. Cancer*, **4**, pp. 806–813.
22. Inapagolla, R., Guru, B. R., Kurtoglu, Y. E., Gao, X., Lieh-Lai, M., Bassett, D. J., and Kannan, R. M. (2010) In vivo efficacy of dendrimer-methylprednisolone conjugate formulation for the treatment of lung inflammation, *Int. J. Pharm.*, **399**, pp. 140–147.
23. Jevprasesphant, R., Penny, J., Jalal, R., Attwood, D., McKeown, N. B., and D'Emanuele, A. (2003) The influence of surface modification on the cytotoxicity of PAMAM dendrimers, *Int. J. Pharm.*, **252**, pp. 263–226.
24. Kaminskas, L. M., Boyd, B. J., Karellas, P., Henderson, S. A., Giannis, M. P., Krippner, G. Y., and Porter, C. J. (2007) Impact of surface derivatization of poly-L-lysine dendrimers with anionic arylsulfonate or succinate groups on intravenous pharmacokinetics and disposition, *Mol. Pharm.*, **4**, pp. 949–961.
25. Kaminskas, L. M., Boyd, B. J., Karellas, P., Krippner, G. Y., Lessene, R., Kelly, B., and Porter, C. J. (2008) The impact of molecular weight and PEG chain length on the systemic pharmacokinetics of PEGylated poly l-lysine dendrimers, *Mol. Pharm.*, **5**, pp. 449–463.
26. Kaminskas, L. M., Boyd, B. J., and Porter, C. J. (2011) Dendrimer pharmacokinetics: The effect of size, structure and surface characteristics on ADME properties, *Nanomedicine (Lond)*, **6**, pp. 1063–1084.

04:32 30 October 2016

27. Kaminskas, L. M., Kelly, B. D., McLeod, V. M., Boyd, B. J., Krippner, G. Y., Williams, E. D., and Porter, C. J. (2009) Pharmacokinetics and tumor disposition of PEGylated, methotrexate conjugated poly-l-lysine dendrimers, *Mol. Pharm.*, **6**, pp. 1190–1204.

28. Kaminskas, L. M., Kelly, B. D., McLeod, V. M., Sberna, G., Boyd, B. J., Owen, D. J., and Porter, C. J. (2011) Capping methotrexate alpha-carboxyl groups enhances systemic exposure and retains the cytotoxicity of drug conjugated PEGylated polylysine dendrimers, *Mol. Pharm.*, **8**, pp. 338–349.

29. Kaminskas, L. M., Kelly, B. D., McLeod, V. M., Sberna, G., Owen, D. J., Boyd, B. J., and Porter, C. J. (2011) Characterisation and tumour targeting of PEGylated polylysine dendrimers bearing doxorubicin via a pH labile linker, *J. Control. Release*, **152**, pp. 241–248.

30. Kaminskas, L. M., Kota, J., McLeod, V. M., Kelly, B. D., Karellas, P., and Porter, C. J. H. (2009) PEGylation of polylysine dendrimers improves absorption and lymphatic targeting following SC administration in rats, *J. Control. Release*, **140**, pp. 108–116.

31. Kaminskas, L. M., McLeod, V. M., Ascher, D. B., Ryan, G. M., Jones, S., Haynes, J. M., Trevaskis, N. L., Chan, L. J., Sloan, E. K., Finnin, B. A., Williamson, M., Velkov, T., Williams, E. D., Kelly, B. D., Owen, D. J., and Porter, C. J. H. (2015) Methotrexate-conjugated PEGylated dendrimers show differential patterns of deposition and activity in tumor-burdened lymph nodes after intravenous and subcutaneous administration in rats, *Mol. Pharm.*, **12**, pp 432–443.

32. Kaminskas, L. M., McLeod, V. M., Kelly, B. D., Sberna, G., Boyd, B. J., Williamson, M., Owen, D. J., and Porter, C. J. H. (2012) A comparison of changes to doxorubicin pharmacokinetics, antitumor activity, and toxicity mediated by PEGylated dendrimer and PEGylated liposome drug delivery systems, *Nanomed. Nanotechnol. Biol. Med.*, **8**, pp. 103–111.

33. Kaminskas, L. M., McLeod, V. M., Ryan, G. M., Kelly, B. D., Haynes, J. M., Williamson, M., Thienthong, N., Owen, D. J., and Porter, C. J. (2014) Pulmonary administration of a doxorubicin-conjugated dendrimer enhances drug exposure to lung metastases and improves cancer therapy, *J. Control. Release*, **183**, pp. 18–26.

34. Kaminskas, L. M., and Porter, C. J. H. (2011) Targeting the lymphatics using dendritic polymers (dendrimers), *Adv. Drug Deliv. Rev.*, **63**, pp. 890–900.

35. Kaminskas, L. M., Wu, Z., Barlow, N., Krippner, G. Y., Boyd, B. J., and Porter, C. J. (2009) Partly-PEGylated Poly-L-lysine dendrimers

04:32 30 October 2016

have reduced plasma stability and circulation times compared with fully PEGylated dendrimers, *J. Pharm. Sci.*, **98**, pp. 3871–3875.

36. Ke, W., Zhao, Y., Huang, R., Jiang, C., and Pei, Y. (2008) Enhanced oral bioavailability of doxorubicin in a dendrimer drug delivery system, *J. Pharm. Sci.*, **97**, pp. 2208–2216.
37. Kitchens, K. M., El-Sayed, M. E., and Ghandehari, H. (2005) Transepithelial and endothelial transport of poly (amidoamine) dendrimers, *Adv. Drug Deliv. Rev.*, **57**, pp. 2163–2176.
38. Kitchens, K. M., Foraker, A. B., Kolhatkar, R. B., Swaan, P. W., and Ghandehari, H. (2007) Endocytosis and interaction of poly (amidoamine) dendrimers with Caco-2 cells, *Pharm. Res.*, **24**, pp. 2138–2145.
39. Kitchens, K. M., Kolhatkar, R. B., Swaan, P. W., Eddington, N. D., and Ghandehari, H. (2006) Transport of poly(amidoamine) dendrimers across Caco-2 cell monolayers: Influence of size, charge and fluorescent labeling, *Pharm. Res.*, **23**, pp. 2818–2826.
40. Kobayashi, H., Kawamoto, S., Bernardo, M., Brechbiel, M. W., Knopp, M. V., and Choyke, P. L. (2006) Delivery of gadolinium-labeled nanoparticles to the sentinel lymph node: Comparison of the sentinel node visualization and estimations of intra-nodal gadolinium concentration by the magnetic resonance imaging, *J. Control. Release*, **111**, pp. 343–351.
41. Kobayashi, H., Kawamoto, S., Brechbiel, M. W., Bernardo, M., Sato, N., Waldmann, T. A., Tagaya, Y., and Choyke, P. L. (2005) Detection of lymph node involvement in hematologic malignancies using micromagnetic resonance lymphangiography with a gadolinum-labeled dendrimer nanoparticle, *Neoplasia*, **7**, pp. 984–991.
42. Kobayashi, H., Kawamoto, S., Choyke, P. L., Sato, N., Knopp, M. V., Star, R. A., Waldmann, T. A., Tagaya, Y., and Brechbiel, M. W. (2003) Comparison of dendrimer-based macromolecular contrast agents for dynamic micro-magnetic resonance lymphangiography, *Magn. Res. Med.*, **50**, pp. 758–766.
43. Kobayashi, H., Kawamoto, S., Saga, T., Sato, N., Hiraga, A., Ishimori, T., Konishi, J., Togashi, K., and Brechbiel, M. W. (2001) Positive effects of polyethylene glycol conjugation to generation-4 polyamidoamine dendrimers as macromolecular MR contrast agents, *Magn. Res. Med.*, **46**, pp. 781–788.
44. Kobayashi, H., Kawamoto, S., Saga, T., Sato, N., Hiraga, A., Konishi, J., Togashi, K., and Brechbiel, M. W. (2001) Micro-MR angiography

of normal and intratumoral vessels in mice using dedicated intravascular MR contrast agents with high generation of polyamidoamine dendrimer core: Reference to pharmacokinetic properties of dendrimer-based MR contrast agents, *J. Magn. Res. Imag.*, **14**, pp. 705–713.

45. Kobayashi, H., Kawamoto, S., Sakai, Y., Choyke, P. L., Star, R. A., Brechbiel, M. W., Sato, N., Tagaya, Y., Morris, J. C., and Waldmann, T. A. (2004) Lymphatic drainage imaging of breast cancer in mice by micro-magnetic resonance lymphangiography using a nano-size paramagnetic contrast agent, *J. Nat. Cancer Inst.*, **96**, pp. 703–708.
46. Kobayashi, H., Sato, N., Hiraga, A., Saga, T., Nakamoto, Y., Ueda, H., Konishi, J., Togashi, K., and Brechbiel, M. W. (2001) 3D-micro-MR angiography of mice using macromolecular MR contrast agents with polyamidoamine dendrimer core with reference to their pharmacokinetic properties, *Magn. Res. Med.,* **45**, pp. 454–460.
47. Kukowska-Latallo, J. F., Candido, K. A., Cao, Z., Nigavekar, S. S., Majoros, I. J., Thomas, T. P., Balogh, L. P., Khan, M. K., and Baker, J. R. (2005) Nanoparticle targeting of anticancer drug improves therapeutic response in animal model of human epithelial cancer, *Cancer Res.*, **65**, pp. 5317–5324.
48. Kwon, M. J., An, S., Choi, S., Nam, K., Jung, H. S., Yoon, C. S., Ko, J. H., Jun, H. J., Kim, T. K., Jung, S. J., Park, J. H., Lee, Y., and Park, J.-S. (2012) Effective healing of diabetic skin wounds by using nonviral gene therapy based on minicircle vascular endothelial growth factor DNA and a cationic dendrimer, *J. Gene Med.*, **14**, pp. 272–278.
49. Lee, C. C., Gillies, E. R., Fox, M. E., Guillaudeu, S. J., Frechet, J. M., Dy, E. E., and Szoka, F. C. (2006) A single dose of doxorubicin-functionalized bow-tie dendrimer cures mice bearing C-26 colon carcinomas, *Proc. Natl. Acad. Sci. U. S. A.*, **103**, pp. 16649–16654.
50. Lee, C. C., MacKay, J. A., Frechet, J. M. J., and Szoka, F. C. (2005) Designing dendrimers for biological applications, *Nat. Biotech.*, **23**, pp. 1517–1526.
51. Lim, J., Guo, Y., Rostollan, C. L., Stanfield, J., Hsieh, J. T., Sun, X., and Simanek, E. E. (2008) The role of the size and number of polyethylene glycol chains in the biodistribution and tumor localization of triazine dendrimers, *Mol. Pharm.*, **5**, pp. 540–547.
52. Maeda, H. (2001) SMANCS and polymer-conjugated macromolecular drugs: Advantages in cancer chemotherapy, *Adv. Drug Deliv. Rev.*, **46**, pp. 169–185.

04:32 30 October 2016

04:32 30 October 2016

53. Malik, N., Wiwattanapatapee, R., Klopsch, R., Lorenz, K., Frey, H., Weener, J. W., Meijer, E. W., Paulus, W., and Duncan, R. (2000) Dendrimers: Relationship between structure and biocompatibility in vitro, and preliminary studies on the biodistribution of I-125-labelled polyamidoamine dendrimers in vivo, *J. Control. Release*, **68**, pp. 299–302.

54. Margerum, L. D., Campion, B. K., Koo, M., Shargill, N., Lai, J. J., Marumoto, A., and Sontum, P. C. (1997) Gadolinium(III) DO3A macrocycles and polyethylene glycol coupled to dendrimers- Effect of molecular weight on physical and biological properties of macromolecular magnetic resonance imaging contrast agents, *J. Alloy Compounds*, **249**, pp. 185–190.

55. Mutalik, S., Shetty, P. K., Kumar, A., Kalra, R., and Parekh, H. S. (2014) Enhancement in deposition and permeation of 5-fluorouracil through human epidermis assisted by peptide dendrimers, *Drug Deliv.*, **21**, pp. 44–54.

56. Myc, A., Douce, T. B., Ahuja, N., Kotlyar, A., Kukowska-Latallo, J., Thomas, T. P., and Baker, J. R., Jr. (2008) Preclinical antitumor efficacy evaluation of dendrimer-based methotrexate conjugates, *Anti-Cancer Drugs*, **19**, pp. 143–149.

57. Nigavekar, S. S., Sung, L. Y., Llanes, M., El-Jawahri, A., Lawrence, T. S., Becker, C. W., Balogh, L., and Khan, M. K. (2004) 3H dendrimer nanoparticle organ/tumor distribution, *Pharm. Res.*, **21**, pp. 476–483.

58. Peer, D., Karp, J. M., Hong, S., FaroKhzad, O. C., Margalit, R., and Langer, R. (2007) Nanocarriers as an emerging platform for cancer therapy, *Nat. Nanotechnol.*, **2**, pp. 751–760.

59. Pisal, D. S., Yellepeddi, V. K., Kumar, A., Kaushik, R. S., Hildreth, M. B., Guan, X., and Palakurthi, S. (2008) Permeability of surface-modified polyamidoamine (PAMAM) dendrimers across Caco-2 cell monolayers, *Int. J. Pharm.*, **350**, pp. 113–121.

60. Quintana, A., Raczka, E., Piehler, L., Lee, I., Myc, A., Majoros, I., Patri, A., Thomas, T., Mulé, J., and Baker, J., Jr. (2002) Design and function of a dendrimer-based therapeutic nanodevice targeted to tumor cells through the folate receptor, *Pharm. Res.*, **19**, pp. 1310–1316.

61. Rameshwer, S., Thommey, P. T., Ankur, M. D., Alina, K., Steve, J. P., and James, R. B., Jr. (2008) HER2 specific delivery of methotrexate by dendrimer conjugated anti-HER2 mAb, *Nanotechnology*, **19**, pp. 295102.

62. Rowland, M., and Tozer, T. N. (1995) *Clinical Pharmacokinetics Concepts and Applications* (Lea and Febiger, Baltimore).

63. Rubin, B. K. (2010) Air and soul: The science and application of aerosol therapy, *Resp. Care*, **55**, pp. 911–921.

64. Ryan, G. M., Kaminskas, L. M., Kelly, B. D., Owen, D. J., McIntosh, M. P., and Porter, C. J. (2013) Pulmonary administration of PEGylated polylysine dendrimers: Absorption from the lung versus retention within the lung is highly size-dependent, *Mol. Pharm.*, **10**, pp. 2986–2995.

65. Ryan, G. M., Kaminskas, L. M., and Porter, C. J. H. (2014) Nano-chemotherapeutics: Maximising lymphatic drug exposure to improve the treatment of lymph-metastatic cancers, *J. Control. Release*, **193**, pp. 241–256.

66. Sadekar, S., and Ghandehari, H. (2012) Transepithelial transport and toxicity of PAMAM dendrimers: Implications for oral drug delivery, *Adv. Drug Deliv. Rev.*, **64**, pp. 571–588.

67. Sadekar, S., Linares, O., Noh, G., Hubbard, D., Ray, A., Janat-Amsbury, M., Peterson, C. M., Facelli, J., and Ghandehari, H. (2013) Comparative pharmacokinetics of PAMAM-OH dendrimers and HPMA copolymers in ovarian-tumor-bearing mice, *Drug Deliv. Translat. Res.*, **3**, pp. 260–271.

68. Sadekar, S., Thiagarajan, G., Bartlett, K., Hubbard, D., Ray, A., McGill, L. D., and Ghandehari, H. (2013) Poly(amido amine) dendrimers as absorption enhancers for oral delivery of camptothecin, *Int. J. Pharm.*, **456**, pp. 175–185.

69. Sandanaraj, B. S., Gremlich, H.-U., Kneuer, R., Dawson, J., and Wacha, S. (2010) Fluorescent nanoprobes as a biomarker for increased vascular permeability: Implications in diagnosis and treatment of cancer and inflammation, *Bioconjug. Chem.*, **21**, pp. 93–101.

70. Schuster, D., Laggner, C., and Langer, T. (2005) Why drugs fail--a study on side effects in new chemical entities, *Curr. Pharm. Des.*, **11**, pp. 3545–3559.

71. Singh, P., Gupta, U., Asthana, A., and Jain, N. K. (2008) Folate and folate-PEG-PAMAM dendrimers: Synthesis, characterization, and targeted anticancer drug delivery potential in tumor bearing mice, *Bioconjug. Chem.*, **19**, pp. 2239–2252.

72. Stacker, S. A., Williams, S. P., Karnezis, T., Shayan, R., Fox, S. B., and Achen, M. G. (2014) Lymphangiogenesis and lymphatic vessel remodelling in cancer, *Nat. Rev. Cancer*, **14**, pp. 159–172.

73. Taratula, O., Garbuzenko, O. B., Kirkpatrick, P., Pandya, I., Savla, R., Pozharov, V. P., He, H., and Minko, T. (2009) Surface-engineered

04:32 30 October 2016

targeted PPI dendrimer for efficient intracellular and intratumoral siRNA delivery, *J. Control. Release*, **140**, pp. 284–293.

74. Tekade, R. K., Dutta, T., Tyagi, A., Bharti, A. C., Das, B. C., and Jain, N. K. (2008) Surface-engineered dendrimers for dual drug delivery: A receptor up-regulation and enhanced cancer targeting strategy, *J. Drug Target*, **16**, pp. 758–772.
75. Thomas, T. P., Shukla, R., Kotlyar, A., Liang, B., Ye, J. Y., Norris, T. B., and Baker, J. R., Jr. (2008) Dendrimer-epidermal growth factor conjugate displays superagonist activity, *Biomacromolecules*, **9**, pp. 603–609.
76. Venuganti, V. V., and Perumal, O. P. (2008) Effect of poly(amidoamine) (PAMAM) dendrimer on skin permeation of 5-fluorouracil, *Int. J. Pharm.*, **361**, pp. 230–238.
77. Venuganti, V. V., and Perumal, O. P. (2009) Poly(amidoamine) dendrimers as skin penetration enhancers: Influence of charge, generation, and concentration, *J. Pharm. Sci.*, **98**, pp. 2345–2356.
78. Venuganti, V. V., Sahdev, P., Hildreth, M., Guan, X., and Perumal, O. (2011) Structure-skin permeability relationship of dendrimers, *Pharm. Res.*, **28**, pp. 2246–2260.
79. Wagner, J. G. (1993) *Pharmacokinetics for the Pharmaceutical Scientist* (Technomic Publishing Co, Lancaster, M. A.).
80. Waite, C. L., and Roth, C. M. (2009) PAMAM-RGD conjugates enhance siRNA delivery through a multicellular spheroid model of malignant glioma, *Bioconjug. Chem.*, **20**, pp. 1908–1916.
81. Wiig, H., and Swartz, M. A. (2012) Interstitial fluid and lymph formation and transport: Physiological regulation and roles in inflammation and cancer, *Physiol. Rev.*, **92**, pp. 1005–1060.
82. Wiwattanapatapee, R., Carreno-Gomez, B., Malik, N., and Duncan, R. (2000) Anionic PAMAM dendrimers rapidly cross adult rat intestine in vitro: A potential oral delivery system?, *Pharm. Res.*, **17**, pp. 991–998.
83. Yang, W., Barth, R. F., Adams, D. M., Ciesielski, M. J., Fenstermaker, R. A., Shukla, S., Tjarks, W., and Caligiuri, M. A. (2002) Convection-enhanced delivery of boronated epidermal growth factor for molecular targeting of EGF receptor-positive gliomas, *Cancer Res.*, **62**, pp. 6552–6558.
84. Yang, W., Barth, R. F., Adams, D. M., and Soloway, A. H. (1997) Intratumoral delivery of boronated epidermal growth factor for neutron capture therapy of brain tumors, *Cancer Res.*, **57**, pp. 4333–4339.

04:32 30 October 2016

85. Zhang, Y., Sun, Y., Xu, X., Zhang, X., Zhu, H., Huang, L., Qi, Y., and Shen, Y. M. (2010) Synthesis, biodistribution, and microsingle photon emission computed tomography (SPECT) imaging study of technetium-99m labeled PEGylated dendrimer poly(amidoamine) (PAMAM)-folic acid conjugates, *J. Med. Chem.*, **53**, pp. 3262–3272.
86. Zölter, H. (2005) Morphology and physiology of lymphatic endothelial cells. In: *Microvascular Research, Biology and Pathology* (Elsevier Science, Burlington).

04:32 30 October 2016

04:32 30 October 2016



Taylor & Francis
Taylor & Francis Group
http://taylorandfrancis.com

# Chapter 10

# Molecular Modeling of Dendrimers

**Matteo Garzoni and Giovanni Pavan**

*Department of Innovative Technologies,*
*University of Applied Sciences and Arts of Southern Switzerland,*
*Galleria 2, CH-6928 Manno, Switzerland*

giovanni.pavan@supsi.ch

## 10.1 Summary

Dendrimers and dendrons are hyperbranched polymers that have recently attracted considerable interest for many applications in nanobiotechnology. However, the rational design of dendrimers with controlled properties is not easy. The high level of structural complexity, their reduced size and their structure offering limited contrast in solution and extremely responsive to the external conditions make the understanding of the dendrimer's properties particularly awkward. Thus, it is typically not easy to understand why dendrimers behave in a determined way, and how to manipulate their structure to control the final properties. Recently, molecular modeling and computer simulations have been increasingly used to study the behavior of dendrimers. The versatility of in silico approaches allows to look at the dendrimer

*Dendrimers in Nanomedicine*
Edited by Delphine Felder-Flesch
Copyright © 2016 Pan Stanford Publishing Pte. Ltd.
ISBN 978-981-4745-49-9 (Hardcover), 978-981-4745-50-5 (eBook)
www.panstanford.com

structure from a privileged point of view. Detailed characterization of the dendrimers in solution can be obtained at the single-molecule level, exceeding the possibilities of other experimental techniques. Simulations can provide unique insight into shape, size and overall features of dendrimers in different conditions, which constitutes the first milestone to understand the dendrimers' properties. Molecular modeling also allows studying the interactions of the dendrimers with other macromolecular targets in great detail. In general, computer-aided simulations constitute an important platform to characterize the dendrimers' behavior on a multiscale level: from understanding the features of the dendrimer, to molecular recognition and self-assembly.

04:36 30 October 2016

## 10.2 Introduction

### 10.2.1 Dendrimers and Their Applications

Dendrimers are hyperbranched polymers with a relatively high monodispersity index characterized by well-defined branching architecture, regular connectivity, and symmetry,[1–4] and grow in generations[5–7] with a structure reminiscent of that of trees. These monodisperse branched polymers have been used for a number of different applications spanning from nanotechnology, to pharmaceuticals and medicinal chemistry.[6] Schematized in Fig. 10.1, the dendritic scaffold can be typically divided into the following sub-domains: the central core, the repetitive units that compose the branches of the scaffold, emanating from the central core, and progressively growing into a series of radially concentric layers, and the terminal surface groups. The "generation number" identifies the increasing level of concentric layers of monomers that compose the dendrimer structure. A higher dendritic generation generally corresponds to a higher number of surface groups and molecular weight, while the entire structure interacts with the external environment and assumes an optimized configuration, depending on the external conditions, controlling the dendrimer size, shape in a given environment.[8]

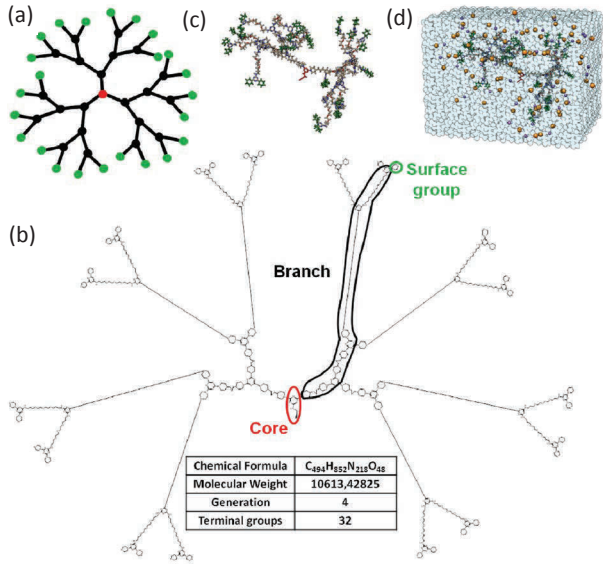



**Figure 10.1** (a) Scheme of the typical structure of a dendrimer, composed of a central core, repetitive branching units and surface groups. (b) Example of a triazine dendrimer. (c) Molecular model of the triazine dendrimer. The core of the dendrimer is colored in red, the repetitive units that compose the branches are colored by element (C: grey, N: blue, O: red, H: white), and the terminal groups in green. (d) Molecular model (starting configuration) of the triazine dendrimer in aqueous solution ($Na^+$ ions in purple, $Cl^-$ in orange, water Oxygen atoms in transparent cyan).

A multitude of dendrimer variants have been synthesized and tested in the last years.[9,10] The most famous examples include poly(propyleneimine) (PPI), poly(amidoamine) (PAMAM), poly(ethyleneimine) (PEI), arborols, poly(lysines), phosphorous-containing dendrimers, triazine dendrimers, aryl ethers, and poly(esters).[11–15]

One of the most interesting characteristics of these macromolecules is that they possess a multivalent surface, where the multiple surface functions at the dendrimer surface can establish strong cooperative binding[16] with other molecular targets such as nucleic acids,[17–19] proteins,[20–22] etc. For example,

04:36 30 October 2016

04:36 30 October 2016

cationic PAMAM dendrimers, first synthesized by Tomalia, are known to be able to establish strong binding with the double strands of nucleic acids, and to allow for successful gene delivery into cells.[23–25] Other molecular variants, such as PEI, possess similar properties and are routinely used for gene delivery.[26,27] Another interesting feature of the dendrimers is that their structure can be customized ad hoc, depending on the molecular target they are going to bind—i.e., the surface units can be used to improve the attraction, and the scaffold can be modified to maximize the simultaneous cooperative binding of multiple ligands to the target (scaffold flexibility/rigidity vs. multivalency). Recently, for example, the strong and natural high-affinity of spermine (natural DNA binder) for DNA has been exploited to produce three-branched spermine-based flexible Newkome-type dendrons capable of ultra-high DNA binding affinity.[28,29]

Several reports in the literature showed that different parameters in the structure of dendrimers might impact molecular behavior. For example, both the scaffold and the surface are crucial to maximize the interaction between a dendritic binder and a molecular target (this will be discussed in more details later on in this chapter). However, a deep comprehension of the structural behavior leading to a real rational design of constructs with controlled properties is still awkward. Important efforts recently pointed at putting some order in this multitude of variables. Tomalia recently proposed the critical nanoscale design parameters (CNDPs)—i.e., size, shape, surface chemistry, flexibility/rigidity and architecture—as parameters that should allow, in principle, to control the dendritic behavior.[30–32] The CNDPs constitute a first interesting framework to try to understand and predict the dendritic effects on different scales.

However, the different CNDPs are somehow intimately interconnected each other in a real environment. For example, the chemistry of the surface groups, and the rigidity/flexibility and overall architecture of the scaffold will clearly control the shape assumed by one dendrimer in one solvent, and the same is true for the dendrimer's size.[33–35] For example, the same dendrimer with a hydrophobic scaffold can assume an open conformation in organic solvent, or more compact one in water solution. Indeed, the rational design of dendrimers for a function is not an easy task.

04:36 30 October 2016

### 10.2.2 Limits of the Experiments in the Characterization of Dendrimers and the Potential of Molecular Modeling

Characterization of dendrimers in solution is not easy to be achieved. This is largely due to the reduced size of these macromolecules (in the range of a few tens of nanometers or smaller), and to the reduced contrast that they offer in the solvent (especially in water). Typically, information on the dendrimer size can be inferred, for example, by dynamic light scattering (DLS). However, the average size provided by DLS accounts also for the solvation shell around the macromolecule, and characterization of macromolecules with diameter below a few nanometers is practically hindered. Transmission electron microscopy (TEM) can also be used to obtain information of the dendrimer size. However, due to the reduced contrast offered by the soft dendrimer scaffold, it is often necessary to use staining, but this may modify the intrinsic characteristics of the dendrimer. Atomic force microscopy (AFM) can also be used, but even at the minimum force measurement, the residual force present on the AFM tip (in the order of pN) can deform the native dendrimers.[36] NMR can also be used to obtain information on the dendrimer structure.[37]

Characterization of the dendrimer interaction with other molecular targets is also awkward. Information on the strength of dendrimers binding can be obtained through different experimental techniques such as, for example, Isothermal Titration Calorimetry (ITC), ethidium bromide (EthBr) displacement assay, etc.[33,34,38–40] However, it is worth noting that dendrimer aggregation in solution, or dendrimer-induced aggregation of other molecules (e.g., nucleic acids, proteins, etc.), are typically very complex multiscale phenomena that may involve multiple types of interactions on different scales.[41] While these experimental approaches can provide an overall estimation of the strength and thermodynamics of binding, they often fail in giving clear understanding of the different interactions involved in multiscale aggregation, going from molecular recognition to self-assembly.

In silico molecular modeling can help filling the gap. The increase of computational power at disposal seen in the last years nowadays allows to build models and to simulate the behavior of large macromolecules in solution, and to study aggregation

and self-assembly phenomena.[33,34,38,39,42,43] The capabilities of molecular simulation are largely dependent on the size of the system that needs to be treated, and on the kind of phenomena to be studied. Certainly, the limitations are still important, but molecular simulation is increasingly becoming a fundamental instrument to support the study and characterization of molecular behavior. As it will be discussed in this chapter, computer simulations can be used in synergy with the experiments to obtain deeper understanding of the behavior of the dendrimers in solution, and of their interaction with the external environment.

04:36 30 October 2016

## 10.3 Molecular Modeling of Dendrimers

### 10.3.1 First Dendrimers Models

The dendrimer scaffold grows in a tree-like fashion in concentric and consecutive generations. However, as the dendritic generation grows, the number of structural defects will also be increased. In fact, the steric congestion at the periphery of the dendrimer will become more and more important while growing the dendrimer, up to the point where growing one more generation will be impossible. The theoretical limits for the growth of these starburst polymers were first described by de Gennes, who proposed a theoretical model to predict the limit of a perfect growth as a function of the monomer structure (Eq. 10.1).[44]

$$G_{\max} = 2.88\ (\ln P + 1.5), \tag{10.1}$$

where $G_{\max}$ is the theoretical defect-free maximum achievable generation, and $P$ is the number of flexible atoms per-monomer chain (monomer length). While it is now well known that structural defects emerge in the dendrimer structure in statistical fashion well before this threshold maximum generation,[45] this simple mathematical model allows to identify what is, in principle, the theoretical largest generation that can be grown depending on the chemical structure of the monomers, which is important to know in dendrimer synthesis.

After these first models, and thanks to the increasing computational power provided by continuously evolving hardware and software, modeling of entire dendrimers with full explicit treatment of all the individual atoms has become

04:36 30 October 2016

possible. Molecular simulation became an important tool, providing the possibility to obtain an atomistic-resolution picture of the dendrimers.

However, soon it became clear that the potential of molecular modeling was not restricted to an additional visual insight. On the contrary, many different parameters could be extracted from the models that were inaccessible to other experimental techniques—e.g., the level of backfolding and internal crowding of the dendrimers, internal hydration, exposure of the surface groups to the solution, etc. Such a high-level characterization allowed for a detailed description of the dendrimer structure that was unconceivable before. For example, the computational work conducted by the group of Likos allowed to locate the macromolecular family of dendrimers in between flexible polymers and rigid colloids, with a molecular behavior strongly dependent on the generation (size) of the dendrimer.[46]

Thanks to the increasing diffusion of computational modeling of the molecular structure understanding, deeper comprehension of the molecular structure is now accessible. The effect of structural modifications can be thus more easily related to molecular behavior. Thanks to recent computational efforts, for example, it is now clear that increasing the dendritic generation, or changing the external conditions such as pH, temperature, etc., may have a direct impact on the density and rigidity of the dendrimer's surface.[47] This delicate and responsive behavior controls the dendrimer's properties, such as, for example, the affinity for other molecules, the ability to strongly bind to a target,[48] or to undergo self-assembly in solution.[49,50]

### 10.3.2 Atomistic Simulation of dendrimers in the Gas-Phase

The group of Goddard performed the first atomistic molecular dynamics (MD) simulations of dendrimers (PAMAMs) in the 1990s. Their MD simulation allowed obtaining an insight into the conformation assumed by the PAMAM structure.[51–53] The large size and structural complexity of dendrimers exceeded the capabilities of the available computational resources. For this reason, the first MD simulations did not consider the presence of the solvent (gas-phase simulations). While the absence of the solvent in the system simplifies the description of the real system,

these models provided for the first time an atomistic picture of the dendrimers at the single-molecule level, and unprecedented insight on the configuration assumed by the dendrimers in vacuum. Since then, the naïve idea of perfectly extended star-like dendrimers provided by the 2D chemical structure often used in scientific papers was surpassed.

Despite the considerable advance in dendrimer characterization brought by these early computer simulations, vacuum modeling did not represent realistically the dendrimers in a real environment. In fact, the presence polar water molecules and salt ions can dramatically change the conformation of the dendrimers, as it happens for proteins and other kind of biomolecules. Thanks to the increase of computational power, further computational attempts allowed to simulate dendrimers as immerged in a model of real solution. The possibility of explicitly accounting for the interactions with the solvent represented a remarkable milestone, and provided a more reliable characterization of the dendrimers in the real environment.[46,47,54–56]

04:36 30 October 2016

Starting from an initial putative model for the dendrimer, the latter typically evolves toward an equilibrium configuration during the MD simulation. Then, from the MD trajectories, several useful parameters can be extracted which provide atomic-resolution details of the dendrimer structure in the real environment. Few examples include the dendrimer radius of gyration ($R_g$), radial distribution functions (RDF) of the dendrimer's atoms, or different groups in the dendrimer's structure, or the moment of inertia, providing information on the overall shape and anisotropy of the macromolecule, etc.[52] Since the first atomistic simulations (mainly MD) accounting for the presence of the solvent in the surrounding of the dendrimer, further computational efforts followed, focusing, for example, on the comparison of the dendrimer generation on the level of backfolding.[48] Other structural parameters were also investigated in detail, such as the role of architecture,[42,57,58] surface chemistry[59] and surrounding conditions[29,47,54,56] (salt concentration, temperature, etc.) on the dendritic structure. In general, understanding the configuration and shape—i.e., the features—of the dendrimers in solution is fundamental to understand the properties, such as, for example, how one dendrimer interacts with other molecules.[29,59–61]

04:36 30 October 2016

### 10.3.3 Characterization of the Dendrimers in Solution

Information on molecular size and shape are easily accessible by all-atom MD simulations of dendrimers in solution. More detailed structural characterizations, such as, for example, atomic density distribution ($g(r)$), information on hydration levels, etc., can also be obtained.[33,34,38,39,47]

The $g(r)$ data extracted from the equilibrated phase MD simulations provide direct indication on the density levels in the dendrimer structure in equilibrium condition (Fig. 10.2d). For example, it is possible to assess the level of surface groups backfolding, of the rigidity/mobility of the surface (Fig. 10.2e), or of water accessibility in the dendrimer interior (Fig. 10.2f,g).

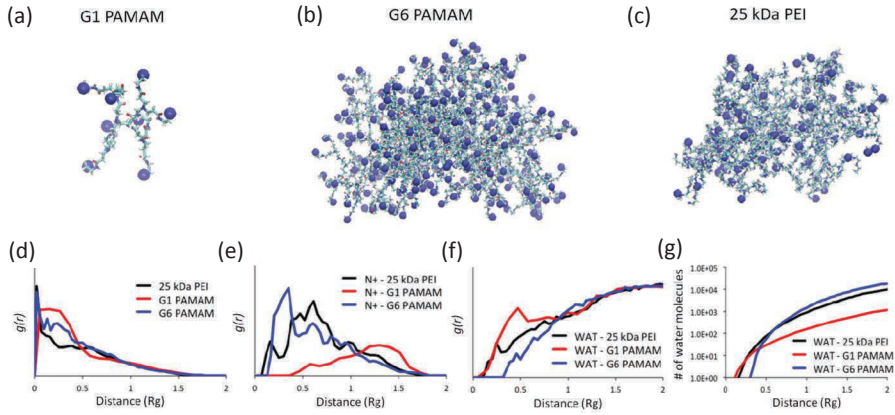



**Figure 10.2** Equilibrated configurations of small and flexible G1 PAMAM (a), large G6 PAMAM (b) and intermediate 25 kDa PEI (c) dendrimers from MD simulations in solution. The cationic surface charged groups are represented as blue spheres. (d–f) Radial distribution function $g(r)$ data as a function of the distance from the dendrimer's center of mass (CM) provide insight into dendrimer's density and on the probability to find precise atoms or groups in space. Distances from CM are expressed in $R_g$ (radius of gyration) units to compare different size dendrimers. The reported $g(r)$ curves are related to the dendrimer's atoms (d), to the surface charged groups (e), and to the water molecules (f) to assess water penetration in the dendrimers interior. (g) Number of water molecules inside the dendrimer's scaffold as a function of the distance from CM.

04:36 30 October 2016

These data are reported in Fig. 10.2 for G1 PAMAM, G6 PAMAM and 25 kDa PEI, used as examples of three dendrimer structures with different levels of rigidity, size and backfolding. The MD data show, for example, that surface group backfolding is directly proportional to the dendrimer's size. In fact, surface groups backfolding (Fig. 10.2e) is found to be negligible in the case of the small G1 PAMAM (the red $g(r)$ maximum peak is found at distance $>R_g$, indicating that the surface groups are most probably found in proximity of the external surface of the dendrimer). Clearly, the level of backfolding in the structure has direct implications for molecular properties. For example, as it will be discussed in more detail in the next sections, this plays an important role in the interaction with other molecules.

The level of hydration in the dendrimer's interior typically decreases while increasing the dendritic generation. This is due to crowding effects, so that, in general, the higher the internal crowding of the dendrimer, the lower the accessibility of water molecules in the dendrimer's interior (this is valid also for other molecular guests).[62] Molecular modeling can also provide other useful information on the hydration state of the dendrimer. This can be typically inferred from the analysis of the solvent accessible surface area (SASA), providing a simple structural estimation of the amount of dendrimer surface in direct contact with the external solution, or from the solvation energy ($G_{sol}$)—partially related to the SASA—which identifies the energy necessary to drag the dendrimer out from the solution.

Extensive experimental and computational investigations demonstrated that shape, size and the overall configuration of the dendrimers somehow depend on the solvent, and change while changing the external environment.[63,64] For example, changing the solution pH usually corresponds to different protonation states in the dendrimer—protonation is increased at lower pH, or *vice versa*. In the atomistic models of cationic dendrimers (e.g., PAMAM, etc.), usual convention is to assume the protonation of the primary amines at pH ≈ 7.4, while at lower pH (<4) the tertiary amines are also protonated.[65,66] Clearly, the charge increase on the branches of the scaffold at low pH produces tension and stretching in the scaffold. While SANS[67,68] and SAXS experiments[69,70–72] demonstrates that the global dimensions of

04:36 30 October 2016

the dendrimer do not change upon pH changes, recent atomistic simulations showed that the increase of positive charge in a **G4** PAMAM at low pH produces an interesting transition in the dendrimer structure from a dense core-flexible surface configuration (neutral and high pH) to a rigid surface-porous core configuration (at low pH).[47] Modification of other external parameters, such as increasing the ionic strength in solution, or changing temperature, etc., may also have an impact on the conformation assumed by the dendrimer. In general, dendrimers are extremely responsive to the external conditions and to the interactions with the external environment. It is thus clear that in order to understand, or somehow predict, the behavior of new dendritic structures (rational design), it is of primary importance to understand "what the dendrimer looks like" in the real environment.

***The impact of the external environment on the on dendrimers' multivalency***. While the environment plays such an important role in controlling the shape and configuration assumed by the dendrimers, it also has a key impact on the multivalent behavior on the dendrimer, and on its interaction/molecular recognition with other macromolecules. This is well illustrated by the case of two generation three-branched Newkome-type dendrons (**3b-G1** and **3b-G2**) reported by Kostiainen et al. bearing spermine surface groups for DNA binding. These low-molecular weight structures are capable of ultra-high affinity for DNA.[28,73] However, when ionic strength in solution is increased from 9.4 to 150 mM NaCl, the smaller dendron, **3b-G1**, lost binding efficiency. This is typical also of other DNA and RNA electrostatic-based binders (e.g., poly-lysine, protamine, and polyamine) both in the absence or in the presence of salt.[74,75] On the other hand, the larger dendron (**3b-G2**) preserved its affinity for DNA—a clear generation-effect.[29]

While the smaller **3b-G1** is capable of strong binding with DNA and RNA in low salt concentration, the larger number of ions is present in solution at 150 mM disturbs the binding. In the case of the larger **3b-G2**, possessing nine surface spermine ligands instead of three, this effect is negligible. In fact, while the most external spermine units are disturbed by the interactions with the ions, the internal one are still sufficient to produce high-affinity binding also at 150 mM NaCl.

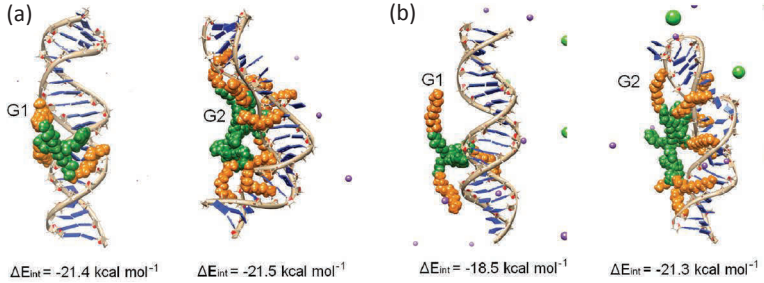



**Figure 10.3** Snapshots taken from MD simulations of the 3b-G1 and 3b-G2 spermine-dendrons binding DNA. MD simulations were conducted starting from the same initial configuration in two different 9.4 mM (a) and 150 mM (b) NaCl concentrations in solution. The $\Delta E_{int}$ data represent the averaged interaction energy between the surface spermine SPM (orange) unit and the DNA expressed in kcal $mol^{-1}$—while G2 is able to compensate the disturbing action of ions due to a higher number of SPM ligands, G1 shows a decrease >10% in $\Delta E_{int}$. The scaffold and the center of the dendrons is colored in green. $Cl^-$ and $Na^+$ ions are represented in florescent green and purple, respectively. The strands of DNA are colored in brown and water molecules are not shown for clarity.

04:36 30 October 2016

This example demonstrates that the multivalency of the dendron, a critical variable for strong binding, is directly dependent of the interaction with the external environment. In this case, the surface spermines have a double role during binding—(i) they actively interact with the target (DNA, RNA), and (ii) some ligands protect the binding site from interferences with the external solution (passive role). Indeed, the whole molecular structure of the dendrons acts in a concerted manner to optimize the interaction in given conditions. These external conditions are thus dramatically important for the final properties.

***Understanding dendrimers in solution***. Understanding what a dendrimer looks like in solution is crucial. Despite the plethora of experimental techniques adopted for the characterization of dendrimers in solution (i.e. DLS, SAXS, SANS, ITC, Eth-Brm essay, etc.), the detail understanding of molecular properties remains obscure in most cases. This is where computer modeling can be helpful. As an example, we report the case of two triazine dendrimers, G2-5 and the F2-1 synthesized by the group of Simanek (Fig. 10.4). While G2-5 is characterized by a

04:36 30 October 2016

rigid core, the interior of F2-1 is composed of long flexible branches.[76,77] F2-1 was designed to obtain strong and tight binding with DNA and RNA thanks to the ability of the dendrimer to "embrace" the target. On the other hand, G2-5 was thought to bind poorly with the nucleic acids. However, the experiments demonstrated an opposite trend.[78]

Molecular simulation was first used to characterize the two dendrimers in solution.[79] MD simulations conducted in the same conditions of the experiments (temperature, solvent, [NaCl], etc.) provided a snapshot of the configuration assumed by the dendrimers in the solvent in equilibrium condition. Starting from an extended configuration, F2-1 evolved into a globular shape during the MD simulation (Fig. 10.4a). Strong folding of the core branches was caused by hydrophobic effects: an attempt by the scaffold to shield the most hydrophobic part (core) from the interaction with the solvent. On the other hand, the rigid core of G2-5 prevented complete folding in solution, and this dendrimer maintained an open configuration (Fig. 10.4b).[79]

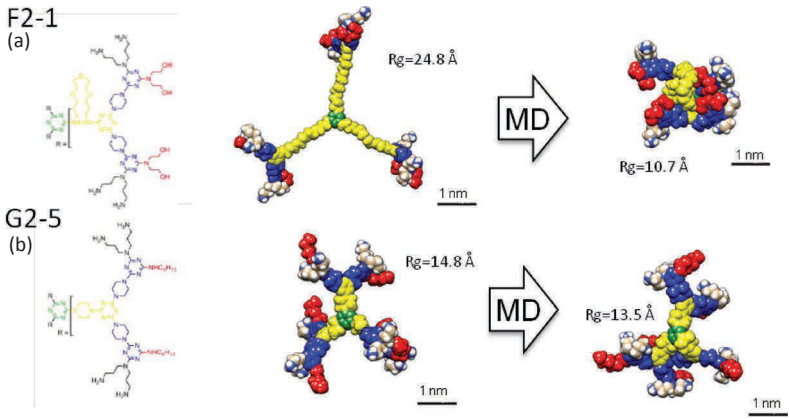



**Figure 10.4** Dendrimers in solution. The rearrangement of "flexible" F2-1 (a) and "rigid" G2-5 (b) once these are immersed in a solution containing water and ions and simulated (MD) to the equilibrium. F2-1 results in a compact globular configuration due to folding the long flexible branches (yellow) around the core (green)—the gyration radius ($R_g$) decreases from 24.8 to 10.7 Å during the MD run. G2-5 maintains its open-core configuration due to the rigidity of the core ($R_g$ changes slightly during MD). Within the dendrimers the charged surface amino groups are colored per atom (N: blue, H: white).

04:36 30 October 2016

The most instructive outcome of this study is represented by the case of F2-1 dendrimer. In this case, a structure originally designed to be flexible resulted in a rigid globular shape due solvent effect.[79] This highlights the importance to account for the interaction with the external environment when designing a novel dendrimer architecture aiming at controlled properties. In one sentence: it is not only important how the dendrimer is designed, but what it will look like in the real environment. A statement sounding even more valid when comparing synthetic branched dendrimers to other biological polymers such as proteins.

***How folding controls properties***. In such an analogy between biological and synthetic polymers, it evident that the primary sequence—i.e., the sequence of amino acids for proteins, or the chemical structure of dendrimers (the typical 2D chemical scheme reported in dendrimer papers)—is not the unique important factor. On the contrary, well demonstrated by the case of proteins, the folding of the primary sequence (chemical structure) into a well-defined secondary and tertiary structure plays a crucial role in molecular recognition, supramolecular aggregation, etc. The same is true also for dendrimers. Molecular modeling allows first to study the folded state of the dendrimers in solution, and then to simulate the interaction with other molecular targets (DNA, proteins, etc.) providing information on molecular recognition.

Back to the previous example, the folded configuration assumed by the F2-1 in solution results in a rigid interaction with the double strands. A limited number of binding points is established by this dendrimer, and the binding interface with DNA and siRNA is quite discontinuous.[77] On the other hand, the open scaffold of G2-5 allows for a more uniform binding interface with the double strands of DNA and siRNA, and overall stronger binding.

The same strong configuration-binding relationship was recently verified also for different small and rigid dendron capable of optimal siRNA binding (Fig. 10.5a),[80] or in the case of dendritic molecular glues binding the surface of microtubules (Fig. 10.5b).[81] Recently, it was also demonstrated that the folded configuration assumed by the dendrimers in the solvent has a direct impact on the biological (anti-inflammatory) activity. In

04:36 30 October 2016

particular, it was demonstrated a direct correlation between the directional conformation assumed by certain dendrimers in solution, with surface groups closely brought together, which can favor multivalent interactions with cells, with their ability to interact with monocytes and to trigger an immunoresponse.[8]

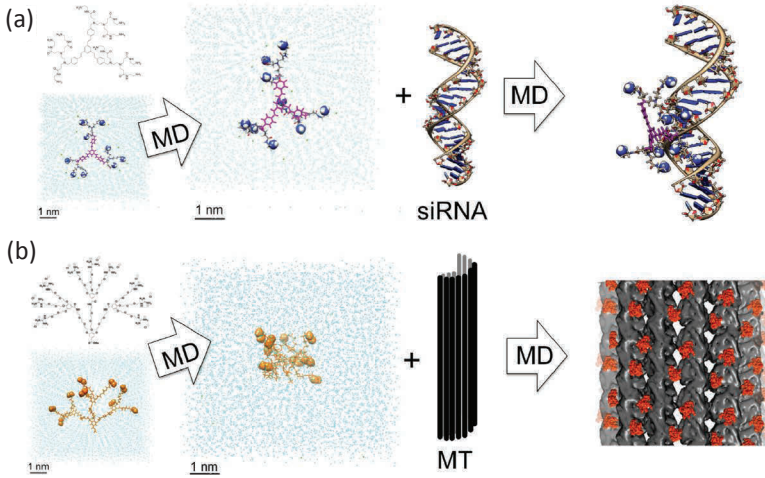



**Figure 10.5** Shape effect on binding. (a) The open configuration of a small and rigid hybrid PPV-PAMAM dendrimer allows for tight and uniform interaction with siRNA.[80] (b) Conversely, a flexible dendritic molecular glue folded in solution into a globular configuration (orange) which perfectly fits with the cavities between the tubulins in the microtubule (MT) assembly.[81]

### 10.3.4 Coarse Graining

The previous sections discussed the advantages provided by computer models at atomistic resolution. However, different models with variable levels of structural simplification can be developed. An important category is that of coarse-grained (CG) models, which has seen recent emergence and diffusion. CG models rely on the simplification of atomistic models. In particular, atoms, or chemical groups, are grouped into single "beads". This simplifies the structure of the model, and makes the interaction potential smoother. As a consequence, larger molecular systems can be simulated for longer times, and it is possible to study phenomena occurring on time and space scales inaccessible to

04:36 30 October 2016

atomistic simulation. CG models of dendrimers have been created in the last years.[82,83] The group of Larson, for example, showed that the interaction of a G5 PAMAM dendrimer with a DPPC membrane model can induce the formation of pores in the membrane. This phenomenon took place during 0.5 μs of MD simulation of a large system containing the dendrimer and the lipid bilayer membrane, which in 2006 was above the capabilities of atomistic simulations.[84] Different CG approaches have also been used, such as, for example, Brownian dynamics and dissipative particle dynamics.[85–87]

Indeed CG approaches, allow studying systems that cannot be treated with atomistic simulations. However, while efficient, these approaches have intrinsic limitations. These are mainly related to the simplified representation of molecular structure in the CG models. CG models also suffer of limited transferability. In fact, differently from atomistic approaches, the CG force field that properly describes one dendrimer can be not well suited for another dendrimer. Thus, CG simulations typically require considerable work for the preparation of the system and parametrization of the CG force field. Another critical point concerns the treatment of the solvent. In the CG models the description of the latter is typically simplified—multiple water molecules are grouped together into larger water beads, treated implicitly, or even completely absent—so that these approaches are not very well suited for the accurate study of molecules in solution.

At the same time, CG approaches allow to treat larger molecular systems, moving the study from the molecular- to the meso-scale. This allows to study hierarchical inter-molecular effects that are typically neglected in atomistic simulations. CG models also allow for a considerable speed-up in the simulations. This is due to the reduced number of particles to be simulated, but also to the fact that, reducing the numbers of degrees of freedom of the system, the potential becomes smoother and larger time steps can be used, resulting in a general speed-up of the simulation, and enhanced sampling of the conformational space of the molecules. In general, CG approaches provide an important platform for modeling and offer considerable advantages, but require deep knowledge of the system (to ensure that the simplifications adopted in the CG model do not compromise the correct behavior of the system), and massive preliminary work for the set-up of the models.

04:36 30 October 2016

### 10.3.5 Advanced Sampling Techniques: Metadynamics

The limited conformational sampling is one weak point of classical atomistic MD simulations, and can be a potential issue for the simulation of semi-flexible dendrimers. During the MD run, it can occur that once the dendrimer folds in solution assuming a configuration that corresponds to a local energy minimum, this can remain trapped in that configuration, and the exploration of different possible configurations during the simulation may be prevented. Typically, this may result in an equilibrated state for the dendrimer that is not optimally folded in solution, or that appears as excessively rigid. While for small dendrimers with a uniform structure this effect is almost negligible in classical MD simulations, this may become more important for very complex and flexible dendrimers that can eventually fold in odd configurations in the solvent. To overcome the typical sampling limitations classical MD simulations, various advanced sampling methods have been developed and used in the last few years. One of the most widely used is metadynamics.[88,89]

Figure 10.6 reports one example of a metadynamics-based method—well-tempered metadynamics (WT-MetaD)[91]—applied to G2 PAMAM dendrimers in two different conditions: high-pH, with unprotonated surface amino-groups (neutral dendrimer: Fig. 10.6a), and at neutral pH (surface $NH_3^+$ groups: Fig. 10.6b).[90] The use of WT-MetaD allows for a better sampling of the conformational space of G2 PAMAM compared to classical MD, and to obtain the free energy surface (FES) of the dendrimer. In Fig. 10.6, the FES of G2 PAMAM in two different conditions (high pH: Fig. 10.6a, and low pH: Fig. 10.6b) is represented as a function of the SASA and the dendrimer size (radius of gyration). Darkest colors in the FES indicate the most energetically favored configurations for the dendrimer in solution. It is clear that the charges present on the surface at neutral pH (where the terminal primary amines are protonated) result in a larger size of the dendrimer, which is more open in solution and is overall more hydrophilic (higher SASA values). Also, the shape of the FES basin provides indication on the flexibility of the dendrimers in solution. The minimum energy conformation for G2 PAMAM at neutral pH occupies a larger region of the FES, and the FES minimum is flatter than at high pH—this this is useful to assess the level of flexibility of the dendrimer in solution (see also Fig. 10.10), which will be discussed in more detail later in this chapter.[90]

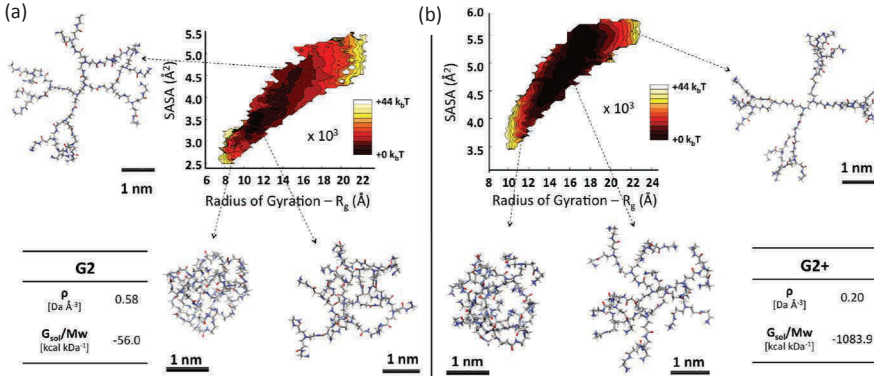



**Figure 10.6** Well-tempered metadynamics (WT-MetaD) simulations of G2 PAMAM dendrimers in solution at two different pHs. (a) WT-MetaD simulation of G2 PAMAM at high pH (neutral dendrimer). (b) WT-MetaD simulation of G2+ PAMAM at neutral pH (surface protonated $NH_3^+$ groups: positively charged dendrimer) dendrimer.[90] From the simulation it is possible to extract the FES of the dendrimers. The darkest colors in the FES identifies the most favored (probable) configuration assumed by the dendrimer in solution. While the dark free energy minimum in the FES is sharp at high pH, the FES basin is flatter and the FES minimum is larger at neutral pH—the charges on the dendrimer surface impart higher flexibility and hydrophilicity to the dendrimer, which stays more open in the solvent.

## 10.4 Some Practical Applications of Molecular Modeling in the Field of Dendrimers

### 10.4.1 Dendritic Host for Small Hydrophobic Guests: Accessibility to the Dendrimer's Interior

All-atom MD simulations have recently been used to study the guest capacity of dendrimers of growing generations.[62] The ability of incorporating guests in their interior is an interesting property for dendrimers, in particular in light of their application as drug nanocarriers. The so-called Meijer's dendritic box is a nice example of a dendritic structure that can trap guests in the interior of the scaffold, and that allows for guest release upon removal of surface groups.[92] The guest-capacity of dendrimers can also show an interesting non-linear behavior, as it is well

04:36 30 October 2016

04:36 30 October 2016

demonstrated by the case of the triazine dendrimers recently reported by Simanek.[51]

At experimental level, the hosting capacity of triazine dendrimers from G3 to G11 was challenged as the ability of incorporating small pyrene and camptothecin hydrophobic guests in the dendrimer scaffold. While a linear increasing trend was expected for the hosting capacity of the dendrimers while growing with the generation, this was not verified for this series of dendrimers. In fact, the accessibility of pyrene and camptothecin was found to increase up to G7, and to decrease again for larger generations. All-atom MD simulations of G3-G11 dendrimers in water solution showed a similar behavior for what pertained to water accessibility in the interior of the dendrimer. Shown in Fig. 10.7c,d pyrene and camptothecin incorporations report a nearly linear trend with water capacity in the dendrimers.

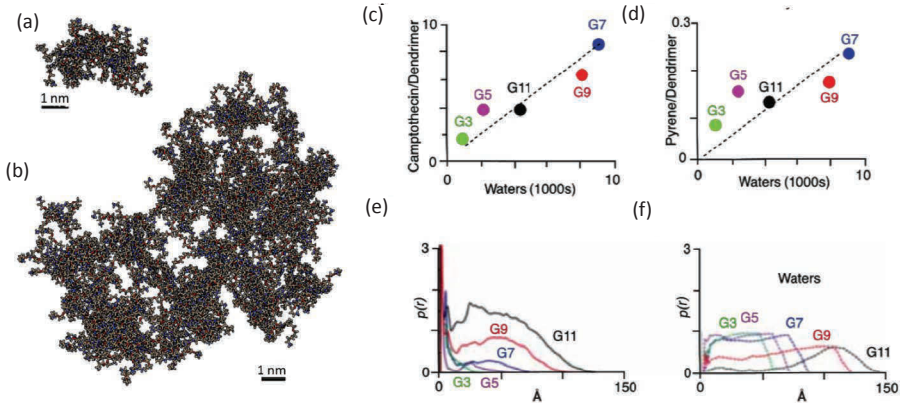



**Figure 10.7** Simulating different generation triazine dendrimers and assessing their level of guest capacity. (a) Equilibrated configuration of G3 dendrimer. (b) Equilibrated configuration of G7 dendrimer. (c,d) Nearly linear correlation between camptothecin (c) and pyrene (d) content (experiment) with water penetration (MD) in the dendrimers as a function of the dendritic generation. (e) Radial distribution function $g(r)$ of the dendrimer atoms. The dendrimer's density increases while increasing the dendritic generation. (f) $g(r)$ of the water molecules respect to the dendrimer's center. A higher dendrimer's density hinders water penetration inside the scaffold for generations larger than G7 (G9, and particularly G11).

This inversion in the guest capacities for dendrimers of generations larger than G7 (Fig. 10.7b) finds consistency with the structural data extracted from the MD simulations. The radial distribution functions, $g(r)$, of the atoms of the dendrimers demonstrate that the density in the dendrimers also increases for larger dendritic generations (Fig. 10.7e,f). In particular, for G9 and G11 the density on the dendrimer surface increases dramatically, while, consistently, there is a drop in water accessibility (Fig. 10.7e,f). Thus, dendrimer's guest capacity reaches a maximum over which further penetration of guests (and water molecules) inside the scaffold is hindered due to increasing structural crowding. In this case, the structural characterization obtained from the simulations provided a molecular rationale useful to explain the guest properties of the dendrimers.

04:36 30 October 2016

### 10.4.2 Dendrimers' Flexibility

Molecular flexibility is one of the CNDPs proposed by Tomalia, and it is highlighted as one intrinsic property of the dendrimers. However, the flexibility/rigidity property of a macromolecule, such as a dendrimer, in solution is not easy to be defined, and proposed controversial interpretations in the last years.

Previously in this chapter, we discussed the controversial rigidity/flexibility of the triazine F2-1 dendrimer (Fig. 10.4), which was designed with three long flexible branches, but once immerged in an aqueous environment, it folded assuming a rigid globular shape. This poses the interesting general question: What is flexibility? This example clearly shows that the simple chemical structure of a dendrimer is not sufficient to answer this question, because it is first necessary to understand how we can define flexibility. What do we mean by "flexibility"? The intrinsic flexibility of the chemical structure of the dendrimer? Which is the same that allows F2-1 undergoing complete folding in water due to hydrophobic effects? Or by "dendrimer flexibility" are we interested into the real flexibility of the folded dendrimer in solution? In the latter case, F2-1 cannot be considered as a flexible molecule, but as a rigid one in water. Similar examples are seen also for different structures, such as, for example, flexible dendritic molecular glues for tubulin binding that are folded, spherical and rigid in water solution.[81] Indeed, the intrinsic flexibility of

04:36 30 October 2016

the chemical structure of the dendrimer, and its real flexibility in solution (folded state) are two different (yet related) properties. While the former is just and intrinsic property of the dendrimer, the latter clearly depends on the chemical structure of the dendrimer and on the external environment.

***Dendrimer's flexibility during binding/adhesion***. Let's consider the case of cationic dendrimers (i.e., $NH_2$-terminated dendrimers) binding negatively charged molecular targets (DNA, proteins, etc.). At neutral pH, let's assume that all the primary amino groups of the dendrimers are protonated ($NH_3^+$). The number of surface groups grows together with the dendritic generation. For this reason, it would be reasonable to imagine that the larger the dendritic generation, the stronger the attraction for an oppositely charged molecule (e.g., DNA, negatively charge proteins, etc.). This is quite widely accepted, and experiments demonstrate that better gene delivery properties can also be achieved at higher dendritic generation.[93] However, together with the number of surface functions, also the dendrimer density and structural crowding increase with the generation, and the higher structural rigidity of large generation dendrimers limits the binding efficiency.[94] In fact, a dense surface with strong backfolding of the surface groups prevents the rearrangement of the dendrimer to optimize the interaction.[48] This is a general effect of dendrimer's rigidity. What is the maximum generation limit separating the flexible generations from large rigid dendrimers[33,34,48]? Understanding the limits of the dendrimer structure can allow, in principle, to control the interactions through different scales.[41]

One interesting lesson on this effect can be extracted from the simulation of the binding between different dendrimers and nucleic acids (Fig. 10.8). Clearly, small dendrimers such as G1 PAMAM are more responsive during binding than a large rigid dendrimer. In Fig. 10.8d, the comparison between the $g(r)$ curves of G1 PAMAM when it is bound to DNA/siRNA or unbound in solution show large discrepancy. This demonstrates that this small dendrimer is very responsive to the interaction with the target (large structural reorganization). On the other hand, a large G6 PAMAM shows negligible structural response to binding. G1 PAMAM completely collapses over the double strand of DNA to optimize the interaction, but at the same time, it also loses all

its degrees of freedom (flexible binding). On the other hand, this is not true for a large dendrimer, which interacts with the target as a rigid sphere (rigid binding). 25 kDa PEI shows an intermediate behavior (Fig. 10.8c,f).

When looking at the energies of binding, the ratio (EF index) between the enthalpy ($\Delta H$) and the entropic cost of binding ($T\Delta S$) – EF = $\Delta H/T\Delta S$—is a good energy descriptor of this effect (Fig. 10.8h).[48,57] While $\Delta H$ captures the electrostatic attraction of the binding, the $T\Delta S$ term represents the "cost" of binding—namely, how structural expensive it is for one molecule to enhance the interaction. EF is typically low for very flexible binders, where the interaction is very strong, but the entropic cost for binding is also very high. EF is low also for rigid binding, where the entropic cost is low, but the interaction is also weaker. EF increases and reaches a maximum for Intermediate generation dendrimers that can optimize the strength of the interaction while limiting the entropic penalty (Fig. 10.8h: 25kDa PEI, G4 and G5 PAMAM).[33,34,38,39,48,57]

From the ratio between the binding energy $\Delta G$ (per-charged group) and the EF parameter, it can be extracted also another interesting parameter—the stickiness index: Stickiness = $(-\Delta G)$/EF (Fig. 10.8i).[41] Higher stickiness values identify more sticky binders—the dendrimer collapses over the surface of the target during adhesion. This index drops for rigid binding. All these analyses provide an interpretation on flexibility based on the energy of binding, and on the interaction with one macromolecular target. Thus, these are based on the interpretation on flexibility as the "reaction to a stimulus" (binding).

As said before, the backfolding of the surface groups is also intrinsically related to dendrimer's rigidity. The more the surface groups are backfolded and surrounded by a crowded environment, the more the binding will be rigid, because for the structure is too expensive to unfold the surface charges to optimize the binding. For example, shown in Fig. 10.9, large dendrimers such as G6 PAMAM have higher level of structural crowding and overall rigidity than small and flexible binders such as G1 PAMAM. For this reason, the former binds in a rigid way while the latter is able to stick tightly to the target. In fact, in the case of G1 PAMAM, the peak of the surface groups $g(r)$, most probable position for the surface groups calculated respect to the dendrimer center, is in the same position of the peak of the P atoms of siRNA, coincident with the hydrodynamic radius ($R_h$) of the dendrimer (Fig. 10.9d).

04:36 30 October 2016

04:36 30 October 2016

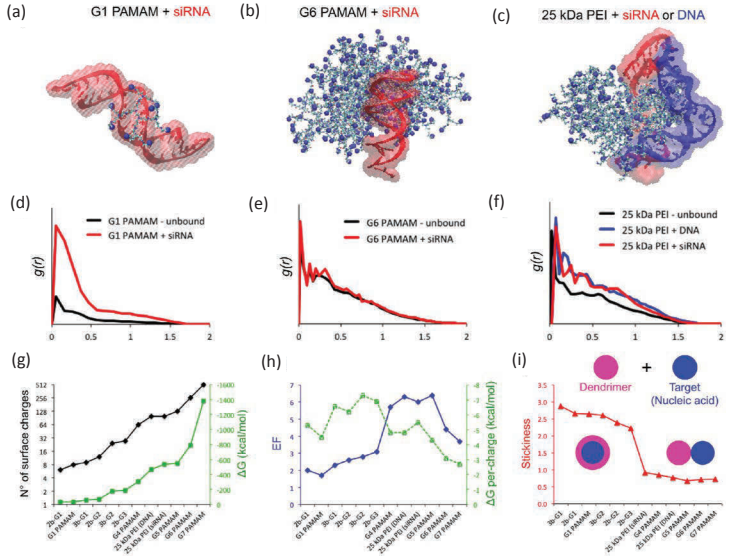



**Figure 10.8** Flexible vs. rigid interaction between dendrimers and nucleic acids (DNA or siRNA). Equilibrated configurations of the complexes of G1 PAMAM (a) and of G6 PAMAM (b) with siRNA (red) and 25 kDa PEI (c) with a slice of DNA (blue) and siRNA (red). The cationic surface charges in the dendrimers are represented as blue spheres. (d-f) The $g(r)$ of the dendrimer's atoms in the unbound (black) and the bound (red) state provide clear evidence of the level of structural rearrangement of the different dendrimers during binding (large difference between black and red curves means that the dendrimer strongly rearrange during binding). (g-i) Effect of dendrimer's flexibility on binding with DNA and siRNA. (g) Binding energy ($\Delta G$: green) obtained from the MD simulations for different dendritic structures with different size and variable number of surface cationic groups (black)—binding strength (green) does not follow strictly the number of surface groups (black). (h) Binding energy ($\Delta G$: green) normalized per-charge and EF indicator (EF = $\Delta H/T\Delta S$: blue) for the different dendrimers. EF represents the ratio between the enthalpic attraction between the cationic charges of the dendrimers and the nucleic acid (mostly electrostatically driven in these cases) and the entropic cost for binding.[48,57] (i) Stickiness calculated as per-charge binding energy ($-\Delta G$) divided for EF of the different dendrimers. This score represents how sticky the adhesion of the dendrimer is onto the nucleic acid—the higher the score, the higher the dendrimer stickiness. Between very small dendrimers (e.g., G1 PAMAM) and dendrons (e.g., 3b-G1), and large dendrimers (e.g., G7 PAMAM) there is net transition between flexible and rigid binders.

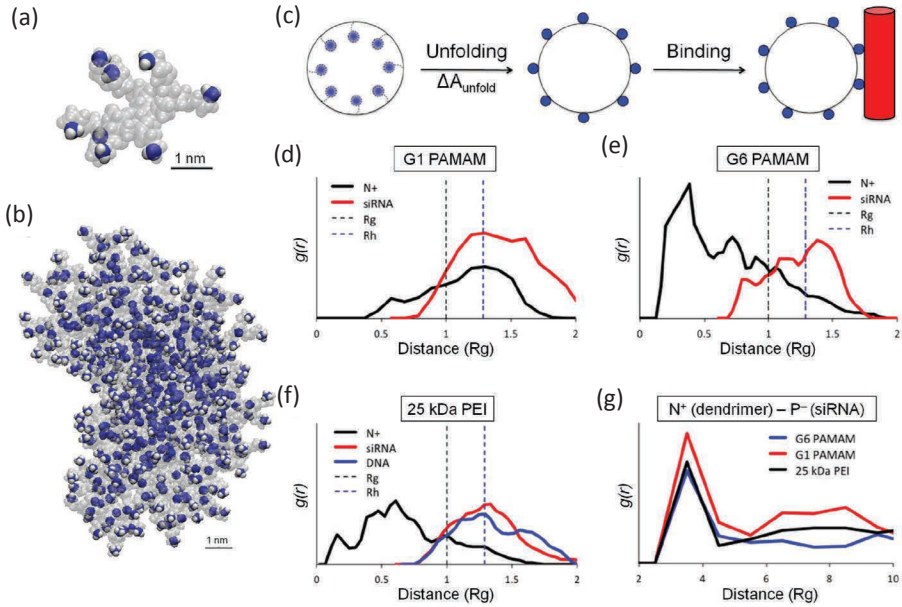



**Figure 10.9** Effect of surface groups backfolding on binding. (a,b) Equilibrated configurations of G1 PAMAM (a) and G6 PAMAM (b)—visually, while surface charges backfolding is absent in G1 PAMAM, many charged groups (blue spheres) are backfolded in the G6 PAMAM interior. (c) Scheme: how much energy $\Delta A_{unfold}$ is necessary to drag out the surface charges from their backfolded state and to make them available for binding? (d–f) Different levels of backfolding: the flexible G1 PAMAM (d) has negligible backfolding (superposition of the black and red $g(r)$ peaks related to the distribution of $N^+$ groups from the dendrimer and the nucleic acid's atoms calculated respect to the dendrimer's CM). On the other hand, strong backfolding is present in the larger G6 PAMAM (e). (f) The 25 kDa PEI has intermediate behavior, invariant whether it binds siRNA or dsDNA. (g) The stronger the surface groups backfolding, the less strong the binding and electrostatic coordination between the $N^+$ groups from the dendrimer and the $P^-$ atoms of siRNA. Higher the $N^+$–$P^-$ coordination peak height ($g(r)$) identifies stronger and more stable coordination during binding. The black and blue dotted lines represent the dendrimers radius of gyration ($R_g$) and the hydrodynamic radius ($R_h$), respectively (calculated according to a spherical colloidal model as $R_h \approx 1.29\ R_g$).[38,39,62]

04:36 30 October 2016

The effect of backfolding on binding can be directly extracted from the $g(r)$ of the surface groups of the dendrimers.[41,95,96] Table 10.1 reports the free energy necessary ($\Delta A_{\text{unfold}}$) to unfold the surface charges (values are per-surface charge) and to make them optimally available for binding for the different cases. The higher the $\Delta A_{\text{unfold}}$, the stronger the backfolding, and the more the dendrimer will interact with the target in a rigid manner.

**Table 10.1** Effect of backfolding on binding. Per-charged group $\Delta A_{\text{unfold}}$ values are reported for the different dendrimers shown in Fig. 10.8 and expressed in kcal/mol

| Dendrimer | G1 PAMAM | G6 PAMAM | 25 kDa PEI (DNA) [a] | 25 kDa PEI (siRNA) [a] |
|---|---|---|---|---|
| $\Delta A_{\text{unfold}}$ [b] | 0 kcal/mol | 1.1 kcal/mol | 0.8 kcal/mol | 0.9 kcal/mol |

[a] $\Delta A_{\text{unfold}}$ is reported for 25 kDa PEI both in the case of DNA and siRNA binding.
[b] $\Delta A_{\text{unfold}}$ values are per-charge energies expressed in kcal/mol.

The values reported in Table 10.1 (per-surface charged group) are consistent with the data in Fig. 10.8. The unfolding energy necessary for the G1 PAMAM case is negligible, as in this small dendrimer the surface charges are always well available at the surface to produce a "sticky" and strong binding. On the other hand, $\Delta A_{\text{unfold}}$ increases with the dendritic generation, and larger dendrimers interact as rigid charged spheres in solution.

***Dendrimer's flexibility in the solvent***. The previous examples provided a description of molecular flexibility as the ability of one dendrimer to react/respond to optimize binding. On the contrary, in this section it will be shown how molecular simulation can give information on the flexibility of the dendrimers in solution.

One possible way to estimate the intrinsic flexibility of a dendrimer in solution is to study its vibrations/oscillations around the equilibrium configuration—the higher the oscillation, the higher the dendrimer flexibility. This can be reliably captured, for example, by using metadynamics simulations.

As an example of complex dendrimers, we report the case of pegylated G2 PAMAM dendrimers. Classical MD simulations have been used to study dendrimer-PEG conjugates in solution.[97,79] In general, both experimental and simulation studies reported that, despite the linear structure of the PEG chains, these tend

04:36 30 October 2016

to fold in solution.[98–104] Recent computational works using WT-MetaD simulations on dendrimers with variable levels of pegylation also demonstrated that the starting star-like open configurations typically reported in many dendrimer works are very unlikely in solution (Fig. 10.10a–d).[90,105]

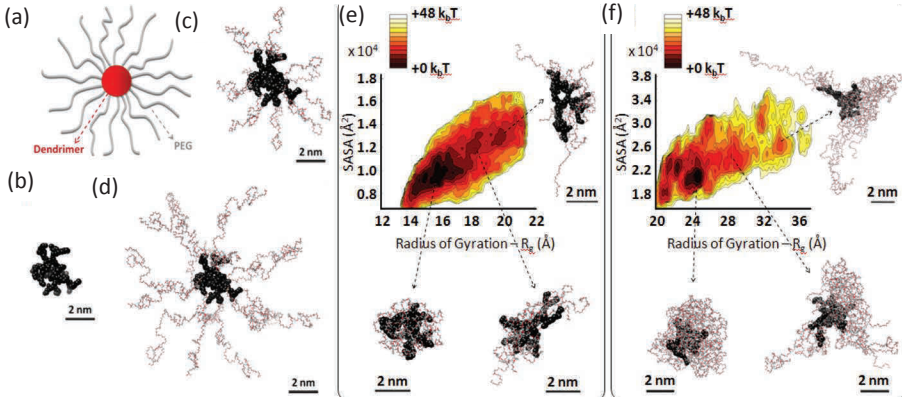



**Figure 10.10** WT-MetaD simulations of pegylated G2 PAMAM dendrimers in solution. (a) Idealized scheme for pegylation—hydrophilic PEG chains (grey) are conjugated to the primary amines of G2 PAMAM (red). The starting structure of **G2**, **G2+** (b) and **G2-550PEG** (c) are obtained by deletion or shortening of the PEG chains of **G2-2kPEG**. (d) The dendrimer atoms are represented as black spheres, PEG is colored by atom (C: grey, O: red and H: white). Explicit water molecules and ions are not shown for clarity. (e–f) The free energy surfaces (FES) of **G2-550PEG** (e) and **G2-2kPEG** (f) obtained from WT-MetaT simulations and calculated with respect to solvent accessible surface area (SASA—$y$ axis) and radius of gyration ($R_g$—$x$ axis). Isolines identify free energy differences of 4 $k_bT$. The darkest the FES regions are the most energetically accessible, and are representative of the most probable molecular configurations. The dendrimer atoms are represented as black spheres, PEG is colored by atom (C: grey, O: red and H: white). Explicit water molecules and $Cl^-$ and $Na^+$ ions are not shown for clarity.

The FES of the pegylated variants G2-550PEG and G2-2kPEG (Fig. 10.10), having 16 PEG chains with MW of 550 Da and 2000 Da, respectively, connected to the surface of the

04:36 30 October 2016

04:36 30 October 2016

dendrimer, show clear minimum energy regions at low $R_g$ and SASA values. This means that these dendrimers are indeed likely to be folded into globular configurations rather than extended in water solution. The shape of the FES basin describes the level of flexibility of the dendrimer in solution. Namely, the larger and the flatter the free energy minimum, the more flexible the dendrimer, as the same dendrimer has the same probability to exist in solution with different sizes. In Fig. 10.6b, G2 PAMAM dendrimer at neutral pH has a size between $R_g$ = 12–19 Å ($R_g$ = 15.5 ± 3.5 Å). On the other hand, when G2 PAMAM is surrounded by the longer PEG chains (G2-2kPEG), the most probable size ranges $R_g$ = 23–25 Å ($R_g$ = 24 ± 1 Å). Clearly, the presence of the positive charges at the surface of G2 at neutral pH imparts a high flexibility to the dendrimer, while a massive pegylation enhances structural rigidity—size fluctuates by ≈20% for G2+ PAMAM and only <5% for the larger G2-2kPEG. Similar results have been recently obtained also for pegylated PPH (poly(phosphorhydrazone)) dendrimers.[105]

### 10.4.3 Dendrimers Self-Assembly Solution

The configuration assumed by the dendrimers can also control the inter-dendrimer interaction and self-assembly in solution. Well illustrated by the work of Glotzer, it is quite accepted that the shape of interacting particles, presence of hydrophobic patches or of charged domains on the particles surface can play a fundamental role triggering inter-particle interactions and self-assembly (Fig. 10.11a).[106–108] Thus, it is clear that the configuration assumed by the dendrimers in solution is of pivotal importance for their interactions and self-assembly. This is what happens in general also for biological molecules (e.g., proteins), where the shape and unique features of each protein is crucial for molecular recognition, inter-protein self-assembly, and the supramolecular formation of higher-scale complex biomaterials such as microtubules, protein capsids, etc. Again, to understand intermolecular interactions and self-assembly, it is first necessary to have sufficient comprehension of the interacting elements in a certain environment.[38,39,81,109]

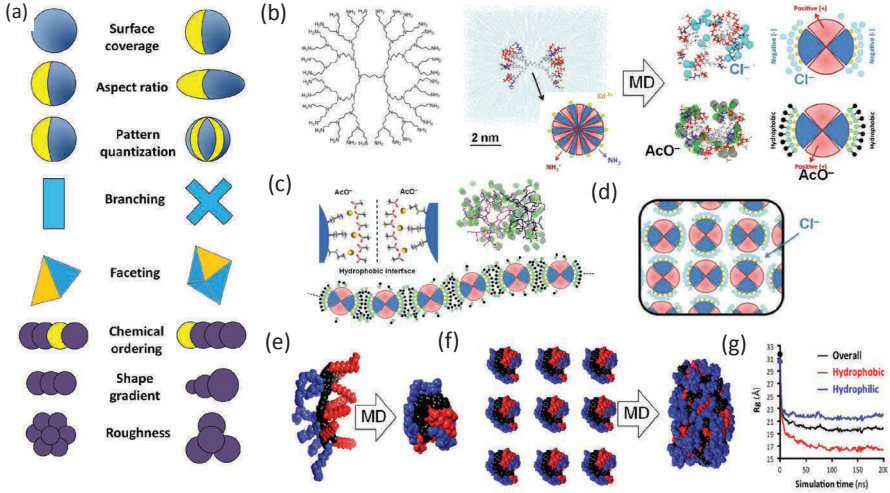



**Figure 10.11** The effect of dendrimer's shape and features in solution on self-assembly. (a) Structural parameters controlling supramolecular aggregation. (b) G4 PPI dendrimers in a solution containing Cadmium acetate assume an anisotropic shape with formation of hydrophobic surface patches due to ionic effects. On the other hand, in the case of Cadmium chloride, the patches are negatively charged. This leads to unidirectional assembly and formation of fibers in solution in the former case, and random electrostatic aggregation in the latter case. (c,d) Asymmetric $AcO^-$ ions generate the 1D assembly of nanofibers in solution while asymmetric $Cl^-$ ions induce 3D aggregation into globular assemblies. (e) Amphiphilic dendrons fold in solution assuming a globular shape in water. The length of the hydrophilic PEG chains (blue) is not sufficient to screen the hydrophobic parts of the structure (red: alkyl chains, black: scaffold). (f) The presence of hydrophobic patches (red and black) triggers dendrons aggregation. (g) Rearrangement upon aggregation demonstrated by the radius of gyration ($R_g$) of the hydrophobic and hydrophilic chains of the dendron aggregate during the MD simulation.

A recent example on dendrimers reported that the shape assumed by G4 PPI dendrimers in aqueous solution and in the presence of cadmium acetate may induce the directional self-assembly of the dendrimers into supramolecular fibers.[109] In this case, the interaction of the dendrimers with the ions in solution led to the formation of ionic clusters on the dendrimer's surface,

04:36 30 October 2016

04:36 30 October 2016

which transformed the dendrimers into interacting particles having different surface patches (Fig. 10.11b). While in the case of $Cl^-$ the patches generated on the dendrimer's surface have opposite charge (negative or positive), $AcO^-$ ions locally neutralize the dendrimers and generate hydrophobic regions on the surface (Fig. 10.11b). While in the former case, a random electrostatic higher-scale aggregation of the dendrimers is obtained (Fig. 10.11d), in the latter case the dendrimer self-assembled in directional manner due to hydrophobic effects (Fig. 10.11c).

Similar effects are seen for the small amphiphilic dendrons shown in Fig. 10.11e–g. While the single dendrons fold in solution into a globular shape, the hydrophilic PEG chains (blue) are not long enough to shield the hydrophobic alkyl tails of the dendrons (red) from the interaction with the solution. Hydrophobic regions remain thus exposed to the solvent, which is the trigger to self-assembly.[110] The $R_g$ data for the different groups of the dendrons as a function of simulation time show that during aggregation the dendrons rearrange toward a configuration where the hydrophobic tails are gathered in the interior of the aggregate and surrounded by hydrophilic PEG chains (micelle).[96] Molecular modeling can also provide deeper details of the self-assembly process, such as how much of this is due to different groups in the structure (tails, scaffold, etc.) or to different types of interactions (electrostatic, H-bonding, hydrophobic).[111]

### 10.4.4 Dendrimers Aggregates Responsive to External Stimuli

During the dendrimers self-assembly process, different kinds of hydrophobic guests can be incorporated into the aggregate (drugs, contrast agents, etc.), which can have broad impact in several applications such as drug delivery, imaging, etc.[112–115] Particularly interesting is the development of a supramolecular structure that can assemble in certain conditions and disassemble in controlled way when the conditions change (release of the guests). In general the development of a multiscale material capable of responsive structural transitions that can be controlled with high precision similar to biological materials (bio-inspired materials) is of high technological interest. Supramolecular systems that disassemble in response to changes in the external conditions (e.g., pH[116,117]

04:36 30 October 2016

or redox[118,119] variations, exposure to light,[120,121] temperature variation,[122–124] or magnetic field[125,126]) have been investigated in the last years. While most of these stimuli can be considered as secondary in several pathologies, primary ones may result from protein or enzymatic activity.[127–129] The rational design of supramolecular materials that can respond to precise biological stimuli in controlled way is thus a hot topic, but very difficult to achieve due to the extreme complexity of the systems.[6,130–136]

As molecular simulation is extremely useful to study intermolecular interactions, solvent effects, and intermolecular self-assembly, it is also the ideal support to understand the responsive behavior of supramolecular dendrimer assemblies to external stimuli. At molecular level, for example, MD simulations allowed to study the structural transition from dense core-flexible surface to porous core-dense surface of PAMAM dendrimers upon changing the pH from neutral to low.[47,48] MD also allowed to understand that surface modifications in catalytic dendrimers can control the catalytic activity by allowing or preventing the access of substrate molecules to the dendrimer's catalytic core.[137] At supramolecular level, molecular simulations can be used to study the variation of the stability in an assembly caused by a change in the external conditions (e.g., temperature, pH, ionic strength, etc.), or by the interaction with other molecules (e.g., proteins, etc.). In this way, this allows to correlate the effect of the external stimulus to the molecular interactions and supramolecular transitions.

For example, all-atom MD simulations have recently been used to explore the self-assembly and disassembly behavior of facially amphiphilic dendrons (Fig. 10.11e–g).[50,96] When one biotin ligand is inserted in the dendron scaffold, the dendron self-assembly become sensitive to the specific interaction with the biotin-complementary protein: avidin.[96] In particular, it was demonstrated that the avidin specific binding to one biotin ligand in the dendron structure compromise the stability of the dendron self-assembly. In particular, from the MD simulations it was extracted the dendron self-assembly energy of the aggregate in the presence (Fig. 10.12a–c) or in the absence (Fig. 10.12d) of a specifically bound avidin protein. The difference between the measured self-assembly energy $\Delta E_{ass}$ in the two cases ($\Delta E_{ass}$) is an indicator

of the destabilization induced by the specific avidin binding in the aggregate (Fig. 10.12e). Data from the simulations show that the presence of even one single specific interaction at the surface of a dendron aggregate locally destabilize the self-assembly by ≈15 kcal/mol (per-dendron)—the self-assembly energy becomes one half (the stability of the unperturbed dendron aggregate is $\Delta E_{ass} \approx -30$ kcal/mol).[96]

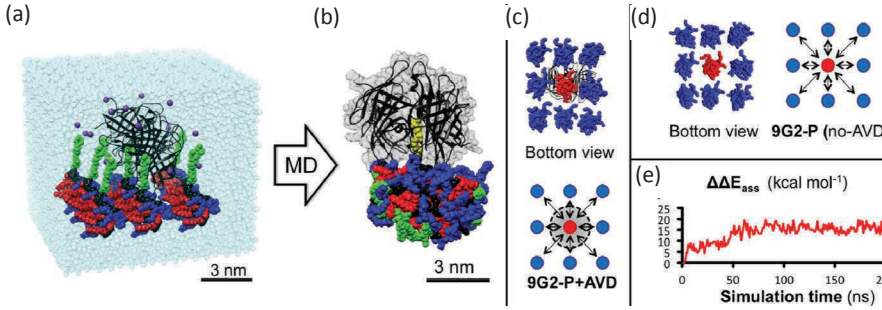



**Figure 10.12** MD simulation of dendron assemblies responsive to protein specific binding. (a) The starting configuration for the molecular system containing nine dendrons and avidin protein (AVD: black ribbons) specifically bound to the biotin ligand (green) of the central dendron. $Cl^-$ ions (purple) were also added for neutralization. (b) Equilibrated configuration of the same system. The same system was also simulated in the absence of the bound avidin and the self-assembly in the two cases was compared. (c, d) The inter-dendron self-assembly energy ($\Delta E_{ass}$) was calculated both in the presence (c) and in the absence (d) of specifically bound AVD. (e) The energetic difference $\Delta E_{ass}$ (red) identifies the dendron self-assembly destabilization due to AVD binding.

This approach can be generalized to study a multitude of different stimuli responsive systems. Different kinds of perturbations can be easily explored by means of in silico simulations, where changes in temperature, pH, ionic strength, etc. can be simulated as modifications in the external conditions. The combination of theory and experiments allows to obtain unique insight into the molecular and supramolecular effect of the stimulus, providing a molecular basis to comprehension that could not be reached without the use of models.

04:36 30 October 2016

04:36 30 October 2016

## 10.5 Conclusions and Future Perspectives

In this chapter we have discussed the opportunities provided by the use of molecular modeling to study the complex behavior of dendrimers in different situations. Computer-aided simulations can tackle the blind spots of the experiments, mainly related to the reduced contrast offered by the dendrimers in solution, their relative monodispersity, and their flexible and responsive structure. On a first step, molecular simulation can provide a unique insight into the solvated state of the dendrimers, and a molecular-level characterization at atomistic resolution that is beyond the possibility of the experiments. On a second step, it allows studying intermolecular interactions in great detail. These include the interactions of the dendrimers with other molecular species (binding), or between themselves (self-assembly). The versatility of the modeling approach also allows to explore multiple spatial and time scales, when more coarse models are employed to simulate larger systems for longer times in spite of acceptable approximations.

The world of in silico molecular modeling is in continuous development. The increasing computational power at disposal granted by more and more powerful hardware and increasingly performant dedicated software pushes nowadays the use of molecular simulation as a crucial part of chemistry research, exactly as it happened in the past with finite element methods and structural modeling for engineering. Clearly, a lot of work still needs to be done both for the calculation performance and accuracy of the models. The efficiency of the simulations toward a better sampling is also under constant development, together the development of reliable CG models with increasing transferability, which could enhance the confidence in modeling multiple scales in a simpler way. All these fields of development still require considerable work, which will hopefully help to improve further the fundamental support provided by molecular modeling and computer simulations to the experimental research.

## References

1. Newkome G. R., Moorefield C. N., Vögtle F., *Dendrimers and Dendrons: Concepts, Syntheses, Applications*, Wiley-VCH, Weinheim, 2001.

04:36 30 October 2016


2. Fréchet J. M. J., Tomalia D. A., *Dendrimers and Other Dendritic Polymers,* John Wiley and Sons, New York, 2002.
3. Smith D. K., *Tetrahedron,* **59**, pp. 3797–3798, 2003.
4. Tomalia D. A., Birth of a new macromolecular architecture: Dendrimers as quantized building blocks for nanoscale synthetic polymer chemistry, *Prog. Polym. Sci.,* **30**, pp. 294–324, 2005.
5. Svenson S., Tomalia D. A., Dendrimers in biomedical applications: Reflections on the field, *Adv. Drug Deliv. Rev.,* **57**, pp. 2106–2129, 2005.
6. Lee C. C., MacKay J. A., Frechet J. M., Szoka F. C., Designing dendrimers for biological applications, *Nat. Biotech.,* **23**(12), pp. 1517–1526, 2005.
7. Fox M. E., Szoka F. C., Frechet J. M., Soluble polymer carriers for the treatment of cancer: The importance of molecular architecture, *Acc. Chem. Res.,* **42**, pp. 1141–1151, 2009.
8. Caminade A. M., Fruchon S.,. Turrin C. O, Poupot M., Ouali A., Maraval A., Garzoni M., Maly M., Furer V., Kovalenko V., Majoral J. P., Pavan G. M. and Poupot R., The key role of the scaffold on the efficiency of dendrimer nanodrugs, *Nat. Commun.,* **6**, p. 7722, 2015.
9. Vogtle F., Richardt G., Werner N., Rackstraw A. J., *Dendrimer Chemistry*, Wiley-VCH, Weinheim, 2009.
10. Newkome G. R., He E. F., Moorefield C. N., Suprasupermolecules with novel properties: metallodendrimers, *Chem. Rev.,***99**, pp. 1689–1746, 1999.
11. Buhleier E., Wehner W., Vögtle F., "Cascade"- and "nonskid-chain-like" syntheses of molecular cavity topologies, *Synthesis,* **2**, pp. 155–158, 1978.
12. Tomalia D. A., Baker H., Dewald J., Hall M., Kallos G., Martin S., Roeck J., Ryder J., Smith P., A new class of polymers: Starburst-dendritic macromolecules, *Polym. J.,* **17**, p. 117, 1985.
13. Tomalia D. A., Christensen J. B., Boas U., *Dendrimers, Dendrons, and Dendritic Polymers: Discovery, Applications, and the Future*, Cambridge University Press, 2012.
14. Newkome G. R., Yao Z., Baker G. R., Gupta V. K., Micelles. Part 1. Cascade molecules: A new approach to micelles. A [27]-arborol, *J. Org. Chem.,* **50**, p. 2003, 1985.
15. Caminade A. M., Turrin C. O., Laurent R., Ouali A., Delavaux-Nicot B., *Dendrimers: Towards Catalytic, Material and Biomedical Uses*, Wiley, 2011.

16. Mammen M., Choi S. K., Whitesides G. M., Polyvalent interactions in biological systems: implications for design and use of multivalent ligands and inhibitors, *Angew. Chem. Int. Ed.,* **37**, p. 2754–2794, 1998.

17. Kukowska-Latallo J. F., Bielinska A. U., Johnson J., Spindler R., Tomalia D. A., Baker J. R., Efficient transfer of genetic material into mammalian cells using Starburst polyamidoamine dendrimers, *Proc. Natl. Acad. Sci. U. S. A.,* **93**, pp. 4897–4902, 1996.

18. Tang M. X., Szoka F. C., The influence of polymer structure on the interactions of cationic polymers with DNA and morphology of the resulting complexes, *Gene Ther.,* **4**, pp. 823–832, 1997.

19. Guillot-Nieckowski M., Eisler S., Diederich F., Dendritic vectors for gene transfection, *New. J. Chem.,* **31**, pp. 1111–1127, 2007.

20. Doni G., Kostiainen M. A., Danani A., Pavan G. M., Generation-dependent molecular recognition controls self-assembly in supramolecular dendron-virus complexes, *Nano Lett.,* **11**, pp. 723–728, 2011.

21. Uchida N., Okuro K., Niitani Y., Ling X., Ariga T., Tomishige M., Aida T., Photoclickable dendritic molecular glue: Noncovalent-to-covalent photochemical transformation of protein hybrids, *J. Am. Chem. Soc.,* **135**, p. 4684–4687, 2013.

22. Okuro K., Kinbara K., Takeda K., Inoue Y., Ishijima A., Aida T., Adhesion effects of a guanidinium ion appended dendritic "molecular glue" on the ATP-driven sliding motion of actomyosin, *Angew. Chem. Int. Ed.,* **49**, p. 3030–3033, 2010.

23. Parekh H. S., The advance of dendrimers: A versatile targeting platform for gene/drug delivery, *Curr. Pharm. Des.,* **13**, pp. 2837–2850, 2007.

24. Luo D., Haverstick K., Belcheva N. Han, E., Saltzman W. M., Poly(ethylene glycol)-conjugated PAMAM dendrimer for biocompatible, high-efficiency DNA delivery, *Macromolecules,* **35**, pp. 3456–3462, 2002.

25. Hsu C. Y., Uludag H., A simple and rapid nonviral approach to efficiently transfect primary tissue-derived cells using polyethylenimine, *Nat. Protoc.,* **7**, pp. 935–945, 2012.

26. Boussif O., Lezoualch F., Zanta M. A., Mergny M. D., Scherman D., Demeneix B., J. P. Behr, A versatile vector for gene and oligonucleotide transfer into cells in culture and in vivo: polyethylenimine, *Proc. Nat. Acad. Sci. U. S. A.,* **92**, pp. 7297–7301, 1995.

27. Rudolph C., Lausier J., Naundorf S., Müller R. H., Rosenecker J., In vivo gene delivery to the lung using polyethlenimine and fractured polyamidoamine dendrimers, *J. Gen. Med.,* **2**, pp. 269–278, 2000.

04:36 30 October 2016

04:36 30 October 2016

28. Kostiainen M. A., Hardy J. G., Smith D. K., High-affinity multivalent DNA binding by using low-molecular-weight dendrons, *Angew. Chem. Int. Ed.,* **44**, pp. 2556–2559, 2005.

29. Pavan G. M., Danani A., Pricl S., et al., Modeling the multivalent recognition between dendritic molecules and DNA: Understanding how ligand "Sacrifice" and screening can enhance binding, *J. Am. Chem. Soc.,* **131**, pp. 9686–9694, 2009.

30. Tomalia D. A., In quest of a systematic framework for unifying and defining nanoscience, *J. Nanopart. Res.,* **11**, pp. 1251–1310, 2009.

31. Tomalia D. A., Dendritic effects: Dependency of dendritic nano-periodic property patterns on critical nanoscale design parameters (CNDPs), *New J. Chem.,* **36**, pp. 264–281, 2012.

32. Tomalia D. A., Dendrons/dendrimers: Quantized, nano-element like building blocks for soft-soft and soft-hard nano-compound synthesis, *Soft Matter,* **6**, pp. 456–474, 2010.

33. Pavan G. M., Danani A., Dendrimers and dendrons for siRNA binding: Computational insights, *J. Drug Deliv. Sci. Technol.,* **22**, pp. 83–89, 2012.

34. Pavan G. M., Danani A., Supporting the design of efficient dendritic DNA and siRNA nanocarriers with molecular modeling, *Curr. Drug Discov. Tech.*, **8**, pp. 314–328, 2011.

35. Shema-Mizrachi M., Pavan G. M., Levin E., Danani A., Lemcoff N. G., Catalytic chameleon dendrimers, *J. Am. Chem. Soc,* **133**, pp. 14359–14367, 2011.

36. Lim J., Kostiainen M. A., Maly J., da Costa V. C. P., Annunziata O., Pavan G. M., Simanek E. E., Synthesis of large dendrimers with the dimensions of small viruses, *J. Am. Chem. Soc.,* **135**, pp. 4660–4663, 2013.

37. Pinto L. F., Correa J., Martin-Pastor M., Riguera R., Fernandez-Megia E., The dynamics of dendrimers by NMR relaxation: Interpretation pitfalls, *J. Am. Chem. Soc.,* **135**, no. 5, p. 1972–1977, 2013.

38. Simanek E. E., Enciso A. E., Pavan G. M., Computational design principles for the discovery of bioactive dendrimers: [s]-triazines and other examples, *Exp. Opin. Drug Discov.,* **8**, pp. 1057–1069, 2013.

39. Lim J., Lo S.-T., Hill S., Pavan G. M., Sun X., Simanek E. E., Antitumor activity and molecular dynamics simulations of paclitaxel-laden triazine dendrimers, *Mol. Pharm.,* **9**, pp. 404–412, 2012.

04:36 30 October 2016


40. Jensen L. B., Pavan G. M., Kasimova M. R.,Rutherford S., Danani A., Nielsen H. M., Foged C., Elucidating the molecular mechanism of PAMAM–siRNA dendriplex self-assembly: Effect of dendrimer charge density, *Int. J. Pharm.,* **416**, pp. 410–418, 2011.
41. Pavan G. M., Modeling the interaction between dendrimers and nucleic acids: A molecular perspective through hierarchical scales, *Chem. Med. Chem.,* **9**, pp. 2623–2631, 2014.
42. Tian W. D., Ma Y. Q., Theoretical and computational studies of dendrimers as drug delivery vectors, *Chem. Soc. Rev.,* **42**, pp. 705–727, 2013.
43. Meneksedag-Erol D., Tang T., Uludag H., Molecular modeling of polynucleotide complexes, *Biomaterials,* **35**, pp. 7068–7076, 2014.
44. De Gennes P. G., Hervet H. J., Statics of "starbust" polymers, *J. Phyisique Lett.,* **44**, pp. 351–359, 1983.
45. van Dongen M. A., Desai A., Orr B. G., Baker J. R. Jr., Banaszak Holl M. M., Quantitative analysis of generation and branch defects in G5 poly(amidoamine) dendrimer, *Polymer,* **54**(16), pp. 4126–4133, 2013.
46. Ballauff M., Likos C. N., Dendrimers in solution: Insight from theory and simulation, *Angew. Chem. Int. Ed.,* **43**, pp. 2998–3020, 2004.
47. Liu Y., Bryantsev V. S., Diallo M. S., Goddard W. A., PAMAM dendrimers undergo pH responsive conformational changes without swelling, *J. Am. Chem. Soc.,* **131**, pp. 2798–2799, 2009.
48. Pavan G. M., Albertazzi L., Danani A., Ability to adapt: Different generations of PAMAM dendrimers show different behaviors in binding siRNA, *J. Phys. Chem. B,* **114**, pp. 2667–2675, 2010.
49. Fuller J., Raghupathi K., Ramireddy R. R., Subrahmanyam A., Yesilyurt V., Thayumanavan S., Temperature-sensitive transitions below LCST in amphiphilic dendritic assemblies: Host-guest implications, *J. Am. Chem. Soc.,* **135**, pp. 8947–8954, 2013.
50. Molla M. R., Rangadurai P., Pavan G. M. and Thayumanavan S., Experimental and theoretical investigations in stimuli responsive dendrimer-based assemblies, *Nanoscale,* **7**, pp. 3817–3837, 2015.
51. Tomalia D. A., Naylor A. M., Goddard W. A., Starburst dendrimers: Molecular-level control of size, shape, surface chemistry, topology, and flexibility from atoms to macroscopic matter, *Angew. Chem. Int. Ed.,* **29**, pp. 138–175, 1990.
52. Maiti P. K., Cagin T., Wang G. F., Goddard W. A., Structure of PAMAM dendrimers: Generations 1 through 11, *Macromolecules,* **37**, pp. 6236–6254, 2004.

04:36 30 October 2016

53. Naylor A. M., Goddard W. A., Kiefer G. E. et al., Starburst dendrimers 5: Molecular shape control, *J. Am. Chem. Soc.,* **111**, pp. 2339–2341, 1989.

54. Maiti P. K., Cagin T., Lin S. T., Goddard W. A., Effect of solvent and pH on the structure of PAMAM dendrimers, *Macromolecules,* **38**, pp. 979–991, 2005.

55. Lin S. T., Maiti P. K., Goddard W. A., Dynamics and thermodynamics of water in PAMAM dendrimers at subnanosecond time scales, *J. Phys. Chem. B,* **109**, pp. 8663–8672, 2005.

56. Tian W. D., Ma Y. Q., Molecular dynamics simulations of a charged dendrimer in multivalent salt solution, *J. Phys. Chem. B,* 2009, pp. 13161–13170, 2009.

57. Pavan G. M., Danani A., The influence of dendron's architecture on the "rigid" and "flexible" behaviour in binding DNA-a modelling study, *Phys. Chem. Chem. Phys.,* **12**, pp. 13914–13917, 2010.

58. Merkel O. M., Zeng M., Mintzer M. A., et al., Molecular modeling and in vivoimaging can identify successful flexible triazine dendrimer-based siRNA delivery systems, *J. Control. Release,* **153**, pp. 23–33, 2011.

59. Jones S. P., Pavan G. M., Danani A., et al., Quantifying the effect of surface ligands on dendron-DNA interactions: Insights into multivalency through a combined experimental and theoretical approach, *Chem. Eur. J.,* **16**, pp. 4519–4532, 2010.

60. Nandy B., Maiti P. K., DNA compaction by a dendrimer, *J. Phys. Chem. B,* **115**, pp. 217–230, 2011.

61. Sun C., Tang T., Uludag H., Probing the effects of lipid substitution on polycation mediated DNA aggregation: A molecular dynamics simulations Study, *Biomacromolecules,* **13**, pp. 2982–2985, 2012.

62. Lim J., Pavan G. M., Annunziata O., et al., Experimental and computational evidence for an inversion of guest capacity in high-generation triazine dendrimer hosts, *J. Am. Chem. Soc.,* **134**, pp. 1942–1945, 2012.

63. Opitz A. W., Wagner N. J., Structural investigations of poly(amido amine) dendrimers in methanol using molecular dynamics, *J. Polym. Sci.,* 44, pp. 3062–3077, 2006.

64. Lee H., Baker J. R., Larson R. G., Molecular dynamics simulations of PAMAM dendrimer-induced pore formation in DPPC bilayers with a coarse-grained model, *J. Phys. Chem. B,* **110**, pp. 4014–4019, 2006.

65. Pavan G. M., Posocco P., Tagliabue A., Maly M., Malek A., Danani A., Ragg E., Catapano C. V., Pricl S., PAMAM dendrimers for siRNA

delivery: Computational and experimental insights, *Chem. Eur. J.,* **16**, pp. 7781–7795, 2010.

66. Cakara D., Kleinmann J., Borkovec M., Microscopic protonation equilibria of poly(amidoamine) dendrimers from macroscopic titrations, *Macromolecules,* **36**, pp. 4201–4207, 2003.
67. Nisato G., Ivkov R., Amis E. J., Size invariance of polyelectrolyte dendrimers, *Macromolecules,* **33**, pp. 4172–4176, 2000.
68. Chen W. R., Porcar L., Liu Y., Butler P. D., Magid L. J., Small angle neutron scattering studies of the counterion effects on the molecular conformation and structure of charged g4 PAMAM dendrimers in aqueous solutions, *Macromolecules,* **40**, pp. 5887–5898, 2007.
69. Prosa T. J., Bauer B. J., Amis E. J., From stars to spheres: A SAXS analysis of dilute dendrimer solutions, *Macromolecules,* **34**, pp. 4897–4906, 2001.
70. Topp A., Bauer B. J., Klimash J. W., Spindler R., Tomalia D. A., Amis E. J., Probing the location of the terminal groups of dendrimers in dilute solution, *Macromolecules,* **32**, pp. 7226–7231, 1999.
71. Topp A., Bauer B. J., Tomalia D. A., Amis E. J., Effect of solvent quality on the molecular dimensions of PAMAM dendrimers, *Macromolecules,* **32**, pp. 7232–7237, 1999.
72. Prosa T. J., Bauer B. J., Amis E. J., Tomalia D. A., Scherrenberg R. J., A SAXS study of the internal structure of dendritic polymer systems, *Polym. Sci.,* **35**, pp. 2913–2924, 1997.
73. Kostiainen M. A., Szilvay G. R., Smith D. K., Linder M. B., Ikkala O., Multivalent dendrons for high-affinity adhesion of proteins to DNA, *Angew. Chem. Int. Ed.,* **45**, pp. 3538–3542, 2006.
74. Akitaya T., Seno A., Nakai T., Hazemoto N., Murata S., Yoshikawa K., Weak interaction induces an ON/OFF switch, whereas strong interaction causes gradual change: Folding transition of a long duplex DNA chain by poly-L-lysine, *Biomacromolecules,* **8**, pp. 273–278, 2007.
75. Makita N., Yoshikawa Y., Takenaka Y., Sakaue T., Suzuki M., Watanabe C., Kanai T., Kanbe T., Imanaka T., Yoshikawa K., Salt has a biphasic effect on the higher-order structure of a DNA-protamine complex, *J. Phys. Chem. B,* **115**, pp. 4453–4459, 2011.
76. Mintzer M. A., Merkel O. M., Kissel T., Simanek E. E., Polycationic triazine-based dendrimers: Effect of peripheral groups on transfection efficiency, *New J. Chem.,* **33**, pp. 1918–1925, 2009.
77. Merkel O. M., Mintzer M. A., Sitterberg J., Bakowsky U., Simanek E. E., Kissel T., Triazine dendrimers as nonviral gene delivery

04:36 30 October 2016

04:36 30 October 2016

systems: Effects of molecular structure on biological activity, *Bioconjug. Chem.,* **20**, pp. 1799–1806, 2009.

78. Merkel O. M., Mintzer M. A., Librizzi D., Samsonova O., Dicke T., Sporat B., Garn H., Barth P. J., Simanek E. E., Kissel T., Triazine dendrimers as nonviral vectors for in vitro and in vivo RNAi: The effects of peripheral groups and core structure on biological activity, *Mol. Pharm.,* **7**, pp. 969–983, 2010.
79. Pavan G. M., Mintzer M. A., Simanek E. E., Merkel O. M., Kissel T., Danani A., Computational insights into the interactions between DNA and RNA, *Biomacromolecules,* **11**, pp. 721–730, 2010.
80. Pavan G. M., Monteagudo S., Guerra J., Carrion B., Ocana V., Rodriguez-Lopez J., Danani A., Perez-Martinez F. C., Cena V., Role of generation, architecture, pH and ionic strength on successful siRNA delivery and transfection by hybrid PPV-PAMAM dendrimers, *Curr. Med. Chem.,* **19**, pp. 4929–4941, 2012.
81. Garzoni M., Okuro K., Ishii N., Aida T., Pavan G. M., Structure and shape effects of molecular glue on supramolecular tubulin assemblies, *ACS Nano,* **8**, pp. 904–914, 2014.
82. Maiti P. K., Li Y., Cagin T., Goddard W. A., Structure of polyamidoamide dendrimers up to limiting generations: A mesoscale description, *J. Chem. Phys.,* **130**, pp. 144902–144911, 2009.
83. Tian W., Ma Y., Coarse-grained molecular simulation of interacting dendrimers, *Soft Matter,* **7**, pp. 500–505, 2011.
84. Lee H., Larson R. G., Molecular dynamics simulations of PAMAM dendrimer-induced pore formation in DPPC bilayers with a coarse-grained model., *J. Phys. Chem.,* **110**, pp. 18204–18211, 2006.
85. Lyulin A. V., Davis G. R., Adolf D. B., Brownian dynamics simulations of dendrimers under shear flow, *Macromolecules,* **33**, pp. 3294–3304, 2000.
86. Lyulin S. V., Evers L. J., van der Schoot P., et al., Effect of solvent quality and electrostatic interactions on size and structure of dendrimers. Brownian dynamics simulation and mean-field theory, *Macromolecules,* **37**, pp. 3049–3063, 2004.
87. Yan L. T., Yu X., Charged dendrimers on lipid bilayer membranes: Insight through dissipative particle dynamics simulations, *Macromolecules,* 2009, pp. 6277–6283, 2009.
88. Laio A., Parrinello M., Escaping free-energy minima, *Proc. Natl. Acad. Sci. U. S. A.,* **99**, pp. 12562–12566, 2002.

89. Barducci A., Bonomi M., Parrinello M., Metadynamics, *Wiley Interdiscip. Rev. Comput. Mol. Sci.,* **1**, p. 826, 2011.

90. Pavan G. M., Barducci A., Albertazzi L., Parrinello M., Combining metadynamics simulation and experiments to characterize dendrimers in solution, *Soft Matter,* **9**, pp. 2593–2597, 2013.

91. Barducci A., Bussi G., Parrinello M., Well-tempered metadynamics: A smoothly converging and tunable, *Phys. Rev. Lett.,* **100**, p. 020603, 2008.

92. Jansen J. F. G. A., de Brabander-van den Berg E. M. M., Meijer E. W., Encapsulation of guest molecules into a dendritic box, *Science,* **266**, pp. 1226–1229, 1994.

93. Sonawane N. D., Szoka F. C., Verkman A. S., Chloride accumulation and swelling in endosomes enhances DNA transfer by polyamine-DNA polyplexes, *J. Biol. Chem.,* **278**, pp. 44826–44831, 2003.

94. Lee I., Athey B. D., Wetzel A. W., Meixner W., Baker J. R., Structural molecular dynamics studies on polyamidoamine dendrimers for a therapeutic application: Effects of pH and generation, *Macromolecules,* **35**, pp. 4510–4520, 2002.

95. Chandler D., *Introduction to Modern Statistical Mechanics*, Oxford University Press, 1987.

96. Torres D. A., Garzoni M., Subrahmanyam A. V., Pavan G. M., Thayumanavan S., Protein-triggered supramolecular disassembly: Insights based on variations in ligand location in amphiphilic dendrons, *J. Am. Chem. Soc.,* **136**, pp. 5385–5399, 2014.

97. Albertazzi L., Brondi M., Pavan G. M., Sulis Sato S., Signore G., Storti B., Ratto G. M., Beltram F., Dendrimer-based fluorescent indicators: In vitro and in vivo applications, *PLoS ONE,* **6**, p. e28450, 2011.

98. Lee C. C., Gillies E. R., Fox M. E., Guilladeu S. J., Fréchet J. M. J., Dy E. E., Szoka F. C., A single dose of doxorubicin-functionalized bow-tie dendrimer cures mice bearing C-26 colon carcinomas, *Proc. Natl. Acad. Sci. U. S. A.,* **106**, p. 16649–16654, 2006.

99. Gitsov I., Wooley K. L., Hawker C. J., Ivanova P. T., Fréchet J. M. J., Synthesis and properties of novel linear-dendritic block copolymers. Reactivity of dendritic macromolecules toward linear polymers, *Macromolecules,* **26**, p. 5621–5627, 1993.

100. Guillaudeu S. J., Fox M. E., Haidar Y. M., Dy E. E., Szoka F. C., Fréchet J. M. J., PEGylated dendrimers with core functionality for biological applications, *Bioconjug. Chem.,* **19**, pp. 461–469, 2008.

04:36 30 October 2016

101. M. F. P. G. H. C. E. A. Albertazzi L., Enhanced bioactivity of internally functionalized cationic dendrimers with PEG cores, *Biomacromolecules,* **19**, pp. 4089–4097, 2012.

102. Natali S., Mijovic J., Molecular dynamics of PEG–dendrimer blends and PEGylated dendrimers, *Macromolecules,* **42**, pp. 6799–6807, 2009.

103. Lee H., Venable R. M., MacKerell A. D., Pastor R. W., Molecular dynamics studies of polyethylene oxide and polyethylene glycol: Hydrodynamic radius and shape anisotropy, *Biophys. J.,* **95**, pp. 1590–1599, 2008.

104. Lee H., Larson R. G., Effects of PEGylation on the size and internal structure of dendrimers: Self-penetration of long PEG chains into the dendrimer core, *Macromolecules,* **44**, pp. 2291–2298, 2011.

105. Hameau A., Fruchon S., Bijani C., Barducci A., Blanzat M., Poupot R., Pavan G. M., Caminade A. M., Turrin C. O., Theoretical and experimental characterization of amino-PEG-phosphonate-terminated Polyphosphorhydrazone dendrimers: Influence of size and PEG capping on cytotoxicity profiles, *J. Polym. Sci. A,* **53**, pp. 761–774, 2015.

106. Glotzer S. C., Nanotechnology: Shape matters, *Nature,* **481**, pp. 450–452, 2012.

107. Glotzer S. C., Solomon M. J., Anisotropy of building blocks and their assembly into complex structures, *Nat. Mater.,* **6**, pp. 557–562, 2007.

108. Zhang Z. L., Glotzer S. C., Self-assembly of patchy particles, *Nano Lett.,* **4**, pp. 1407–1413, 2004.

109. Garzoni M., Cheval N., Fahmi A., Danani A., Pavan G. M., Ion-selective controlled assembly of dendrimer-based functional nanofibers and their ionic-competitive disassembly, *J. Am. Chem. Soc.,* **134**, pp. 3349–3357, 2012.

110. Zhang S., Zhao Y., Rapid release of entrapped contents from multi-functionalizable, surface cross-linked micelles upon different stimulation, *J. Am. Chem. Soc.,* **132**, p. 10642–10644, 2010.

111. Baker M. B., Albertazzi L., Voets C. I., Leenders K. M. A., Palmans A. R. A., Pavan G. M., Meijer E. W., Consequences of chirality on the dynamics of a water-soluble supramolecular polymer, *Nat. Commun.,* **6**, p. 6234, 2015.

112. Sorrenti A., Illa O., Ortuño R. M., Amphiphiles in aqueous solution: Well beyond a soap bubble, *Chem. Soc. Rev.,* **42**, pp. 8200–8219, 2013.

113. Zhao Y., Sakai F., Su L., Yijiang L., Wei K., Chen G., Jiang M., Progressive macromolecular self-assembly: From biomimetic chemistry to bio-inspired materials, *Adv. Mater.,* **25**, pp. 5215–5256, 2013.

04:36 30 October 2016

04:36 30 October 2016

114. Busseron E., Ruff Y., Moulin E., Giuseppone N., Supramolecular self-assemblies as functional nanomaterials, *Nanoscale,* **5**, pp. 7098–7140, 2013.

115. Bai C., Liu M., From chemistry to nanoscience: Not just a matter of size, *Angew. Chem. Int. Ed.,* **52**, pp. 2678–2683, 2013.

116. Almutairi A., Guillaudeu S. J., Berezin M. J., Achilefu S., Fréchet J. M. J., Biodegradable pH-sensing dendritic nanoprobes for near-infrared fluorescence lifetime and intensity imaging, *J. Am. Chem. Soc.,* **130**, pp. 444–445, 2008.

117. Qiao Z., Ji R., Huang X., Du F., Zhang R., Liang D., Li Z., Polymersomes from dual responsive block copolymers: Drug encapsulation by heating and acid-triggered release, *Biomacromolecules,* **14**, pp. 1555–1563, 2013.

118. Zhang H., Shen J., Liu Z., Hao A., Bai Y., An W., Multi-responsive cyclodextrin vesicles assembled by "supramolecular bola-amphiphiles", *Supramol. Chem.,* **22**, pp. 297–310, 2010.

119. Wang Y., Xu H., Zhang X., Tuning the amphiphilicity of building blocks: Controlled self-assembly and disassembly for functional supramolecular materials, *Adv. Mater.,* **21**, pp. 2849–2864, 2009.

120. Yesilyurt V., Ramirredy R., Thayumanavan S., Photoregulated release of noncovalent guests from dendritic amphiphilic nanocontainers, *Angew. Chem. Int. Ed.,* **50**, pp. 3038–3042, 2011.

121. Raghupathi K. R., Azagarsamy M. A., Thayumanavan S., Guest-release control in enzyme-sensitive, amphiphilic-dendrimer-based nanoparticles through photochemical crosslinking, *Chem. Eur. J.,* **17**, pp. 11752–11760, 2011.

122. Kojima C., Tsumura S., Harada A., Kono K., A collagen-mimic dendrimer capable of controlled release, *J. Am. Chem. Soc.,* **131**, pp. 6052–6053, 2009.

123. Huang X., Du F., Cheng J., Dong Y., Liang D., Ji S., Lin S., Li Z., Acid-sensitive polymeric micelles based on thermoresponsive block copolymers with pendent cyclic orthoester groups, *Macromolecules,* **42**, pp. 783–790, 2009.

124. Li Y., Lokitz B. S., McCormick C., Thermally responsive vesicles and their structural "locking" through polyelectrolyte complex formation, *Angew. Chem. Int. Ed.,* **45**, pp. 5792–5795, 2006.

125. Meng F., Zhong Z., Feijen J., Stimuli-responsive polymersomes for programmed drug delivery, *Biomacromolecules,* **10**, pp. 197–209, 2009.

04:36 30 October 2016

126. Nam J.-M., Thaxton C. S., Mirkin C. A., Nanoparticle-based bio-bar codes for the ultrasensitive detection of proteins, *Science*, **301**, pp. 1884–1886, 2003.

127. da Silva Cardeal L. B., Boccardo E., Termini L., Rabachini T., Andreoli M. A., di Loreto C., Filho A. L., Villa L. L., Maria-Engler S. S., HPV16 oncoproteins induce MMPs/reck-timp-2 imbalance in primary keratinocytes: Possible implications in cervical carcinogenesis, *PLoS One,* **7**, p. e33585, 2012.

128. Hayes G. M., Carrigan P. E., Miller L. J., Serine-arginine protein kinase 1 overexpression is associated with tumorigenic imbalance in mitogen-activated protein kinase pathways in breast, colonic, and pancreatic carcinomas, *Cancer Res.,* **67**, pp. 2072–2080, 2007.

129. Mao J-H., Kim I-J., Wu D., Climent J., Kang H. C., DelRosario R., Balmain A., FBXW7 targets mTOR for degradation and cooperates with PTEN in tumor suppression, *Science,* **321**, pp. 1499–1502, 2008.

130. Mintzer M. A., Grinstaff M. W., Biomedical applications of dendrimers: A tutorial, *Chem. Soc. Rev.,* **40**, pp. 173–190, 2011.

131. Chan D. P. Y., Owen S. C., Shoichet M. S., Double click: Dual functionalized polymeric micelles with antibodies and peptides, *Bioconjug. Chem.,* **24**, pp. 105–113, 2013.

132. Ramireddy R. R., Raghupathi K. R., Amado Torres D., Thayumanavan S., Stimuli sensitive amphiphilic dendrimers, *New J. Chem.* 2012*,* **36**, pp. 340–349, 2012.

133. Tomalia D. A., Reyna L. A., Svenson S., Dendrimers as multi-purpose nanodevices for oncology drug delivery and diagnostic imaging, *Biochem. Soc. Trans.,* **35**, pp. 61–67, 2007.

134. Patri A. K., Kukowska-Latallo J. F., Baker Jr. J. R., Targeted drug delivery with dendrimers: Comparison of the release kinetics of covalently conjugated drug and non-covalent drug inclusion complex, *Adv. Drug Deliv. Rev.,* **57**, pp. 2203–2214, 2005.

135. D'Emanuele A., Attwood D., Dendrimer-drug interactions, *Adv. Drug Deliv. Rev.,* **57**, pp. 2147–2162, 2005.

136. Kojima C., Design of stimuli-responsive dendrimers, *Exp. Opin. Drug Deliv.,* **7**, pp. 307–319, 2010.

137. Mizrachi M. S., Pavan G. M., Levin E., Danani A., Lemcoff N. G., Catalytic chameleon dendrimers, *J. Am. Chem. Soc.,* **133**, pp. 14359–14367, 2011.

04:36 30 October 2016



Taylor & Francis
Taylor & Francis Group
http://taylorandfrancis.com